

UNIVERSITAT DE BARCELONA

Biogeochemical controls on organic contaminants in the Atlantic and Southern Oceans

Núria Trilla i Prieto

ADVERTIMENT. La consulta d'aquesta tesi queda condicionada a l'acceptació de les següents condicions d'ús: La difusió d'aquesta tesi per mitjà del servei TDX (**www.tdx.cat**) i a través del Dipòsit Digital de la UB (**diposit.ub.edu**) ha estat autoritzada pels titulars dels drets de propietat intel·lectual únicament per a usos privats emmarcats en activitats d'investigació i docència. No s'autoritza la seva reproducció amb finalitats de lucre ni la seva difusió i posada a disposició des d'un lloc aliè al servei TDX ni al Dipòsit Digital de la UB. No s'autoritza la presentació del seu contingut en una finestra o marc aliè a TDX o al Dipòsit Digital de la UB (framing). Aquesta reserva de drets afecta tant al resum de presentació de la tesi com als seus continguts. En la utilització o cita de parts de la tesi és obligat indicar el nom de la persona autora.

ADVERTENCIA. La consulta de esta tesis queda condicionada a la aceptación de las siguientes condiciones de uso: La difusión de esta tesis por medio del servicio TDR (**www.tdx.cat**) y a través del Repositorio Digital de la UB (**diposit.ub.edu**) ha sido autorizada por los titulares de los derechos de propiedad intelectual únicamente para usos privados enmarcados en actividades de investigación y docencia. No se autoriza su reproducción con finalidades de lucro ni su difusión y puesta a disposición desde un sitio ajeno al servicio TDR o al Repositorio Digital de la UB. No se autoriza la presentación de su contenido en una ventana o marco ajeno a TDR o al Repositorio Digital de la UB (framing). Esta reserva de derechos afecta tanto al resumen de presentación de la tesis como a sus contenidos. En la utilización o cita de partes de la tesis es obligado indicar el nombre de la persona autora.

WARNING. On having consulted this thesis you're accepting the following use conditions: Spreading this thesis by the TDX (**www.tdx.cat**) service and by the UB Digital Repository (**diposit.ub.edu**) has been authorized by the titular of the intellectual property rights only for private uses placed in investigation and teaching activities. Reproduction with lucrative aims is not authorized nor its spreading and availability from a site foreign to the TDX service or to the UB Digital Repository. Introducing its content in a window or frame foreign to the TDX service or to the UB Digital Repository is not authorized (framing). Those rights affect to the presentation summary of the thesis as well as to its contents. In the using or citation of parts of the thesis it's obliged to indicate the name of the author.

Biogeochemical controls on organic contaminants in the Atlantic and Southern Oceans



Núria Trilla i Prieto

Universitat de Barcelona
CSIC
Consejo Superior de Investigaciones Científicas

Programa de doctorat:
Ciències del Mar

Biogeochemical controls on organic contaminants in the Atlantic and Southern Oceans

Memòria de tesi presentada per optar al grau de Doctora per la Universitat de Barcelona per

Núria Trilla i Prieto

Barcelona, 12 de febrer de 2025

Directors:

Prof. Jordi Dachs
(IDAEA-CSIC)

Dra. Begoña Jiménez
(IQOG-CSIC)

Tutora:

Dra. Montserrat Vidal
(UB - Facultat de Biologia)

La Dra. Begoña Jiménez, investigadora científica de l'Institut de Química Orgànica General (IQOG) i el Prof. Jordi Dachs, professor d'investigació de l'Institut de Diagnòstic Ambiental i Estudis de l'Aigua (IDAEA), pertanyents el Consell Superior d'Investigacions Científiques (CSIC), certifiquen:

Que la present memòria presentada per optar el títol de Doctora, titulat: "*Biogeochemical controls on organic contaminants in the Atlantic and Southern Oceans*" ha estat realitzada sota la nostra direcció per la Núria Trilla i Prieto a l'IDAEA-CSIC i IQOG-CSIC, i que tots els resultats presentats són fruit del treball experimental realitzat per la mencionada doctoranda.

Barcelona, 12 de febrer del 2025

Portada dissenyada per Clàudia Sanz
Sueñaflores / @suenaflores

Aquesta tesi ha estat suportada pel Ministeri de Ciència, Innovació i Universitats del Gobierno de España a través dels projectes ANTOM (PGC2018-096612-B-I00) i PANTOC (PID2021-127769NB-I00). La Núria Trilla i Prieto ha estat receptora de una ajuda per part del Ministeri de Ciència, Innovació i Universitats del Gobierno de España amb una beca predoctoral FPI (PRE2019-089641).

This thesis was supported by Spanish Ministry of Science, Innovation and Universities through project ANTOM (PGC2018-096612-B-I00) and PANTOC (PID2021-127769NB-I00). Núria Trilla i Prieto has been funded through the Spanish Ministry of Science, Innovation and Universities, as a recipient of an FPI predoctoral scholarship (PRE2019-089641).

«La frase tan repetida de "viure dels records" crec que es vàlida, sempre i quant s'hagi fet una acumulació d'experiències que hagin omplert tota una vida. Aquestes vivències son les que cap decisió administrativa podrà esborrar mai. Amb tota seguretat puc dir que jo he viscut a l'Antàrtida. I em sento capaç d'alimentar-me dels seus records la resta de la meva vida.»

Josefina Castellví i Piulachs

A la meva Sagrada Familia



TABLE OF CONTENTS

ABSTRACT / RESUM 14
LIST OF ABBREVIATIONS 22
LIST OF TABLES & FIGURES 24

PART 01 - INTRODUCTION 34

1.1. General Introduction 36
1.1.1. The anthropogenic impact on Earth system's processes 36
1.1.2. The planetary boundaries 38
1.1.3. Chemical pollution 39
1.1.4. Regulatory frameworks 41
1.1.5. Properties of priorization of chemical pollutants 44
1.1.6. POPs cycling in the environment 46

1.2. Selected oceanic regions 52
1.2.1. The Atlantic Ocean 52
1.2.2. The Southern Ocean and Antarctica 53

1.3. Targeted contaminants 56
1.3.1. Aromatic Compounds 56
1.3.2. Perfluoroalkyl Substances 58
1.3.3. Organophosphate Esters 62

1.4. Objectives and thesis structure 68
1.4.1. Objectives 68
1.4.2. Thesis structure 68

1.5. References 71

PART 02 - METHODOLOGICAL APPROACH 88

2.1. The ANTOM Project 90
2.2. The ANTOM oceanographic cruises 90
2.3. Sampling overview 91
2.3.1. Seawater: surface and water column 93
2.3.2. Sea surface microlayer and sub-surface layers 94
2.3.3. Wet Deposition 95
2.3.4. Other samplings 95

2.4. Sample treatment and analysis 95
2.4.1. PFAS analysis 96
2.4.2. OPE analysis 97

2.5. Quality Control and Quality Assurance 100
2.6. References 101

PART 03 - MAIN CHAPTERS 101

GUIDE TO THE MAIN CHAPTERS *103*

CHAPTER I. OCCURRENCE OF AROMATIC-LIKE COMPOUNDS IN THE GLOBAL OCEAN *105*

3.1.1. Paper I. *Dissolved Black Carbon and Semivolatile Aromatic Hydrocarbons in the Ocean: Two Entangled Biogeochemical Cycles?* *109*
3.1.2. Paper I. Supplementary Materials *117*

CHAPTER 2. TRANSPORT AND BIOGEOCHEMISTRY OF PFAAs IN THE OCEANS *121*

3.2.1. Paper II. *Accumulation of Perfluoroalkyl Acid "Forever Chemicals" in Antarctic Waters* *122*
3.2.2. Paper II. Supplementary Materials *135*

CHAPTER 3. TRANSPORT AND BIOGEOCHEMISTRY OF OPEs IN THE OCEANS *148*

3.3.1. Paper III. *Enrichment of Organophosphate Esters in the Sea Surface Microlayer from the Atlantic and Southern Oceans* *151*
3.3.2. Paper III. Supplementary Materials *161*
3.3.3. Paper IV. *Biogeochemical Controls on Latitudinal (42°N to 70°S) and Depth Distribution of Organophosphate Esters in the Atlantic and Southern Oceans* *167*
3.3.4. Paper IV. Supplementary Materials *205*

CHAPTER 4. SCIENTIFIC OUTREACH WITHIN ACADEMY *234*

3.4.1. Paper V. *Balancing the equation: A tool for evaluating effective scientific outreach* *237*
3.4.2. Paper V. Supplementary Materials *247*

PART 04 - GENERAL DISCUSSION AND CONCLUSIONS 259

4.1. Global discussion of the results *261*
4.2. Conclusions *273*
4.3. References *275*

AKNOWLEDGMENTS 280

ABSTRACT

During the last two centuries, the increase of human population and economic development has led to a rising demand for goods and resources. Such development has also led to the synthesis of millions of new organic chemicals, with hundreds of thousands of these currently used in agriculture and industrial applications, as well as in consumer products. A fraction of this myriad of synthetic chemicals, together with hydrocarbons derived from the use of fossil fuels, reach the environment. This mixture of organic compounds with diverse properties and uses, invisible to the human eye, constitutes a form of pollution to the Earth system of unusual complexity. Addressing chemical pollution is a major challenge due to the large number of chemicals involved, which in addition have different and diverse physico-chemical properties and present different mechanisms of toxicity to organisms, ecosystems and humans.

For decades, researchers, environmental agencies and regulatory bodies have sought to prioritize those organic contaminants that need to be regulated because of their potential for long-range transport, ubiquitous occurrence, persistence, bioaccumulation potential, toxicity, and ecological impact. However, the massive production and release of these substances into the environment surpass research and regulatory capacities, endangering the sustainability of the Earth's system. This mismatch has led to the definition of "novel entities" as one of the planetary boundaries in the current context of global change, essential for the planet's resilience. A recent study confirms that this threshold, along with five others, has already been exceeded, increasing the risk of irreversible changes to the Earth system.

Mostly during the last century, some synthetic chemicals were regulated and banned, even though they are still found in the environment. However, just in the recent decades, an increasing number of chemicals, potentially thousands of contaminants of emerging concern (CECs), have dispersed globally, accumulating in various environmental compartments, with transport, biogeochemical cycles and sinks strongly dependent on their physicochemical properties and chemical structure. They are found in soils, fresh and sea water, ice, air, and biota, from microorganisms to large predators. Many CECs originate from common consumer products such as clothing, cosmetics, furniture, and paints. Among CECs, organophosphate esters (OPEs) and perfluoroalkyl acids (PFAAs) have raised increasing concern due to their ubiquity, persistence, toxicity and bioaccumulation in food webs. Nevertheless, knowledge not only on their occurrence, but their transport, cycling and sinks in the oceans is limited. The study of persistent organic pollutants (POPs) and CECs in the ocean is important, especially in remote regions, as these are sentinels of global pollution, which can only occur for chemicals persistent enough to undergo long-range transport. For instance, candidates for regulation as POPs under the Stockholm Convention should meet the criteria on persistence, toxicity, long-range transport, and biomagnification.

This thesis contributes to the study of oceanic and Antarctic pollution with the overall objective of assessing the occurrence, biogeochemistry and sinks of three families of organic pollutants in the ocean: PFAAs, OPEs and semivolatile aromatic compounds (SALCs) within the dissolved black carbon (DBC). Despite their differences in sources and physicochemical properties, these three families share the ability for long-range transport, persistence , and toxic effects on ecosystems and human health.

Polycyclic aromatic hydrocarbons (PAHs), as part of SALCS, and DBC, all originate from the incomplete combustion of organic matter, including fossil fuels and wildfires. By means of a meta-analysis of previous studies, the coupling and entanglement between the biogeochemical cycles of DBC and SALCs in the ocean was assessed, showing that SALCs account for 16% of oceanic DBC, a key feature neglected in previous works. The main source of these compounds to the ocean is air-water diffusive exchange, with photo- and bio-degradation in the top 200 m as their main sinks. This work shows that there is a semi-volatile and labile fraction of DBC which is relevant for the study of this fraction of anthropogenic and biogenic condensed organic matter in the ocean.

The assessment of PFAAs and OPEs was based on field measurements performed during an extensive latitudinal transect, covering from 42°N to 70.1°S, encompassing the Atlantic and Southern Oceans, including the South Shetland Islands, the Bransfield Strait, and the Bellingshausen Sea. The samples were collected from two oceanographic cruises covering this transect, and were analyzed for OPEs and PFAAs, allowing the determination of their latitudinal and depth distribution from the surface down to 2000 m. Such unique data set is among the largest available to date, and covers different oceanic regions receiving different anthropogenic pressures from source regions to the remote Antarctic waters, driven by different biogeochemical conditions.

OPEs, which have been used as plasticizers and flame retardants for the last decades, showed a decreasing concentration trend when moving from the Northern to the Southern Hemisphere, with peaks in concentrations near primary source regions (off-shore Iberian Peninsula and Brazil). Concentrations in the surface waters of the Southern Ocean were significantly lower, consistent with its remoteness and the role of the Antarctic circumpolar current limiting the oceanic transport of contaminants to the Southern Ocean. In terms of vertical distribution, a correlation between surface and depth concentrations, and between concentrations in the deep chlorophyll maximum depth and chlorophyll a concentrations suggested the role of the biological pump as a relevant sink by sequestering OPEs in the photic zone and releasing them in the mesopelagic and bathypelagic waters as organic matter re-mineralize and OPE partition to the dissolved phase. Additionally, significant accumulation of OPEs in the sea surface microlayer (SML) (the upper mm of the ocean) was observed, especially in the Southern Ocean consistent with higher phytoplankton biomass which release surfactant active substances favoring a developed SML. It is also suggested that OPEs can be transferred to the atmosphere by sea spray formation, which would contribute to their long-range transport potential, favoring atmospheric transport to remote regions. This work shows that OPEs are ubiquitous in the ocean, demonstrating their persistence and potential for long range transport.

PFAAs, actually known as “forever chemicals”, have been widely used for their water-repellent properties especially for the last five decades. In this study, PFAAs showed an unexpected distribution pattern in which concentrations in the Southern Ocean were of a comparable magnitude to those in the North Atlantic, which is closer to major emission sources. This suggested that PFAAs are accumulating in Antarctic waters as PFAAs concentrations were very low in earlier reports. A mechanism for the transport of PFAAs to the Southern Ocean

is suggested, consisting on aerosolization of PFAAs during sea spray formation, and their wet atmospheric deposition via rain and snow. These processes would result in a grasshopping behavior, even though PFAAs are swimmers, mediated by sea spray formation and wet deposition, but not by successive cycles of volatilization and deposition. This mechanism facilitates their arrival and accumulation in Antarctica, where they may be retained by the Antarctic Circumpolar Current and the Antarctic Divergence. This process raise concern on the potential impact and accumulation of other thousands of persistent poly- and per-fluorinated substances (PFAS) which have not yet been assessed. In addition, it confirms persistence as the key property for the priorization of organic contaminants.

PFAAs stand out as the contaminants studied with the highest apparent persistence, and having less relevant sinks, as evidenced by their high concentrations in Antarctica. This accumulation occurs even for some individual PFAAs that have already been included in the Stockholm convention. The problematic of the larger group of PFAS is especially troublesome as addressing their occurrence and sinks in the ocean may not be attainable for such a large number of individual chemicals. This will present a significant challenge for the future and highlights the lack of agents and policies capable of effectively regulating chemical pollution on a global scale.

This study highlights the widespread presence and impact of persistent organic pollutants in the global ocean, including remote regions like Antarctica. Identifying the mechanisms regulating their distribution, transport, and removal is essential for understanding their persistence and environmental effects. The results of this thesis provide key information for the future management and regulation of these compounds, underscoring the need for coordinated global action to reduce their emissions and minimize their impacts.

Lastly, driven by my personal concern about the need of bigger efforts to bring science closer to the general public, my PhD research journey have led to multiple initiatives aimed at explaining the motivations, findings, and significance of environmental chemistry and Antarctic research to a broad range of audiences. These efforts have had a considerable impact in terms of audience, and have leaded to the development of an evaluation tool designed to assist both researchers and science communicators in optimizing and enhancing science dissemination strategies, with the goal of achieving greater reach and impact. This endeavor is essential for fostering scientific vocations, stimulating critical thinking, and strengthening society's engagement with socio-environmental causes that are crucial for our future.

This work underscores the pervasive presence, persistence, and transport of organic pollutants in the global ocean, revealing key mechanisms that govern their distribution and accumulation, even in remote Antarctic waters. By integrating scientific research with science communication, this thesis not only advances our understanding of chemical pollution but also promotes broader public engagement, contributing to the urgent need for informed policy action and environmental stewardship.

RESUM

Durant els darrers dos segles, l'augment de la població humana i el desenvolupament econòmic han generat una creixent demanda de béns i recursos. Aquest desenvolupament també ha conduït a la síntesi de milions de nous compostos orgànics, centenars de milers dels quals s'utilitzen actualment en aplicacions agrícoles, industrials i en productes de consum. Una fracció d'aquesta miríada de substàncies sintètiques, juntament amb hidrocarburs derivats de l'ús de combustibles fòssils, arriba al medi ambient. Aquesta barreja de compostos orgànics amb propietats i usos diversos, invisibles a l'ull humà, constitueix una forma de contaminació d'una complexitat inusual per al sistema terrestre. Abordar la contaminació química representa un repte majúscul a causa del gran nombre de substàncies implicades, que, a més, presenten propietats fisicoquímiques diferents i mecanismes de toxicitat diversos per als organismes, els ecosistemes i la salut humana.

Durant dècades, investigadors, agències ambientals i organismes reguladors han treballat per prioritzar aquells contaminants orgànics que han de ser regulats a causa del seu potencial de transport a llarga distància, la seva presència ubiqua, persistència, bioacumulació, toxicitat i impacte ecològic. No obstant això, la producció massiva i el vessament d'aquestes substàncies al medi ambient superen la capacitat d'investigació i regulació, posant en perill la sostenibilitat del sistema terrestre. Aquest desajust ha portat a la definició de les "noves entitats" com un dels límits planetaris en el context actual del canvi global, essencials per a l'estabilitat del planeta. Un estudi recent confirma que aquest llindar, juntament amb cinc altres, ja han estat superats, augmentant el risc de canvis irreversibles en el sistema terrestre.

Majoritàriament durant el darrer segle, alguns compostos sintètics han estat regulats i prohibits, tot i que encara es detecten en el medi ambient. No obstant això, només en les últimes dècades, un nombre creixent de compostos, potencialment milers de contaminants emergents (CEs), s'han dispersat globalment, acumulant-se en diversos compartiments ambientals, amb transports, cicles biogeoquímics i embornals fortament dependents de les seves propietats fisicoquímiques i estructura química. Aquests contaminants es troben en sòls, aigües dolces i marines, gel, aire i biota, des de microorganismes fins a grans depredadors. Molts CEs tenen origen en productes de consum habituals com la roba, els cosmètics, el mobiliari i les pintures. Entre els CEs, els èsters organofosforats (OPEs, de l'anglès "organophosphate esters") i els àcids perfluoroalquilats (PFAAs, de l'anglès "perfluoroalkyl acids") han suscitat una preocupació creixent a causa de la seva ubiqüitat, persistència, toxicitat i capacitat de bioacumulació en les xarxes tròfiques. No obstant això, el coneixement no només sobre la seva presència, sinó també sobre el seu transport, cicle i embornals als oceans és limitat. L'estudi dels contaminants orgànics persistents (COPs) i dels CEs a l'oceà és crucial, especialment en regions remotes, ja que aquestes actuen com a sentinelles de la contaminació global, que només pot tenir lloc per a compostos prou persistents per experimentar transport a llarga distància. Per exemple, els candidats per a la regulació com a COPs en el marc del Conveni d'Estocolm han de complir els criteris de persistència, toxicitat, transport a llarga distància i biomagnificació.

Aquesta tesi contribueix a l'estudi de la contaminació oceànica i antàrtica amb l'objectiu general d'avaluar la presència, biogeoquímica i embornals de tres famílies de contaminants orgànics en l'oceà: PFAAs, OPEs i compostos aromàtics semivolàtils (SALCs, de l'anglès "semivolatile aromatic-like compounds") dins del carboni negre dissolt (DBC, de l'anglès "dissolved black carbon"). Malgrat les seves diferències en fonts i propietats fisicoquímiques, aquestes tres famílies comparteixen la capacitat de transport a llarga distància, persistència i efectes tòxics sobre els ecosistemes i la salut humana.

Els hidrocarburs aromàtics policíclics (PAHs, de l'anglès "polycyclic aromatic hydrocarbons"), com a part dels SALCs, i el carboni negre dissolt s'originen en la combustió incompleta de matèria orgànica, inclosos els combustibles fòssils i els incendis forestals. Mitjançant una meta-anàlisi d'estudis previs, s'ha avaluat la interacció entre els cicles biogeoquímics del DBC i els SALCs a l'oceà, mostrant que els SALCs representen un 16% del DBC oceànic, un aspecte clau que havia estat negligit en estudis anteriors. La font principal d'aquests compostos a l'oceà és l'intercanvi difusiu aire-aigua, amb la fotodegradació i la biodegradació en els primers 200 metres com a principals embornals. Aquest treball demostra l'existència d'una fracció semivolàtil i làbil del DBC rellevant per a l'estudi d'aquesta fracció de matèria orgànica condensada d'origen antropogènic i biogènic a l'oceà.

L'avaluació dels PFAAs i OPEs s'ha basat en mesures de camp realitzades durant un extens transsecte latitudinal, des de 42°N fins a 70.1°S, cobrint els oceans Atlàntic Austral, incloent les illes Shetland del Sud, l'estret de Bransfield i el mar de Bellingshausen. Les mostres es van recollir durant dues campanyes oceanogràfiques que van cobrir aquest transsecte i es van analitzar per a OPEs i PFAAs, permetent determinar la seva distribució latitudinal i en profunditat, des de la superfície fins als 2000 m. Aquest conjunt de dades és un dels més amplis disponibles fins avui i cobreix diferents regions oceàniques que reben diverses pressions antropogèniques, des de les zones on es troben les principals fonts fins a les aigües remotes de l'Antàrtida, influenciades per diferents condicions biogeoquímiques.

Els OPEs, emprats com a plastificants i retardants de flama durant les darreres dècades, han mostrat una tendència decreixent de concentració en desplaçar-se de l'hemisferi nord al sud, amb màxims prop de les regions on hi ha les fonts primàries (al llarg de les costes de la Península Ibèrica i el Brasil). Les concentracions a les aigües superficials de l'oceà Austral han estat significativament més baixes, fet que concorda amb la seva llunyania i amb el paper de la Corrent Circumpolar Antàrtica com a barrera que limita el transport oceànic de contaminants cap a l'oceà Austral.

Pel que fa a la distribució vertical, s'ha observat una correlació entre les concentracions en superfície i en profunditat, així com entre les concentracions a la profunditat del màxim de clorofil·la (DCM, de l'anglès "depth of chloropyll maximum") i les concentracions de clorofil·la *a*. Això suggereix que la bomba biològica actua com un embornal rellevant, segrestant els OPEs a la zona fòtica i alliberant-los a les aigües mesopelàgiques i batipelàgiques a mesura que la matèria orgànica es remineralitza i els OPEs re-entren a la fase dissolta. A més, s'ha observat una acumulació significativa d'OPEs en la microcapa superficial marina (els mil·límetres superiors de l'oceà), especialment a l'oceà Austral, d'acord amb una major biomassa fitoplanctònica que podria alliberar substàncies actives com a tensioactius. També es suggereix que els OPEs poden ser transportats cap a l'atmosfera mitjançant la formació d'aerosols marins, la qual cosa contribuiria al seu potencial de transport a llarga distància, afavorint-ne el transport atmosfèric cap a regions remotes. Aquest treball demostra que els OPEs són pervasius a l'oceà, evidenciant la seva persistència i capacitat de transport a llarga distància.

Els PFAAs, coneguts com a "químics eterns", han estat àmpliament utilitzats per les seves propietats hidrorepel·lents, especialment durant les darreres cinc dècades. En aquest estudi, els PFAAs han mostrat un patró de distribució inesperat, en què les concentracions a l'oceà Austral eren d'una magnitud comparable a les de l'Atlàntic Nord, que es troba més a prop de les principals fonts d'emissió.

Aquest resultat suggereix que els PFAAs s'estan acumulant a les aigües antàrtiques, ja que les seves concentracions en treballs anteriors eren molt baixes. S'ha proposat un mecanisme per al transport dels PFAAs cap a l'oceà Austral que inclou la seva aerosolització durant la formació d'aerosols marins i la seva deposició atmosfèrica humida a través de la pluja i la neu. Aquests processos generarien un comportament de "saltadors" (grasshopping), tot i que els PFAAs són considerats "nedadors", mediat per la formació d'aerosols marins i deposició humida, i no per cicles successius de volatilització i deposició. Aquest mecanisme facilitaria la seva arribada i acumulació a l'Antàrtida, on podrien quedar retinguts per la Corrent Circumpolar Antàrtica i la Divergència Antàrtica. Aquest fenomen genera preocupació per l'impacte potencial i l'acumulació de milers d'altres substàncies per- i poli- fluoralquilades (PFAS, de l'anglès "per- and poly-fluoroalkyl substances") que encara no han estat avaluades. A més, confirma que la persistència és la propietat clau per a la priorització dels contaminants orgànics.

Els PFAAs es destaquen com els contaminants estudiats amb la persistència aparent més elevada i amb embornals menys significatius, com es reflecteix en les seves altes concentracions a l'Antàrtida. Aquesta acumulació es produeix fins i tot per a alguns PFAAs individuals que ja han estat inclosos en el Conveni d'Estocolm. La problemàtica del conjunt més ampli dels PFAS és especialment preocupant, ja que abordar-ne la presència i els embornals a l'oceà pot resultar inassolible a causa del gran nombre d'aquests compostos. Això suposarà un repte significatiu per al futur i posa en relleu la manca d'agents i polítiques capaços de regular eficaçment la contaminació química a escala global.

Aquest estudi destaca la presència i l'impacte generalitzat dels contaminants orgànics persistents a l'oceà global, incloses regions remotes com l'Antàrtida. Identificar els mecanismes que regulen la seva distribució, transport i eliminació és essencial per comprendre la seva persistència i efectes ambientals. Els resultats d'aquesta tesi proporcionen informació clau per a la futura gestió i regulació d'aquests compostos, subratllant la necessitat d'una acció global coordinada per reduir-ne les emissions i minimitzar-ne els impactes.

Finalment, impulsada per una unquietud personal sobre la necessitat de fer més esforços per apropar la ciència al públic general, la meva trajectòria com a investigadora durant el doctorat m'ha portat a promoure múltiples iniciatives dirigides a explicar les motivacions, els resultats i la importància de la química ambiental i la recerca antàrtica a un públic ampli. Aquests esforços han tingut un impacte considerable en termes d'audiència i han conduït al desenvolupament d'una eina d'avaluació dissenyada per ajudar tant investigadors com comunicadors científics a optimitzar i millorar les estratègies de divulgació científica, amb l'objectiu d'aconseguir un abast i un impacte més grans. Aquesta tasca és fonamental per fomentar vocacions científiques, estimular el pensament crític i enfortir el compromís de la societat amb les causes socioambientals crucials per al nostre futur.

Aquest treball posa de manifest la presència generalitzada, la persistència i el transport dels contaminants orgànics a l'oceà global, revelant els mecanismes clau que en regulen la distribució i acumulació, fins i tot en aigües remotes de l'Antàrtida. Mitjançant la integració de la recerca científica amb la comunicació de la ciència, aquesta tesi no només aprofundeix en el coneixement sobre la contaminació química, sinó que també fomenta una major implicació pública, contribuint a la necessitat urgent d'una acció política informada i d'una gestió ambiental responsable

LIST OF ABBREVIATIONS

1PAR / 1%PAR	Depth of 1% of radiation
ACC	Antarctic Circumpolar Current
AP	Antarctic Peninsula
AO	Atlantic Ocean
BA	Bacterial abundance
BAF	Bioaccumulation Factor
BP	Bacterial production
CFCs	Chlorofluorocarbons
Chl a	Chlorophyll *a*
Cl-OPEs	Halogenated / Chlorinated Organophosphate Esters
CLRTAP	Convention on Long-Range Transboundary Air Pollution
CSIC	Consejo Superior de Investigaciones Científicas
DBC	Dissolved Black Carbon
DCM	Depth of Maxymum Chlorophyll
DDE	Dichlorodiphenyldichloroethylene
DDT	Dichloro-diphenyl-trichloroethane
ECHA	European Chemicals Agency
EU	European Union
EF	Enrichment Factor
EF_{SML}	Enrichment Factor in the Sea Surface Microlayer
EF_{SSA}	Enrichment Factor in the Sea Spray Aerosols
EPA	Environmental Protection Agency
FR	Flame Retardants
GC	Gas chromatography
GC-Ms/Ms	Gas chromatography coupled to Tandem Mass Spectrometry
GF/F	Glass fiber filter
H	Henry's Law constant
H'	Dimensionless Henry's Law constant
HCB	Hexachlorobenzene
HCH	Hexachlorocyclohexane
HLB cartridge	Hydrophyllic - Lipophyllic balance
HMW	High Molecular Weight
IDAEA	Institute for Environmental Assessment and Water Research
IQOG	Institute of General Organic Chemistry
IPCC	Intergovernmental Panel on Climate Change
IS	Internal Standard
K_{ow}	Octanol-Water Partition Coefficient
K_{OA}	Octanol-Air Partition Coefficient
K_{AW}	Air-Water Partition Coefficient
K_{RP}	Rain-aerosol partition coefficient
LC	Liquid Chromatography
LC-Ms/Ms	Liquid Chromatography coupled to Tandem Mass Spectrometry
LC-PFCAs	Long chain perfluorocarboxylic acids
LMW	Low Molecular Weight

LOD	Limit of Detection
LOQ	Limit of Quantification
LRAT	Long-range Atmospheric Transport
MM	Molar Mass
MOx	Depth of Minimum Oxygen
MW	Molecular weight
N Atlantic	North Atlantic basin
OCs	Organochlorine Compounds
OM	Organic Matter
OPEs	Organophosphate Esters
P / P-val	P-value
P_v	Vapor pressure
PAHs	Polycyclic Aromatic Hydrocarbons
PBDEs	Polybrominated Diphenyl Ethers
PCBs	Polychlorinated Biphenyls
PCDDs	Polychlorinated Dibenzo-p-dioxins
PCDFs	Polychlorinated Dibenzofurans
PFAS	Perfluoroalkyl Substances
PFAAs	Perfluoroalkyl Acids
PFCAs	Perfluoroalkyl carboxylic acids
PFOA	Perfluorooctanoic acid
PFOS	Perfluorooctanesulfonic acid
PFSAs	Perfluoroalkyl sulfonic acids
POPs	Persistent Organic Pollutants
PP	Polypropelene
PTFE	Polytetrafluoroethylene
QqQ	Triple quadrupole
REACH	Registration, Evaluation, Authorisation, and Restriction of Chemicals
S Atlantic	South Atlantic basin
SALCs	Semi Volatile Aromatic-Like Compounds
SC	Stockholm Convention
SML	Sea Surface Microlayer
SO	Southern Ocean
SOCs	Semivolatile Organic Compounds
SPE	Solid Phase Extraction
SPP	Science-Poly Panel
SSA	Sea Spray Aerosols
SSL	Subsurface Layer / Subsurface Waters
T	Temperature
UNECE	United Nations Economic Commission for Europe
UNEA	United Nations Environment Assembly
UNEP	United Nations Environmental Program
UPLC	Ultraperformance liquid chromatography
X^2	Chi-square Test

LIST OF TABLES & FIGURES

PART 01. INTRODUCTION

LIST OF FIGURES

Figure 1.1 | Responses of the Earth System to increasing pressure from human activities: a nitrogen fixation (Vitousek, 1994); b species extinctions (Smith, 2002); c northern hemisphere surface temperature (Mann et al., 1999); and d atmospheric CO_2 concentration (adapted from Keeling and Whorf, 2000). From Steffen et al. (2005)

Figure 1.2 | Current status of control variables for all nine planetary boundaries. Richardson et al. (2023) (left panel) and Persson et al. (2022) (right panel).

Figure 1.3 | Major modes of transport of perfectly persistent, hypothetical chemicals defined by their partitioning properties log K_{AW} and log K_{OA}, when calculated with the Globo-POP model (Wania, 2003) assuming 10 years of steady emissions into air. Graphics modified from Wania (2006), with copyright by the American Chemical Society. (A) Legacy organochlorine compounds. (B) Some chemicals in current use. (The arrow for perfluoro acids illustrates that these degradation products of the polyfluoro alcohols have log K_{AW} << - 5 and log K_{OA} << 3, and are thus off scale). From Lohmann et al. (2007).

Figure 1.4 | DOC and ADOC cycling in the upper ocean. Orange and green arrows show the sources, transport and transformation processes of anthropogenic dissolved organic carbon (ADOC) and biogenic dissolved organic carbon (BDOC) respectively. tADOC accounts for the transformed ADOC, thus those transformation products due to biotic and abiotic degradation. Black arrows show the overall DOC processes resulting from contributions from ADOC and DOC. The lower panel shows the adsorption and absorption of ADOC compounds to cell membranes due to hydrophobicity. Reported effects of ADOC on microbes are depicted. From Vila-Costa et al. (2020).

Figure 1.5 | Global distillation with fractionation according to global mobility. Adapted from Nash et al. (2013).

Figure 1.6 | The Atlantic meridional overturning circulation (AMOC) fingerprint, sea surface temperature (SST) and global mean (GM). Black contour marks subpolar gyre (SG) region on top of the Hadley Centre Sea Ice and Sea Surface Temperature data set (HadISST) SST reconstruction for December 2020.

Figure 1.7 | A schematic representation of the current systems in the Southern Ocean. The Antarctic Circumpolar Current (ACC) flows from west to east around Antarctica in two major branches, the Polar Front and Subantarctic Front. Clockwise gyres fill the deep basins between the Antarctic continent and the ACC. Adapted from Rintoul et al. (2001).

Figure 1.8 | A schematic of the three-dimensional flow between ocean basins. The figure illustrates the two key roles the Southern Ocean plays in the global overturning circulation: (1) the circumpolar link connects the ocean basins, and (2) water mass formation transforms deep water to intermediate and bottom water. From Schmitz (1996).

Figure 1.9 | The PFAS life cycle. PFAS product flows from primary producer to commercial user to consumers to disposal. Each step is attended by atmospheric and aqueous fugitive releases. Soils constitute a long-term environmental sink, slowly releasing PFAS to the hydrosphere and allowing uptake in biota, but the ultimate reservoir is deep marine sediment. From Evich et al. (2022).

Figure 1.10 | Major sources and pathways of OPEs in coastal and open oceans. The primary continental sources of organophosphate esters (OPEs) include industry, wastewater treatment plants, electronic waste recycling plants and ambient emissions. Major environmental pathways for OPE dispersal include atmospheric and oceanic transport, air–water exchange, atmospheric dry and wet deposition, sedimentation, bioaccumulation and microbial interactions. OPEs can be transported from continental sources to the open ocean and undergo biogeochemical cycling in various environmental compartments. UV, ultraviolet. From Xie et al. (2022a).

Figure 1.11 | Thesis structure.

LIST OF TABLES

Table 1.1 | Compounds listed under the CLRTAP-POPs Protocol (UNECE, 1998).

Table 1.2 | Persistent Organic Pollutants (POPs) listed in the Stockholm Convention. The chemicals targeted by the Stockholm Convention are listed in the annexes of the convention text. In May 2023, the Conference of the Parties amended Annex A to include Methoxychlor, Dechlorane Plus, and UV-328, following previous proposals for their listing.

Table 1.3 | Summary of characteristics and requirements to define a POP according to UNECE (Stockholm Convention on POPs). Text and Annexes revised in 2023.

Table 1.4 | US EPA's 16 priority PAHs and selected physico-chemical properties by ASTDR, 1995. Italics refers to compounds classified as probable human carcinogenic by National Toxicological Program (USA), 2005.

Table 1.5 | Physicochemical properties of the selected PFAS. Data extracted from [a]Kin et al., 2015, and [b]Wang et al., 2011. Blank cells indicate no data available.

Table 1.6 | Physicochemical properties of the selected OPEs. Data extracted from Zhang et al. 2016. Those marked in bold are from EPISuite ChemSpider Royal Society of Chemistry.Blank cells indicate no data available.

Table 1.7 | Chemical structure of the selected OPEs.

LIST OF EQUATIONS

[1] Air-water partition coefficient (K_{AW})

[2] Octanol-water partition coefficient (K_{OW})

[3] Octanol-air partition coefficient (K_{OA})

[4] Octanol-air partition coefficient (K_{OA})

[5] Bioconcentration factor (BCF [kg L^{-1}])

[6] Dry deposition of particulate-bound pollutants (F_{DD})

[7] Diffusive air-water exchange (F_{AW})

[8] Wet Deposition flux (F_{WD})

[9] Wet Deposition flux (F_{WD})

[10] Rain-air partition constant (K_{RA})

[11] Rain-air partition constant ($K_{RP, air, P}$)

[12] Rain-air partition constant ($K_{RG, air, G}$)

[13] Enrichment factor in the SML (EF_{SML})

[14] Enrichment factor in the SSA (EF_{SSA})

PART 02.METHODOLOGICAL APPROACH

LIST OF FIGURES

Figure 2.1 | Map (left) and details of the stations (right) from the transect performed during the oceanographic ANTOM-I cruise.

Figure 2.2 | Map (left) and details of the stations (right) from the transect performed during the oceanographic ANTOM-I cruise.

Figure 2.3 | Schematics of the sampling processes during both ANTOM I and II campaigns.

Figure 2.4 | Cast (left) and sampling (right) from the Niskin rossete from the R/V Hespérides.

Figure 2.5 | Pictures of the SML and SSL sampling processes during ANTOM-I (left picture) and Southern Ocean (right picture).

Figure 2.6 | Schematics illustration of how the wet deposition is collected (left), and picture of the installation in the RV Sarmiento de Gamboa (right).

Figure 2.7 | Pictures on the plankton sampling nets (top), plankton sample (middle), and the high-volume samplers (bottom).

Figure 2.8 | Schematic workflow diagram illustrating the analytical process for chemical analysis of environmental samples.

Figure 2.9 | Schematic overview of the samples pre-treatment in the vessels for PFAS analysis in sea-water.

Figure 2.10 | Schematic overview of the analytical procedure for the extraction, concentration, and analysis of PFAS from environmental samples in the ultra-clean lab and instrumental analysis.

Figure 2.11 | Schematic overview of the samples pre-treatment in the vessels for OPE analysis in sea-water.

Figure 2.12 | Schematic overview of the analytical procedure for the extraction, concentration, and analysis of OPEs from environmental samples in the ultra-clean lab and instrumental analysis.

LIST OF TABLES

Table 2.1 | Information of labelled PFAAs compounds used as surrogate.

Table 2.2 | Information of labelled PFAAs compounds used as Internal Standard.

Table 2.3 | Information of labelled OPE compounds used as surrogate.

Table 2.4 | Information of labelled OPE compounds used as Internal Standard.

PART 03. MAIN CHAPTERS

CHAPTER I

Paper I. Main text

LIST OF FIGURES

Figure 0 | Toc Art

Figure 1 | Comparison of dissolved black carbon and semivolatile aromatic-like hydrocarbons (SALCs) in the ocean.

Figure 2 | Abundance of key genes, from the Tara Oceans metagenomes, responsible of the metabolic routes for the degradation of aromatic hydrocarbons.

Paper I. Supplementary Materials

LIST OF FIGURES

Figure S1 | Global distribution of concentrations of DBC (upper panel) and SALCs (lower panel) in the oceans for the eight regions were DBC and SALCs could be compared.

LIST OF TABLES

Table S1 | Summary of the DBC and SALC concentrations for the eight oceanic regions where SALCs and DBC were compared.

CHAPTER II

Paper II. Main text

LIST OF FIGURES

Figure 1 | Latitudinal composition of PFAAs.

Figure 2 | PFAAs at surface versus the deep chlorophyll maximum (DCM) depth.

Figure 3 | Latitudinal and depth distribution of PFAAs.

Figure 4 | Transport of PFAAs from the South Atlantic Ocean to the Southern Ocean.

Paper II. Supplementary Materials

LIST OF TABLES

Table S1 | Sampling stations information.

Table S2 | Target PFSAs and PFCAs, and Surrogate and Injection Standards used in the present study with their acronyms, parent and product ions and retention times.

Table S3 | Individual PFAAs concentrations (pg L^{-1}) at 5 m and DCM samples from the Atlantic Ocean.

Table S4 | Individual PFAAs concentrations (pg L^{-1}) at vertical profile samples from the Atlantic Ocean.

Table S5 | Individual PFAAs concentrations (pg L^{-1}) at 5 m and DCM samples from the Southern Ocean.

Table S6 | Individual PFAAs concentrations (pg L^{-1}) at vertical profile samples from the Southern Ocean.

Table S7 | Mean relative contribution of individual PFAAs to the total PFAA's pool (%), separated by ocean.

Table S8 | PFAAs values (pg) from field blanks and procedural blanks.

Table S9 | Limits of Quantification (LOQs) for PFAAs compounds for the Atlantic and Southern Ocean samples.

CHAPTER III

Paper III. Main text

LIST OF FIGURES

Figure 0 | Toc Art

Figure 1 | (A) Locations of sampling sites and station codes in the Atlantic Ocean; (B) individual OPE concentrations (ng L^{-1}) at the SML and SSL in the Atlantic Ocean; (C) locations of sampling sites and station codes in the Southern Ocean. (D) Individual OPE concentrations (ng L^{-1}) at the SML and SSL in the Southern Ocean.

Figure 2 | (A) Enrichment factors in the surface microlayer (EF_{SML}) for individual OPEs in the Atlantic Ocean; (B) enrichment factors in sea spray aerosols (EF_{SSA}) for samples in the Atlantic Ocean; (C) enrichment factors in the surface microlayer ($EF_{SML)}$ for individual OPEs in the Southern Ocean.

Figure 3 | Heatmap of correlation (Spearman test) between individual OPE concentrations at the SML and SSL (ng L^{-1}) and environmental and biological conditions at the sampling sites.

Paper III. Supplementary Materials

LIST OF FIGURES

Figure S1 | Pictures of SML sampling in the Atlantic (left) and Southern Ocean (right) with the SML sampler.

Figure S2 | Relative abundance (%) of OPEs in SML, SSL and SSA samples.

Figure S3 | Correlation plot between Na^+ concentration and log $\sum_{24}$OPEs concentration in the Atlantic Ocean aerosols.

Figure S4 | Heatmap of correlations between individual OPE EFSML with environmental and biological conditions.

Figure S5 | $\sum_{10}$OPE paired concentrations (ng L^{-1}) at the SML and SSL in the Atlantic (left panel) and Southern Ocean (right panel).

LIST OF TABLES

Table S1 | Sampling sites and environmental variables at time and site of sampling for the Atlantic Ocean (top table) and the Southern Ocean samples (bottom table).

Table S2 | Target OPEs in the present study, their acronyms, Log KOW and molecular weight (MW).

Table S3 | Blanks (ng) for Atlantic (top table) and Southern Ocean (bottom table).

Table S4 | Limits of quantification (LOQs) in ng.

Table S5 | Information of labelled OPE compounds used as surrogate (top table) and as internal standard (bottom table).

Table S6 | Surrogate recoveries from the Atlantic Ocean samples (top table) and Southern Ocean samples (bottom table).

Table S7 | Presence, absence and <LOQ number of samples per each compound and campaign.

Table S8 | Individual and $\sum_{24}$OPE concentrations (ng L^{-1}) in SML.

Table S9 | Individual and $\sum_{24}$OPE concentrations (ng L^{-1}) in SSL.

Table S10 | Mean, median and standard deviation of individual and $\sum_{24}$OPE in SML and SSL for the Atlantic Ocean (top table) and Southern Ocean (bottom table).

Table S11 | Mean SML and SSL concentrations (ng L^{-1}) and T-test p-value results for statistical comparison of individual and $\sum_{24}$OPE between the two layers in the Atlantic Ocean. differences.

Table S12 | Mean SML and SSL concentrations (ng L^{-1}) and T-test p-value results for statistical comparison of individual and $\sum_{24}$OPE between the two layers in the Southern Ocean.

Table S13 | Mean SML and SSL concentrations (ng L^{-1}) and T-test p-value results for statistical comparison of individual and $\sum_{24}$OPE between the two layers in both Atlantic and Southern Ocean.

Table S14 | Enrichment factor of SML (EF_{SML}) for individual OPE for the Atlantic samples (top table) and Southern Ocean samples (bottom table).

Table S15 | Spearman correlation between EF_{SML} for individual OPEs and total chlorophyll content (mg L^{-1}).

Table S16 | Sea spray aerosols (SSA), seawater (SW) from SSA volumes (V_{SW}), Na^+, OPEs in SSA ($\sum_{14}OPE_{SSA}$) and OPEs in SW from SSA ($\sum_{14}OPE_{sw}$).

Table S17 | Individual and $\sum_{14}$OPE in SWSSA (ng L^{-1}) [1].

Table S18 | Enrichment factor of SSA (EF_{SSA}) for individual OPEs.

CHAPTER III

Paper IV. Main text

LIST OF FIGURES

Figure 0 | Toc Art

Figure 1 | Latitudinal variability of OPEs at 5 m depth. (A) Location of stations in the Atlantic Ocean; (B) surface concentrations of individual and $\sum_{24}$OPE (ng L^{-1}) in the Atlantic Ocean; (C) Location of stations in the Southern Ocean; and (D) surface concentrations of individual and $\sum_{24}$OPE (ng L^{-1}) in the Southern Ocean.

Figure 2 | Spearman correlation heatmap showing the relationships between individual OPEs, $\sum_{24}$OPE concentrations, and various biological (e.g., bacterial abundance, bacterial production, chlorophyll a) and environmental variables (e.g., water temperature, air temperature, and wind speed).

Figure 3 | Latitudinal distribution of log Cl-OPE concentrations (ng L^{-1}) at five different depths.

Figure 4 | Linear regressions between Σ_{24}OPE concentrations (ng L^{-1}) and Chl a (mg m^{-3}) (panel A), and oxygen levels (mg L^{-1}) at the DCM (panel B). Panel C shows the linear regression between Σ_{24}OPE concentrations (ng L^{-1}) and oxygen levels (mg L^{-1}) at the MOx layer (panel C).

Figure 5 | Vertical profiles of concentrations (ng L^{-1}) of grouped OPEs categorized as alkyl-OPEs, aryl-OPEs, Cl-OPEs, and minor OPEs. The left panel shows the vertical profiles sampled in the Atlantic Ocean, whereas the right panel shows profiles sampled in the Southern Ocean.

Paper IV. Supplementary Materials

LIST OF FIGURES

Figure S1 | Log-transformed concentrations of grouped OPEs vs latitude, colored by depth (m). Panel top left plots Cl-OPES, top right Alkyl-OPEs, bottom left Aryl-OPEs and bottom right Minor-OPEs. The color gradient represents the sampling depth, with shallower depths depicted in yellow and deeper depths in purple. The shaded area around the regression line represents the 95% confidence interval.

Figure S2 | Rainfall and 5 m depth seawater (Surface) individual and $\sum_{24}$OPE concentrations (ng L^{-1}) from Atlantic Ocean stations AN1_ST10 and AN1_ST11.

Figure S3 | Surface microlayer (SML), subsurface layer (SSL), and 5m depth OPE concentrations (ng L^{-1}) of individual and $\sum_{24}$OPE at nine stations sampled in the Atlantic Ocean (top panel) and the Southern Ocean (bottom panel).

Figure S4 | Scatter plots comparing the individual and $\sum_{24}$OPE log-transformed concentrations between the 5 m depth (Surface) and DCM layers across three ocean regions.

Figure S5 | Vertical profiles of concentrations (in ng L^{-1}) of $\sum_{24}$OPEs plotted over the bathymetry of the sampling site where each vertical profile was sampled.

Figure S6 | Log-transformed surface (5 m depth) and deep (2000 m) OPE concentrations for different OPE groups (Cl-OPEs, Alkyl-OPEs, Aryl-OPEs, and Minor OPEs). Spearman correlation coefficients (r) and p-values are displayed for each group.

Figure S7 | Major ocean gyres (top) and global winds circulation (bottom).

LIST OF TABLES

Table S1 | Stations information from the Atlantic Ocean (top table) and Southern Ocean (bottom table) where samples for OPE analysis were collected.

Table S2 | Information of labelled OPE compounds used as surrogate (top table) and as Internal Standard (bottom table).

Table S3 | Names, acronym molecular weight (MW) and Log K_{OW} of the targeted compounds.

Table S4 | Individual OPE contribution (%) to the total pool for each for the Atlantic and Southern Ocean samples.

Table S5 | Field and procedural blanks OPE abundance (ng).

Table S6 | Limits of quantification (LOQs) in ng.

Table S7 | Surrogate and matrix spike recoveries (%) from the Atlantic Ocean samples (top table) and Southern Ocean samples (bottom table).

Table S8 | Individual and $\sum_{24}$OPE concentration in surface and DCM samples from the Atlantic Ocean (ng L^{-1}).

Table S9 | Mean and SD of surface and DCM concentrations (ng L^{-1}) in the three ocean basins sampled.

Table S10 | Individual and $\sum_{24}$OPE concentration in surface and DCM samples from the Southern Ocean (ng L^{-1}).

Table S11 | Environmental variables measured at surface waters and atmospheric conditions in the Atlantic and Southern Oceans.

Table S12 | Summary of the polynomial regression models applied to log-transformed grouped OPEs concentrations across different depths (5 m, DCM, 1% PAR, MOx, and Deep) with latitude.

Table S13 | Wet Deposition and related surface sample concentrations (in ng L^{-1}) of individual and $\sum_{24}$OPE in the Atlantic Ocean and calculation of EFWD (C_{WD}/C_{SURF}) for those samples.

Table S14 | Atmospheric aerosol concentrations of $\sum_{14}$OPEs (ng m^{-3}) from Malaspina (Castro-Jiménez et al., 2016) from latitudes ranging between 7°N and 0°N (top table) and rain water $\sum_{14}$OPEs (ng m-3) concentrations from AN1_ST10 and AN1_ST11 2021 Atlantic campaign.

Table S15 | Log K_{RP} values from the Atlantic Ocean.

Table S16 | Mean ± SD of group OPE concentrations (ng L^{-1}) separated by ocean and depth.

Table S17 | Individual and $\sum_{24}$OPE concentration in vertical profiles from the Atlantic Ocean (ng L^{-1}).

Table S18 | Individual and $\sum_{24}$OPE concentration in vertical profiles from the Southern Ocean (ng L^{-1}).

CHAPTER IV

Paper V. Main text

LIST OF FIGURES

Figure 1 | Flowchart illustrating the ideal process for developing and refining outreach activities.

Figure 2 | Overview of the evaluation tool and scoring system for assessing scientific outreach activities.

Paper V. Supplementary Materials

LIST OF TABLES

Table S1 | Evaluation criteria for scientific outreach activities. The table provides a description for each parameter evaluated to assess the execution and results of outreach activities. Each activity receives a score from 1 to 5 based on its performance relative to the criteria below.

Table S2 | Summary of outreach activity scores and ranking. The table provides a proposed ranking based on the total scores from the evaluation in Table S1, guiding prioritization and assessing the overall impact and effectiveness of each outreach activity.

Table S3 | Activity evaluation model.

Table S4 | Evaluation of outreach activities conducted within our project. This table presents the parameters and scores for outreach activities that were implemented as part of our project, highlighting the performance of each real-world initiative.

PART 04. GENERAL DISCUSSION AND CONCLUSIONS

LIST OF FIGURES

Figure 4.1 | $\sum_5$Cl-OPEs, $\sum_6$Alkyl-OPEs and $\sum_9$Aryl-OPEs concentrations (pg L^{-1}) (left panels), and $\sum_6$PFSAs and $\sum_{11}$PFCAs concentrations (pg L^{-1}) (middle panels) across the Atlantic Ocean (top panel) and Southern Ocean (bottom panel). Right panels show the stations locations in the Atlantic Ocean (top) and Southern Ocean (bottom).

Figure 4.2 | Distribution of PFOS and PFOA concentrations (pg L^{-1}) across the Atlantic Ocean (AN1_ST01 to ST24) and Southern Ocean (AN2_ST00 to ST12) and corresponding PFOS/PFOA ratios (right panel).

Figure 4.3 | $\sum_{64}$PAH concentrations (pg L^{-1}) (left panel) across the Atlantic Ocean (St 1 to 17) and Southern Ocean, sampled at four different stations around Livingston Island in the South Shetland Islands (Antarctic Peninsula) and maps of stations locations (right panels).

Figure 4.4 | Bar plots showing the ratios of $\sum_5$Cl-OPEs (Cl-OPEs) and total $\sum_{22}$OPEs (OPEs) relative to $\sum_{17}$PFAAs (PFAAs), $\sum_{11}$PFCAs (PFCAs), and $\sum_6$PFSAs (PFSAs) concentrations (pg L^{-1}) along an Atlantic Ocean (AN1, stations St01 to St24) and Southern Ocean (AN2 stations St01 to ST12) transects. Each panel represents a different ratio: Cl-OPEs/PFAAs, Cl-OPEs/PFCAs, Cl-OPEs/PFSAs, OPEs/PFAAs, OPEs/PFCAs, and OPEs/PFSAs.

Figure 4.5 | Bar plots of pollutant ratios across latitude categories. The plots illustrate PAH/PFCA, PAH/PFSA, and PAH/PFAA ratios, respectively, from left to right. Each plot shares a consistent y-axis scale ranging from 0 to 1000 for easy comparison.

LIST OF TABLES

Table 4.1 | Stations, coordinates, and dates of sampling (dd-mm-yyyy) of surface waters at 5 m depth from the Atlantic Ocean (AN1_ST01 to ST24) and Southern Ocean (AN2_ST01 to AN2_ST12) where both PFAAs and OPEs were analyzed.

Table 4.2 | Stations and coordinates from González-Gaya et al. (2016) and Iriarte et al. (2023) for measured PAH concentrations.

INTRODUCTION

01



TABLE OF CONTENTS

1.1. General Introduction
1.1.1. The anthropogenic impact on Earth system's processes
1.1.2. The planetary boundaries
1.1.3. Chemical pollution
1.1.4. Regulatory frameworks
1.1.5. Properties of priorization of chemical pollutants
1.1.6. POPs cycling in the environment

1.2. Selected oceanic regions
1.2.1. The Atlantic Ocean
1.2.2. The Southern Ocean

1.3. Targeted contaminants
1.3.1. Aromatic compounds
1.3.2. Perfluoroalkyl Acids
1.3.3. Organophosphate Esters

1.4. Objectives and thesis structure
1.4.1. Objectives
1.4.2. Thesis structure

1.5. References

PART 01. INTRODUCTION

1.1. GENERAL INTRODUCTION

1.1.1. THE ANTHROPOGENIC IMPACT ON EARTH SYSTEM'S PROCESSES

Throughout Earth's history, natural processes have governed the planet's chemical composition and shaped its environment. From the formation of the oceans to the evolution of atmospheric gases, the Earth's system has been in a constant state of chemical perturbations, and in occasions, major changes. During the Holocene interglacial epoch, which began approximately 11700 years ago, the planet entered a relatively stable climatic period, with profound implications for evolution and the development of civilizations (Petit et al., 1999). However, this balance began to change dramatically with the onset of the Industrial Revolution in the late 18th century.

The Industrial Revolution marked a pivotal moment in human history, where advancements in technology, mechanized production, and increased energy consumption enabled rapid societal growth (Durlauf et al., 2010). This period also marked the beginning of large-scale chemical production and fossil fuel use, greatly increasing the variety and volume of chemicals released into the environment. Processes like the mass production of sulfuric acid, the Leblanc process for soda ash, and the use of chlorine for bleaching textiles opened new avenues for chemical innovation. In the late 19th century, breakthroughs in organic synthesis, driven by the textile industry, led to the discovery of synthetic dyes, transitioning from natural products to lab-made compounds. This period also saw the development of fertilizers, explosives, and medicines, spurring chemical production. The 20th century saw exponential growth in anthropogenic chemicals, with industries like petrochemicals, agriculture, and manufacturing expanding rapidly. Innovations such as Bakelite in 1907 and increased plastic production transformed consumer goods (Sperling et al., 2011). During the post-World War II period, production of synthetic chemicals like pesticides, flame retardants, and solvents intensified, bringing both benefits and unintended consequences due to their persistence and toxicity.

By the late 20th century, industrial and technological advancements had profoundly transformed society, raising concerns about the environmental impacts of synthetic chemicals. Rachel Carson was among the first to bring this issue to public attention in her groundbreaking work, Silent Spring (1962), which catalyzed awareness of the ecological consequences of human activity. Building on this growing recognition of major environmental changes, many scientists argued that humanity had entered a new epoch known as the **Anthropocene**, defined by the dominant role of human activities in shaping the Earth's systems and atmosphere (Crutzen and Stoemer, 2000; Steffen et al., 2011; Malm and Hornborg, 2014; Waters et al., 2016). This epoch is considered to mark a profound shift in the planet's biosphere dynamics, introducing a new

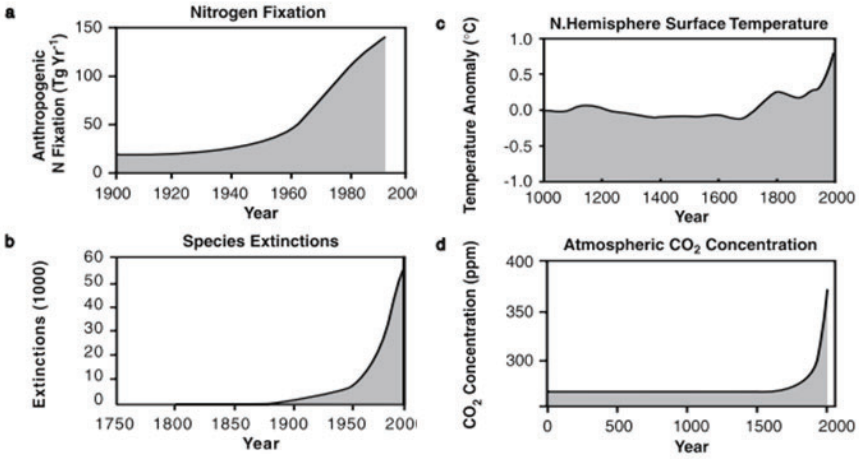


Figure 1.1 | Responses of the Earth System to increasing pressure from human activities: a nitrogen fixation (Vitousek et al., 1994); b species extinctions (Smith et al., 2002); c northern hemisphere surface temperature (Mann et al., 1999); and d atmospheric CO_2 concentration (adapted from Keeling and Whorf, 2000). From Steffen et al. (2005).

anthropogenic perturbation into the Earth's system. Historically, this system consisted of five interconnected subsystems: the atmosphere, hydrosphere, geosphere, biosphere, and cryosphere, which interact in complex and dynamic ways, regulating the Earth's climate and sustaining life.

The **anthroposphere**, however, has become an additional functional component of Earth system, capable of altering its state (Steffen et al., 2021). It represents the human-made environment, encompassing human activities, infrastructure, and technological systems. It increasingly influences other subsystems through greenhouse gas emissions, land-use changes, and the introduction of synthetic chemicals, pushing the Earth system toward the new, less stable conditions **(Figure 1.1)**. Before the proposed Anthropocene era, some human driven changes were already taking place in the biosphere, such as emissions of CO and CO_2, metals, nutrients and other organic compounds composition (Sarmiento and Gruber, 2006; Steffen et al., 2007), but increased industrial, agricultural and other anthropogenic activities led to the introduction of thousands of new synthetic compounds, most of them organic, in the environment (Daughton et al., 2005; Muir and Howard 2006; Dachs and Mejánelle, 2010). These human-induced alterations across various subsystems reflect a larger phenomenon often referred to as **global change.** Global change encompasses not only climate change, but also a multitude of interrelated environmental shifts driven by industrialization, urbanization, and the intensification of agriculture. This concept captures the cumulative effects of human activities on Earth's physical, chemical, and biological systems, disrupting natural processes and accelerating environmental degradation at a planetary scale **(Box 1.1)** (Vitousek et al., 1997; Steffen et al., 2004).

GLOBAL CHANGE: THEN vs NOW

In 1997 Peter M. Vitousek published the following data on global change:

"Human alteration of Earth is substantial and growing. Between one-third and one-half of the land surface has been transformed by human action; the carbon dioxide concentration in the atmosphere has increased by nearly 30% since the beginning of the Industrial Revolution; more atmospheric nitrogen is fixed by humanity than by all natural terrestrial sources combined; more than half of all accessible surface fresh water is put to use by humanity; and about one-quarter of the bird species on Earth have been driven to extinction. By these and other standards, it is clear that we live on a human-dominated planet."

Since Vitousek's pivotal work in 1997, the understanding of global change has significantly evolved. The most recent updates from the Intergovernmental Panel on Climate Change (IPCC, 2023) in their 6th evaluation report provide alarming insights into the scale of human impacts on Earth's ecosystems. Their key findings include the following points:

- Human activities have unequivocally caused global warming, with the Earth's surface temperature reaching 1.1°C above pre-industrial levels (1850-1900) during the period 2011-2020.
- Greenhouse gas emissions have continued to rise, with fossil fuel combustion and industrial processes being the largest contributors.
- Climate change is already causing widespread adverse impacts, including ecosystem degradation, reduced food security, and increasing water scarcity.
- 3.3 to 3.6 billion people live in areas highly vulnerable to climate change, with disproportionate impacts on low-income communities and developing nations.
- Every increment of global warming will escalate risks, with significant impacts on ecosystems, food production, and human health. Some ecosystems, such as coral reefs, are approaching irreversible damage.
- Global sea levels have risen by 0.2 m between 1901 and 2018, and sea-level rise is virtually certain to continue, further threatening coastal regions.
- While adaptation efforts are progressing, they are insufficient to address the full scale of the problem, particularly in low-income countries. Finance gaps and unequal implementation are major barriers.
- Warming is likely to exceed 1.5°C during the 21st century if current trends continue, with extreme weather events becoming more frequent and severe. Immediate and sustained reductions in GHG emissions are necessary to avoid catastrophic changes.

Box 1.1 | Global Change: Then vs. Now

1.1.2. THE PLANETARY BOUNDARIES

On this context, the main question that arises is: “are we still on time to reverse climate change?”. To answer this, Rockström and colleagues (2009) introduced the "planetary boundaries" framework, outlining critical thresholds for Earth System processes that must not be exceeded to maintain planetary stability. These boundaries define the safe operating space for humanity, beyond which the risk of abrupt or irreversible changes significantly increases.

The authors identified **nine key global processes,** estimating thresholds that must not be transgressed to avoid undesired global changes. These include climate change, biodiversity loss, biogeochemical flows, land-use change, freshwater use, ocean acidification, stratospheric ozone depletion, atmospheric aerosol loading, and novel entities.

"Novel entities" refer to substances and compounds introduced by human activity, such as industrial chemicals, pesticides, pharmaceuticals, plastics, and engineered nanoparticles, which are not naturally present in the Earth system (Richardson et al., 2023). Many of these synthetic chemicals resist natural breakdown, accumulating in air, water, soil, and biota. Novel entities have even become geological markers of the Anthropocene (Waters et al., 2016), and its production has doubled since 2020, increasingly endangering human health and ecosystems (Persson et al., 2022). For many novel entities, potential effects on Earth system processes—particularly on the biosphere integrity and functioning—are not well known (Richardson et al., 2023). In 2022, Persson and colleagues argued that humanity had already exceeded the safe operating space for novel entities **(Figure 1.2)**, as the rate of chemical production far surpasses our capacity to assess and monitor these substances. This transgression poses a significant threat to ecosystems and biodiversity. A few months later, in 2023, an updated assessment by the same team found that six of the nine planetary boundaries had been crossed **(Figure 1.2)**, threatening Earth systems' stability (Richardson et al., 2023). Specifically, the boundaries for climate change, biosphere integrity, biogeochemical flows, land-system change, freshwater use, and novel entities have been breached. The update also highlighted the interdependencies among these boundaries, noting that breaching one often exacerbates others.

Within the broader planetary boundaries' framework, this thesis focuses on the boundary of novel entities, also referred to as **chemical pollution**. These substances, introduced by human activity, have become a key challenge of the Anthropocene, becoming one of the “triple planetary crises” together with climate change and biodiversity loss. By examining the current state of occurrence, biogeochemistry, and transport processes of selected pollutant families across a vast oceanic region, this work aims to contribute to the understanding of how chemical pollution impacts Earth at large scale.

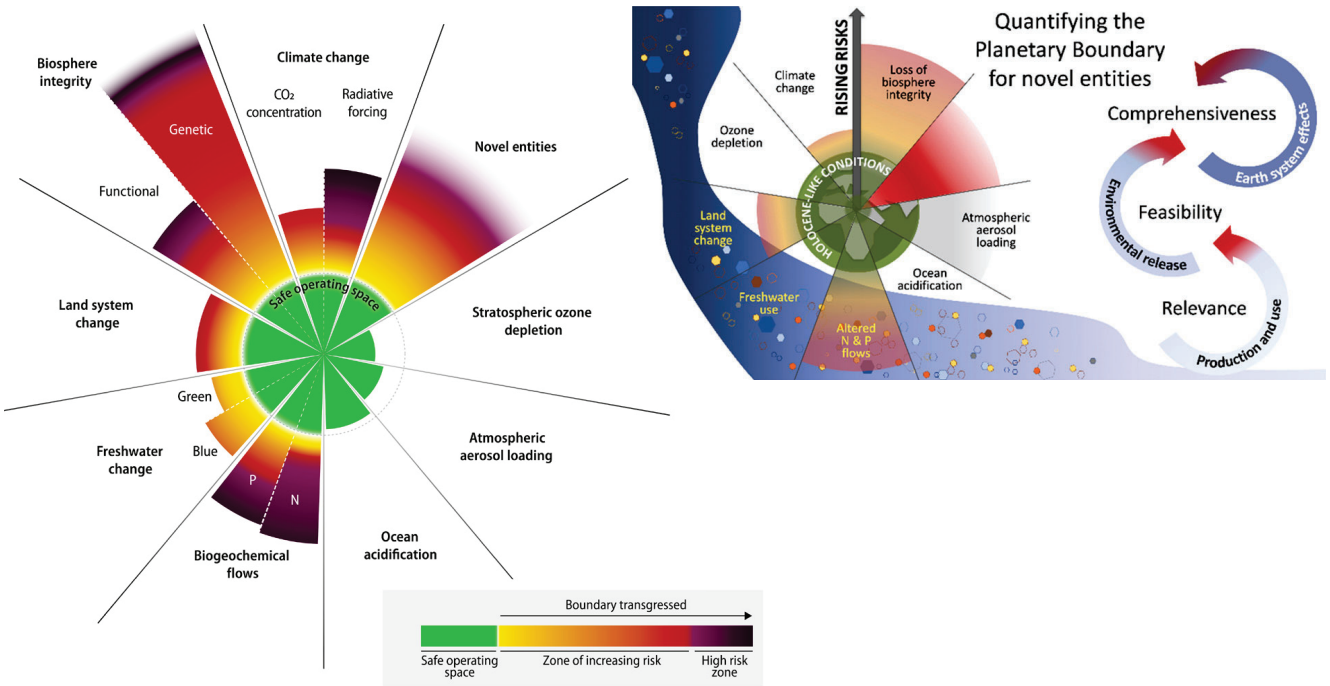


Figure 1.2 | Current status of control variables for all nine planetary boundaries. Richardson et al. (2023) (left panel) and Persson et al. (2022) (right panel).

1.1.3. CHEMICAL POLLUTION

Humanity has often been caught off guard by the unintended consequences of releasing chemical compounds into the environment without fully understanding their impacts. Rachel Carson's landmark book from 1962, "**Silent Spring**," was one of the first warnings about this situation. Carson highlighted the environmental damage caused by the widespread use of pesticides like Dichlorodiphenyltrichloroethane (commonly known as DDT), showing how our actions can have far-reaching and harmful effects when their full consequences are not considered. The story of chlorofluorocarbons (CFCs) is another example—these compounds caused serious damage to the ozone layer before action was taken to regulate them. Richardson and colleagues (2023) argued that the only truly safe approach for novel entities is to avoid releasing them into the environment unless their potential impacts on Earth system processes have been thoroughly evaluated, meaning the aim should be a zero release of synthetic chemical compounds unless they are proven safe and can be carefully monitored. However, this approach is not realistic for developed societies, as many chemicals also contribute to human wellbeing and health.

From a simplified source perspective, POPs and related organic chemicals may belong to two principal source categories. Either they are **intentionally produced** for one or multiple purposes, or they are unintentionally or **accidentally formed as by-products** in other (industrial) processes or by human activities. In addition, minor quantities of very specific POPs may originate from natural processes (Breivik et al., 2004). Primary sources, such as the ones mentioned can be direct or "diffusive", such as volatilization from consumer products while these are used. After their release generally to air or water, these are transported and eventually, these chemicals can be "stored" in environmental reservoirs such as soils, sediments, glaciers, or oceans. These reservoirs, however, can re-release the POPs back to the environment, and this cycling constitutes the so-called secondary sources (Jones & de Voogt., 1999).

Humans are constantly exposed to a multitude of chemicals, both naturally occurring and synthetically produced, which are released daily into the environment (Muir and Howard, 2006; Wang et al., 2020). While many of these substances have been beneficial in industrial processes and household products, they also pose significant environmental and health risks due to their persistence and bioaccumulative nature. In response to these concerns, various local and global regulations, including the Stockholm Convention on Persistent Organic Pollutants (POPs), have prohibited or restricted the production and use of certain highly persistent and toxic compounds.

Despite these regulatory efforts, many of these historically used but now-regulated or banned substances continue to be detected in the environment due to their extreme chemical stability, slow degradation rates, and long-range environmental transport (LRET) (Xie et al., 2022b; Zhang et al., 2024). These substances, known as **legacy pollutants,** are a subset of POPs and include polychlorinated biphenyls (PCBs), organochlorine (OC) pesticides and their metabolites such as DDT and DDE (dichlorodiphenyldichloroethylene), polybrominated diphenyl ethers (PBDEs), and polycyclic aromatic hydrocarbons (PAHs) (Dachs et al., 2002a; Xie et al., 2022b). Some phthalates have also been subject to regulatory restrictions due to concerns over their environmental persistence and potential health effects.

Legacy pollutants are particularly concerning because they undergo long-range environmental transport via atmospheric deposition, ocean currents, and ice remobilization, leading to their detection in remote areas, including the Arctic and Antarctic (Xie et al., 2022b). Even decades after being phased out, these pollutants continue to cycle between air, water, and sediments, contributing to their prolonged presence in marine ecosystems (Zhang et al., 2024). Due to their lipophilic nature, they bioaccumulate and biomagnify in marine food webs, posing risks to top predators, including seabirds, marine mammals, and humans through dietary exposure (Zhang et al., 2024).

Understanding the environmental fate and impact of legacy pollutants is essential for assessing long-term contamination trends and guiding future regulatory actions. The following sections provide an overview of the most well-documented legacy pollutants, highlighting their sources, regulatory history, and occurrence in the environment.

Legacy and emerging contaminants

Some legacy POPs such as PCBs, PCDDs (Polychlorinated Dibenzo-p-dioxins), PCDFs (Polychlorinated Dibenzofurans), and OC pesticides have been widely detected in the environment since the late 1980s or earlier in many cases, as part of regional, national, and global research and monitoring programs (Muir et al., 2023). Several studies have assessed their occurrence and distribution across all oceans and seas (Manodori et al., 2006; García-Flor et al., 2009; Ge et al., 2014; Lohmann et al., 2009a; Gioia et al., 2007). But also, have shown its presence in human tissues, plants and trophic webs (van der Ber et al., 2017; Altshul et al., 2004; Fängström et al., 2005; Ulaszewska et al., 2011) showing its bioaccumulation potential and effects on

human and ecosystem health.

DDT (Dichloro-diphenyl-trichloroethane) was developed in the 1940s as the first modern synthetic insecticide and was initially used with great success to combat malaria, typhus, and other insect-borne diseases, as well as controlling pests in agriculture and households. Rachel Carson's Silent Spring (1962) amplified public concern about the dangers of pesticide overuse and its ecological consequences. In response to mounting evidence of DDT's harmful effects on wildlife and potential human health risks, the U.S. Environmental Protection Agency (EPA) restricted its use in 1972. Despite these restrictions, DDT remains persistent in the environment, mainly its main metabolite, and is still detected in remote locations globally (Geisz et al., 2008; Galbán-Malacón et al., 2023; Cui et al., 2020; Ge et al., 2021). Moreover, large quantities of DDT were legally disposed of through barrel dumping or direct discharge into deep ocean basins and continental slopes, further contributing to its long-term environmental persistence and ecological damage (Schmidt et al., 2024; Neira et al., 2024).

Although its current restriction to production and use under the Stockholm Convention, DDT continues to be legally used for public health purposes, specifically for indoor residual spraying against malaria-carrying mosquitoes in certain countries under WHO guidance (Stockholm Convention, 2024; WHO, 2006). This exemption allows malaria-endemic regions to temporarily use DDT when no effective alternatives are available.

Flame retardants are a diverse group of substances, including both inorganic and organic chemicals, that are used in a wide range of applications including furniture, building materials, and electronic goods. Many molecules acquire flame retardant properties through the addition of halogens such as bromine and chlorine (Page et al., 2023). Polybrominated diphenyl ethers **(PBDEs)** have been used as flame retardants for several decades providing longer escapes times in case of fire and thus saving lives as well as reducing the damages from the fire. Bromine acts by reaction with the free radicals in the gas phase and thus slows down the ignition and combustion process (Frederiksen et al., 2008). The commercial formulations of PBDEs includes penta-, octa- and deca-BDE technical mixtures. As classical environmental pollutants, these compounds have been widely studied in different environmental matrixes (Wania, 2003; Lohmann et al., 2013; 2020) and have shown to have several toxicological effects and a high bioaccumulation potential (Strid et al., 2013).

PAHs (Polycyclic Aromatic Hydrocarbons) are a well-known and extensively studied group of pollutants that are primarily generated through the incomplete combustion of organic materials, including fossil fuels, biomass, and industrial processes. These compounds are categorized sometimes as legacy pollutants due to their long-standing presence in the environment and their potential to cause adverse health effects, even though these are still being emitted largely due to use of fossil fuels. PAHs have been studied extensively, with their latitudinal, longitudinal and depth distributions described across oceans and seas (Dachs et al., 1996; 1997; 2002; Gigliotti et al., 2000; del Vento et al., 2007; Berrojalbiz et al., 2011a; González-Gaya et al., 2019a, Iriarte et al., 2023). Their ubiquity in the environment, large concentrations and the resulting human exposure over time have been linked to significant health risks (Menzie et al., 1992; Xia et al., 2010; Peng et al., 2023; Gómez et al., 2024; Wu et al., 2024).

During the last decades, thanks to the development of instrumental analytical techniques, particularly linked to high resolution mass spectrometry, researchers have identified thousands of chemicals in the environment. The scrutiny and development of data science tools have also allowed to identify hundreds to millions of synthetic substances in chemical data bases, with an unknown number of them potentially reaching the environment (Yang et al., 2020; Schymanski et al., 2023). These compounds, the so-called **contaminants of emerging concern (CECs)**, a term first used by Sauvé and Desrosiers in 2014, are characterized by limited knowledge regarding their environmental behavior, eventual disposition, and biological consequences. CECs include a broad range of substances, such as: pharmaceuticals and personal care products, endocrine-disrupting chemicals, nanomaterials, and certain industrial chemicals and flame retardants. The mechanisms governing their presence, distribution, and impact on organisms remain largely unexplored. The limitations of current analytical chemical methods, the sheer number of substances, and the low environmental concentrations at which some of these compounds are found pose an enormous challenge to researchers to realistically quantify the magnitude of these complex environmental hazard (Fenner and Scheringer, 2021). Among the CECs that are ubiquitous in the environment, toxic, bioaccumulative, and show moderate persistence, OPEs and PFAS are receiving increased attention by researchers and environmental agencies.

Indeed, **Perfluoroalkyl Substances** (**PFAS)** have been extensively studied for decades, but they represent a complex group that includes both legacy and emerging compounds. While some PFAS, such as the perfluorooctanesulfonic acid (PFOS), perfluorooctanoic acid (PFOA), and perfluorohexanesulfonic acid (PFHxS), have been banned or restricted under the Stockholm Convention, newer generations of PFAS,

often designed to replace these older compounds, are increasingly in focus. These newer PFAS are generally considered CECs.

Similarly, **Organophosphate Esters (OPEs)**, widely used as flame retardants and plasticizers, are gaining attention as CECs. Recent studies highlight their persistence and potential to bioaccumulate, suggesting that OPEs may pose risks comparable to legacy POPs, warranting stricter evaluation and regulation.

Both PFAS and OPEs are addressed in greater detail later in this chapter, as they are the selected target compounds of this thesis.

1.1.4.REGULATORY FRAMEWORKS

Estimating the total number and environmental concentrations of synthetic organic chemicals is challenging, if not impossible. Few studies have addressed the number of chemicals on the market, and often underestimating this figure. A recent study revealed that **350,000 chemicals and mixtures are registered for production and use**, up to three times previous estimates (Wang et al., 2020). These chemicals vary widely in physicochemical properties, with multiple sources, life cycles, and sinks. Only dozens of these chemicals are currently regulated or planned to be eventually regulated in the coming years. However, an even smaller fraction has undergone comprehensive risk assessment, highlighting how current regulations address only the tip of the iceberg in terms of potential environmental and human health risks.

In the late 20th century, as scientific understanding of environmental pollution advanced, it became clear that many harmful chemicals were not confined to the regions where they were produced or used. Instead, they were carried across borders by winds and water currents, spreading toxic substances far and wide. This realization sparked international concern, particularly within Europe and North America, where regulation agencies and scientists recognized the urgent need to cooperate in reducing the spread of these pollutants. In response, the UNECE Aarhus Protocol on POPs was born under the **Convention on Long-Range Transboundary Air Pollution** (CLRTAP) in 1998.

The protocol was a groundbreaking step in tackling the cross-border pollution problem. It focused on controlling, reducing, or eliminating the release of certain persistent organic pollutants, substances that resist degradation and can travel long distances through the atmosphere. The initial list of 16 chemicals **(Table 1.1)** included industrial and agricultural pollutants such as PCBs or DDT, and dangerous by-products like dioxins and furans, all of which were found to accumulate in the environment and living organisms, posing serious health risks. Countries that signed the protocol committed to phasing out, or severely restricting, the use of these substances, and to adopting the best available techniques to reduce emissions from industrial processes.

While the CLRTAP-UNECE on POPs Protocol marked a significant progress, it became clear that a more global, comprehensive approach was needed. This paved the way for the adoption of the **Stockholm Convention (SC) on Persistent Organic Pollutants** in 2001, a landmark treaty that would take the regulation of these hazardous chemicals to the global stage, addressing not just regional but worldwide concerns.

The criteria and physicochemical properties described below are the characteristics and requirements to define a POP according to Stockholm Convention on POPs (Annex D revised in 2023):

1) Persistence. The ability of a chemical to remain in the environment for extended periods without breaking down. Persistent pollutants resist natural degradation processes, leading to long-term contamination of soil, water, and air, and can affect ecosystems and human health for generations.

Table 1.1 | Compounds listed under the CLRTAP-POPs Protocol (UNECE, 1998).

CLRTAP-POPs Protocol (UNECE, 1998)		
Banned or restricted		
Aldrin ◆	Chlordane ◆	Chlordecone ◆
DDT ◆	Dieldrin ◆	Heptachlor ◆
Hexachlorocyclohexane (including Lindane) ◆	HCB ◆ ▼ ◆	Hexabromobiphenyl ◆
Mirex ◆	Toxaphene ◆	PCBs ▼
Emission reduction		
PCDD/Fs ◆	HCB ◆	PAHs ◆

◆ Pesticide ▼ Industrial chemical ◆ Unintentional by-product Production

2) Bioaccumulation. Is the process by which chemicals build up in the tissues of living organisms over time, often because they are stored in fat or other tissues. Substances with high bioaccumulation potential can reach harmful concentrations in organisms, especially those at higher levels in the food chain. Hydrophobicity goes directly with bioaccumulation potential, as the more hydrophobic chemicals are more prone to attach to fatty tissues and accumulate in biota at higher concentrations than those found in the environment. Biomagnification describes the increasing concentration of a substance as it moves up the food chain. As predators consume contaminated prey, the pollutants accumulate at higher levels in each successive level of the food web, posing risks to top predators, including humans.

3) Potential for Long Range Transport. This criterion assesses a pollutant's ability to travel long distances from its source regions through air or water currents, allowing their spread across continents and oceans, and often reaching regions where it was never used or produced.

4) Adverse effects. This refers to the potential of a substance to cause harmful effects to organisms, including acute effects like death or chronic effects such as cancer, reproductive harm, or developmental issues. High-toxicity chemicals pose significant risks to both ecosystems and human health.

The SC was established with the primary objective of safeguarding human health and the environment from the adverse effects of POPs. By targeting chemicals that are carbon-based, persistent, bioaccumulative, and capable of long-range transport, it seeks to eliminate or restrict their production, use, and release. It also ensures the environmentally sound management of stockpiles and waste to prevent further contamination. The Convention also includes mechanisms for assessing and adding new POPs as scientific knowledge evolves, emphasizing global cooperation and best practices to address this multigenerational threat.

The convention initially targeted a group of chemicals known as "the dirty dozen" **(Box 1.2),** a list of twelve highly toxic, bioaccumulative and persistent substances. As of the time of this thesis is being written (2024), the SC lists forty chemicals as POPs. These chemicals have been subject to strict regulations, with many of them being either banned or severely restricted in most countries **(Table 1.2)**.

Within the European Union, the European Chemicals Agency (ECHA) plays a key role in identifying and proposing new POPs for inclusion under the Stockholm Convention. ECHA was established in 2007 to implement REACH *(Registration, Evaluation, Authorisation, and Restriction of Chemicals)*, a comprehensive EU regulation aimed at ensuring the safe production, use, and disposal of chemicals while protecting human health and the environment.

THE DIRTY DOZEN

The dirty dozen refers to a group of 12 highly toxic chemicals initially targeted by the Stockholm Convention on Persistent Organic Pollutants. The dirty dozen includes:

1. Aldrin[1]
2. Chlordane[1]
3. Dichlorodiphenyltrichloroethane[1] (DDT)
4. Dieldrin[1]
5. Endrin[1]
6. Heptachlor[1]
7. Hexachlorobenzene[1,2] (HCB)
8. Mirex[1]
9. Toxaphene[1]
10. Polychlorinated Biphenyls[2] (PCBs)
11. Polychlorinated Dibenzo-p-dioxins[3] (PCDDs)
12. Polychlorinated Dibenzofurans[3] (PCDFs)

[1]pesticide [2]industrial chemical [3]byproduct

Box 1.2 | The Dirty Dozen. Stockholm Convention on POPs. *The 12 initial POPs under the Stockholm Convention. Visited October 2024.*

Under the REACH framework, ECHA compiles data from Member States, creates a Union-wide overview, and supports future EU actions under the POPs Union Implementation Plan. By managing the assessment and restriction of harmful chemicals through REACH, ECHA complements POPs regulations, working to minimize chemical-related risks.

Among the POPs included after "the dirty dozen", three compounds from the Per- and Polyfluoroalkyl Substances group have been gradually listed under the SC. **Perfluorooctane sulfonic acid (PFOS)** was the first PFAS compound added to Annex B in 2009, with certain exemptions due to its widespread use in firefighting foams and stain repellents. **Perfluorooctanoic acid (PFOA)**, used in non-stick cookware and water-resistant fabrics, was listed in Annex A for elimination in 2019, with specific exemptions, due to its links to cancer and other health risks. More recently, in 2022, **Perfluorohexane sulfonic acid (PFHxS)**, commonly found in firefighting foams and textiles, was included in Annex A because of its persistence and harmful effects on immune and thyroid function. Currently, there is growing attention to include the broader group of long-chain perfluorocarboxylic acids (LC-PFCAs), such as perfluoro nonanoic acid (PFNA) and perfluoro decanoic

acid (PFDA), under Annex A. These compounds, with carbon chains longer than 7, share similar properties with PFOA and PFHxS, raising concerns due to their extreme environmental persistence and adverse health impacts, signaling a shift toward regulating broader classes of PFAS rather than individual compounds.

In response to growing concerns about the persistence and harmful effects of PFAS, a comprehensive restriction proposal under REACH is currently being evaluated. The proposal targets a broad range of PFAS compounds, seeking to limit their use in industries such as textiles, firefighting foams, and food packaging. This initiative reflects the EU's commitment to addressing the environmental and health impacts of PFAS, building on earlier regulatory actions such as those in the Stockholm Convention. If adopted, the REACH restriction would significantly reduce PFAS usage across the EU.

Outside Europe, other countries have implemented regulatory frameworks to address the challenges posed by POPs. In the United States, the Environmental Protection Agency (EPA) plays a central role in regulating these chemicals under laws like the Toxic Substances Control Act (TSCA) and the Clean Water Act. The EPA has also initiated significant actions to phase out specific PFAS compounds and impose limits on their presence in drinking water. Similarly, Canada has developed a Chemicals Management Plan (CMP), which evaluates and manages the risks associated with chemicals, including POPs, in alignment with international conventions like the Stockholm Convention. Both frameworks emphasize the need for

Table 1.2 | POPs listed in the Stockholm Convention. *The chemicals targeted by the Stockholm Convention are listed in the annexes of the convention text. In May 2023, the Conference of the Parties amended Annex A to include Methoxychlor, Dechlorane Plus, and UV-328, following previous proposals for their listing.*

Annex A (Elimination)	*Parties must take measures to eliminate the production and use of the chemicals listed under Annex A. Specific exemptions are available in Annex A and apply only to Parties that have registered for them.*		
Aldrin ◆	Chlordane ◆	Chlordecone ◆	
Decabromodiphenyl ether ▼ (commercial mixture, c-decaBDE)	Dechlorane Plus ▼	Dicofol ◆	
Dieldrin ◆	Endrin ◆	Heptachlor ◆	
Hexabromobiphenyl ▼	Hexabromocyclododecane ▼ (HBCDD)	Hexabromodiphenyl ether and heptabromodiphenyl ether ▼	
Hexachlorobenzene ◆ (HCB)	Hexachlorobutadiene ▼	Alpha hexachlorocyclohexane ◆	
Beta hexachlorocyclohexane ◆	Lindane ◆	Methoxychlor ◆	
Mirex ◆	Pentachlorobenzene ◆	Pentachlorophenol and its salts and esters ◆	
Polychlorinated biphenyls ◆ ▼ ◆ (PCBs)	Polychlorinated naphthalenes ▼	Perfluorooctanoic acid ▼ (PFOA), its salts and PFOA-related compounds	
Perfluorohexane sulfonic acid ▼ (PFHxS), its salts and PFHxS-related compounds	Short-chain chlorinated paraffins ▼ (SCCPs)	Technical endosulfan and its related isomers ◆	
Tetrabromodiphenyl ether and pentabromodiphenyl ether ▼	Toxaphene ◆	UV-328 ▼	
Annex B (Restriction)	*Parties must take measures to restrict the production and use of the chemicals listed under Annex B in light of any applicable acceptable purposes and/or specific exemptions listed in the Annex.*		
DDT ◆	Perfluorooctane sulfonic acid (PFOS) and its salts ◆	Perfluorooctane sulfonyl fluoride ◆ (PFOSF)	
Annex C (Unintentional production)	*Parties must take measures to reduce the unintentional releases of chemicals listed under Annex C with the goal of continuing minimization and, where feasible, ultimate elimination.*		
Hexachlorobenzene ◆ ▼ ◆ (HCB)	Hexachlorobutadiene ◆ (HCBD)	Pentachlorobenzene ◆	Polychlorinated naphthalenes ◆
Polychlorinated biphenyls ◆ (PCB)	Polychlorinated dibenzo-p-dioxins ◆ (PCDD)	Polychlorinated dibenzofurans ◆ (PCDF)	
Chemicals proposed for listing under the Convention	*Any Party may submit proposal for listing a new chemical in Annex A, B, or C of the Convention. The POPs Review Committee evaluates the proposals and makes recommendations to the Conference of the Parties on such listing in accordance with Article 8 of the Convention.*		
Chlorinated paraffins	LC-PFCAs	Chlorpyrifos	

◆ Pesticide ▼ Industrial chemical ◆ Unintentional by-product Production

comprehensive monitoring, public transparency, and risk-based regulations to mitigate the impacts of POPs and safeguard human and environmental health.

Recognizing the gaps in global chemical governance, the United Nations Environment Assembly (UNEA) has mandated the creation of a Science-Policy Panel (SPP) on Chemicals, Waste, and Pollution Prevention, a body that could play a role analogous to the Intergovernmental Panel on Climate Change (IPCC) (Diamond et al., 2024). The SPP is intended to provide timely, authoritative, and policy-relevant scientific assessments on chemical pollution, guiding regulatory decisions and international efforts to manage hazardous substances. Unlike existing treaties such as the Stockholm Convention, which focus on specific chemicals and waste, the SPP aims to take a more integrative and forward-looking approach, including horizon scanning to anticipate emerging risks before they become widespread issues. This would result on an enhancing of global cooperation, improvement of risk assessment frameworks, and contribution to the management of chemicals and waste at a planetary scale.

1.1.5. PROPERTIES OF PRIORIZATION OF CHEMICAL POLLUTANTS

Within the vast and complex array of chemicals present in the environment, clear and objective criteria are crucial for scientists and regulators to effectively prioritize pollutants and pollutant families. Potential priority organic contaminants are screened based on their chemical and physical properties, along with ecotoxicological profiles, which collectively determine their transport, fate, and overall environmental impact (Wania et al., 2003; 2006).

As described previously, there are some criteria and physicochemical properties described to define a POP according to UNECE (Stockholm Convention on POPs, Annex D revised in 2023). These are compounds' persistence, bioaccumulation and biomagnification potential, their adverse effects to organisms and the environment, and their potential for long-range transport **(Table 1.3)**.

For an exploratory assessment of these criteria and predict a pollutant's environmental fate, scientists use specific physicochemical parameters, which allow to predict partitioning constants between environmental media. These helps underscore a compounds tendency to move between air, water and biota (organic phase). This compartmentalization is described as the ratio of concentrations of a specific compound between the two matrixes at equilibrium and are expressed using the following partition constants:

Air-water partition coefficient (K_{AW})

The ratio of a chemical's vapor pressure to its water solubility is named Henry's law constant. The air-water partitioning coefficient (K_{AW}) or dimensionless Henry's Law Constant (H') is given by the ratio between the concentrations in air and water at equilibrium. It defines the chemical's tendency to move from a water solution into air, thus it is a measure of the compound's **volatility**. The lower this value is, the more prone is the chemical to be dissolved into water. It is empirically calculated as follows:

$$K_{AW} = H' = \frac{C_G}{C_W} \qquad [1]$$

where C_W is the compound's concentration in water (ng o µg L^{-1}) and C_G is the compound's concentration in the atmospheric gas phase (ng o µg L^{-1}). K_{AW} it is usually expressed as Log K_{AW}, and it is dimensionless.

Table 1.3 | Summary of characteristics and requirements to define a POP according to UNECE (Stockholm Convention on POPs). *Text and Annexes revised in 2023.*

PROPERTY	PARAMETER	CRITERIA
Persistence	Half-life time of the chemical in water Half-life time of the chemical in soil Half-life time of the chemical in sediment	$t_{1/2}$ in water > 2 months $t_{1/2}$ in soil > 6 months $t_{1/2}$ in sediment > 6 months
Bioaccumulation	Bio-concentration factor (BCF) in aquatic species Bio-accumulation factor (BAF) in aquatic species Log K_{OW} High BAF in other species, high toxicity or ecotoxicity Presence in biota	BCF > 5000 BAF > 5000 Log K_{OW} > 5
LRT Potential	Half-life time of the chemical in air Presence of the chemical in locations distant from the sources Data showing LRT via air, water or migratory species	$t_{1/2}$ in air > 2 days
Adverse effects	Evidence of adverse effects to human health or the environment Toxicity or ecotoxicity data	

Octanol-water partition coefficient (K_{OW})

The octanol-water partition coefficient, often represented as K_{OW}, is a key measure used to estimate how likely a chemical is to migrate from water into organic tissues, which also describes how hydrophobic it is. Octanol has traditionally been used as a surrogate of fats and lipids found in living tissues. Consequently, octanol-water partition K_{OW} is used to represent the equilibrium distribution of organic chemicals between organic phases and water, and is widely applied as a correlation parameter for bioaccumulation and sediments sorption (McDonald et al., 2000). It is estimated by,

$$K_{OW} = \frac{C_O}{C_W} \quad [2]$$

where C_o is the compound concentration in the octanol phase (ng o µg L^{-1}) and C_W is the compound's concentration in the aqueous phase (ng o µg L_{-1}). K_{OW} it is usually expressed as $LogK_{OW}$.

Octanol-air partition coefficient (K_{OA})

In addition, octanol-air partition coefficient (K_{OA}) estimates a chemical's tendency to move between air and organic phases like soil or biological tissues. It also measures the compounds **hydrophobicity** in terrestrial environments. This partition coefficient is particularly useful for understanding the behavior of volatile organic compounds in the environment. K_{OA} is given by:

$$K_{OA} = \frac{C_O}{C_A} \quad [3]$$

where C_o is the compound concentration in the octanol phase (ng o µg L^{-1}) and C_A is the compound's concentration in the gas phase (ng o µg L^{-1}) at equilibrium. If measures of K_{OA} are missing, K_{OA} can also be estimated as follows:

$$K_{OA} = \frac{K_{OW}}{H'} \quad [4]$$

These partition coefficients can be obtained through laboratory studies under controlled conditions, or, in the absence of data or the possibility of measuring it in the field or lab, they can be estimated from the physicochemical or molecular properties of the compounds, when that information is available.

Bioconcentration factor (BCF [kg L^{-1}])

The bioconcentration factor is the ratio of concentrations at steady state of a chemical in an aquatic organism to the corresponding freely dissolved chemical concentration in the water column. BCF can be calculated as follows:

$$BCF = \frac{C_B}{C_W} \quad [5]$$

where C_B (typically ng kg^{-1}) is the compound's concentration in biota, and C_W (typically ng L^{-1}) is the compound's concentration water at steady state.

Depending of these partition coefficients a chemical will be more or less likely to be in a particular phase and to be transported or migrate into this phase. For some legacy pollutants, relationship among physicochemical variables and their partitioning properties have been studied (Wania et al., 2003). For example, for PBDEs, as molar mass (MM) increases, vapor pressure (P_L) and water solubility (S_L) decrease, indicating that heavier PBDEs are less volatile and less water-soluble. The air–water partition coefficient (K_{AW}) also decreases with MM, suggesting that heavier compounds are less likely to partition into the air from water. Conversely, both the octanol–water partition coefficient (K_{OW}) and the octanol–air partition coefficient (K_{OA}) increases with molar mass, implying that heavier PBDEs are more lipophilic and tend to accumulate in fatty tissues, as well as favor organic over gaseous phases.

POPs can be classified as flyers, multi- or single hoppers and swimmers **(Figure 1.3)**. This assignment was based on the major modes of chemical transport behavior at large and global scale according to their specific partitioning property combinations by Wania (2003). Most classical POPs such as PCBs, DDT or HCB, can be classified as **multi-hoppers** (Wania et al., 2003; 2006) with their main transport route being LRAT. Others, such as HCHs or PFAS, with low log K_{AW} fall into the **swimmer**'s category, while most volatile compounds with high log K_{AW} and low K_{OA} are described as **flyers**.

Nevertheless, this classification as flyers, hoppers and swimmers is nowadays discussed, as volatile chemicals can be deposited by rain and snow (Casal et al. 2019, Casas et al. 2021), and swimmers can be transferred to the atmosphere by sea spray aerosol and ultimately be deposited by wet deposition (Casal et al. 2017, Casas et al. 2020, Casas et al. 2023).

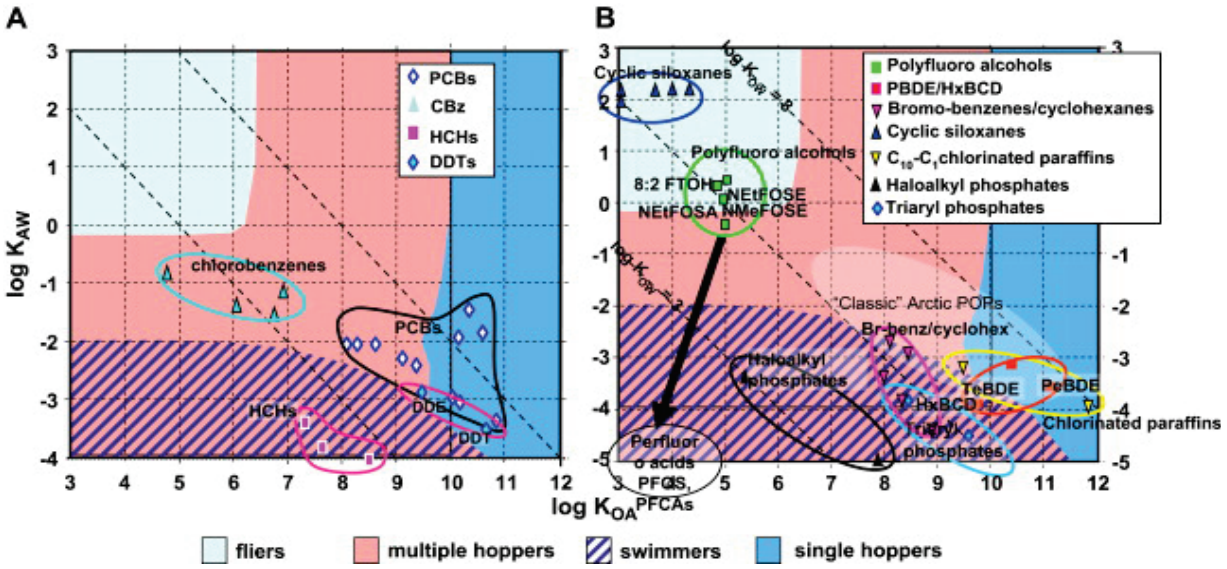


Figure 1.3 | Major modes of transport of perfectly persistent, hypothetical chemicals defined by their partitioning properties log K_{AW} and log K_{OA}, when calculated with the Globo-POP model (Wania, 2003) assuming 10 years of steady emissions into air. *Graphics modified from Wania (2006), with copyright by the American Chemical Society. (A) Legacy organochlorine compounds. (B) Some chemicals in current use. (The arrow for perfluoro acids illustrates that these degradation products of the polyfluoro alcohols have log K_{AW} << - 5 and log K_{OA} << 3, and are thus off scale). From Lohmann et al. (2007).*

1.1.6. POPs CYCLING IN THE ENVIRONMENT

This section explores the processes that govern the cycling, transformation, and fate of POPs in the marine environment, providing a foundation for understanding their dynamics and impacts within the ocean.

Sources and Transport Pathways of POPs into the Ocean

The oceans cover 70% of the ocean surface and have important reservoirs of organic carbon (preferred sorbing phase for many POPs) (Gioia et al., 2011). Numerous studies have examined how POPs are transported and cycle in the environment, with the world's oceans acting as a net sink for POPs, the study of which attracts increasing interest as research topic (Muir et al., 2021; Galbán-Malagón et al., 2012). As a result, oceans serve as a crucial environment for evaluating the enduring consequences and environmental effects of these substances (Lohmann et al., 2023; Muir et al., 2021; Galbán-Malagón et al., 2012; 2013a; 2013b; Ya et al., 2019; Luek et al., 2017; Carrizo et al., 2017; Jantunen et al., 2015; Zhang et al., 2024).

Once a chemical is released into the environment, its transport processes and ultimate fate are determined by the environmental temperature of the atmosphere and ocean, the pools and cycling of organic matter, as well as its specific physicochemical properties (Wania and Mackkay, 1996; Dachs et al., 2002b) **(Figure 1.3)**. Generally, pollutants with high K_{AW} and low K_{OA} (flyers) will volatilize to the atmosphere and remain in a gas phase, being subject to long-range atmospheric transport (Jurado et al., 2004) unless they undergo wet deposition. In contrast, chemicals with low K_{AW} and K_{OA} (swimmers) will deposit and stay in the water bodies where they are transported by oceanic currents. Formation of **sea spray aerosol (SSA)** is the only known process that can transfer important quantities of swimmers to the atmosphere (Casas et al., 2021; Sha et al., 2020; 2022; 2024). The chemicals with intermediate values of K_{OA} and K_{AW} are transported by a process called **"grasshopping" (Figure 1.3)** (Lohmann et al., 2007, Jurado et al., 2008b) which implies that they partition between hydrosphere/land and atmosphere while are transported at regional and global scale. This repeated volatilization/deposition is driven not only by temperature, but also by the pools of organic matter, its fluxes due to the biological pump, precipitation, and formation of aerosols. While originally, grasshopping was defined as repeated volatilization/absorption, nowadays it needs to take into account all these processes, which eventually will drive POP's short- and long-range transport **(Figure 1.4)**.

In warmer, lower-mid latitude areas, where most sources are found, these chemicals can volatilize, then move south or north with atmospheric currents, depositing temporarily in cooler, mid-latitude regions before re-volatilizing. In addition to temperature, POPs also accumulate preferentially in regions with higher amounts of organic matter (Jurado et al., 2004). As they reach south-high latitudes, where temperatures are colder, equilibrium conditions of the air-water

and air-soil partitioning moves to the water and land side. Increased fluxes will occur in regions with a more intense biological pump or other processes that deplete the water column concentrations, inducing an air-water dis-equilibrium that increase the deposition flux. Grasshopping results in a gradual global transport of pollutants toward colder regions, including polar regions, and also to those regions with a higher capacity to hold POPs (higher organic matter content, lower temperatures). Degradation is generally lower at low temperatures, increasing the POP's persistence in the environment **(Figure 1.5).**

Air-sea Exchange of POPs

The atmosphere has been regarded as the most important and rapid route of transport for POPs to surface waters. Semivolatile organic compounds can be removed from the atmosphere to the ocean by **three main processes** that play a key role in the transport and fate of POPs at the global scale. These highly efficient mechanisms are able to deposit POPs onto the ocean's surface in both dissolved and particulate forms, but are subject to substantial regional and seasonal fluctuations in their intensity. In areas characterized by high industrial activities or close to urban centers, deposition rates are often elevated due to increased atmospheric concentrations of POPs and higher aerosol concentrations. Furthermore, seasonal variations significantly influence scavenging dynamics.

(1) Dry deposition of particulate-bound pollutants

Dry deposition is the process by which aerosol-bound pollutants are deposited to the surface ocean in the absence of precipitation. Dry aerosol deposition fluxes (F_{DD}, pg m^{-2} d^{-1}) are often estimated by:

$$F_{DD} = V_D x C_P \quad [6]$$

Where V_D is the aerosol dry deposition velocity (m d^{-1}) and C_P is the POP aerosol-phase concentration (pg m^{-3}).

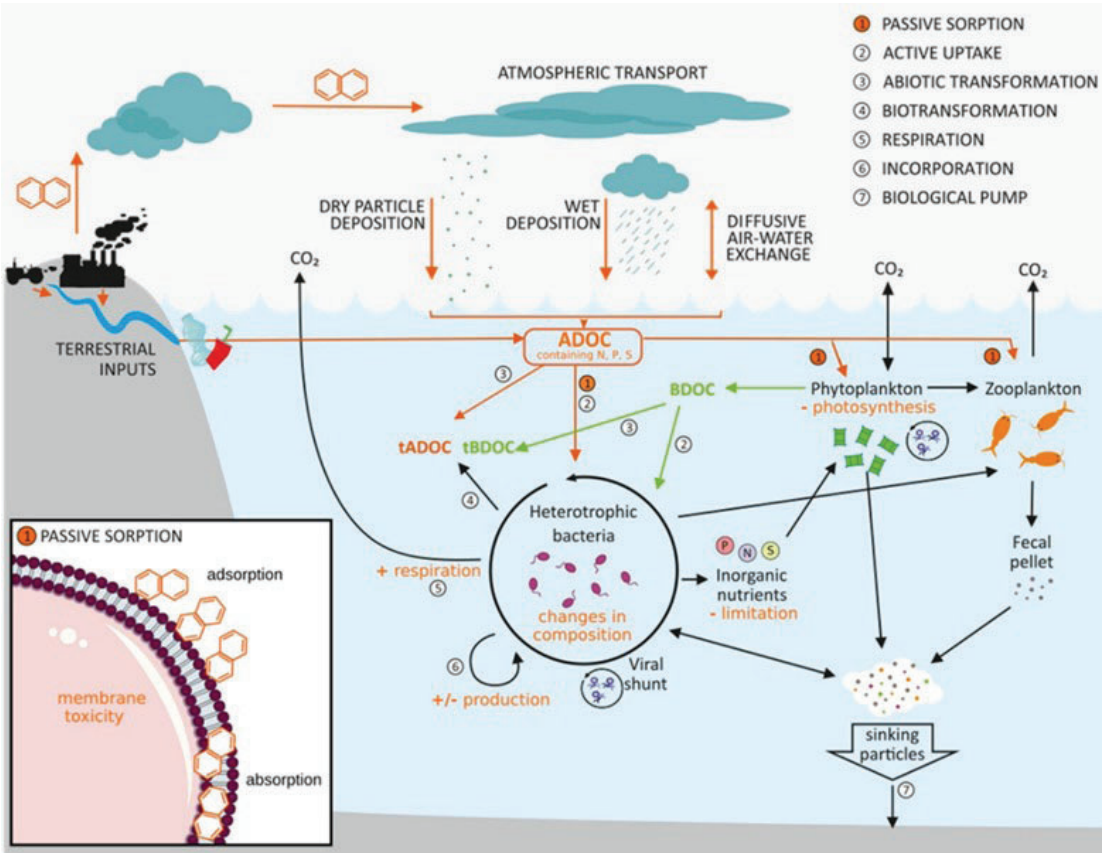


Figure 1.4 | DOC and ADOC cycling in the upper ocean. Orange and green arrows show the sources, transport and transformation processes of anthropogenic dissolved organic carbon (ADOC) and biogenic dissolved organic carbon (BDOC) respectively. tADOC accounts for the transformed ADOC, thus those transformation products due to biotic and abiotic degradation. Black arrows show the overall DOC processes resulting from contributions from ADOC and DOC. The lower panel shows the adsorption and absorption of ADOC compounds to cell membranes due to hydrophobicity. Reported effects of ADOC on microbes are depicted. From Vila-Costa et al. (2020).

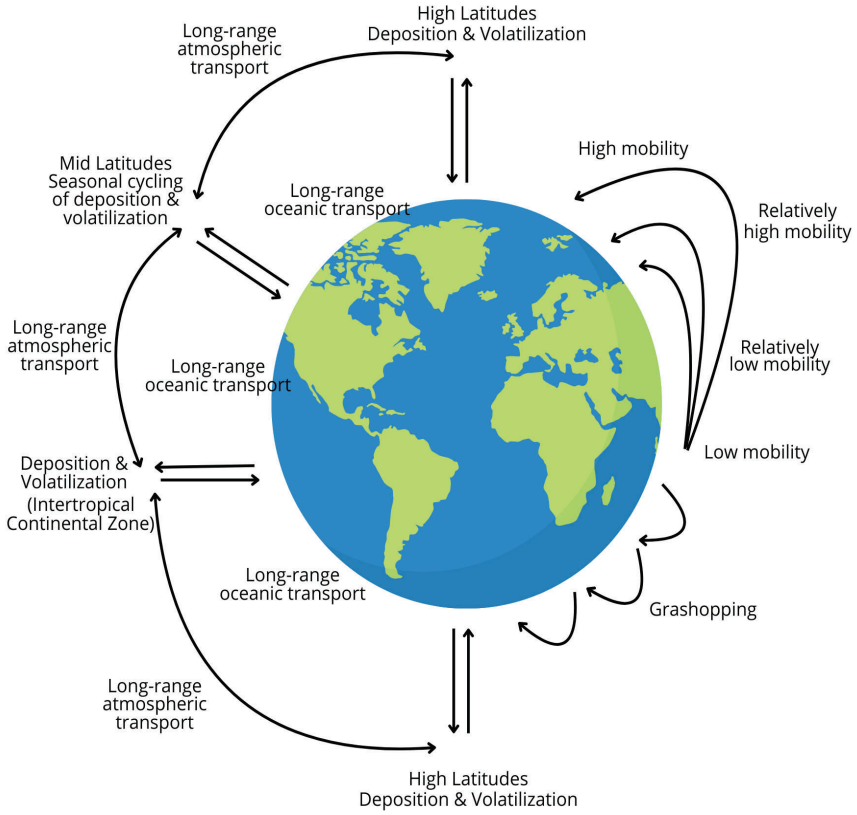


Figure 1.5 | Global distillation with fractionation according to global mobility. Adapted from Nash et al. (2013).

(2) Diffusive air-water exchange between the atmospheric boundary layer and the surface ocean

Diffusive air-water exchange has been traditionally estimated by:

$$F_{AW}=k_{AW}\left(\frac{C_A}{H'}-c_W\right) \quad [7]$$

where C_A and C_W are the dissolved and gas-phase POP concentrations (ng m^{-3}), respectively H' is the dimensionless Henry's law constant, and K_{AW} is the air-water mass transfer rate (m d^{-1}), which is parameterized from wind speed, temperature and chemical properties.

(3) Scavenging by rain and snow (either from gas or particulate phases)

Even though earlier studies suggested that snow was more efficient than rain scavenging POPs (Lei and Wania, 2004; Herbert et al., 2005, 2006; Jurado et al., 2005), a recent compilation of the scavenging washout ratios has shown that the efficiency of snow and rain is similar (Casal et al., 2019, Casas et al., 2021). Both rain and snow play critical roles in the scavenging and amplification of POPs across different environments. Rain significantly enhances POP concentrations in various climatic regions, while snow is particularly effective in polar and alpine areas, impacting the global distribution and cycling of these chemicals (Casas et al., 2021; Casal et al., 2019).

The wet deposition fluxes (F_{WD}, ng m^{-2} d^{-1}) can experimentally be estimated by:

$$F_{WD}=p_0 C_{rain} \quad [8]$$

where C_{rain} (pg m^{-3}) is the concentration of POPs in the rain and p_0 (m d^{-1}) is the precipitation's depth per day.

Consequently, the wet deposition flux can be estimated by:

$$F_{WD_rain} = K_{RA}\left(C_{air,G}+C_{air,P}\right)\frac{P_0}{f} \quad [9]$$

where $C_{air,P}$ is the concentration in particulate phase of air (aerosols), $C_{air,G}$ is the concentration in gas phase, and *f* is the fractional occurrence of rain.

The rain-air partition constant (K_{RA}), which is also named water/air scavenging ratio, or washout ratio, is given by (Ligocki et al., 1985),

$$K_{RA} = \frac{C_{rain}}{C_{air,P} + C_{air,G}} = K_{RP} + K_{RG}(1 - \theta) \quad [10]$$

Where K_{RP} and K_{RG} are the rain-air partition constants for gas and particulate phase, respectively. θ (dimensionless) is the fraction of aerosol-bound POPs to total atmospheric concentration of POPs ($C_{air,P}/C_{air,P} + C_{air,G}$).

These partition constants (dimensionless) can be given by,

$$K_{RP} = \frac{C_{rain}}{C_{air,P}} \quad [11]$$

$$K_{RG} = \frac{C_{rain}}{C_{air,G}} \quad [12]$$

Particle-water and biota-water partitioning

Once POPs enter the ocean via air-sea exchange, their behavior in the surface layers is governed by their partitioning between dissolved, particulate phases and organisms. Dissolved-phase POPs may be absorbed by marine organisms, particularly phytoplankton and bacteria, be transferred to upper levels of the trophic web, or undergo photochemical or biotic transformations in the upper layers **(Figure 1.4)**. These processes may gradually alter the chemical composition and toxicity of the pollutants. The dynamic nature of surface waters also allows for dissolved pollutants to re-enter the atmosphere through volatilization or accumulate at unique interfaces, such as the sea surface microlayer (SML), and eventually be transferred to sea spray aerosols.

Sea Surface Microlayer

One such crucial interface is the sea surface microlayer (SML), which acts as an accumulation layer for dissolved and particulate POPs and plays a pivotal role in their cycling, distribution, degradation and potential re-emission back into the atmosphere. The SML, a distinct biogeochemical layer (Liss and Duce et al., 1997; Zhang et al., 2003; Nakajima et al., 2013; Martínez-Varela et al., 2022), only 1-1000 μm thick at the ocean's surface, accumulates deposited particles and gases, as well as POPs transported from underlying waters. Here, POPs accumulate and interact complexly with both particles, dissolved organic matter and microorganisms, with an impact on marine and atmospheric chemistry (Calace et al., 2007; Sabbaghzade et al., 2017; Uning et al., 2018; Engel et al., 2017). The SML is generally enriched in a wide variety of organic pollutants compared to the underlying subsurface seawater (SSL), especially due to their surfactant nature, but also due to their hydrophobic character, or processes leading to high concentrations at the surface such as bubbles' scavenging. Previous works have reported the enrichment of semivolatile chemicals in the SML, such as polychlorinated biphenyls (Garcia-Flor et al., 2005; Fuoco et al., 2005), as well of polycyclic aromatic hydrocarbons (Fuoco et al., 2005; Cincinelli et al., 2001; 2005; Stortini et al., 2009). Recent research has extended the assessment of enrichment in the SML to emerging pollutants such as PFAS (Casas et al., 2020; Li et al., 2024).

To calculate the potential enrichment of a chemical in the SML in comparison to the subsurface layer (SSL), a dimensionless enrichment factor is defined (EF_{SML}):

$$EF_{SML} = \frac{C_{SML}}{C_{SSL}} \quad [13]$$

where C_{SML} and C_{SSL} are the individual POPs concentrations at the SML (ng L^{-1}) and SSL (ng L^{-1}), respectively.

Sea Spray Aerosols

The SML is thought to play an important role in the composition of sea spray aerosol (SSA). When the ocean surface is disturbed, tiny droplets are ejected, carrying with them the concentrated POPs from the SML (Casas et al., 2020), however, the potential role that SSA plays as a source of atmospheric semi-volatile contaminants, such as OPEs, remains unknown, even tough has been already quantified for PFAS (Casas et al., 2020; Johansson et al., 2019; Sha et al., 2020; 2022; 2024).

Assuming that the POPs measured in aerosols are due to SSA formation, it is then possible to estimate their apparent enrichment in SSA, to explore the relevance of this process for the long-range transport of OPEs. The apparent enrichment of OPEs in the SSA (EF_{SSA}, unitless) is given by:

$$EF_{SSA} = \frac{C_{SSA}}{C_{SML}} \quad [14]$$

where C_{SSA} and C_{SML} are the POP concentrations at the SSA (ng L^{-1}) and SML (ng L^{-1}), respectively.

Biological Pump and Sinks of POPs in the Ocean

As POPs interact with organic particles in the surface ocean, they can adhere to particulate matter and cells, forming aggregates that sink to deeper ocean layers. Sinking particles transport POPs to deeper waters, where they may settle in sediments, thus sequestering them for extended periods. Some studies have detected POPs at depths below 2000 m (McDonough et al., 2018; Savvidou et al., 2023), but these findings remain scare and are limited to specific families and locations. The role of sinking particles, along with natural processes such as phytoplankton uptake, collectively known as the biological pump, in the global cycling remains insufficiently explored (Dachs et al., 2022b, Galbán-Malagón et al., 2012) for most CECs.

The biological pump term in the POPs field is slightly different than the generally used in oceanography, in which the biological pump refers to the process of carbon dioxide fixation and subsequent transport of a fraction of the newly formed organic matter to deeper ocean layers via settling particles (Sarmiento & Gruber, 2006). However, as many CECs and POPs are hydrophobic, the settling of organic matter is linked to the settling of contaminants. This process plays a significant role in regulating the dissolved-phase concentrations of POPs in the water column, which, in turn, influences air-water concentration gradients (Dachs et al., 2002b; Jurado et al., 2004). By moving POPs from the surface to deeper waters, the biological pump reduces their potential for re-emission into the atmosphere (Dachs et al., 2002b; Jurado et al., 2004, 2008a). Studies have shown that decreases in dissolved POP concentrations often correlate with higher biomass or chlorophyll *a* levels, emphasizing the role of biological activity in sequestering POPs within the water column (Dachs et al., 2002b; González-Gaya et al., 2019b). Although this mechanism has been extensively studied for legacy POPs (Dachs et al., 2002b; Jurado et al., 2007; Berrojalbiz et al., 2011b), its effectiveness in modulating POP pollution in the mesopelagic and deep ocean remains unexamined in field studies.

Once POPs settle into the ocean's water column, their ultimate fate is compound dependent. Potential sinks include photolysis (Stubbins et al., 2012) and biodegradation (González-Gaya et al., 2019a; Cerro-Gálvez et al., 2019), though these processes are most active within the photic zone (0–200 m depth). Microbial degradation, in particular, serves as a significant sink for certain organic contaminants in marine environments. For instance, microbial communities in surface seawater play a primary role in the removal of polycyclic aromatic hydrocarbons, underscoring their importance in the natural attenuation of these compounds (González-Gaya et al., 2019a). Specific bacterial communities have also been shown to partially degrade perfluorooctane sulfonate (PFOS) via desulfurization, contributing to its breakdown in Antarctic water under the influence of volcanic sulfur-rich waters (Cerro-Gálvez et al., 2019). Additionally, marine bacteria are capable of degrading some organophosphate esters—commonly used as flame retardants and plasticizers—that are increasingly detected within marine dissolved organic matter (Vila-Costa et al., 2019; Iriarte et al., 2025). While this biodegradation is most effective in the photic zone, where microorganisms interact with dissolved organic pollutants, the extent of microbial degradation in deeper ocean layers remains largely unexplored.

Effects of Climate Change in the POPs cycling

The cycling of POPs in marine environments is deeply influenced by physical, chemical, and biological processes, all of which are being reshaped by climate change. As the ocean responds to rising temperatures, increasing stratification, changing circulation patterns, and declining ice cover, the dynamics of POP transport, transformation, and sequestration are likely to shift significantly. These changes have far-reaching implications for the persistence, distribution, and ecological impacts of POPs in marine ecosystems.

Rising sea surface temperatures directly influence the partitioning and bioavailability of POPs. Increased temperatures will increase Henry's law constant, promoting partitioning from water into air (Macdonald et al., 2005, Kallenborn et al., 2012). Additionally, warming intensifies ocean stratification, reducing vertical mixing and limiting the exchange of nutrients and dissolved pollutants between surface and deeper waters. This could decrease the efficiency of the biological pump, reducing the downward transport of POPs associated with organic matter. At the same time, microbial degradation processes, particularly in surface waters, are sensitive to temperature changes (Kallenborn, et al., 2012).

Shifts in global ocean circulation, such as the weakening of the Atlantic Meridional Overturning Circulation (AMOC) (Bonnet et al., 2021), may alter the transport and distribution of POPs, especially those that behave as swimmers, such as PFAS. Ocean currents play a crucial role in redistributing POPs globally, often delivering them to remote and environmentally sensitive regions like the Arctic. A slowdown in major currents could prolong the residence time of POPs in surface waters, increasing their bioavailability and potential ecological impacts (AMAP, 2016).

The Arctic and Antarctic serve as critical reservoirs for POPs, with sea ice trapping atmospheric deposition and acting as a temporary storage medium. Melting sea ice, driven by climate change, releases POPs into surrounding waters, leading to localized spikes in concentrations (Geisz et al., 2008; Pawlak et al., 2021, Corsolini et al., 2022). The accelerated ice loss in polar regions is expected to enhance air-sea exchange, increasing the re-volatilization of POPs into the atmosphere. This phenomenon could intensify global cycling, redistributing POPs to other parts of the world.

Climate change-induced shifts in primary production could have cascading effects on the biological pump and POPs cycling. Changes in phytoplankton community composition, such as a decline in diatoms and an increase in smaller phytoplankton species, may reduce the efficiency of carbon export to the deep ocean (Laufkötter et al., 2016). Since POPs are often bound to organic material, these changes could alter their transport to deeper waters, leaving higher concentrations in surface waters where they can interact with marine organisms. Furthermore, disruptions to food web dynamics could impact the bioaccumulation and biomagnification of POPs in marine ecosystems.

Ocean acidification, resulting from increased CO_2 absorption, may affect the solubility and partitioning of some POPs in seawater. Acidification also has direct impacts on marine organisms, potentially weakening calcifying organisms like planktonic foraminifera, which play a role in particle aggregation and sinking (Doney et al., 2009). As these natural processes are disrupted, the sequestration of POPs through sinking particles could decline, leading to prolonged residence times in surface layers.

1.2. SELECTED OCEANIC REGIONS

1.2.1. THE ATLANTIC OCEAN

The Atlantic Ocean (AO) is the second-largest ocean on Earth, covering approximately 106.5 million square kilometers, which represents about 20% of the Earth's surface. It extends from the Arctic Ocean in the north to the Southern Ocean in the south, bounded by America to the west and Europe and Africa to the east. The Atlantic is characterized by its unique S-shaped basin and includes notable bodies such as the Caribbean Sea, the Gulf of Mexico, and the Mediterranean Sea, which are part of its broader geographic system.

The Atlantic Ocean plays a critical role in the transport and distribution of POPs due to its complex system of currents, wind-driven circulation, and inputs from riverine sources. These interconnected mechanisms not only facilitate the movement of POPs from temperate and tropical regions toward higher latitudes but also drive their long-term cycling within the marine environment.

Rivers act as significant conduits for introducing POPs into the AO. Major river systems such as the Amazon, Congo, and Mississippi transport pollutants from industrial, agricultural, and urban areas into coastal zones (Schmidt et al., 2019; 2020). These inputs often include pesticides, PCBs, and PAHs originating from runoff, atmospheric deposition, and direct discharge (Lohmann et al., 2021). In tropical and subtropical regions, high precipitation levels can further amplify concentrations in the coastal and open-ocean (Jurado, 2005). Once in the marine environment, POPs can be transported across vast distances.

In the Atlantic, the easterly trade winds, part of the global wind system, play a pivotal role in driving surface currents and shaping the transport pathways of POPs. These winds generate Ekman transport, which moves surface waters westward along the equatorial Atlantic and creates the North Equatorial Current (NEC) and South Equatorial Current (SEC). These currents transport POPs from nearshore sources into open-ocean gyres, where they can accumulate in convergence zones such as the North Atlantic Gyre (Lohmann et al., 2007). The interplay of the trade winds and seasonal shifts, such as the Intertropical Convergence Zone (ITCZ), further influences pollutant transport across the equator. Atmospheric deposition driven by these winds ensures that POPs originating

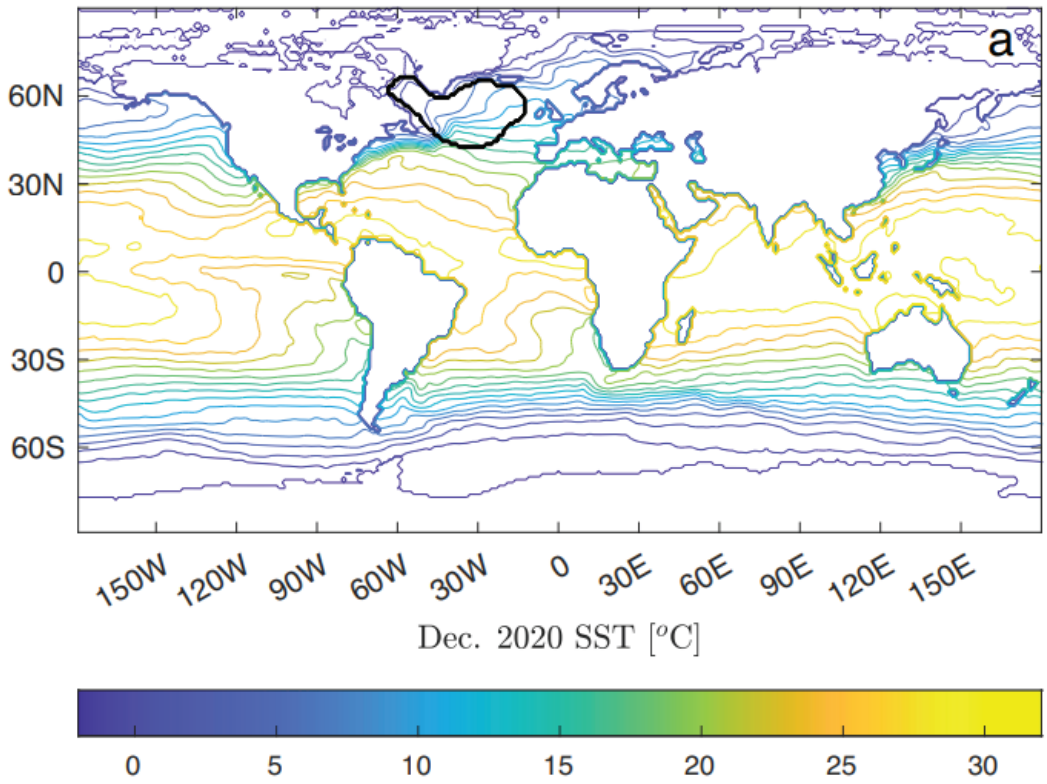


Figure 1.6 | | The Atlantic meridional overturning circulation (AMOC) fingerprint, sea surface temperature (SST) and global mean (GM). Black contour marks subpolar gyre (SG) region on top of the Hadley Centre Sea Ice and Sea Surface Temperature data set (HadISST) SST reconstruction for December 2020. From Ditlevsen & Ditlevsen (2023).

from tropical and subtropical regions are continuously introduced into the oceanic system.

As surface currents carry POPs northward, the dynamics of the Atlantic Meridional Overturning Circulation (AMOC) **(Figure 1.6)** and its associated branches, such as the Gulf Stream, the sub-polar gyre and the North Atlantic Drift, transport pollutants toward polar regions. However, recent studies suggest that the AMOC is undergoing significant weakening, with projections indicating a potential collapse by mid-century (Ditlevsen & Ditlevsen, 2023). This weakening could disrupt the northward transport of heat and pollutants, modifying deposition patterns and increasing pollutant accumulation in subtropical gyres. Additionally, a weaker AMOC would enhance ocean stratification, reducing vertical mixing and the biological sequestration of pollutants, thereby prolonging their residence time in surface waters (Boot et al., 2025).

At higher latitudes, POPs encounter the polar front, a dynamic boundary where cold polar waters meet warmer subtropical waters. This region acts as a sink for POPs due to the high biological activity and particle aggregation that facilitate their sequestration into deeper waters (Dachs et al., 2002b; Gonzalez-Gaya et al., 2019). Additionally, the convergence and upwelling processes along the polar front enhance the partitioning of POPs into organic matter, further driving their sequestration by the biological pump.

In the Southern Ocean, the South Atlantic Gyre and its convergence with the Antarctic Circumpolar Current (ACC) create another pathway for POP transport toward the Southern Ocean. Nevertheless, the ACC acts as a barrier, limiting the mixing of pollutants in the south subtropical Atlantic into Antarctic waters.

1.2.1. THE SOUTHERN OCEAN AND ANTARCTICA

The Southern Ocean (SO), encircling Antarctica, is a unique and vital component of the Earth's climate and ocean systems. Occupying approximately 20.3 million square kilometers, it is the fourth-largest ocean and serves as a critical boundary between the warmer waters of the Atlantic, Pacific, and Indian Oceans and the frigid, isolated waters surrounding Antarctica. This

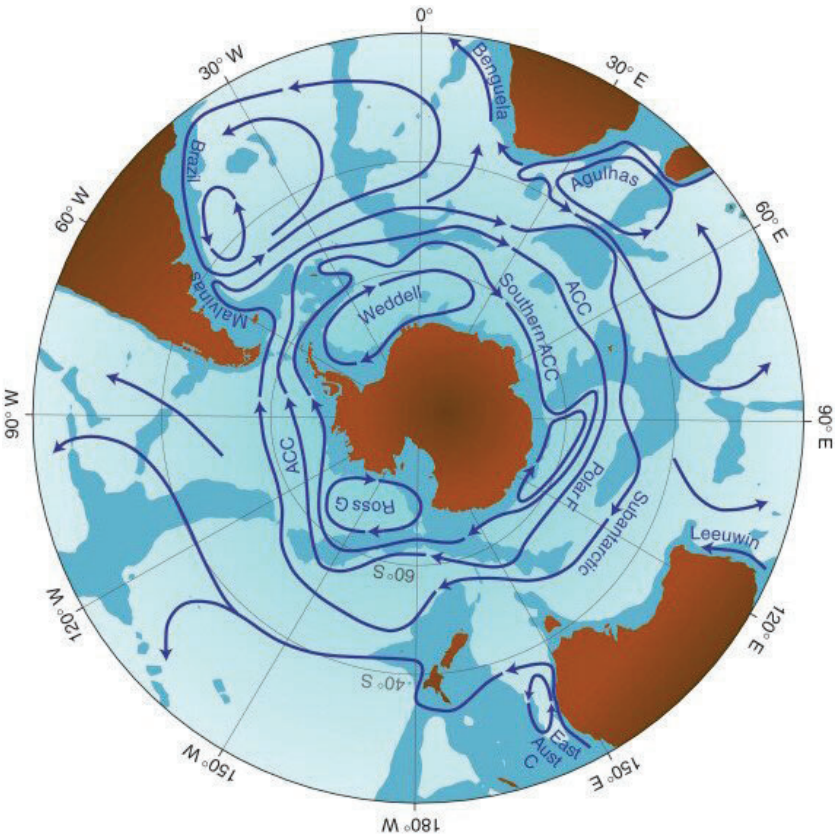


Figure 1.7 | A schematic representation of the current systems in the Southern Ocean. The Antarctic Circumpolar Current (ACC) flows from west to east around Antarctica in two major branches, the Polar Front and Subantarctic Front. Clockwise gyres fill the deep basins between the Antarctic continent and the ACC. Adapted from Rintoul et al. (2001).

dynamic region is shaped by extreme temperatures, powerful currents, and distinct biological and geochemical properties, making it integral to global ocean circulation and climate regulation (Rintoul et al., 2001, 2011; Gutt et al., 2015). The SO is among the coldest marine environments on Earth, with surface water temperatures ranging from approximately 10°C near its northern boundary to near -2°C in areas adjacent to the Antarctic continent.

Seasonal sea ice expansion and contraction significantly influence the region's physical and ecological processes. During the austral winter, sea ice expands to cover an average maximum of approximately 18 million square kilometers, while in summer, it recedes to around 2–3 million square kilometers (Parkinson et al., 2019). This annual variability drives energy exchange between the ocean and atmosphere, alters surface albedo, and insulates the ocean below, contributing to ocean stratification. Recent research highlights changes in the extent and duration of sea ice cover, with some regions, particularly in the western Antarctic Peninsula, experiencing significant declines due to warming waters and shifting wind patterns, while others have seen localized increases (Parkinson & Cavalieri, 2012). These spatial and temporal variations in sea ice are critical for marine ecosystems, regulating nutrient availability, primary production, and habitat structure.

The Southern Ocean's most defining feature is the Antarctic Circumpolar Current (ACC) (Orsi et al., 1994), the world's largest and strongest ocean current. Driven by persistent westerly winds, the ACC flows eastward around Antarctica, transporting an estimated 135–145 million cubic meters of water per second (Rintoul et al., 2001). This current acts as a barrier, limiting the mixing of warmer subtropical waters with cold Antarctic waters and maintaining the unique physical and ecological characteristics of the region.

The SO is characterized by distinct water masses **(Figures 1.7 and 1.8)** that interact to form a complex circulation system. Key water masses include:

- **Antarctic Bottom Water** (AABW): Formed by the cooling and sinking of dense, salty water around Antarctica, AABW flows into the deep basins of the world's oceans, driving global thermohaline circulation.
- **Antarctic Intermediate Water** (AAIW): A lighter water mass that forms as surface waters mix with intermediate layers, contributing to the transport of nutrients and heat.
- **Circumpolar Deep Water** (CDW): A relatively warm and saline water mass that upwells near the Antarctic Divergence zone, bringing nutrient-rich waters to the surface and fueling biological productivity.

Semivolatile POPs reach Antarctica primarily via long-range atmospheric transport (LRAT), facilitated by the grasshopper effect—a process of repeated volatilization and absorption that allows these pollutants to travel vast distances, as well toward colder regions. Once deposited, Antarctica's low temperatures, the biological pump, and the barrier effect of the Antarctic Circumpolar Current (ACC) minimize their re-volatilization, leading to their accumulation in local ecosystems. The temperature influence on these processes has been named as "cold-trapping" (Wania & Mackay, 1995), but grasshopping of semivolatile POPs is also driven by the biological pump (Jurado et al. 2008). Monitoring in East Antarctica has highlighted the dominance of semi-volatile agricultural pesticides, such as hexachlorobenzene (HCB) and endosulfan, which exhibit seasonal variations linked to temperature-driven volatilization (Bengtson Nash et al., 2017). Wet deposition processes, such as snow scavenging and sea spray aerosols, further contribute to the delivery of POPs into Antarctic marine environments, particularly in maritime regions like the Antarctic Peninsula (Casal et al., 2019; Casas et al., 2021), and this wet deposition is not limited to grasshoppers, but also to swimmers and flyers.

Unlike the Arctic, contamination in the Antarctic does not primarily reflect chemical usage in a hemisphere with relatively little landmass, a smaller human population, and a limited history of industrial activity. Generally, contaminants in Antarctica are the result of long-range atmospheric transport and deposition. Additionally, the shorter food chains typical of the Antarctic and the absence of permanent human populations have contributed to a lower perceived chemical risk for its ecosystems and organisms. As a result, research investment regarding POPs in Antarctica has been comparatively lower (Bengston-Nash, 2011) than in the Arctic.

Certain regions, such as the Antarctic Peninsula, are more exposed to air masses from northern latitudes, resulting in elevated atmospheric concentrations of POPs compared to other parts of maritime Antarctica (Galbán-Malagón et al., 2013a; Casal et al., 2017). Seasonal snowmelt during warmer periods has been linked to increased POP levels in both the atmosphere and surface seawater (Wang et al., 2015; Sanchís et al., 2015; Casal et al., 2017). Climate change exacerbates these dynamics by accelerating ice melt, which releases legacy POPs trapped in glaciers and snow, increasing their bioavailability and amplifying bioaccumulation in local biota (Corsolini & Ademollo, 2022).

The Antarctic Peninsula is especially significant as a "sentinel" of global pollution. The detection of synthetic pollutants in this region highlights their global distribution and amplifies concern about their persistence. Despite a smaller number of studies compared to temperate regions, research in Antarctica has been crucial in advancing understanding of pollutant dynamics, influencing international legislation on POPs. These investigations underscore the role of polar regions as early indicators of global environmental change (UNEP, 2009; IPCC, 2019).

For this thesis, the Southern Ocean, specifically the Bellingshausen Sea and the region around the South Shetland Islands up to 71.02ºN, has been chosen as the study area. These regions are recognized as key sentinels of global pollution due to their role in capturing and integrating atmospheric and oceanic contaminants, offering a unique perspective on the interactions between anthropogenic pollution and polar marine ecosystems.

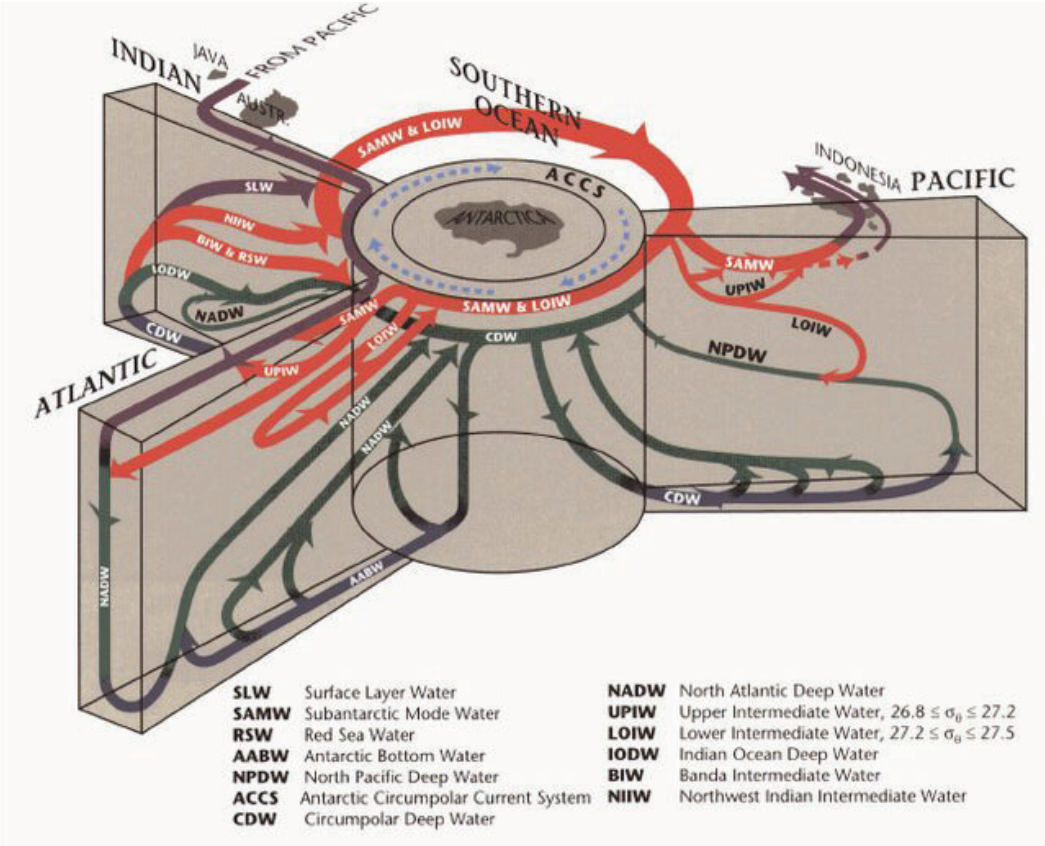


Figure 1.8 | A schematic of the three-dimensional flow between ocean basins. The figure illustrates the two key roles the Southern Ocean plays in the global overturning circulation: (1) the circumpolar link connects the ocean basins, and (2) water mass formation transforms deep water to intermediate and bottom water. From Schmitz (1996).

1.3. TARGET CONTAMINANTS STUDIED IN THIS THESIS

Three families of chemical pollutants were selected for this thesis. The first, **aromatic compounds**, including Dissolved Black Carbon (DBC), polycyclic aromatic hydrocarbons (PAHs), and other semi-volatile aromatic like compounds (SALCs), were chosen due to its dual origin. DBC is naturally produced through processes such as wildfires and volcanic activity; however, human activities—especially the incomplete combustion of fossil fuels and biomass—have exponentially increased its presence in the environment. This anthropogenic contribution amplifies its environmental impact, making DBC an essential focus for studies on both natural and human-driven pollution. DBC was assessed in a meta-analysis in **Chapter 1 - Paper I,** in conjunction with PAHs and SALCs.

As particularly persistent, bioaccumulative, toxic and with potential for long range transport, Perfluoroalkyl Substances (PFAS) and Organophosphate Esters (OPEs) were also selected as target organic contaminants for this study, focusing on the biogeochemical controls of these organic contaminants through the Atlantic and Southern oceans.

Perfluoroalkyl Substances (PFAS) are a group of chemicals of emerging concern that have been widely used over the past few decades. Their extreme persistence in the environment has led to significant research and the establishment of regulations for certain compounds within this group. As a result, a few PFAS are now classified as legacy pollutants, even as thousands of new replacements continue to be developed, marketed, and used. The study of PFAS is addressed in **Chapter 2 - Paper II**.

Organophosphate Esters (OPEs), as chemicals of emerging concern, were selected as a class of chemicals representing plasticizers and flame retardants. OPEs have gained attention in recent years due to their widespread use and potential adverse environmental and health effects but data on their occurrence and distribution across the global ocean are needed to better understand their behavior, persistence and risks. Research regarding OPEs is presented in **Chapter 3 - Papers III & IV**.

1.3.1. AROMATIC COMPOUNDS (DBC, SALCs AND PAHs)

Natural and Anthropogenic Pollutants

The study of combustion-derived organic aromatic compounds in the environment has long focused on understanding their sources, transport, and impacts on ecosystems. Polycyclic aromatic hydrocarbons (PAHs), a major group of combustion by-products, were among the earliest identified contaminants originating from both natural and anthropogenic sources, including wildfires, fossil fuel combustion, and industrial emissions. Structurally composed of multiple aromatic rings, PAHs exhibit notable stability and persistence, allowing for long-range atmospheric transport. While PAHs were initially studied primarily for their toxicity and carcinogenic properties in both biota and humans (Menzie & Potocki, 1992; Ding et al., 2007; Kim et al., 2013), research has expanded to include their role in the broader class of semi-volatile aromatic-like compounds (SALCs), encompassing a range of aromatic hydrocarbons with similar chemical structures and combustion origins (González-Gaya et al., 2016).

PAHs are nonpolar, lipophilic compounds, whose physicochemical properties vary with molecular weight (MW). Generally, PAHs with low molecular weights (LMW), with two or three aromatic rings, show slightly higher water solubility, though still limited to only a few milligrams per liter, whereas high molecular weight (HMW), with four to six condensed aromatic rings are less soluble. As MW increases, PAHs exhibit lower melting points, boiling points, and vapor pressures. In contrast, their log K_{OW} values rise with MW, indicating a greater tendency to partition into organic materials where HMW PAHs can accumulate and persist (Mackay & Callcott, 1998).

Despite a tendency to bioaccumulate at lower trophic levels, such as mollusks and crustaceans, PAHs can be metabolized by fish and other organisms, reducing their persistence as they move up in the food chain (Lee et al., 1972). The U.S. Environmental Protection Agency (EPA) has identified 16 priority PAHs **(Table 1.4)** based on their toxicity to human health, with seven classified as probable human carcinogens, including benzo[a]pyrene, benzo[b]fluoranthene, and dibenzo[a,h] anthracene. The European Commission also monitors PAH levels in food, with regular assessments of 15 HMW PAHs plus one methylated PAH in various environmental matrices and consumer goods (EU Commission, Regulation No. 835/2011).

Dissolved Black Carbon (DBC) has emerged as a significant component of marine dissolved organic carbon (DOC), generated from the incomplete combustion of organic matter such as biomass and fossil fuels. DBC can persist in marine systems over extended periods, influencing oceanic carbon cycling (Dittmar & Paeng, 2009; Jaffé et al., 2013).

Quantification of DBC is generally done through analysis of benzene polycarboxylic acids (BPCAs) as surrogate (Dittmar et al., 2008a; 2008b). This approach

has provided insights into the distribution of this stable carbon form in marine environments (Coppola et al., 2014; Wagner & Jaffé, 2015). Recent studies show that PAHs and SALCs contribute to significant atmosphere-ocean fluxes, of a magnitude relevant for the marine carbon cycle, (González-Gaya et al., 2016). To certain degree, PAHs, SALCs and DBC all refer to chemicals originating from incomplete combustion of organic matter (biogenic or anthropogenic), but it is unclear the relationship between DBC and PAHs.

Compound name	Structure (number of rings)	Molecular Weight (g mole^{-1})	Solubility (mg L^{-1})	Vapor pressure (mm Hg)	Log K_{ow}
Naphthalene	2	128.17	31	8.89E-02	3.37
Acenaphthene	3	154.21	3.8	3.75E-03	4.00
Acenaphthylene	3	152.20	16.1	2.90E-02	3.62
Anthracene	3	178.23	0.045	2.55E-05	4.54
Phenanthrene	3	178.23	1.1	6.80E-04	4.57
Fluorene	3	166.22	1.9	3.24E-03	4.18
Fluoranthene	4	202.26	0.26	8.13E-06	5.23
Benzo(a)anthracene	4	228.29	0.011	1.54E-07	5.91
Chrysene	4	228.29	0.0015	7.80E-09	5.75
Pyrene	4	202.26	0.132	4.25E-06	5.18
Benzo(a)pyrene	5	252.32	0.0038	4.89E-09	6.04
Benzo(b)fluoranthene	5	252.32	0.0015	8.06E-08	6.2
Benzo(k)fluoranthene	5	252.32	0.0008	9.59E-11	6.2
Dibenz(a,h)anthracene	6	278.35	0.0005	2.10E-11	6.86
Benzo(g,h,i)perylene	6	276.34	0.00026	1.00E-10	6.22
Indeno[1,2,3-cd]pyrene	6	276.34	0.062	1.40E-10	6.65

Table 1.4 | US EPA's 16 priority PAHs and selected physico-chemical properties by ASTDR, 1995. Italics refers to compounds classified as probable human carcinogenic by National Toxicological Program (USA), 2005.

1.3.2. PER- AND POLYFLUOROALKYL SUBSTANCES (PFAS)

The "Forever Chemicals"

Per- and polyfluoroalkyl substances (PFAS) are a large group of synthetic organofluorine compounds that have been used since the 1940s due to their unique "repellent" properties, extreme stability, and surfactant characteristics (Lindstrom et al., 2011). These properties make PFAS effective in a variety of applications, including waterproofing, stain resistance, non-stick coatings, and firefighting foams. However, their chemical resilience, which provides durability in consumer products, also contributes to their environmental persistence, bioaccumulation, and widespread distribution—posing significant ecological and health challenges worldwide.

The chemical structure of PFAS consists of poly- and per-fluoroalkyl chains with an external hydrophilic head. PFAS can be divided into two main groups: neutral and ionic PFAS. Neutral PFAS include fluorotelomers and perfluorosulfonamides among others, which have higher vapor pressure and lower water solubility, allowing them to undergo transformation through hydrolysis, photolysis, and biodegradation (Martin et al., 2006; Rhoads et al., 2008). In contrast, ionic PFAS, including the well-studied **perfluoroalkyl acids (PFAAs)**, exhibit high water solubility and are exceptionally persistent, making them significant bioaccumulative pollutants with potential health impacts.

Among ionic PFAS, two main groups stand out **perfluoroalkyl sulfonates (PFSAs)** and **perfluoroalkyl carboxylic acids (PFCAs)**. PFSAs, including PFOS (perfluorooctanesulfonic acid), follow the structure $C_nF2_{n+1}SO_3H$, while PFCAs, such as PFOA (perfluorooctanoic acid), follow the structure $C_nF2_{n+1}CO_2$. Both groups exhibit resistance to breakdown, making them bioaccumulative and persistent pollutants with known potential health impacts. This high resistance to degradation, as argued by Cousins et al., 2020, supports the need to manage PFAS collectively as a chemical class rather than individually, suggesting that the persistence of PFAS alone is reason enough to justify their phased removal from non-essential applications to limit further accumulation in ecosystems and food chains (Cousins et al., 2020).

The widespread use of PFAS can be traced back to the invention of Teflon in 1938, which marked the beginning of their application in products resistant to heat, oil, stains, and water. PFAS production expanded in 1949 with 3M's manufacturing of PFOS as a surfactant, followed by PFOA in 1951. Due to health concerns,

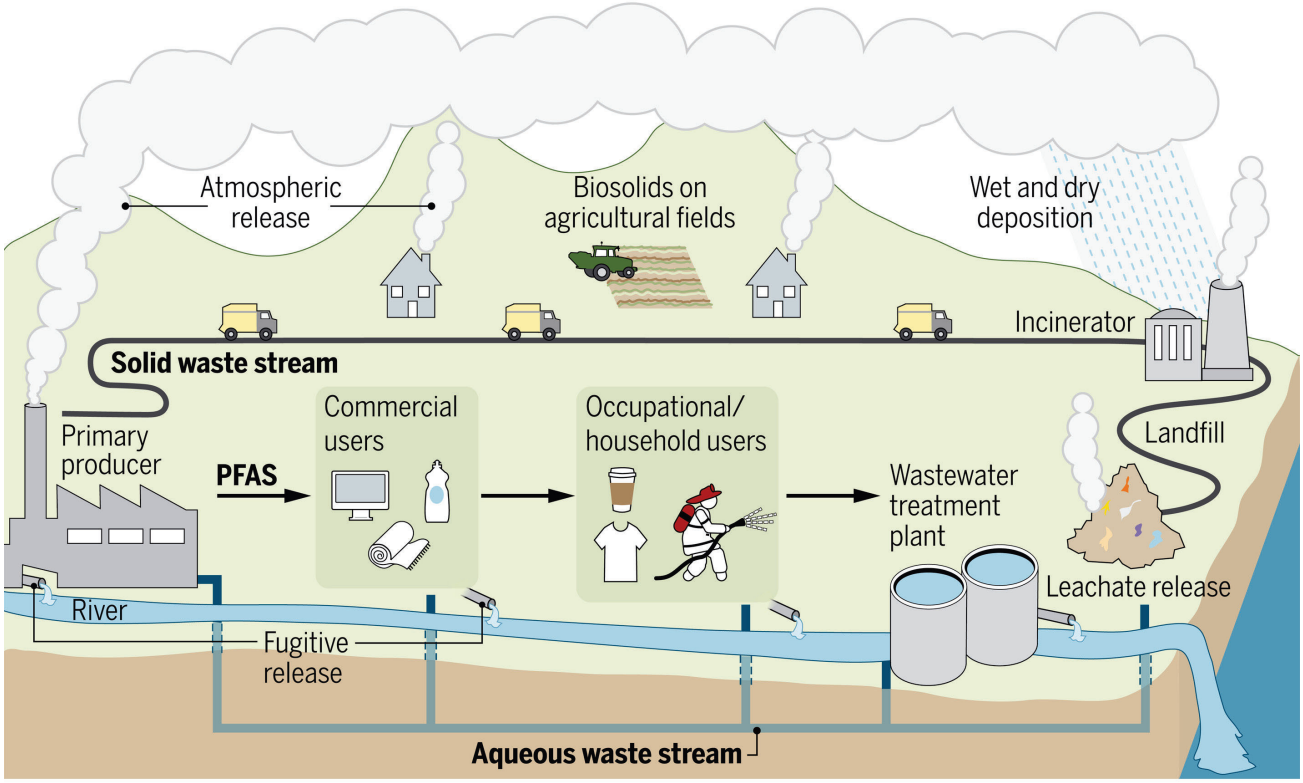


Figure 1.9 | The PFAS life cycle. PFAS product flows from primary producer to commercial user to consumers to disposal. Each step is attended by atmospheric and aqueous fugitive releases. Soils constitute a long-term environmental sink, slowly releasing PFAS to the hydrosphere and allowing uptake in biota, but the ultimate reservoir is deep marine sediment. From Evich et al. (2022).

additional PFAS compounds, such as PFNA and PFTrDA, were developed from 1975 onward. In 1998, the EPA raised concerns about PFOS after detecting it in human serum near production sites (Gaines et al., 2022). Despite these concerns, PFAS have continued to be extensively used in consumer, commercial, and industrial applications.

PFAS are introduced into the environment through a variety of sources, including releases during manufacturing, industrial emissions, wastewater discharge, landfill leachate, and consumer products such as firefighting foams, non-stick cookware, and waterproof textiles **(Figure 1.9)**. These emissions have resulted in the global distribution of PFAS, with both atmospheric and aqueous releases contributing to their spread. Neutral PFAS compounds, which are volatile, undergo long-range atmospheric transport, traveling significant distances from their source before deposition through precipitation and dust particles. Upon release, PFAS compounds can undergo complex environmental transformations, often leading to recalcitrant transformation products, which are PFAS that resist degradation. In aquatic environments, PFAS persist in surface and groundwater, bioaccumulating within marine and freshwater food webs and serving as major exposure pathways for wildlife and humans. Soil and sediment also act as long-term sinks, retaining PFAS for decades. These persistent sources and transport pathways contribute to PFAS's classification as "forever chemicals," underscoring their global ecological and health impacts (Evich et al., 2022).

PFAS can be found in all environmental media. They can be present in water, soil, air, and food as well as in materials found in our homes or workplaces, including: drinking water, soil and water at or near waste sites, fire extinguishing foams, food, food packaging, household products and dust or personal care products (EPA, 2024). A recent study (Glüge et al., 2020) identified that PFAS have or have had 200 different uses within 64 categories, five times as many uses previously proposed by Kissa et al., 2001. While previous works proposed that the number of PFAS in use was about a few thousands of individual compounds (Wang et al., 2016), under the most recent revised definition by the Organization for Economic Co-Operation and development (OECD), which included any chemical containing at least one saturated CF2 or CF3 moiety, there are currently 7 million of such chemicals in use according to PubChem (Schymanski et al., 2023). Further emphasizing their global impact, Cousins et al. (2022) highlighted PFAS within the planetary boundaries' framework proposed by Rockström et al., identifying PFAS as a pollutants family that has likely exceeded safe environmental limits due to its widespread, lasting presence. This boundary transgression implies that PFAS pollution, if left unmanaged, poses a systemic risk to planetary health and underscores the need for precautionary regulation.

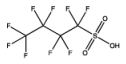
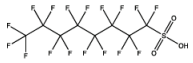
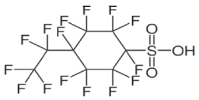
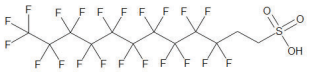
Several studies have demonstrated the widespread presence of PFAS across global oceans (Yamashita, et al., 2007; Ahrens et al., 2010; Benskin et al., 2012; González-Gaya et al., 2014; Muir & Miaz, 2021; Khan et al., 2023), in deeper water bodies (González-Gaya et al., 2019b; Savvidou et al., 2023), and even in remote regions (Zhao et al., 2012; Joerss et al., 2020; Casas et al., 2023; Xie et al., 2023). Their ubiquity, and capacity for LRAT (Prevedouros et al., 2006; Ahrens et al., 2011), combined with evidence of bioaccumulation through the food chain and toxicity to both marine organisms and humans (Lindstrom et al., 2011; Roth et al., 2020; Fenton et al., 2020; Podder et al., 2021; Truong et al., 2022; Khan et al., 2023), underscores the ecological and health risks associated with PFAS. Recent research has tested microbial degradation as a possible method for PFAS breakdown (Cerro-Galvez et al., 2020; Berhanu et al., 2023). However, the extreme stability of PFAS, especially ionic forms, has proven challenging for biodegradation efforts.

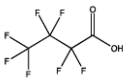
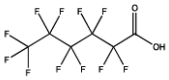
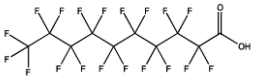
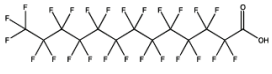
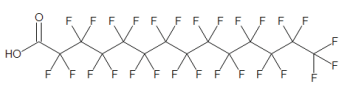
Currently, **twelve chemical companies** account for the majority of global PFAS production: AGC, Arkema, Chemours, Daikin, 3M, Solvay, Dongyue, Archroma, Merck, Bayer, BASF, and Honeywell. Despite their substantial role in PFAS production, most of these companies rarely mention "PFAS" on their public websites. In fact, seven of the twelve do not mention PFAS at all, while three others reference it fewer than ten times. The two exceptions are 3M and Chemours, both of which are involved in litigation related to PFAS production and therefore obligated to disclose information in their reporting (ChemSec, 2023). In fact, in December 2022, 3M announced it would cease manufacturing PFAS and eliminate them from its product portfolio by the end of 2025 (3M News Center, 2022). This decision aligns with global regulatory efforts, including the Stockholm Convention on Persistent Organic Pollutants, which has progressively listed various PFAS compounds for elimination or restriction.

In this thesis, nineteen PFAAs have been targeted, including thirteen PFCAs (C_4–C_{18}) and six PFSAs (C_4, C_6, C_8, C_8, C_{12}), with individual compounds and their physicochemical properties shown in **Table 1.5**

Table 1.5 | Physicochemical properties of the selected PFAS. *Data extracted from [a]Kin et al., 2015, and [b]Wang et al., 2011. Blank cells indicate no data available.*

Analyte	Acronym	#C	MW (g mole^{-1})[a]	Log K_{AW}[b]	Log K_{OW}[b]	Log K_{OA}[b]
Perfluoroalkyl sulfonic acids	**PFSAs**					
Perfluorobutane sulfonic acid	PFBS	4	300.10	-2.59	3.90	6.49
Perfluorohexane sulfonic acid	PFHxS	6	400.11	-2.38	5.17	7.55
Perfluorooctane sulfonic acid	PFOS	8	500.13	-1.65	6.43	8.07
Perfluoroethylcyclohexane sulfonate	PFECHS	8	462.1		3.8	4.92
Perfluorodecane sulfonic acid	PFDS	10	563.00	-1.15	7.66	8.82
Perfluorododecane sulfonic acid	PFDoDS	12	700.16			
Perfluoroalkyl carboxylic acids	**PFCAs**					
Perfluorobutanoic acid	PFBA	4	214.04	-3.23	2.82	6.04
Perfluoropentanoic acid	PFPeA	5	264.06	-2.90	3.43	6.33
Perfluorohexanoic acid	PFHxA	6	314.05	-2.58	4.06	6.63
Perfluoroheptanoic acid	PFHpA	7	364.06	-2.25	4.67	6.92
Perfluorooctanoic acid	PFOA	8	414.07	-1.93	5.30	7.23
Perfluorononanoic acid	PFNA	9	464.08	-1.58	5.92	7.50
Perfluorodecanoic acid	PFDA	10	514.08	-1.27	6.50	7.77
Perfluoroundecanoic acid	PFUnDA	11	564.09	-0.92	7.15	8.08
Perfluorododecanoic acid	PFDoDA	12	614.10	-0.58	7.77	8.36
Perfluorotridecanoic acid	PFTrDA	13	664.10	-0.38	8.25	8.63
Perfluorotetradecanoic acid	PFTeDA	14	714.11	0.03	8.90	8.87
Perfluorohexadecanoic acid	PFHxDA	16	814.13			
Perfluorooctadecanoic acid	PFODA	18	914.10			

Log S (mol L^{-1})[a]	Chemical structure
-1.64	
-3.23	
-4.81	
0.0014	
-5.39	
	

-0.64	
-1.43	
-2.22	
-3.01	
-3.81	
-4.60	
-5.39	
-6.05	
-6.97	
-8.40	
	
	
	

1.3.3. ORGANOPHOSPHATE ESTERS (OPEs)

Plasticizers and Flame Retardants

Organophosphate esters (OPEs) are a class of organophosphorus compounds with a central phosphate molecule structured as $O=P(OR)_3$, where each OR group is either an alkyl or aromatic substituent (Greaves et al., 2016). Following the effective regulation of polybrominated diphenyl ethers (PBDEs), widely used flame retardants until 2003, the use of OPEs surged, with global demand increasing from 300 kilotons in 2004 to 620 kilotons in 2013, accounting for 30% of the global flame retardant market (Sühring et al., 2016; Makinen et al., 2009).

OPEs are used extensively for two main reasons: chlorinated (Cl-OPEs) and brominated (Br-OPEs) variants serve as flame retardants, while non-halogenated alkyl and aryl OPEs are mainly used as plasticizers (Andresen et al., 2004). Non-derivatized alkyl phosphates, such as tributyl phosphine oxide (TBPO), tris-iso-butyl phosphate (TiBP), triphenyl phosphate (TPhP), and tris (2-butoxyethyl) phosphate (TBEP), are primarily used as plasticizers, lubricants, and pore size regulators, though some also function as flame retardants (Andresen et al., 2004). Others, such as tris (2-isopropylphenyl) phosphate (TPPP), are incorporated into commercial flame retardant mixtures, often in polyurethane foam (van der Veen & de Boer, 2012).

The low production cost and compatibility with various polymers have led to widespread OPE use across industries, including textiles, furniture, and electronics, where they serve as plasticizers and flame retardants. OPEs are typically added physically rather than chemically bonded to the final product (Wang et al., 2019a). Applications include floor polish (TBEP), lacquers (TBEP and tri-n-butyl phosphate [TNBP]), hydraulic fluids (TPhP), PVC plasticizers (triethyl phosphate [TEP], TPhP, tris (2-chloroethyl) phosphate [TCEP], tris (2-ehylhexyl) phosphate [TEHP], tri-o-cresyl phosphate [ToCP], TPPP and 2-ethylhexyldiphenyl phosphate [EHDPP]), as well as textiles, rubber, polyurethane foam, antistatic agents, electronics, engineering thermoplastics, epoxy, and phenolic resins (van der Veen & de Boer, 2012).

Despite evidence of OPEs in marine environments (Bollmann et al., 2012; Li et al., 2017; Gao et al., 2019; 2020; McDonough et al., 2018; Schmidt et al., 2019; 2021; Na et al., 2020; Xie et al., 2024), data on their oceanic large-scale distribution remains limited. The ubiquity of OPEs in the environment has raised concerns regarding their toxicological effects (van der Veen & de Boer, 2012; Wei et al., 2015; Tran et al., 2021; Wang et al., 2019a; Greaves et al., 2017), bioaccumulation potential (Bekele et al., 2021; Ding et al., 2020; Wang et al., 2019b; Garcia-Garín et al., 2020), and persistence in ecosystems (Sühring et al., 2016; Wei et al., 2015; Schmidt et al., 2019, 2020; Marklund et al., 2005; Meyer & Bester, 2004). Studies have shown that certain OPEs exhibit endocrine-disrupting properties, with evidence of developmental, reproductive, and neurological toxicity in aquatic species (Noyes et al., 2015; Sun et al., 2016; Dishaw et al., 2014; Jarema et al., 2015).

OPEs are typically released from land-based sources (Wei et al., 2015) and so they have been detected in various terrestrial environmental matrices, including air (Castro-Jiménez et al., 2016), indoor dust (Carlsson et al., 1997; Marklund et al., 2003) or soil (Zhang et al., 2022). The releasing processes are typically volatilization (Zeng et al., 2020) or riverine inputs (Wang et al., 2015; Schmidt et al., 2019; 2020). The riverine pathways integrate different processes such as sewage treatment effluents (Brommer et al., 2012; Wei et al., 2015; Gravel et al., 2019; Fries & Puttmann, 2001; Bester et al., 2004), industrial leakages, plastics or e-waste runoff or atmospheric deposition. OPEs can also be directly released in the marine environment through leaching from oceanic plastic debris (Fauvelle et al., 2021; Palusselli et al., 2019). Once OPEs reach the marine environment, they can accumulate in the water, sea surface microlayer, sediment (Ma et al., 2017; Sutton et al., 2019; Schmidt et al., 2021) or biota (Castro et al., 2020; Schmidt et al., 2021), even at higher trophic levels (Aznar-Alemany et al., 2019; Sala et al., 2019, Garcia-Garin et al., 2020).

Once they are released in the atmosphere via volatilization, OPEs have been shown to have the potential for LRAT **(Figure 1.10)**, which has proven to be a crucial pathway for OPEs, contradicting early assumptions that their short atmospheric half-lives would prevent their global distribution. Initial assessments, such as the EU's 2008 study on tris (1.3-dichlor-2-propyl) phosphate's (TDCIPP) short half-life (8.6 hours), led to the assumption that OPEs had low LRAT potential. However, recent studies reveal that particle-bound OPEs, like TPhP, TEHP, and TDCIPP, have atmospheric lifetimes of several days, indicating they can travel considerable distances, showing that certain OPEs are indeed capable of reaching remote areas.

During LRAT, OPEs also undergo significant atmosphere-ocean exchanges. These processes include diffusive air-water exchange, dry deposition of particle-bound OPEs, and wet deposition via rain and snow (Li et al., 2017; Castro-Jiménez et al., 2016; Na et al., 2020; McDonough et al., 2018). Notably, studies have shown that rain and snow have the potential to amplify the concentrations of OPEs in the receiving

waters (Casas et al., 2021; Casal et al., 2019), due to the high specific surface area of snowflakes and raindrops, which increases the snow-air and rain–air washout ratios (generally close to 10^5 for OPEs) (Casas et al., 2021).

Another process affecting OPE distribution is ice and snow melting. As global temperatures rise, this process release chemical contaminants, including OPEs, trapped within them, directly discharging these pollutants into nearby water columns (Casal et al. 2019). This process can significantly increase OPE concentrations in coastal seawater and enhance their fugacity gradient between seawater and air (Li et al., 2017; Castro-Jiménez et al., 2016).

OPEs can also undergo significant long-range transport via ocean currents, especially Cl-OPEs, which are highly persistent in water due to low degradation rates. Coastal seas often contain elevated levels of OPEs, influenced by riverine inputs, which can be carried across thousands of kilometers by currents. Floating debris may also transport OPEs, potentially introducing them to remote regions like the Southern Ocean (Cheng et al., 2013).

The primary known sinks of OPEs are photodegradation, which may occur predominantly in the photic zone and upper waters (Regnery and Püttman, 2010; Su et al., 2016; Cristale et al., 2017), and microbial degradation (Vila-Costa et al., 2019, Iriarte et al. 2025) **(Figure 1.10)**. However, the complexities of these processes, especially in marine environments, are not fully understood, and further in situ and field-based explorations are required to accurately assess OPE potential degradation dynamics.

Individual OPEs selected in this study are presented in **Tables 1.6 and 1.7.**

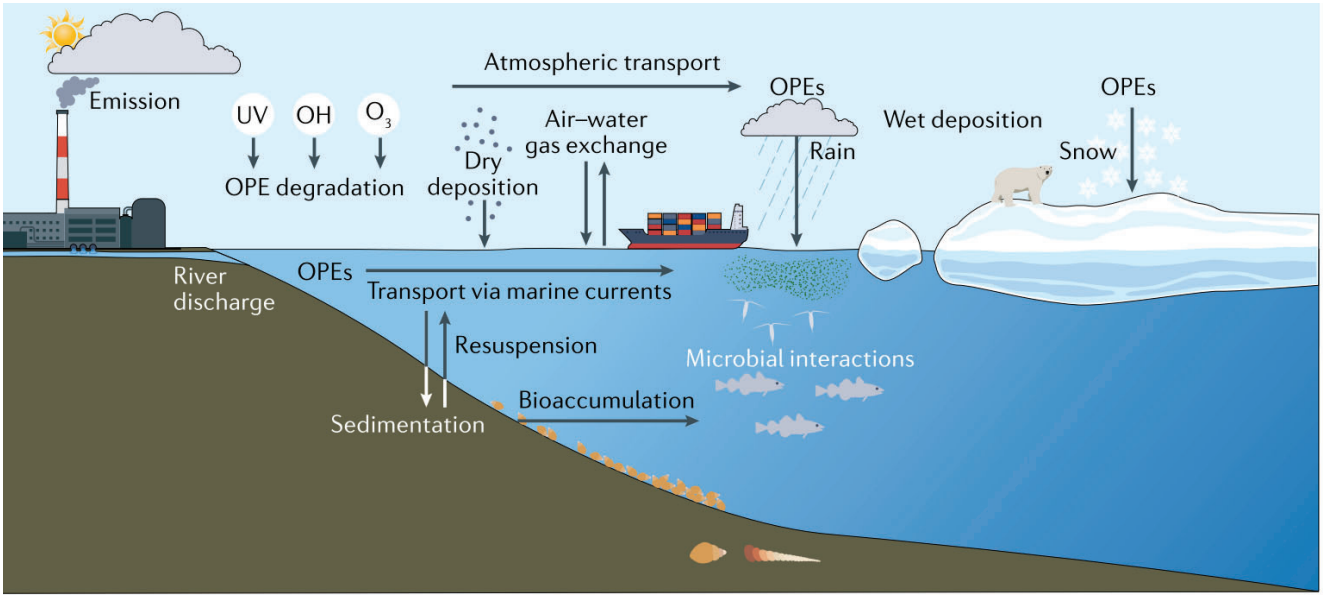
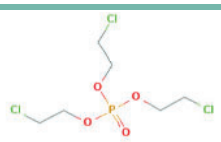
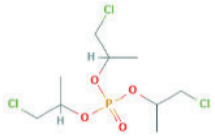
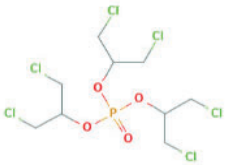
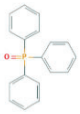
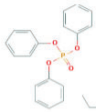
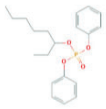
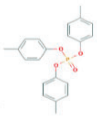
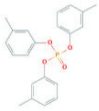
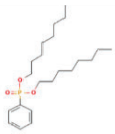
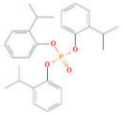
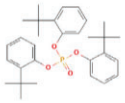


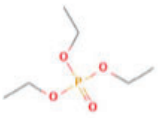
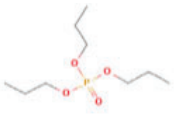
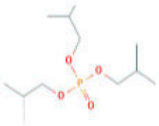
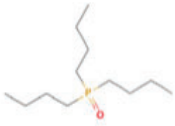
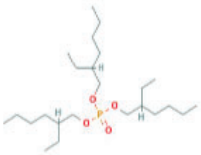
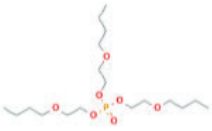
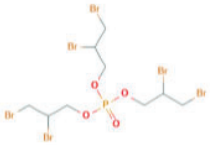
Figure 1.10 | Major sources and pathways of OPEs in coastal and open oceans. *The primary continental sources of organophosphate esters (OPEs) include industry, wastewater treatment plants, electronic waste recycling plants and ambient emissions. Major environmental pathways for OPE dispersal include atmospheric and oceanic transport, air–water exchange, atmospheric dry and wet deposition, sedimentation, bioaccumulation and microbial interactions. OPEs can be transported from continental sources to the open ocean and undergo biogeochemical cycling in various environmental compartments. UV, ultraviolet. From Xie et al. (2022).*

Table 1.6 | Physicochemical properties of the selected OPEs. *Data extracted from Zhang et al. 2016. Those marked in bold are from EPISuite ChemSpider Royal Society of Chemistry. Blank cells indicate no data available.*

Analyte	Acronym	MW (g mol^{-1})	Log K_{AW}	Log K_{OW}	Log K_{OA}	Log S (mol L^{-1})
Cl-OPEs						
Tris (2-chloroethyl) phosphate	TCEP	285.5	-6	1.6	7.6	1.1
Tris (2-choloroisopropyl) phosphate	TCPP-1.2.3	327.6	-5.6	2.9	8.5	1.7
Tris (1.3-dichlor-2-propyl) phosphate	TDCIPP	430.9	-7	3.7	10.6	-0.9
Alkyl-OPE						
Triethyl phosphate	TEP	182.2	-4.6	0.9	5.5	1.2
Tripropyl phosphate	TPrP	224.2	**-4.3**	**2.1**	**6.4**	**2.7**
Tris-iso-butyl phosphate	TiBP	266.3	**-3.9**	**3.6**	**7.5**	**1.2**
Tri-n-butyl phosphate	TNBP	266.3	-3.9	3.8	7.7	-1.2
Tributyl phosphine oxide	TBPO	218.3	-1.8	3.9		1.2
Tris (2-ehylhexyl) phosphate	TEHP	434.6	-2.4	9.5	11.9	-5.9
Tris (2-butoxyethyl) phosphate	TBEP	398.5	-9.3	3	12.3	0.1
Aryl-OPEs						
Triphenyl phosphine oxide	TPPO	278.3	**-7.7**	**2.9**	**10.5**	**1.8**
Triphenyl phosphate	TPhP	326.3	-5.8	4.7	10.5	-2.1
2-Ethylhexyldiphenyl phosphate	EHDPP	362.4	-5.0	6.3	11.5	-1.2
Chlorpyrifos	Chlor	350.6		4.96	8.6	
Tri-p-cresyl phosphate	TpCP	368.4	-5.7	6.3	12.0	-3.7
Tri-o-cresyl phosphate	ToCP	368.4	-5.7	6.3	12.0	-3.7
Tri-m-cresyl phosphate	TmCP	368.4	-5.7	6.3	12.0	-3.7
Dioctylphenyl phosphonate	DOPP	382.5		7.5		
Tris (3.5-dimethylphenyl) phosphate	TDMPP	410.4	-5.5	8	13.5	-5.2
Tris (2-isopropylphenyl) phosphate	TPPP	452.5	-4.9	9.1	14.0	-5.7
Tris (4-tert-butylphenyl) phosphate	TTBPP	494.6	-4.6	10.4	15.0	-7.3
Br-OPE						
Tris (2.3-dibromopropyl) phosphate	TDBPP	697.6	-9.9	9.1	14.1	-2.4

Table 1.7 | Chemical structure of the selected OPEs.

Cl-OPEs	
Tris (2-chloroethyl) phosphate (TCEP)	
Tris (2-choloroisopropyl) phosphate (TCPP)	
Tris (1.3-dichlor-2-propyl) phosphate (TDCIPP)	
Aryl-OPEs	
Triphenyl phosphine oxide (TPPO)	
Triphenyl phosphate (TPhP)	
2-Ethylhexyldiphenyl phosphate (EHDPP)	
Tri-o-cresyl phosphate (ToCP)	
Tri-p-cresyl phosphate (TpCP)	
Tri-m-cresyl phosphate (TmCP)	
Dioctylphenyl phosphonate (DOPP)	
Tris (3.5-dimethylphenyl) phosphate (TDMPP)	
Tris (2-isopropylphenyl) phosphate (TPPP)	
Tris (4-tert-butylphenyl) phosphate (TTBPP)	

Alkyl-OPE	
Triethyl phosphate (TEP)	
Tripropyl phosphate (TPrP)	
Tris-iso-butyl phosphate (TiBP)	
Tri-n-butyl phosphate (TNBP)	
Tributyl phosphine oxide (TBPO)	
Tris (2-ehylhexyl) phosphate (TEHP)	
Tris (2-butoxyethyl) phosphate (TBEP)	
Br-OPE	
Tris (2.3-dibromopropyl) phosphate	

1.4. OBJECTIVES AND THESIS STRUCTURE

1.4.1. OBJECTIVES

Given the complex issues surrounding chemical pollution in the oceans, particularly in the high seas and Southern Ocean, the overarching objective of this thesis was to study the occurrence, transport and biogeochemical controls on dissolved hydrocarbons, black carbon, organophosphate esters, and perfluoroalkyl substances in the Atlantic and Southern Oceans.

In order to accomplish this goal, the following **specific objectives** were defined:

1. To evaluate the previously unquantified contribution of Semivolatile Aromatic-Like Compounds (SALCs) and Polycyclic Aromatic Hydrocarbons (PAHs) to the pool and cycle of Dissolved Black Carbon (DBC) in the oceans.
2. To elucidate the transport, sinks, sources and processes affecting PFAS occurrence in the Atlantic and Southern oceans, and provide a mechanistic explanation for PFAS occurrence in the Bransfield Strait and Bellinghausen Sea.
3. To assess the biogeochemical controls affecting the latitudinal and depth distribution of OPEs in the oceans. This objective was divided into two sections:
    - To identify the enrichment of OPEs at the surface microlayer (SML) in comparison to the subsurface layer (SSL) in the Atlantic and Southern Oceans, and explore the potential role of sea spray aerosol in OPE's cycling.
    - To study the vertical and latitudinal transport and biogeochemistry of OPEs in the Atlantic and Southern Oceans.

1.4.2. THESIS STRUCTURE

To address the proposed objectives and provide valuable insights, this thesis is structured into four parts **(Figure 1.11)**. The first, **Part 01. Introduction**, establishes the context of the research and outlines the main objectives and the thesis structure. Next, **Part 02. Methodological Approach**, provides an overview of the field and analytical methods used in this study.

The core of the thesis is presented in **Part 03. Main Chapters**, which comprises the main work divided into four chapters: **Chapters 1, 2, 3, and 4**.

Each chapter includes the corresponding publication(s) and their supplementary materials.

Chapter 1 entitled **"Occurrence of aromatic-like compounds in the global ocean"** highlights the contribution of Dissolved Black Carbon (DBC) to the total Polycyclic Aromatic Hydrocarbon (PAH) pool. It includes **one published article** in Environmental Science & Technology Letters (ACS) entitled "Dissolved Black Carbon and Semivolatile Aromatic Hydrocarbons in the Ocean: Two Entangled Biogeochemical Cycles?", that investigates how DBC, a significant fraction of dissolved organic matter, influences the transport and fate of PAHs in the global ocean, contributing to their persistence and biogeochemical cycling.

Chapter 2 entitled **"Transport and biogeochemistry of PFAAs in the oceans"** examines the transport and the latitudinal and vertical distribution of Perfluoroalkyl Acids (PFAAs) in the Atlantic and Southern Oceans, based on analyses of seawater samples collected during two oceanographic campaigns. This chapter provides novel insights into the long-range transport mechanisms of PFAAs, and their distribution patterns across the two oceans. Specifically, it suggests a mechanism for PFAAs transport to Antarctica. It includes **one article** entitled "Accumulation of Perfluoroalkyl Acids 'Forever Chemicals' in Antarctic Waters," which was submitted to Science Advances in January 2025.

Chapter 3 entitled **"Transport and biogeochemistry of OPEs in the oceans"** focuses on the transport and biogeochemistry of Organophosphate Esters (OPEs) across the Atlantic and Southern Oceans, also based on analyses of seawater samples collected during two oceanographic campaigns. This chapter emphasizes their environmental distribution and biogeochemical processes. This chapter is structured into two separate publications:

- **Chapter 3.1** explores the enrichment potential of OPEs in the **sea surface microlayer (SML)**, including the potential role of the SML mediating the transfer of OPEs to sea spray aerosols. It includes **one published article** in Environmental Science & Technology Letters (ACS), entitled "Enrichment of Organophosphate Esters in the Surface Microlayer from the Atlantic and Southern Oceans."
- **Chapter 3.2** describes the processes influencing the **vertical and latitudinal distribution of OPEs**, examining their occurrence in deep and surface waters and the factors governing their transport. It includes **one article** entitled "Biogeochemical Controls on Latitudinal (42°N to 70°S) and Depth Distribution of Organophosphate Esters in the Atlantic and Southern Oceans" submitted to Environmental Science & Technology (ACS) in December 2024.

Chapter 4 entitled **"Scientific outreach within academy"** explores the challenge of balancing outreach activities within academia. While not directly related to the scientific core of the thesis, this chapter has been included due to the significant efforts made to disseminate the thesis findings to the general public. It highlights the importance of science communication as an integral part of research, reflecting on the strategies used to engage diverse audiences and maximize the societal impact of scientific discoveries. Furthermore, this chapter serves as a guide for researchers seeking to improve their outreach efforts, offering insights into effective communication practices that bridge the gap between academia and society. It includes **one article** entitled "Balancing the Equation: A tool for evaluating effective scientific outreach.

The final section of the thesis, **Part 04. General Discussion and Conclusions**, adds additional discussion on the contributions of this work, synthesizing and complementing the knowledge gained from the publications and research conducted during this PhD.

Specific references used in each chapter and part of the thesis are presented at the end of each respective section.

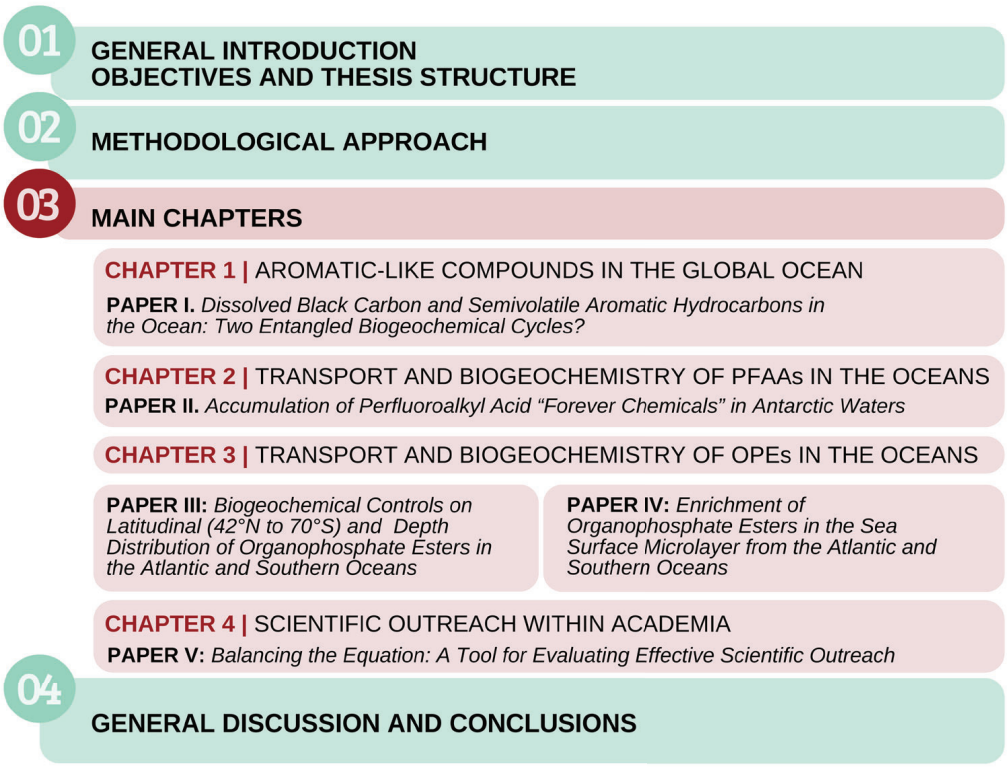


Figure 1.11 | Thesis structure.

REFERENCES

- A -

Agency for Toxic Substances and Disease Registry (ATSDR). (1995). Toxicological Profile for Polycyclic Aromatic Hydrocarbons (PAHs). U.S. Department of Health and Human Services, Public Health Service.

Altshul, L., Covaci, A., & Hauser, R. (2004). The relationship between levels of PCBs and pesticides in human hair and blood: Preliminary results. Environmental Health Perspectives, 112(11), 1193–1199.

Ahrens, L., Xie, Z., & Ebinghaus, R. (2010). Distribution of perfluoroalkyl compounds in seawater from Northern Europe, Atlantic Ocean, and Southern Ocean. Chemosphere, 78(8), 1011–1016.

AMAP. (2016). AMAP Assessment 2016: Chemicals of Emerging Arctic Concern. Arctic Monitoring and Assessment Programme, Oslo, Norway.

Andresen, J. A., Grundmann, A., & Bester, K. (2004). Organophosphorus flame retardants and plasticizers in surface waters. Science of the Total Environment, 332 (1–3), 155–166.

Aznar-Alemany, Ò., Sala, B., Plön, S., Bouwman, H., Barceló, D., & Eljarrat, E. (2019). Halogenated and organophosphorus flame retardants in cetaceans from the southwestern Indian Ocean. Chemosphere, 226, 791–799.

- B -

Bao, H., Niggemann, J., Luo, L., Dittmar, T., & Kao, S. J. (2017). Aerosols as a source of dissolved black carbon to the ocean. Nature Communications, 8(1).

Bengtson Nash, S. (2011). Persistent organic pollutants in Antarctica: Current and future research priorities. In Journal of Environmental Monitoring, 13, 3, 497–504.

Bengtson Nash, S. M., Wild, S. J., Hawker, D. W., Cropp, R. A., Hung, H., Wania, F., Xiao, H., Bohlin-Nizzetto, P., Bignert, A., & Broomhall, S. (2017). Persistent organic pollutants in the east antarctic atmosphere: Inter-annual observations from 2010 to 2015 using high-flow-through passive sampling. Environmental Science and Technology, 51(23), 13929–13937.

Berhanu, A., Mutanda, I., Taolin, J., Qaria, M. A., Yang, B., & Zhu, D. (2023). A review of microbial degradation of per- and polyfluoroalkyl substances (PFAS): Biotransformation routes and enzymes. In Science of the Total Environment (Vol. 859). Elsevier B.V.

Bekele, T. G., Zhao, H., & Wang, Q. (2021). Tissue distribution and bioaccumulation of organophosphate esters in wild marine fish from Laizhou Bay, North China: Implications of human exposure via fish consumption. Journal of Hazardous Materials, 401, 123410.

Benskin, J. P., Muir, D. C. G., Scott, B. F., Spencer, C., de Silva, A. O., Kylin, H., Martin, J. W., Morris, A., Lohmann, R., Tomy, G., Rosenberg, B., Taniyasu, S., & Yamashita, N. (2012). Perfluoroalkyl acids in the atlantic and Canadian arctic oceans. Environmental Science and Technology, 46(11), 5815–5823.

Berrojalbiz, N., Lacorte, S., Calbet, A., Saiz, E., Barata, C., & Dachs, J. (2009). Accumulation and cycling of polycyclic aromatic hydrocarbons in zooplankton. Environmental Science and Technology, 43(7), 2295–2301.

Berrojalbiz, N., Dachs, J., Ojeda, M. J., Valle, M. C., Castro-Jiménez, J., Wollgast, J., Ghiani, M., Hanke, G., & Zaldivar, J. M. (2011). Biogeochemical and physical controls on concentrations of polycyclic aromatic hydrocarbons in water and plankton of the Mediterranean and Black Seas. Global Biogeochemical Cycles, 25(4).

Berrojalbiz, N., Dachs, J., del Vento, S., Ojeda, M. J., Valle, M. C., Castro-Jiménez, J., Mariani, G., Wollgast, J., & Hanke, G. (2011b). Persistent organic pollutants in mediterranean seawater and processes affecting their accumulation in plankton. Environmental Science and Technology, 45(10), 4315–4322.

Boyd, P. W., Watson, A. J., Law, C. S., Abraham, E. R., Trull, T., Murdoch, R., Bakker, D. C. E., Bowie, A. R., Buesseler, K. O., Chang, H., Charette, M., Croot, P., Downing, K., Frew, R., Gall, M., Hadfield, M., Hall,

J., Harvey, M., Jameson, G., … Zeldis, J. (2000). A mesoscale phytoplankton bloom in the polar Southern Ocean stimulated by iron fertilization. Nature, 407.

Bollmann, U. E., Möller, A., Xie, Z., Ebinghaus, R., & Einax, J. W. (2012). Occurrence and fate of organophosphorus flame retardants and plasticizers in coastal and marine surface waters. Water Research, 46(2), 531–538.

Bonnet, R., Swingedouw, D., Gastineau, G., Boucher, O., Deshayes, J., Hourdin, F., Mignot, J., Servonnat, J., & Sima, A. (2021). Increased risk of near term global warming due to a recent AMOC weakening. Nature Communications, 12(1).

Bosch, C.; Andersson, A.; Krusa, M.; Bandh, C.; Hovorkova, I.; Klanova, J.; Knowles, T.D.J., Pancost, R.D., Evershed, R.P., & Gustafsson, Ö. (2015). Source apportionment of polycyclic aromatic hydrocarbons in central European soils with compound-specific triple isotopes (δ13C, Δ14C, δ2H). Environ. Sci. Technol. 49, 7657–7665.

Boot, A. A., Steenbeek, J., Coll, M., von der Heydt, A. S., & Dijkstra, H. A. (2025). Global Marine Ecosystem Response to a Strong AMOC Weakening Under Low and High Future Emission Scenarios. Earth's Future, 13(1).

Breivik, K., Alcock, R., Li, Y. F., Bailey, R. E., Fiedler, H., & Pacyna, J. M. (2004). Primary sources of selected POPs: Regional and global scale emission inventories. Environmental Pollution, 128(1–2), 3–16.

Brommer, S., Harrad, S., van den Eede, N., & Covaci, A. (2012). Concentrations of organophosphate esters and brominated flame retardants in German indoor dust samples. Journal of Environmental Monitoring, 14(9), 2482–2487.

- C -

Cabrerizo, A., Dachs, J., Barceló, D., & Jones, K. C. (2012). Influence of organic matter content and human activities on the occurrence of organic pollutants in antarctic soils, lichens, grass, and mosses. Environmental Science and Technology, 46(3), 1396–1405.

Cabrerizo, A., Galbán-Malagõn, C., del Vento, S., & Dachs, J. (2014). Sources and fate of polycyclic aromatic hydrocarbons in the Antarctic and Southern Ocean atmosphere. Global Biogeochemical Cycles, 28(12), 1424–1436.

Calace, N., Catrambone, T., Petronio, B. M., & Pietroletti, M. (2007). Fulvic acid in microlayer waters of the Gerlache Inlet Sea (Antarctica): Their distribution in dissolved and particulate phases. Water Research, 41(1), 152–158.

Calvin, K., Dasgupta, D., Krinner, G., Mukherji, A., Thorne, P. W., Trisos, C., Romero, J., Aldunce, P., Barrett, K., Blanco, G., Cheung, W. W. L., Connors, S., Denton, F., Diongue-Niang, A., Dodman, D., Garschagen, M., Geden, O., Hayward, B., Jones, C., … Ha, M. (2023). IPCC, 2023: Climate Change 2023: Synthesis Report. Contribution of Working Groups I, II and III to the Sixth Assessment Report of the Intergovernmental Panel on Climate Change [Core Writing Team, H. Lee and J. Romero (eds.)]. IPCC, Geneva, Switzerland. (P. Arias, M. Bustamante, I. Elgizouli, G. Flato, M. Howden, C. Méndez-Vallejo, J. J. Pereira, R. Pichs-Madruga, S. K. Rose, Y. Saheb, R. Sánchez Rodríguez, D. Ürge-Vorsatz, C. Xiao, N. Yassaa, J. Romero, J. Kim, E. F. Haites, Y. Jung, R. Stavins, … C. Péan, Eds.).

Carrizo, D., Sobek, A., Salvadó, J. A., & Gustafsson, Ö. (2017). Spatial Distributions of DDTs in the Water Masses of the Arctic Ocean. Environmental Science and Technology, 51(14)

Carson, R. Silent Spring; Houghton Mifflin: Boston, 1962.

Carsson, H., Nilsson, U., Becker, G., & Östman, C (1997). Organophosphate Ester Flame Retardants and Plasticizers in the Indoor Environment: Analytical Methodology and Occurrence. 7913–7919.

Casal, P., Cabrerizo, A., Vila-Costa, M., Pizarro, M., Jiménez, B., & Dachs, J. (2018). Pivotal Role of Snow Deposition and Melting Driving Fluxes of Polycyclic Aromatic Hydrocarbons at Coastal Livingston Island (Antarctica). Environmental Science and Technology, 52(21), 12327–12337.

Casal, P., Casas, G., Vila-Costa, M., Cabrerizo, A., Pizarro, M., Jiménez, B., & Dachs, J. (2019). Snow amplification of persistent organic pollutants at coastal antarctica. Environmental Science and Technology, 53(15), 8872–8882.

Casas, G., Martínez-Varela, A., Roscales, J. L., Vila-Costa, M., Dachs, J., & Jiménez, B. (2020). Enrichment of perfluoroalkyl substances in the sea-surface microlayer and sea-spray aerosols in the Southern Ocean. Environmental Pollution, 267, 1–30.

Casas, G., Martinez-Varela, A., Vila-Costa, M., Jiménez, B., & Dachs, J. (2021). Rain Amplification of Persistent Organic Pollutants. Environmental Science and Technology, 55(19), 12961–12972.

Casas, G., Iriarte, J., D'Agostino, L. A., Roscales, J. L., Martinez-Varela, A., Vila-Costa, M., Martin, J. W., Jiménez, B., & Dachs, J. (2023). Inputs, amplification and sinks of perfluoroalkyl substances at coastal Antarctica. Environmental Pollution, 338, 122608.

Castro, Ó., Pocurull, E., & Borrull, F. (2020). Determination of organophosphate ester flame retardants and plasticisers in fish samples by QuEChERs followed by gas chromatography-tandem mass spectrometry. Exposure and risk assessment through fish consumption. Journal of Chromatography A, 1626.

Castro-Jiménez, J., González-Gaya, B., Pizarro, M., Casal, P., Pizarro-Álvarez, C., & Dachs, J. (2016). Organophosphate ester flame retardants and plasticizers in the global oceanic atmosphere. Environmental Science and Technology, 50(23), 12831–12839.

Cerro-Gálvez, E., Roscales, J. L., Jiménez, B., Sala, M. M., Dachs, J., & Vila-Costa, M. (2019). Microbial responses to perfluoroalkyl substances and perfluorooctanesulfonate (PFOS) desulfurization in the Antarctic marine environment. Water Research, 171, 115434.

Chen, D., Hale, R. C., la Guardia, M. J., Luellen, D., Kim, S., & Geisz, H. N. (2015). Hexabromocyclododecane flame retardant in Antarctica: Research stations as sources. Environmental Pollution, 206, 611–618.

ChemSec. (2023). ChemSec identifies the top 12 PFAS producers in the world and reveals shocking societal costs. [Consulted on Nov 4th 2024]. Retrieved from https://chemsec.org/chemsec-identifies-the-top-12-pfas-producers-in-the-world-and-reveals-shocking-societal-costs/

Cheng, W., Xie, Z., Blais, J. M., Zhang, P., Li, M., Yang, C., Huang, W., Ding, R., & Sun, L. (2013). Organophosphorus esters in the oceans and possible relation with ocean gyres. Environmental Pollution, 180, 159–164.

Cincinelli, A., Stortini, A. M., Perugini, M., Checchini, L., & Lepri, L. (2001). Organic pollutants in sea-surface microlayer and aerosol in the coastal environment of Leghorn - (Tyrrhenian Sea). Marine Chemistry, 76(1–2), 77–98.

Cincinelli, A., Stortini, A. M., Checchini, L., Martellini, T., del Bubba, M., & Lepri, L. (2005). Enrichment of organic pollutants in the sea surface microlayer (SML) at Terra Nova Bay, Antarctica: Influence of SML on superficial snow composition. Journal of Environmental Monitoring, 7(12), 1305–1312.

Clark, G. (2010). Industrial Revolution. In: Durlauf, S.N., Blume, L.E. (eds.) Economic Growth. The New Palgrave Economics Collection. Palgrave Macmillan, London.

Crutzen, P. J. & Stoermer, E. F. IGBP Newsletter 41. Royal Swedish Academy of Sciences, Stockholm, 2000.

Coppola, A. I., Walker, B. D., & Druffel, E. R. M. (2015). Solid phase extraction method for the study of black carbon cycling in dissolved organic carbon using radiocarbon. Marine Chemistry, 177, 697–705.

Coppola, A. I., & Druffel, E. R. M. (2016). Cycling of black carbon in the ocean. Geophysical Research Letters, 43(9), 4477–4482.

Coppola, A. I., Druffel, E. R. M., Broek, T. A., Haghipour, N., Eglinton, T. I., McCarthy, M., & Walker, B. D. (2024). Variable aging and storage of dissolved black carbon in the ocean. Proceedings of the National Academy of Sciences of the United States of America, 121(13).

Corsolini, S., & Ademollo, N. (2022). POPs in Antarctic ecosystems: is climate change affecting their temporal trends? In Environmental Science: Processes and Impacts, 24, 10, 1631–1642)

Cory, R. M.; Ward, C.P., Crump, B.C., & Kling, G.W. (2014). Sunlight controls water column processing of carbon in arctic fresh waters. Science, 345, 925-928.

Cousins, I. T., Dewitt, J. C., Glüge, J., Goldenman, G., Herzke, D., Lohmann, R., Ng, C. A., Scheringer, M., & Wang, Z. (2020). The high persistence of PFAS is sufficient for their management as a chemical class. In Environmental Science: Processes and Impacts, 22, 12, 2307–2312..

Cousins, I. T., Johansson, J. H., Salter, M. E., Sha, B. & Scheringer, M. (2022). Outside the Safe Operating Space of a New Planetary Boundary for Per- and Polyfluoroalkyl Substances (PFAS). Environmental Science And Technology, 56 11172–11179.

Cristale, J., Dantas, R. F., de Luca, A., Sans, C., Esplugas, S., & Lacorte, S. (2017). Role of oxygen and DOM in sunlight induced photodegradation of organophosphorous flame retardants in river water. Journal of Hazardous Materials, 323, 242–249.

Crutzen, P. J. (2002) Geology of mankind. Nature, 415, 23.

Crutzen, P. J. (2006) The 'Anthropocene'. In: Ehlers, E. & Kraftt, T. Earth System Science in the Anthropocene: Emerging Issues and Problems. Berlin: Springer, 13–18.

Cui, J., Yu, Z., Mi, M., He, L., Sha, Z., Yao, P., Fang, J., & Sun, W. (2020). Occurrence of Halogenated Organic Pollutants in Hadal Trenches of the Western Pacific Ocean. Environmental Science and Technology, 54(24), 15821–15828.

- D -

Dachs, J., Bayona, J. M., Fowler, S. W., Miquel, J.-C., & Albaig6s, J. (1996). Vertical fluxes of polycyclic aromatic hydrocarbons and organochlorine compounds in the western Alboran Sea. In Marine Chemistry, 52.

Dachs, J.; Bayona, J.M., Raoux, C., Albaigés, J. (1997). Spatial, Vertical Distribution and Budget of Polycyclic Aromatic Hydrocarbons in the Western Mediterranean Seawater. Environmental Science And Technology, 31, 682-688.

Dachs, J. and Eisenreich, S.J. (2000). Adsorption onto Aerosol Soot Carbon Dominates Gas-Particle Partitioning of Polycyclic Aromatic Hydrocarbons. Environmental Science And Technology, 34, 3690-3697.

Dachs, J., Glenn Iv, T. R., Gigliotti, C. L., Brunciak, P., Totten, L. A., Nelson, E. D., Franz, T. P., & Eisenreich, S. J. (2002). Processes driving the short-term variability of polycyclic aromatic hydrocarbons in the Baltimore and northern Chesapeake Bay atmosphere, USA. In Atmospheric Environment, 36.

Dachs, J., Lohmann, R., Ockenden W. A., Méjanelle, L., Eisenreich S. J., Jones, K. C. (2002b). Oceanic Biogeochemical Controls on Global Dynamics of Persistent Organic Pollutants. Environmental Science And Technology, 36, 4229-4237.

Dachs, J., Ribes, S., van Drooge, B., Grimalt, J., Eisenreich, S. J., & Gustafsson, Ø. (2004). Response to the comment on "influence of soot carbon on the soil-air partitioning of polycyclic aromatic hydrocarbons." In Environmental Science and Technology, 38, 5, 1624–1625.

Dachs, J., & Méjanelle, L. (2010). Organic pollutants in coastal waters, sediments, and biota: A relevant driver for ecosystems during the anthropocene? Estuaries and Coasts, 33(1), 1–14.

Daughton, C.G. (2005). "Emerging" Chemicals as Pollutants in the Environment: a 21st Century Perspective. Renewable Resources Journey, Winter 2005, 6 - 23.

del Vento, S., & Dachs, J. (2007). Atmospheric occurrence and deposition of polycyclic aromatic hydrocarbons in the northeast tropical and subtropical Atlantic Ocean. Environmental Science and Technology, 41(16), 5608–5613.

Diamond, M. L., Sigmund, G., Bertram, M. G., Ford, A. T., Ågerstrand, M., Carlini, G., Lohmann, R., Šebková, K., Soehl, A., Starling, M. C. V. M., Suzuki, N., Venier, M., Vlahos, P., & Scheringer, M. (2024). Exploring Outputs of the Intergovernmental Science-Policy Panel on Chemicals, Waste, and Pollution Prevention. Environmental Science And Technology Letters, 11, 7664–672).

Ding, Y. S., Ashley, D. L., & Watson, C. H. (2007). Determination of 10 carcinogenic polycyclic aromatic hydrocarbons in mainstream cigarette smoke. Journal of Agricultural and Food Chemistry, 55(15), 5966–5973.

Ding, Y. (2013). Environmental Dynamics of Dissolved Black Carbon in Aquatic Ecosystems. FIU Electronic Theses and Dissertations. 846.

Ding, Y., Han, M., Wu, Z., Zhang, R., Li, A., Yu, K., Wang, Y., Huang, W., Zheng, X., & Mai, B. (2020). Bioaccumulation and trophic transfer of organophosphate esters in tropical marine food web, South China Sea. Environment International, 143.

Dishaw, L. v., Hunter, D. L., Padnos, B., Padilla, S., & Stapleton, H. M. (2014). Developmental exposure to organophosphate flame retardants elicits overt toxicity and alters behavior in early life stage zebrafish (danio rerio). Toxicological Sciences, 142(2), 445–454.

Ditlevsen, P., & Ditlevsen, S. (2023). Warning of a forthcoming collapse of the Atlantic meridional overturning circulation. Nature Communications, 14(1).

Dittmar, T., Koch, B., Hertkorn, N., & Kattner, G. (2008a). A simple and efficient method for the solid-phase extraction of dissolved organic matter (SPE-DOM) from seawater. Limnology and Oceanography: Methods, 6(6), 230–235.

Dittmar, T. (2008b). The molecular level determination of black carbon in marine dissolved organic matter. Organic Geochemistry, 39(4), 396–407.

Dittmar, T., & Paeng, J. (2009). A heat-induced molecular signature in marine dissolved organic matter. Nature Geoscience, 2(3), 175–179.

Dittmar, T.; Paeng, J.; Gihring, T. M.; Suryaputra, I. G. N. A., & Huettel, M. (2012). Discharge of Dissolved Black Carbon from a Fire-Affected Intertidal System. Limnology Oceanografy, 57 (4), 1171–1181.

Dittmar, T.; De Rezende, C. E.; Manecki, M.; Niggemann, J.; Coelho Ovalle, A. R.; Stubbins, A., & Bernardes, M. C. (2012b). Continuous Flux of Dissolved Black Carbon from a Vanished Tropical Forest Biome. Nature Geosciences, 5 (9), 618–622.

Doney, S. C., Fabry, V. J., Feely, R. A., & Kleypas, J. A. (2009). Ocean acidification: The other CO_2 problem. Annual Review of Marine Science, 1, 169–192.

- E -

Engel, A., Bange, H. W., Cunliffe, M., Burrows, S. M., Friedrichs, G., Galgani, L., Herrmann, H., Hertkorn, N., Johnson, M., Liss, P. S., Quinn, P. K., Schartau, M., Soloviev, A., Stolle, C., Upstill-Goddard, R. C., van Pinxteren, M., & Zäncker, B. (2017). The ocean's vital skin: Toward an integrated understanding of the sea surface microlayer. Frontiers in Marine Science, 4, 1–14.

Evich, M. G., Davis, M. J. B., McCord, J. P., Acrey, B., Awkerman, J. A., Knappe, D. R. U., Lindstrom, A. B., Speth, T. F., Tebes-Stevens, C., Strynar, M. J., Wang, Z., Weber, E. J., Henderson, W. M., & Washington, J. W. (2022). Per- and polyfluoroalkyl substances in the environment. Science, 375 (6580).

- F -

Fauvelle, V., Garel, M., Tamburini, C., Nerini, D., Castro-Jiménez, J., Schmidt, N., Paluselli, A., Fahs, A., Papillon, L., Booth, A. M., & Sempéré, R. (2021). Organic additive release from plastic to seawater is lower under deep-sea conditions. Nature Communications, 12(1).

Fängström, B., Strid, A., Grandjean, P., Weihe, P., & Bergman, Å. (2005). A retrospective study of PBDEs and PCBs in human milk from the Faroe Islands. Environmental Health: A Global Access Science Source, 4.

Fenner, K., & Scheringer, M. (2021). The Need for Chemical Simplification As a Logical Consequence of Ever-Increasing Chemical Pollution. In Environmental Science and Technology, 55, 21, 14470–14472.

FireSafetyInfo, 2006. Flame retardants – mode of action. FireSafetyInfo, accessed May 25, 2006.

Frederiksen, M., Vorkamp, K., Thomsen, M., & Knudsen, L. E. (2009). Human internal and external exposure to PBDEs - A review of levels and sources. In International Journal of Hygiene and Environmental Health, 212, 2, 109–134.

Fries, E., & Püttmann, W. (2001). Occurrence of organophosphate esters in surface water and ground water in Germany. Journal of Environmental Monitoring, 3(6), 621–626.

Frölicher, T. L., Sarmiento, J. L., Paynter, D. J., Dunne, J. P., Krasting, J. P., & Winton, M. (2015). Dominance of the Southern Ocean in anthropogenic carbon and heat uptake in CMIP5 models. Journal of Climate, 28(2), 862–886.

Frömel, T., & Knepper, T.P. (2019). Biodegradation of fluorinated alkyl substances. Review of Environmental Contamination and Toxicology Vol. 208, 161-177.

Fuoco, R., Giannarelli, S., Wei, Y., Abete, C., Francesconi, S., & Termine, M. (2005). Polychlorobiphenyls and polycyclic aromatic hydrocarbons in the sea-surface micro-layer and the water column at Gerlache Inlet, Antarctica. Journal of Environmental Monitoring, 7(12), 1313–1319.

- G -

Gaines, L. G. T. (2023). Historical and current usage of per- and polyfluoroalkyl substances (PFAS): A literature review. American Journal of Industrial Medicine, 66, 5, 353–378.

Galbán-Malagón, C., Berrojalbiz, N., Ojeda, M. J., & Dachs, J. (2012). The oceanic biological pump modulates the atmospheric transport of persistent organic pollutants to the Arctic. Nature Communications, 3.

Galbán-Malagón, C. J., Berrojalbiz, N., Gioia, R., & Dachs, J. (2013a). The "degradative" and "biological" pumps controls on the atmospheric deposition and sequestration of hexachlorocyclohexanes and hexachlorobenzene in the North Atlantic and Arctic Oceans. Environmental Science and Technology, 47(13), 7195–7203.

Galbán-Malagón, C., Cabrerizo, A., Caballero, G., & Dachs, J. (2013b). Atmospheric occurrence and deposition of hexachlorobenzene and hexachlorocyclohexanes in the Southern Ocean and Antarctic Peninsula. Atmospheric Environment, 80, 41–49.

Galbán-Malagón, C. J., del Vento, S., Cabrerizo, A., & Dachs, J. (2013c). Factors affecting the atmospheric occurrence and deposition of polychlorinated biphenyls in the Southern Ocean. Atmospheric Chemistry and Physics, 13(23), 12029–12041.

Galbán-Malagón, C., Gómez-Aburto, V. A., Hirmas-Olivares, A., Luarte, T., Berrojalbiz, N., & Dachs, J. (2023). Dichlorodiphenyltrichloroethane (DDT) and Dichlorodiphenyldichloroethylene (DDE) levels in air and surface sea waters along the Antarctic Peninsula. Marine Pollution Bulletin, 197.

García-Flor, N., Dachs, J., Bayona, J. M., & Albaigés, J. (2009). Surface waters are a source of polychlorinated biphenyls to the coastal atmosphere of the North-Western Mediterranean Sea. Chemosphere, 75(9), 1144–1152.

Garcia-Garin, O., Sala, B., Aguilar, A., Vighi, M., Víkingsson, G. A., Chosson, V., Eljarrat, E., & Borrell, A. (2020). Organophosphate contaminants in North Atlantic fin whales. Science of the Total Environment, 721.

Gao, X., Huang, P., Huang, Q., Rao, K., Lu, Z., Xu, Y., Gabrielsen, G. W., Hallanger, I., Ma, M., & Wang, Z. (2019). Organophosphorus flame retardants and persistent, bioaccumulative, and toxic contaminants in Arctic seawaters: On-board passive sampling coupled with target and non-target analysis. Environmental Pollution, 253, 1–10.

Gao, X., Xu, Y., Ma, M., Huang, Q., Gabrielsen, G. W., Hallanger, I., Rao, K., Lu, Z., & Wang, Z. (2020). Distribution, sources and transport of organophosphorus flame retardants in the water and sediment of Ny-Ålesund, Svalbard, the Arctic. Environmental Pollution, 264.

Ge, J., Liu, M., Yun, X., Yang, Y., Zhang, M., Li, Q. X., & Wang, J. (2014). Occurrence, distribution and seasonal variations of polychlorinated biphenyls and polybrominated diphenyl ethers in surface waters of the East Lake, China. Chemosphere, 103, 256–262.

Ge, M., Wang, X., Yang, G., Wang, Z., Li, Z., Zhang, X., & Xu, Q. (2021). Persistent organic pollutants (POPs) in deep-sea sediments of the tropical western Pacific Ocean. Chemosphere, 277.

Geisz, H. N., Dickhut, R. M., Cochran, M. A., Fraser, W. R., & Ducklow, H. W. (2008). Melting glaciers: A probable source of DDT to the Antarctic marine ecosystem. Environmental Science and Technology, 42(11), 3958–3962.

Gigliotti, C. L., Dachs, J., Nelson, E. D., Brunciak, P. A., & Eisenreich, S. J. (2000). Polycyclic aromatic hydrocarbons in the New Jersey coastal atmosphere. Environmental Science and Technology, 34(17), 3547–3554.

Gioia, R., Nizzetto, L., Lohmann, R., Dachs, J., Temme, C., & Jones, K. C. (2007). Polychlorinated biphenyls (PCBs) in air and seawater of the Atlantic Ocean: Sources, trends and processes. Environmental Science and Technology, 42(5), 1416–1422.

Gioia, R., Dachs, J., Nizzeto, L, Berrojalbiz, N., Galbán-Malacón, C., Del Vento, S., Méjanelle, L., Jones, C. K. (2011). Sources, Transport and Fate of Organic Pollutants in the Oceanic Environment, in book Persistent Pollution – Past, Present and Future. School of Environmnetal Research – Organized by Helmholtz-Zentrum Geesthacht. Ed. Springer. 111-141.

Glüge, J., Scheringer, M., Cousins, I. T., Dewitt, J. C., Goldenman, G., Herzke, D., Lohmann, R., Ng, C. A., Trier, X., & Wang, Z. (2020). An overview of the uses of per- And polyfluoroalkyl substances (PFAS). Environmental Science: Processes and Impacts, 22(12), 2345–2373.

Gómez, Ó., Ramírez, N., Vallecillos, L., & Borrull, F. (2024). Determining personal exposure to high production volume chemicals (HPVCs) and polycyclic aromatic hydrocarbons (PAHs) with silicone wristbands: A pilot study. Environmental Research, 263.

González-Gaya, B., Dachs, J., Roscales, J. L., Caballero, G., & Jiménez, B. (2014). Perfluoroalkylated substances in the global tropical and subtropical surface oceans. Environmental Science and Technology, 48(22), 13076–13084.

González-Gaya, B., Fernández-Pinos, M. C., Morales, L., Méjanelle, L., Abad, E., Piña, B., Duarte, C. M., Jiménez, B., & Dachs, J. (2016). High atmosphere-ocean exchange of semivolatile aromatic hydrocarbons. Nature Geoscience, 9(6), 438–442.

González-Gaya, B., Martínez-Varela, A., Vila-Costa, M., Casal, P., Cerro-Gálvez, E., Berrojalbiz, N., Lundin, D., Vidal, M., Mompeán, C., Bode, A., Jiménez, B., & Dachs, J. (2019a). Biodegradation as an important sink of aromatic hydrocarbons in the oceans. Nature Geoscience, 12(2), 119–125.

González-Gaya, B., Casal, P., Jurado, E., Dachs, J., & Jiménez, B. (2019b). Vertical transport and sinks of perfluoroalkyl substances in the global open ocean. Environmental Science: Processes and Impacts, 21(11), 1957–1969.

Gravel, S., Lavoué, J., Bakhiyi, B., Diamond, M. L., Jantunen, L. M., Lavoie, J., Roberge, B., Verner, M. A., Zayed, J., & Labrèche, F. (2019). Halogenated flame retardants and organophosphate esters in the air of electronic waste recycling facilities: Evidence of high concentrations and multiple exposures. Environment International, 128, 244–253.

Greaves, A. K., Letcher, R. J., Chen, D., McGoldrick, D. J., Gauthier, L. T., & Backus, S. M. (2016). Retrospective analysis of organophosphate flame retardants in herring gull eggs and relation to the aquatic food web in the Laurentian Great Lakes of North America. Environmental Research, 150, 255–263.

Grunfeld, D. A., Gilbert, D., Hou, J., Jones, A. M., Lee, M. J., Kibbey, T. C. G., & Carroll, D. M. O. (2024). Underestimated burden of per- and polyfluoroalkyl substances in global surface waters and groundwaters. Gutt, J., Bertler, N., Bracegirdle, T. J., Buschmann, A., Comiso, J., Hosie, G., Isla, E., Schloss, I. R., Smith, C. R., Tournadre, J., & Xavier, J. C. (2015). The Southern Ocean ecosystem under multiple climate change stresses - an integrated circumpolar assessment. Global Change Biology, 21(4), 1434–1453.

Gutt, J., Bertler, N., Bracegirdle, T. J., Buschmann, A., Comiso, J., Hosie, G., Isla, E., Schloss, I. R., Smith, C. R., Tournadre, J., & Xavier, J. C. (2015). The Southern Ocean ecosystem under multiple climate change stresses - an integrated circumpolar assessment. Global Change Biology, 21(4), 1434–1453.

- H -

Herbert, B. M. J., Halsall, C. J., Villa, S., Jones, K. C., & Kallenborn, R. (2005). Rapid changes in PCB and OC pesticide concentrations in arctic snow. Environmental Science and Technology, 39(9), 2998–3005.

Herbert, B. M. J., Villa, S., & Halsall, C. J. (2006). Chemical interactions with snow: Understanding the behavior and fate of semi-volatile organic compounds in snow. Ecotoxicology and Environmental Safety, 63(1), 3–16.

Hylland, K., et al. (2006). Polycyclic aromatic hydrocarbon (PAH) ecotoxicology in marine ecosystems. Journal of Toxicology and Environmental Health, Part A, 69(1-2), 109-123.

Hung, H., Katsoyiannis, A. A., Brorström-Lundén, E., Olafsdottir, K., Aas, W., Breivik, K., Bohlin-Nizzetto, P., Sigurdsson, A., Hakola, H., Bossi, R., Skov, H., Sverko, E., Barresi, E., Fellin, P., & Wilson, S. (2016). Temporal trends of Persistent Organic Pollutants (POPs) in arctic air: 20 years of monitoring under the Arctic Monitoring and Assessment Programme (AMAP). Environmental Pollution, 217, 52–61.

- I -

Iriarte, J., Dachs, J., Casas, G., Martínez-Varela, A., Berrojalbiz, N., & Vila-Costa, M. (2023). Snow-Dependent Biogeochemical Cycling of Polycyclic Aromatic Hydrocarbons at Coastal Antarctica. Environmental Science and Technology, 57(4), 1625–1636.

Iriarte, J., Trilla-Prieto, N., Berrojalbiz, N., Vila-Costa, M., & Dachs, J. (2025). Bacterial Production Modulates the Persistence of Organophosphate Ester Flame Retardants and Plasticizers in the Ocean. Environmental Science & Technology Letters.

IPCC, 2022: Summary for Policymakers [H.-O. Pörtner, D.C. Roberts, E.S. Poloczanska, K. Mintenbeck, M. Tignor, A. Alegría, M. Craig, S. Langsdorf, S. Löschke, V. Möller, A. Okem (eds.)]. In: Climate Change 2022: Impacts, Adaptation, and Vulnerability. Contribution of Working Group II to the Sixth Assessment Report of the Intergovernmental Panel on Climate Change [H.-O. Pörtner, D.C. Roberts, M. Tignor, E.S. Poloczanska, K. Mintenbeck, A. Alegría, M. Craig, S. Langsdorf, S. Löschke, V. Möller, A. Okem, B. Rama (eds.)]. Cambridge University Press, Cambridge, UK and New York, NY, USA, pp. 3-33.

- J -

Jaffé, R., Ding, Y., Niggemann, J., Vähätalo, A. v., Stubbins, A., Spencer, R. G. M., Campbell, J., & Dittmar, T. (2013). Global charcoal mobilization from soils via dissolution and riverine transport to the oceans. Science, 340(6130), 345–347.

Jantunen, L. M., Wong, F., Gawor, A., Kylin, H., Helm, P. A., Stern, G. A., Strachan, W. M. J., Burniston, D. A., & Bidleman, T. F. (2015). 20 Years of Air-Water Gas Exchange Observations for Pesticides in the Western Arctic Ocean. Environmental Science and Technology, 49(23), 13844–13852.

Jarema, K. A., Hunter, D. L., Shaffer, R. M., Behl, M., & Padilla, S. (2015). Acute and developmental behavioral effects of flame retardants and related chemicals in zebrafish. Neurotoxicology and Teratology, 52, 194–209.

Johansson, J. H., Salter, M. E., Acosta Navarro, J. C., Leck, C., Nilsson, E. D., & Cousins, I. T. (2019). Global transport of perfluoroalkyl acids via sea spray aerosol. Environmental Science: Processes and Impacts, 21(4), 635–649.

Jones, K. C., & de Voogt, P. (1999). Persistent organic pollutants (POPs): state of the science. Environmental Pollution ,100 209±221.

Jurado, E., Jaward, F. M., Lohmann, R., Jones, K. C., Simó, R., & Dachs, J. (2004). Atmospheric dry deposition of persistent organic pollutants to the atlantic and inferences for the global oceans. Environmental Science and Technology, 38 (21), 5505–5513.

Jurado, E., Jaward, F., Lohmann, R., Jones, K. C., Simó, R., & Dachs, J. (2005). Wet deposition of persistent organic pollutants to the global oceans. Environmental Science and Technology, 39(8), 2426–2435.

Jurado, E., Zaldívar, J. M., Marinov, D., & Dachs, J. (2007). Fate of persistent organic pollutants in the water column: Does turbulent mixing matter? Marine Pollution Bulletin, 54(4), 441–451.

Jurado, E., Dachs, J., Duarte, C. M. & Simo, R. (2008a). Atmospheric deposition of organic and black carbon to the global oceans. Atmospheric Environment, 42, 7931–7939

Jurado, E., & Dachs, J. (2008b). Seasonality in the "grasshopping" and atmospheric residence times of persistent organic pollutants over the oceans. Geophysical Research Letters, 35(17).

- K -

Kallenborn, R., Halsall, C., Dellong, M., & Carlsson, P. (2012). The influence of climate change on the global distribution and fate processes of anthropogenic persistent organic pollutants. In Journal of Environmental Monitoring (Vol. 14, Issue 11, pp. 2854–2869).

Keeling, C. D., & Whorf, T. P. (2000). Monthly carbon dioxide measurements on Mauna Loa, Hawaii from 1958 to 1998 [dataset]. PANGAEA

Kim, K. H., Jahan, S. A., Kabir, E., & Brown, R. J. C. (2013). A review of airborne polycyclic aromatic hydrocarbons (PAHs) and their human health effects. In Environment International, 60, 71–80.

Kissa, E. (2001). Fluorinated surfactants and repellents. Surfactant Science series, 97.

Khan, B., Burgess, R. M., & Cantwell, M. G. (2023). Occurrence and Bioaccumulation Patterns of Per- and Polyfluoroalkyl Substances (PFAS) in the Marine Environment. Environmental Science and Technology Water, 3, 5, 1243–1259.

- L -

Lee, R. F., Sauerheber, R. & Dobbs, G. H. (1972). Uptake, metabolism and discharge of polycyclic aromatic hydrocarbons by marine fish. Marine Biology, 17, 201-8.

Li, J., Xie, Z., Mi, W., Lai, S., Tian, C., Emeis, K. C., & Ebinghaus, R. (2017). Organophosphate Esters in Air, Snow, and Seawater in the North Atlantic and the Arctic. Environmental Science and Technology, 51(12), 6887–6896.

Li, Y., Zhao, X., Li, X., Zhang, Y., & Niu, Z. (2024). The investigation of the enrichment behavior of identified PFAS and unknown PFAA-precursors in water and suspended particulate matter of the surface microlayer: A case study in Tianjin (China). Water Research, 260, 121944.

Ligocki, M. P.; Leuenberger, C.; Pankow, J. F. Trace Organic Compounds in Rain-II. Gas Scavenging of Neutral Organic Compounds. Atmospheric Environment, 1985, 19, 1609–1617.

Lindstrom, A. B., Strynar, M. J., & Libelo, E. L. (2011). Polyfluorinated compounds: Past, present, and future. Environmental Science and Technology, 45(19), 7954–7961.

Liss, P. S. & Duce, R. A. (1997) The Sea Surface and Global Change; Cambridge University Press.

Logan, D. T. (2007). Perspective on ecotoxicology of PAHs to fish. Human and Ecological Risk Assessment: An International Journal, 13(2), 302-316.

Lohmann, R., Breivik, K., Dachs, J., & Muir, D. (2007). Global fate of POPs: Current and future research directions. Environmental Pollution, 150(1), 150–165.

Lohmann, R., Gioia, R., Jones, K. C., Nizzetto, L., Temme, C., Xie, Z., Schulz-Bull, D., Hand, I., Morgan, E., & Jantunen, L. (2009). Organochlorine pesticides and PAHs in the surface water and atmosphere of the North Atlantic and Arctic Ocean. Environmental Science and Technology, 43(15), 5633–5639.

Lohmann, R.; Bollinger, K.; Cantwell, M.; Feichter, J.; Fischer-Bruns, I. & Zabel, M. (2009b). Fluxes of soot black carbon to South Atlantic sediments. Global Biogeochemical Cycles, 23, GB1015.

Lohmann, R., Klanova, J., Kukucka, P., Yonis, S., & Bollinger, K. (2013). Concentrations, fluxes, and residence time of PBDEs across the tropical Atlantic Ocean. Environmental Science and Technology, 47(24), 13967–13975.

Lohmann, R., Markham, E., Klanova, J., Kukucka, P., Pribylova, P., Gong, X., Pockalny, R., Yanishevsky, T., Wagner, C. C., & Sunderland, E. M. (2021). Trends of Diverse POPs in Air and Water across the Western Atlantic Ocean: Strong Gradients in the Ocean but Not in the Air. Environmental Science and Technology, 55(14), 9498–9507.

Lohmann, R., Vrana, B., Muir, D., Smedes, F., Sobotka, J., Zeng, E. Y., Bao, L. J., Allan, I. J., Astrahan, P., Barra, R. O., Bidleman, T., Dykyi, E., Estoppey, N., Fillmann, G., Greenwood, N., Helm, P. A., Jantunen, L., Kaserzon, S., Macías, J. V., … Wong, C. S. (2023). Passive-Sampler-Derived PCB and OCP Concentrations in the Waters of the World-First Results from the AQUA-GAPS/MONET Network. Environmental Science and Technology, 57(25), 9342–9352.

Luek, J. L., Dickhut, R. M., Cochran, M. A., Falconer, R. L., & Kylin, H. (2017). Persistent organic pollutants in the Atlantic and southern oceans and oceanic atmosphere. Science of the Total Environment, 583, 64–71.

- M -

Macdonald, R. W., Harner, T., & Fyfe, J. (2005). Recent climate change in the Arctic and its impact on contaminant pathways and interpretation of temporal trend data. Science of the Total Environment, 342, 1–3, 5–86.

Mackay, D., Callcott, D. (1998). Partitioning and Physical Chemical Properties of PAHs. In: Neilson, A.H. (eds) PAHs and Related Compounds. The Handbook of Environmental Chemistry, 3, 3I.

Makinen, M. S. E., Makinen, M. R. A., Koistinen, J. T. B., Pasanen, A. L., Pasanen, P. O., Kalliokoski, P. J., & Korpi, A. M. (2009). Respiratory and dermal exposure to organophosphorus flame retardants and tetrabromobisphenol A at five work environments. Environmental Science and Technology, 43(3), 941–947.

Malm, A., & Hornborg, A. (2014). The geology of mankind? A critique of the anthropocene narrative. Anthropocene Review, 1(1), 62–69.

Mann, M. E., Bradley, R. S., & Hughes, M. K. (1999). Northern hemisphere temperatures during the past millennium: Inferences, uncertainties, and limitations. Geophysical Research Letters, 26(6), 759–762.

Mannino, A., & Harvey, H. R. (2004). Black Carbon in Estuarine and Coastal Ocean Dissolved Organic Matter. Limnology Oceanography, 49 (3), 735–740.

Manodori, L., Gambaro, A., Piazza, R., Ferrari, S., Stortini, A. M., Moret, I., & Capodaglio, G. (2006). PCBs and PAHs in sea-surface microlayer and sub-surface water samples of the Venice Lagoon (Italy). Marine Pollution Bulletin, 52(2), 184–192.

Marklund, A., Andersson, B., & Haglund, P. (2005). Organophosphorus flame retardants and plasticizers in Swedish sewage treatment plants. Environmental Science and Technology, 39(19), 7423–7429.

Martin, J. W., Ellis, D. A., Mabury, S. A., Hurley, M. D., & Wallington, T. J. (2006). Atmospheric chemistry of perfluoroalkanesulfonamides: Kinetic and product studies of the OH radical and Cl atom initiated oxidation of N-ethyl perfluorobutanesulfonamide. Environmental Science and Technology, 40(3), 864–872.

Martinez-Varela, A., Casas, G., Piña, B., Dachs, J., & Vila-Costa, M. (2020). Large Enrichment of Anthropogenic Organic Matter Degrading Bacteria in the Sea-Surface Microlayer at Coastal Livingston Island (Antarctica). Frontiers in Microbiology, 11, 1–13.

McDonough, C. A., de Silva, A. O., Sun, C., Cabrerizo, A., Adelman, D., Soltwedel, T., Bauerfeind, E., Muir, D. C. G., & Lohmann, R. (2018). Dissolved Organophosphate Esters and Polybrominated Diphenyl Ethers in Remote Marine Environments: Arctic Surface Water Distributions and Net Transport through Fram Strait. Environmental Science and Technology, 52(11), 6208–6216.

Menzie, C. A., & Potocki, B. B. (1992). Exposure to Carcinogenic PAHs in the Environment. Environ. Sci. and Techno., 26(7), 1278–1284.

Meyer, J. & Bester, K. (2004) Organophosphate flame retardants and plasticisers in wastewater treatment plants. Journal of Environmental Monitoring, 6, 599–605.

Muir, D. C. G., & Howard, P. H. (2006). Are there other persistent organic pollutants? A challenge for environmental chemists. Environmental Science and Technology, 40, 23, 7157–7166.

Muir, D., & Miaz, L. T. (2021). Spatial and Temporal Trends of Perfluoroalkyl Substances in Global Ocean and Coastal Waters. Environmental Science and Technology, 55(14), 9527–9537.

Muir, D. C. G., Getzinger, G. J., McBride, M., & Ferguson, P. L. (2023). How Many Chemicals in Commerce Have Been Analyzed in Environmental Media? A 50 Year Bibliometric Analysis. In Environmental Science and Technology, 57, 25, 9119–9129.

- N -

Na, G., Hou, C., Li, R., Shi, Y., Gao, H., Jin, S., Gao, Y., Jiao, L., & Cai, Y. (2020). Occurrence, distribution, air-seawater exchange and atmospheric deposition of organophosphate esters (OPEs) from the Northwestern Pacific to the Arctic Ocean. Marine Pollution Bulletin, 157, 111243.

Nakajima, R., Tsuchiya, K., Nakatomi, N., Yoshida, T., Tada, Y., Konno, F., Toda, T., Kuwahara, V. S., Hamasaki, K., Ross Othman, B. H., Segaran, T. C., & Mohd Effendy, A. W. (2013). Enrichment of microbial abundance in the sea-surface microlayer over a coral reef: Implications for biogeochemical cycles in reef ecosystems. Marine Ecology Progress Series, 490, 11–22.

Nash, R. (2013). The Oceans and Their Challenge to Conserve Marine Biodiversity. In book: Living with Water: Targeting Quality in a dynamic world. Edition: 1st. Chapter: 5. Publisher: Springer. Editors: Pechan, P & de Vries, G.

National Toxicology Program. Federal Register. (2005). Report on Carcinogens, Eleventh Edition. U.S. Department of Health and Human Services. February 8, 2005, Vol. 70, No. 25, pp. 6721-6723. Available at: https://www.govinfo.gov/content/pkg/FR-2005-02-08/

pdf/05-2393.pdf

Neira, C., Mendoza, G. F., Bradley, A., Gossett, R., Rouse, G. W., & Levin, L. A. (2024). Waste barrel contamination and macrobenthic communities in the San Pedro Basin DDT dumpsite. Marine Pollution Bulletin, 203.

Noyes, P. D., Haggard, D. E., Gonnerman, G. D., & Tanguay, R. L. (2015). Advanced morphological - behavioral test platform reveals neurodevelopmental defects in embryonic zebrafish exposed to comprehensive suite of halogenated and organophosphate flame retardants. Toxicological Sciences, 145(1), 177–195.

- O -

Orsi, A. H., Whitworth III, T., & Nowlin Jr, W. D. (1994). On the meridional extent and fronts of the Antarctic Circumpolar Current (Vol. 42, Issue 5).

- P -

Paluselli, A., Fauvelle, V., Galgani, F., & Sempéré, R. (2019). Phthalate Release from Plastic Fragments and Degradation in Seawater. Environmental Science and Technology, 53(1), 166–175.

Page, J., Whaley, P., Bellingham, M., Birnbaum, L. S., Cavoski, A., Fetherston Dilke, D., Garside, R., Harrad, S., Kelly, F., Kortenkamp, A., Martin, O., Stec, A., & Woolley, T. (2023). A new consensus on reconciling fire safety with environmental & health impacts of chemical flame retardants. Environment International, 173.

Parkinson, C. L., & Cavalieri, D. J. (2012). Antarctic sea ice variability and trends, 1979-2010. Cryosphere, 6, 4, 871–880.

Parkinson, C. L. (2019). A 40-y record reveals gradual Antarctic sea ice increases followed by decreases at rates far exceeding the rates seen in the Arctic. Proceedings of the National Academy of Sciences of the United States of America, 116(29), 14414–14423.

Pawlak, F., Koziol, K., & Polkowska, Z. (2021). Chemical hazard in glacial melt? The glacial system as a secondary source of POPs (in the Northern Hemisphere). A systematic review. Science of the Total Environment, 778.

Peng, B., Dong, Q., Li, F., Wang, T., Qiu, X., & Zhu, T. (2023). A Systematic Review of Polycyclic Aromatic Hydrocarbon Derivatives: Occurrences, Levels, Biotransformation, Exposure Biomarkers, and Toxicity. In Environmental Science and Technology, 57, 41, 15314–15335.

Persson, L., Carney Almroth, B. M., Collins, C. D., Cornell, S., de Wit, C. A., Diamond, M. L., Fantke, P., Hassellöv, M., MacLeod, M., Ryberg, M. W., Søgaard Jørgensen, P., Villarrubia-Gómez, P., Wang, Z., & Hauschild, M. Z. (2022). Outside the Safe Operating Space of the Planetary Boundary for Novel Entities. Environmental Science and Technology, 56(3), 1510–1521.

Pesant, S. (2015) Open science resources for the discovery and analysis of Tara Oceans data. Scientific Data 2, 150023.

Petit, J. R., Jouzel, J., Raynaud, D., Barkov, N. I., Barnola, J. M., Basile, I., Bender, M., Chappellaz, J., Davis, M., Delaygue, G., Delmotte, M., Kotiyakov, V. M., Legrand, M., Lipenkov, V. Y., Lorius, C., Pépin, L., Ritz, C., Saltzman, E., & Stievenard, M. (1999). Climate and atmospheric history of the past 420,000 years from the Vostok ice core, Antarctica. Nature, 399, 6735, 429–436.

Podder, A., Sadmani, A. H. M. A., Reinhart, D., Chang, N. bin, & Goel, R. (2021). Per and poly-fluoroalkyl substances (PFAS) as a contaminant of emerging concern in surface water: A transboundary review of their occurrences and toxicity effects. In Journal of Hazardous Materials (Vol. 419). Elsevier B.V.

- Q -

Qi, Y., Fu, W., Tian, J., Luo, C., Shan, S., Sun, S., Ren, P., Zhang, H., Liu, J., Zhang, X., & Wang, X. (2020). Dissolved black carbon is not likely a significant refractory organic carbon pool in rivers and oceans. Nature Communications, 11(1).

- R -

Reemtsma, T., García-López, M., Rodríguez, I., Quintana, J. B., & Rodil, R. (2008). Organophosphorus flame retardants and plasticizers in water and air I. Occurrence and fate. TrAC - Trends in Analytical Chemistry, 27(9), 727–737.

Regnery, J. & Püttmann, W. (2010). Occurrence and Fate of Organophosphorus Flame Retardants and Plasticizers in Urban and Remote Surface Waters in Germany. Water Research, 44 (14), 4097–4104.

Richardson, K., Steffen, W., Lucht, W., Bendtsen, J., Cornell, S. E., Donges, J. F., Drüke, M., Fetzer, I., Bala, G., von Bloh, W., Feulner, G., Fiedler, S., Gerten, D., Gleeson, T., Hofmann, M., Huiskamp, W., Kummu, M., Mohan, C., Nogués-Bravo, D., … Rockström, J. (2023). Earth beyond six of nine planetary boundaries. Science Advances, 9, eaddh2459.

Rintoul, S. R., Church, J., Fahrbach, E., Garcia, M., Gordon, A., King, B., Morrow, R., Orsi, A. H., & Speer, K. (2001). Monitoring and Understanding Southern Ocean Variability and its Impact on Climate: A Strategy for Sustained Observations.

Rintoul, S. R. (2011). The Southern Ocean in the Earth System.

Rockström J., Steffen, W., Noone, K., Persson Å., Chapin, S., Lambin, E. F., Lenton, T. M., Scheffer, M., Folke, C., Schellnhuber, J., Nykvist, B., DeWit, C. A., Hughes, T., van der Leeuw, S., Rodhe, H., Sörlin, S., Snyder, P. K., Costanza, P. K., Svedin, U., Falkenmark, M., Karlberg, L., Corell, R. W., Fabry, V. J., Hansen, J., Liverman, D., Richardson, K., Crutzen, P., Foley, J. (2009). A safe operating space for humanity. Nature 461, 472–475.

Rhoads, K. R., Janssen, E. M. L., Luthy, R. G., & Criddle, C. S. (2008). Aerobic biotransformation and fate of N-ethyl perfluorooctane sulfonamidoethanol (N-EtFOSE) in activated sludge. Environmental Science and Technology, 42(8).

Roth, K., Imran, Z., Liu, W., & Petriello, M. C. (2020). Diet as an Exposure Source and Mediator of Per- and Polyfluoroalkyl Substance (PFAS) Toxicity. In Frontiers in Toxicology, 2.

- S -

Sabbaghzadeh, B., Upstill-Goddard, R. C., Beale, R., Pereira, R., & Nightingale, P. D. (2017). The Atlantic Ocean surface microlayer from 50°N to 50°S is ubiquitously enriched in surfactants at wind speeds up to 13 m s−1. Geophysical Research Letters, 44(6), 2852–2858.

Sala, B., Giménez, J., de Stephanis, R., Barceló, D., & Eljarrat, E. (2019). First determination of high levels of organophosphorus flame retardants and plasticizers in dolphins from Southern European waters. Environmental Research, 172, 289–295.

Sarmiento, J. L. & Gruber, N. (2006). Ocean Biogeochemical Dynamics (Princeton University Press).

Sauvé, S., & Desrosiers, M. (2014). A review of what is an emerging contaminant. Chemistry Central Journal, 8.

Savvidou, E. K., Sha, B., Salter, M. E., Cousins, I. T., & Johansson, J. H. (2023). Horizontal and Vertical Distribution of Perfluoroalkyl Acids (PFAAs) in the Water Column of the Atlantic Ocean. Environmental Science and Technology Letters, 10(5), 418–424.

Schmidt, N., Fauvelle, V., Ody, A., Castro-Jiménez, J., Jouanno, J., Changeux, T., Thibaut, T., & Sempéré, R. (2019). The Amazon River: A Major Source of Organic Plastic Additives to the Tropical North Atlantic? Environmental Science and Technology, 53(13), 7513–7521.

Schmidt, N., Castro-Jiménez, J., Fauvelle, V., Ourgaud, M., & Sempéré, R. (2020). Occurrence of organic plastic additives in surface waters of the Rhône River (France). Environmental Pollution, 257.

Schmidt, N., Castro-Jiménez, J., Oursel, B., & Sempéré, R. (2021). Phthalates and organophosphate esters in surface water, sediments and zooplankton of the NW Mediterranean Sea: Exploring links with microplastic abundance and accumulation in the marine food web. Environmental Pollution, 272.

Schymanski, E. L., Zhang, J., Thiessen, P. A., Chirsir, P., Kondic, T., & Bolton, E. E. (2023). Per- and Polyfluoroalkyl Substances (PFAS) in PubChem: 7 Million and Growing. Environmental Science and Technology, 57(44), 16918–16928.

Sha, B., Johansson, J. H., Benskin, J. P., Cousins, I. T., & Salter, M. E. (2021). Influence of Water Concentrations of Perfluoroalkyl Acids (PFAAs) on Their Size-Resolved Enrichment in Nascent Sea Spray Aerosols. Environmental Science and Technology, 55(14), 9489–9497.

Sha, B., Johansson, J. H., Tunved, P., Bohlin-Nizzetto, P., Cousins, I. T., & Salter, M. E. (2022). Sea Spray Aerosol (SSA) as a Source of Perfluoroalkyl Acids (PFAAs) to the Atmosphere: Field Evidence from Long-Term Air Monitoring. Environmental Science and Technology, 56(1), 228–238.

Sha, B., Johansson, J. H., Salter, M. E., Blichner, S. M., & Cousins, I. T. (2024). Constraining global transport of perfluoroalkyl acids on sea spray aerosol using field measurements. Science Advances, 10(14), 1–10.

Sperling, L. H. (2011). History of interpenetrating polymer networks starting with bakelite-Based compositions. ACS Symposium Series, 1080, 69–82.

Sharkey, M., Harrad, S., Abou-Elwafa Abdallah, M., Drage, D. S., & Berresheim, H. (2020). Phasing-out of legacy brominated flame retardants: The UNEP Stockholm Convention and other legislative action worldwide. Environment International, 144.

Steffen, W., Sanderson, A., Tyson, P. D., Jäger, J., Matson, P. A., Moore III, B., Oldfield, F., Richardson, K., Schellnhuber, H. J., Turner, B. L., & Wasson, R. J. (2004). Global Change and the Earth System: A Planet Under Pressure. Springer-Verlag, Berlin, Heidelberg.

Steffen, w:, Sanderson, A., Tyson, P., Jäger, K., Matson, P., Moore, B., Oldfield, F., Richardson, K., Schellnhuber, H.J., Turner, B.L.,& Wasson, R.J. (2005). Global Change and the Earth System. A Planet Under Pressure. The IGBP Series.

Steffen, W., Grinevald, J., Crutzen, P., & Mcneill, J. (2011). The anthropocene: Conceptual and historical perspectives. In Philosophical Transactions of the Royal Society A: Mathematical, Physical and Engineering Sciences, 369, 1938, 842–867.

Steffen, W., Richardson, K., Rockström, J., Schellnhuber, H. J., Dube, O. P., Dutreuil, S., Lenton, T. M., & Lubchenco, J. (2020). The emergence and evolution of Earth System Science. In Nature Reviews Earth and Environment (Vol. 1, Issue 1, pp. 54–63). Springer Nature.

Stockholm Convention on Persistent Organic Pollutants (POPs). (2024). Acceptable Purposes for DDT Under the Stockholm Convention. Retrieved from: https://chm.pops.int/Implementation/Exemptions/AcceptablePurposes/AcceptablePurposesDDT/tabid/456/Default.aspx

Stortini, A. M., Martellini, T., del Bubba, M., Lepri, L., Capodaglio, G., & Cincinelli, A. (2009). n-Alkanes, PAHs and surfactants in the sea surface microlayer and sea water samples of the Gerlache Inlet sea (Antarctica). Microchemical Journal, 92(1), 37–43.

Strid, A., Bruhn, C., Sverko, E., Svavarsson, J., Tomy, G., & Bergman, Å. (2013). Brominated and chlorinated flame retardants in liver of Greenland shark (Somniosus microcephalus). Chemosphere, 91(2), 222–228.

Stubbins, A., Niggemann, J., & Dittmar, T. (2012). Photo-lability of deep ocean dissolved black carbon. Biogeosciences, 9(5), 1661–1670.

Su, G., Letcher, R. J., & Yu, H. (2016). Organophosphate Flame Retardants and Plasticizers in Aqueous Solution: PH-Dependent Hydrolysis, Kinetics, and Pathways. Environmental Science and Technology, 50(15), 8103–8111.

Sühring, R., Wolschke, H., Diamond, M. L., Jantunen, L. M., & Scheringer, M. (2016). Distribution of Organophosphate Esters between the Gas and Particle Phase-Model Predictions vs Measured Data. Environmental Science and Technology, 50(13), 6644–6651.

Sun, L., Xu, W., Peng, T., Chen, H., Ren, L., Tan, H., Xiao, D., Qian, H., & Fu, Z. (2016). Developmental exposure of zebrafish larvae to organophosphate flame retardants causes neurotoxicity. Neurotoxicology and Teratology, 55, 16–22.

Sutton, R., Chen, D., Sun, J., Greig, D. J., & Wu, Y. (2019). Characterization of brominated, chlorinated, and phosphate flame retardants in San Francisco Bay, an urban estuary. Science of the Total Environment, 652, 212–223.

- T -

Tran, C. M., Lee, H., Lee, B., Ra, J. S., & Kim, K. T. (2021). Effects of the chorion on the developmental toxicity of organophosphate esters in zebrafish embryos. Journal of Hazardous Materials, 401, 123389.

Truong, L., Rericha, Y., Thunga, P., Marvel, S., Wallis, D., Simonich, M. T., Field, J. A., Cao, D., Reif, D. M., & Tanguay, R. L. (2022). Systematic developmental toxicity assessment of a structurally diverse library of PFAS in zebrafish. Journal of Hazardous Materials, 431.

- U -

Ulaszewska, M. M., Zuccato, E., & Davoli, E. (2011). PCDD/Fs and dioxin-like PCBs in human milk and estimation of infants' daily intake: A review. Chemosphere, 83(6), 774–782.

UNEP. (2009, 2019). Stockholm Convention on Persistent Organic Pollutants. United Nations Environment Programme.

Uning, R., Latif, M. T., Yu, K. L., Cheng, S. Y., Ahamad, F., Khan, M. F., Bedurus, E. A., & Suratman, S. (2018). Surfactants in the Sea Surface Microlayer, Underlying Water and Atmospheric Particles of Tropical Coastal Ecosystems. Water, Air, and Soil Pollution, 229(9).

United Nations Environment Programme (UNEP), "Stockholm Convention on Persistent Organic Pollutants (POPs)" (UNEP/POPS/COP, UNEP, 2019); https://chm.pops.int/ TheConvention/Overview/TextoftheConvention/tabid/2232/Default.aspx.

U.S. Environmental Protection Agency. (2024, March 12). DDT - A brief history and status. EPA. https://www.epa.gov/ingredients-used-pesticide-products/ddt-brief-history-and-status.

- V -

van der Veen, I., & de Boer, J. (2012). Phosphorus flame retardants: Properties, production, environmental occurrence, toxicity and analysis. Chemosphere, 88(10), 1119–1153.

Vitousek, P. M., Mooney, H. A., Lubchenco, J., & Melillo, J. M. (1997). Human Domination of Earth's Ecosystems. Science, 277(5325), 494-499.

van den Berg, M., Kypke, K., Kotz, A., Tritscher, A., Lee, S. Y., Magulova, K., Fiedler, H., & Malisch, R. (2017). WHO/UNEP global surveys of PCDDs, PCDFs, PCBs and DDTs in human milk and benefit–risk evaluation of breastfeeding. Archives of Toxicology, 91, 1, 83–96.

Varner, J. (2014, April 1). Scientific outreach: Toward effective public engagement with biological science. BioScience. Oxford University Press.

Vila-Costa, M., Sebastián, M., Pizarro, M., Cerro-Gálvez, E., Lundin, D., Gasol, J. M., & Dachs, J. (2019). Microbial consumption of organophosphate esters in seawater under phosphorus limited conditions. Scientific Reports, 9(1), 1–11.

Vila-Costa, M., Cerro-Gálvez, E., Martínez-Varela, A., Casas, G., & Dachs, J. (2020). Anthropogenic dissolved organic carbon and marine microbiomes. The ISME Journal, 14, 2646–2657.

Vitousek, P.M. (1994). Beyond Global Warming: Ecology and Global Change. In Centennial Sepecial: Notable Papers in ESA History MacArthur Award Series, 75. 7.

- W -

Wagner, S. & Jaffé, R. (2015). Effect of photodegradation on molecular size distribution and quality of dissolved black carbon. Organic Chemistry, 86, 1-4.

Wagner, S., Jaffé, R., Stubbins, A., Stanley, E., & del Giorgio, P. (2018). SPECIAL ISSUE-CURRENT EVIDENCE Dissolved black carbon in aquatic ecosystems. Limnology and Oceanography Letters, 3, 168–185.

Wang, R.; Tao, S.; Wang, W.; Liu, J.; Shen, H.; Shen, G.; Wang, B.; Liu, X.; Li, W.; Huang, Y.; Zhang, Y.; Lu, Y.; Chen, H.; Chen, Y.; Wang, C.; Zhu, D.; Wang, X.; Li, B.; Liu, W., & Ma, J. (2012). Black carbon emissions in China from 1949 to 2050. Environmental Science and Technology, 46, 7595–7603.

Wang, Z., MacLeod, M., Cousins, I. T., Scheringer, M., & Hungerbühler, K. (2011). Using COSMOtherm to predict physicochemical properties of poly- and perfluorinated alkyl substances (PFASs). Environmental Chemistry, 8(4), 389–398.

Wang, Z., Dewitt, J. C., Higgins, C. P., & Cousins, I. T. (2017). A Never-Ending Story of Per- and Polyfluoroalkyl Substances (PFASs)? Environmental Science and Technology, 51(5), 2508–2518.

Wang, Y., Li, W., Martínez-Moral, M. P., Sun, H., & Kannan, K. (2019). Metabolites of organophosphate esters in urine from the United States: Concentrations, temporal variability, and exposure assessment. Environment International, 122, 213–221.

Wang, X., Zhong, W., Xiao, B., Liu, Q., Yang, L., Covaci, A., & Zhu, L. (2019). Bioavailability and biomagnification of organophosphate esters in the food web of Taihu Lake, China: Impacts of chemical properties and metabolism. Environment International, 125, 25–32.

Wang, Z., Walker, G. W., Muir, D. C. G., & Nagatani-Yoshida, K. (2020). Toward a Global Understanding of Chemical Pollution: A First Comprehensive Analysis of National and Regional Chemical Inventories. Environmental Science and Technology, 54(5), 2575–2584.

Wania, F. & Mackay, D. (1996). Tracking the distribution of persistent organic pollutants. Environmental Science and Technology, 30, 390–397.

Wania, F., & Dugani, C. B. (2003). Assessing the long-range transport potential of polybrominated diphenyl ethers: A comparison of four multimedia models. Environmental Toxicology and Chemistry, 22(6), 1252–1261.

Wania, F. (2006). Potential of degradable organic chemicals for absolute and relative enrichment in the Arctic. Environmental Science and Technology, 40(2), 569–577.

Waters, C. N., Zalasiewicz, J., Summerhayes, C., Barnosky, A. D., Poirier, C., Gałuszka, A., Cearreta, A., Edgeworth, M., Ellis, E. C., Ellis, M., Jeandel, C., Leinfelder, R., McNeill, J. R., Richter, D. D. B., Steffen, W., Syvitski, J., Vidas, D., Wagreich, M., Williams, M., … Wolfe, A. P. (2016). The Anthropocene is functionally and stratigraphically distinct from the Holocene. In Science, 351, 6269.

Wei, G. L., Li, D. Q., Zhuo, M. N., Liao, Y. S., Xie, Z. Y., Guo, T. L., Li, J. J., Zhang, S. Y., & Liang, Z. Q. (2015). Organophosphorus flame retardants and plasticizers: Sources, occurrence, toxicity and human exposure. In Environmental Pollution, 196, 29–46.

Wild, S., McLagan, D., Schlabach, M., Bossi, R., Hawker, D., Cropp, R., King, C. K., Stark, J. S., Mondon, J., & Nash, S. B. (2015). An antarctic research station as a source of brominated and perfluorinated persistent organic pollutants to the local environment. Environmental Science and Technology, 49(1), 103–112.

World Health Organization (WHO), Environmental Health Criteria 218, WHO, Geneva, 2000.

World Health Organization (WHO). (2006). Indoor Residual Spraying: Use of Indoor Residual Spraying for Scaling Up Global Malaria Control and Elimination. WHO/HTM/MAL/2006.1112. Retrieved from: https://

apps.who.int/iris/bitstream/handle/10665/69386/WHO_HTM_MAL_2006.1112_eng.pdf

Wu, Z., Chen, X., Wang, Z., Chen, H., Wang, Z., Mu, Q., Wu, L., Wang, W., Tang, X., Li, J., Li, Y., Wu, Q., Wang, Y., Zou, Z., & Jiang, Z. (2024). Modeling of PAHs From Global to Regional Scales: Model Development and Investigation of Health Risks from 2013 to 2018 in China.

- X -

Xia, Z., Duan, X., Qiu, W., Liu, D., Wang, B., Tao, S., Jiang, Q., Lu, B., Song, Y., & Hu, X. (2010). Health risk assessment on dietary exposure to polycyclic aromatic hydrocarbons (PAHs) in Taiyuan, China. Science of the Total Environment, 408(22), 5331–5337.

Xie, C., Qiu, N., Xie, J., Guan, Y., Xu, W., Zhang, L., & Sun, Y. (2024). Organophosphate esters in seawater and sediments from the low-latitude tropical sea. Science of the Total Environment, 907, 167930.

Xie, Z., Wang, P., Wang, X., Castro-Jiménez, J., Kallenborn, R., Liao, C., Mi, W., Lohmann, R., Vila-Costa, M., & Dachs, J. (2022). Organophosphate ester pollution in the oceans. Nature Reviews Earth and Environment, 3, 5, 309–322.

Xie, Z., Zhang, P., Wu, Z., Zhang, S., Wei, L., Mi, L., Kuester, A., Gandrass, J., Ebinghaus, R., Yang, R., Wang, Z., & Mi, W. (2022). Legacy and emerging organic contaminants in the polar regions. In Science of the Total Environment, 835.

Xie, Z., & Kallenborn, R. (2023). Legacy and emerging per- and poly-fluoroalkyl substances in polar regions. In Current Opinion in Green and Sustainable Chemistry (Vol. 42).

- Y -

Ya, M., Wu, Y., Wu, S., Li, Y., Mu, J., Fang, C., Yan, J., Zhao, Y., Qian, R., Lin, X., & Wang, X. (2019). Impacts of Seasonal Variation on Organochlorine Pesticides in the East China Sea and Northern South China Sea. Environmental Science and Technology, 53, 13088-13097.

Yamashita, Y., Nakane, M., Mori, Y., Nishioka, J., & Ogawa, H. (2022). Fate of dissolved black carbon in the deep Pacific Ocean. Nature Communications, 13(1).

- Z -

Zhang, Z., Liu, L., Liu, C., & Cai, W. (2003). Studies on the sea surface microlayer: II. The layer of sudden change of physical and chemical properties. Journal of Colloid and Interface Science, 264(1), 148–159.

Zhang, X., Sühring, R., Serodio, D., Bonnell, M., Sundin, N., & Diamond, M. L. (2016). Novel flame retardants: Estimating the physical-chemical properties and environmental fate of 94 halogenated and organophosphate PBDE replacements. Chemosphere, 144, 2401–2407.

Zhang, X., Li, L., Xie, Z., Ma, J., Li, Y.-F., Cai, M., Ren, N.-Q., Kallenborn, R., Zhang, Z.-F., Zhang, X., & Muir, D. C. G. (2024). Exploring global oceanic persistence and ecological effects of legacy persistent organic pollutants across five decades. Science Advances 10, eado5534.

Zhang, Z., Lin, G., Lin, T., Zhang, R., Jin, L., & Di, Y. (2020). Occurrence, behavior, and fate of organophosphate esters (OPEs) in subtropical paddy field environment: A case study in Nanning City of South China. Environmental Pollution, 267.

Zhao, Z., Xie, Z., Möller, A., Sturm, R., Tang, J., Zhang, G., & Ebinghaus, R. (2012). Distribution and long-range transport of polyfluoroalkyl substances in the Arctic, Atlantic Ocean and Antarctic coast. Environmental Pollution, 170, 71–77.

- # -

3M. (2022, December 20). 3M to exit PFAS manufacturing by the end of 2025. [Consulted Nov 11th 2024]. Retrieved from https://news.3m.com/2022-12-20-3M-to-Exit-PFAS-Manufacturing-by-the-End-of-2025

METHODOLOGICAL APPROACH

02



TABLE OF CONTENTS

2.1. The ANTOM Project
2.2. The ANTOM oceanographic cruises
2.3. Sampling overview
2.3.1. Seawater: surface and the water column
2.3.2. Sea surface microlayer and subsurface layers
2.3.3. Wet Deposition
2.3.4. Other samplings

2.4. Sample treatment and instrumental analyses
2.4.1. PFAS analysis
2.4.2. OPE analysis

2.5. Quality Control and Quality Assurance
2.6. References

PART 02. METHODOLOGICAL APPROACH

2.1. THE ANTOM PROJECT

This thesis has been performed under the framework of the ANTOM Project (2019-2022), "Transport and biogeochemistry of ANThropogenic Organic Matter in the Southern Ocean and Antarctica" (Ref. PGC2018-096612-B-I00).

The project aimed to advance our understanding of the transport, deposition, and biogeochemical impact of semivolatile organic compounds (SOCs) in the Southern Ocean and Antarctica. Anthropogenic organic matter, including persistent organic pollutants (POPs), emerging contaminants, and unresolved complex mixtures, reach remote environments via atmospheric and oceanic transport, yet its environmental significance remains largely unquantified. The project challenged the current paradigm of the global carbon cycle by considering the atmospheric input of anthropogenic organic carbon as a major, yet overlooked, driver of ecosystem change.

The general objective of the project was to quantify the anthropogenic perturbation of the organic matter due to inputs of organic contaminants. The project's region of study was the Southern Ocean and maritime Antarctica, but to understand the transport mechanisms and biogeochemistry in the austral region, the study was addressed as a latitudinal transect from the Atlantic to the Southern Ocean, as the anthropogenic perturbation in the Southern Ocean's chemosphere depends on the transport of contaminants from source regions.

Specific objectives

- Quantify atmosphere-ocean fluxes of aliphatic, aromatic, and polar SOCs.
- Characterize the latitudinal fractionation of SOCs in a Spain-Antarctica transect.
- Investigate the fate and transport of emerging polar pollutants (e.g., organophosphate esters, perfluoroalkyl substances).
- Assess the role of snow deposition in air-sea and air-land exchanges of SOCs.
- Examine microbial community responses to atmospheric inputs of organic carbon and phosphorus.
- Develop gene-inclusive biogeochemical models for SOCs in the marine water column.
- Analyze long-term trends of anthropogenic organic pollutants in Antarctica to evaluate historical and future changes.

Within the framework of this project, this thesis has specifically focused on the biogeochemical processes governing the behavior and fate of organic contaminants, with particular attention to organophosphate esters (OPEs) and perfluoroalkyl acids (PFAAs), which were experimentally measured for this work. On the other hand, aromatic like compounds, including Polycyclic Aromatic Hydrocarbons, and Dissolved Black Carbon, were assessed by a meta-analysis from previously published data.

Hence, in this section we will detail all the field work and analytical methods used in the thesis. Even though the specific analytical methods are provided in each chapter within the publications, this section provides a general overview of all the experimental work performed.

2.2. THE ANTOM OCEANOGRAPHIC CRUISES

All samples used for the analyses performed in this thesis were collected during two oceanographic campaigns: ANTOM-I and ANTOM-II.

ANTOM-I, on board the R/V Sarmiento de Gamboa, took place from December 15th, 2020, to January 15th, 2021, covering a broad region of the Atlantic Ocean, spanning from Vigo (Spain) at 42°N, to Punta Arenas (Chile) at 52°S. **ANTOM-II**, conducted on the R/V Hespérides, explored the Southern Ocean during the Austral summer, from the South Shetland Islands at 62°S through the Gerlache Strait and the Bellingshausen Sea, reaching up to 71°S, from January 14th to February 7th, 2022.

Twenty-four stations in the Atlantic and fourteen in the Southern Ocean were selected within the project **(Figures 2.1 and 2.2)** to provide extensive coverage in both oceans. Although the sampling schedule was planned in advance on land, it required adaptability to changing weather conditions, which were particularly challenging in Antarctica.

During each campaign, a coordinated effort by a team of scientists ensured the collection, treatment, and processing of more than 1000 environmental samples for chemical and biological analysis, including seawater, air, and plankton. Additionally, diverse in-situ experiments were planned and conducted during both campaigns to complement the environmental characterization with new data on the potential biodegradation of pollutants by marine microbial communities

Sampling stations in both oceans were designated according to the following coding system:

Atlantic Ocean: AN1_ST[01 - 24]

Southern Ocean: AN2_ST[01 – 14].

Sampling locations were carefully selected to provide broad and consistent coverage of open ocean waters. In the Atlantic Ocean, stations were located at international waters off the coasts of Spain, northwestern Africa, and the eastern coast of South America. In the Southern Ocean, stations were positioned around the South Shetland Islands, Bransfield Strait extending south to Marguerite Bay, reaching 71.02ºS in the Bellingshausen Sea, and then heading north through open Antarctic waters **(Figures 2.1 and 2.2)**.

This latitudinal transect in the Atlantic and Southern Ocean represented a significant environmental gradient, spanning from oceanic regions proximate to populated and industrialized regions with high anthropogenic and pollution pressures, to some of the most pristine marine environments on the planet, allowing for a comprehensive assessment of pollutant distribution and behavior across contrasting ecological and pollution scenarios. The transect also included different biogeochemical provinces and climatic regimes.

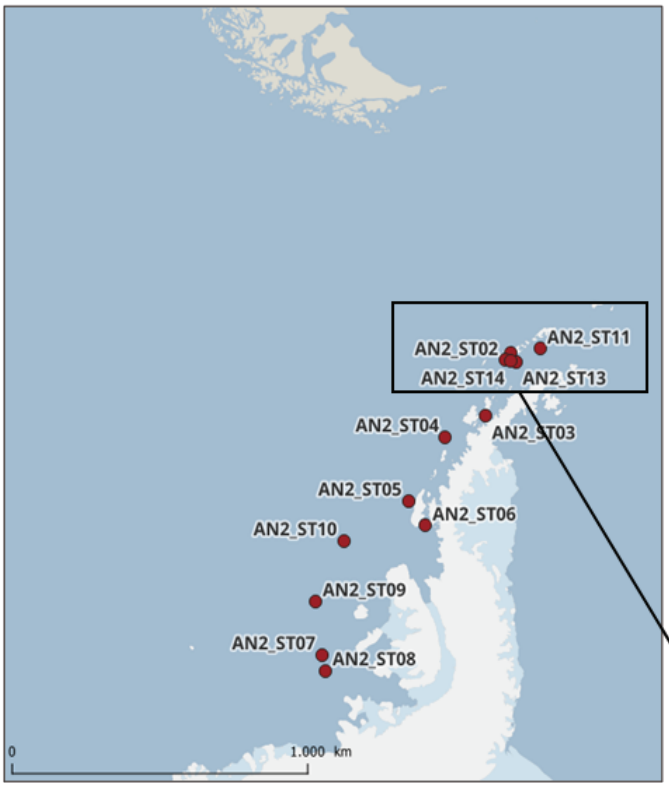
2.3. SAMPLING OVERVIEW

After the planification and preparation of the oceanographic campaigns, largely performed during the COVID pandemics, a detailed sampling planning was elaborated to cover a wide range of environmental matrixes and variables allowing a comprehensive characterization of chemical and biological parameters in the atmosphere and ocean. The planning included the sampling of sea water (particulate and dissolved phase), from surface and the water column, as well the sea surface microlayer and subsurface waters, in order to characterize the top ocean's layers. It also included sampling of air (aerosols and gas phase), and



ANTOM-I (Atlantic Ocean)				
Station number	St Code	Date	Latitude	Longitude
1	AN1_ST01	18/12/2020	37.91	-15.97
2	AN1_ST02	19/12/2020	35.73	-19.06
3	AN1_ST03	20/12/2020	32.18	-21.53
4	AN1_ST04	21/12/2020	28.65	-23.39
5	AN1_ST05	22/12/2020	25.63	-24.89
6	AN1_ST06	23/12/2020	22.22	-26.63
7	AN1_ST07	24/12/2020	18.86	-28.31
8	AN1_ST08	25/12/2020	14.98	-28.77
9	AN1_ST09	26/12/2020	10.87	-29.23
10	AN1_ST10	27/12/2020	7.34	-29.58
11	AN1_ST11	28/12/2020	3.82	-29.86
12	AN1_ST12	29/12/2020	0.15	-30.50
13	AN1_ST13	30/12/2020	-2.97	-30.95
14	AN1_ST14	31/12/2020	-6.77	-31.33
15	AN1_ST15	02/01/2021	-14.36	-33.91
16	AN1_ST16	03/01/2021	-17.77	-35.26
17	AN1_ST17	04/01/2021	-21.29	-36.81
18	AN1_ST18	05/01/2021	-24.91	-38.71
19	AN1_ST19	06/01/2021	-27.79	-40.65
20	AN1_ST20	07/01/2021	-30.98	-42.96
21	AN1_ST21	08/01/2021	-34.40	-45.63
22	AN1_ST22	09/01/2021	-37.24	-48.09
23	AN1_ST23	11/01/2021	-43.79	-54.75
24	AN1_ST24	12/01/2021	-46.78	-58.46

Figure 2.1 | Map (left) and details of the stations (right) from the transect performed during the ANTOM-I oceanographic cruise.



ANTOM-II (Southern Ocean)

Station number	St Code	Date	Latitude	Longitude
1	AN2_ST01	23/01/2022	-62.71	-60.64
2	AN2_ST02	24/01/2022	-62.92	-61.04
3	AN2_ST03	25/01/2022	-64.58	-62.57
4	AN2_ST04	26/01/2022	-65.15	-65.64
5	AN2_ST05	27/01/2022	-66.92	-69.10
6	AN2_ST06	28/01/2022	-67.75	-68.03
7	AN2_ST07	30/01/2022	-70.85	-79.89
8	AN2_ST08	30/01/2022	-70.85	-79.89
9	AN2_ST09	31/01/2022	-69.21	-78.84
10	AN2_ST10	01/02/2022	-67.70	-75.00
11	AN2_ST11	04/02/2022	-62.57	-58.62
12	AN2_ST12	04/02/2022	-62.57	-58.62
13	AN2_ST13	05/02/2022	-62.97	-60.29
14	AN2_ST14	06/02/2022	-62.95	-60.64



Figure 2.2. | Map (left) and details of the stations (right) from the transect performed during the ANTOM-II oceanographic cruise.

plankton. For all samples, a chemical and biological characterization was performed.

The chemical characterization included the quantification of specific chemicals, the total organic carbon (TOC), and nutrients. Biological characterization included DNA and RNA analyses, bacterial abundance (BA) and bacterial production (BP), chlorophyll *a* (Chl *a*), and the extra-cellular enzymatic activity. Environmental and water column parameters were systematically measured for surface waters through all the transect, and for the water column at each sampling station. All sampling strategies are summarized in **Figure 2.3.** This multidisciplinary approach and analysis have been the result of a team work by numerous scientist with different background and expertise.

Surface seawater samples were collected at a depth of 4 to 5 meters (below the influence of the boat) at twenty-four, and fourteen stations in the Atlantic and Southern oceans, respectively. Moreover, at specific locations, seawater samples from the water column were collected at four selected depths to capture vertical distribution patterns, resulting in vertical profiles of five depths down to 2000 m. Furthermore, whenever oceanic and meteorological conditions permitted, SML and SSL samplings were conducted from an inflatable boat. In the Atlantic Ocean, air and plankton samples were collected daily. However, in

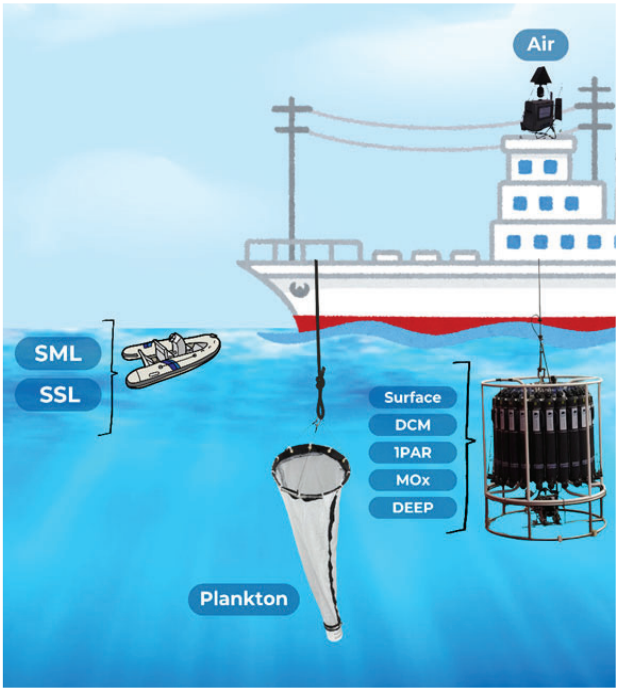


Figure 2.3 | Schematics of the sampling processes during both ANTOM I and II campaigns.

the Southern Ocean, due to meteorological limitations, air samples were not collected, while plankton samples were also collected. Atmospheric inputs were measured through the collection of wet deposition samples (rain) and air samples, which are critical for evaluating atmospheric transport pathways

All information regarding the measurements performed to each water sample, as well as any relevant success happening during the analysis were systematically noted in a complex yet effective system of field logbooks. Descriptive meteorological and ocean conditions were also noted at each SML and SSL sampling due to their relevant effect on the marine surface's microlayer state.

All samples were processed in the vessel's laboratory as much as feasible, and labelled and stored at the corresponding temperature (4ºC, -20ºC or -80ºC) until further transportation to the research institute facilities where further processing and analyses were performed.

2.3.1. SEAWATER: SURFACE AND THE WATER COLUMN

For surface and water column seawater sampling, a Niskin rosette equipped with a Sea-Bird SBE 9 CTD sensor was used **(Figure 2.4)**. The CTD was programmed to continuously measure conductivity, fluorescence, oxygen, temperature, and depth, providing real-time data essential for characterizing the water column. These continuous measurements allowed for the identification of key oceanographic features and the determination of sampling depths.

The Niskin rosette consisted of a circular frame holding twenty-four 15 L polypropylene (PP) Niskin bottles, enabling the collection of up to 288 L of water per cast. The bottles were closed at specific depths from the ship laboratory. This allowed the sampling of water depths with specific characteristics. Water samples were collected from five specific depth layers:

- Surface layer (~ 4 to 5 m)
- Depth of the Chlorophyll Maximum (DCM)
- Depth of 1% Photosynthetically Active Radiation (1% PAR)
- Minimum Oxygen Layer (MOx)
- Deep layer (DEEP), closest to the seafloor

These layers were identified in real-time based on in situ monitoring of temperature, oxygen, fluorescence, and salinity during the CTD cast.

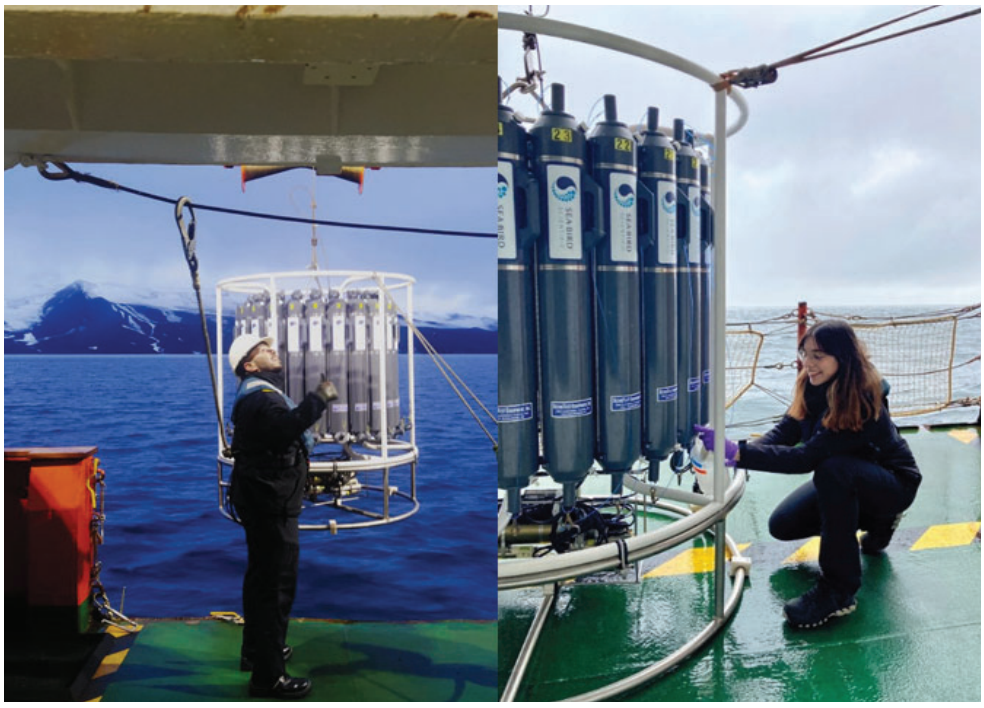


Figure 2.4 | Cast (left) and sampling (right) from the Niskin rossete from the R/V Hespérides.

Once the CTD was retrieved on deck, water samples were immediately drawn directly from the Niskin bottles into pre-rinsed containers designated for different analyses. This careful handling ensured sample integrity for subsequent chemical and biological measurements **(Figure 2.4).**

2.3.2. SEA SURFACE MICROLAYER AND SUBSURFACE LAYER

Sea surface microlayer (SML), and subsurface layer For the collection of the SML samples, a glass plate SML sampler was used, adopting a method initially described by Harvey and Burzell in 1972 and since then used by many researchers. Briefly, this method involves vertically dipping a pre-rinsed glass plate (40 x 30 cm) into the water surface, allowing the SML to adhere to the plate during a slow withdrawal driven by the surface tension. The water retained on the glass is then swiftly scraped between two polytetrafluoroethylene (PTFE) wipers **(Figure 2.5)**, facilitating drainage into a pre-rinsed 500 mL PTFE bottle. The process is repeated until obtaining a volume of 500 mL of SML seawater.

After collecting the SML samples, the SSL was collected at the exact same location, at between 0.3 and 0.4 m depth, with a 2 L PTFE pre-rinsed bottle by simply submerging it in the ocean water. SML and SSL samples were then processed following the methodology described in Section 2.4.2 for OPEs analysis.

To mitigate the risk of contamination from the ship, SML and SSL sampling operations were executed from a rigid inflatable boat at 500 m upwind of the ship. Samples were taken from the upwind side of the inflatable boat, and drifting with the engine turned off. Operations conducted from the inflatable boat were always carried out with the mandatory use of life jackets to ensure safety at sea. In the Southern Ocean, all activities involving embarking or disembarking the research vessels (R/Vs), as well as any operations performed from the inflatable boat, required the use of a Viking survival suit, which provides essential protection against the extreme cold **(Figure 2.5)**.

2.3.3. WET DEPOSITION

Wet deposition (WD) samples were collected for the analysis of organophosphate esters (OPEs). During rain events, samples were collected using a pre-combusted 2.5 L glass bottle fitted with a stainless-steel funnel (0.2 m diameter) that had been pre-cleaned with methanol (MeOH) and acetone. The collection system was securely installed on the vessel's deck using ropes prior to each rain event and removed during periods without precipitation to minimize the risk of contamination **(Figure 2.6)**.

Coordinates marking the start and end of each rain event were recorded to document the sample collection period. The WD samples were processed using solid-phase extraction (SPE), following the methodology described in Section 2.4.2, with one modification: the filtering step was omitted to prevent potential losses of target compounds. The samples were loaded onto HLB cartridges and processed following the standard protocol for OPE extraction, elution, and analysis.

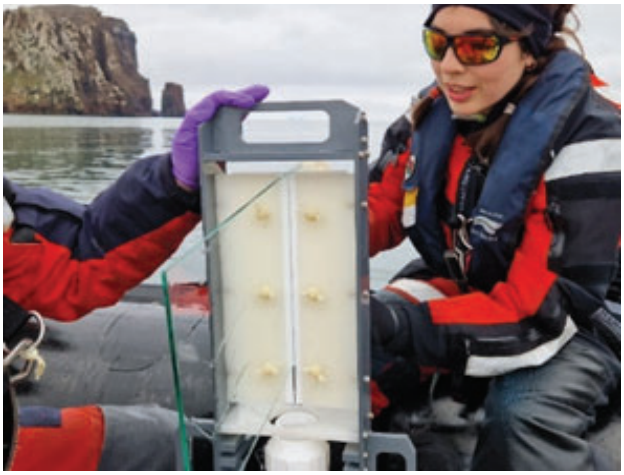


Figure 2.5 | Picture of the SML sampling process in the Southern Ocean.



Figure 2.6 | Schematics illustration of how the wet deposition is collected (left), and picture of the installation in the RV Sarmiento de Gamboa (right).

2.3.4. OTHER SAMPLINGS

During the campaigns, other environmental matrixes were sampled for pollutants analysis though they are not included in this thesis.

Air samples were collected using a high-volume sampler (MCV, Collbató, Spain) **(Figure 2.7)** that operated at 40 m^3 h^{-1} for 48-hour intervals. The air was first directed through a pre-combusted and pre-weighed quartz microfiber filter (QMA) to capture aerosol-bound substances. Subsequently, it passed through a polyurethane foam (PUF) to collect compounds in the gas phase. QMA filters and PUF foams were then stored with aluminum foil and zip-lock bags at -20ºC until further analysis.

Plankton samples were obtained by vertically dragging 100 and 200 µm mesh nets **(Figure 2.7)** into the water column down to the DCM depth, on average around 60 m depth. The collected sample was then transferred into glass bottles. Once in the laboratory, samples were filtered through a GF/D filter (47 mm, 2.7 µm mesh size, Whatmann), using a stainless-steel filtration ramp system connected to a vacuum pump. GF/D filters were wrapped in pre-combusted aluminum foil, and stored at -20ºC in zip lock bags.

Water continuum samples were collected using a filtration system designed to separate particulate and dissolved phases of pollutants. The system consisted of a stainless-steel filter holder (142 mm diameter) equipped with a GF/F filter (142 mm, 0.7 µm mesh size, Whatmann), connected in series to a pre-cleaned stainless-steel column packed with XAD-2 resin (Supelco). Approximately 200 L of seawater were passed through the system via a continuous tap that drew water from a depth of 1 meter below the vessel's influence zone, with the assistance of a vacuum pump to maintain steady flow.

GF/F filters were replaced after every 50 L of water to ensure optimal filtration efficiency and avoid clogging. The XAD-2 columns, used for trapping dissolved-phase pollutants, were stored at 4°C until further analysis. GF/F filters, which retained the particulate phase, were wrapped in pre-combusted aluminum foil and stored at -20°C in zip-lock bags to preserve sample integrity prior to laboratory processing.

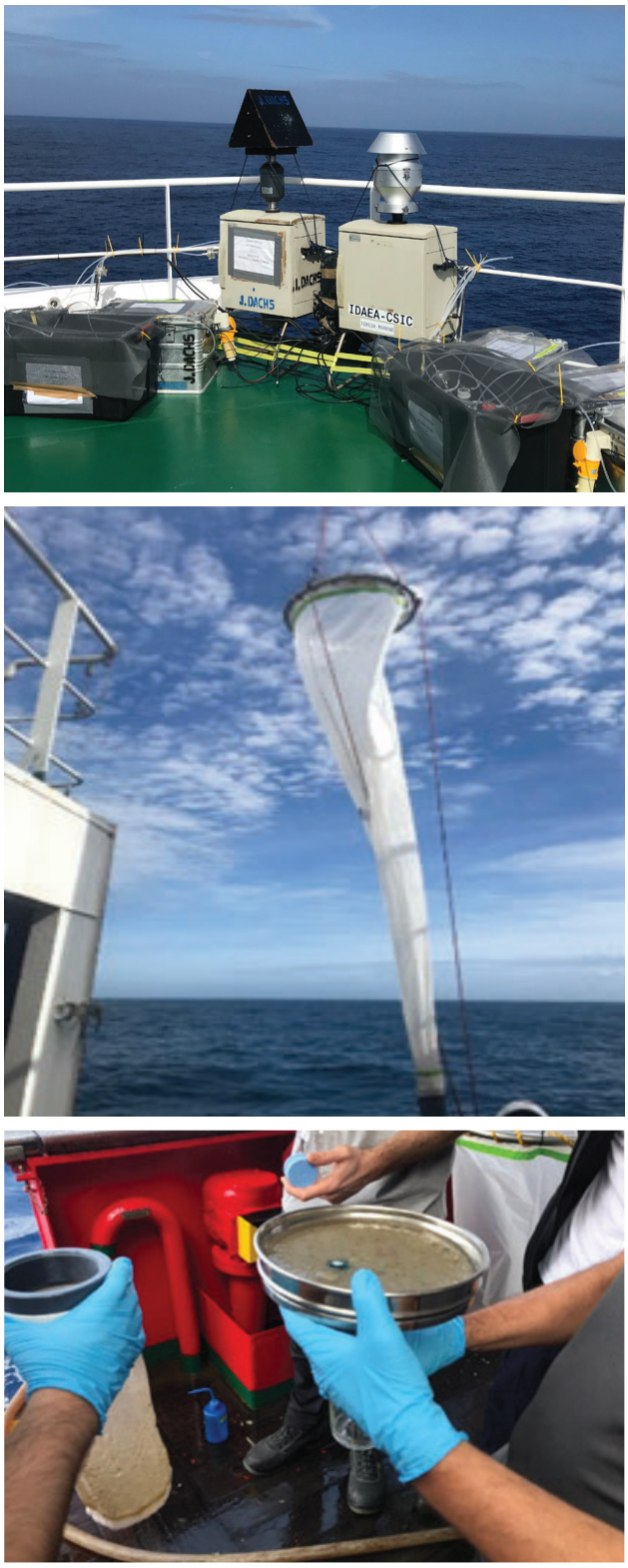


Figure 2.7 | Pictures of a) high-volume sampler attached to the vessel's deck (top); b) plankton sampling net casting (middle) and, c) plankton sample (bottom). All three pictures belong to the ANTOM-I cruise on board R/V Sarmiento de Gamboa.

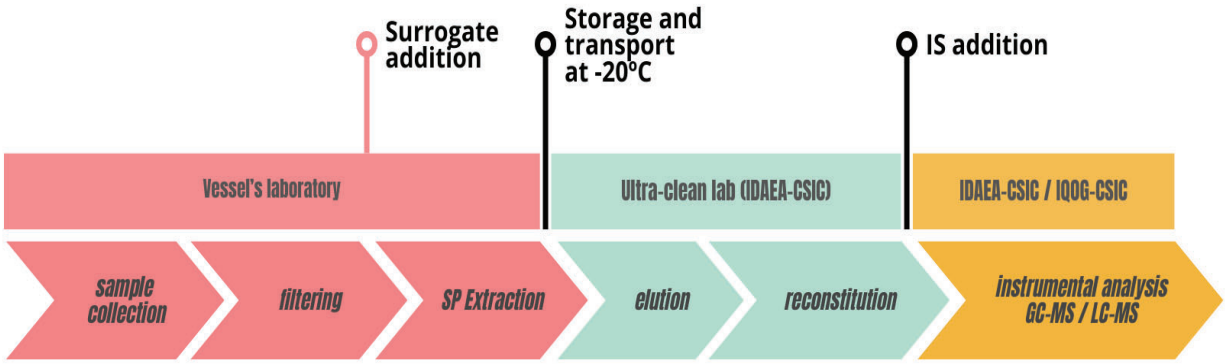


Figure 2.8 | Schematic workflow diagram illustrating the analytical process for chemical analysis of environmental samples.

2.4. SAMPLE TREATMENT AND INSTRUMENTAL ANALYSES

All sample treatments followed the general steps outlined in **Figure 2.8**. This section describes the initial sample processing conducted at the research station, subsequent clean-up and fractionation steps performed in the ultraclean laboratory at the Institute of Environmental Assessment and Water Research (IDAEA-CSIC), and the instrumental analysis of the different chemicals performed both at the instrumental laboratories of IDAEA-CSIC (for OPEs analysis) and IQOG-CSIC (for PFAS analysis)

2.4.1. PFAS ANALYSIS

For the analysis of PFAS, 2 L of water samples collected from the Niskin were directly transferred to a 2 L PP pre-rinsed bottle. Then, samples were filtered through pre-combusted glass fiber filters (GF/F, 0.7 µm mesh size, Whatman) and spiked directly in the PP bottle with 50 µL of a ^{13}C-labeled mixture of 9 recovery standards **(Table 2.1)** at a concentration of 20 pg µL^{-1}. PFAS were extracted using an established SPE method using OASIS WAX cartridges (Bond Elut, 6 cm^3, 150 mg; Waters) with minor modifications (González-Gaya et al., 2019b; Casas et al., 2020; 2021; 2023).

Briefly, cartridges were pre-conditioned with 6 ml of 0.1% ammonia in MeOH, 6 mL of MeOH and 6 mL of HPLC-grade water. Next, the sample was passed through the cartridges at a flowrate of 1 mL min^{-1}. After loading the sample, salts were washed with 6 mL of HPLC-grade water, and the cartridge was vacuum-dried for 10 mins. Cartridges and GF/F filters were labeled, protected with aluminum foil and zip lock bags, and stored at -20ºC until further treatment **(Figure 2.9)**.

Once in the ultra-clean laboratory **(Figure 2.10)**, cartridges were unfrozen for two hours. Each cartridge was then conditioned with 6 mL of ammonium acetate buffer (25 mM, pH=4), and centrifuged 4 minutes at 3500 rpm to eliminate excess water. Samples were eluted with 8 mL MeOH containing 0.1% ammonia. Eluents were dry-evaporated under a gentle stream of

Table 2.1 | Information of labelled PFAS compounds used as surrogate.

Surrogate standards	Acronym	Concentration (pg µL^{-1})
Perfluoro-n- [$^{13}C_4$] butanoic acid	PFBA-$^{13}C_4$	20
Perfluoro-n- [1,2-$^{13}C_2$] hexanoic aic	PFHxA-$^{13}C_2$	20
Perfluoro-n- [1,2,3,4-$^{13}C_4$] octanoic acid	PFOA-$^{13}C_4$	20
Perfluoro-n- [1,2,3,4,5-$^{13}C_5$] nonanoic acid	PFNA-$^{13}C_5$	20
Perfluoro-n- [1,2-$^{13}C_2$] decanoic acid	PFDA-$^{13}C_2$	20
Perfluoro-n- [1,2-$^{13}C_2$] undecanoic acid	PFUnDA-$^{13}C_2$	20
Perfluoro-n- [1,2-$^{13}C_2$] dodecanoic acid	PFDoDA-$^{13}C_2$	20
Sodium perfluoro-1- hexane[$^{18}C_2$] sulfonate	PFHxS-$^{18}C_2$	20
Sodium perfluoro-1- [1,2,3,4-$^{13}C_4$] octanesulfonate	PFOS-$^{13}C_4$	20

N^2. Each sample was reconstituted in 300 µl PP vials with 70:30 MeOH/HPLC grade water.

Samples were analyzed using a UPLC-MS/MS system equipped with a Xevo TQS (Waters, Milford, MA) based on an established method with minor modifications (González-Gaya et al., 2019b, Casas et al., 2021).

For chromatographic separation, extracts were injected into an Acquity UPLC BEH C18 column (1.7 µm, 2.1 x 50 mm; Waters). A C18 pre-column (Acquity UPLC BEH C18 1.7 µm VanGuard™, 2.1 x 5 mm) was used to protect the analytical column and an Isolator Column (Waters ACQUITY UPLC, 2.1 x 50 mm) to prevent contamination, ensuring reliable results. A gradient mobile phase of water and methanol including a constant 1% of ammonium acetate in water (0.2 M, pH 4) as buffer was used at a flow rate of 0.4 mL min^{-1}. The gradient water:organic phase for each 12-min injection was 72:28 at the initial conditions, 15:85 at 4.5 min, 1:99 at 4.6 min, and returned to the initial conditions from 10.0 min.

Analytes were ionized with an electrospray ionization (ESI) source operating in negative ion mode. Multiple-reaction-monitoring (MRM) mode was used for data acquisition. Prior to injection, 1000 pg of a mixture containing six C-labelled internal standards was added to each vial **(Table 2.2)**. Samples were analyzed in duplicate, with an injection volume of 10 µL, and quantification was performed using a 12-point calibration curve ranging from 0.005 to 100 pg. The calibration curve was injected prior and after each 10 samples batch. To eliminate any potential carryover, acetonitrile was injected in duplicate and passed through the system after every sample or calibration standard.

2.4.2. OPE ANALYSIS

For surface and water column OPE analysis, 2 L of For surface and water column OPE analysis, 2 L of water were collected into 2 L PTFE pre-rinsed bottles directly poured from the Niskin rosette's bottle. For the SSL, a 2 L volume of sample was collected manually with 2

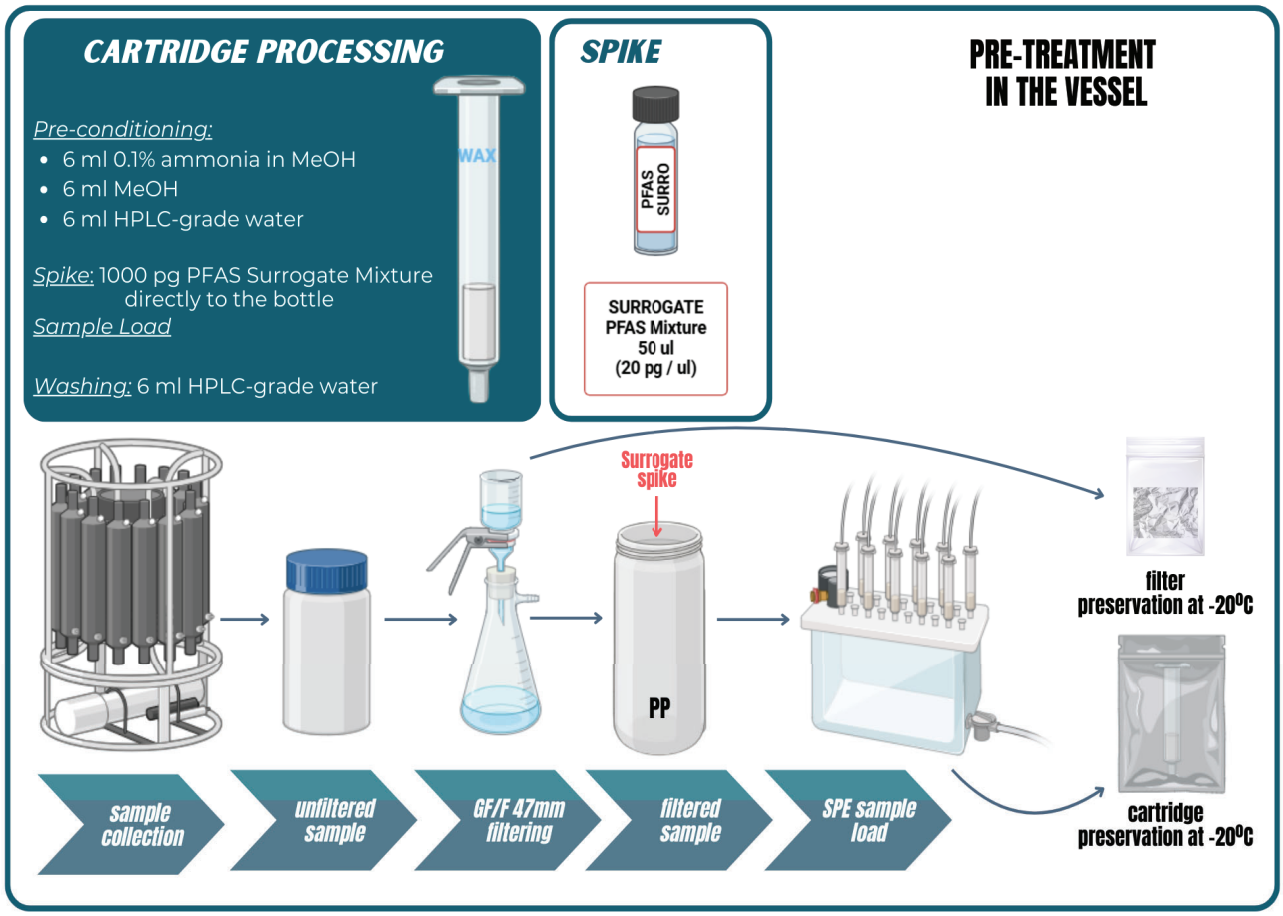


Figure 2.9. | Schematic overview of the samples pre-treatment in the vessels for PFAS analysis in sea-water. *Created with https://BioRender.com.*

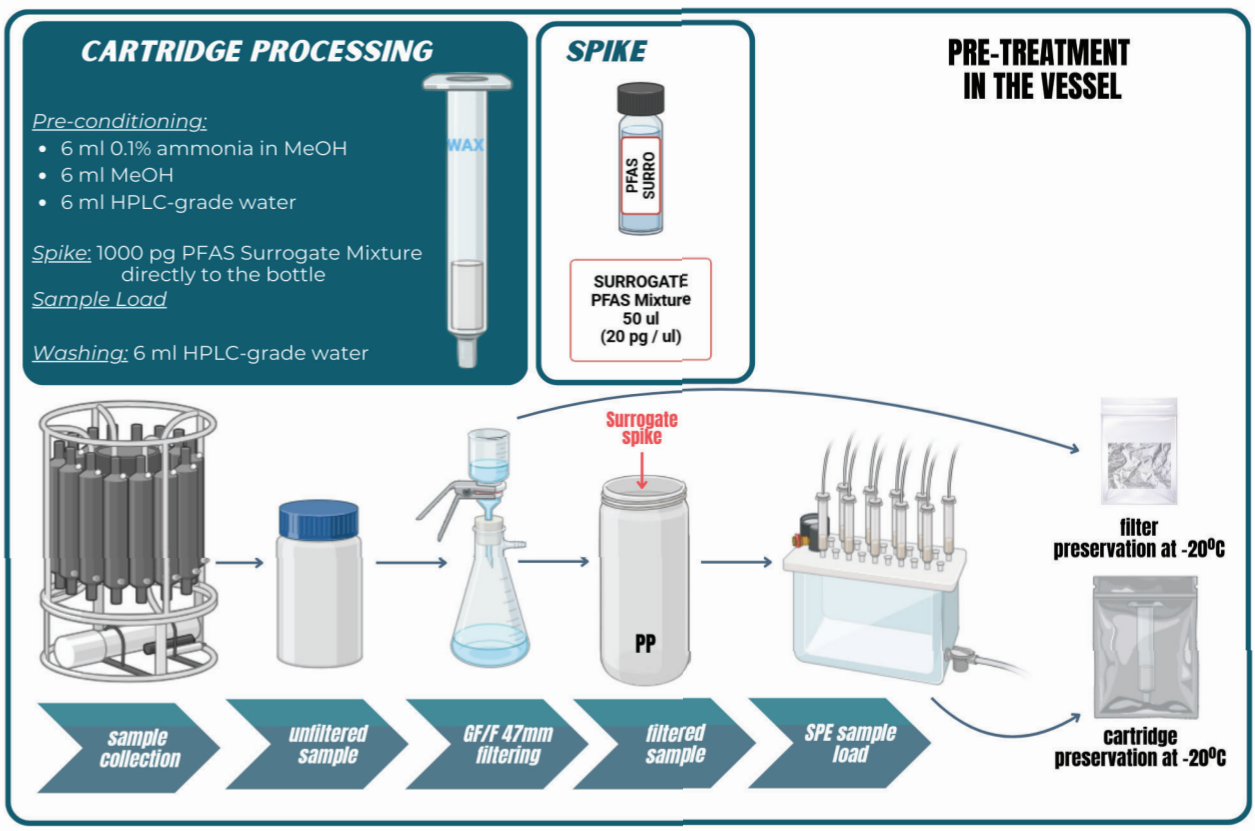


Figure 2.10 | Schematic overview of the analytical procedure for the extraction, concentration, and analysis of PFAS from environmental samples in the ultra-clean lab and instrumental analysis. *Created with https://BioRender.com.*

Table 2.2 | Information of labelled PFAS compounds used as Internal Standard.

Surrogate standards	Acronym	Concentration (pg μL^{-1})
Perfluoro-n-[2,3,4-$^{13}C_3$] butanoic acid	PFBA-$^{13}C_3$	40
Perfluoro-n-[$^{13}C_5$] pentanoic acid	PFPeA-$^{13}C_5$	40
Sodium perfluoro-1-[$^{13}C_8$] octanesulfonate	PFOS-$^{13}C_8$	40
Perfluoro-n-[$^{13}C_8$] octanoic acid	PFOA-$^{13}C_8$	40
Sodium perfluoro-1-[1,2,3-$^{13}C_3$] hexanesulfonate	PFHxS-$^{13}C_3$	40
Perfluoro-n-[1,2,3,4,5,6,7-$^{13}C_7$] undecanoic acid	PFUnDA-$^{13}C_7$	40

Table 2.3 | Information of labelled OPE compounds used as surrogate.

OPE Surrogate Mixture			
Compound name	Abbreviation	Concentration (ng μL^{-1})	Mass added (ng)
Tri-n-buthyl phosphate - d27	D27-TNBP	1	50
Triphenyl phosphate – d15	D15-TPhP	1	50
Tris (2-chloroethyl) phosphate - d12	D12-TCEP	1	50
Tri-n-propyl phosphate - d21	D21-TPrP	1	50
Tris (2-chloroisoprpyl) phosphate – d18	D18-TCPP	1	50
Tris (2-ethylhexyl) phosphate – d51	D51-TEHP	1	50
Triphenylphosphine oxide – d15	D15-TPPO	1	50

L pre-rinsed PTFE bottles from the inflatable boat at a depth of approximately 0.4 m depth. For the SML, 500 mL volume of sample were collected in 500 ml PTFE pre-rinsed bottles with the SML sampling technic previously described. Rain samples were collected in 2.5 L glass pre-rinsed bottles. The final volume collected depended on the intensity and duration of the rain event.

All samples were pre-processed in the vessel's laboratory following an established methodology with minor modifications (Casas et al., 2021) **(Figure 2.11)**. Briefly, all seawater samples (surface, DCM, 1PAR, MOx, DEEP, SML and SSL) were filtered through pre-combusted glass fiber filters (47 mm, GF/F, 0.7 µm mesh size, Whatman). Rain samples were not filtered but followed the same procedure as the other from this point on.

Next, samples were processed using a stablished solid phase extraction (SPE) method with Oasis HLB cartridges (Hydrophilic-Lipophilic-Balanced, 6 cm^3, 200 mg; Waters). Cartridges were preconditioned with 6 ml Propanol-2, and 6 ml HPLC-grade water, and then spiked with 50 ng of a mix of labelled recovery standards **(Table 2.3)** directly in the cartridge. Samples were then loaded into the cartridge at a flow rate of 1 ml min^{-1} After loading the 2 L samples, cartridges were washed with 6 mL of chromatographic-grade water at 5% of methanol, dried under vacuum for 10 - 15 minutes, and stored at -20ºC in sealed bags for further treatment.

In the ultra-clean laboratory, HLB cartridges were unfrozen for 2h at room temperature, centrifuged at 3500 rpm for 4' and eluted with 12 mL of methyl tert butyl ether:methanol (3:1; v/v). The residual water was removed by adding 3 g of pre-baked sodium sulfate. The final eluents were concentrated under a gentle stream of N_2 and reconstituted in 100 µL of toluene **(Figure 2.12).**

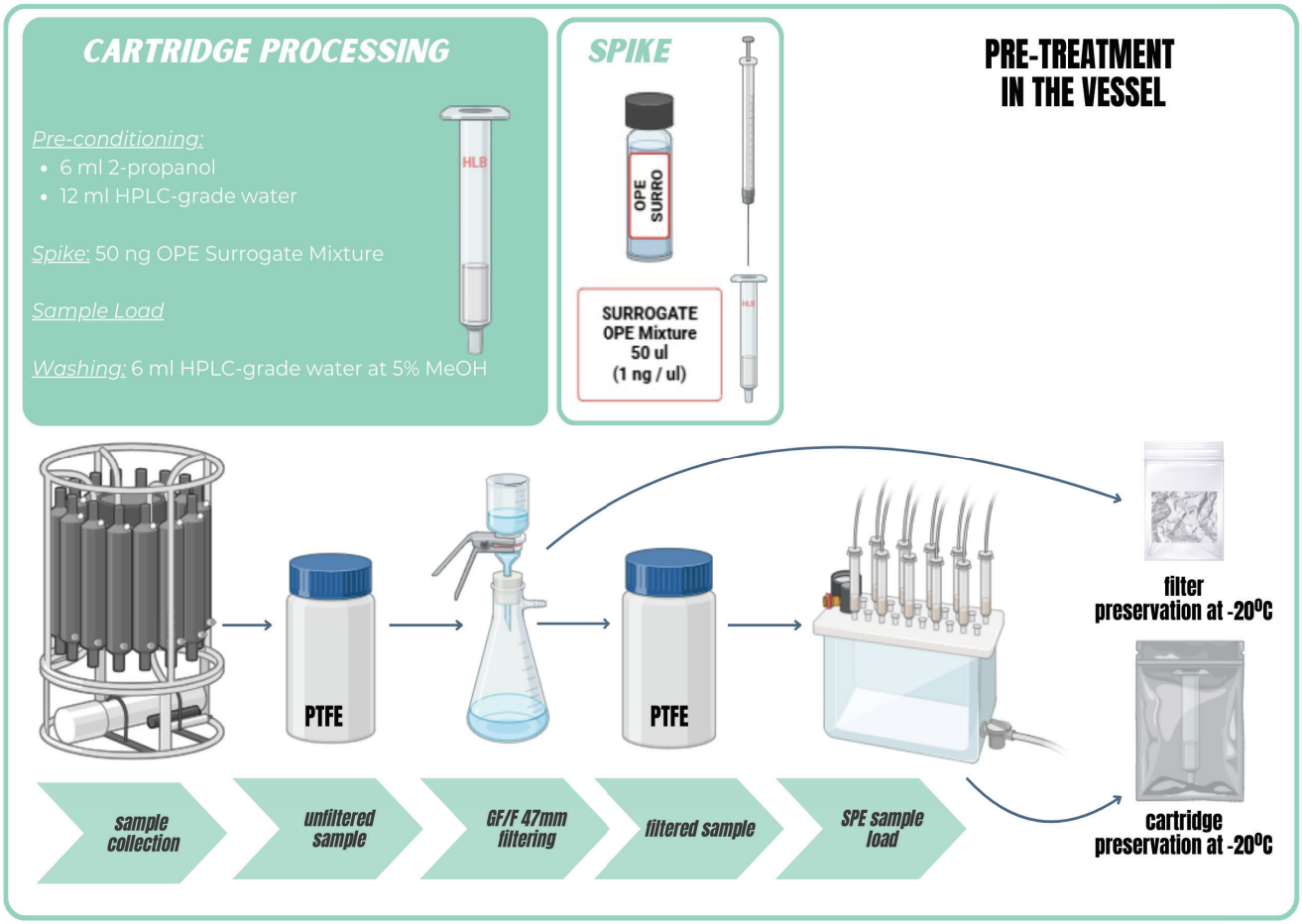


Figure 2.11 | Schematic overview of the samples pre-treatment in the vessels for OPE analysis in sea-water. *Created with https://BioRender.com.*

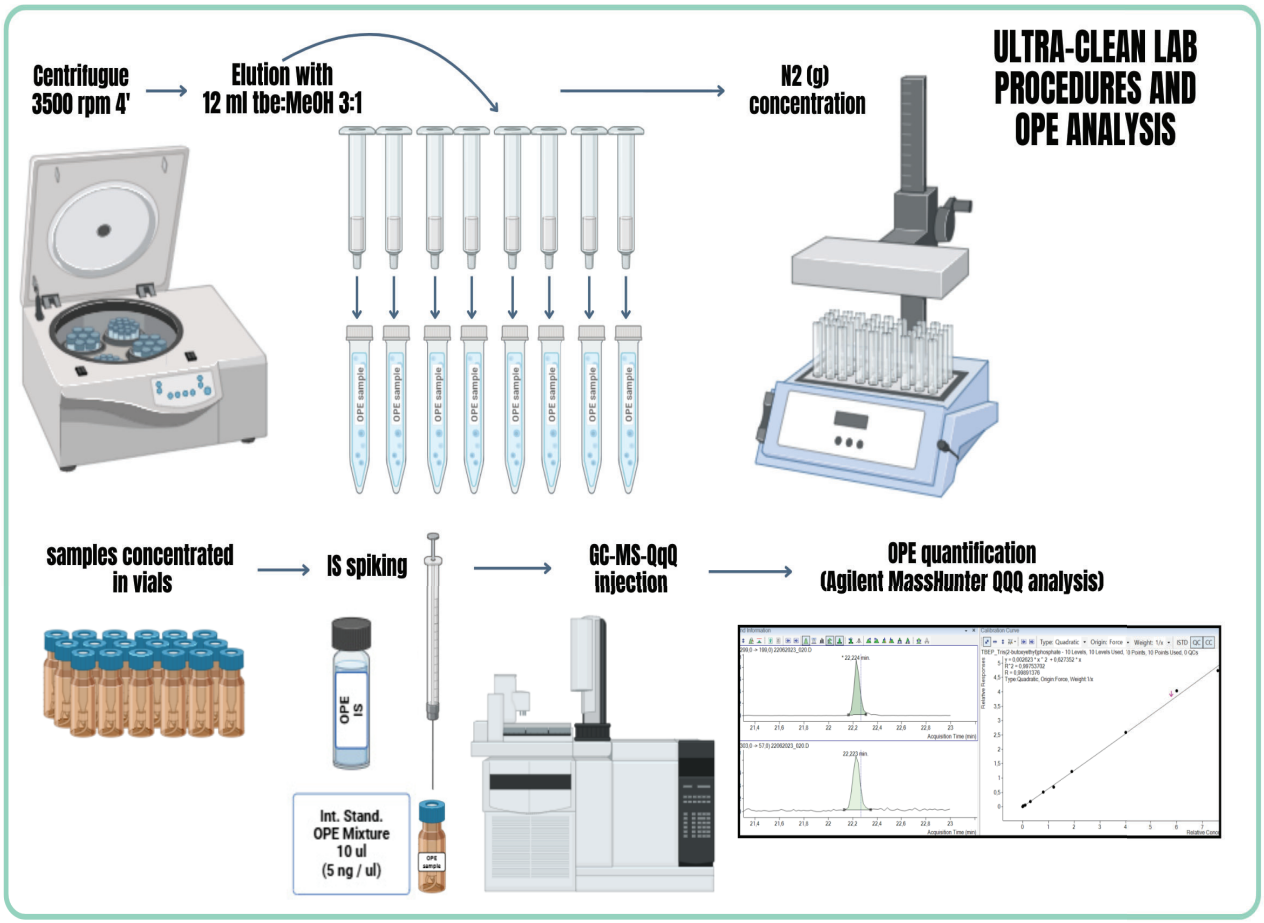


Figure 2.12 | Schematic overview of the analytical procedure for the extraction, concentration, and analysis of organophosphate esters (OPEs) from environmental samples in the ultra-clean lab and instrumental analysis. *Created with https://BioRender.com.*

OPE instrumental analysis was conducted by gas chromatography coupled to a triple quadrupole mass spectrometer in tandem (GC-MS/MS-QqQ). The chromatographic separation was carried out using a HP-5MS column (30m, 0.25 mm internal diameter, 0.25 µm film thickness) on an Agilent 7890A gas chromatograph. Methane was used as ionization gas and helium was used as a carrier gas at a constant flow mode of 20 mL min^{-1}. Five µl of sample were injected in split less mode at an injection port temperature of 280°C. The column temperatures were: 90°C for 1 min, increased at 15 °C min^{-1} to 200°C held for 6 min, then at 5°C min^{-1} to 250 °C, held for 6 min and then at 10°C min^{-1} to 315°C, held for 10 min. The detection was carried out with an Agilent 7000B triple quadrupole mass spectrometer using electronic impact ionization (EI) mode in positive mode. The EI source, transfer line and quadrupole temperature were 230°C, 280 °C and 300 °C, respectively. Acquisition was performed in multiple reaction monitoring (MRM). 50 ng of a mixture of three labelled compounds was used as Internal Standard **(Table 2.4).** Samples were quantified using a 12-point calibration curve ranging from 0.01 to 2 ng µl-1. Recoveries were monitored using TNBP-d27, TCEP-d12, TCPP-d18, TEHP-d51 and TPhP-d15 as recovery standards prior to the extraction.

2.5. QUALITY CONTROL AND QUALITY ASSURANCE

Due to the relatively low environmental concentrations of OPEs and PFAS in the ocean (up to a few ng L^{-1} for OPEs, and a few pg L^{-1} for PFAS) sample concentrations are often close to the method's limit of quantification (LOQ). For this reason, good quality control procedures are essential both in the vessel, and laboratory to ensure the quality of the data presented.

All containers, tubes, and connections for sampling and chemical analysis were made of stainless steel, glass, PP or PTFE (for PFAAs and OPEs, respectively).

Table 2.4 | Information of labelled OPE compounds used as Internal Standard.

OPE Internal Standard Mixture			
Compound name	**Abbreviation**	**Concentration (ng µL^{-1})**	**Mass added (ng)**
Tris (1.3-dichloro-2-propyl) phosphate - d15	D15-TDCPP	5	50
Tris (2-butoxyethyl) phosphate - $^{13}C_2$	M6TBEP	5	50
Triphenyl phosphate - $^{13}C_{18}$	MTPhP	5	50

Prior to the campaigns, glass material was pre-cleaned with detergent and rinsed with distilled water, dried under the fume hood, and rinsed with MeOH and acetone. GF/F and GF/D filters and all glass material was combusted at 450°C for 4h before their use and protected with pre-combusted aluminum foil. PP and PTFE material was pre-cleaned with detergent and rinsed with distilled water, and then rinsed with acetone and let it dry until evaporation under a fume hood. SPE material (Baker system, capillary, valves, and tubing) was pre-cleaned with MeOH and acetone. All material was protected with aluminum foil and zip-lock bags during the transport to the RVs. During the oceanographic cruises, all material was cleaned with MeOH and acetone every two days and rinsed with seawater between each swap of samples.

All environmental samples were processed in an ultra-clean lab environment under strict contamination control protocols. The clean lab was equipped with negative pressure to minimize the risk of airborne contaminants, ensuring that the integrity of the samples was maintained. A clean lab-coat and clogs were used only inside the clean lab to ensure no contamination entered from outside.

Field blanks (FBs) consisted of GF/D filters and cartridges that followed the same procedure and analysis as the samples from the vessel's lab the ultra-clean lab. No water was loaded into the cartridges; however, they were connected to the SPE system during the same time than the samples to replicate handling conditions. Field blank GF/F and GF/D filters were performed by placing them in the same suction flask and leaving then connected during 3' to the vacuum pump. Then, they were folded and protected with foil inside a zip-lock bag along the rest of the GF/F filter from the samples. Procedural blanks consisted in samples where the same elution solvent (tert:metyl butyl eter, in the case of OPEs; MeOH with 0.1% ammonia for PFAS) was loaded through the pre-conditioned cartridge into a vial, and followed the same extraction and analysis procedures as the rest of the samples. A procedural and field blank were analyzed for each batch of samples to monitor potential contamination from the field and laboratory. The limits of quantification (LOQs) were defined as the mean concentration of field and procedural blanks plus three times the standard deviation.

Only samples above LOQ were considered. For statistical analysis, nd and <loq values were replaced by their loq/2. Samples were also recovery corrected with the recoveries from the Surrogate Standards.

Matrix spike tests (Quality Controls) were performed during both cruises to evaluate potential losses of target analytes throughout the entire sampling and analytical process, from collection to injection. These tests involved spiking cartridges with both the Surrogate Standard and a mixture containing the same native compounds analyzed in the samples. The matrix spikes were processed alongside environmental samples to assess the recovery rates of the target analytes and identify any potential degradation or loss during sample handling, extraction, and analysis. This procedure ensured the accuracy and reliability of the analytical results by providing a measure of the method's efficiency under real sampling conditions.

2.6. REFERENCES

Casas, G., Martínez-Varela, A., Roscales, J. L., Vila-Costa, M., Dachs, J., & Jiménez, B. (2020). Enrichment of perfluoroalkyl substances in the sea-surface microlayer and sea-spray aerosols in the Southern Ocean. Environmental Pollution 267, 1–30.

Casas, G., Martinez-Varela, A., Vila-Costa, M., Jiménez, B., & Dachs, J. (2021). Rain Amplification of Persistent Organic Pollutants. Environmenal Science and Technologies, 55(19), 12961–12972.

Casas, G., Iriarte, J., D'Agostino, L. A., Roscales, J. L., Martinez-Varela, A., Vila-Costa, M., Martin, J. W., Jiménez, B., & Dachs, J. (2023). Inputs, amplification and sinks of perfluoroalkyl substances at coastal Antarctica. Environmental Pollution 338.

González-Gaya, B., Casal, P., Jurado, E., Dachs, J., & Jiménez, B. (2019). Vertical transport and sinks of perfluoroalkyl substances in the global open ocean. Environmental Sciences: Processes and Impacts, 21(11), 1957–1969.

Harvey, G., & Burzell. (1966). Simple microlayer method for Small Samples. 156–157.

MAIN CHAPTERS

03



GUIDE TO THE MAIN CHAPTERS

CHAPTER	PUBLICATION	PAGE
CHAPTER I	**OCCURRENCE OF AROMATIC-LIKE COMPOUNDS IN THE GLOBAL OCEAN**	107
	Paper I: Dissolved Black Carbon and Semivolatile Aromatic Hydrocarbons in the Ocean: Two Entangled Biogeochemical Cycles? **Authors:** Núria Trilla-Prieto, Maria Vila-Costa, Gemma Casas, Begoña Jiménez, and Jordi Dachs **Published** in ES&T-letters (Environ. Sci. Technol. Lett. 2021, 8, 918−923) doi: 10.1021/acs.estlett.1c00658	
CHAPTER II	**TRANSPORT AND BIOGEOCHEMISTRY OF PFAAs IN THE OCEANS**	123
	Paper II: Accumulation of Perfluoroalkyl Acid "Forever Chemicals" in Antarctic Waters **Authors**: Núria Trilla-Prieto, Jordi Dachs, Jon Iriarte, Naiara Berrojalbiz, Pere Colomer-Vidal, Gemma Casas, Odei Garcia-Garin, Maria Vila-Costa and Begoña Jiménez Submitted to Science Advances in January 2025	
CHAPTER III	**TRANSPORT AND BIOGEOCHEMISTRY OF OPEs IN THE OCEANS**	150
	Paper III: Enrichment of Organophosphate Esters in the Sea Surface Microlayer from the Atlantic and Southern Oceans **Authors**: Núria Trilla-Prieto, Jon Iriarte, Naiara Berrojalbiz, Gemma Casas, Cristina Sobrino, Maria Vila-Costa, Begoña Jiménez, and Jordi Dachs **Published** in ES&T-letters (Environ. Sci. Technol. Lett. 2024, 11, 1008−1015) doi: 10.1021/acs.estlett.4c00636w	
		188
	Paper IV: Biogeochemical Controls on Latitudinal (42°N to 70°S) and Depth Distribution of Organophosphate Esters in the Atlantic and Southern Oceans **Authors**: Núria Trilla-Prieto, Naiara Berrojalbiz, Jon Iriarte, Antonio Fuentes-Lema, Cristina Sobrino, Maria Vila-Costa, Begoña Jiménez, and Jordi Dachs Submitted to ES&T in November 2024	
CHAPTER IV	**SCIENTIFIC OUTREACH WITHIN ACADEMIA**	239
	Paper V: Balancing the equation: A tool for evaluating effective scientific outreach **Authors**: Núria Trilla-Prieto, Maria Paula Carrillo, Clara Serrano, Jon Iriarte, Jessica Patrone, and Naiara Berrojalbiz *To submit at Frontiers in Science and Environmental Communication*	





PART 03

CHAPTER 1.

Ocurrence of aromatic-like compounds in the global ocean.

3.1.1. Paper I. *Dissolved Black Carbon and Semivolatile Aromatic Hydrocarbons in the Ocean: Two Entangled Biogeochemical Cycles?*

3.1.2. Paper I. Supplementary Materials

PART 03 - CHAPTER 1. OCCURRENCE OF AROMATIC-LIKE COMPOUNDS IN THE GLOBAL OCEAN

3.1.1. Paper I. *Dissolved Black Carbon and Semivolatile Aromatic Hydrocarbons in the Ocean: Two Entangled Biogeochemical Cycles?*

Núria Trilla-Prieto[1], Maria Vila-Costa[1], Gemma Casas[1], Begoña Jiménez[2], and Jordi Dachs[1]*.

[1]Department of Environmental Chemistry, IDAEA-CSIC, Barcelona, Catalunya, Spain.
[2]Department of Instrumental Analysis and Environmental Chemistry, IQOG-CSIC, Madrid, Spain
*Corresponding author email: jordi.dachs@idaea.csic.es

State: Published in ES&T-letters (Environ. Sci. Technol. Lett. 2021, 8, 918−923)
Accesible at doi: 10.1021/acs.estlett.1c00658

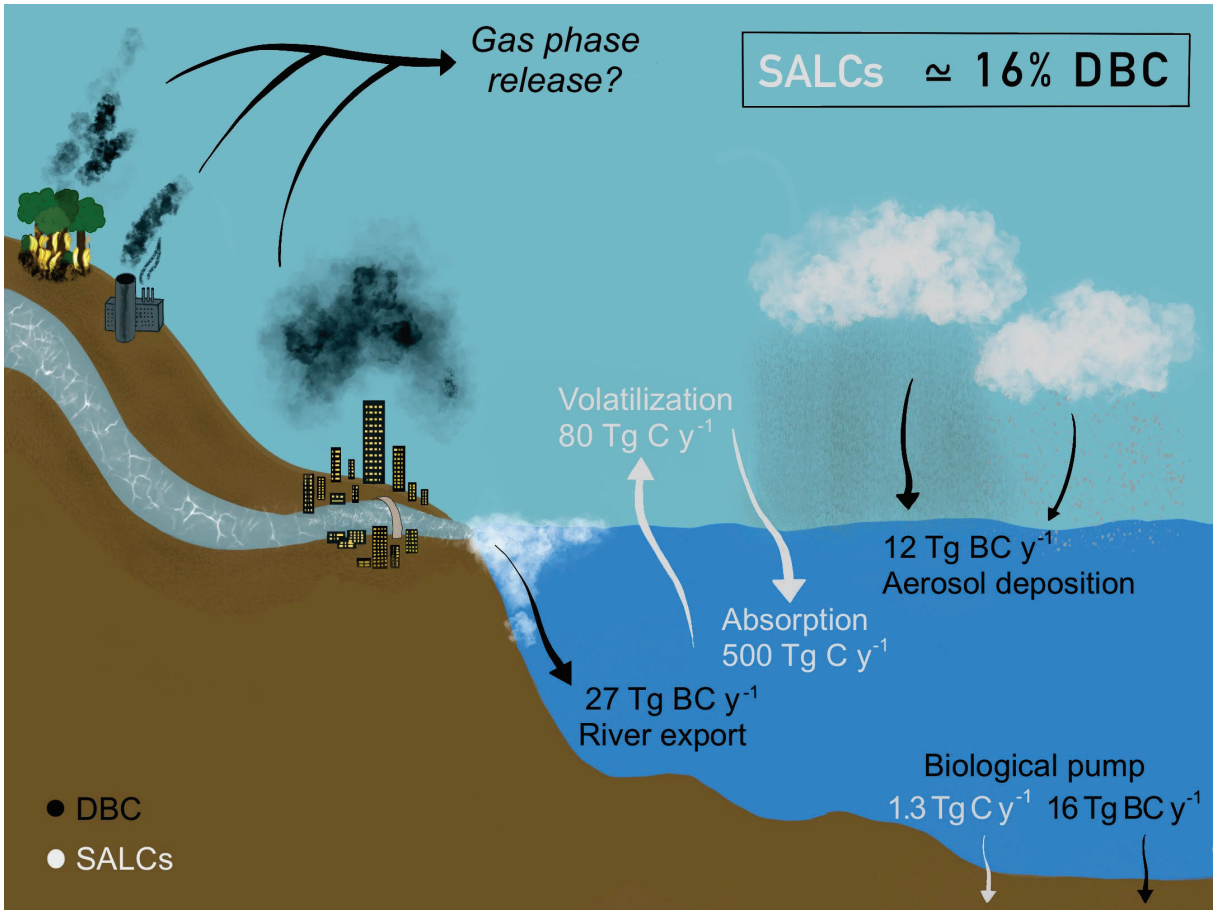


Figure 0 | Toc Art

Environmental Science & Technology Letters

pubs.acs.org/journal/estlcu

Letter

Dissolved Black Carbon and Semivolatile Aromatic Hydrocarbons in the Ocean: Two Entangled Biogeochemical Cycles?

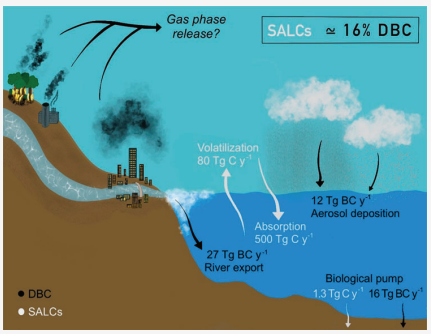
Núria Trilla-Prieto, Maria Vila-Costa, Gemma Casas, Begoña Jiménez, and Jordi Dachs*

Cite This: *Environ. Sci. Technol. Lett.* 2021, 8, 918–923

Read Online

ACCESS | Metrics & More | Article Recommendations | Supporting Information

ABSTRACT: Dissolved black carbon (DBC) plays a role in the oceanic carbon cycle. DBC originates from the heating and incomplete combustion of organic matter, including fossil fuels, a shared origin with polycyclic aromatic hydrocarbons (PAH). DBC is quantified using the benzene polycarboxylic acids produced by oxidation of the organic extract, a fraction of which derive from PAHs and other semivolatile aromatic-like compounds (SALCs). However, the current view of the DBC cycle does not take into account the inputs and sinks known for PAHs, such as diffusive air−water exchange and degradation. A meta-analysis of oceanic PAHs, SALCs, and DBC concentrations shows that SALCs account for 16% of DBC (ranging from 5% to 31%). Such a large contribution of semivolatile aromatic hydrocarbons to DBC is consistent with the large atmospheric input of SALCs (estimated as 400 Tg C y^{-1}). Furthermore, photodegradation at the surface ocean and microbial degradation in the water column of semivolatile DBC can be important sinks, consistent with the ubiquitous occurrence of the degradation genes of the metabolic routes for aromatic hydrocarbons. Future work should focus on the characterization of semivolatile DBC and its degradation in order to constrain its contribution to refractory organic matter and the anthropogenic perturbation of the carbon cycle.



INTRODUCTION

Black carbon originates from the heating and combustion of organic matter, such as during forest fires or use of fossil fuels. Semivolatile polycyclic aromatic hydrocarbons (PAHs) are also produced during these combustion processes, even though PAHs can also be released to the environment due to oil spills or even from natural sources. Particulate black carbon has been extensively studied in soils and the atmosphere due to its role in Earth radiation balance, health effects, and as an environmental sorbent for PAHs and other pollutants.[1−3] During recent years, there has been an increasing interest in dissolved black carbon (DBC) in the ocean.[3] Oceanic DBC accounts for between 0.1% and 4−7% of dissolved organic carbon (DOC).[3] DBC is old carbon, as determined by $\Delta^{14}C$ isotopic determinations,[4,5] and it has been suggested that DBC contributes to refractory organic matter and plays a key role in the slow cycle of DOC in the ocean.[5] Even though the major identified sources of DBC are riverine inputs, followed by atmospheric deposition of aerosol-bound black carbon,[3,6] the $\delta^{13}C$ signal of oceanic DBC is different than that of rivers, suggesting unaccounted sources of oceanic DBC.[7]

DBC is generally quantified by using benzene polycarboxylic acids (BPCA) as a proxy, and the determination of BPCA has become an operational definition of DBC, as the condensed aromatic fraction of DOC. BPCA are produced during the oxidation of pyrogenic organic matter[8,9] from well-known PAHs such as phenanthrene, pyrene, or benzo[a]pyrene but also from complex aromatic molecules present within the DBC pool of organic matter. Even though PAHs are known to be oxidized to BPCA, the accumulated knowledge of the biogeochemical cycle of PAHs and other semivolatile aromatic-like compounds (SALCs)[10,11] has been largely omitted when deciphering the transport, biogeochemical cycling, and fate of DBC.[3] While rivers and aerosol-bound PAHs are a known source of SALCs to the ocean, diffusive air−water exchange accounts for most of the input of SALCs, including PAHs and a large aromatic unresolved complex mixture (UCM), to the open ocean.[10] The relative importance of the different atmospheric inputs of aromatic compounds depend on their gas-particle partitioning, which is proportional to molecular weight and volatility. High MW PAHs are mainly deposited bound to aerosols, while PAHs with 2−5 aromatic rings are mainly deposited through diffusive exchange.[10] Concerning the oceanic sinks of PAHs, direct photolysis is important in the surface ocean,[11] but microbial degradation is the main sink in the overall water column.[11] The relevance of

Received: August 14, 2021
Published: September 9, 2021



Downloaded via 161.111.60.152 on October 11, 2022 at 16:32:52 (UTC).
See https://pubs.acs.org/sharingguidelines for options on how to legitimately share published articles.

PART 03

ACS Publications

© 2021 The Authors. Published by American Chemical Society

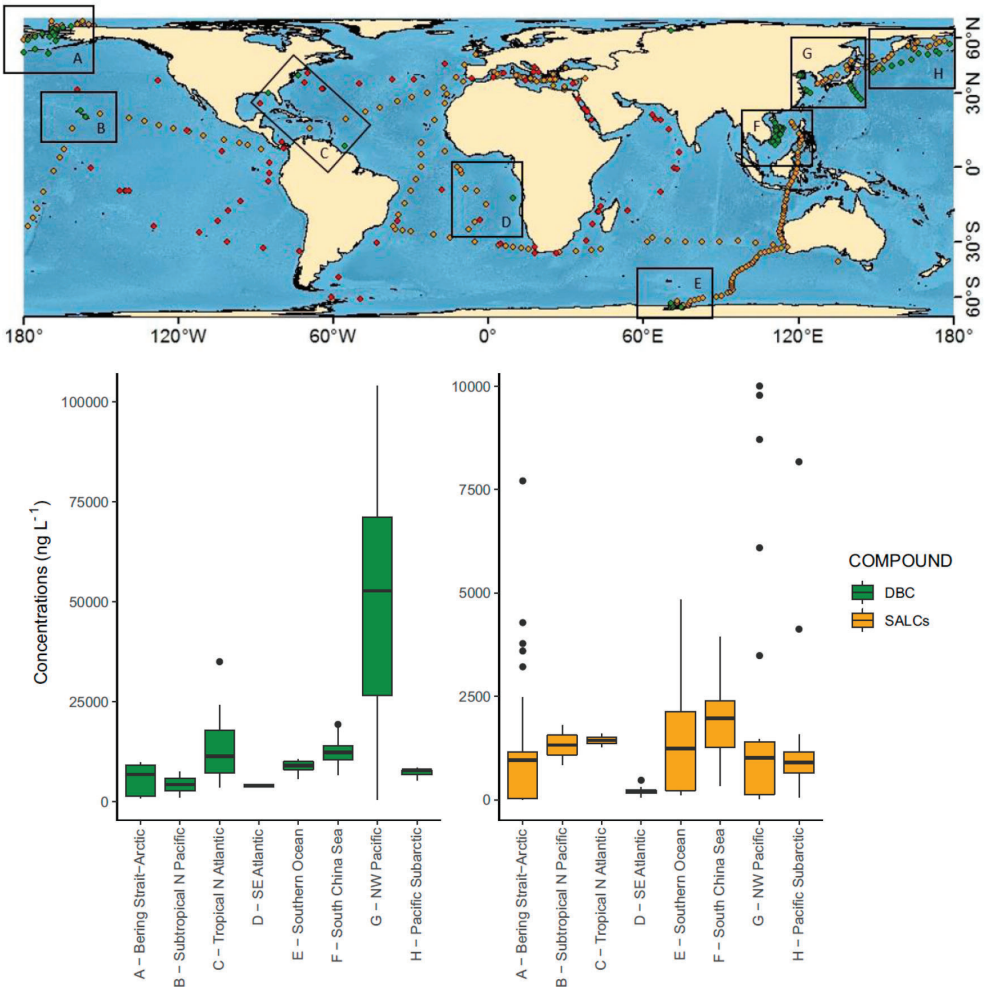


Figure 1. Comparison of dissolved black carbon and semivolatile aromatic-like hydrocarbons (SALCs) in the ocean. Upper panel shows all data points collected in the compilation. Green dots mark all DBC measurements, orange dots all PAHs measurements, and red dots all gene data points from Tara Oceans. Lower panel shows the box-plots of the dissolved black carbon and dissolved aromatic hydrocarbons for the eight oceanic regions shown in the upper panel.

biodegradation of DBC in the ocean is unclear. While charcoal leachates can partly be photo- and biodegraded,[12] as these contain a large suite of organic chemicals and not only condensed aromatic organic matter, its relevance for the persistence of oceanic DBC is under debate.[13,14]

The objective of this work was to compare the marine occurrence of SALCs and DBC, assess how the known biogeochemical cycle of PAHs can shed light to the sources and fate of oceanic DBC by addressing the feasibility of DBC photo- and biodegradation, the latter derived from oceanic metagenomes, and the implications of semivolatile DBC for this important pool of refractory DOC.

MATERIALS AND METHODS

Meta-Analysis of DBC and PAH Concentrations. The meta-analysis of DBC and PAH concentrations considered those papers reporting the dissolved phase concentrations of BC and PAHs. DBC and PAH literature sources were limited to those reporting concentrations in surface waters (0−25m for the DBC and 0−10m for PAHs) from the open ocean and coastal regions.[4,5,7−30] Reports of DBC and PAHs in rivers and estuaries were not considered. Generally, there are more oceanic measurements for PAHs than for DBC. However, all the DBC reports used the BPCA approach, with similar sampling and analysis methods, while PAHs sampling and the number of targeted compounds differ between studies. In this work, we take the operational definition of DBC as derived from the use of BPCA as a proxy, which defines DBC as the fraction of DOC with condensed aromatics. Validation of the DBC extraction methods and BPCA determination has demonstrated that not only high MW aromatic chemicals are quantified as DBC but also PAHs with a number of aromatic rings ranging from 3 to 7.[8,9] For example, the BPCA method has been validated for phenanthrene, pyrene, and fluoranthenes,[9] which are semivolatile PAHs with important diffusive inputs to the ocean.[10]

The different number of targeted PAHs in the different reports of marine PAHs needs to be taken into account when

https://doi.org/10.1021/acs.estlett.1c00658
Environ. Sci. Technol. Lett. 2021, 8, 918−923

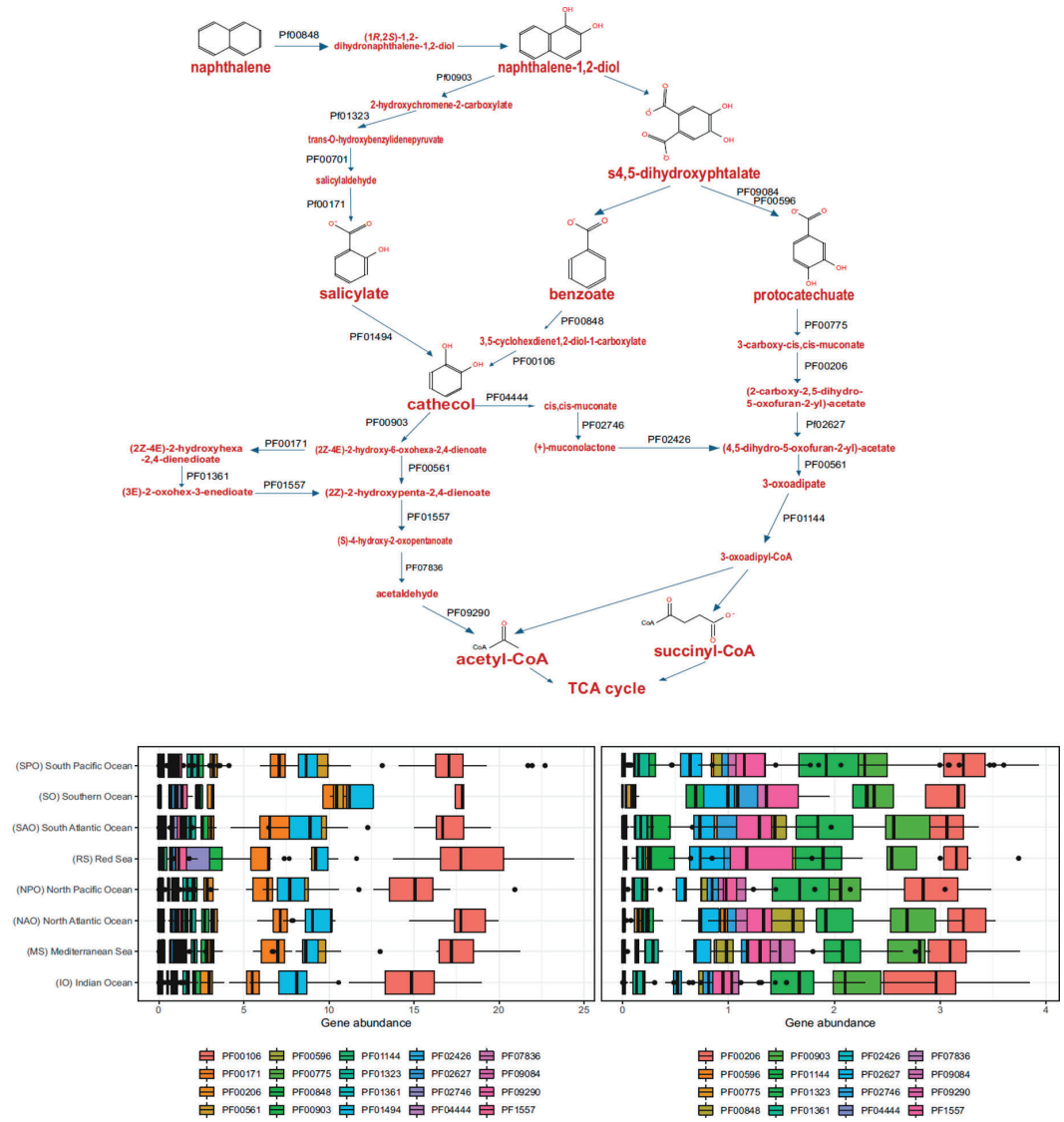


Figure 2. Abundance of key genes, from the Tara Oceans metagenomes, responsible for the metabolic routes of the degradation of aromatic hydrocarbons. Upper panel shows the PAH degradation route, and the lower panel the single-copy normalized abundance of the genes (notice the lower panel on the right zooms the less abundant genes). From the most abundant genes to the lowest, mean surface concentrations (copies/cell) are PF00106 at 16.7, PF00561 at 9.06, PF01494 at 8.89, PF00171 at 6.71, PF00206 at 3.13, PF00903 at 2.44, PF01323 at 1.94, PF09084 at 1.81, PF1557 at 1.69, PF02746 at 1.03, PF00848 at 1.01, PF00596 at 0.928, PF02627 at 0.650, PF01144 at 0.276, PF01361 at 0.190, PF00775 at 0.131, PF07836 at 0.0199, PF09290 at 0.0192, PF02426 at 0.0145, and PF0444 at 0.0628.

estimating the total SALCs. Phenanthrene, anthracene, fluoranthene, and pyrene were taken as the reference compounds for comparing the different works reporting PAHs (as $\sum_4$PAH), as the concentrations for these individual hydrocarbons are commonly reported in all previous field assessments of PAHs. Other works report up to 64 individual PAHs.[10,11,27] For the SALCs estimation, we used a mean ratio for the $\sum_{64}$PAH/$\sum_4$PAH of 2.46 and a mean ratio SALCs/$\sum_{64}$PAH of 456 as reported elsewhere.[9,10,24] This approach allowed us to undertake a conversion of the PAH concentrations to the total SALCs, so the comparison of SALCs and DBC could be done. The data set compiled did not include the values under the detection limit. Only DBC and PAH concentrations determined from active solid phase extraction of seawater were considered.

From all the compiled data, eight specific zones were selected where data from DBC and PAHs were available (Figure 1). Mean and SD were calculated for each zone and chemical class. In order to assess the contribution from SALCs to DBC, the ratios of SALCs/DBC were calculated for each zone (Table S1).

Bioinformatics. Relative abundances of PAH-degrading genes were quantified using hidden Markov models (HMMs) which are sensitive tools for the identification of protein and

https://doi.org/10.1021/acs.estlett.1c00658
Environ. Sci. Technol. Lett. 2021, 8, 918−923

protein domain sequences. HMMs corresponding to the complete degradation of naphthalene (as model PAH molecule, Figure 2) were downloaded from the Pfam website.[31] Similarly, HMMs corresponding to five single-copy marker genes were also downloaded (namely, PF00154, PF00204, PF04561, PF04563, and PF04565). The HMMs were used to search all protein sequences from metagenomes from the Tara Oceans expedition (2009−2013)[32] using HMMER[33] with score thresholds built into the Pfam profiles. The identified proteins were subsequently quantified in surface and deep-chlorophyll maximum (DCM) samples of the free-living bacterial fraction (cells collected on an 0.22 μm filter after prefiltration through a 3 μm filter). The PAH-degrading gene abundances were normalized by division with the mean abundance of the five single-copy genes.

RESULTS AND DISCUSSION

Our meta-analysis of reported concentrations of DBC shows that most previous measurements have so far covered continental shelf regions in the western and northern Pacific Ocean regions, in the eastern North Atlantic, and some measurements in the maritime Antarctica (Figure 1). There are large open ocean regions that remain unassessed in terms of DBC occurrence and cycling. Concentrations of oceanic DBC range between 0.0005 and 0.104 mg C L^{-1}, with the highest concentrations in the Northwest Pacific (regional average of 0.048 mg C L^{-1}). This is consistent with the available data of global carbon emissions, as China, with a gross population of 1.36 billion in East Asia, is the world's largest BC emitter.[34] In the Southern Ocean and maritime Antarctica, the values ranged between 0.005 and 0.01 mg C L^{-1}, while in the Arctic region DBC ranged between 0.0009 and 0.009 mg C L^{-1} in the Bering Sea and between 0.005 and 0.008 mg C L^{-1} in the Subarctic North Pacific. No other latitudinal trends were found a part from the lower values found in the Arctic and Antarctica.

Previous PAH measurements show a more complete spatial coverage of the vast oceanic regions thanks to measures performed during north−south latitudinal transects in the eastern Atlantic and western Pacific, in polar regions, and during the Malaspina circumnavigation. Depending on the research group performing the analysis, a different number of targeted PAHs are considered. In this work, we took the sum of phenanthrene, anthracene, pyrene, and fluoranthene as reference for comparison purposes, as these four PAHs are commonly targeted in all studies. The $\sum_4$PAH ranged from 0.003 to 11.3 ng L^{-1}, with a mean of 1.34 ng L^{-1}. Concentrations of PAHs in the Southern Ocean and maritime Antarctica ranged from 0.011 to 4.3 ng L^{-1} and in the Arctic from 0.4 to 6.8 ng L^{-1}. The number of individual PAHs reported in the literature usually range between 16 and 64,[10,27] as determined by target analysis, but these account for a small fraction of the total SALCs in natural waters. The estimated SALCs in the ocean, including PAHs and the aromatic UCM (see Materials and Methods), average 2500 ng L^{-1}, ranging between 350 and 4500 ng L^{-1}.[10]

The comparison of DBC and SALC concentrations was feasible for eight oceanic regions (Figure 1 and Figure S1). For these regions, SALCs account for 16% of reported DBC concentrations, ranging between 5% and 31% of DBC (Table S1). The ratio of SALCs/DBC shows a remarkable variability (Table S1). The lowest SALCs/DBC ratios were found in the Atlantic (Zones C and D in Figure 1), especially in the South Atlantic Ocean (SALCs/DBC = 5, zone D), which receives inputs of DBC from Africa and South America (probably important sources from forest fires). The ratios in the Northwest Pacific (SALCs/DBC = 4.6, zone G) are also low, comparable to those in the South Atlantic. The sources of atmospheric particulate black carbon are enormous in eastern Asia (China and India among other countries), which suggest that sources of DBC through rivers and/or the atmosphere may also be important, thus resulting in a lower SALCs/DBC ratio. This would mean that those oceanic regions receiving higher inputs of DBC from biomass (maybe anthropogenic as well) may have lower SALCs/DBC ratios. On the contrary, in the Arctic and Subarctic (Zones A, B, and H), the ratios of SALCs/DBC were the highest (ranging from 22 to 31), which suggest that these regions have higher input of PAHs and other semivolatile aromatic compounds. The ratio in other remote regions such as in the Southern Ocean is also high (15.7, zone E) but lower than in the Arctic. In any case, the Southern Ocean is the most distant region to known sources of both DBC and PAHs.

A number of PAHs with 3−7 aromatic rings have been used to validate the BPCA analytical methods commonly used to quantify DBC.[8,9] As DBC can be viewed as the condensed aromatic fraction of DOC, this comparison shows that there is a significant and relevant fraction of DBC that is composed of semivolatile aromatic compounds. This contrasts with the current view of the DBC cycle in the ocean,[3] which neglects those processes and sources known to be important for semivolatile aromatic compounds. Semivolatile DBC exchanges diffusively between the atmosphere and the ocean. Rivers have been thought, so far, to be the main input of DBC, estimated as 27 Tg C y^{-1} [3], followed by partial dissolution of aerosol black carbon in seawater, as DBC after atmospheric deposition, estimated as an input of 1.8 Tg C y^{-1} [3]. In comparison, the atmospheric deposition of aerosol BC is of 12 Tg C y^{-1} [1]. The estimated atmospheric deposition input of aerosol-bound SALCs to the ocean is of 6 Tg C y^{-1}, thus about 50% the deposition of aerosol BC. Part of these SALCs, together with yet unquantified oxidized SALCs present in aerosols, account for the observed water-soluble BC fraction (or DBC). However, most of PAHs and SALCs enter the ocean by diffusive air−water exchange,[9] which has been estimated as an input of 400 Tg C y^{-1}, much larger than previously reported inputs of DBC. This suggests that in the open ocean, atmospheric deposition, rather than rivers, will be the main input of DBC. Furthermore, diffusive air−water exchange accounts for a direct input to the dissolved phase, without the redissolution and partitioning processes between deposited aerosols and water.

An important issue is to discern to which degree this large input of semivolatile DBC is consistent with our current knowledge of the DBC cycle in the ocean. The δ^{13}C signal of oceanic DBC is enriched when compared with rivers. A large input by diffusive air−water exchange could account for a fraction of the missing source of DBC in the ocean as indicated by the δ^{13}C signal of oceanic DBC. Unfortunately, the δ^{13}C signal of gas phase SALCs remains unknown. However, the few available δ^{13}C measurements for PAHs in soils have been reported to range between −23.81‰ and −24.19‰.[35] The potential importance of an anthropogenic source of DBC in the ocean is also consistent with δ^{13}C of −23.2 ‰ for coal pyrolysis at low temperature and −25.3‰ for liquid fuel combustion.[35] The Δ^{14}C of BPCA in the ocean shows old carbon,[3] which would also be consistent with a relevant

https://doi.org/10.1021/acs.estlett.1c00658
Environ. Sci. Technol. Lett. 2021, 8, 918−923

contribution from anthropogenic SALCs. Future work should resolve the isotopic signal of semivolatile DBC inputs. Second, the assessment of oceanic sinks can provide further evidence of the key controls of oceanic DBC. The biological pump fluxes of DBC and SALCs, referred here as settling to deep waters due to DBC and SALC partitioning to sinking particles, have been estimated to be 16 and 1.3 Tg C y^{-1}, respectively.[3,10] These figures are much lower than the atmospheric inputs of aromatic compounds; therefore, there are large sinks that account for more than 96% and 99% of the DBC and SALCs removal in the photic zone, respectively. For SALCs, photo- and biodegradation can account for this large degradation of SALCs. Direct photodegradation of PAHs is important in the surface ocean, while biodegradation has been suggested to dominate in the top 200 m of the ocean.[11] Photodegradation has also been reported to be relevant as a transformation mechanism of DOC in the top ocean[36] and could be analogously relevant for DBC. Experiments done by irradiating deep oceanic waters showed that a fraction of DBC can be photodegraded, suggesting that this is limited by the short time period that DBC molecules spend in the surface ocean.[18] The microbial degradation routes of aromatic compounds in seawater are fairly well known,[37,38] and the first step in this degradation is performed by ring hydroxylating dioxygenase, widespread in the surface ocean.[11] While hydroxylated PAHs are not quantified by target analysis of PAHs, they would still be quantified as DBC using BPCA as a proxy. A more complete degradation of aromatic compounds is needed in order to quantify the removal of DBC from the water column. Analysis of oceanic metagenomes show that there is widespread occurrence of the genes involved in the metabolic routes of aromatic compounds in oceanic microbiomes (Figure 2). As far as we know, this is the first time that the ubiquity of the genes responsible for complete degradation of aromatic hydrocarbons are assessed in the ocean. Such ubiquity of degradation genes suggests that this degradation of DBC is feasible, even though the fact that some genes have very low abundance (Figure 2) may limit the degree of respiration of DBC. However, large aromatic compounds show slower biodegradation than smaller aromatic molecules and independent of their oxidation degree will partition to particulate organic matter (including soot), which may significantly decrease the bioavailable fraction of DBC for microbial degradation. Therefore, there is the possibility of a contrasting fate of two DBC pools. On one side are the semivolatile DBC pool (SALCs), with lower MW aromatic molecules which are largely degraded in the ocean, and on the other side are the high MW condensed aromatic compounds, also being part of DBC which may be recalcitrant in the marine environment. These biogeochemical controls on the fate of DBC degradation will require further experimental confirmation in the future. Current field evidence shows, however, that BC/OC in sediments can be as high as 0.35,[2] while in the surface ocean, the DBC/DOC range is between 0.001 and 0.07.[3] As part of the biogeochemical cycle of DBC, there is a continuous partitioning between the dissolved and particulate phases (also for the transformation products), as known for PAHs. Thus, the oceanic cycles of dissolved and particulate BC are closely coupled. Despite an important degradation of DBC in surface waters, mainly the semivolatile component (SALCs), there is a preferential degradation of organic matter in comparison to BC, thus rendering DBC and particulate black carbon key components of the refractory carbon in the ocean. The consideration of a semivolatile component of the black carbon cycle, previously neglected, has important implications for the understanding of the marine cycle of this ultimately recalcitrant pool of organic matter and its anthropogenic perturbation.

■ ASSOCIATED CONTENT

Supporting Information

The Supporting Information is available free of charge at https://pubs.acs.org/doi/10.1021/acs.estlett.1c00658.

Summary of DBC and PAH concentrations (Table S1) and global distribution of DBC and SALC concentrations (Figure S1) (PDF)

■ AUTHOR INFORMATION

Corresponding Author

Jordi Dachs − *Department of Environmental Chemistry, IDAEA-CSIC, Barcelona, Catalunya 08034, Spain;* orcid.org/0000-0002-4237-169X; Email: jordi.dachs@idaea.csic.es

Authors

Núria Trilla-Prieto − *Department of Environmental Chemistry, IDAEA-CSIC, Barcelona, Catalunya 08034, Spain;* orcid.org/0000-0001-6973-9514

Maria Vila-Costa − *Department of Environmental Chemistry, IDAEA-CSIC, Barcelona, Catalunya 08034, Spain*

Gemma Casas − *Department of Environmental Chemistry, IDAEA-CSIC, Barcelona, Catalunya 08034, Spain*

Begoña Jiménez − *Department of Instrumental Analysis and Environmental Chemistry, IQOG-CSIC, Madrid 28006, Spain;* orcid.org/0000-0002-2401-4648

Complete contact information is available at: https://pubs.acs.org/10.1021/acs.estlett.1c00658

Notes

The authors declare no competing financial interest.

■ ACKNOWLEDGMENTS

This work was supported by the ANTOM project funded by the Spanish Research Agency from the Ministry of Science (PGC2018-096612-B-I00). N.T. and G.C. acknowledge FPI Ph.D. fellowships from the Spanish Research Agency. The research group of Global Change and Genomic Biogeochemistry receives support from the Catalan Government (2017SGR800). This research is part of POLARCSIC activities. IDAEA-CSIC is a Centre of Excellence Severo Ochoa (Spanish Ministry of Science and Innovation, Project CEX2018-000794-S).

■ REFERENCES

(1) Jurado, E.; Dachs, J.; Duarte, C. M.; Simó, R. Atmospheric deposition of organic and black carbon to the global oceans. *Atmos. Environ.* **2008**, *42*, 7931−7939.

(2) Lohmann, R.; Bollinger, K.; Cantwell, M.; Feichter, J.; Fischer-Bruns, I.; Zabel, M. Fluxes of soot black carbon to South Atlantic sediments. *Global Biogeochem. Cycles* **2009**, *23*, GB1015.

(3) Wagner, S.; Jaffé, R.; Stubbins, A. Dissolved black carbon in aquatic ecosystems. *Limnol. Oceanogr. Lett.* **2018**, *3*, 168−185.

(4) Ziolkowski, L. A.; Druffel, E. R. M. Aged black carbon identified in marine dissolved organic carbon. *Geophys. Res. Lett.* **2010**, *37*, 4−7.

(5) Coppola, A. I.; Druffel, E. R. M. Cycling of black carbon in the ocean. *Geophys. Res. Lett.* **2016**, *43*, 4477−4482.

(6) Bao, H.; Niggemann, J.; Luo, L.; Dittmar, T.; Kao, S. J. Aerosols as a source of dissolved black carbon to the ocean. *Nat. Commun.* **2017**, *8*, 8.
(7) Wagner, S.; Brandes, J.; Spencer, R. G. M.; Ma, K.; Rosengard, S. Z.; Moura, J. M. S.; Stubbins, A. Isotopic composition of oceanic dissolved black carbon reveals non-riverine source. *Nat. Commun.* **2019**, *10*, 1−8.
(8) Dittmar, T. The molecular level determination of black carbon in marine dissolved organic matter. *Org. Geochem.* **2008**, *39*, 396−407.
(9) Ziolkowski, L. A.; Chamberlin, A. R.; Greaves, J.; Druffel, E. R. M. Quantification of black carbon in marine systems using the benzene polycarboxylic acid method: a mechanistic and yield study. *Limnol. Oceanogr.: Methods* **2011**, *9*, 140−149.
(10) González-Gaya, B.; Fernández-Pinos, M.-C.; Morales, L.; Méjanelle, L.; Abad, E.; Piña, B.; Duarte, C. M.; Jiménez, B.; Dachs, J. High atmosphere-ocean exchange of semivolatile aromatic hydrocarbons. *Nat. Geosci.* **2016**, *9*, 438−442.
(11) González-Gaya, B.; Martínez-Varela, A.; Vila-Costa, M.; Casal, P.; Cerro-Gálvez, E.; Berrojalbiz, N.; Lundin, D.; Vidal, M.; Mompeán, C.; Bode, A.; Jiménez, B.; Dachs, J. Biodegradation as an important sink of aromatic hydrocarbons in the oceans. *Nat. Geosci.* **2019**, *12*, 119−125.
(12) Qi, Y.; Fu, W.; Tian, J.; Luo, C.; Shan, S.; Sun, S.; Ren, P.; Zhang, H.; Liu, J.; Zhang, X.; Wang, X. Dissolved Black Carbon Is Not Likely a Significant Refractory Organic Carbon Pool in Rivers and Oceans. *Nat. Commun.* **2020**, *11*, 5051.
(13) Bostick, K. W.; Zimmerman, A. R.; Goranov, A. I.; Mitra, S.; Hatcher, P. G.; Wozniak, A. S. Biolability of fresh and photodegraded pyrogenic dissolved organic matter from laboratory-prepared chars. *J. Geophys. Res.: Biogeosci.* **2021**, *126*, e2020JG005981.
(14) Wagner, S.; Coppola, A. I.; Stubbins, A.; Dittmar, T.; Niggemann, J.; Drake, T. W.; Seidel, M.; Spencer, R. G. M.; Bao, H. Questions remain about the biolability of dissolved black carbon along the combustion continuum. *Nat. Commun.* **2021**, *12*, 4281.
(15) Fang, Y.; Chen, Y.; Tian, C.; Wang, X.; Lin, T.; Hu, L.; Li, J.; Zhang, G.; Luo, Y. Cycling and Budgets of Organic and Black Carbon in Coastal Bohai Sea, China: Impacts of Natural and Anthropogenic Perturbations. *Global Biogeochem. Cycles* **2018**, *32*, 971−986.
(16) Fang, Z.; Yang, W.; Chen, M.; Ma, H. Source and Fate of Dissolved Black Carbon in the Western South China Sea During the Southwest Monsoon Prevailing Season. J. Geophys. Res. *J. Geophys. Res.: Biogeosci.* **2017**, *122*, 2817−2830.
(17) Fang, Z.; Yang, W.; Chen, M.; Stubbins, A.; Ma, H.; Jia, R.; Li, Q.; Chen, Q. Transport of Dissolved Black Carbon from the Prydz Bay Shelf, Antarctica to the Deep Southern Ocean. *Limnol. Oceanogr.* **2018**, *63*, 2179−2190.
(18) Stubbins, A.; Niggemann, J.; Dittmar, T. Photo-Lability of Deep Ocean Dissolved Black Carbon. *Biogeosciences* **2012**, *9*, 1661−1670.
(19) Nakane, M.; Ajioka, T.; Yamashita, Y. Distribution and Sources of Dissolved Black Carbon in Surface Waters of the Chukchi Sea, Bering Sea, and the North Pacific Ocean. *Front. Earth Sci.* **2017**, *5*, 1−12.
(20) Dittmar, T.; Paeng, J.; Gihring, T. M.; Suryaputra, I. G. N. A.; Huettel, M. Discharge of Dissolved Black Carbon from a Fire-Affected Intertidal System. *Limnol. Oceanogr.* **2012**, *57* (4), 1171−1181.
(21) Dittmar, T.; De Rezende, C. E.; Manecki, M.; Niggemann, J.; Coelho Ovalle, A. R.; Stubbins, A.; Bernardes, M. C. Continuous Flux of Dissolved Black Carbon from a Vanished Tropical Forest Biome. *Nat. Geosci.* **2012**, *5* (9), 618−622.
(22) Mannino, A.; Harvey, H. R. Black Carbon in Estuarine and Coastal Ocean Dissolved Organic Matter. *Limnol. Oceanogr.* **2004**, *49* (3), 735−740.
(23) Dittmar, T.; Paeng, J. A Heat-Induced Molecular Signature in Marine Dissolved Organic Matter. *Nat. Geosci.* **2009**, *2* (3), 175−179.
(24) Ke, H.; Chen, M.; Liu, M.; Chen, M.; Duan, M.; Huang, P.; Hong, J.; Lin, Y.; Cheng, S.; Wang, X.; Huang, M.; Cai, M. Fate of Polycyclic Aromatic Hydrocarbons from the North Pacific to the Arctic: Field Measurements and Fugacity Model Simulation. *Chemosphere* **2017**, *184*, 916−923.
(25) Ma, Y.; Xie, Z.; Yang, H.; Möller, A.; Halsall, C.; Cai, M.; Sturm, R.; Ebinghaus, R. Deposition of Polycyclic Aromatic Hydrocarbons in the North Pacific and the Arctic. *J. Geophys. Res. Atmos.* **2013**, *118* (11), 5822−5829.
(26) Zheng, H.; Cai, M.; Zhao, W.; Khairy, M.; Chen, M.; Deng, H.; Lohmann, R. Net Volatilization of PAHs from the North Pacific to the Arctic Ocean Observed by Passive Sampling. *Environ. Pollut.* **2021**, *276*, 116728.
(27) Casal, P.; Cabrerizo, A.; Vila-Costa, M.; Pizarro, M.; Jiménez, B.; Dachs, J. Pivotal Role of Snow Deposition and Melting Driving Fluxes of Polycyclic Aromatic Hydrocarbons at Coastal Livingston Island (Antarctica). *Environ. Sci. Technol.* **2018**, *52*, 12327−12337.
(28) Casal, P.; Casas, G.; Vila-Costa, M.; Cabrerizo, A.; Pizarro, M.; Jiménez, B.; Dachs, J. Snow Amplification of Persistent Organic Pollutants at Coastal Antarctica. *Environ. Sci. Technol.* **2019**, *53* (15), 8872−8882.
(29) Nizzetto, L.; Lohmann, R.; Gioia, R.; Jahnke, A.; Temme, C.; Dachs, J.; Herckes, P.; Di Guardo, A.; Jones, K. C. PAHs in Air and Seawater along a North-South Atlantic Transect: Trends, Processes and Possible Sources. *Environ. Sci. Technol.* **2008**, *42* (5), 1580−1585.
(30) Berrojalbiz, N.; Dachs, J.; Ojeda, M. J.; Valle, M. C.; Castro-Jiménez, J.; Wollgast, J.; Ghiani, M.; Hanke, G.; Zaldivar, J. M. Biogeochemical and Physical Controls on Concentrations of Polycyclic Aromatic Hydrocarbons in Water and Plankton of the Mediterranean and Black Seas. *Global Biogeochem. Cycles* **2011**, *25* (4), 1−14.
(31) Finn, R. D.; Coggill, P.; Eberhardt, R. Y.; Eddy, S. R.; Mistry, J.; Mitchell, A. L.; Potter, S. C.; Punta, M.; Qureshi, M.; Sangrador-Vegas, A.; Salazar, G. A.; Tate, J.; Bateman, A. The Pfam protein families database: towards a more sustainable future. *Nucleic Acids Res.* **2016**, *44*, D279−D285.
(32) Pesant, S.; Not, F.; Picheral, M.; Kandels-Lewis, S.; Le Bescot, N.; Gorsky, G.; Iudicone, D.; Karsenti, E.; Speich, S.; Trouble, R.; Dimier, C.; Searson, S. Open science resources for the discovery and analysis of Tara Oceans data. *Sci. Data* **2015**, *2*, 150023.
(33) Eddy, S. R. Accelerated profile HMM searches. *PLoS Comput. Biol.* **2011**, *7*, e1002195.
(34) Wang, R.; Tao, S.; Wang, W.; Liu, J.; Shen, H.; Shen, G.; Wang, B.; Liu, X.; Li, W.; Huang, Y.; Zhang, Y.; Lu, Y.; Chen, H.; Chen, Y.; Wang, C.; Zhu, D.; Wang, X.; Li, B.; Liu, W.; Ma, J. Black carbon emissions in China from 1949 to 2050. *Environ. Sci. Technol.* **2012**, *46*, 7595−7603.
(35) Bosch, C.; Andersson, A.; Krusa, M.; Bandh, C.; Hovorkova, I.; Klanova, J.; Knowles, T. D. J.; Pancost, R. D.; Evershed, R. P.; Gustafsson, Ö. Source apportionment of polycyclic aromatic hydrocarbons in central European soils with compound-specific triple isotopes ($\delta^{13}C$, $\Delta^{14}C$, $\delta^{2}H$). *Environ. Sci. Technol.* **2015**, *49*, 7657−7665.
(36) Cory, R. M.; Ward, C. P.; Crump, B. C.; Kling, G. W. Sunlight controls water column processing of carbon in arctic fresh waters. *Science* **2014**, *345*, 925−928.
(37) Ghosal, D.; Ghosh, S.; Dutta, T. K.; Ahn, Y. Current state of knowledge in microbial degradation of polycyclic aromatic hydrocarbons (PAHs): a review. *Front. Microbiol.* **2016**, *7*, 1369.
(38) Dombrowski, N.; Donaho, J. A.; Gutierrez, T.; Seitz, K. W.; Teske, A. P.; Baker, B. J. Reconstructing metabolic pathways of hydrocarbon-degrading bacteria from the Deepwater Horizon oil spill. *Nature microbial.* **2016**, *1*, 1−7.

https://doi.org/10.1021/acs.estlett.1c00658
Environ. Sci. Technol. Lett. 2021, 8, 918−923

PART 03 - CHAPTER 1. OCCURRENCE OF AROMATIC-LIKE COMPOUNDS IN THE GLOBAL OCEAN

3.1.2. Paper I. Supplementary Information

Table S1 and Figure S1.

Supplementary Information

Dissolved Black Carbon and Semivolatile Aromatic Hydrocarbons in the Ocean: Two Entangled Biogeochemical Cycles?

Núria Trilla-Prieto[1], Maria Vila-Costa[1], Gemma Casas[1], Begoña Jiménez[2], Jordi Dachs[1]*.

1 Department of Environmental Chemistry, IDAEA-CSIC, Barcelona, Catalunya, Spain.

2 Department of Instrumental Analysis and Environmental Chemistry, IQOG-CSIC, Madrid, Spain

* Corresponding author email: jordi.dachs@idaea.csic.es

This supplementary material contains Table S1 and Figure S1

Table S1 | Summary of the DBC and SALCs concentrations for the eight oceanic regions where DBC and SALCs were compared. The concentrations are the mean for the region. *SD stands for standard deviation. N is the number of measurments in that given region.*

		N	[DBC] ngL-1	SD	N	[SALC] ng L-1	SD	[SALCS]/[DBC](%)
Bering Strait-Arctic	**A**	18	5456	3731	30	1322	1704	24.2
Subtropical North Pacific	**B**	2	4285	4523	2	1322	665	30.9
Tropical North Atlantic	**C**	8	14394	10508	2	1438	217	10.0
Eastern South Atlantic	**D**	1	3983	0	8	210	129	5.3
Southern Ocean	**E**	7	8777	1743	26	1379	1229	15.7
South China Sea	**F**	41	12518	3008	12	1883	963	15.0
Nortwest Pacific	**G**	44	49268	27902	22	2247	3251	4.6
Pacific Subarctic	**H**	10	7368	1001	12	1653	1653	22.4
MEAN			**13256**			**1432**		**16.0**

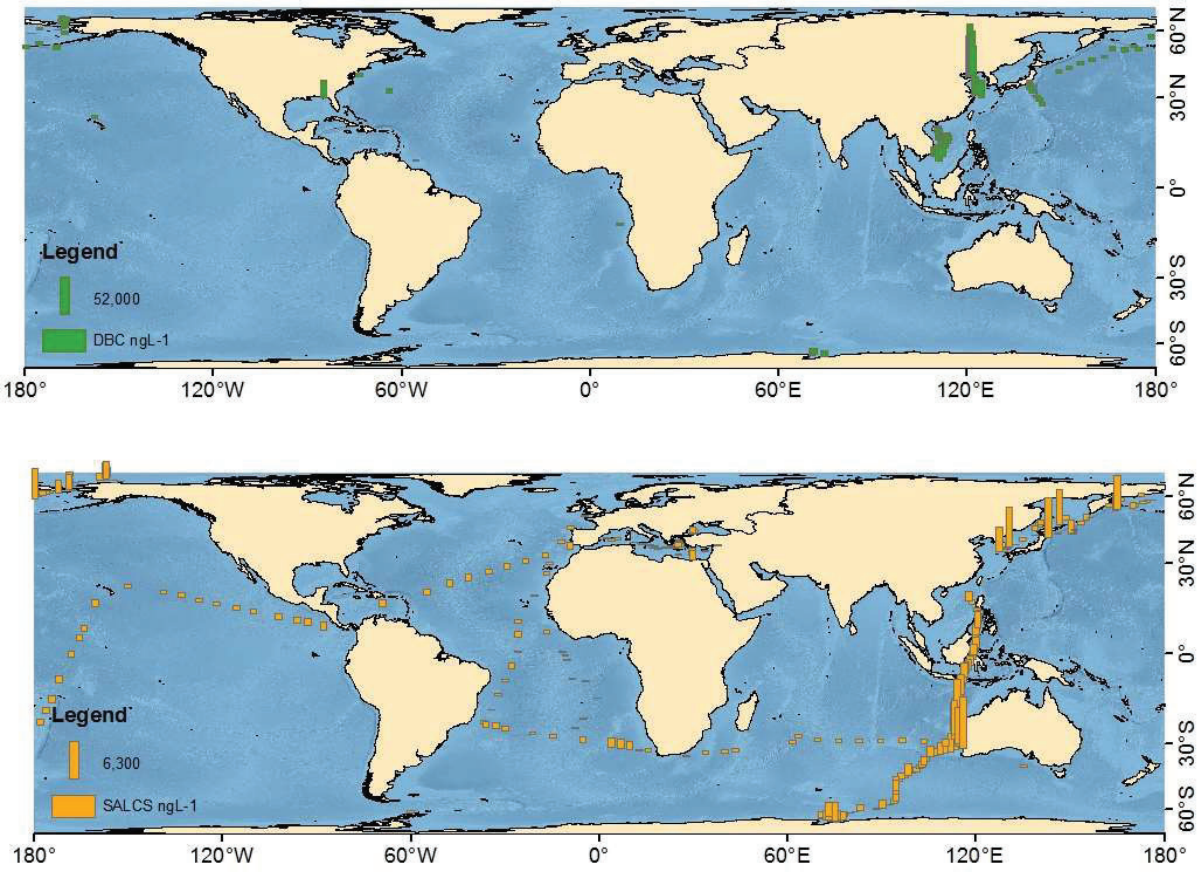


Figure S1 | Global distribution of concentrations of DBC (upper panel) and SALCs (lower panel) in the oceans for the eight regions where DBC and SALCs could be compared.





PART 03

CHAPTER 2.
Transport and biogeochemistry of PFAAs in the oceans.

3.2.1. Paper II. *Accumulation of Perfluoroalkyl Acid "Forever Chemicals" in Antarctic Waters*

3.2.2. Paper II. Supplementary Materials

PART 03 - CHAPTER 2. TRANSPORT AND BIOGEOCHEMISTRY OF PFAAs IN THE OCEANS

3.2.1. Paper II. *Accumulation of Perfluoroalkyl Acid "Forever Chemicals" in Antarctic Waters.*

Núria Trilla-Prieto[1,2], Jordi Dachs[1*], Jon Iriarte[1], Naiara Berrojalbiz[1], Pere Colomer-Vidal 3, Gemma Casas[1,4], Odei Garcia-Garin[5], Maria Vila-Costa[1], Begoña Jiménez[3]

[1]Department of Environmental Chemistry, IDAEA-CSIC, 08034, Barcelona, Catalunya, Spain

[2]Department of Evolutionary Biology, Ecology and Environmental Sciences, Faculty of Earth Sciences, Universitat de Barcelona, 08028, Barcelona, Catalunya, Spain

[3]Department of Instrumental Analysis and Environmental Chemistry, IQOG-CSIC, 28006, Madrid, Spain

[4]Present Address: Institute de Ciències del Mar, ICM-CSIC, 08003, Barcelona, Catalunya, Spain

[5]Department of Evolutionary Biology, Ecology and Environmental Sciences, Biodiversity Research Institute (IRBio), Universitat de Barcelona, 08028, Barcelona, Catalunya, Spain

State: *Submitted to Science Advances in February 2025*

ABSTRACT

Perfluoroalkyl Acids (PFAAs) have been widely used during the last fifty years in a myriad of industrial and consumer applications. PFAAs are a paradigm of persistent "forever chemicals", yet their impact on the global environment remains unknown. Early studies suggested a limited occurrence in the Southern Ocean as a consequence of the Antarctic Circumpolar Current (ACC) preventing their oceanic transport southwards. Here we show PFAAs in the water column of the Bransfield Strait and Bellingshausen Sea (west of Antarctic Peninsula) at concentrations not only higher than those in the central Atlantic, but of comparable magnitude to those measured in the North Atlantic, a region traditionally impacted by historical sources. Furthermore, PFAAs are ubiquitous in the water column with occurrence unrelated to proximate and direct sources from human activities. Atmospheric wet deposition of previously PFAAs aerosolized by sea spray arises as the main PFAAs source to Antarctica, while the prevailing marine currents and atmospheric regime in the region encapsulate these chemicals in the Antarctic region once these have crossed the Antarctic Divergence. The biological pump and biodegradation, key sinks for other persistent organic pollutants, do not compensate wet deposition inputs of PFAAs, resulting in the long-term accumulation of PFAAs in Antarctic waters. This work underscores the importance of persistence as the key property driving chemical's environmental risk, and raises concern on the long-term impact of the much larger pool of currently used poly- and per- fluoroalkyl substances.

INTRODUCTION

Per- and polyfluoroalkyl substances (PFAS) are a large group of synthetic organic chemicals widely used in the industry, household consumer products, and in a myriad of other applications[1–5]. Among PFAS, some Perfluoroalkyl Acids (PFAAs) have received increasing attention. They are known to be widely distributed in the ocean[6–9], and are extremely persistent in the environment[4]. PFAAs have been reported in the Arctic[10,11], but to a lesser extend in Antarctica[9,12–14].

Oceans are a major reservoir of PFAAs[15,16], and long-range transport by oceanic currents has generally been assumed to drive their global occurrence and long-term trends. This contrasts with the successive volatilization and deposition processes, a process known as grasshopping, which is the dominant transport mechanism for semi-volatile persistent organic pollutants (POPs), such as legacy polychlorinated biphenyls (PCBs), hexachlorocyclohexanes (HCHs), or polycyclic aromatic hydrocarbons (PAHs)[17–19]. Known oceanic sinks of perfluoroalkyl sulfonates (PFSAs) and perfluoroalkyl carboxylates (PFCAs) in the marine environment are vertical eddy diffusion[20], deep water formation[20,21], and settling of particle bound PFAAs (known as biological pump)[9,15,22]. However, despite these sinks, their persistence is estimated to range between decades and centuries in the marine environment[16,23].

Disparate PFAAs concentrations in coastal and open Antarctic waters have been reported[11,24,25], ranging from high concentrations close to the anthropically impacted King George Island[14], to extremely low levels in early reports of PFAAs in the open Southern Ocean[11,24,26]. Research stations account for a point source of PFAAs, but limited to the perimeter of the facilities[12,27]. Generally, it is thought that the Antarctic Circumpolar Current (ACC) acts as a barrier for the north-south transport of PFAAs by oceanic currents[28]. Neutral PFAS, precursors of PFAAs, have been reported in the Southern Ocean's atmosphere around the Antarctic Peninsula with a potential role as a source of PFAAs to this region[29–31]. Only recently, the potential role of wet deposition of sea spray aerosol-bound PFAAs has been identified as an additional mechanism accounting for a source of PFAAs in the Southern Shetland's coastal waters[12,32]. Nevertheless, the relevance of these atmospheric sources to the larger Antarctic Peninsula region remains unquantified, as well as how the occurrence of PFAAs in the open Southern Ocean compares with that in other oceanic regions.

The main goals of this work were i) to provide a unique set of measurements of PFCAs and PFSAs in the Atlantic Ocean, Bransfield Strait and Bellingshausen Sea, extending from 37°N to 71°S, covering latitudes in the Southern Ocean never sampled before for PFAAs, (ii) to assess the PFAAs depth distribution, and iii) to elucidate the processes driving the long-term occurrence and accumulation of PFAAs in Antarctic waters within the framework of the general atmospheric and oceanic patterns in the Atlantic-Southern Ocean continuum.

MATERIALS AND METHODS

Sampling. Seawater from 5 m depth (below the influence of the ship), and along the water column down to a depth of 2000 m, was collected during two oceanographic expeditions. During the ANTOM-I cruise (January-February 2021), from Vigo (Spain) to Punta Arenas (Chile), a total of 19 stations were sampled along a latitudinal transect in the Atlantic Ocean onboard the R/V Sarmiento de Gamboa. The second campaign, ANTOM-II, focused on the Southern Ocean west of the Antarctic Peninsula, covering 9 stations in the Bransfield Strait and the Bellingshausen Sea, conducted onboard the R/V Hespérides from January to February 2022 **(Table S1)**. Seawater samples were collected using a Niskin-rossete system equipped with a Sea-bird SBE 9 CTD, which measured salinity, temperature, fluorescence, depth, and oxygen concentrations, enabling characterization of the water column. The 5 m depth water samples were collected at 28 stations (19 in the Atlantic, and 9 in the Southern Ocean). In addition, seawater from the DCM, determined using the fluorescence from the CTD, was sampled at thirteen stations in the Atlantic Ocean, and seven stations in the Southern Ocean. Vertical profiles (5 depths) were obtained at six stations in the Atlantic Ocean and at three stations in the Southern Ocean. These profiles included samples from the layer with 1% of photosynthetic active radiation (1% PAR), the layer with minimum of oxygen (MOx), and at a depth of 2000 m depth, in addition to surface and DCM.

Sample Treatment. Samples were extracted on board following a previously published procedure[15, 32, 44] with minor modifications. Briefly, samples were filtered with pre-combusted glass fiber filters (GF/F, 0.7 µm, Whatman) and spiked with 1000 pg of a 13C-labeled mixture of nine recovery standards **(Table S2)**. Then, filtered samples were extracted by solid phase extraction at a flow rate of 1 mL min^{-1} using Oasis Wax 6cc cartridges pre-conditioned with 6 ml of 0.1% ammonia in MeOH, 6 mL of MeOH and 6 mL HPLC-grade water. Salts were washed with one cartridge volume of HPLC-grade water, and cartridges were vacuum-dried for 10 minutes before being labelled and frozen at -20°C until final treatment in an ultraclean laboratory.

After unfreezing, each cartridge was conditioned in a clean laboratory with 6 mL of ammonium acetate buffer (25 mM) at pH 4, and centrifuged 4 minutes at 3500 rpm to eliminate excess water. Samples were then eluted with 8 mL MeOH containing 0.1% ammonia and dry-evaporated under N_2 stream, and reconstituted in 300 µl PP vials with 50:50 MeOH-H_2O.

Instrumental Analysis. Samples were analysed using a UPLC-MS/MS system equipped with a Xevo TQS (Waters, Milford, MA) based on an established method with minor modifications.[15, 32, 44]

For chromatographic separation, extracts are injected into a high-resolution Acquity UPLC BEH C18 column (1.7 µm, 2.1 x 50 mm; Waters), optimized for exceptional sensitivity and throughput. The system incorporates features like the VanGuard™ C18 pre-column (Acquity UPLC BEH C18 1.7 µm VanGuardTM Pre-Column, 2.1 x 5 mm) to protect the analytical column and an Isolator Column (Waters ACQUITY UPLC, 2.1 x 50 mm) to prevent contamination, ensuring reliable results. The organic phase was methanol, while the mobile phase was a continuous 1% ammonium acetate buffer in water (200 mM, pH 4) at a flow rate of 0.4 mL min-1. The gradient water:organic phase for each 12-min injection was 72:28 at the initial conditions, 15:85 at 4.5 min, 1:99 at 4.6 min, and returned to the initial conditions from 10.0 min.

Analytes were ionized with an electrospray ionization (ESI) source operating in negative ion mode. Multiple-reaction-monitoring (MRM) mode was used for data acquisition. Each sample was injected in duplicate and calibration curve was injected prior and after each 10 samples batch. To eliminate any potential carryover, acetonitrile was injected in duplicate and passed through the system after every sample or calibration standard.

Statistical analysis. The normality of concentrations was assessed using the Shapiro-Wilk test, which revealed a non-normal distribution. Consequently, non-parametric statistical tests were employed to compare groups of samples. To determine statistically significant differences among groups, t-test and Mann-Whitney U test were used with a significance level of 0.05. Linear regression models were used to assess the linear relation among groups of paired samples. The statistical analysis was carried out using R-Studio (version 2024.09.1+394).

Quality Assurance and Quality Control. All field and sampling material were rinsed with MeOH and seawater in-situ before sampling. Polypropylene (PP) bottles for water collection, were also cleaned with MeOH and acetone, and then rinsed with sea-water. GF/F filters were pre-combusted at 450º for 4h and protected with foil and air-sealed PP zip-bags. Capillary and SPE system were cleaned with MeOH. At the ultra-clean laboratory, all PP materials were cleaned with MeOH. Other metallic material such as tweezers and evaporation needles were cleaned with MeOH.

Field blanks and procedural blanks were collected to monitor the potential contamination during the whole process. Blanks concentrations are reported in Table S8. Field blanks consisted in an Oasis WAX cartridge processed along the rest of the samples.

The limits of quantification (LOQ) were defined as the mean individual log transformed PFAAs values (pg) obtained in the procedural and field blanks, plus three times the standard deviation of the blank response, which covers 95% of the sample population. For the analytes that were not found in blanks, LOQs were derived from the lowest point in the calibration curve where the compound was detected.

Samples were blank corrected. Only values above the limit of quantification (>loq) were considered. Empty values were replaced by "nd" (non-detected). LOQs are presented in **Table S9**. Nineteen PFAAs were targeted at this study **(Table S2)**. Among them, PFHxA was excluded due to analytical uncertainty due to a potential co-elution, and PFBA wasn't found in any sample.

RESULTS AND DISCUSSION

Occurrence of PFCAs and PFSAs in the Atlantic Ocean. Seventeen of the nineteen targeted PFAAs were detected in seawater (see list of sampling stations in **Table S1** and chemicals and acronyms in **Table S2**). At 5 m depth in the Atlantic Ocean, $\sum_{17}$PFAAs concentrations ranged from 36.0 to 810.0 pg L^{-1} with an average of 203.9 pg L^{-1}, among which, the $\sum_{6}$PFSAs (PFBS, PFHxS, PFECHS, PFOS, PFDS, PFDoDS) ranged from 3.0 to 38.2 pg L^{-1} and $\sum_{11}$PFCAs (PFPeA, PFHpA, PFOA, PFNA, PFDA, PFUnDA, PFDoDA, PFTrDA, PFTeDA, PFHxDA, PFODA) ranged from 15.0 to 801.3 pg L^{-1}. The highest concentrations were found off-shore Brazil and Argentina (21°S and 43°S), with 466.8 and 810.0 pg L^{-1} of $\sum_{17}$PFAAs, respectively **(Figure 1 and Table S3)**.

PFAAs concentrations at 5 m depth (surface) showed a north-south latitudinal decrease from 40°N to the Equator (0°), and concentrations were high but variable off-shore Argentina between 21 and 46°S. The range of concentrations reported here is consistent, but in the lower end, of those previously reported for the Atlantic Ocean[8,10,33,34]. For example, during the Malaspina circumnavigation cruise in 2010, $\sum_{21}$PFAS at surface in the Atlantic ranged from 131 to 10900 pg L^{-1}, with the highest concentrations off-shore Brazil[8], consistent with the high values reported here in terms of

geographical distribution, even though with significant lower maximum concentration in 2021 than in 2010. Concentrations in the North Atlantic measured were generally higher than in the Central and South Atlantic, with the exception of water masses under the influence of South American inputs, and higher than those reported for the open Pacific and Indian Oceans[8,35]. The concentrations measured in the Atlantic Ocean show no evidence of a long-term increasing concentration of PFAAs, consistent with the compilation of oceanic PFAAs measures done recently[16].

For the Atlantic Ocean stations, the deep chlorophyll maximum (DCM) depth ranged from 50 to 145 m. $\sum_{17}$PFAA concentrations at the DCM showed a mean of 143.2 pg L^{-1} (ranging 48.7 – 444.0 pg L^{-1}) with $\sum_{6}$PFSAs and $\sum_{11}$PFCAs ranging from 0.7 to 53.2 pg L^{-1}, and from 38.2 to 390.7 pg L^{-1}, respectively **(Table S3)**. The concentrations of $\sum_{17}$PFAAs in the DCM were significantly correlated with those at surface (R^2 = 0.77, $p < 0.05$) **(Figure 2)**. Concentrations of some of the most abundant PFAAs (PFHpA, PFOA, PFNA, PFDA, PFBS, PFOS) were not significantly different between surface and the DCM, while those with lower contributions to $\sum_{17}$PFAAs (PFBS, PFNA and PFDA), showed higher concentrations (about 10 pg L-1 higher) at surface than at the DCM ($p < 0.05$). This is consistent with previous patterns of PFAAs occurrences at surface and the DCM for the Atlantic, Indian and Pacific oceans[15].

At six stations from the Atlantic Ocean, additional measurements were performed along the vertical profile, when sea conditions allowed them, at the depth with 1% photosynthetic active radiation (1% PAR), at the minimum of oxygen depth (MOx), and at 2000 m depth. Such coverage of PFAAs in the meso-pelagic and deep ocean provides further information on the extent of the distribution of PFAS in the ocean, and the biogeochemical controls on their transport and sinks.

The vertical profiles showed distinct trends **(Table S4)**. At 37°N, a surface enrichment depth depletion profile was present, consistent with PFAAs sources at surface, with $\sum_{17}$PFAAs concentrations at 5 m depth of 369.0 pg L^{-1}, and descending to 317.2 pg L^{-1} at 2000 m depth. This decrease was mainly driven by PFOA, PFNA and PFDA. At 28°N and 10°N, no discernible vertical trends were found, with especially low concentrations in the latter, ranging from 36.0 pg L^{-1} at surface to 120.0 pg L^{-1} at 400 m depth.

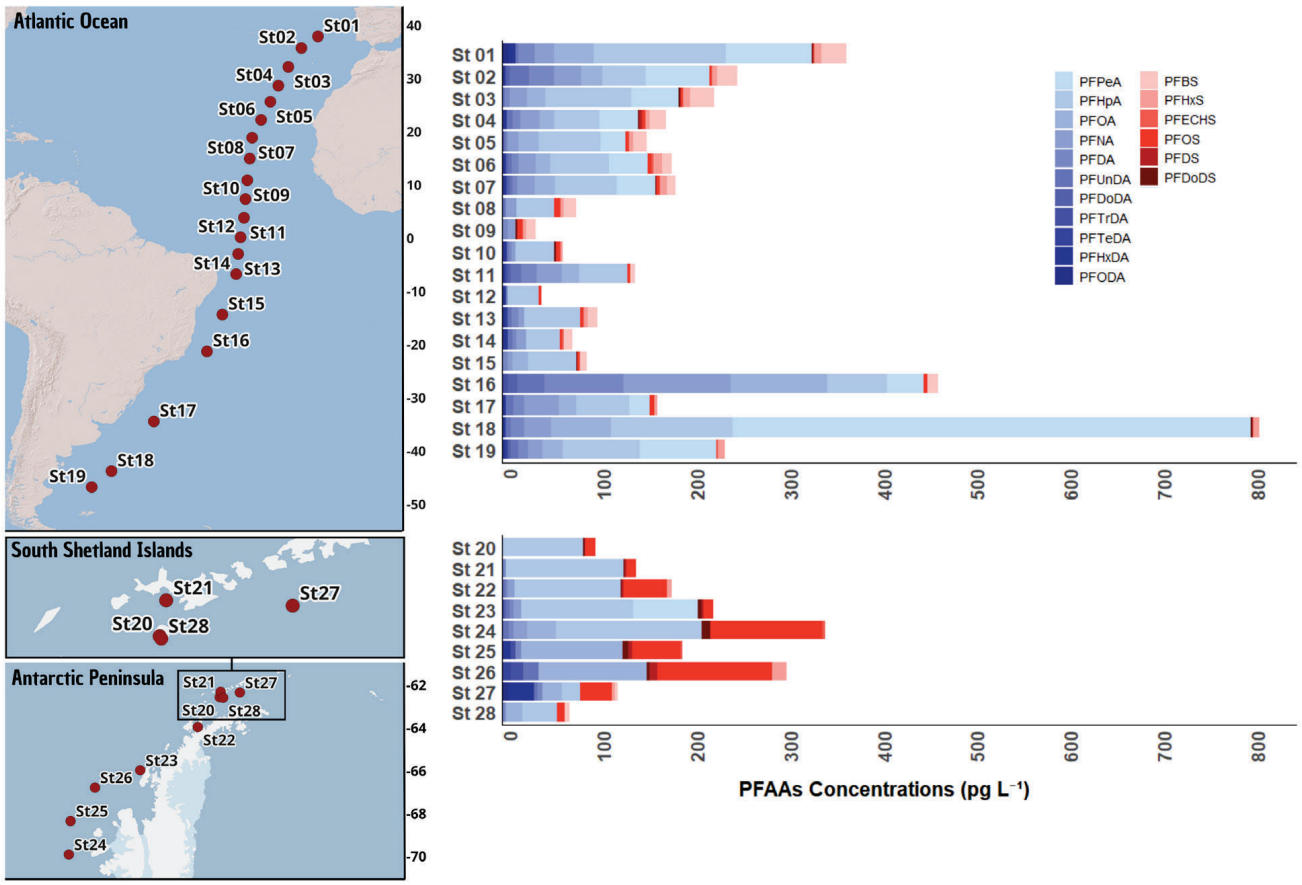


Figure 1. Latitudinal composition of PFAAs. Sampling sites and surface concentrations (pg L^{-1}) for PFCAs and PFSAs in the Atlantic Ocean (top panels) and Southern Ocean (bottom panels).

Low concentrations were also found at Equator (station 12), slightly increasing from 42.7 pg L^{-1} at the surface to 125.2 pg L^{-1} at 2000 m depth. The lower occurrence of PFAAs at 10°N and 0°N is consistent with their distance from potential source regions in Europe and North America. Conversely, at 14°S and 46°S, maximum concentrations within the profile, of 144.0 pg L^{-1} and 461.4 pg L^{-1} were found at 350 m and 200 m depth, respectively. The diverse profiles at different stations may reflect different influences of sources, with the highest at 37°N and 46°S, but also related to the fact that sampling was performed at different stages of the physical and biological seasonal succession. The profiles at latitudes 37°N, 28°N and 10°N (stations 1, 4 and 9) account for the conditions during winter, while the profiles at 14°S and 46°S (stations 15 and 19) account for vertical profiles in summer conditions. The relative contribution of individual PFAAs at Equator (0°S, station 12) was characterized by a higher contribution of PFCAs (91%) to $\sum_{17}$PFAAs, than in the other stations **(Table S7)**. The Equator is one of the few oceanic regions receiving significant wet deposition events36, and rain is generally enriched in PFCAs in comparison to PFSAs[12,32].

Despite the decreasing trend in PFAAs concentrations that arise when comparing early with recent reports from the Atlantic Ocean[11,16,24,34], a notable variability of $\sum_{12}$PFAS concentrations at surface, meso-pelagic and deep waters occur as shown in this work and elsewhere (n.d to 224 pg L^{-1})[34]. In the Indian Ocean, a general pattern of surface enrichment and depth depletion, with concentrations decreasing to a few pg L^{-1} at depths deeper than 1000 m, has been described[35].

The deep ocean integrates long-term inputs, mainly originating from the biological pump transport of PFAS[22]. As settling particles release PFAAs when organic matter is remineralized, PFAAs can build up their concentrations in deep waters. At 2000 m depth, $\sum_{17}$PFAAs averaged 142.2 pg L^{-1}, with the maximum value at 37°N, off-shore the Iberian Peninsula. The range of concentrations at 5 m depth measured in the vertical profiles (average of 158.7 pg L^{-1}, ranging from 36.0 to 369.0 pg L^{-1}), was not significantly different than at 2000 m depth. Furthermore, the relative contributions of PFHpA (58%), PFPeA (26%) and PFOA (9%) at 2000 m depth were similar than at surface (46%, 27% and 12%, respectively).

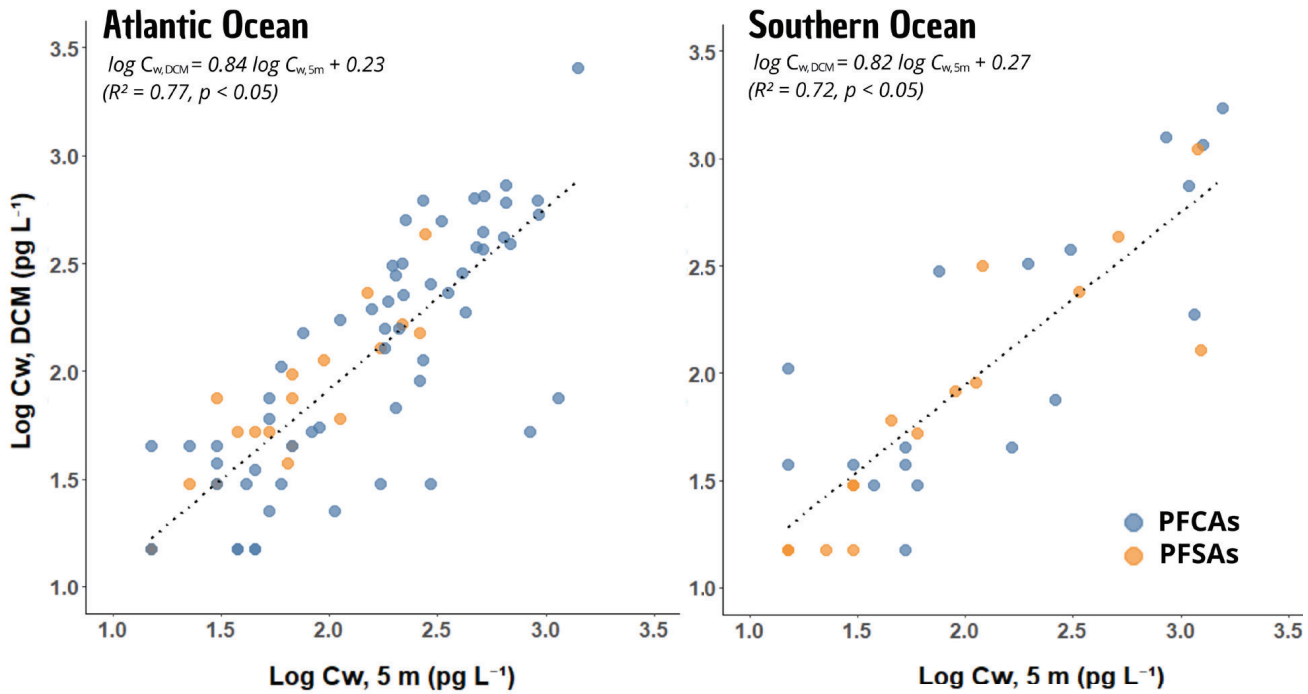


Figure 2. PFAAs at surface versus the deep chlorophyll maximum (DCM) depth. Correlations between concentrations (pg L^{-1}) at 5 m and DCM. Orange dots account for PFSAs (PFBS, PFHxS, PFOS, PFECHS, PFDS, and PFDoDS) and blue dots for PFCAs (PFPeA, PFHpA, PFOA, PFNA, PFDA, PFUnDA, PFDoDA, PFTrDA, PFTeDA, PFHxDA, and PFODA).

Such similarities between the surface and deep ocean in terms of concentrations and patterns are strong indicators of the persistence of PFAAs under oceanic conditions. The low concentrations of PFAS reported previously for the Indian Ocean, may be related to lower historical inputs in this region, and different oceanographic conditions.

Occurrence of PFCAs and PFSAs in the Southern Ocean. In the Southern Ocean, $\sum_{17}$PFAAs averaged 188.6 pg L^{-1} at 5 m depth (ranging from 72.7 to 343.3 pg L^{-1}), with $\sum_{6}$PFSAs ranging from 13.6 to 149.3 pg $L^{-1}$and $\sum_{11}$PFCAs ranging from 59.1 to 214.2 pg L^{-1} **(Table S5)**. At the DCM, $\sum_{17}$PFAAs averaged 188.9 pg L^{-1} (with a range of 72.7 - 336.0 pg L^{-1}), with $\sum_{6}$PFSAs ranging from 15.8 to 121.5 pg L^{-1} and $\sum_{11}$PFCAs ranging from 51.7 to 286.5 pg L^{-1} **(Table S5)**. As in the Atlantic Ocean, PFAAs concentrations at surface were correlated with those at the DCM (R^2=0.72, $p < 0.05$) **(Figure 2)**, with no significantly different concentrations between both depths.

The measurements in the Southern Ocean were conducted away from research stations, with the exception of station 28 (Deception Island), and were, therefore, not affected by their localized impact[12,27]. At the inner harbour of Deception Island (station 28), $\sum_{17}$PFAAs concentrations were not significantly higher than those in the proximate open ocean stations, despite the presence of two research stations inside the volcano caldera and the visits of thousands of tourists during the austral summer.

PFAAs in the open Southern Ocean reported here are the only recent measurements for open waters in the Southern Ocean. These concentrations are comparable to those reported previously in the Southern and False Bays from Livingston Island, and Port Foster in Deception Island[9,12], but significantly lower than those reported by others at King George Island[14]. Generally, these concentrations in Western Antarctic seawaters are higher than those in Eastern Antarctica[13], and significantly higher than those reported for the Southern Ocean in early reports of PFAAs in north-south transects[11,24,26]. Legacy POPs have previously been reported in Western Antarctic seawaters, including PCBs[37], HCHs[38] or PAHs[39,40], with concentrations higher than in other Antarctic regions. This occurrence of semi-volatile POPs is driven by the larger influence of air masses entering from the north, which bring POPs to the Antarctic region by atmospheric transport[32,39,41,42] and are associated with wet deposition events[9,12,41], even though for semi-volatile chemicals diffusive air-water exchange is a key input to the region[37,38]. Indeed, for semi-volatile chemicals, such PCBs, HCHs, and PAHs, long range atmospheric transport is driven by successive volatilization and deposition processes (grasshopping)[17,43]. Conversely, PFAAs are highly soluble compounds at environmental pH values, and their volatilization-absorption fluxes are negligible.

Three Southern Ocean vertical profiles were measured at stations 24, 27, and 28 **(Figure 1 and 3, and Table S6)**. At station 27 (62°S), there were relatively constant $\sum_{17}$PFAAs concentrations through the water column averaging 93.5 pg L^{-1} (123.7, 79.5, 110.2, 76.5, and 77.4 pg L^{-1}, from 5 to 1620 m depth, respectively) with no significant changes of the relative abundance of individual PFCAs. Conversely, PFOS showed a decreasing pattern from 33.7 pg L^{-1} at surface to 7.5 pg L^{-1} at 1620 m. Inside the proximate Deception Island volcano (62°S, station 28), $\sum_{17}$PFAAs concentrations were not significantly different between 5 and 40 m depth, and decreased at 155 m depth close to the bottom (72.0, 72.7, and 38.2 pg L^{-1}, respectively). The vertical profile at station 24 (70.8°S, 79.9°W), situated at the southernmost station 71°S, showed a surface enrichment depth depletion distribution with $\sum_{17}$PFAAs concentration of 345.7, 265.5, 157.7, and 94.5 pg L^{-1} at 5, 75, 210, and 584 m (close to bottom) depths, respectively. Such decrease was mainly driven by PFCAs.

Generally, there were higher contributions of PFCAs than PFSAs in Antarctic waters. This is consistent with rain and snow PFAAs inputs, as these are enriched in PFCAs to a greater extent than PFSAs[9,12,32], being these the main sources of PFAAs to the Southern Ocean, south of the Antarctic Circumpolar Current (Antarctic Divergence).

North-south transport of PFAAs and accumulation in the Southern Ocean. The transport of PFAAs from the South Atlantic to the Southern Ocean can be explained by taking into account the observed PFAAs distribution together with the general oceanic and atmospheric circulation pattern **(Figure 4)**. In the Atlantic Ocean, $\sum_{17}$PFAAs concentrations at 5 m depth decreased from 37°N to 14°S (from 369.0 pg L^{-1} to 90.7 pg L^{-1}). The higher concentrations in the North Atlantic in comparison to Equatorial and intertropical regions are consistent with larger potential sources from Europe, while the sampling points at low latitudes were distant from continents, reflecting lower influence from potential sources. The high $\sum_{17}$PFAAs concentrations at stations 16 and 18 (466.8 and 810.0 pg L^{-1}, respectively) reflect the influence from proximate Argentina and Brazil, as well as the influence of the warm current descending along the eastern coast of South America, transporting water masses from Brazil to the South Atlantic. Further south, in Antarctic waters south of the Antarctic Divergence, unexpected $\sum_{17}$PFAAs concentrations, comparable to those measured in the Northern Atlantic, were found. These are not consistent with the suggested role of the Antarctic Circumpolar Current as a barrier for the transport of PFAAs to Antarctica.

Recently, it has been suggested that both snow and rain deposition events could be relevant sources of PFAAs to Antarctica[12,32,44]. For example, PFCAs concentrations are more than one order of magnitude higher in freshly deposited snow (760-3600 pg L^{-1}) than in seawater (94-420 pg L^{-1})[12]. Wet deposition arises as the only process that can explain the large-scale occurrence of PFAAs in the Southern Ocean, especially for PFCAs. The transport of PFAAs from the southern subtropical Atlantic Ocean to the sub-Antarctic current will occur by oceanic transport, with a contribution from sea spray mediated grasshopping. Such grasshopping is different than that responsible for the transport of semi-volatile POPs which is driven by volatilization-absorption. For PFAAs, the grasshopping would occur by aerosolization mediated by sea spray formation and deposition of the sea spray aerosols after atmospheric transport **(Figure 4).** The Southern Ocean, and especially the sub-Antarctic waters, are characterized by high wind speeds, and is the world region of a larger emission flux of PFAAs associated with sea spray[45]. In the region around the Antarctic peninsula, there are incursions of air masses from the north that are humid, with such moisture originating in the sub-Antarctic zone (around 50°S)[46], and resulting in wet deposition of PFAAs by rain or snow[12,32,44]. Such wet deposition increases the concentrations of PFAAs in Antarctic coastal surface waters[12], and the widespread occurrence of PFAAs in the open Bellingshausen Sea and Bransfield Strait shows that it is also relevant for the Southern Ocean surrounding the Antarctic peninsula. Wet deposition of PFAAs neutral precursors or their oxidation products may also contribute to the PFAAs inputs in the region.

An accumulation of PFAAs to the levels observed in this work, higher than in early studies of PFAAs in the Southern Ocean, can only occur if the inputs are larger than sinks and sustained over time. A potential sink for PFAAs is the biological pump, but even if this is relevant in explaining the occurrence of PFAAs in the deep ocean, the resulting residence times in the water column due to this sink are longer for PFAAs[15,22] than for other legacy POPs such as PCBs, for which the biological pump effectively depletes the surface concentrations in the ocean[18,37]. Microbial degradation has been suggested for PFOS in seawater from Deception Island , but its relevance for the rest of Antarctic waters is unclear. In any case, generally, PFCAs concentrations are much higher than those

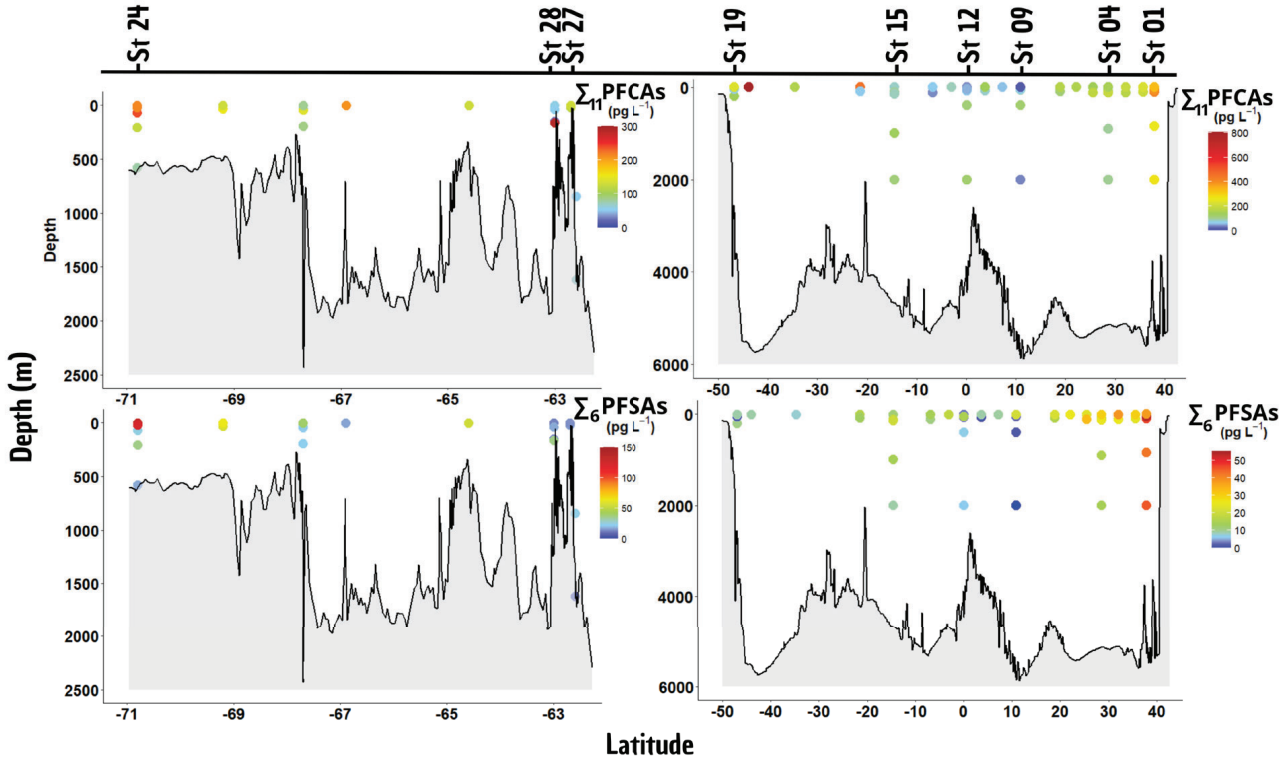


Figure 3. Latitudinal and depth distribution of PFAAs. Latitudinal and depth distribution of concentrations (pg L-1) for $\sum_{11}$PFCAs (top panels) and $\sum_{6}$PFSAs (bottom panels), in the Atlantic Ocean (right panels) and Southern Ocean (left panels). The circle's color accounts for concentrations of different magnitude. Black line and shadow show the bathymetry of the ocean.

of PFSAs in the ocean. PFCAs arise as perfectly persistent, truly forever chemicals. Once PFAAs reach Antarctica, wind speeds are lower in Antarctic waters than in the region north of the Antarctic Divergence, and therefore, the aerosolization of PFAAs from Antarctic waters and their transport out of the region will be of lower magnitude than the atmospheric inputs in the opposite direction. Therefore, the Antarctic Circumpolar Current has a dual role as both a barrier for the input and output of PFAAs to/from Antarctica by oceanic currents **(Figure 1)** but there is a net atmospheric input to the region. For other POPs, the biological pump for PCBs[37], or degradation for PAHs or HCHs[38,48], lower their concentrations and prevent their

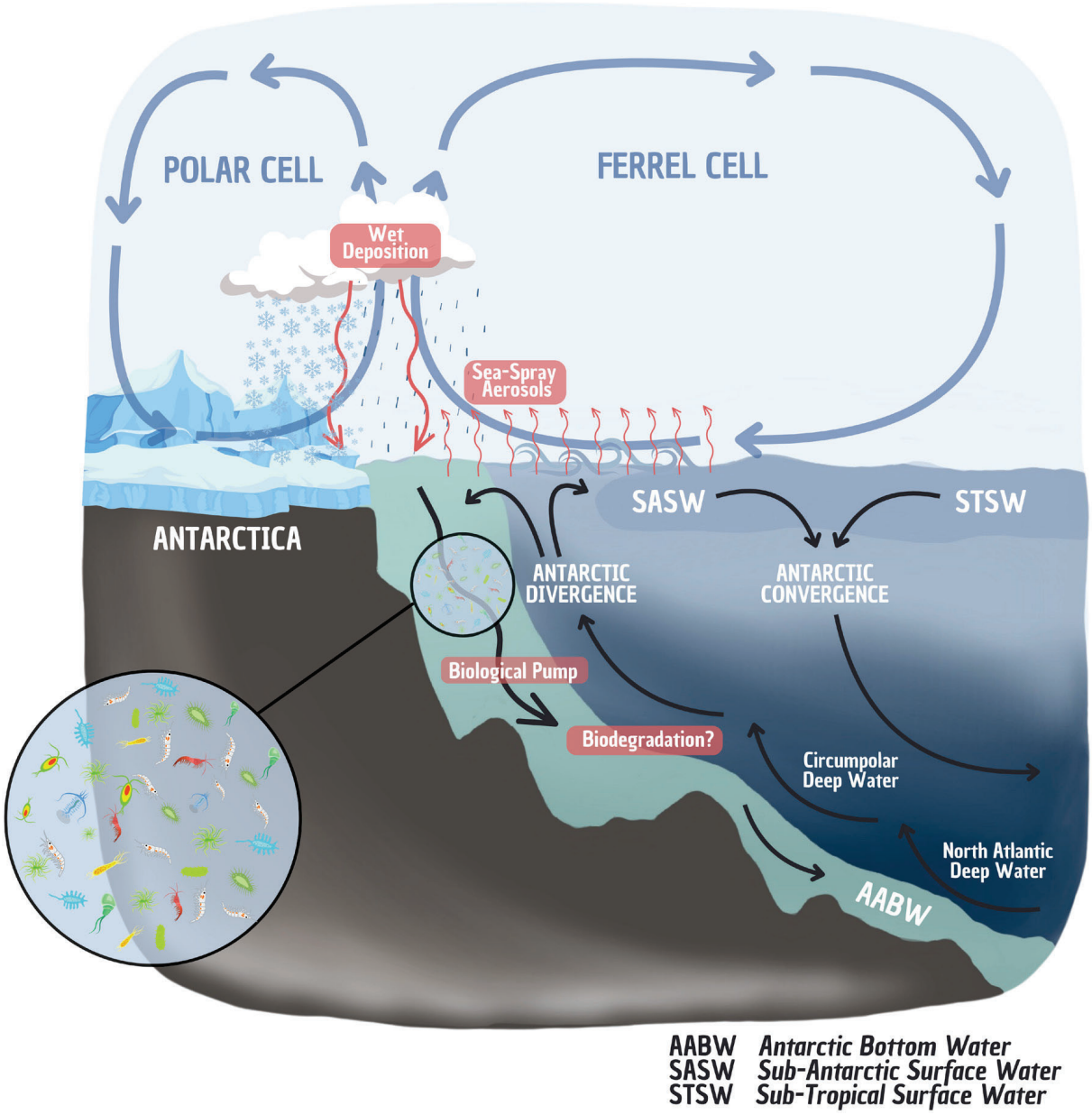


Figure 4. Transport of PFAAs from the South Atlantic Ocean to the Southern Ocean. The accumulation of PFAAs to Antarctica arise from their aerosolization mediated by sea spray aerosols in the sub-Antarctic surface water, followed by atmospheric transport and wet deposition in the Antarctic Peninsula region. Once in Antarctic waters, the Antarctic Divergence prevents their transport out of the region.

long-term increasing accumulation in Antarctic waters. For these semivolatile POPs, their concentrations in Antarctica are lower, thus generally not comparable, to those observed in the North Atlantic Ocean. However, for extremely persistent chemicals such as PFAAs, this results in a long-term accumulation around the Antarctic Peninsula. The fact that concentrations were higher at the southernmost stations **(Figure 1)** is consistent with increasing inputs from deposition or melting, which supports the levels of the East Wind Drift current along the Antarctic Peninsula. The Antarctic Peninsula receives more precipitation events than other Antarctic regions[49], which is also consistent with the generally higher levels of PFAAs and other contaminants here than in other Antarctic sectors.

This unexpected accumulation evidences the global risk posed by persistent chemicals, raises concerns on the risk posed to the Antarctic ecosystem, and will require further research on the occurrence of many persistent contaminants of emerging concern, such as the thousands of per- and poly- fluoroalkyl substances currently used by the contemporaneous society[2,50].

REFERENCES

1. Lindstrom, A. B., Strynar, M. J. & Libelo, E. L. Polyfluorinated compounds: Past, present, and future. Environ. Sci. Technol. 45, 7954–7961 (2011).

2. Glüge, J. et al. An overview of the uses of per- And polyfluoroalkyl substances (PFAS). Environ. Sci. Process Impacts 22, 2345–2373 (2020).

3. Cousins, I. T., Johansson, J. H., Salter, M. E., Sha, B. & Scheringer, M. Outside the Safe Operating Space of a New Planetary Boundary for Per- and Polyfluoroalkyl Substances (PFAS). Environ. Sci. Technol. 56 11172–11179 (2022).

4. Cousins, I. T. et al. The high persistence of PFAS is sufficient for their management as a chemical class. Environ. Sci.: Proc. Impacts 22 2307–2312 (2020).

5. Ackerman Grunfeld, D. et al. Underestimated burden of per- and polyfluoroalkyl substances in global surface waters and groundwaters. Nat. Geosci. 17, 340–346 (2024).

6. Ahrens, L. & Bundschuh, M. Fate and effects of poly- and perfluoroalkyl substances in the aquatic environment: A review. Environ. Toxicol. Chem. 33, 1921–1929 (2014).

7. Yamashita, N., Kannan, K., Taniyasu, S. & Horii, Y. A global survey of perfluorinated acids in oceans. Mar. Pollut. Bull. 51, 658–668 (2005).

8. González-Gaya, B., Dachs, J., Roscales, J. L., Caballero, G. & Jiménez, B. Perfluoroalkylated substances in the global tropical and subtropical surface oceans. Environ. Sci. Technol. 48, 13076–13084 (2014).

9. Casas, G. et al. Inputs, amplification and sinks of perfluoroalkyl substances at coastal Antarctica. Environ. Poll. 338, 122608 (2023).

10. Benskin, J. P. et al. Perfluoroalkyl acids in the atlantic and Canadian arctic oceans. Environ. Sci. Technol. 46, 5815–5823 (2012).

11. Zhao, Z. et al. Distribution and long-range transport of polyfluoroalkyl substances in the Arctic, Atlantic Ocean and Antarctic coast. Environ. Poll. 170, 71–77 (2012).

12. Casal, P. et al. Role of Snow Deposition of Perfluoroalkylated Substances at Coastal Livingston Island (Maritime Antarctica). Environ. Sci. Technol. 51, 8460–8470 (2017).

13. Shan, G. et al. Legacy and emerging per- and poly-fluoroalkyl substances in surface seawater from northwestern Pacific to Southern Ocean: Evidences of current and historical release. J. Hazard. Mater. 411, 125049 (2021).

14. Cai, M. et al. Per- and polyfluoroalkyl substances in snow , lake , surface runoff water and coastal seawater in Fildes Peninsula , King George Island , Antarctica. J. Hazard. Mater. 209–210, 335–342 (2012).

15. González-Gaya, B., Casal, P., Jurado, E., Dachs, J. & Jiménez, B. Vertical transport and sinks of perfluoroalkyl substances in the global open ocean. Environ. Sci. Process. Impacts 21, 1957–1969 (2019).

16. Muir, D. & Miaz, L. T. Spatial and Temporal Trends of Perfluoroalkyl Substances in Global Ocean and Coastal Waters. Environ. Sci. Technol. 55, 9527–9537 (2021).

17. Jurado, E. & Dachs, J. Seasonality in the 'grasshopping' and atmospheric residence times of persistent organic pollutants over the oceans. Geophys. Res. Lett. 35, L17805 (2008).

18. Galbán-Malagón, C., Berrojalbiz, N., Ojeda, M. J. & Dachs, J. The oceanic biological pump modulates the atmospheric transport of persistent organic pollutants to the Arctic. Nat. Commun. 3, 862 (2012).

19. González-Gaya, B. et al. High atmosphere-ocean exchange of semivolatile aromatic hydrocarbons. Nat. Geosci 9, 438–442 (2016).

20. Lohmann, R., Jurado, E., Dijkstra, H. A. & Dachs, J. Vertical eddy diffusion as a key mechanism

for removing perfluorooctanoic acid (PFOA) from the global surface oceans. Environ. Poll. 179, 88–94 (2013).

21. Armitage, J. M., Schenker, U. R. S., Scheringer, M., Martin, J. W. & Macleod, M. Modeling the Global Fate and Transport of Perfluorooctane Sulfonate (PFOS) and Precursor Compounds in Relation to Temporal Trends in Wildlife Exposure. Environ. Sci. Technol. 43, 9274–9280 (2009).

22. Casal, P. et al. Accumulation of Perfluoroalkylated Substances in Oceanic Plankton. Environ. Sci. Technol. 51, 2766–2775 (2017).

23. Yamashita, N. et al. Perfluorinated acids as novel chemical tracers of global circulation of ocean waters. Chemosphere 70, 1247–1255 (2008).

24. Ahrens, L., Xie, Z. & Ebinghaus, R. Distribution of perfluoroalkyl compounds in seawater from Northern Europe, Atlantic Ocean, and Southern Ocean. Chemosphere 78, 1011–1016 (2010).

25. Xie, Z. & Kallenborn, R. Legacy and emerging per- and poly-fluoroalkyl substances in polar regions. Current Opinion Green and Sustain. Chem. 42, 100840 (2023).

26. Wei, S. et al. Baseline Distribution of Perfluorinated Compounds in Surface Seawaters between Asia and Antarctica. Mar. Poll. Bull. 54, 1813-1818 (2007).

27. Wild, S. et al. An antarctic research station as a source of brominated and perfluorinated persistent organic pollutants to the local environment. Environ. Sci. Technol. 49, 103–112 (2015).

28. Bengtson Nash, S. et al. Perfluorinated compounds in the Antarctic region: Ocean circulation provides prolonged protection from distant sources. Environ. Poll. 158, 2985–2991 (2010).

29. Dreyer, A., Weinberg, I., Temme, C. & Ebinghaus, R. Polyfluorinated compounds in the atmosphere of the Atlantic and Southern Oceans: Evidence for a global distribution. Environ. Sci. Technol. 43, 6507–6514 (2009).

30. Del Vento, S., Halsall, C., Gioia, R., Jones, K. & Dachs, J. Volatile per- and polyfluoroalkyl compounds in the remote atmosphere of the western Antarctic Peninsula: An indirect source of perfluoroalkyl acids to Antarctic waters? Atmos. Pollut. Res. 3, 450–455 (2012).

31. Wang, Z. et al. Neutral Poly/Per-Fluoroalkyl Substances in Air from the Atlantic to the Southern Ocean and in Antarctic Snow. Environ. Sci. Technol. 49, 7770–7775 (2015).

32. Casas, G., Martinez-Varela, A., Vila-Costa, M., Jiménez, B. & Dachs, J. Rain Amplification of Persistent Organic Pollutants. Environ. Sci. Technol. 55, 12961–12972 (2021).

33. Zhang, X., Lohmann, R. & Sunderland, E. M. Poly- And Perfluoroalkyl Substances in Seawater and Plankton from the Northwestern Atlantic Margin. Environ. Sci. Technol. 53, 12348–12356 (2019).

34. Savvidou, E. K., Sha, B., Salter, M. E., Cousins, I. T. & Johansson, J. H. Horizontal and Vertical Distribution of Perfluoroalkyl Acids (PFAAs) in the Water Column of the Atlantic Ocean. Environ. Sci. Technol. Lett. 10, 418–424 (2023).

35. Han, T. et al. Spatial distribution, vertical profiles and transport of legacy and emerging per- and polyfluoroalkyl substances in the Indian Ocean. J. Hazard. Mater. 437, 129264 (2022).

36. Jurado, E. et al. Wet deposition of persistent organic pollutants to the global oceans. Environ. Sci. Technol. 39, 2426–2435 (2005).

37. Galbán-Malagón, C. J., Del Vento, S., Cabrerizo, A. & Dachs, J. Factors affecting the atmospheric occurrence and deposition of polychlorinated biphenyls in the Southern Ocean. Atmos. Chem. Phys. 13, 12029–12041 (2013).

38. Galbán-Malagón, C., Cabrerizo, A., Caballero, G. & Dachs, J. Atmospheric occurrence and deposition of hexachlorobenzene and hexachlorocyclohexanes in the Southern Ocean and Antarctic Peninsula. Atmos. Environ. 80, 41–49 (2013).

39. Casal, P. et al. Pivotal Role of Snow Deposition and Melting Driving Fluxes of Polycyclic Aromatic Hydrocarbons at Coastal Livingston Island (Antarctica). Environ. Sci. Technol. 52, 12327–12337 (2018).

40. Iriarte, J. et al. Snow-Dependent Biogeochemical Cycling of Polycyclic Aromatic Hydrocarbons at Coastal Antarctica. Environ. Sci. Technol. 57, 1625–1636 (2023).

41. Casal, P. et al. Snow amplification of persistent organic pollutants at coastal antarctica. Environ. Sci. Technol. 53, 8872–8882 (2019).

42. Khairy, M. A., Luek, J. L., Dickhut, R. & Lohmann, R. Levels, sources and chemical fate of persistent organic pollutants in the atmosphere and snow along the western Antarctic Peninsula. Environ. Poll. 216, 304–313 (2016).

43. Wania, F. & Mackay, D. Tracking the Distribution of Persistent Organic Pollutants. Environ. Sci. Technol. 30, 390A-396A (1996).

44. Casas, G. et al. Rain amplification of persistent

organic pollutants. Environ. Sci. Technol. 55, 12961-12972 (2023).

45. Sha, B., Johansson, J. H., Salter, M. E., Blichner, S. M. & Cousins, I. T. Constraining global transport of perfluoroalkyl acids on sea spray aerosol using field measurements. Sci. Adv. 10, 1–10 (2024).

46. Sodemann, H. & Stohl, A. Asymmetries in the moisture origin of Antarctic precipitation. Geophys Res Lett 36, L22803 (2009).

47. Cerro-Gálvez, E. et al. Microbial responses to perfluoroalkyl substances and perfluorooctanesulfonate (PFOS) desulfurization in the Antarctic marine environment. Water Res. 171, 115434 (2020).

48. González-Gaya, B. et al. Biodegradation as an important sink of aromatic hydrocarbons in the oceans. Nat. Geosci. 12, 119–125 (2019).

49. Thomas, E. R., Marshall, G. J. & McConnell, J. R. A doubling in snow accumulation in the western Antarctic Peninsula since 1850. Geophys. Res. Lett. 35, L01706 (2008).

50. Schymanski, E. L. et al. Per- and Polyfluoroalkyl Substances (PFAS) in PubChem: 7 Million and Growing. Environ. Sci. Technol. 57, 16918–16928 (2023).

Acknowledgments

We thank the UTM-CSIC and the crew from R/V Sarmiento de Gamboa and R/V Hespérides for technical support, and all the ANTOM cruises' participants for their collaboration on the field work. Funding: This work has been funded by Ministry of science, innovation and universities of the Spanish Government with project ANTOM (PGC2018-096612-B-I00) and PANTOC (PID2021-127769NB-I00). N.T.P. and JI acknowledge predoctoral fellowship (PRE2019-089641 and FPU19/02782) funded by the Spanish Ministry of Science, Innovation and Universities.

Author contributions:

Conceptualization: NTP, JD, MVC, BJ

Methodology: NTP, JI, NB, GC, PC, OGG

Investigation: NTP, JD, BJ, NB, PC

Visualization: NTP

Funding acquisition: JD, BJ, MVC

Project administration: JD, BJ, MVC

Supervision: JD, BJ, MVC

Writing – original draft: NTP, JD, BJ

Writing – review & editing: NTP, JD, JI, NB, GC, PC, OGG, MVC

Competing interests: The authors declare that they have no competing interests.

Data and materials availability: All data are available in the manuscript or the supplementary materials.

Supplementary Materials:

Supplementary Text (Note S1)
Tables S1 to S9
References (51)

PART 03 - CHAPTER 2. TRANSPORT AND BIOGEOCHEMISTRY OF PFAAs IN THE OCEANS

3.2.2. Paper II. Supplementary Information

Supplementary Text (Note S1)
Tables S1 to S9
References (51)

Supplementary Material

Accumulation of Perfluoroalkyl Acid "forever chemicals" in Antarctic Waters

Núria Trilla-Prieto[1,2], Jordi Dachs[1]*, Jon Iriarte[1], Naiara Berrojalbiz[1], Pere Colomer-Vidal[3], Gemma Casas[1,4], Odei Garcia-Garin[5], Maria Vila-Costa[1], Begoña Jiménez[3]

[1]Department of Environmental Chemistry, IDAEA-CSIC, 08034, Barcelona, Catalunya, Spain

[2]Department of Evolutionary Biology, Ecology and Environmental Sciences, Faculty of Earth Sciences, Universitat de Barcelona, 08028, Barcelona, Catalunya, Spain

[3]Department of Instrumental Analysis and Environmental Chemistry, IQOG-CSIC, 28006, Madrid, Spain

[4]Present Address: Institute de Ciències del Mar, ICM-CSIC, 08003, Barcelona, Catalunya, Spain

[5]Department of Evolutionary Biology, Ecology and Environmental Sciences, Biodiversity Research Institute (IRBio), Universitat de Barcelona, 08028, Barcelona, Catalunya, Spain

Corresponding author email: jordi.dachs@idaea.csic.es

Table of Contents

Supplementary Text

Note S1. Details on the calculation of LOQ.

Tables

Table S1. Sampling stations information.

Table S2. Target PFSAs and PFCAs, and Surrogate and Injection Standards used in the present study with their acronyms, parent and product ions and retention times.

Table S3. Individual PFAAs concentrations (pg L^{-1}) at 5 m and DCM samples from the Atlantic Ocean.

Table S4. Individual PFAAs concentrations (pg L^{-1}) at vertical profile samples from the Atlantic Ocean.

Table S5. Individual PFAAs concentrations (pg L^{-1}) at 5 m and DCM samples from the Southern Ocean.

Table S6. Individual PFAAs concentrations (pg L^{-1}) at vertical profile samples from the Southern Ocean.

Table S7. Mean relative contribution of individual PFAAs to the total PFAA's pool (%), separated by ocean.

Table S8. PFAAs values (pg) from field blanks and procedural blanks.

Table S9. Limits of Quantification (LOQs) for PFAAs compounds for the Atlantic and Southern Ocean samples.

References

Supplementary Text

Note S1. Details on the calculation of LOQ.

The following protocol[51] was followed to calculate LOQs and blank correction. Procedural and field blank results (pg) were log-transformed (LN) to ensure a normal distribution of the data. From the log-transformed data, the mean (μ) and standard deviation (σ) of the log-normal data set were calculated, and the variance (Var) was estimated by:

$$Var = (e^{\sigma^2} - 1)\, x\, e^{(2\mu+\sigma^2)} \qquad [1]$$

where σ represents the standard deviation of the log-transformed blank values, and μ represents the mean of the log-transformed blank values.

To calculate the limits of quantification (LOQs), the mean ($\bar{x}$) and standard deviation (SD) on the original blank values (previous to log-transformation) were derived by (Pavlovic 2022):

$$\bar{x} = e^{(\mu+(\frac{1}{2}*\sigma^2)} \qquad [2]$$

$$\text{SD} = \sqrt{Var} \qquad [3]$$

Finally, individual LOQs were calculated as follow:

$$LOQ = \bar{x} + (3\, x\, SD) \qquad [4]$$

This method ensures accurate back-transformation of log data to the original scale for quantifying blank levels, determining LOQs, and performing corrections on the sample data.

Table S1. Sampling stations information.

Code	Original cruise code	Date	Lat	Long
St 01	AN1_ST01	201218	37.91	-15.97
St 02	AN1_ST02	201219	35.73	-19.07
St 03	AN1_ST03	201220	32.18	-21.53
St 04	AN1_ST04	201221	28.65	-23.40
St 05	AN1_ST05	201222	25.63	-24.90
St 06	AN1_ST06	201223	22.22	-26.64
St 07	AN1_ST07	201224	18.87	-28.32
St 08	AN1_ST08	201225	14.95	-28.78
St 09	AN1_ST09	201226	10.87	-29.23
St 10	AN1_ST10	201227	7.34	-29.58
St 11	AN1_ST11	201228	3.83	-29.86
St 12	AN1_ST12	201229	0.15	-30.50
St 13	AN1_ST13	201230	-2.97	-30.95
St 14	AN1_ST14	201231	-6.77	-31.33
St 15	AN1_ST15	210102	-14.37	-33.92
St 16	AN1_ST17	210104	-21.30	-36.81
St 17	AN1_ST21	210108	-34.46	-46.79
St 18	AN1_ST23	210111	-43.79	-54.75
St 19	AN1_ST24	210112	-46.79	-58.46

Code	Original cruise code	Date	Lat	Long
St 20	AN2_ST00	220121	-62.98	-60.65
St 21	AN2_ST01	220123	-62.71	-60.64
St 22	AN2_ST03	220125	-64.58	-62.57
St 23	AN2_ST05	220127	-66.92	-69.10
St 24	AN2_ST07	220130	-70.85	-79.89
St 25	AN2_ST09	220131	-69.21	-78.84
St 26	AN2_ST10	220201	-67.70	-75.00
St 27	AN2_ST11	220204	-62.58	-58.62
St 28	AN2_ST12	220206	-62.98	-60.27

Table S2. Target PFSAs and PFCAs, and Surrogate and Injection Standards used in the present study with their acronyms, parent and product ions and retention times.

Compound	Acronym	Parent Ion (m/z)	Product Ion (m/z)	Retention Time
Perfluoroalkyl sulfonic acids	**PFSAs**			
Perfluorobutane sulfonic acid	PFBS	299	80	2.32
Perfluorohexane sulfonic acid	PFHxS	399	80	3.81
Perfluorooctane sulfonic acid	PFOS	599	80	4.63
Perfluorodecane sulfonic acid	PFDS	563	519	5.18
Perfluorododecane sulfonic acid	PFDoDS	699	80	5.51
Perfluoroethylcyclohexane sulfonate	PFECHS	461	381	4.18
Perfluoroalkyl carboxylic acids	**PFCAs**			
Perfluorobutanoic acid	PFBA	213	169	0.88
Perfluoropentanoic acid	PFPeA	263	219	2.03
Perfluorohexanoic acid	PFHxA	131	269	3.06
Perfluoroheptanoic acid	PFHpA	363	319	3.75
Perfluorooctanoic acid	PFOA	413	369	4.23
Perfluorononanoic acid	PFNA	463	419	4.61
Perfluorodecanoic acid	PFDA	513	469	4.93
Perfluoroundecanoic acid	PFUnDA	563	519	5.19
Perfluorododecanoic acid	PFDoDA	613	569	5.38
Perfluorotridecanoic acid	PFTrDA	663	619	5.52
Perfluorotetradecanoic acid	PFTeDA	713	669	5.64
Perfluorohexadecanoic acid	PFHxDA	813	769	5.77
Perfluorooctadecanoic acid	PFODA	913	369	5.84
Surrogate Standards				
Perfluoro-n-[$^{13}C_4$]butanoic acid	PFBA-$^{13}C_4$	216	172	0.88
Perfluoro-n-[1,2-$^{13}C_2$]hexanoic aic	PFHxA-$^{13}C_2$	315	270	3.06
Perfluoro-n-[1,2,3,4-$^{13}C_4$]octanoic acid	PFOA-$^{13}C_4$	417	372	4.23
Perfluoro-n-[1,2,3,4,5-$^{13}C_5$]nonanoic acid	PFNA-$^{13}C_5$	468	423	4.61
Perfluoro-n-[1,2-$^{13}C_2$]decanoic acid	PFDA-$^{13}C_2$	515	470	4.93
Perfluoro-n-[1,2-$^{13}C_2$]undecanoic acid	PFUnDA-$^{13}C_2$	570	252	5.18
Perfluoro-n-[1,2-$^{13}C_2$]dodecanoic acid	PFDoDA-$^{13}C_2$	615	570	5.37
Sodium perfluoro-1-hexane[$^{18}C_2$]sulfonate	PFHxS-$^{18}C_2$	403	84	3.81
Sodium perfluoro-1-[1,2,3,4-$^{13}C_4$]octanesulfonate	PFOS-$^{13}C_4$	503	80	4.63
Injection Standard				
Perfluoro-n-[2,3,4-$^{13}C_3$]butanoic acid	PFBA-$^{13}C_3$	216	172	0.89
Perfluoro-n-[$^{13}C_5$]pentanoic acid	PFPeA-$^{13}C_5$	268	223	2.03
Sodium perfluoro-1-[$^{13}C_8$]-octanesulfonate	PFOS-$^{13}C_8$	507	80	3.81
Perfluoro-n-[$^{13}C_8$]octanoic acid	PFOA-$^{13}C_8$	421	376	4.23
Sodium perfluoro-1-[1,2,3-$^{13}C_3$]-hexanesulfonate	PFHxS-$^{13}C_3$	402	99	4.62
Perfluoro-n-[1,2,3,4,5,6,7-$^{13}C_7$]undecanoic acid	PFUnDA-$^{13}C_7$	570	525	5.18

Table S3. Individual PFAAs concentrations (pg L^{-1}) at 5 m and DCM samples from the Atlantic Ocean.

Sample	Type	Station Code	Depth (m)	PFBS	PFHxS	PFECHS	PFOS	PFDS	PFDoDS	PFPeA	PFHpA	PFOA	PFNA	PFDA	PFUnDA	PFDoDA	PFTrDA	PFTeDA	PFHxDA	PFODA	∑17PFAA
AN1WPFAS_002	DCM	St 01	60	43.50	4.50	1.50	3.00	nd	0.75	53.25	255.00	18.75	27.75	15.75	4.50	nd	nd	0.75	15.00	nd	444.00
AN1WPFAS_003	5 m	St 01	4	27.75	6.75	1.50	<loq	0.75	0.75	92.25	141.00	42.75	20.25	18.00	2.25	nd	<loq	nd	7.50	7.50	369.00
AN1WPFAS_006	DCM	St 02	105	16.50	5.25	1.50	<loq	0.75	nd	39.00	63.75	50.25	25.50	11.25	6.75	1.50	<loq	nd	<loq	nd	222.00
AN1WPFAS_007	5 m	St 02	5	21.75	5.25	0.75	2.25	nd	nd	68.25	46.50	22.50	29.25	27.00	20.25	3.75	<loq	1.50	3.00	nd	252.00
AN1WPFAS_009	5 m	St 03	5	26.25	6.75	1.50	2.25	nd	1.50	51.00	91.50	19.50	18.75	5.25	3.00	nd	<loq	nd	nd	nd	227.25
AN1WPFAS_010	DCM	St 03	115	15.00	7.50	1.50	<loq	nd	1.50	44.25	62.25	30.75	21.00	6.00	4.50	nd	nd	nd	<loq	nd	194.25
AN1WPFAS_011	DCM	St 04	85	12.75	5.25	1.50	<loq	nd	nd	28.50	37.50	19.50	15.75	5.25	3.00	nd	<loq	nd	7.50	nd	136.50
AN1WPFAS_013	5 m	St 04	5	17.25	4.50	0.75	3.00	3.00	1.50	41.25	48.00	15.75	21.00	8.25	6.00	nd	<loq	nd	5.25	nd	175.50
AN1WPFAS_016	5 m	St 05	5	15.00	3.75	1.50	3.00	nd	nd	27.00	65.25	21.75	11.25	3.00	1.50	nd	2.25	nd	<loq	nd	155.25
AN1WPFAS_017	DCM	St 05	120	23.25	5.25	0.75	3.00	nd	0.75	62.25	60.75	31.50	17.25	3.75	4.50	nd	nd	nd	<loq	nd	213.00
AN1WPFAS_019	5 m	St 06	5	9.75	9.75	1.50	4.50	nd	nd	41.25	63.00	15.75	18.75	6.75	3.75	2.25	<loq	nd	4.50	nd	181.50
AN1WPFAS_020	5 m	St 07	5	9.38	6.38	1.13	3.38	nd	1.50	41.25	65.63	22.00	18.00	5.25	3.75	2.25	<loq	1.50	4.13	nd	185.50
AN1WPFAS_021	DCM	St 07	85	11.25	3.75	<loq	<loq	nd	0.75	nd	72.75	22.50	12.75	2.25	1.50	nd	nd	nd	3.00	nd	130.50
AN1WPFAS_022	5 m	St 08	5	13.50	3.00	1.50	5.25	nd	nd	nd	40.50	nd	12.00	<loq	3.00	nd	<loq	0.75	<loq	nd	79.50
AN1WPFAS_023	5 m	St 09	5	10.50	3.00	0.75	5.25	nd	1.50	nd	nd	<loq	9.00	4.50	nd	nd	<loq	1.50	<loq	nd	36.00
AN1WPFAS_024	DCM	St 09	50	<loq	<loq	0.75	<loq	nd	1.50	nd	46.50	<loq	5.50	3.50	2.25	nd	<loq	1.50	7.13	<loq	68.63
AN1WPFAS_028	5 m	St 10	5	<loq	2.50	0.38	4.88	nd	1.50	nd	41.63	<loq	4.50	3.00	2.00	nd	<loq	nd	4.88	<loq	65.25
AN1WPFAS_029	5 m	St 11	5	5.25	nd	0.75	3.00	nd	nd	nd	51.00	19.13	26.25	17.25	10.50	3.75	2.25	0.75	3.00	<loq	142.88
AN1WPFAS_030	DCM	St 11	77	<loq	<loq	0.75	nd	nd	nd	22.50	36.75	<loq	9.00	3.00	2.25	nd	<loq	1.50	3.00	<loq	78.75
AN1WPFAS_032	5 m	St 12	5	<loq	nd	0.75	2.25	nd	nd	nd	33.00	<loq	nd	1.50	1.50	nd	<loq	nd	3.75	nd	42.75
AN1WPFAS_033	DCM	St 12	50	6.75	4.50	0.75	3.00	nd	nd	nd	49.50	<loq	nd	<loq	1.50	nd	<loq	nd	<loq	nd	66.00
AN1WPFAS_037	5 m	St 13	5	9.75	4.50	0.75	3.00	nd	nd	nd	60.00	<loq	6.00	7.50	4.50	nd	<loq	1.50	4.50	nd	102.00
AN1WPFAS_038	5 m	St 14	5	9.75	nd	1.50	3.00	nd	nd	nd	35.25	<loq	10.50	4.50	4.50	nd	nd	0.75	6.00	nd	75.75
AN1WPFAS_039	DCM	St 14	120	<loq	<loq	1.50	7.50	nd	1.50	nd	23.25	<loq	nd	1.50	1.50	nd	nd	1.50	10.50	nd	48.75
AN1WPFAS_041	5 m	St 15	5	6.75	nd	1.50	2.25	nd	0.75	nd	51.75	16.50	4.50	6.75	nd	nd	nd	nd	<loq	nd	90.75
AN1WPFAS_042	DCM	St 15	145	9.75	3.75	1.50	<loq	4.50	0.75	nd	65.25	<loq	nd	4.50	6.00	nd	3.00	nd	4.50	<loq	103.50
AN1WPFAS_047	5 m	St 16	5	11.25	nd	0.75	4.05	nd	nd	39.00	63.75	103.50	114.75	84.00	29.25	10.50	4.50	1.50	<loq	nd	466.80
AN1WPFAS_048	DCM	St 16	90	6.00	3.75	1.50	<loq	nd	1.50	nd	42.00	<loq	7.50	5.25	3.00	nd	<loq	1.50	nd	<loq	72.00
AN1WPFAS_057	5 m	St 17	5	nd	3.00	nd	4.50	nd	nd	21.75	57.00	18.75	36.75	12.00	7.50	nd	nd	0.75	3.75	nd	165.75
AN1WPFAS_061	5 m	St 18	5	nd	6.00	1.50	nd	nd	1.50	554.25	130.50	63.75	28.50	14.25	5.25	nd	<loq	1.50	3.00	nd	810.00
AN1WPFAS_064	5 m	St 19	5	<loq	7.50	1.50	nd	nd	nd	81.75	82.50	21.75	15.75	10.50	8.25	3.00	<loq	1.50	4.50	<loq	238.50
AN1WPFAS_065	DCM	St 19	50	<loq	nd	1.50	nd	nd	nd	nd	55.50	<loq	9.00	2.25	3.00	nd	nd	1.50	<loq	nd	72.75

nd stands for *non detected*; <loq stands for samples *below limit of quantification*

Table S4. Individual PFAAs concentrations (pg L^{-1}) at vertical profile samples from the Atlantic Ocean.

Sample	Type	Station Code	Depth (m)	PFBS	PFHxS	PFECHS	PFOS	PFDS	PFDoDS	PFPeA	PFHpA	PFOA	PFNA	PFDA	PFUnDA	PFDoDA	PFTrDA	PFTeDA	PFHxDA	PFODA	∑17PFAA
AN1WPFAS_003	5 m	St 01	4	27.75	6.75	1.50	<loq	0.75	0.75	92.25	141.00	42.75	20.25	18.00	2.25	nd	<loq	nd	7.50	7.50	369.00
AN1WPFAS_002	DCM	St 01	60	43.50	4.50	1.50	3.00	nd	0.75	53.25	255.00	18.75	27.75	15.75	4.50	nd	nd	0.75	15.00	nd	444.00
AN1WPFAS_001	1%PAR	St 01	100	32.25	6.00	0.75	3.75	3.00	0.75	117.75	195.75	47.25	30.00	14.25	2.25	nd	nd	nd	3.75	nd	457.50
AN1WPFAS_005	MOx	St 01	850	28.50	6.75	0.75	4.50	nd	1.50	59.25	132.75	23.25	18.75	12.00	4.50	1.50	<loq	0.75	3.00	nd	297.75
AN1WPFAS_004	Deep	St 01	2000	35.25	3.00	nd	3.00	2.25	1.50	79.50	140.25	15.75	12.00	10.50	6.75	1.50	2.25	nd	3.75	nd	317.25
AN1WPFAS_013	5 m	St 04	5	17.25	4.50	0.75	3.00	3.00	1.50	41.25	48.00	15.75	21.00	8.25	6.00	nd	<loq	nd	5.25	nd	175.50
AN1WPFAS_011	DCM	St 04	85	12.75	5.25	1.50	<loq	nd	nd	28.50	37.50	19.50	15.75	5.25	3.00	nd	<loq	nd	7.50	nd	136.50
AN1WPFAS_012	1%PAR	St 04	125	10.88	5.25	2.25	5.63	nd	1.00	35.25	60.75	31.50	23.63	6.00	3.75	nd	<loq	0.75	12.75	15.00	214.38
AN1WPFAS_014	MOx	St 04	900	12.75	nd	0.75	nd	1.50	nd	29.25	57.00	<loq	3.00	1.50	3.00	1.50	<loq	nd	nd	nd	110.25
AN1WPFAS_015	Deep	St 04	2000	12.00	<loq	nd	2.25	nd	nd	29.25	60.00	<loq	3.00	3.00	2.25	nd	<loq	nd	nd	nd	111.75
AN1WPFAS_023	5 m	St 09	5	10.50	3.00	0.75	5.25	nd	1.50	nd	nd	<loq	9.00	4.50	nd	nd	<loq	1.50	<loq	nd	36.00
AN1WPFAS_024	DCM	St 09	50	<loq	<loq	0.75	<loq	nd	1.50	nd	46.50	<loq	5.50	3.50	2.25	nd	<loq	1.50	7.13	<loq	68.63
AN1WPFAS_025	1%PAR	St 09	60	5.63	2.63	0.75	3.00	nd	1.50	nd	48.75	16.80	8.63	3.00	nd	nd	<loq	1.50	7.13	<loq	99.30
AN1WPFAS_026	MOx	St 09	400	nd	<loq	0.38	<loq	nd	0.75	40.50	65.25	<loq	5.25	1.50	2.63	nd	<loq	nd	3.75	<loq	120.00
AN1WPFAS_027	Deep	St 09	2000	nd	<loq	nd	nd	nd	nd	nd	29.25	<loq	nd	nd	<loq	nd	<loq	nd	6.75	nd	36.00
AN1WPFAS_032	5 m	St 12	5	<loq	nd	0.75	2.25	nd	nd	nd	33.00	<loq	nd	1.50	1.50	nd	<loq	nd	3.75	nd	42.75
AN1WPFAS_033	DCM	St 12	50	6.75	4.50	0.75	3.00	nd	nd	nd	49.50	<loq	nd	<loq	1.50	nd	<loq	nd	<loq	nd	66.00
AN1WPFAS_034	1%PAR	St 12	78	nd	<loq	1.50	nd	nd	nd	nd	44.25	<loq	6.00	3.00	3.00	nd	<loq	1.50	nd	nd	59.25
AN1WPFAS_035	MOx	St 12	400	<loq	3.00	1.50	<loq	2.25	nd	37.50	55.50	<loq	4.50	5.25	6.00	nd	nd	0.75	4.50	<loq	120.75
AN1WPFAS_036	Deep	St 12	2000	<loq	4.50	1.50	nd	nd	nd	27.75	71.25	16.50	nd	2.25	nd	nd	nd	1.50	<loq	<loq	125.25
AN1WPFAS_041	5 m	St 15	5	6.75	nd	1.50	2.25	nd	0.75	nd	51.75	16.50	4.50	6.75	nd	nd	nd	nd	<loq	nd	90.75
AN1WPFAS_042	DCM	St 15	145	9.75	3.75	1.50	<loq	4.50	0.75	nd	65.25	<loq	nd	4.50	6.00	nd	3.00	nd	4.50	<loq	103.50
AN1WPFAS_043	1%PAR	St 15	110	8.85	7.50	1.50	<loq	nd	nd	nd	45.00	27.00	3.75	4.50	5.25	nd	nd	0.75	7.50	nd	111.60
AN1WPFAS_044	MOx	St 15	350	6.75	3.00	1.50	nd	2.25	0.75	48.00	63.00	<loq	6.00	5.25	4.50	nd	3.00	nd	<loq	nd	144.00
AN1WPFAS_045	Deep	St 15	2000	<loq	6.00	0.75	nd	2.25	nd	37.50	66.75	<loq	nd	3.75	3.00	nd	<loq	nd	<loq	nd	120.00
AN1WPFAS_064	5 m	St 19	5	<loq	7.50	1.50	nd	nd	nd	81.75	82.50	21.75	15.75	10.50	8.25	3.00	<loq	1.50	4.50	<loq	238.50
AN1WPFAS_065	DCM	St 19	50	<loq	nd	1.50	nd	nd	nd	nd	55.50	<loq	9.00	2.25	3.00	nd	nd	1.50	<loq	nd	72.75
AN1WPFAS_066	1%PAR	St 19	200	5.25	nd	0.75	4.20	nd	nd	318.00	93.00	20.70	11.25	5.25	3.00	nd	<loq	nd	nd	nd	461.40

nd stands for *non detected*; <loq stands for samples *below limit of quantification*

Table S5. Individual PFAAs concentrations (pg L^{-1}) at 5 m and DCM samples from the Southern Ocean.

Sample	Type	Station Code	Depth (m)	PFBS	PFHxS	PFECHS	PFOS	PFDS	PFDoDS	PFBA	PFPeA	PFHpA	PFOA	PFNA	PFDA	PFUnDA	PFDoDA	PFTrDA	PFTeDA	PFHxDA	PFODA	∑17PFAA
AN2WPFAS_001	5 m	St 20	5	nd	nd	nd	12.00	nd	1.50	nd	85.50	<loq	nd	1.50	<loq	nd	<loq	<loq	<loq	nd	nd	100.50
AN2WPFAS_002	DCM	St 20	165	nd	nd	0.75	31.50	3.00	0.75	138.75	126.00	<loq	13.50	3.75	3.00	1.50	<loq	<loq	<loq	nd	nd	322.50
AN2WPFAS_013	5 m	St 21	5	nd	nd	nd	11.25	1.50	1.50	nd	126.00	<loq	nd	3.75	<loq	nd	<loq	nd	<loq	nd	nd	144.00
AN2WPFAS_014	DCM	St 21	25	nd	3.00	0.75	9.00	1.50	1.50	nd	115.50	<loq	nd	3.00	<loq	nd	<loq	nd	<loq	nd	nd	134.25
AN2WPFAS_023	5 m	St 22	5	nd	4.50	nd	47.25	1.50	0.75	nd	114.00	<loq	7.50	2.25	3.00	0.75	<loq	nd	<loq	nd	nd	181.50
AN2WPFAS_028	5 m	St 23	6	nd	nd	nd	10.50	1.50	4.50	69.00	120.00	<loq	8.25	3.75	4.50	1.50	2.25	<loq	<loq	nd	nd	225.75
AN2WPFAS_033	5 m	St 24	5	nd	nd	3.00	120.00	nd	9.00	nd	156.00	30.75	14.25	5.25	6.00	nd	<loq	1.50	<loq	nd	nd	345.75
AN2WPFAS_034	DCM	St 24	22	nd	nd	3.00	110.25	nd	8.25	nd	171.00	37.50	nd	1.50	3.00	nd	<loq	<loq	<loq	1.50	nd	336.00
AN2WPFAS_039	5 m	St 25	5	nd	nd	2.25	51.00	4.50	6.00	nd	nd	108.75	nd	6.00	nd	nd	5.25	nd	7.50	1.50	nd	192.75
AN2WPFAS_040	DCM	St 25	33	nd	nd	1.50	43.50	6.00	5.25	nd	nd	74.25	nd	nd	33.00	nd	4.50	1.50	30.00	10.50	nd	210.00
AN2WPFAS_042	5 m	St 26	5	nd	15.00	nd	123.75	7.50	3.00	nd	nd	115.50	nd	nd	16.50	nd	14.25	9.00	nd	nd	nd	304.50
AN2WPFAS_043	DCM	St 26	50	6.75	nd	nd	12.75	nd	1.50	17.25	54.00	18.75	3.00	6.00	4.50	nd	<loq	0.00	27.00	10.50	6.75	162.00
AN2WPFAS_044	5 m	St 27	5	3.00	3.00	nd	33.75	nd	nd	nd	19.50	21.00	nd	5.25	3.00	1.50	<loq	0.00	26.25	7.50	3.00	123.75
AN2WPFAS_045	DCM	St 27	37	nd	3.00	nd	24.00	nd	0.75	nd	32.25	<loq	4.50	3.75	3.75	nd	<loq	nd	7.50	nd	nd	79.50
AN2WPFAS_049	5 m	St 28	5	4.50	nd	nd	8.25	nd	0.75	nd	36.75	18.00	nd	3.75	<loq	nd	nd	<loq	<loq	nd	4.50	72.00
AN2WPFAS_050	DCM	St 28	40	3.75	3.00	nd	10.50	nd	nd	nd	54.00	<loq	nd	1.50	<loq	nd	nd	nd	<loq	nd	3.75	72.75

nd stands for *non detected*; <loq stands for samples *below limit of quantification*

Table S6. Target PFAAs concentrations (pg L^{-1}) at vertical profile samples from the Southern Ocean.

Sample	Type	Station Code	Depth (m)	PFBS	PFHxS	PFECHS	PFOS	PFDS	PFDoDS	PFPeA	PFHpA	PFOA	PFNA	PFDA	PFUnDA	PFDoDA	PFTrDA	PFTeDA	PFHxDA	PFODA	∑17PFAA
AN2WPFAS_033	5 m	St 24	5	nd	nd	3.00	120.00	nd	9.00	nd	156.00	30.75	14.25	5.25	6.00	nd	<loq	1.50	<loq	nd	345.75
AN2WPFAS_034	DCM	St 24	22	nd	nd	3.00	110.25	nd	8.25	nd	171.00	37.50	nd	1.50	3.00	nd	<loq	<loq	<loq	1.50	336.00
AN2WPFAS_035	1%PAR	St 24	75	nd	nd	1.50	21.00	nd	2.25	nd	193.50	26.25	9.00	6.00	3.75	nd	<loq	1.50	<loq	0.75	265.50
AN2WPFAS_036	MOx	St 24	210	nd	3.00	1.50	28.50	2.25	0.75	nd	75.75	40.50	nd	nd	3.00	nd	2.25	nd	nd	nd	157.50
AN2WPFAS_037	Deep	St 24	584	nd	3.00	0.75	12.00	1.50	nd	nd	54.00	23.25	nd	nd	<loq	nd	<loq	nd	nd	nd	94.50
AN2WPFAS_044	5 m	St 27	5	3.00	3.00	nd	33.75	nd	nd	nd	19.50	21.00	nd	5.25	3.00	1.50	<loq	0.00	26.25	7.50	123.75
AN2WPFAS_045	DCM	St 27	37	nd	3.00	nd	24.00	nd	0.75	nd	32.25	<loq	4.50	3.75	3.75	nd	<loq	nd	7.50	nd	79.50
AN2WPFAS_046	1%PAR	St 27	200	3.00	2.25	nd	17.25	nd	0.75	22.50	44.25	15.00	nd	2.25	3.00	nd	nd	nd	<loq	nd	110.25
AN2WPFAS_047	MOx	St 27	850	3.00	<loq	nd	19.50	nd	1.50	nd	41.25	<loq	4.50	3.00	3.00	0.75	nd	nd	<loq	nd	76.50
AN2WPFAS_048	Deep	St 27	1620	5.25	nd	nd	7.50	nd	nd	nd	31.50	17.55	6.00	3.75	2.85	1.50	nd	1.50	<loq	nd	77.40
AN2WPFAS_049	5 m	St 28	5	4.50	nd	nd	8.25	nd	0.75	nd	36.75	18.00	nd	3.75	<loq	nd	nd	<loq	<loq	nd	71.25
AN2WPFAS_050	DCM	St 28	40	3.75	3.00	nd	10.50	nd	nd	nd	54.00	<loq	nd	1.50	<loq	nd	nd	nd	<loq	nd	72.75
AN2WPFAS_051	1%PAR	St 28	155	3.75	nd	nd	8.25	nd	nd	nd	26.25	<loq	nd	nd	<loq	nd	<loq	nd	<loq	nd	38.25

nd stands for *non detected*; <loq stands for samples *below limit of quantification*

Table S7. Mean relative contribution of individual PFAAs to the total PFAA's pool (%), for the Atlantic and Southern oceans.

Ocean	PFBS	PFHxS	PFECHS	PFOS	PFDS	PFDoDS	PFPeA	PFHpA	PFOA	PFNA	PFDA	PFUnDA	PFDoDA	PFTrDA	PFTeDA	PFHxDA	PFODA
Atlantic	5.99	1.98	0.59	1.20	0.27	0.33	22.2	39.2	9.43	8.31	4.61	2.53	0.37	0.23	0.38	1.96	0.38
Southern	0.87	1.06	0.39	20.1	0.80	1.31	6.51	43.6	14.4	1.84	1.72	2.51	0.19	0.76	0.40	2.67	0.84

Table S8. PFAAs values (pg) from field blanks and procedural blanks.

Name	PFBS	PFHxS	PFECHS	PFOS	PFDS	PFDoDS	PFPeA	PFHpA	PFOA	PFNA	PFDA	PFUnDA	PFDoDA	PFTrDA	PFTeDA	PFHxDA	PFODA
ANIWPFAS_008	nd	nd	nd	nd	nd	nd	0.10	nd	0.45	nd	nd	nd	nd	0.10	nd	0.10	nd
ANIWPFAS_018	0.50	nd	nd	nd	nd	nd	nd	nd	0.55	nd	nd	nd	nd	nd	nd	nd	nd
ANIWPFAS_031	0.10	0.10	nd	0.05	nd	nd	nd	nd	0.85	nd	nd	0.05	nd	0.10	nd	nd	nd
ANIWPFAS_040	0.05	0.05	nd	nd	nd	0.35	0.10	nd	0.80	nd	nd	0.05	nd	0.10	0.60	nd	nd
ANIWPFAS_049	0.10	nd	nd	nd	nd	nd	nd	nd	0.35	nd	nd	nd	nd	0.10	0.05	nd	1.35
ANIWPFAS_053	0.15	0.05	nd	0.30	nd	nd	nd	nd	1.00	nd	nd	0.05	nd	nd	0.05	nd	0.60
ANIWPFAS_062	0.05	0.15	nd	0.10	nd	nd	0.70	nd	0.85	nd	nd	nd	nd	0.10	0.05	0.70	nd
ANIWPFAS_063	0.20	0.05	nd	0.05	nd	nd	0.15	nd	0.50	nd	nd	0.05	nd	0.10	0.05	nd	nd
ANIWPFAS_067	0.10	0.05	nd	nd	nd	nd	0.10	nd	0.50	nd	nd	0.05	nd	0.10	nd	0.05	nd
ANIWPFAS_068	0.05	nd	nd	nd	nd	nd	nd	nd	0.55	nd	nd	0.05	nd	0.10	nd	0.20	0.20
ANIWPFAS_069	0.70	nd	nd	0.05	nd	nd	nd	0.10	0.90	nd	nd	0.05	nd	0.10	nd	0.15	nd
ANIWPFAS_070	nd	0.15	nd	0.10	nd	nd	0.10	nd	0.90	nd	nd	0.05	nd	0.10	0.05	0.50	nd
AN2WPFAS_003	0.05	0.10	nd	0.10	nd	nd	nd	0.10	0.80	nd	nd	0.10	nd	0.10	nd	nd	nd
AN2WPFAS_005	0.10	0.10	nd	nd	nd	nd	nd	0.10	0.80	nd	nd	0.05	nd	0.10	nd	0.10	nd
AN2WPFAS_006	0.10	0.10	nd	nd	nd	nd	0.10	0.10	0.70	nd	nd	0.10	nd	0.10	nd	0.10	nd
AN2WPFAS_007	nd	nd	nd	nd	nd	nd	0.60	nd	0.60	nd	nd	0.05	nd	0.10	0.05	1.00	nd
AN2WPFAS_008	nd	nd	nd	nd	nd	nd	0.50	nd	0.25	nd	nd	nd	nd	0.10	nd	1.35	0.10
AN2WPFAS_052	nd	nd	nd	nd	nd	nd	nd	nd	0.15	nd	nd	nd	nd	0.10	nd	nd	nd
AN2WPFAS_041	nd	nd	nd	nd	nd	0.05	nd	nd	0.45	nd	nd	nd	nd	0.10	nd	nd	nd
ANPFAS_PB01	nd	0.10	nd	nd	nd	nd	0.15	nd	0.60	nd	nd	nd	nd	0.10	nd	0.20	nd
ANPFAS_PB02	nd	0.10	nd	nd	nd	nd	nd	0.10	0.85	nd	0.05	0.20	nd	nd	0.20	0.25	nd
ANPFAS_PB03	nd	0.10	nd	0.30	nd	nd	0.10	0.85	0.30	nd	nd	0.05	nd	nd	0.10	0.05	nd
ANPFAS_PB04	nd	0.15	nd	0.20	nd	nd	nd	0.10	0.95	nd	nd	0.25	nd	0.10	0.10	0.40	nd
ANPFAS_PB05	nd	0.15	nd	nd	nd	nd	nd	nd	0.20	nd	nd	0.05	nd	0.10	nd	nd	nd

nd stands for *non detected*; <loq stands for samples *below limit of quantification*

Table S9. Limits of Quantification (LOQs) (pg) for PFAAs compounds for the Atlantic and Southern Ocean samples.

	Atlantic Ocean	Southern Ocean
PFBS	0.530	0.110
PFHxS	0.210	0.180
PFECHS	0.001	0.001
PFOS	0.200	0.260
PFDS	0.001	0.001
PFDoDS	0.010	0.020
PFHpA	0.310	0.450
PFPeA	0.330	0.550
PFOA	1.340	1.330
PFNA	0.010	0.010
PFDA	0.010	0.020
PFUnDA	0.120	0.260
PFDoDA	0.001	0.001
PFTrDA	0.140	0.120
PFTeDA	0.290	0.110
PFHxDA	0.260	0.700
PFODA	0.650	0.050

LOQs were calculated from the log transformed mean and SD values from the field and procedural blanks. LOQs are the result of the mean plus three times the standard deviation.

References

51. Pavlov, M. Log-normal Distribution - A simple explanation. How to calculate μ & σ, the mode, mean, median & variance. Published in Towards Data Science. Medium. (2022). Retrieved from https://towardsdatascience.com/log-normal-distribution-a-simple-explanation-7605864fb67c on June 2024.





PART 03

CHAPTER 3.

Transport and biogeochemistry of OPEs in the oceans.

3.3.1. Paper III. *Enrichment of Organophosphate Esters in the Sea Surface Microlayer from the Atlantic and Southern Oceans*

3.3.2. Paper III. Supplementary Materials

3.3.3. Paper IV. *Biogeochemical Controls on Latitudinal (42°N to 70°S) and Depth Distribution of Organophosphate Esters in the Atlantic and Southern Oceans*

3.3.4. Paper IV. Supplementary Materials

PART 03 - CHAPTER 3. TRANSPORT AND BIOGEOCHEMISTRY OF OPEs IN THE OCEANS

3.3.1. Publication III. *Enrichment of Organophosphate Esters in the Sea Surface Microlayer from the Atlantic and Southern Oceans*

Núria Trilla-Prieto[1,2], Jon Iriarte[1], Naiara Berrojalbiz[1], Gemma Casas[2,3], Cristina Sobrino[4], Maria Vila-Costa[1], Begoña Jiménez[5], Jordi Dachs[1]

[1]Department of Environmental Chemistry, IDAEA-CSIC, Barcelona, Catalunya Spain.

[2]Departament of Ecology, Faculty of Marine Sciences, Universitat de Barcelona, Barcelona, Catalunya, Spain.

[3]Department of Marine Biology and Oceanography, Institut de Ciències del Mar, CSIC, Pg. Marítim de la Barceloneta, 37-49, E08003, Barcelona, Catalunya, Spain.

[4]Grupo de Oceanografía Biolóxica, Centro de Investigación Mariña (CIM), Universidade de Vigo (UVigo), Vigo, Spain.

[5]Department of Instrumental Analysis and Environmental Chemistry, IQOG-CSIC, Juan de la Cierva, 3, 28006, Madrid, Spain.

State: Published in ES&T-letters in August 2024 (Environ. Sci. Technol. Lett. 2024, 11, 1008−1015)
Available at doi: 10.1021/acs.estlett.4c00636

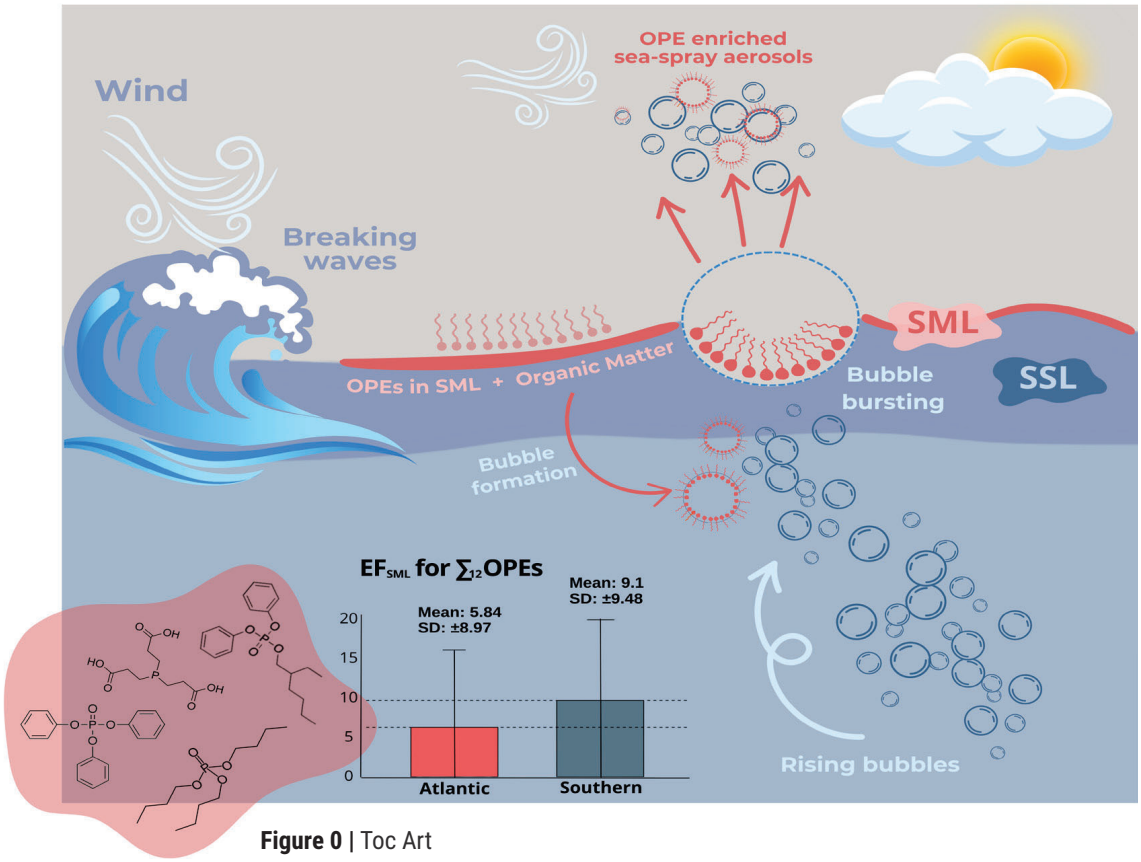


Figure 0 | Toc Art

Environmental Science & Technology Letters

pubs.acs.org/journal/estlcu

Letter

Open Access

This article is licensed under CC-BY 4.0

Enrichment of Organophosphate Esters in the Sea Surface Microlayer from the Atlantic and Southern Oceans

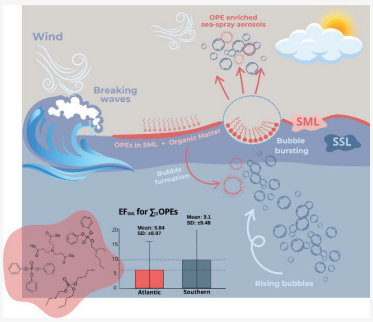
Núria Trilla-Prieto, Jon Iriarte, Naiara Berrojalbiz, Gemma Casas, Cristina Sobrino, Maria Vila-Costa, Begoña Jiménez, and Jordi Dachs*

Cite This: *Environ. Sci. Technol. Lett.* 2024, 11, 1008−1015

Read Online

ACCESS | Met ics & Mo e | A ticle Recommendations | - uppo ting 1n2o mation

ABSTRACT: The sea surface microlayer (SML) is the thin interface between the ocean and the atmosphere, exhibiting an enrichment of hydrophobic and surfactant-like chemicals. Here we report the concentrations of organophosphate esters (OPEs), widely used flame retardants and plasticizers, in the SML and underlying waters from a north−south transect in the Atlantic and Southern Oceans. Generally, concentrations of OPEs in the SML were higher than in the underlying waters. Concentrations in the SML were correlated with the chlorophyll α content for some OPEs, consistent with biogenic surfactants at the SML. The enrichment factors (ratio of concentrations in SML over concentrations in underlying waters) were 5.84 ± 8.97 and 9.10 ± 9.48 for the Atlantic and Southern Oceans, respectively. The average enrichment factors in sea spray aerosols (SSA), estimated using previously reported aerosol-phase concentrations, ranged from 3.69×10^4 to 3.33×10^6. These OPE enrichments in SSA are high and suggest that the formation of SSA, mediated by the enrichment in the SML, could be relevant for many semivolatile organic pollutants. Future research is needed to elucidate the variables driving the enrichment in the SML, its large variability, as well as its role in the fate of organic pollutants.



KEYWORDS: *organophosphate esters, sea surface microlayer, sea-spray aerosol, Atlantic Ocean, Southern Ocean*

PART 03

Downloaded via 83.50.55.101 on January 9, 2025 at 10:36:13 (UTC).
See https://pubs.acs.org/sharingguidelines for options on how to legitimately share published articles.

INTRODUCTION

Organophosphate esters (OPEs) are synthetic chemicals extensively used as flame retardants and plasticizers in many consumer products.[1] Due to their extensive application, OPEs have emerged as ubiquitous environmental contaminants, sparking concern over their widespread occurrence, toxic properties, bioaccumulative potential and persistence.[2−5]

OPEs impact marine ecosystems and major biogeochemical cycles,[6,7] and have been detected not only in surface, but also in deep-seawaters.[7−10] Previous studies have reported diverse levels of OPEs in the Atlantic, Pacific, and Indian oceans, as well as in the Mediterranean and Black Seas, reflecting diverse sources and contrasting transport and biogeochemical processes.[6,11−24] OPE concentrations have previously been reported in oceanic transects from both the Atlantic and the Southern Ocean, with the highest concentrations close to river mouths such as the Amazon River.[4]

Atmospheric deposition explains their ubiquitous distribution in the ocean.[14,16,26,27] Nevertheless, the occurrence of OPEs in the surface microlayer (SML), the thin seawater layer between the air and sea,[27,28] remains uncharacterized. The SML displays unique physicochemical properties[29,30] and biological communities,[31,32] and it is a critical interface for the exchange of matter and energy between the ocean and the atmosphere.[33−36] The SML is generally enriched in a wide variety of organic pollutants compared to the underlying subsurface seawater (SSL), due to their surfactant nature, hydrophobic character, or processes leading to high concentrations at the surface such as bubbles' scavenging.[37] Previous works have reported the enrichment of semivolatile chemicals in the SML, such as polychlorinated biphenyls,[38,39] as well of polycyclic aromatic hydrocarbons.[39−44] Recent research has extended the assessment of enrichment in the SML to emerging pollutants such as perfluoroalkyl substances (PFAS).[45−47]

The SML is thought to play an important role in the composition of sea spray aerosol (SSA). SSA has been shown to account for an important vector for the aerosolization, and long-range transport of SSA-enriched chemicals such as PFAS.[46,48,49] To date, no information on the OPE-enrichment in the SML and the potential role that SSA plays as a source of atmospheric OPEs exist, limiting the current knowledge of their oceanic transport and biogeochemistry.

Here, we provide a unique data set of OPEs and other organophosphorus pollutants in the SML and SSL, as well as

Received: August 1, 2024
Revised: August 13, 2024
Accepted: August 13, 2024
Published: August 16, 2024



ACS Publications

© 2024 The Authors. Published by American Chemical Society

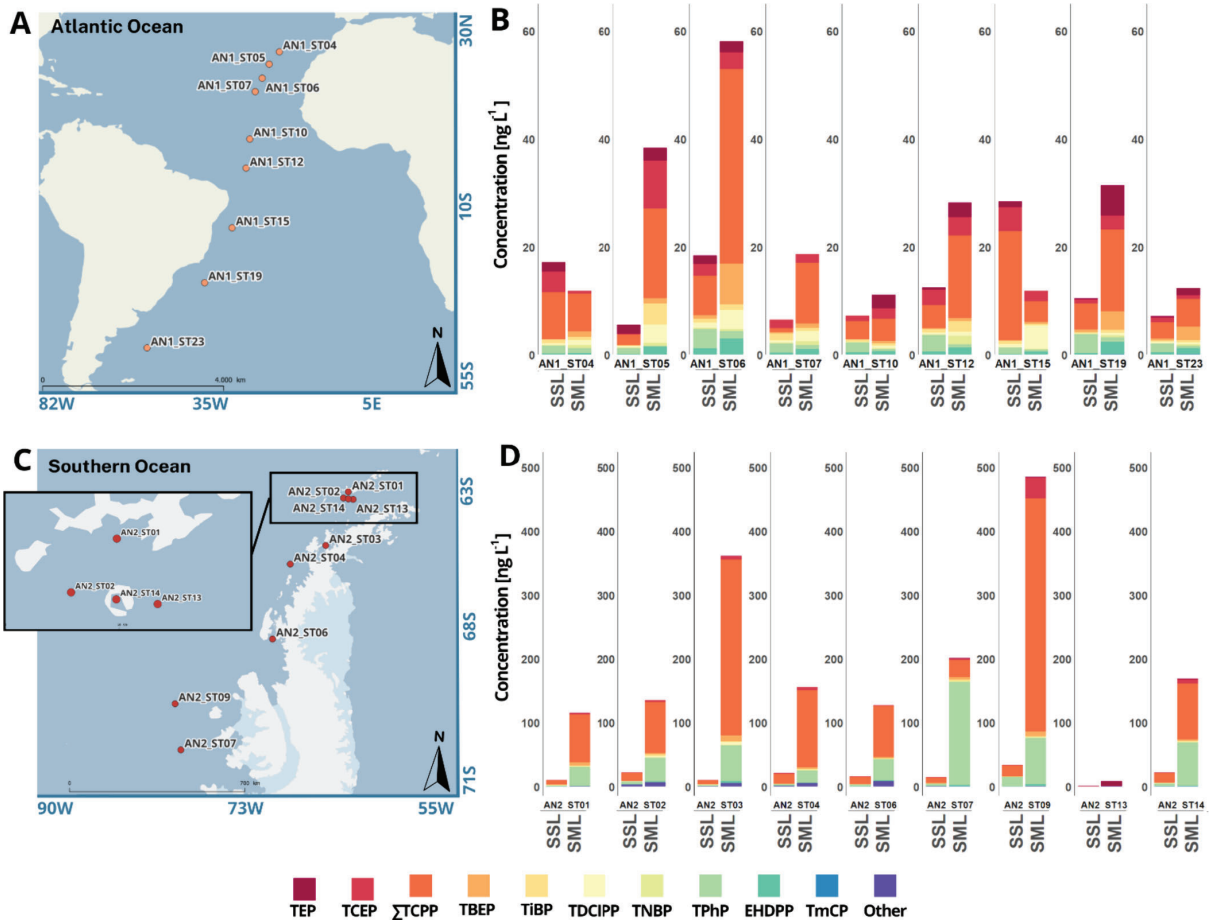


Figure 1. (A) Locations of sampling sites and station codes in the Atlantic Ocean; (B) individual OPE concentrations (ng L^{-1}) at the SML and SSL in the Atlantic Ocean; (C) locations of sampling sites and station codes in the Southern Ocean. (D) Individual OPE concentrations (ng L^{-1}) at the SML and SSL in the Southern Ocean; Category "other" results from the sum of TEHP, TPPO, TPrP, TpCP, TPPP, TBPO, Chlorpyrifos, ToCP, DOPP, TDMPP, TDBPP and TTBPP (see Table S2 for acronyms).

the corresponding enrichment factors, covering the Atlantic Ocean (from 35°N to 55°S) and the Southern Ocean (from 63°S to 70°S). The goals of this study are (i) to compare the distribution of OPEs between the SML and SSL, (ii) to estimate whether SSA formation has the potential for accounting for the occurrence of OPEs in the oceanic atmosphere, using previously reported aerosol-phase concentrations,[14] and (iii) to evaluate the drivers of OPE enrichment in the SML.

METHODS AND MATERIALS

Site Description. The SML and SSL samples were taken during the two ANTOM cruises on board of the RV Sarmiento de Gamboa and the RV Hespérides, respectively. ANTOM-I (December 15th, 2020 to January 15th 2021) involved a latitudinal oceanic transect from Vigo (41°N, Spain) to Punta Arenas (53°S, Chile), covering a vast region of the Atlantic Ocean. ANTOM-II (January 22th to February 6th, 2022) covered the Bransfield Strait and the Bellingshausen sea from 60°S to 71°S, in the Southern Ocean surrounding the western Antarctic peninsula. Nine pairs of SML and SSL samples were collected during each cruise (Figure 1). The Atlantic and Southern Ocean transects covered sites of contrasting environmental conditions (see Table S1 for ancillary data).

The SML sampling was performed with a glass plate SML sampler, adapting a method initially described by Harvey and Burzell in 1972[50] and since then used by many researchers.[32,35,38,45,46,51] This method involved vertically dipping a prerinsed glass plate (40 × 30 cm) into the water surface, allowing the SML to adhere to the plate during a slow withdrawal driven by the surface tension. The water retained on the glass was then swiftly scraped between two polytetrafluoroethylene (PTFE) wipers (Figure S1), facilitating drainage into a prerinsed 500 mL PTFE bottle. The process was repeated until obtaining a volume of 500 mL of SML seawater. SSL seawater samples were collected at the exact same location, at between 0.3 and 0.4 m depth, with a 2 L PTFE prerinsed bottle.

To mitigate the risk of contamination from the ship, SML and SSL sampling operations were executed from a rigid inflatable boat at 500 m upwind of the ship. Samples were taken from the upwind side of the inflatable boat, and drifting with the engine turned off.

https://doi.org/10.1021/acs.estlett.4c00636
Environ. Sci. Technol. Lett. 2024, 11, 1008−1015

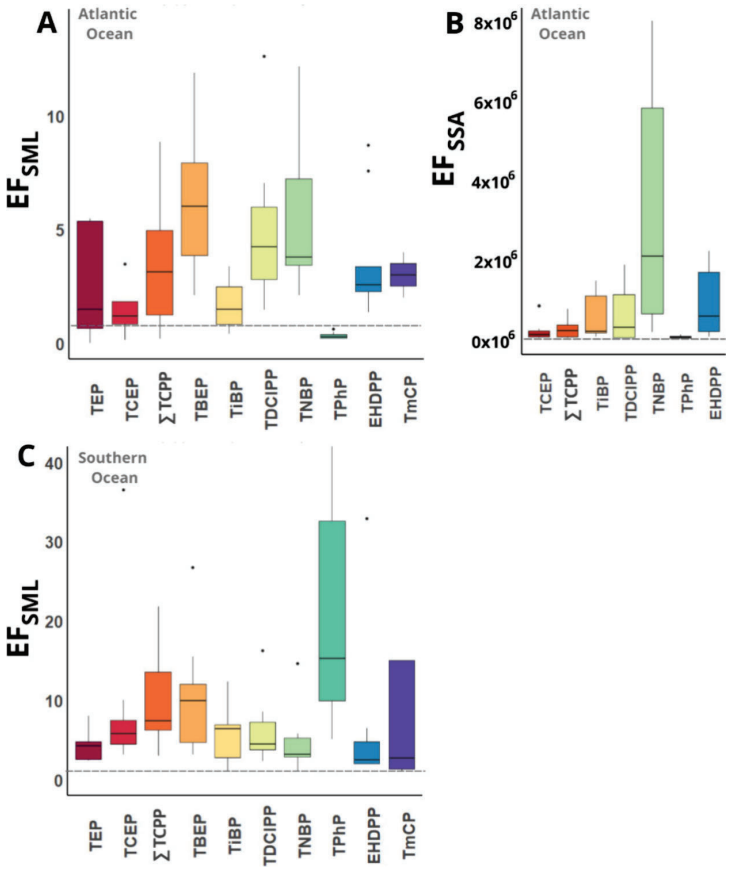


Figure 2. (A) Enrichment factors in the surface microlayer (EF_{SML}) for individual OPEs in the Atlantic Ocean; (B) enrichment factors in sea-spray aerosols (EF_{SSA}) for samples in the Atlantic Ocean; (C) enrichment factors in the surface microlayer (EF_{SML}) for individual OPEs in the Southern Ocean. Gray dashed line marks EF = 1.

Analysis, and Quality Assurance/Quality Control. Laboratory procedures and chemical analysis are detailed in Supplementary Notes S1 and S2, respectively. A total of 24 analytes were targeted in this study: five chlorinated-OPEs (TCEP, TDClPP and TCPP-1, 2 and 3), one brominated-OPE (TDBPP), eight alkylated-OPEs (TPhP, EHDPP, ToCP, TpCP, TmCP, TDMPP, TPPP, TTBPP) and six aryl-OPEs (TEP, TPrP, TiBP, TNBP, TBEP, TEHP) (see Table S2 for acronyms). In addition to OPEs, four organophosphorus chemicals were targeted (TPPO, DOPP, Chlorpyrifo,s and TBPO). For simplification, when we refer to OPEs in the discussion below, all targeted organophosphorus compounds are included.

Concentrations were recovery and blank corrected. Field blanks consisted of GF/F filters and Oasis HLB cartridges that followed the same field procedure, transport to the field and back to the laboratory, and analyzed as the field samples. Laboratory blanks (procedural blanks) followed the same extraction and analysis as the samples. A procedural and field blank were analyzed for each batch of 10 samples to monitor potential contamination. Blank concentrations are presented in Table S3. The limits of quantification (LOQs) were defined as the mean concentration of field and procedural blanks plus three times the standard deviation (Table S4). All concentrations below LOQ were not included in the statistical analysis. Recoveries were monitored using five surrogate standards prior to the extraction (Table S5). Surrogate recoveries averaged 70% and 73% for the samples from the Atlantic and Southern Ocean, respectively (Table S6).

RESULTS AND DISCUSSION

Occurrence of OPEs in the Atlantic and Southern Oceans. Among the 24 targeted analytes, a subset of 12 compounds were found in more than 50% of the samples, specifically TEP, TCEP, the three isomers of TCPP (TCPP-1, TCPP-2 and TCPP-3), TBEP, TiBP, TDCIPP, TNBP, TPhP, EHDPP, and TmCP. The remaining 12 analytes, were detected in less than 50% of the samples, and subsequently collectively grouped and categorized as "other" in this work, which encompass TEHP, TPPO, TPrP, TpCP, TPPP, TBPO, Chlorpyrifos, ToCP, DOPP, TDMPP, TDBPP, and TTBPP (Table S7).

In the Atlantic Ocean, concentrations of $\sum_{24}$OPEs in the SML averaged 24.7 ng L^{-1} (N = 9, median = 18.7 ± 16.0 ng L^{-1}), ranging from 11.2 to 58.1 ng L^{-1}. In the SSL, $\sum_{24}$OPEs averaged 12.7 ng L^{-1} (N = 9, median = 10.5 ± 7.54 ng L^{-1}) and ranged from 5.60 to 28.5 ng L^{-1} (Figures 1 and S5 and Tables S8, S9 and S10). The main contributing OPEs in the SSL were ∑TCPP (59%), followed by TCEP (10%), TPhP (6%) and TEP (6%). The trend in the SML was similar, with

https://doi.org/10.1021/acs.estlett.4c00636
Environ. Sci. Technol. Lett. 2024, 11, 1008−1015

also ∑TCPP as the main contributor (47%) followed by TPhP (16%), TCEP (15%) and TEP (6%) (Figure S2).

Regarding the samples collected in the Southern Ocean, concentrations of $\sum_{24}$OPEs in the SML were on average 196 ng L^{-1} (N = 9, median = 156 ± 143 ng L^{-1}) and ranged from 10 to 485 ng L^{-1}. Concentrations of $\sum_{24}$OPEs in the SSL averaged 17.15 ng L^{-1} (N = 9, median = 15.8 ± 9.13 ng L^{-1}), ranging from 2.5 to 34 ng L^{-1} (Figure 1 and S5 and Tables S8, S9, and 10). The distribution pattern was slightly different when compared to the Atlantic: ∑TCPP and TPhP were the main contributors to the total pool at the SML, with 63% and 26% of $\sum_{24}$OPEs, respectively. Similarly, in the SSL, these OPEs accounted for 61% and 21% of $\sum_{24}$OPEs, respectively. These percentages of ∑TCPP and TPhP are higher than those observed in the Atlantic (Figure S2).

The SSL concentrations reported here are within the same range as those published previously for oceanic regions.[17,20,23−25] For example, concentrations of $\sum_{8}$OPEs in the North Atlantic and Arctic ranged from 0.35 to 8.40 ng L^{-1}, with high contributions of TCPP and TCEP in 2014.[24] $\sum_{9}$OPEs ranged from 74 to 1340 ng L^{-1}, in the North Atlantic, being the highest concentrations from stations closer to the Amazon River estuary.[4] $\sum_{11}$OPEs ranged from 8.47 to 143.4 ng L^{-1} in the northwestern Pacific and Arctic Ocean in 2020.[23] In the Southern Ocean, $\sum_{11}$OPE surface concentrations ranged from 1 to 28.97 ng L^{-1}, in the Fildes Peninsula in 2023 (King George Island, Antarctica)[16] and from 4.54 to 70.0 ng L^{-1} in the Ross Sea[17] in 2024.

Enrichment of OPEs in the SML. Concentrations of $\sum_{24}$OPEs did not show significant differences between the SML and SSL (t test, p-value = 0.07) in the Atlantic Ocean. However, concentrations for TBEP, TDCIPP, TNBP and EHDPP were significantly higher in the SML than in the SSL, with an opposite trend for TPhP (Table S11). For the Southern Ocean, concentrations of $\sum_{24}$OPEs (t test, p-value = 0.0044), and all individual compounds, except for TEP, TCEP and TmcP, were significantly higher in the SML than in SSL (Table S12). There were positive correlations between concentrations of TPhP, TBEP, TmCP, TDCIPP, TNBP, and ∑TCPP in the SML with those in the SSL (Table S13).

The enrichment of OPEs in the SML (EF_{SML}) is given by

$$EF_{SML} = \frac{C_{SML}}{C_{SSL}} \quad (1)$$

where C_{SML} and C_{SSL} are the individual OPE concentrations at the SML (ng L^{-1}) and SSL (ng L^{-1}), respectively. EF_{SML} was calculated only for the compounds present at >50% of the samples (TEP, TCEP, ∑TCPP, TBEP, TiBP, TDCIPP, TNBP, TPhP, EHDPP, TmCP) (Figure 2).

EF_{SML} in the Atlantic Ocean ranged from 0.32 ± 0.15 (TPhP) to 16.3 ± 33.9 (TEP) (Table S14). TPhP was the only with a mean EF_{SML} bellow unity, while the rest of individual OPEs had EF_{SML} higher than 1, indicating enrichment at the SML. Nevertheless, EF_{SML} showed a high variability, such large variability in the SML has also been observed for other classes of organic pollutants.[39,41,44,45,48,52,53] The large standard deviation suggests sporadic and significant enrichment events and points out to the unstable character and nonuniform distribution of the SML, or of pollutant burdens in the SML. The patchy character of the SML has been reported before[30,35,54] and is influenced by the concentrations of surfactant-like compounds and wind speed, among other environmental variables.

In the Southern Ocean, OPEs showed significantly higher EF_{SML} than in the Atlantic Ocean, with EF_{SML} (mean ± sd) ranging from 4.5 ± 3.9 (TNBP) to 22.3 ± 16.9 (TPhP). TmCP and EHDPP also exhibited large enrichments with EF_{SML} of 13.4 ± 16.8 and 7.2 ± 10.4, respectively (Figure 2 and Table S14).

Enrichment of OPEs in the Sea-Spray Aerosols (SSA). The enrichment of organic compounds in the SML is a key process in the transfer of chemicals associated with SSA. Assuming that the OPEs measured in aerosols are due to SSA formation, it is then possible to estimate the apparent enrichment of OPEs in SSA, and explore the relevance of this process for the long-range transport of OPEs. The enrichment of OPEs in the SSA (EF_{SSA}) is given by

$$EF_{SSA} = \frac{C_{SSA}}{C_{SML}} \quad (2)$$

where C_{SSA} is the ∑OPE concentrations in SSA (ng L^{-1}) (Figure 2). As aerosols from our cruise were not analyzed for OPEs, the assessment of OPE enrichment in the SSA compared to those in the SML was done using the aerosol-phase concentrations reported in the same Atlantic sector during the Malaspina circumnavigation campaign.[14] Even though interannual variability of aerosol-phase concentrations occurs, atmospheric concentration of semivolatile compounds do not change dramatically over long time periods in remote regions.[55] Therefore, the obtained EF_{SSA} would provide an estimate of the order of magnitude of the apparent enrichment in SSA if this was the main source of OPEs in the atmosphere, but not a precise measurement as when measurements are done in SSA and SML simultaneously.[46]

In eq 2, C_{SSA} is normalized to the liters of seawater that the SSA had when it was ejected from the sea surface. This volume of ejected seawater can be estimated using the salt content (Na^+ ions) in the aerosol samples as reported before[56] and the Na^+ content in seawater (11.18 g Na^+ L^{-1}). The average estimated amount of water in the SSA (Table S16) when it was formed was of 1.6×10^{-6} L m^{-3} ± 1.4×10^{-6} ranging from 1.6×10^{-7} L m^{-3} to 3.9×10^{-6} L m^{-3}.

Assuming that all aerosol-phase OPEs were bound to SSA, the concentrations of $\sum_{10}$OPEs in SSA averaged 6.9×10^{6} ng L^{-1} ± 8.7×10^{6} ng L^{-1} ranging from 6.6×10^{5} ng L^{-1} to 2.4×10^{7} ng L^{-1} (Table S17). If these concentrations were indeed due to SSA-bound OPEs and not due to OPEs bound to other aerosol pools (terrestrial organic matter or black carbon), the concentration of ∑OPEs in the seawater associated with the SSA would be very high, suggesting a significant transfer of OPEs from the SML to the atmosphere. EF_{SSA} for TCEP, ∑TCPP, TiBP, TNBP, TPhP, and EHDPP ranged between 2.81×10^{3} (TCEP) to 8.08×10^{6} (TNBP) (Figure 2, Table S18). Recently, EF_{SSA} have been reported for PFAS in the field,[46] and in experiments.[48] EF_{SSA} for OPES are from comparable to 2 orders of magnitude larger than those of PFAS determined previously.[46,48] PFAS are surfactant active chemicals, but some OPEs are more hydrophobic than PFAS favoring their sorption to organic matter in the SML and SSA. The Pearson's correlations of OPE concentrations in aerosols and Na^+ concentrations were significant for ∑OPEs (Figure S3) and for the individual OPES: TCEP, TiBP, TnBP, TPhP, and TEHP (Figure S3). These observations are consistent with

https://doi.org/10.1021/acs.estlett.4c00636
Environ. Sci. Technol. Lett. 2024, 11, 1008−1015

SSA formation as a source of atmospheric OPEs over the ocean, but the elucidation of its relative relevance when compared with other aerosol sources (probably from continents followed by atmospheric long-range transport of other organic aerosols) will require future research work. Nevertheless, the exploratory analysis performed here suggest that SSA could play a role in the long-range transport of semivolatile chemicals as well, in addition to the now accepted role of SSA formation as a key transport mechanism for PFAS.

Drivers of OPEs Enrichment in the SML and Relevance. The enrichment of OPEs in the SML may not only be relevant as intermediate step in their transfer to the atmosphere, but also because the SML has been identified as a compartment with particular biogeochemical characteristics and it harbors an increased potential microbial degradation, as demonstrated for other pollutants.[32]

To provide a wider picture of the relationship between concentrations, EF_{SML} and environmental conditions, particularly in terms of explaining the larger EF_{SML} and concentrations in the SML in the Southern than the Atlantic Ocean, these were compared with chlorophyll α (Chl α), bacterial abundance (BA), wind speed and other environmental variables measured during the cruises (Table S1). For example, BA in the Southern Ocean was higher than in the Atlantic Ocean, consistent with the mesotrophic and oligotrophic character of the sampled regions. Consistently, Chl α concentrations were generally higher in the Southern Ocean (0.07 to 3.63 $\mu g\ L^{-1}$) compared to the Atlantic (0.07 to 0.24 $\mu g\ L^{-1}$) (Supporting Information, Note S3). This is consistent with higher autochthonous sources of organic matter in the Southern Ocean than in the Atlantic, as well as a more intense biological activity and production of extracellular polymeric substances and other biosurfactants which accumulate in the SML.[57] These compounds can bind OPEs more effectively, thus increasing their enrichment. Indeed, Chl α concentrations were significantly positively correlated (spearman, $p < 0.05$) with the SML concentrations of TPhP, $\sum$TCPP, TmCP, and TNBP (Figure 3), and with the EF_{SML} of TPhP, TmCP, TiBP and TCEP (Figure S4 and Table S15). A significant negative correlation was also found between air and water-side temperatures with the EF_{SML} of TmCP, TCEP, TPhP, and TiBP. Higher temperatures in the Atlantic, could increase volatilization of OPEs from the SML to air due to larger Henry's law constants, reducing their enrichment. In contrast, colder Southern Ocean temperatures decrease volatilization and increase SML viscosity, potentially enhancing OPE retention and enrichment. Wind speed plays a role by destabilizing or disrupting the SML, and the variable wind speeds during both cruises are consistent with the large variability in EF_{SML} observed at both oceans, even though there was not a significant correlation between wind speed and enrichment factors of individual OPEs. The main known sinks of OPEs are photodegradation[58,59] and microbial degradation.[60] It is feasible to consider that both may also affect differently the occurrence of OPEs in Antarctic and Atlantic seawaters, as solar irradiance and OH radical generation is higher in the tropical and subtropical Atlantic than in the Southern Ocean, and microbial communities may be more active in warmer waters. There was a negative significant correlation between $\sum$TCPP, TNBP, TBEP, and TPhP concentrations at the SML and the BA in that same layer (Figure 3), consistent with a potential biodegradation of these compounds, which cannot be confirmed here. This work shows

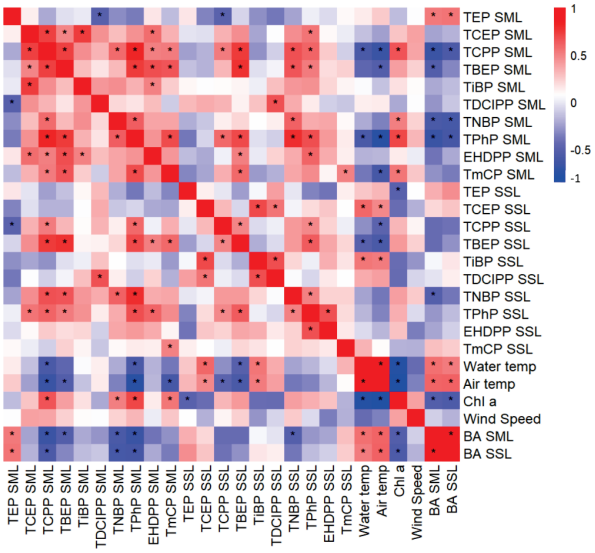


Figure 3. Heatmap of correlation (Spearman test) between individual OPE concentrations at the SML and SSL ($ng\ L^{-1}$) and environmental and biological conditions at the sampling sites. * mark significant correlations. Blue shows negative correlations, while red shows positive correlations.

that there is an ubiquitous occurrence of OPEs in the oceanic SML, with a remarkable variability which is consistent with the environmental biogeochemical and physical conditions in a complex manner. The enrichment of semivolatile contaminants in the SML will require further field and experimental work to elucidate its drivers as well as the environmental relevance in the transport and fate of chemical pollution.

■ ASSOCIATED CONTENT

Supporting Information

The Supporting Information is available free of charge at https://pubs.acs.org/doi/10.1021/acs.estlett.4c00636.

Additional text on methods (notes S1−S3). Additional tables with ancillary data, quality assurance, individual OPE's concentrations, enrichment factors, and correlations (Tables S1−S18). Additional figures showing concentrations, correlations, and photographs of sampling (Figures S1−S5) (PDF)

■ AUTHOR INFORMATION

Corresponding Author

Jordi Dachs − *Department of Environmental Chemistry, IDAEA-CSIC, 08034 Barcelona, Catalunya, Spain;* orcid.org/0000-0002-4237-169X; Email: Jordi.dachs@idaea.csic.es

Authors

Núria Trilla-Prieto − *Department of Environmental Chemistry, IDAEA-CSIC, 08034 Barcelona, Catalunya, Spain; Departament of Ecology, Faculty of Earth Sciences, Universitat de Barcelona, 08034 Barcelona, Spain;* orcid.org/0000-0001-6973-9514

Jon Iriarte − *Department of Environmental Chemistry, IDAEA-CSIC, 08034 Barcelona, Catalunya, Spain; Department of Chemical Engineering and Analytical Chemistry, Faculty of Chemistry, Universitat de Barcelona,*

08034 Barcelona, Spain; orcid.org/0000-0003-2315-1920

Naiara Berrojalbiz − *Department of Environmental Chemistry, IDAEA-CSIC, 08034 Barcelona, Catalunya, Spain*

Gemma Casas − *Department of Environmental Chemistry, IDAEA-CSIC, 08034 Barcelona, Catalunya, Spain;* Present Address: (G.C.) Institut de Ciències del Mar, ICM-CSIC, 08003, Barcelona, Catalunya, Spain

Cristina Sobrino − *Grupo de Oceanografía Biolóxica, Centro de Investigación Mariña (CIM), Universidade de Vigo, 36310 Vigo, Spain*

Maria Vila-Costa − *Department of Environmental Chemistry, IDAEA-CSIC, 08034 Barcelona, Catalunya, Spain*

Begoña Jiménez − *Department of Instrumental Analysis and Environmental Chemistry, IQOG-CSIC, 28006 Madrid, Spain;* orcid.org/0000-0002-2401-4648

Complete contact information is available at: https://pubs.acs.org/10.1021/acs.estlett.4c00636

Notes

The authors declare no competing financial interest.

■ ACKNOWLEDGMENTS

We thank the staff of the Marine Technology Unit (UTM-CSIC) and the crew of the research ships *Sarmiento de Gamboa* and *Hespérides* for their logistical support during the sampling campaigns. Antonio Fuentes (Univ. Vigo) is acknowledged for technical support during Chl analysis. N.T.P. acknowledges a predoctoral fellowship (PRE2019-089641) from the Spanish Ministry of Science. This work was supported by the Spanish Research Agency through projects ANTOM (PGC2018-096612-B-I00), PANTOC (PID2021-127769NB-I00) and MIQAS (PID2021-128084OB-I00). The research group of Global Change and Genomic Biogeochemistry receives support from the Catalan Government (2021-SGR-00448).

■ REFERENCES

(1) van der Veen, I.; de Boer, J. Phosphorus Flame Retardants: Properties, Production, Environmental Occurrence, Toxicity, and Analysis. *Chemosphere* **2012**, *88* (10), 1119−1153.

(2) Sühring, R.; Diamond, M. L.; Scheringer, M.; Wong, F.; Pućko, M.; Stern, G.; Burt, A.; Hung, H.; Fellin, P.; Li, H.; Jantunen, L. M. Organophosphate Esters in Canadian Arctic Air: Occurrence, Levels and Trends. *Environ. Sci. Technol.* **2016**, *50* (14), 7409−7415.

(3) Wei, G. L.; Li, D. Q.; Zhuo, M. N.; Liao, Y. S.; Xie, Z. Y.; Guo, T. L.; Li, J. J.; Zhang, S. Y.; Liang, Z. Q. Organophosphorus Flame Retardants and Plasticizers: Sources, Occurrence, Toxicity and Human. *Exposure. Environ. Pollut.* **2015**, *196*, 29−46.

(4) Schmidt, N.; Fauvelle, V.; Ody, A.; Castro-Jiménez, J.; Jouanno, J.; Changeux, T.; Thibaut, T.; Sempéré, R. The Amazon River: A Major Source of Organic Plastic Additives to the Tropical North Atlantic? *Environ. Sci. Technol.* **2019**, *53* (13), 7513−7521.

(5) Schmidt, N.; Castro-Jiménez, J.; Fauvelle, V.; Ourgaud, M.; Sempéré, R. Occurrence of Organic Plastic Additives in Surface Waters of the Rhône River (France). *Environ. Pollut.* **2020**, *257*, 113637.

(6) Salamova, A.; Hermanson, M. H.; Hites, R. A. Organophosphate and Halogenated Flame Retardants in Atmospheric Particles from a European Arctic Site. *Environ. Sci. Technol.* **2014**, *48* (11), 6133−6140.

(7) Xie, Z.; Wang, P.; Wang, X.; Castro-Jiménez, J.; Kallenborn, R.; Liao, C.; Mi, W.; Lohmann, R.; Vila-Costa, M.; Dachs, J. Organophosphate Ester Pollution in the Oceans. *Nat. Rev. Earth Environ.* **2022**, *3*, 309−322.

(8) Aminot, Y.; Tao, L.; Héas-Moisan, K.; Pollono, C.; O'Loghlin, M.; Munschy, C. Organophosphate Esters (OPEs) in the Marine Environment: Spatial Distribution and Profiles in French Coastal Bivalves. *Chemosphere* **2023**, *330*, 138702.

(9) Rodgers, T. F. M.; Truong, J. W.; Jantunen, L. M.; Helm, P. A.; Diamond, M. L. Organophosphate Ester Transport, Fate, and Emissions in Toronto, Canada, Estimated Using an Updated Multimedia Urban Model. *Environ. Sci. Technol.* **2018**, *52* (21), 12465−12474.

(10) Sühring, R.; Scheringer, M.; Rodgers, T. F. M.; Jantunen, L. M.; Diamond, M. L. Evaluation of the OECD P OV and LRTP Screening Tool for Estimating the Long-Range Transport of Organophosphate Esters. *Environ. Sci. Process. Impacts* **2020**, *22* (1), 207−216.

(11) Möller, A.; Sturm, R.; Xie, Z.; Cai, M.; He, J.; Ebinghaus, R. Organophosphorus Flame Retardants and Plasticizers in Airborne Particles over the Northern Pacific and Indian Ocean toward the Polar Regions: Evidence for Global Occurrence. *Environ. Sci. Technol.* **2012**, *46* (6), 3127−3134.

(12) Kim, U. J.; Kannan, K. Occurrence and Distribution of Organophosphate Flame Retardants/Plasticizers in Surface Waters, Tap Water, and Rainwater: Implications for Human Exposure. *Environ. Sci. Technol.* **2018**, *52* (10), 5625−5633.

(13) Castro-Jiménez, J.; Berrojalbiz, N.; Pizarro, M.; Dachs, J. Organophosphate Ester (OPE) Flame Retardants and Plasticizers in the Open Mediterranean and Black Seas Atmosphere. *Environ. Sci. Technol.* **2014**, *48* (6), 3203−3209.

(14) Castro-Jiménez, J.; González-Gaya, B.; Pizarro, M.; Casal, P.; Pizarro-Álvarez, C.; Dachs, J. Organophosphate Ester Flame Retardants and Plasticizers in the Global Oceanic Atmosphere. *Environ. Sci. Technol.* **2016**, *50* (23), 12831−12839.

(15) Sühring, R.; Diamond, M. L.; Bernstein, S.; Adams, J. K.; Schuster, J. K.; Fernie, K.; Elliott, K.; Stern, G.; Jantunen, L. M. Organophosphate Esters in the Canadian Arctic Ocean. *Environ. Sci. Technol.* **2021**, *55* (1), 304−312.

(16) Li, R.; Gao, H.; Hou, C.; Fu, J.; Shi, T.; Wu, Z.; Jin, S.; Yao, Z.; Na, G.; Ma, X. Occurrence, Source, and Transfer Fluxes of Organophosphate Esters in the South Pacific and Fildes Peninsula, Antarctic. *Sci. Total Environ.* **2023**, *894*, 164263.

(17) Shi, T.; Li, R.; Fu, J.; Hou, C.; Gao, H.; Cheng, G.; Zhang, H.; Jin, S.; Kong, L.; Na, G. Fate of Organophosphate Esters from the Northwestern Pacific to the Southern Ocean: Occurrence, Distribution, and Fugacity Model Simulation. *J. Environ. Sci. (China)* **2024**, *137*, 347−357.

(18) Xie, C.; Qiu, N.; Xie, J.; Guan, Y.; Xu, W.; Zhang, L.; Sun, Y. Organophosphate Esters in Seawater and Sediments from the Low-Latitude Tropical Sea. *Sci. Total Environ.* **2024**, *907*, 167930.

(19) Schmidt, N.; Castro-Jiménez, J.; Oursel, B.; Sempéré, R. Phthalates and Organophosphate Esters in Surface Water, Sediments and Zooplankton of the NW Mediterranean Sea: Exploring Links with Microplastic Abundance and Accumulation in the Marine Food Web. *Environ. Pollut.* **2021**, *272*, 115970.

(20) Bollmann, U. E.; Möller, A.; Xie, Z.; Ebinghaus, R.; Einax, J. W. Occurrence and Fate of Organophosphorus Flame Retardants and Plasticizers in Coastal and Marine Surface Waters. *Water Res.* **2012**, *46* (2), 531−538.

(21) Sutton, R.; Chen, D.; Sun, J.; Greig, D. J.; Wu, Y. Characterization of Brominated, Chlorinated, and Phosphate Flame Retardants in San Francisco Bay, an Urban Estuary. *Sci. Total Environ.* **2019**, *652*, 212−223.

(22) Cheng, W.; Xie, Z.; Blais, J. M.; Zhang, P.; Li, M.; Yang, C.; Huang, W.; Ding, R.; Sun, L. Organophosphorus Esters in the Oceans and Possible Relation with Ocean Gyres. *Environ. Pollut.* **2013**, *180*, 159−164.

(23) Na, G.; Hou, C.; Li, R.; Shi, Y.; Gao, H.; Jin, S.; Gao, Y.; Jiao, L.; Cai, Y. Occurrence, Distribution, Air-Seawater Exchange and Atmospheric Deposition of Organophosphate Esters (OPEs) from the Northwestern Pacific to the Arctic Ocean. *Mar. Pollut. Bull.* **2020**, *157*, 111243.

(24) Li, J.; Xie, Z.; Mi, W.; Lai, S.; Tian, C.; Emeis, K. C.; Ebinghaus, R. Organophosphate Esters in Air, Snow, and Seawater in the North Atlantic and the Arctic. *Environ. Sci. Technol.* **2017**, *51* (12), 6887−6896.
(25) Garbe, C.; Rutgersson, A.; Boutin, J.; Leeuw, G.; Delille, B. Transfer across the air-sea interface. In *Ocean-Atmosphere Interactions of Gases and Particles*; Liss, P., Johnson, M., Eds.; Springer, Berlin, 2014; pp 55−112.
(26) Castro-Jiménez, J.; Sempéré, R. Atmospheric Particle-Bound Organophosphate Ester Flame Retardants and Plasticizers in a North African Mediterranean Coastal City (Bizerte, Tunisia). *Sci. Total Environ.* **2018**, *642*, 383−393.
(27) Duce, R. A.; Hoffman, E. J. Chemical Fractionation at the Air/Sea Interface. *Annual Review of Earth and Planetary Sciences* **1976**, *4*, 187.
(28) Hunter, K. A. Processes Affecting Particulate Trace Metals in the Sea Surface Microlayer. *Mar. Chem.* **1980**, *9* (1), 49−70.
(29) Liss, P. S.; Duce, R. A. *The Sea Surface and Global Change*; Cambridge University Press, 1997. DOI: 10.1017/CBO9780511525025.
(30) Zhang, Z.; Liu, L.; Liu, C.; Cai, W. Studies on the Sea Surface Microlayer: II. The Layer of Sudden Change of Physical and Chemical Properties. *J. Colloid Interface Sci.* **2003**, *264* (1), 148−159.
(31) Nakajima, R.; Tsuchiya, K.; Nakatomi, N.; Yoshida, T.; Tada, Y.; Konno, F.; Toda, T.; Kuwahara, V. S.; Hamasaki, K.; Ross Othman, B. H.; Segaran, T. C.; Mohd Effendy, A. W. Enrichment of Microbial Abundance in the Sea-Surface Microlayer over a Coral Reef: Implications for Biogeochemical Cycles in Reef Ecosystems. *Mar. Ecol.: Prog. Ser.* **2013**, *490*, 11−22.
(32) Martinez-Varela, A.; Casas, G.; Berrojalbiz, N.; Piña, B.; Dachs, J.; Vila-Costa, M. Polycyclic Aromatic Hydrocarbon Degradation in the Sea-Surface Microlayer at Coastal Antarctica. *Front. Microbiol.* **2022**, *13*, 907265.
(33) Calace, N.; Catrambone, T.; Petronio, B. M.; Pietroletti, M. Fulvic Acid in Microlayer Waters of the Gerlache Inlet Sea (Antarctica): Their Distribution in Dissolved and Particulate Phases. *Water Res.* **2007**, *41* (1), 152−158.
(34) Sabbaghzadeh, B.; Upstill-Goddard, R. C.; Beale, R.; Pereira, R.; Nightingale, P. D. The Atlantic Ocean Surface Microlayer from 50°N to 50°S Is Ubiquitously Enriched in Surfactants at Wind Speeds up to 13 m S−1. *Geophys. Res. Lett.* **2017**, *44* (6), 2852−2858.
(35) Uning, R.; Latif, M. T.; Yu, K. L.; Cheng, S. Y.; Ahamad, F.; Khan, M. F.; Bedurus, E. A.; Suratman, S. Surfactants in the Sea Surface Microlayer, Underlying Water and Atmospheric Particles of Tropical Coastal Ecosystems. *Water. Air. Soil Pollut.* **2018**, *229*, 305.
(36) Engel, A.; Bange, H. W.; Cunliffe, M.; Burrows, S. M.; Friedrichs, G.; Galgani, L.; Herrmann, H.; Hertkorn, N.; Johnson, M.; Liss, P. S.; Quinn, P. K.; Schartau, M.; Soloviev, A.; Stolle, C.; Upstill-Goddard, R. C.; van Pinxteren, M.; Zäncker, B. The Ocean's Vital Skin: Toward an Integrated Understanding of the Sea Surface Microlayer. *Front. Mar. Sci.* **2017**, *4*, 1−14.
(37) Cunliffe, M.; Engel, A.; Frka, S.; Gašparović, B. Ž.; Guitart, C.; Murrell, J. C.; Salter, M.; Stolle, C.; Upstill-Goddard, R.; Wurl, O. Sea Surface Microlayers: A Unified Physicochemical and Biological Perspective of the Air-Ocean Interface. *Prog. Oceanogr.* **2013**, *109*, 104−116.
(38) García-Flor, N.; Guitart, C.; Ábalos, M.; Dachs, J.; Bayona, J. M.; Albaigés, J. Enrichment of Organochlorine Contaminants in the Sea Surface Microlayer: An Organic Carbon-Driven Process. *Mar. Chem.* **2005**, *96* (3−4), 331−345.
(39) Fuoco, R.; Giannarelli, S.; Wei, Y.; Abete, C.; Francesconi, S.; Termine, M. Polychlorobiphenyls and Polycyclic Aromatic Hydrocarbons in the Sea-Surface Micro-Layer and the Water Column at Gerlache Inlet, Antarctica. *J. Environ. Monit.* **2005**, *7* (12), 1313−1319.
(40) Cincinelli, A.; Stortini, A. M.; Perugini, M.; Checchini, L.; Lepri, L. Organic Pollutants in Sea-Surface Microlayer and Aerosol in the Coastal Environment of Leghorn - (Tyrrhenian Sea). *Mar. Chem.* **2001**, *76* (1−2), 77−98.
(41) Cincinelli, A.; Stortini, A. M.; Checchini, L.; Martellini, T.; Del Bubba, M.; Lepri, L. Enrichment of Organic Pollutants in the Sea Surface Microlayer (SML) at Terra Nova Bay, Antarctica: Influence of SML on Superficial Snow Composition. *J. Environ. Monit.* **2005**, *7* (12), 1305−1312.
(42) Stortini, A. M.; Martellini, T.; Del Bubba, M.; Lepri, L.; Capodaglio, G.; Cincinelli, A. N-Alkanes PAHs and Surfactants in the Sea Surface Microlayer and Sea Water Samples of the Gerlache Inlet Sea (Antarctica). *Microchem. J.* **2009**, *92* (1), 37−43.
(43) Wurl, O.; Obbard, J. P. A Review of Pollutants in the Sea-Surface Microlayer (SML): A Unique Habitat for Marine Organisms. *Mar. Pollut. Bull.* **2004**, *48* (11−12), 1016−1030.
(44) Sakellari, A.; Karavoltsos, S.; Moutafis, I.; Koukoulakis, K.; Dassenakis, M.; Bakeas, E. Occurrence and Distribution of Polycyclic Aromatic Hydrocarbons in the Marine Surface Microlayer of an Industrialized Coastal Area in the Eastern Mediterranean. *Water* **2021**, *13*, 3174−3189.
(45) Ju, X.; Jin, Y.; Sasaki, K.; Saito, N. Perfluorinated Surfactants in Surface, Subsurface Water and Microlayer from Dalian Coastal Waters in China. *Environ. Sci. Technol.* **2008**, *42* (10), 3538−3542.
(46) Casas, G.; Martínez-Varela, A.; Roscales, J. L.; Vila-Costa, M.; Dachs, J.; Jiménez, B. Enrichment of Perfluoroalkyl Substances in the Sea-Surface Microlayer and Sea-Spray Aerosols in the Southern Ocean. *Environ. Pollut.* **2020**, *267*, 115512.
(47) Li, Y.; Zhao, X.; Li, X.; Zhang, Y.; Niu, Z. The Investigation of the Enrichment Behavior of Identified PFAS and Unknown PFAA-Precursors in Water and Suspended Particulate Matter of the Surface Microlayer: A Case Study in Tianjin (China). *Water Res.* **2024**, *260* (May), 121944.
(48) Johansson, J. H.; Salter, M. E.; Acosta Navarro, J. C.; Leck, C.; Nilsson, E. D.; Cousins, I. T. Global Transport of Perfluoroalkyl Acids via Sea Spray Aerosol. *Environ. Sci. Process. Impacts* **2019**, *21* (4), 635−649.
(49) Sha, B.; Johansson, J. H.; Salter, M. E.; Blichner, S. M.; Cousins, I. T. Constraining Global Transport of Perfluoroalkyl Acids on Sea Spray Aerosol Using Field Measurements. *Sci. Adv.* **2024**, *10* (14), 1−10.
(50) Harvey, G.; Burzell, L. A. A Simple Microlayer Method for Small Samples. *Limnol. Oceanogr.* **1972**, *17*, 156−157.
(51) Knulst, J. C.; Rosenberger, D.; Thompson, B.; Paatero, J. Intensive Sea Surface Microlayer Investigations of Open Leads in the Pack Ice during Arctic Ocean 2001 Expedition. *Langmuir* **2003**, *19* (24), 10194−10199.
(52) Guitart, C.; García-Flor, N.; Dachs, J.; Bayona, J. M.; Albaigés, J. Evaluation of Sampling Devices for the Determination of Polycyclic Aromatic Hydrocarbons in Surface Microlayer Coastal Waters. *Mar. Pollut. Bull.* **2004**, *48* (9−10), 961−968.
(53) Manodori, L.; Gambaro, A.; Piazza, R.; Ferrari, S.; Stortini, A. M.; Moret, I.; Capodaglio, G. PCBs and PAHs in Sea-Surface Microlayer and Sub-Surface Water Samples of the Venice Lagoon (Italy). *Mar. Pollut. Bull.* **2006**, *52* (2), 184−192.
(54) Wurl, O.; Wurl, E.; Miller, L.; Johnson, K.; Vagle, S. Formation and Global Distribution of Sea-Surface Microlayers. *Biogeosciences* **2011**, *8* (1), 121−135.
(55) Luarte, T.; Gomez-Aburto, V. A.; Poblete-Castro, I.; Castro-Nallar, E.; Huneeus, N.; Molina-Montenegro, M.; Egas, C.; Azcune, G.; Perez-Parada, A.; Lohmann, R.; Bohlin-Nizzetto, P.; Dachs, J.; Bengtson-Nash, S.; Chiang, G.; Pozo, K.; Galban-Malagon, C. J. Levels of Persistent Organic Pollutants (POPs) in the Antarctic Atmosphere over Time (1980 to 2021) and Estimation of Their Atmospheric Half-Lives. *Atmos. Chem. Phys.* **2023**, *23* (14), 8103−8118.
(56) Chen, Q.; Geng, L.; Schmidt, J.; Xie, Z.; Kang, H.; Dachs, J.; Cole-Dai, J.; Schauer, A.; Camp, M.; Alexander, B. Isotopic Constraints on the Role of Hypohalous Acids in Sulfate Aerosol Formation in the Remote Marine Boundary Layer. *Atmos. Chem. Phys.* **2016**, *16* (17), 11433−11450.

(57) Frew, N.; Nelson, R. K. Isolation of Marine Microlayer Film Surfactants for ex Situ Study of Their Surface Physical and Chemical Properties. *J. Geophys. Res.* **1992**, *97* (C4), 5281−5290.
(58) Regnery, J.; Püttmann, W. Occurrence and Fate of Organophosphorus Flame Retardants and Plasticizers in Urban and Remote Surface Waters in Germany. *Water Res.* **2010**, *44* (14), 4097−4104.
(59) Cristale, J.; Dantas, R. F.; De Luca, A.; Sans, C.; Esplugas, S.; Lacorte, S. Role of Oxygen and DOM in Sunlight Induced Photodegradation of Organophosphorous Flame Retardants in River Water. J. *Hazard. Mater.* **2017**, *323*, 242−249.
(60) Vila-Costa, M.; Sebastián, M.; Pizarro, M.; Cerro-Gálvez, E.; Lundin, D.; Gasol, J. M.; Dachs, J. Microbial Consumption of Organophosphate Esters in Seawater under Phosphorus Limited Conditions. *Sci. Rep.* **2019**, *9* (1), 233.

https://doi.org/10.1021/acs.estlett.4c00636
Environ. Sci. Technol. Lett. 2024, 11, 1008−1015

PART 03 - CHAPTER 3. TRANSPORT AND BIOGEOCHEMISTRY OF OPEs IN THE OCEANS

3.3.2. Paper III. Supplementary Information

Notes S1 - S3, Figures S1 - S5, and Tables S1 - S18

Supplementary Information

Enrichment of Organophosphate Esters in the Sea Surface Microlayer from the Atlantic and Southern Oceans

Núria Trilla-Prieto[1,2], Jon Iriarte[1], Naiara Berrojalbiz[1], Gemma Casas[2,3], Cristina Sobrino[4], Maria Vila-Costa[1], Begoña Jiménez[5], Jordi Dachs[1]

[1]Department of Environmental Chemistry, IDAEA-CSIC, Barcelona, Catalunya Spain.

[2]Departament of Ecology, Faculty of Marine Sciences, Universitat de Barcelona, Barcelona, Catalunya, Spain.

[3]Department of Marine Biology and Oceanography, Institut de Ciències del Mar, CSIC, Pg. Marítim de la Barceloneta, 37-49, E08003, Barcelona, Catalunya, Spain.

[4]Grupo de Oceanografía Biolóxica, Centro de Investigación Mariña (CIM), Universidade de Vigo (UVigo), Vigo, Spain.

[5]Department of Instrumental Analysis and Environmental Chemistry, IQOG-CSIC, Juan de la Cierva, 3, 28006, Madrid, Spain.

Supplementary Information

Supplementary Notes

Note S1. OPEs extraction laboratory procedure.
Note S2. OPEs analytical method.
Note S3. Chlorophyll a concentration determination method.

Figures

Figure S1. Pictures of SML sampling in the Atlantic (left) and Southern Ocean (right) with the SML sampler.
Figure S2. Relative abundance (%) of OPEs in SML, SSL and SSA samples.
Figure S3. Correlation plot between Na+ concentration and log $\sum_{24}$OPEs concentration in the Atlantic Ocean aerosols.
Figure S4. Heatmap of correlations between individual OPE EFSML with environmental and biological conditions.
Figure S5. $\sum_{10}$OPE paired concentrations (ng L^{-1}) at the SML and SSL in the Atlantic (left panel) and Southern Ocean (right panel).

Tables

Table S1. Sampling sites and environmental variables at time and site of sampling for the Atlantic Ocean (top table) and the Southern Ocean samples (bottom table).
Table S2. Target OPEs in the present study, their acronyms, Log K_{OW} and molecular weight (MW).
Table S3. Blanks (ng) for Atlantic (top table) and Southern Ocean (bottom table).
Table S4. Limits of quantification (LOQs) in ng.
Table S5. Information of labelled OPE compounds used as surrogate (top table) and as internal standard (bottom table).
Table S6. Surrogate recoveries from the Atlantic Ocean samples (top table) and Southern Ocean samples (bottom table).
Table S7. Presence, absence and <LOQ number of samples per each compound and campaign.
Table S8. Individual and $\sum_{24}$OPE concentrations (ng L^{-1}) in SML.
Table S9. Individual and $\sum_{24}$OPE concentrations (ng L^{-1}) in SSL.
Table S10. Mean, median and standard deviation of individual and ∑24OPE in SML and SSL for the Atlantic Ocean (top table) and Southern Ocean (bottom table).
Table S11. Mean SML and SSL concentrations (ng L^{-1}) and T-test p-value results for statistical comparison of individual and $\sum_{24}$OPE between the two layers in the Atlantic Ocean. differences.
Table S12. Mean SML and SSL concentrations (ng L^{-1}) and T-test p-value results for statistical comparison of individual and $\sum_{24}$OPE between the two layers in the Southern Ocean.
Table S13. Mean SML and SSL concentrations (ng L^{-1}) and T-test p-value results for statistical comparison of individual and $\sum_{24}$OPE between the two layers in both Atlantic and Southern Ocean.
Table S14. Enrichment factor of SML (EF_{SML}) for individual OPE for the Atlantic samples (top table) and Southern Ocean samples (bottom table).
Table S15. Spearman correlation between EF_{SML} for individual OPEs and total chlorophyll content (mg L^{-1}).
Table S16. Sea spray aerosols (SSA), seawater (SW) from SSA volumes (V_{SW}), Na+, OPEs in SSA ($\sum_{14}OPE_{SSA}$) and OPEs in SW from SSA ($\sum_{14}$OPEsw).
Table S17. Individual and $\sum_{14}$OPE in SW_{SSA} (ng L^{-1}).
Table S18. Enrichment factor of SSA (EF_{SSA}) for individual OPEs.

References

Note S1. OPE extraction laboratory procedure.

After the sampling, samples were taken to the vessel laboratory where were filtered through pre-combusted glass fiber filters (47 mm, GF/F Whatman) and extracted using a stablished solid phase extraction (SPE) method with Oasis HLB cartridges (6 cm^3, 200 mg; Waters). Cartridges were conditioned with 6 mL of 2-propanol and 12 ml of HPLC-grade water, and then spiked with 50 ng of a mix of labelled recovery standards (D27-TNBP, D15-TPhP, D12-TCEP, D21-TPrP, D18-TCPP and D51-TEHP). After loading the samples (500 ml for the SML samples and the 2 L for the SSL), cartridges were washed with 6 mL of chromatographic-grade water at 5% of methanol, dried under vacuum for 10 to 15 minutes, and stored at -20ºC in sealed bags before further treatment analysis in an ultraclean laboratory.

Once in the ultraclean laboratory, HLB cartridges were unfreeze for 3 hours at room temperature, centrifuged at 3500 rpm for 4' and eluted with 12 ml methyl tert-butyl ether:methanol (3:1; v/v). The residual water was removed by adding 3 g of pre-baked sodium sulfate. The final eluents were concentrated under N_2 and reconstituted in 100 µL of toluene. Recoveries were monitored using the recovery standards prior to the extraction **(Tables S5 and 6)**. Six and four matrix spike recovery samples were done at Atlantic and Antarctic cruises, respectively, to assess the recoveries of the native analytes. Surrogate recoveries from matrix spikes were of 54% ± 8% and 78% ± 29% for the Atlantic and Southern Ocean, respectively. Analytes showed recoveries ranging from 73% ± 11% and 77 ± 13% for the Atlantic and Southern Ocean, respectively.

All containers, tubes, and connections used during sampling and chemical analysis were made of stainless steel, glass or PTFE, and were rinsed with methanol and acetone in order to avoid contamination. In addition, all filters and all glass material were combusted at 450°C for 4h before their use.

Note S2. OPEs analytical method.

OPEs instrumental analysis was conducted by gas chromatography coupled to a tandem mass spectrometry GC-MS/MS with a triple quadrupole analyzer (qQq). The chromatographic separation was carried out using a HP-5MS column (30 m, 0.25 mm internal diameter, 0.25 µm film thickness) on an Agilent 7890A gas chromatograph. Methane was used as ionization gas and helium was used as carrier gas at a constant flow mode of 20ml min^{-1}. Two µl of sample were injected in splitless mode and injection port temperature of 280 °C. The column temperatures were: 90 °C for 1 min, increased at 15 °C min^{-1} to 200°C held for 6 min, then at 5 °C min^{-1} to 250 °C, held for 6 min and then at 10°C min^{-1} to 315°C, held for 10 min. The detection was carried out with an Agilent 7000B triple quadrupole mass spectrometer using electronic impact ionization (EI) mode in positive mode. The EI source, transfer line and quadrupole temperature were 230°C, 280 °C and 300 °C, respectively. Acquisition was performed in multiple reaction monitoring (MRM). 50 ng of perdeuterated Internal standards (d15-TDCPP, M6TBEP and MTPHP) were added before the instrumental analysis **(Table S3)**.

Note S3. Chlorophyll α concentration determination method.

Chlorophyll α (Chl α) concentration was measured in surface water samples collected with a Niskin bottle attached to the boat oceanographic rosette. For each sample, 250 mL were gently filtered under dim light in triplicate through a size fraction cascade system with 20, 2 and 0.22 µm size pore 47-mm Filter-Lab polycarbonate filters, and immediately stored at -20 °C until further analysis. Chl α extraction was carried out with 90% acetone and the concentration in each sample (µg L^{-1}) was estimated following the protocol in Strickland and Parsons (1972) using a Turner A10 fluorometer previously calibrated with a pure Chl α standard (SIGMA C5753-1mg).



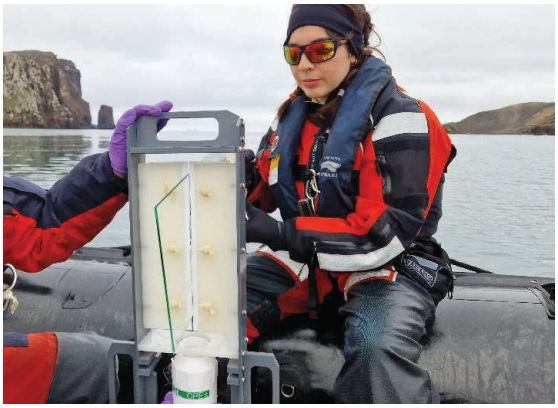
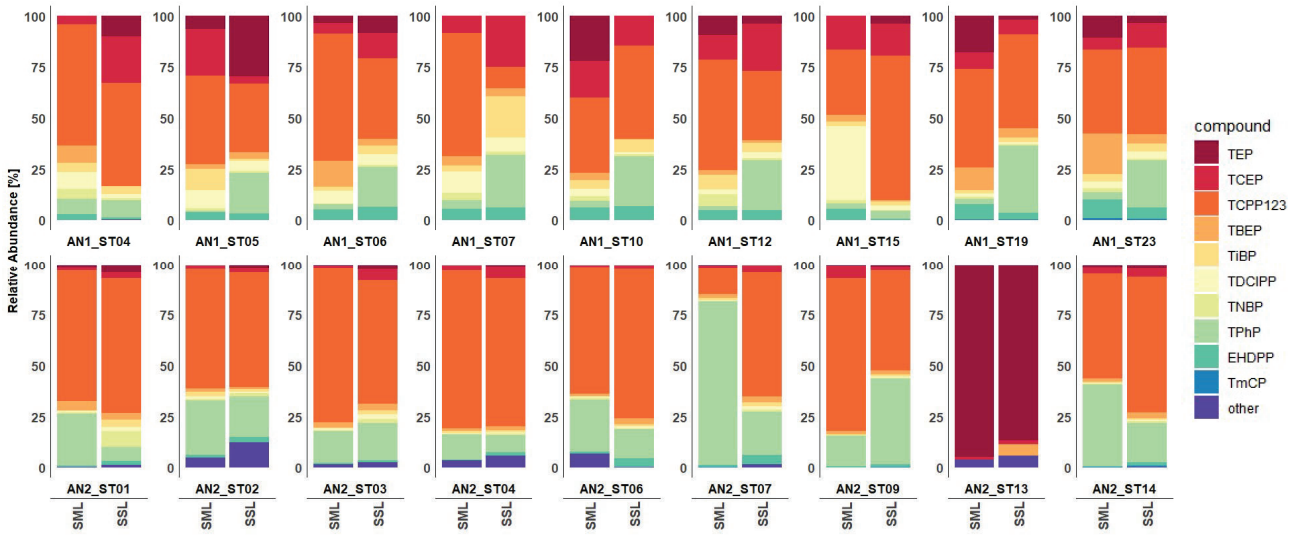


Figure S1. Pictures of SML sampling in the Atlantic (left) and Southern Ocean (right) with the SML sampler.



**Category "other" include all individual OPEs that contribute <5% to total pool: TEHP, TPPO, TPrP, TpCP, TPPP, TBPO, Chlorpyrifos, ToCP, DOPP, TDMPP, TDBPP and TTBPP.*

Figure S2. Relative abundance (%) of OPEs in SML and SSL samples.

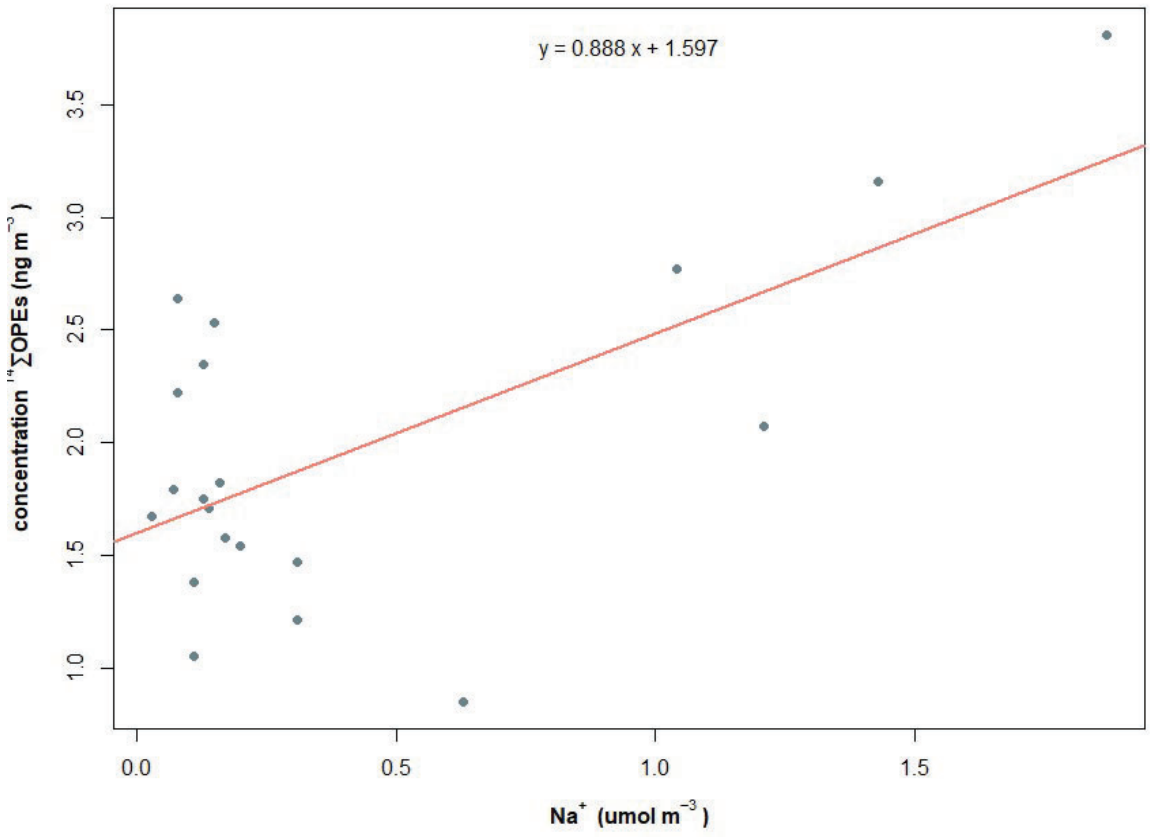


Figure S3. Aerosol phase OPE concentrations versus sea-salt (Na^+) concentrations. Pearson correlation (r2 = 0.64, p-value=0.002) and regression plot between Na^+ concentration (µmol m^3) and $\sum_{13}$OPEs (ng m^3) concentration in the Atlantic Ocean aerosol samples. The Pearson's correlations for individual OPEs were (* marks statistically significant correlation): TCEP with a p-value = **0.01*** and r = 0.56, ∑TCPP with a p-value = 0.24 and r = 0.27, TiBP with a p-value = **9.233e-05*** and r = 0.76, TNBP with a p-value = **0.001*** and r = 0.68, TPhP with a p-value = **0.01*** and r2 = 0.52, EHDPP with a p-value = 0.88 and r = -0.03, TEHP with a p-value = **0.0005*** and r = 0.70, ∑TcPs with a p-val = 0.26 and r = 0.26. Generally, four or five sampling points had a remarkable influence on the correlation, suggesting that log-log correlations may better fit the results, but this is not the case, as the person correlation for $\sum_{13}$OPEs has a p-value =0.06 and r = 0.2, and the log-log correlations were only significant for TiBP with p-values **= 0.028*** and r = 0.49, TNBP with p-value **= 0.018*** and r = 0.52, and TEHP with p-value **= 0.005*** and r = 0.61.

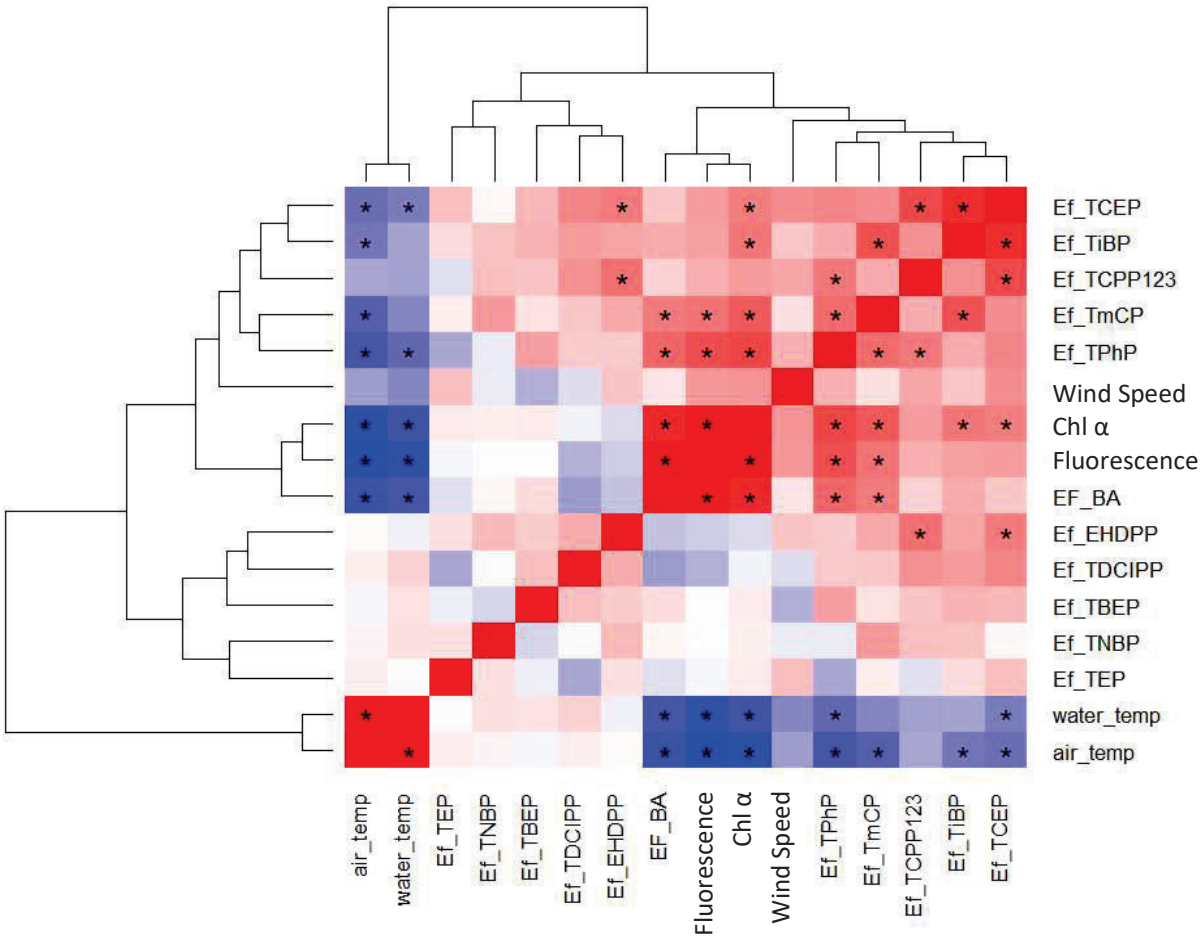


Figure S4. Heatmap of correlations between individual OPE EF_{SML} with environmental and biological conditions.

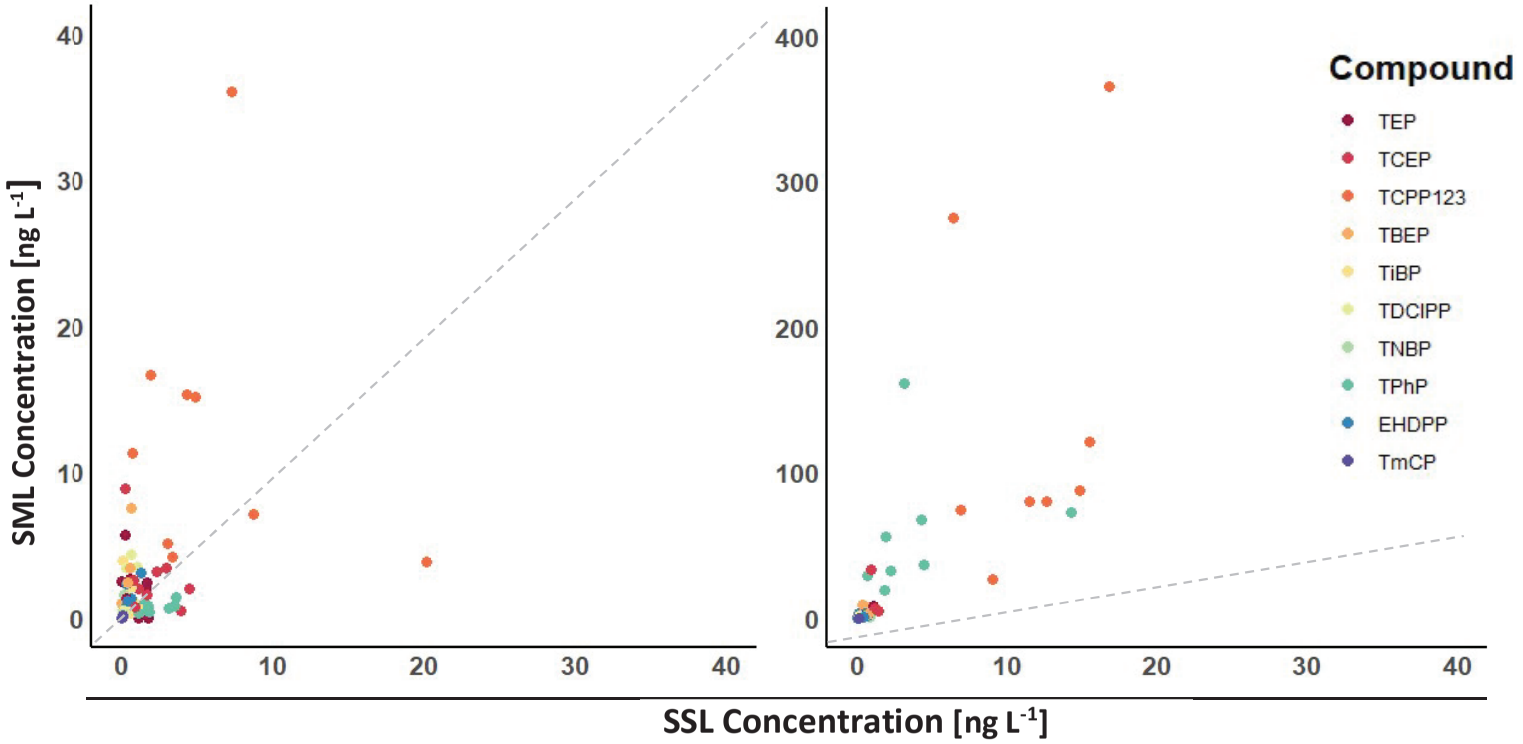


Figure S5. *$\sum_{10}$OPE paired concentrations (ng L^{-1}) at the SML and SSL in the Atlantic (left panel) and Southern oceans (right panel).*

Table S1. Sampling sites and environmental variables at time and site of sampling for Atlantic Ocean (top table) and the Southern Ocean (bottom table).

Atlantic Ocean										
Station code	**Cruise**	**Sampling date**	**LAT**	**LONG**	**Water temperature** *ºC*	**Air temperature** *ºC*	**Chlorophyll** *µg L^{-1}*	**Wind speed** *m/s*	**Bacterial Abundance** *(SML)*	**Bacterial Abundance** *(SSL)*
AN1_ST4	ANTOM-I	21/12/2020	28.66	-28.41	21.19	20.99	0.114	4.41	553000	541333
AN1_ST5	ANTOM-I	22/12/2020	25.63	-24.89	20.42	21.00	0.118	6.42	673500	701500
AN1_ST6	ANTOM-I	23/12/2020	22.22	-26.63	19.53	21.80	0.155	2.96	595000	1270000
AN1_ST7	ANTOM-I	24/12/2020	18.87	-28.32	20.73	26.50	0.157	6.10	627500	634500
AN1_ST10	ANTOM-I	27/12/2020	7.35	-29.58	25.41	26.65	0.165	1.94	1105000	1050000
AN1_ST12	ANTOM-I	29/12/2020	0.14	-30.50	25.77	27.05	0.190	7.55	900000	890000
AN1_ST15	ANTOM-I	02/01/2021	-14.37	-33.91	25.11	26.68	0.066	5.51	756500	781500
AN1_ST19	ANTOM-I	06/01/2021	-27.79	-40.65	24.41	24.82	0.092	3.37	656500	682000
AN1_ST23	ANTOM-I	11/01/2021	-43.79	-54.75	18.53	17.65	0.239	3.67	2630000	2505000

Southern Ocean										
Station code	**Cruise**	**Sampling date**	**LAT**	**LONG**	**Water temperature** *ºC*	**Air temperature** *ºC*	**Chlorophyll** *µg L^{-1}*	**Wind speed** *m/s*	**Bacterial Abundance** *(SML)*	**Bacterial Abundance** *(SSL)*
AN2_ST1	ANTOM-II	23/01/2022	-62.71	-60.63	1.41	1.95	0.68	8.06	411000	312000
AN2_ST2	ANTOM-II	24/01/2022	-62.92	-61.03	1.52	1.31	0.95	1.81	468000	457000
AN2_ST3	ANTOM-II	25/01/2022	-64.58	-62.56	0.97	1.48	1.16	9.80	237000	235000
AN2_ST4	ANTOM-II	26/01/2022	-65.15	-65.63	0.97	0.21	1.86	6.65	258000	220000
AN2_ST6	ANTOM-II	28/01/2022	-67.75	-68.03	0.34	-0.55	2.64	3.70	200000	169000
AN2_ST7	ANTOM-II	30/01/2022	-70.85	-79.89	0.52	-0.87	3.63	6.82	253000	195000
AN2_ST9	ANTOM-II	31/01/2022	-69.21	-78.84	-0.04	-0.01	0.72	10.1	361000	312000
AN2_ST13	ANTOM-II	05/02/2022	-62.97	-60.28	0.37	2.40	0.62	8.07	1160000	1130000
AN2_ST14	ANTOM-II	06/02/2022	-62.95	-60.64	1.76	1.05	0.95	11.33	1160000	1130000

Table S2. Target OPES in the present study, acronyms, Log K_{OW} and molecular weight (MW).

Analyte	Acronym	Log Kow	MW (g/mol)
Cl-OPEs			
Tris (2-chloroethyl) phosphate	TCEP	1.6	285.48
Tris (2-choloroisopropyl) phosphate	TCPP-1.2.3	2.9	327.56
Tris (1.3-dichlor-2-propyl) phosphate	TDCIPP	3.7	430.89
Alkyl-OPE			
Triethyl phosphate	TEP	0.9	182.16
Tripropyl phosphate	TPrP	2.1	224.23
Tris (2-butoxyethyl) phosphate	TBEP	3	398.48
Tris-iso-butyl phosphate	TiBP	3.6	266.32
Tri-n-butyl phosphate	TNBP	3.8	266.32
Tributyl phosphine oxide	TBPO	3.9	218.3
Tris (2-ehylhexyl) phosphate	TEHP	9.5	434.64
Aryl-OPE			
Triphenyl phosphine oxide	TPPO	2.9	278.28
Triphenyl phosphate	TPhP	4.7	326.29
Chlorpyrifos	CPS	4.96	350.59
Tri-p-cresyl phosphate	TpCP	6.3	368.36
Tri-o-cresyl phosphate	ToCP	6.3	368.36
Tri-m-cresyl phosphate	TmCP	6.3	368.36
2-Ethylhexyldiphenyl phosphate	EHDPP	6.3	362.41
Dioctylphenyl phosphonate	DOPP	7.5	382.52
Tris (3.5-dimethylphenyl) phosphate	TDMPP	8	410.40
Tris (2-isopropylphenyl) phosphate	TPPP	9.1	452.50
Tris (4-tert-butylphenyl) phosphate	TTBPP	10.4	494.60
Br-OPE			
Tris (2.3-dibromopropyl) phosphate	TDBPP	9.1	697.60

Table S3. Blanks (ng) for Atlantic (top table) and Southern Ocean (bottom table).

**PB for Procedure blank, nd = non detected*

Atlantic Ocean blanks																							
Sample code	TEP	TPrP	TiBP	TNBP	TBPO	TCEP	TCPP1	TCPP2	TCPP3	Chlor	TDCIPP	TPhP	TBEP	EHDPP	TEHP	TPPO	ToCP	DOPP	TmCP	TpCP	TPPP	TDMPP	TDBPP	TTBPP
ANIWOPE_010	nd	0.01	nd	0.01	0.29	nd	0.27	0.04	0.002	nd	0.01	0.03	0.111	0.02	nd	nd	nd	nd	nd	nd	nd	nd	nd	nd
ANIWOPE_024	nd	0.01	nd	0.02	0.05	nd	0.32	0.08	0.04	nd	0.02	0.11	nd	0.19	nd	nd	0.00	nd	0.003	nd	0.05	nd	0.02	nd
ANIWOPE_050	0.004	0.03	0.07	0.06	0.11	0.16	1.32	0.30	0.02	nd	0.02	0.27	nd	0.40	nd	nd	0.00	nd	nd	0.00	0.00	nd	nd	nd
ANIWOPE_051	0.003	0.02	0.07	0.09	0.18	0.38	1.15	0.50	0.30	nd	0.01	0.16	nd	0.27	nd	nd	nd	nd	nd	nd	0.00	nd	nd	nd
ANIWOPE_064	0.002	0.01	nd	0.04	0.24	1.59	0.76	0.09	0.006	nd	0.01	0.16	nd	0.12	nd	nd	0.00	nd	0.001	nd	nd	nd	0.04	0.00
ANIWOPE_066	0.003	0.01	nd	0.08	0.55	nd	0.82	0.10	0.006	nd	0.06	0.33	nd	0.38	nd	nd	0.00	nd	0.002	0.00	0.00	nd	0.05	nd
ANIWOPE_082	0.004	0.01	nd	0.04	0.40	0.28	0.45	0.11	0.007	nd	0.03	0.16	nd	0.21	nd	nd	nd	nd	nd	nd	nd	nd	nd	nd
ANIWOPE_083	0.006	0.02	nd	0.08	0.86	0.51	0.71	0.18	0.007	nd	0.001	0.15	nd	0.15	nd	nd	0.00	nd	nd	nd	nd	nd	nd	nd
ANIWOPE_090	nd	0.03	nd	0.03	0.14	0.30	0.91	0.51	0.03	nd	nd	0.14	nd	0.22	nd	nd	nd	nd	nd	0.00	0.00	nd	0.05	nd
ANIWOPE_121	nd	0.01	nd	0.03	0.23	5.13	0.54	0.06	0.004	nd	0.02	0.07	nd	0.09	nd	nd	0.00	nd	0.005	nd	0.01	0.03	nd	nd
ANIWOPE_134	0.0001	0.00	nd	0.01	0.11	0.11	0.18	0.03	0.001	nd	Nd	0.06	nd	0.04	nd	nd	0.00	nd	0.001	0.00	0.00	0.03	0.03	0.00
ANIWOPE_140	nd	0.00	0.06	0.08	0.17	0.07	1.17	0.16	0.10	nd	0.001	0.11	nd	0.10	nd	nd	0.00	nd	nd	nd	0.00	nd	nd	nd
ANIWOPE_142	0.001	0.01	nd	0.02	0.12	0.002	0.33	0.18	0.03	nd	nd	0.07	nd	0.03	nd	nd	nd	nd	nd	nd	0.00	nd	nd	nd
ANIWOPE_174	nd	0.01	0.02	0.04	0.23	0.02	0.40	0.04	0.02	nd	0.08	0.10	0.09	0.05	nd	nd	0.03	nd	0.02	0.01	0.01	0.04	nd	nd
ANIWOPE_175	0.000	0.00	nd	0.02	0.19	nd	0.17	0.11	0.01	nd	0.06	0.10	Nd	0.09	nd	nd	0.00	nd	0.002	nd	0.00	0.03	nd	nd
ANIWOPE_217	0.005	0.00	0.01	0.01	0.08	nd	0.09	0.04	0.01	nd	Nd	0.04	Nd	0.009	nd	nd	nd	nd	nd	nd	nd	nd	nd	nd
ANIWOPE_219	0.007	0.01	no	0.03	0.19	0.43	0.40	0.24	0.04	nd	Nd	0.10	Nd	0.03	nd	nd	0.00	nd	nd	0.00	0.00	nd	nd	nd
ANIWOPE_248	0.07	0.01	0.01	0.01	nd	0.57	0.24	0.06	0.004	nd	0.04	1.04	Nd	0.59	nd	nd	nd	nd	nd	nd	0.09	nd	nd	nd
ANIWOPE_PB001	0.09	nd	0.02	0.37	nd	nd	0.10	0.02	0.13	nd	0.006	0.03	0.03	0.003	nd	nd	nd	nd	0.002	nd	nd	nd	nd	nd
ANIWOPE_PB002	0.05	nd	0.02	0.31	nd	nd	0.10	0.01	0.12	nd	0.02	0.03	0.05	0.01	nd	nd	nd	nd	0.002	nd	nd	nd	nd	nd
ANIWOPE_PB003	nd	nd	0.03	0.36	nd	d	0.08	0.01	0.10	nd	0.06	0.03	0.07	0.006	nd	nd	nd	nd	nd	nd	nd	nd	nd	nd
ANIWOPE_PB004	0.005	nd	0.04	0.45	nd	nd	0.16	0.03	0.19	nd	0.03	0.08	0.10	0.004	nd	nd	nd	nd	0.01	nd	nd	nd	nd	nd
ANIWOPE_PB005	0.005	nd	0.03	0.51	nd	nd	0.13	nd	0.16	nd	nd	0.03	Nd	0.002	nd	nd	nd	nd	nd	nd	nd	nd	nd	nd
ANIWOPE_PB006	0.002	nd	0.02	0.29	nd	nd	0.08	0.01	0.10	nd	0.01	0.03	0.05	0.01	nd	nd	nd	nd	nd	nd	nd	nd	nd	nd
ANIWOPE_PB007	nd	nd	0.08	0.86	nd	0.002	nd	nd	0.05	nd	nd	0.02	Nd	nd	nd	nd	nd	nd	nd	nd	nd	nd	nd	nd
ANIWOPE_PB008	nd	nd	0.02	0.24	nd	nd	0.05	0.06	0.06	nd	0.006	0.04	0.32	0.005	nd	nd	nd	nd	nd	nd	nd	nd	nd	nd
ANIWOPE_PB009	nd	nd	0.03	0.24	nd	nd	0.04	0.05	0.05	nd	0.01	0.04	Nd	0.007	nd	nd	nd	nd	nd	nd	nd	nd	nd	nd
ANIWOPE_PB010	nd	nd	0.05	0.02	nd	nd	0.09	0.06	0.13	nd	0.006	0.008	Nd	0.003	nd	nd	nd	nd	nd	nd	nd	nd	nd	nd
ANIWOPE_PB011	nd	nd	0.03	0.01	nd	nd	0.05	0.02	0.07	nd	0.006	0.02	0.04	0.01	nd	nd	nd	nd	nd	nd	nd	nd	nd	nd
ANIWOPE_PB012	nd	nd	0.05	0.02	nd	nd	0.06	0.03	0.09	nd	0.008	0.008	0.16	0.004	nd	nd	nd	nd	nd	nd	nd	nd	nd	nd
ANIWOPE_PB013	nd	nd	0.05	0.02	nd	nd	0.06	0.03	0.08	nd	0.009	0.01	0.07	0.008	nd	nd	nd	nd	nd	nd	nd	nd	nd	nd
ANIWOPE_PB014	nd	nd	0.06	0.38	nd	nd	0.07	0.09	0.09	nd	nd	0.02	0.24	0.003	nd	nd	nd	nd	nd	nd	nd	nd	nd	nd
ANIWOPE_PB015	nd	nd	0.06	0.43	nd	nd	0.11	0.14	0.15	nd	nd	nd	nd	nd	nd	nd	nd	nd	nd	nd	nd	nd	nd	nd
ANIWOPE_PB016	nd	nd	0.06	0.10	nd	nd	0.03	0.03	0.04	nd	nd	nd	nd	0.003	nd	nd	nd	nd	nd	nd	nd	nd	nd	nd
ANIWOPE_PB017	nd	nd	0.10	0.44	nd	nd	0.10	0.08	0.02	nd	nd	0.005	nd	nd	nd	nd	nd	nd	nd	nd	nd	nd	nd	nd
ANIWOPE_PB018	nd	nd	0.007	0.11	nd	nd	0.01	0.01	0.01	nd	0.005	0.02	nd	0.003	nd	nd	nd	nd	nd	nd	nd	nd	nd	nd
ANIWOPE_PB019	nd	nd	0.007	0.12	nd	nd	0.01	0.01	0.01	nd	0.002	0.009	nd	nd	nd	nd	nd	nd	0.06	nd	nd	nd	nd	nd
AN2WOPE_003	0.31	nd	0.13	nd	nd	0.04	1.35	0.12	0.06	nd	0.02	0.13	nd	nd	0.01	1.84	nd	nd	nd	nd	nd	nd	nd	nd
AN2WOPE_015	0.15	nd	0.06	0.05	nd	0.04	1.55	0.12	nd	nd	0.04	0.19	nd	nd	0.02	1.16	nd	nd	nd	nd	nd	nd	nd	nd
AN2WOPE_031	0.12	0.02	0.07	0.07	nd	0.02	0.82	0.08	0.05	nd	0.02	0.08	0.10	nd	0.01	1.17	nd	nd	nd	nd	nd	nd	nd	nd
AN2WOPE_032	0.06	0.02	0.04	0.04	nd	0.02	0.91	0.09	0.02	nd	0.02	0.15	0.11	nd	0.01	0.61	nd	nd	nd	nd	nd	nd	nd	nd
AN2WOPE_033	0.07	0.02	0.05	nd	nd	0.02	0.59	0.06	0.02	nd	nd	0.07	nd	nd	nd	1.34	nd	nd	nd	nd	nd	nd	nd	nd
AN2WOPE_042	0.04	0.01	0.02	0.06	nd	0.02	0.73	0.08	0.05	nd	0.01	0.09	nd	nd	nd	0.72	nd	nd	nd	nd	nd	nd	nd	nd
AN2WOPE_048	0.02	0.01	0.01	0.01	nd	0.02	0.19	0.03	0.03	nd	nd	0.06	0.04	nd	0.00	0.18	nd	nd	nd	nd	nd	nd	nd	nd
AN2WOPE_097	0.07	nd	0.04	nd	nd	0.02	0.67	0.06	0.04	nd	nd	0.07	nd	nd	nd	0.86	nd	nd	nd	nd	nd	nd	nd	nd
AN2WOPE_141	0.21	0.01	0.02	0.01	nd	0.01	0.98	0.06	0.01	nd	0.01	0.35	nd	nd	0.01	0.28	nd	nd	nd	nd	nd	nd	nd	nd

Table S4. Limits of quantification (LOQs) in ng.

	LOQs	
OPEs	**Atlantic**	**Southern**
TEP	0,03	0,29
TPrP	0,02	0,02
TiBP	0,08	0,11
TNBP	0,06	0,08
TBPO	0,31	0,00
TCEP	0,64	0,04
TCPP1	0,89	1,84
TCPP2	0,25	0,14
TCPP3	0,21	0,07
Chlorpyrifos	0,00	0,00
TDCIPP	0,05	0,03
TPhP	0,26	0,26
TBEP	0,12	0,09
EHDPP	0,32	0,00
TEHP	0,00	0,01
TPPO	0,00	2,16
ToCP	0,00	0,00
DOPP	0,00	0,00
TmCP	0,01	0,00
TpCP	0,00	0,00
TPPP	0,02	0,00
TDMPP	0,01	0,00
TDBPP	0,02	0,00
TTBPP	0,00	0,00

The limits of quantification (LOQs) were defined as the mean concentration of log 10 transformed field blanks, plus three times the standard deviation of the blank response. For the analytes which were not found in procedural blanks, LOQs were derived from the lowest standard in the calibration curve.

Table S5. Information of labelled OPE compounds used as surrogate (top table) and as internal standard (bottom table).

Compound name	Abbreviation	Concentration (ng / µL)	V added (µL)	Mass added (ng)
Tri-n-buthyl phosphate - d27	D27-TNBP	1	50	50
Triphenyl phosphate – d15	D15-TPhP	1	50	50
Tris (2-chloroethyl) phosphate - d12	D12-TCEP	1	50	50
Tri-n-propyl phosphate - d21	D21-TPrP	1	50	50
Tris (2-chloroisoprpyl) phosphate – d18	D18-TCPP	1	50	50
Tris (2-ethylhexyl) phosphate – d51	D51-TEHP	1	50	50

Compound name	Abbreviation	Concentration (ng / µL)	V added (µL)	Mass added (ng)
Tris (1.3-dichloro-2-propyl) phosphate - d15	D15-TDCPP	5	10	50
Tris (2-butoxyethyl) phosphate - $^{13}C_2$	M6TBEP	5	10	50
Triphenyl phosphate - $^{13}C_{18}$	MTPhP	5	10	50

Table S6. Surrogate recoveries (%) from the Atlantic Ocean samples (top table) and Southern Ocean samples (bottom table).

Atlantic Ocean samples					
Recoveries	d27-TNBP	d12-TCEP	d18-TCPP	d15-TPHP	d51-TEHP
Mean (%)	46.2	66.9	28.2	85.3	123.9
SD	21.9	66.0	21.8	39.7	50.9

Southern Ocean samples					
Recoveries	d27-TNBP	d12-TCEP	d18-TCPP	d15-TPHP	d51-TEHP
Mean (%)	63.5	57.8	71.3	78.2	96.0
SD	19.1	18.1	22.0	21.5	51.9

Table S7. Presence, absence and <LOQ number of samples per each compound and campaign.

ALL																						
	TEP	TCEP	TCPP123	TBEP	TiBP	TDCIPP	TNBP	TPhP	EHDPP	TmCP	TEHP	TPPO	TPrP	TpCP	TPPP	TBPO	Chlor	ToCP	DOPP	TDMPP	TDBPP	TTBPP
PRESENT (N)	32	53	52	48	52	50	52	50	51	31	13	13	24	3	15	0	0	1	1	5	1	6
N.D (N)	2	1	0	4	0	2	0	2	3	5	28	28	30	39	34	54	54	53	53	48	53	48
<LOQ (N)	20	0	2	2	2		2	2	0	18	13	13	0	12	5	0	0	0	0	1	0	0
N = 54	54	54	54	54	54	54	54	54	54	54	54	54	54	54	54	54	54	54	54	54	54	54
% PRESENCE	59.3	98.1	96.3	88.9	96.3	92.6	96.3	92.6	94.4	57.4	24.1	24.1	44.4	5.6	27.8	0.0	0.0	1.9	1.9	9.3	1.9	11.1
% N.D	3.7	1.9	0.0	7.4	0.0	3.7	0.0	3.7	5.6	9.3	51.9	51.9	55.6	72.2	63.0	100.0	100.0	98.1	98.1	88.9	98.1	88.9
% <LOQ	37.0	0.0	3.7	3.7	3.7	3.7	3.7	3.7	0.0	33.3	24.1	24.1	0.0	22.2	9.3	0.0	0.0	0.0	0.0	1.9	0	0

ATLANTIC																						
	TEP	TCEP	TCPP123	TBEP	TiBP	TDCIPP	TNBP	TPhP	EHDPP	TmCP	TEHP	TPPO	TPrP	TpCP	TPPP	TBPO	Chlor	ToCP	DOPP	TDMPP	TDBPP	TTBPP
PRESENT (N)	16	26	27	23.0	27.0	25.0	27.0	25.0	26	7	1	0	0	0	0	0	0.0	0.0	0.0	2.0	0.0	3.0
N.D (N)	2	1	0	2.0	0.0	2.0	0.0	2.0	1	5	26	27	27	27	27	27	27.0	27.0	27.0	9.0	10.0	8.0
<LOQ (N)	9	0	0	2.0	0.0	0.0	0.0	0.0	0	15	0	0	0	0	0	0	0.0	0.0	0.0	0.0	1.0	0.0
N = 27	27	27	27	27	27	27	27	27	27	27	27	27	27	27	27	27	27.0	27.0	27	27	27	27
% PRESENCE	59.3	96.3	100.0	85.2	100.0	92.6	100.0	92.6	96.3	25.9	3.7	0.0	0.0	0.0	0.0	0.0	0.0	0.0	0.0	7	0.0	11
% N.D	7.4	3.7	0.0	7.4	0.0	7.4	0.0	7.4	3.7	18.5	96.3	100.0	100.0	100.0	100.0	100.0	100.0	100.0	100.0	93	100	89
% <LOQ	33.3	0.0	0.0	7.4	0.0	0.0	0.0	0.0	0.0	55.6	0.0	0.0	0.0	0.0	0.0	0.0	0.0	0.0	0.0	0.0	0	0.0

SOUTHERN OCEAN																						
	TEP	TCEP	TCPP123	TBEP	TiBP	TDCIPP	TNBP	TPhP	EHDPP	TmCP	TEHP	TPPO	TPrP	TpCP	TPPP	TBPO	Chlor	ToCP	DOPP	TDMPP	TDBPP	TTBPP
PRESENT (N)	16.0	27.0	25.0	25.0	25.0	25.0	25.0	25.0	25.0	24.0	12.0	13.0	24.0	3.0	15.0	0.0	0.0	1.0	1.0	3.0	1.0	3.0
N.D (N)	0.0	0.0	0.0	2.0	0.0	0.0	0.0	0.0	2.0	0.0	2.0	1.0	3.0	12.0	7.0	27.0	27.0	26.0	26.0	12.0	15.0	13.0
<LOQ (N)	11.0	0.0	2.0	0.0	2.0	2.0	2.0	2.0	0.0	3.0	13.0	13.0	0.0	12.0	5.0	0.0	0.0	0.0	0.0	1.0	0.0	0.0
N = 27	27.0	27.0	27.0	27.0	27.0	27.0	27.0	27.0	27.0	27.0	27.0	27.0	27.0	27.0	27.0	27.0	27.0	27.0	27.0	27	27	27
% PRESENCE	59.3	100.0	92.6	92.6	92.6	92.6	92.6	92.6	92.6	88.9	44.4	48.1	88.9	11.1	55.6	0.0	0.0	3.7	3.7	11	4	11
% N.D	0.0	0.0	0.0	7.4	0.0	0.0	0.0	0.0	7.4	0.0	7.4	3.7	11.1	44.4	25.9	100.0	100.0	96.3	96.3	85	96	89
% <LOQ	40.7	0.0	7.4	0.0	7.4	7.4	7.4	7.4	0.0	11.1	48.1	48.1	0.0	44.4	18.5	0.0	0.0	0.0	0.0	4	0	0

Table S8. Individual and $\sum_{24}$OPE concentrations (ng L^{-1}) in SML.

Station code	Date (yymmdd)	LAT	LONG	TEP	TCEP	∑TCPP	TBEP	TiBP	TDCIPP	TNBP	TPhP	EHDPP	TmCP	TEHP	TPPO	TPrP	TpCP	TPPP	TBPO	Chlor	ToCP	DOPP	TDMPP	TDBPP	TTBPP	$\sum_{24}$OPE
AN1_ST04	201221	28.66	-28.41	<loq	0.81	7.05	0.99	0.58	0.95	0.58	0.9	0.33	<loq	n.d	n.d	n.d	n.d	n.d	n.d	n.d	n.d	n.d	n.d	n.d	n.d	11.9
AN1_ST05	201222	25.63	-24.90	2.44	8.80	16.6	0.93	3.94	3.41	0.47	0.24	1.47	<loq	n.d	n.d	n.d	n.d	n.d	n.d	n.d	n.d	n.d	n.d	n.d	n.d	38.4
AN1_ST06	201223	22.22	-26.63	2.02	3.15	36.0	7.49	1.12	3.50	0.36	1.36	3.04	n.d	n.d	n.d	n.d	n.d	n.d	n.d	n.d	n.d	n.d	nd	n.d	n.d	58.1
AN1_ST07	201224	18.87	-28.32	<loq	1.57	11.2	0.85	0.55	1.95	0.65	0.81	1.02	<loq	n.d	n.d	n.d	n.d	n.d	n.d	n.d	n.d	n.d	n.d	n.d	n.d	18.6
AN1_ST10	201227	7.35	-29.58	2.45	1.98	4.12	0.41	0.44	0.42	0.34	0.38	0.67	n.d	n.d	n.d	n.d	n.d	n.d	n.d	n.d	n.d	n.d	n.d	n.d	n.d	11.1
AN1_ST12	201229	0.14	-30.50	2.68	3.42	15.3	0.56	2.03	0.71	1.57	0.61	1.33	<loq	n.d	n.d	n.d	n.d	n.d	n.d	n.d	n.d	n.d	n.d	n.d	n.d	28.2
AN1_ST15	210102	-14.37	-33.92	<loq	1.97	3.82	0.36	0.3	4.3	0.39	0.31	0.64	<loq	n.d	n.d	n.d	n.d	n.d	n.d	n.d	n.d	n.d	n.d	n.d	n.d	11.9
AN1_ST19	210106	-27.79	-40.65	5.63	2.57	15.2	3.44	0.52	0.49	0.34	0.79	2.35	0.08	n.d	n.d	n.d	n.d	n.d	n.d	n.d	n.d	n.d	n.d	n.d	n.d	31.4
AN1_ST23	210111	-43.79	-54.75	1.31	0.76	5.11	2.44	0.45	0.42	0.24	0.44	1.12	0.12	n.d	n.d	n.d	n.d	n.d	n.d	n.d	n.d	n.d	n.d	n.d	n.d	12.3
AN2_ST01	220123	-62.71	-60.64	0.99	2.54	74.5	5.43	0.37	0.67	0.86	29.4	0.88	0.02	0.09	n.d	0.14	n.d	n.d	n.d	n.d	n.d	n.d	n.d	n.d	n.d	115.9
AN2_ST02	220124	-62.92	-61.04	<loq	3.41	79.8	2.17	3.09	1.45	1.07	36.4	1.41	0.04	0.04	6.49	0.07	n.d	0.05	n.d	n.d	n.d	n.d	n.d	n.d	n.d	135.5
AN2_ST03	220125	-64.58	-62.57	0.64	5.91	275.1	9.1	1.73	3.74	1.12	55.7	3.29	0.11	n.d	4.78	N.d	n.d	0.36	n.d	n.d	n.d	n.d	n.d	n.d	0.004	361.6
AN2_ST04	220126	-65.15	-65.64	<loq	5.10	120.9	2.17	1.14	0.83	0.37	19.3	0.63	0.02	0.05	4.81	0.37	n.d	0.08	n.d	n.d	n.d	n.d	n.d	n.d	n.d	155.8
AN2_ST06	220128	-67.75	-68.03	<loq	1.17	80.0	1.6	0.22	0.55	1.17	32.4	1.27	0.02	n.d	8.34	0.28	n.d	0.02	n.d	n.d	n.d	n.d	n.d	n.d	n.d	127.0
AN2_ST07	220130	-70.85	-79.89	0.65	2.69	26.9	3.84	1.94	0.51	0.92	161.6	1.64	0.49	<loq	<loq	0.1	<loq	0.02	n.d	n.d	n.d	n.d	n.d	n.d	n.d	201.2
AN2_ST09	220131	-69.21	-78.84	0.90	32.9	365.3	7.55	0.8	0.99	0.5	72.5	3.27	0.07	0.12	<loq	0.07	n.d	0.08	n.d	n.d	n.d	n.d	n.d	n.d	n.d	485.0
AN2_ST13	220205	-62.97	-60.29	8.30	0.12	<loq	n.d	<loq	<loq	<loq	<loq	n.d	<loq	<loq	<loq	0.34	n.d	n.d	n.d	n.d	n.d	n.d	n.d	n.d	n.d	8.76
AN2_ST14	220206	-62.95	-60.65	1.31	6.61	87.6	2.61	1.05	0.87	0.58	67.8	0.78	0.14	<loq	<loq	0.09	n.d	n.d	n.d	n.d	n.d	n.d	0.02	n.d	0.03	169.4

nd = not detected. <loq = below limit of detection

Table S9. Individual and $\sum_{24}$OPE concentrations (ng L^{-1}) SSL.

Station code	Date (yymmdd)	LAT	LONG	TEP	TCEP	∑TCPP	TBEP	TiBP	TDCIPP	TNBP	TPhP	EHDPP	TmCP	TEHP	TPPO	TPrP	TpCP	TPPP	TBPO	Chlor	ToCP	DOPP	TDMPP	TDBPP	TTBPP	$\sum_{24}$OPE
AN1_ST04	201221	28.66	-28.41	1.73	3.92	8.69	<loq	0.69	0.34	0.16	1.44	0.23	<loq	nd	nd	nd	nd	nd	nd	nd	nd	nd	nd	0.01	nd	17.19
AN1_ST05	201222	25.63	-24.90	1.65	<loq	1.88	0.18	<loq	0.27	0.19	1.11	0.17	<loq	nd	nd	nd	nd	nd	nd	nd	nd	nd	nd	nd	nd	5.58
AN1_ST06	201223	22.22	-26.63	1.56	2.25	7.27	0.63	0.75	0.99	0.16	3.59	1.21	<loq	nd	nd	nd	nd	nd	nd	nd	nd	nd	nd	0.01	nd	18.4
AN1_ST07	201224	18.87	-28.32	<loq	1.64	0.89	0.25	1.32	0.46	0.09	1.70	0.40	<loq	nd	nd	nd	nd	nd	nd	nd	nd	nd	nd	nd	nd	6.56
AN1_ST10	201227	7.35	-29.58	<loq	1.08	3.31	0.14	0.44	0.06	0.17	1.78	0.50	nd	nd	nd	nd	nd	nd	nd	nd	nd	nd	nd	nd	nd	7.27
AN1_ST12	201229	0.14	-30.50	0.49	2.89	4.26	0.14	0.60	0.36	0.13	3.06	0.59	<loq	nd	nd	nd	nd	nd	nd	nd	nd	nd	nd	nd	nd	12.5
AN1_ST15	210102	-14.37	-33.92	1.08	4.49	20.2	0.17	0.57	0.61	0.16	1.12	0.19	<loq	nd	nd	nd	nd	nd	nd	nd	nd	nd	nd	nd	nd	28.4
AN1_ST19	210106	-27.79	-40.65	0.20	0.74	4.83	0.47	0.21	0.10	0.09	3.45	0.31	0.04	nd	nd	nd	nd	nd	nd	nd	nd	nd	0.01	nd	nd	10.5
AN1_ST23	210111	-43.79	-54.75	0.25	0.86	3.02	0.33	0.27	0.26	0.14	1.67	0.39	0.03	nd	nd	nd	nd	nd	nd	nd	nd	nd	nd	nd	nd	7.14
AN2_ST01	220123	-62.71	-60.64	0.42	0.34	6.91	0.35	0.36	0.21	0.82	0.70	0.21	0.02	0.01	<loq	0.11	<loq	<loq	nd	nd	nd	nd	nd	nd	nd	10.5
AN2_ST02	220124	-62.92	-61.04	0.25	0.65	12.6	0.20	0.25	0.17	0.34	4.46	0.58	0.008	0.02	2.711	0.02	<loq	0.007	nd	nd	nd	nd	nd	nd	nd	22.3
AN2_ST03	220125	-64.58	-62.57	0.25	0.59	6.38	0.34	0.23	0.23	0.22	1.89	0.10	0.003	0.07	<loq	0.21	<loq	0.005	nd	nd	nd	nd	nd	nd	nd	10.5
AN2_ST04	220126	-65.15	-65.64	0.15	1.37	15.5	0.44	0.17	0.17	0.13	1.84	0.32	0.002	<loq	1.217	0.03	<loq	<loq	nd	nd	nd	nd	nd	nd	nd	21.3
AN2_ST06	220128	-67.75	-68.03	<loq	0.37	11.5	0.50	0.14	0.14	0.08	2.21	0.67	0.005	<loq	<loq	0.03	<loq	0.005	nd	nd	nd	nd	nd	nd	nd	15.6
AN2_ST07	220130	-70.85	-79.89	<loq	0.60	9.03	0.42	0.29	0.22	0.16	3.12	0.65	0.01	<loq	<loq	0.23	0.003	0.002	nd	nd	nd	nd	nd	nd	nd	14.7
AN2_ST09	220131	-69.21	-78.84	0.19	0.90	16.8	0.70	0.25	0.24	0.16	14.3	0.51	0.004	0.01	<loq	0.015	nd	0.005	nd	nd	nd	nd	nd	nd	nd	34.0
AN2_ST13	220205	-62.97	-60.29	1.04	0.02	<loq	0.07	<loq	<loq	<loq	<loq	Nd	<loq	<loq	<loq	0.069	nd	nd	nd	nd	nd	nd	nd	nd	nd	1.20
AN2_ST14	220206	-62.95	-60.65	0.31	1.14	14.8	0.64	0.17	0.13	0.21	4.29	0.39	0.10	<loq	<loq	0.04	nd	nd	nd	nd	0.01	0.03	nd	nd	nd	22.2

nd = not detected. <loq = lower than limit of detection

Table S10. Mean, median and standard deviation of individual and $\sum_{24}$OPE SML and SSL for the Atlantic Ocean (top table) and Southern Ocean (bottom table).

ATLANTIC OCEAN																						
		TEP	TCEP	∑TCPP	TBEP	TiBP	TDCIPP	TNBP	TPhP	EHDPP	TmCP	TEHP	TPPO	TPrP	TpCP	TPPP	TBPO	Chlor	ToCP	DOPP	TDMPP	TDBPP	TTBPP	$\sum_{24}$OPE
SML	MEAN	1.84	2.74	12.7	1.94	1.10	1.79	0.52	0.65	1.33	0.03	0.01	0.01	0.01	0.01	0.01	0.01	0.01	0.01	0.01	0.01	0.01	0.01	24.7
	MEDIAN	2.02	1.98	11.2	0.93	0.55	0.95	0.36	0.61	1.12	0.01	0.01	0.01	0.01	0.01	0.01	0.01	0.01	0.01	0.01	0.01	0.01	0.01	18.7
	SD	1.80	2.48	10.1	2.32	1.19	1.55	0.43	0.36	0.87	0.04	0.00	0.00	0.00	0.00	0.00	0.00	0.00	0.00	0.00	0.00	0.00	0.00	16.0
SSL	MEAN	0.78	2.01	6.01	0.26	0.54	0.38	0.09	2.10	0.44	0.01	0.01	0.01	0.01	0.01	0.01	0.01	0.01	0.01	0.01	0.01	0.01	0.01	12.7
	MEDIAN	0.49	1.64	4.26	0.18	0.57	0.34	0.09	1.70	0.39	0.01	0.01	0.01	0.01	0.01	0.01	0.01	0.01	0.01	0.01	0.01	0.01	0.01	10.5
	SD	0.72	1.49	5.86	0.19	0.37	0.28	0.04	0.99	0.32	0.01	0.00	0.00	0.00	0.00	0.00	0.00	0.00	0.00	0.00	0.00	0.00	0.00	7.54

SOUTHERN OCEAN																								
		TEP	TCEP	∑TCPP	TBEP	TiBP	TDCIPP	TNBP	TPhP	EHDPP	TmCP	TEHP	TPPO	TPrP	TpCP	TPPP	TBPO	Chlor	ToCP	DOPP	TDMPP	TDBPP	TTBPP	$\sum_{24}$OPE
SML	MEAN	1.47	6.71	123.4	3.83	1.15	1.07	0.74	52.8	1.47	0.10	0.03	2.71	0.16	0.00	0.07	0.01	0.01	0.01	0.01	0.01	0.01	0.01	195.8
	MEDIAN	0.65	3.41	80.0	2.61	1.05	0.83	0.87	36.5	1.27	0.04	0.00	0.00	0.11	0.01	0.02	0.01	0.01	0.01	0.01	0.01	0.01	0.01	155.9
	SD	2.60	10.0	119.0	2.98	0.97	1.07	0.39	46.9	1.14	0.15	0.04	3.38	0.13	0.00	0.12	0.00	0.00	0.00	0.00	0.00	0.00	0.01	142.6
SSL	MEAN	0.32	0.66	10.5	0.41	0.21	0.17	0.24	3.66	0.38	0.02	0.01	0.44	0.08	0.00	0.00	0.01	0.01	0.01	0.01	0.00	0.00	0.00	17.1
	MEDIAN	0.25	0.59	11.5	0.42	0.23	0.17	0.16	2.21	0.37	0.01	0.00	0.00	0.04	0.00	0.00	0.01	0.01	0.01	0.01	0.01	0.01	0.01	15.8
	SD	0.28	0.42	5.13	0.20	0.09	0.07	0.23	4.23	0.24	0.03	0.02	0.94	0.08	0.00	0.00	0.00	0.00	0.00	0.01	0.00	0.00	0.00	9.13

Table S11. Mean SML and SSL concentrations (ng L^{-1}) and T-test p-value results for statistical comparison of individual and $\sum_{24}$OPE between the two layers in the Atlantic Ocean.

	TEP	TCEP	TCPP123	TBEP	TiBP	TDCIPP	TNBP	TPhP	EHDPP	TmCP	$\sum_{24}$OPES
SML_average	1.85	2.74	12.7	1.94	1.10	1.79	0.52	0.65	1.33	0.03	24.7
SSL_average	0.78	2.01	6.01	0.26	0.54	0.38	0.10	2.10	0.44	0.01	12.7
P-value	0.17	0.53	0.14	**0.04***	0.26	**0.01***	**0.01***	**0.0005***	**0.004***	0.19	0.07

** marks statistically significant differences*

Table S12. Mean SML and SSL concentrations (ng L^{-1}) and T-test p-value results for statistical comparison of individual and $\sum_{24}$OPE between the two layers in the Southern Ocean.

	TEP	TCEP	TCPP123	TBEP	TiBP	TDCIPP	TNBP	TPhP	EHDPP	TmCP	$\sum_{24}$OPES
SML_average	1.47	6.71	123.4	3.83	1.15	1.07	0.736	52.81	1.46	0.099	195.80
SSL_average	0.32	0.66	10.5	0.407	0.21	0.17	0.24	3.65	0.38	0.017	17.14
P-value	0.17	0.10	**0.02***	**0.01***	**0.02***	**0.03***	**0.004***	**0.01***	**0.02***	0.13	**0.004***

** marks statistically significant differences*

Table S13. Mean SML and SSL concentrations (ng L^{-1}) and T-test p-value results for statistical comparison of individual and $\sum_{24}$OPE between the two layers in the Atlantic and Southern Oceans.

	TEP	TCEP	TCPP123	TBEP	TiBP	TDCIPP	TNBP	TPhP	EHDPP	TmCP	$\sum_{24}$OPES
SML_average	1.65	4.72	68.07	2.88	1.12	1.43	0.62	26.73	1.39	0.06	110.26
SSL_average	0.55	1.33	8.25	0.33	0.37	0.27	0.17	2.87	0.41	0.01	14.92
P-value	**0.04***	0.08	**0.018***	**0.001***	**0.014***	**0.001***	**0.0001***	**0.02***	**0.0002***	0.07	**0.005***

** marks statistically significant differences*

Table S14. Enrichment factor of SML (EF_{SML}) for individual OPE [1] for the Atlantic samples (top table) and Southern Ocean samples (bottom table).

ATLANTIC OCEAN										
Station Code	TEP	TCEP	∑TCPP	TBEP	TiBP	TDCIPP	TNBP	TPhP	EHDPP	TmCP
AN1_ST04	0.01	0.13	0.81	9.24	0.83	2.79	3.66	0.62	1.53	1.00
AN1_ST05	1.48	43.7	8.86	5.14	69.91	12.46	8.32	0.21	8.69	1.00
AN1_ST06	1.29	1.40	4.95	11.9	1.50	3.54	2.16	0.38	2.51	0.78
AN1_ST07	1.00	0.96	16.22	3.36	0.42	4.24	7.07	0.48	2.56	1.00
AN1_ST10	103	1.84	1.25	10.8	1.01	6.44	3.44	0.21	1.35	1.00
AN1_ST12	5.47	1.18	3.58	3.96	3.35	1.98	11.8	0.20	2.26	1.00
AN1_ST15	0.02	0.44	0.19	2.12	0.52	7.02	2.93	0.28	3.38	1.00
AN1_ST19	28.5	3.49	3.14	6.94	2.42	4.72	3.79	0.23	7.62	2.22
AN1_ST23	5.16	0.82	1.69	7.28	1.70	1.43	5.96	0.26	2.85	3.75
MEAN	16.2	5.99	4.52	6.76	9.07	4.96	5.46	0.32	3.64	1.42
MEDIAN	1.48	1.18	3.14	6.94	1.50	4.24	3.79	0.26	2.56	1.00
MAX	103	43.7	16.2	11.9	69.9	12.5	11.8	0.62	8.69	3.75
MIN	0.01	0.13	0.19	2.12	0.42	1.43	2.16	0.20	1.35	0.78
ST DEV	33.9	14.2	5.12	3.41	22.8	3.38	3.13	0.14	2.65	0.97

SOUTHERN OCEAN										
Station Code	TEP	TCEP	∑TCPP	TBEP	TiBP	TDCIPP	TNBP	TPhP	EHDPP	TmCP
AN2_ST01	2.36	7.55	10.8	15.7	1.03	3.28	1.05	41.9	4.24	0.80
AN2_ST02	0.54	5.22	6.31	10.9	12.4	8.48	3.10	8.17	2.43	5.20
AN2_ST03	2.57	10.0	43.1	26.9	7.40	16.2	5.11	29.5	31.5	36.92
AN2_ST04	0.91	3.72	7.79	4.89	6.52	4.96	2.79	10.5	1.98	7.37
AN2_ST06	1.00	3.15	6.96	3.18	1.62	3.94	13.9	14.7	1.89	3.32
AN2_ST07	4.70	4.51	2.98	9.07	6.66	2.26	5.63	51.7	2.52	43.50
AN2_ST09	36.4	21.8	10.7	3.17	4.17	3.08	5.08	6.41	17.5	8.97
AN2_ST13	5.22	1.00	0.00	1.00	1.00	1.00	1.00	-	1.00	-
AN2_ST14	4.22	5.79	5.92	4.07	6.31	6.66	2.81	15.8	2.02	1.47
MEAN	6.43	6.97	10.5	8.77	5.24	5.54	4.51	22.3	7.23	13.4
MEDIAN	2.57	5.22	6.96	4.89	6.31	3.94	3.10	15.2	2.43	6.28
MAX	36.4	21.80	43.1	26.9	12.4	16.2	13.9	51.7	31.5	43.5
MIN	0.54	1.00	0.00	1.00	1.00	1.00	1.00	6.41	1.00	0.80
ST DEV	11.3	6.13	12.7	8.24	3.72	4.59	3.93	16.9	10.4	16.8

$$[1]\ EF_{SSA}\frac{OPE\ C\ SW_{SML}\ (ng\ L^{-1})}{OPE\ C\ SW_{SSL}\ (ng\ L^{-1})}$$

Table S15. Pearson's and Spearman correlation between EF_{SML} for individual OPEs and total chlorophyll α content (μg L^{-1}).

Atlantic + Southern samples (N=18)		
Ef	**Spearman**	**Pval**
TEP	0.07	0.08
TCEP	0.47	**0.04***
TCPP123	0.37	0.13
TBEP	0.07	0.77
TiBP	0.51	**0.03***
TDCIPP	-0.04	0.86
TNBP	0.05	0.84
TPhP	0.73	**0.001***
EHDPP	-0.13	0.59
TmCP	0.68	**0.002***

Atlantic Ocean samples (N=9)		
Ef	**Spearman**	**Pval**
TEP	0.45	0.23
TCEP	0.03	0.94
TCPP123	0.3	0.43
TBEP	0.23	0.55
TiBP	0.21	0.58
TDCIPP	-0.6	0.09
TNBP	0.41	0.26
TPhP	-0.34	0.36
EHDPP	-0.41	0.27
TmCP	0.14	0.70

Southern Ocean samples (N=9)		
Ef	**Spearman**	**Pval**
TEP	-0.28	0.46
TCEP	-0.20	0.61
TCPP123	-0.03	0.94
TBEP	0.21	0.58
TiBP	0.5	0.17
TDCIPP	0.23	0.55
TNBP	0.75	**0.02***
TPhP	0.30	0.46
EHDPP	-0.01	0.98
TmCP	0.5	0.21

*Statistically significant correlations are marked with an *.*

Table S16. Sea-spray aerosols (SSA). seawater (SW) from SSA volumes (V_{SW}). Na^+. OPEs in SSA ($\sum_{13}OPE_{SSA}$) and OPEs in SW from SSA ($\sum_{14}OPEsw$).

Station code	LAT	LON	Air sampled**	$\sum_{13}OPE_{SSA}$***	Na^{+****}	$[Na^+]_{SSA}$ [1]	Vsw [2]	$\sum_{13}OPEsw$ [4]	$\sum_{13}OPE/Na^+$ [3]
			m^3	$ng\ m^{-3}$	μmol	$\mu mol\ m^{-3}$	$L\ m^{-3}$	$ng\ L^{-1}$	$\mu mol\ m^{-3}$
MA8	-3.03	-27.33	945	2.78	145.60	0.15	3.17E-07	8,66E+06	18,04
MA9	-4.78	-28.17	960	0.87	601.00	0.63	1.29E-06	6,66E+05	1,39
MA10	-15.83	-33.40	632	1.61	109.20	0.17	3.56E-07	4,47E+06	9,32
MA11	-18.42	-34.64	525	3.61	751.35	1.43	2.94E-06	1,21E+06	2,52
MA12	-21.09	-35.97	275	4.35	515.35	1.87	3.86E-06	1,11E+06	2,32
MA13	-24.32	-36.22	866	3.20	897.08	1.04	2.13E-06	1,48E+06	3,09
MA14	-25.43	-30.07	927	2.79	71.37	0.08	1.58E-07	1,74E+07	36,22

**Data from Malaspina (Castro-Jiménez et al.. 2016). nd = non-detected*

Air sampled (m^3): Air volume sampled by High Volume Sampler. ***14$\sum OPE_{SSA}$ ($ng\ m^{-3}$): $\sum$OPE concentrations in SSA.. **Na^+ (μmol): Na^+ content in SSA

$$[\mathbf{1}]\ Na^+_{SSA}\ (\mu mol\ m^{-3}) = \frac{Na^+\ (\mu mol)}{Air\ sampled\ (m^3)} \quad [\mathbf{2}]\ V_{SW}\ (L\ m^{-3}) = \frac{Na^+_{SSA}\ (\mu mol\ m^{-3})}{11.18\ g\ L^{-1} \Big/ 22.98\ g\ mol^{-1}} \quad [\mathbf{3}]\ {}^{13}\sum OPEs/Na^+\ (\mu mol\ m^{-3}) = \frac{{}^{13}\sum OPE_{SSA}\ (ng\ m^{-3})}{Na^+\ (\mu mol)}$$

$$[\mathbf{4}]\ 13\sum OPE_{SW}\ (ng\ L^{-1}) = \frac{{}^{13}\sum OPE_{SSA}\ (ng\ m^{-3})}{V_{SW}\ (L\ m^{-3})}$$

Table S17. Individual and ∑OPE in SW_{SSA} (ng L^{-1}) [1].

Station code	TCEP	$\sum_3$TCPP	TiBP	TnBP	TPhP	EHDPP	TEHP	$\sum_3$TCrP	$\sum_{13}OPE_{SSA}$
MA8	483961	789304	451553	1972194	27759	1322827	497999	58362	8657083
MA9	9612	15637	106939	248107	5014	n.d	280801	n.d	666113
MA10	303286	79860	344592	901658	27618	545232	659679	n.d	4473181
MA11	71869	149949	54558	395953	8093	167182	76459	10466	1209558
MA12	120106	137356	71800	186581	1626	117291	229229	14547	1114187
MA13	248270	201510	70727	246828	3495	375232	91998	n.d	1483650
MA14	2122830	908335	761494	2399077	43833	5225412	1518621	102277	17383553

**Data from Malaspina (Castro-Jiménez et al., 2016). nd = non-detected*

$$[\mathbf{1}] OPE_{SW}\ (ng\ L^{-1}) = \frac{OPE_{SSA}\ (ng\ m^{-3})}{V_{SW}\ (L\ m^{-3})}$$

Table S18. Enrichment factor of SSA (EF_{SSA}) for individual OPEs [1].

Area	Code	SSA sample	SML sample	TCEP	∑TCPP	TiBP	TNBP	TPhP	EHDPP
Z1	**Ef1**	SSA_MA8	AN1_ST10	2,44E+05	1,87E+06	7,41E+05	1,02E+06	8,08E+06	7,29E+04
Z1	**Ef2**	SSA_MA9	AN1_ST12	2,81E+03	2,21E+04		5,28E+04	1,57E+05	8,20E+03
Z2	**Ef3**	SSA_MA10	AN1_ST15	1,54E+05	1,86E+04	4,22E+05	1,16E+06	4,75E+06	8,96E+04
Z2	**Ef4**	SSA_MA11	AN1_ST15	3,65E+04	3,49E+04	7,21E+04	1,83E+05	2,08E+06	2,63E+04
Z3	**Ef5**	SSA_MA12	AN1_ST19	4,66E+04	2,77E+05	1,55E+04	1,39E+05	5,42E+05	2,05E+03
Z3	**Ef6**	SSA_MA13	AN1_ST19	9,64E+04	4,07E+05	1,62E+04	1,37E+05	7,17E+05	4,40E+03
Z3	**Ef7**	SSA_MA14	AN1_ST19	8,24E+05	1,83E+06	2,84E+05	1,47E+06	6,97E+06	5,51E+04
AVERAGE				2.01E+05	2,58E+05	5.95E+05	3.33E+06	3.69E+04	9.20E+05
SD				2.87E+05	2,87E+05	5.98E+05	3.27E+06	3.56E+04	9.56E+05
MIN				2.81E+03	1,55E+04	5.28E+04	1.57E+05	2.05E+03	4.99E+04
MAX				8.24E+05	7,41E+05	1.47E+06	8.08E+06	8.96E+04	2.22E+06

[1] $$EF_{SSA} \frac{OPE\ C\ SW_{SSA}\ (ng\ L^{-1})}{OPE\ C\ SW_{SML}\ (ng\ L^{-1})}$$

References

Strickland, J.D.H. and Parsons, T.R. (1972) A Practical Handbook of Seawater Analysis. 2nd edition. Ottawa, Canada, Fisheries Research Board of Canada, 310pp. (Bulletin Fisheries Research Board of Canada, Nr. 167 (2nd ed)).

PART 03 - CHAPTER 3. TRANSPORT AND BIOGEOCHEMISTRY OF OPEs IN THE OCEANS

3.3.3. Paper IV. *Biogeochemical Controls on Latitudinal (42°N to 70°S) and Depth Distribution of Organophosphate Esters in the Atlantic and Southern Oceans*

Núria Trilla-Prieto[1,2], Naiara Berrojalbiz[1], Jon Iriarte[1], Antonio Fuentes-Lema[3], Cristina Sobrino[4], Maria Vila-Costa[1], Begoña Jiménez[5], and Jordi Dachs[1]*

[1]Department of Environmental Chemistry, IDAEA-CSIC, 08034, Barcelona, Catalunya, Spain.

[2]Departament of Ecology, Faculty of Earth Sciences, Universitat de Barcelona, 08034, Barcelona, Catalunya, Spain.

[3]Centro de Investigación Mariña (CIM), Universidade de Vigo, 36310, Vigo, Spain

[4]Grupo de Oceanografía Biolóxica, Centro de Investigación Mariña (CIM), Universidade de Vigo, 36310, Vigo, Spain.

[5]Department of Instrumental Analysis and Environmental Chemistry, IQOG-CSIC, 28006, Madrid, Spain.

*Corresponding Author: jordi.dachs@idaea.csic.es

State: Submitted to ES&T in November 2024

ABSTRACT

Large scale oceanic assessments are key for determining persistence and long-range transport potential of organic pollutants, but there is a dearth of these for organophosphate esters (OPEs), widely used as flame retardants and plasticizers. This work reports the latitudinal distribution (42°N-70°S) and vertical profiles (from surface to 2000 m depth) of OPEs in the Atlantic and Southern Oceans, and explore their biogeochemical controls. The latitudinal gradient shows higher surface OPE concentrations near the equator than at higher latitudes, the prevailing oceanic and atmospheric circulation, and measured wet deposition events. At the deep chlorophyll maximum depth, there was an inverse correlation between OPEs and phytoplankton biomass, with the lowest concentrations in the Southern Ocean, consistent with the role of the biological pump depleting OPEs from the photic zone. OPE latitudinal trends in the deep ocean (2000 m depth) resembled those at surface with maximum intertropical concentrations. Analysis derived from OPE concentrations at the bottom of the photic zone and in the minimum oxygen layer, suggested a complex dynamic biogeochemical cycling driven by transport, degradation, and re-dissolution of OPEs with depth. OPEs are persistent enough to reach all oceanic compartments, but a quantitative resolution of the sources, sinks, seasonality and biogeochemical cycles will require future research.

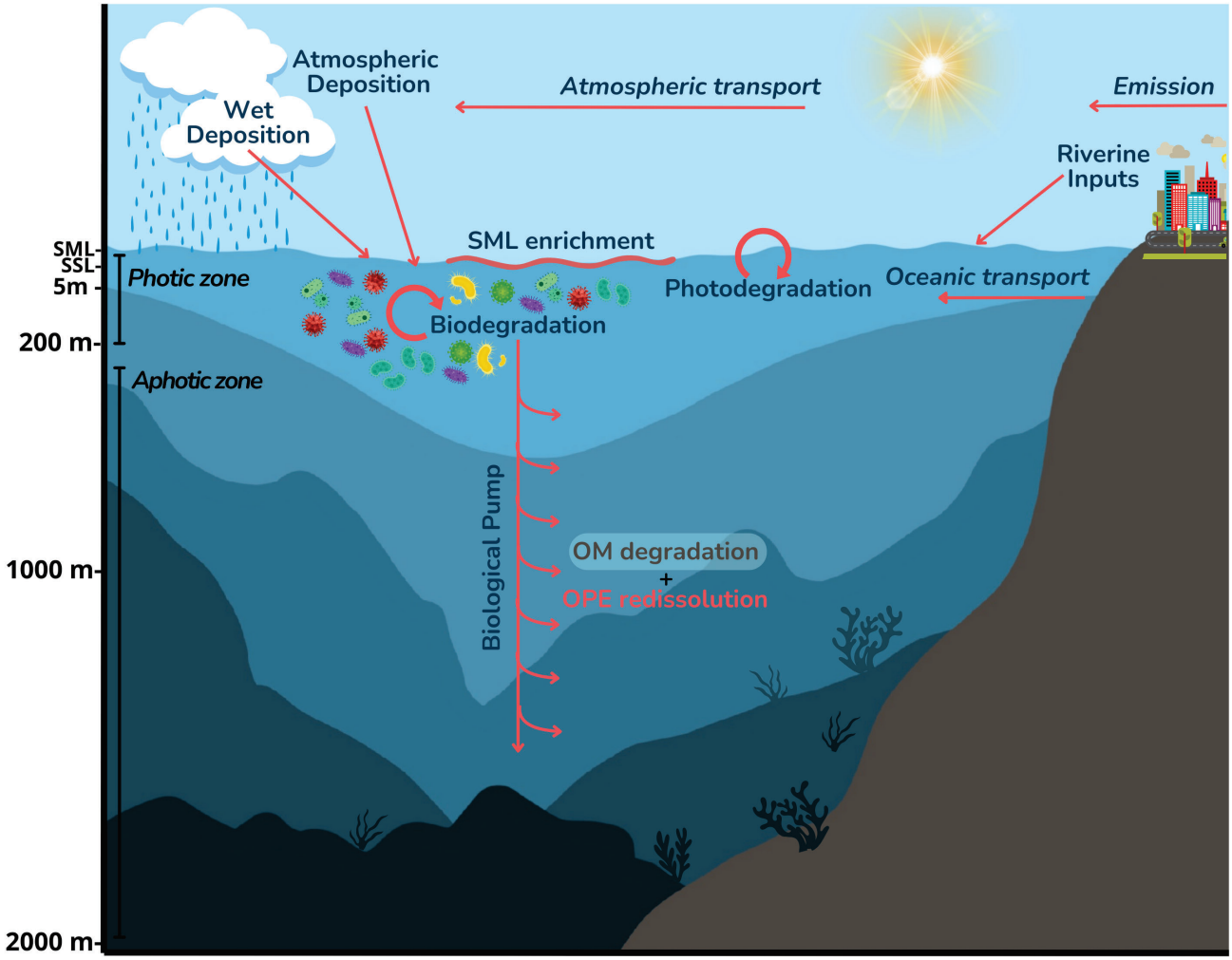


Figure 0 | Toc Art

Keywords

Organophosphate esters, OPEs, Atlantic Ocean, Southern Ocean, plasticizers.

Synopsis

Latitudinal trends in the Atlantic and Southern Oceans at different depths provide information on sources and biogeochemistry of the widely used organophosphate ester flame retardants and plasticizers

INTRODUCTION

Contemporaneous societies use hundreds of thousands of organic chemicals, and many of them reach the environment[1]. Persistence and potential for long-range transport are two key criteria for prioritizing the regulation of persistent organic pollutants (POPs) among the myriad of synthetic chemicals. Assessments of organic contaminants at the oceanic scale, including POPs, are essential for understanding their persistence, mobility and impacts[2,3]. Legacy POPs[2–7], polycyclic aromatic hydrocarbons (PAHs)[4,8–11], plastics[12–15] and perfluoroalkyl substances (PFAS)[16–24] are among the anthropogenic contaminants that have received more attention in terms of their biogeochemistry and occurrence in the ocean.

OPEs have been reported in many marine environments[25–33], but assessments at oceanic scale are limited[33]. OPEs are widely used as flame retardants, plasticizers, and lubricants in many consumer products and applications[34–37]. OPEs are ubiquitous in the environment, raising concerns due to their toxicological effects[35,36,38–40], bioaccumulative potential[41–44], and persistence in ecosystems[30,36,45–48]. Previous assessment in the marine environment report variable concentrations of OPEs[25–28,30–32,49], suggesting heterogeneous sources and biogeochemical pathways. For example, $\sum_{14}$OPE concentrations ranged from 40.0 to 60.8 ng L^{-1} in the Atlantic Ocean off New York State[50] , while in the remote Canadian Arctic [51], $\sum_{7}$OPE concentrations ranged from 0.02 to 306 ng L^{-1}, with drivers of such variability largely unknown. Few studies have investigated OPE concentrations in the Southern Ocean. Li et al. (2023)[52] reported $\sum_{11}$OPE surface concentrations at coastal Antarctica (Fildes Peninsula, King George Island) and in the Ross Sea (1 to 70 ng L^{-1}), which were comparable to the Arctic[26,53]. A north-south oceanic transect of OPEs has been reported for the concentrations in the surface microlayer (SML) and subsurface layer (SSL) of the Atlantic and Southern Oceans[54], thus only covering the top half meter of the water column.

Even though vertical profiles of contaminant concentrations provide important information on their transport and biogeochemical cycling[55–58], few studies report OPEs for depths other than the top few meters of the water column. A wide range of $\sum_{11}$OPE concentrations (0.006 to 0.44 ng L^{-1}) were measured at five different depths (between 221 and 2513 m) in the North Atlantic's Fram Strait, without a clear trend with depth[29]. When evaluating biogeochemical processes, the deep chlorophyll maximum (DCM), where there is a phytoplankton biomass maxima[59], provides clues on the transport to deep waters by the biological pump[19,60]. For instance, maximums of particle-phase PAHs and PCBs concentrations at the DCM in the Mediterranean Sea showed that there was a maximum of particle-phase PAHs and PCBs at the DCM[55,56]. While the influence of the biological pump has been reported for legacy pollutants, PAHs and PFAS[19,61–63], it remains unexplored for OPEs. The primary known sinks of OPEs are photodegradation and hydrolysis, the former may occur predominantly close to surface[64–66], as well as microbial degradation[67]. Other regions in the mesopelagic ocean, such as the layer with minimum of oxygen, remain unexplored in terms of biogeochemistry of contaminants. Furthermore, it is unclear how the occurrence at surface relates to the other depths of the water column, which is an important issue as most oceanic measurements are made at 4-5 m depth[25–28,30,31,49].

OPEs exhibit a broad spectrum of physicochemical properties, such as volatility, aqueous solubility, and octanol-water partition coefficients (K_{OW}), attributed to the varying substituents on their side chains[68]. Such variability in properties and potential for being degraded, may introduce variations in their biogeochemistry and eventually their oceanic sinks, even though K_{ow} is often a poor descriptor for polar chemicals. Measurements in large scale transects and vertical profiles are useful to identify regions with under a larger influence of sources (rivers, atmospheric inputs including rain), potential for long-range transport, and cycling. Wet deposition has barely been quantified for OPEs in the open ocean, as previous measurements focused on continents and coastal zones, even though rain-air washout ratios are high.[69]

Here, we provide a large dataset of concentrations for twenty-four targeted OPEs in the dissolved phase at 5 m depth and the DCM covering a latitudinal transect from 42°N to 53°S in the Atlantic Ocean, and from 60°S to 70.2°S in the Southern Ocean. In addition, we provide eleven vertical profiles of concentrations from surface to 2000 m depth. The objectives of this work are a) to describe the latitudinal and depth distribution of OPEs in the Atlantic and Southern Ocean, b) to assess the biogeochemical controls on the latitudinal and depth occurrence of OPEs, c) and to provide measurements of wet deposition of OPEs over the ocean.

MATERIALS AND METHODS

Sampling

Seawater from 5 m depth (below the influence of the ship), and at additional depths down to 2000 m, as well as wet deposition samples were collected during two oceanographic expeditions. During the ANTOM-I cruise (December 2020-January 2021), from Vigo (Spain) to Punta Arenas (Chile), a total of 24 stations were sampled

along a latitudinal transect in the Atlantic Ocean onboard the R/V Sarmiento de Gamboa. The second campaign, ANTOM-II onboard the R/V Hespérides (January-February 2022), covered the Southern Ocean, west of the Antarctic Peninsula, sampling at 13 stations in the Bransfield Strait and the Bellinghausen Sea **(Table S1)**. Seawater samples were collected using a Niskin-rosette system equipped with a Sea-bird SBE 9 CTD, which measured salinity, temperature, fluorescence, depth, and oxygen concentrations, enabling the characterization of the water column. The 5 m depth water samples were collected at all the stations (N = 37). In addition, seawater from the DCM, determined using the fluorescence sensor from the CTD, was sampled at sixteen stations in the Atlantic Ocean, and ten stations in the Southern Ocean. Vertical profiles (5 depths) were obtained at seven stations in the Atlantic Ocean and at four stations in the Southern Ocean. These depth profiles included samples, in addition to surface and DCM, from the layer receiving 1% of photosynthetic active radiation (1% PAR), the layer with minimum of oxygen concentration (MOx), and at a depth of 2000 m. At two stations from the Southern Ocean stations (AN2_ST08 and ST11, see **Figure 1**), intense water mixing disrupted the oxygen gradient, and only a weak minimum was observed.

2 L of seawater were collected from Niskin bottles into pre-rinsed 2 L polytetrafluoroethylene (PTFE) bottles and seawater was pre-processed in the vessel's laboratory. First, the seawater was filtered through pre-combusted glass fiber filters (47 mm, GF/F Whatmann). The dissolved phase was then collected using Oasis HLB solid-phase extraction (SPE) cartridges (6 cm^3, 200 mg; Waters). The cartridges were pre-conditioned with 6 mL of 2-propanol and 12 mL of HPLC-grade water and then spiked with 50 ng of a mix of labelled recovery standards **(Table S2)**. After sample loading, cartridges were washed with 6 mL of HLPC-grade water containing 5% methanol, dried under vacuum for 10 min and stored at -20 °C in sealed bags until processed ashore in a clean laboratory.

During the only two rain episodes that occurred during the campaigns, wet deposition (WD) samples were collected using a pre-combusted 2.5 L glass-bottle and a MeOH and acetone pre-cleaned stainless-steel funnel (diameter of 0.2 m). The WD samples were treated equal to the rest of the seawater samples, with the exception of the GF/F filtering step, which was not performed. Two samples were collected from the Atlantic Ocean (station 10 at latitude 7°N, and 11 at latitude 4°S). The first was collected during the night (8 h) from December 26 to 27th 2020, and the second was collected the following night (8h), from December 27 to the 28th. For both rain events, 1 L of rain was analyzed, but during the rain events 1 and 1.2 L of rainwater were collected. There weren't WD events during the Southern Ocean campaign.

OPE analysis

After transport of the samples to the clean lab, HLB cartridges were unfrozen for 3h at room temperature, centrifuged at 3500 rpm for 4 min, and eluted with 12 mL methyl tert-butyl ether:methanol (3:1, v/v). Residual water was removed from the extracts by adding 3 g of pre-baked sodium sulfate. The final eluents were concentrated under N_2 avoiding dryness and reconstituted in 300 µL of toluene.

OPE identification and quantification was conducted using gas chromatography coupled to a triple quadrupole mass spectrometer (GC-MS/MS-QqQ). Chromatographic separation was carried out using a HP-5MS column (30 m, 0.25 mm internal diameter, 0.25 µm film thickness) on an Agilent 7890A gas chromatograph. Methane was used as the ionization gas, and helium was used as the carrier gas at a constant flow rate of 20 mL min^{-1}. Two microliters of sample were injected in split-less mode at an injection port temperature of 280°C. The column temperatures were: 90°C for 1 min, increased at 15 °C min^{-1} to 200°C, held for 6 min, then at 5°C min^{-1} to 250 °C, held for 6 min, and then at 10°C min^{-1} to 315°C, held for 10 min. Detection was carried out with an Agilent 7000B triple quadrupole mass spectrometer using the electronic impact ionization (EI) mode in positive mode. Acquisition was performed by multiple reaction monitoring (MRM). Fifty nanograms of internal standards **(Table S2)** were added before the analysis. Concentrations were recovery corrected and only concentrations above limits of quantification (LOQ) were considered.

A total of 24 OPEs were targeted in this study (acronyms in **Table S3**). These include five chlorinated OPEs (TCEP, TDCIPP, and three TCPP isomers), one brominated OPE (TDBPP), eight aryl OPEs (TPhP, EHDPP, ToCP, TpCP, TmCP, TDMPP, TPPP, and TTBPP), and six alkylated OPEs (TEP, TPrP, TiBP, TNBP, TBEP, and TEHP). In addition, four organophosphorus chemicals were targeted: TPPO, DOPP, Chlorpyrifos, and TBPO. For this analysis, the three TCPP isomers were grouped together as ∑TCPP, and the three cresyl isomers (TmCP, ToCP, and TpCP) were grouped as ∑TcPs. Furthermore, analytes contributing less than 0.5% on average to the total OPE pool were grouped under name "Minor-OPEs", which included TEHP, TPrP, TPPP, DOPP, TBPO, TPPO, Chlorpyrifos, TDMPP, TDBPP, and TTBPP **(see Table S4)**. For simplification, the term "OPEs" in the discussion encompasses all targeted organophosphorus compounds, and i) Cl-OPEs includes TCEP, ∑TCPP, and TDCIPP; ii) aryl-OPEs includes TPhP, EHDPP, and ∑TcPs; iii) alkyl-OPEs

includes TEP, TiBP, TNBP, and TBEP.

Quality Assurance and Quality Control

All containers, tubes, and connections used during sampling and chemical analysis were made of stainless steel, glass, or PTFE, and were rinsed with methanol and acetone to avoid contamination. To minimize contamination, all filters and glass materials were combusted at 450°C for 4h before their use.

A minimum of a field blank and a procedural blank were analyzed for each batch of 10 samples to monitor potential contamination from the laboratories and during transport. Field blanks consisted of HLB cartridges that followed the same pre-conditioning, transport, and analysis as the samples, but no seawater was loaded into the cartridges even though they were connected to the SPE system for the same time as the sample cartridges to replicate handling conditions. Procedural blanks followed the same extraction and analysis procedures conducted in the clean laboratory. The limits of quantification (LOQs) were defined as the mean concentrations of field/procedural blanks **(Table S5)** plus three times the standard deviation **(Table S6)**. The recoveries were monitored using TNBP-d27, TCEP-d12, TCPP-d18, TEHP-d51, and TPhP-d15 as surrogate standards added to the cartridge prior to the loading of the sample, with mean recoveries of 71% ± 44% and 74% ± 20% in the Atlantic and Southern Ocean, respectively **(Table S7)**. Six and four matrix spikes were performed during the Atlantic and Southern Ocean campaigns, respectively. The recoveries of the native analytes ranged from 18.3% ± 2.8% to 144.6% ± 13.2 in the Atlantic, and from 41.4% ± 1.2% to 113.8% ± 8.7% in the Southern Ocean **(Table S7)**.

Biological measurements

Bacterial Abundance (BA), bacterial production (BP), and chlorophyll a (Chl a) were also measured to provide further information about the biological interaction between marine microbial plankton assemblages and OPEs (see **Note S1** for methods).

Statistical analysis

Due to the non-normal distribution of concentrations (confirmed by Shapiro-Wilk normality test, $p < 0.01$), non-parametric statistical analysis, or log-transformation of the data was conducted using RStudio 2023.12.1+402. The Mann-Whitney U test and Kruskal-Wallis test were used to detect significant differences between independent groups, whereas the Wilcoxon Signed-Rank test was used for paired comparisons. Additional analyses included the utilization of polynomial and linear regression models, and Spearman, and Pearson's correlation tests.

RESULTS AND DISCUSSION

Latitudinal distribution of OPEs at 5 m depth

The dissolved phase concentrations of $\sum_{24}$OPE at 5 m depth ranged from 2.12 to 78.5 ng L^{-1} in the Atlantic Ocean (AN1_ST01 to ST24) with an average of 23.4 ng L^{-1} (**Table S8 and S9** for complete statistics). In the Southern Ocean (stations AN2_ST01 to ST14), 5 m depth $\sum_{24}$OPE concentrations were significantly lower, ranging from 1.42 to 20.1 ng L^{-1}, averaging 9.14 ng L^{-1} **(Table S9 and S10)**. The highest $\sum_{24}$OPE concentrations at 5 m depth were recorded along the Brazilian coast at stations AN1_ST15, AN1_ST16, AN1_ST12, and AN1_ST18 **(Figure 1)**. This spatial pattern aligns with rivers' influence, such as the Amazon, identified as a significant source of OPEs in the tropical Atlantic Ocean. High dissolved-phase concentrations of OPEs, reaching up to 1 µg L^{-1}, have been reported before within the Amazon River plume[30].

In the Atlantic Ocean, OPE patterns at 5 m depth were dominated by ∑TCPP, TCEP and, TPhP, the first particularly prevalent at most stations. Previous studies for seawater, air and sediment compartments have highlighted the predominance of Cl-OPE within the total OPE pool[26,29,70,71], which is consistent with the large production of TCEP and TCPPs, and Cl-OPEs being less prone to degradation than alkyl and aryl-OPE by photolysis and/or hydrolysis[65,66,72]. In the Southern Ocean, the OPEs profile was dominated by ∑TCPP, EHDPP and TBEP, suggesting different sources and potentially distinct biogeochemistry in the water column.

Several studies have documented OPE concentrations in surface seawater (measured at 4 - 5 m depth), highlighting a large variability across marine regions. For example, Xie et al. (2024)[49] reported $\sum_{14}$OPE concentrations ranging from 7.65 to 270 ng L^{-1} in the Pearl River Estuary and South China Sea. In the North Atlantic, near the Amazon River plume, Schmidt et al. (2019)[30] observed $\sum_{9}$OPE concentrations between 74 and 1340 ng L^{-1}. Similarly, in Marseille Bay (NW Mediterranean Sea), $\sum_{9}$OPE concentrations ranged from 9 to 1013 ng L^{-1} [31]. Bollmann et al. (2012)[25] found $\sum_{16}$OPE concentrations in the North Sea ranging between 5 and 50 ng L^{-1}, while Na et al. (2020)[32] measured $\sum_{11}$OPE concentrations between 8.47 and 143.4 ng L^{-1} from the Northwestern Pacific to the Arctic Ocean. In the North Atlantic and Arctic, Li et al. (2017)[26] reported lower $\sum_{8}$OPE concentrations, ranging from 0.35 to 8.40 ng L^{-1}. The concentrations reported here are in the lower range of those reported in the South China Sea, lower than sites near to the Amazon River, and comparable to those in the Pacific. These studies emphasize potential influences from regional sources, and probably a

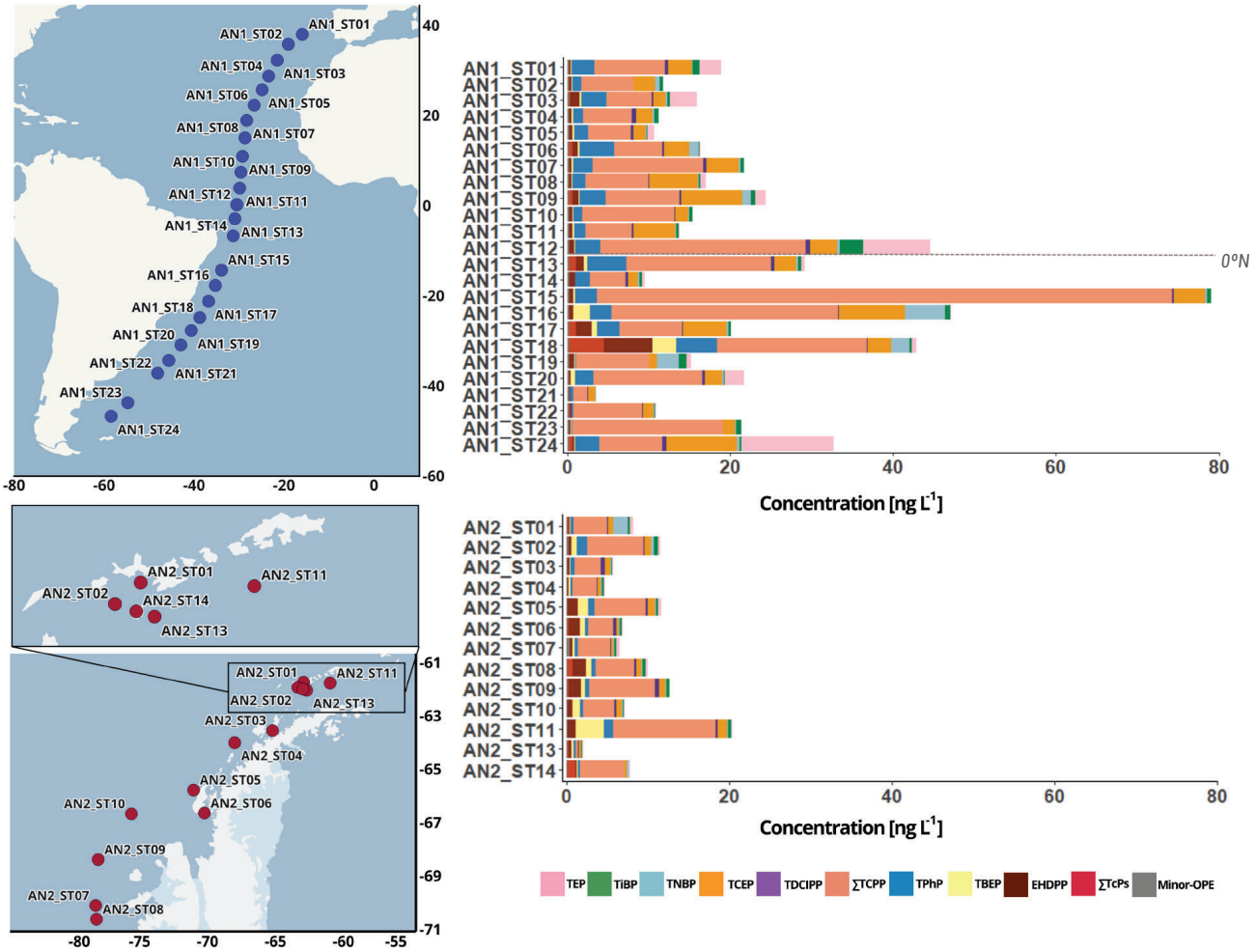


Figure 1 | Latitudinal variability of OPEs at 5 m depth. (A) Location of stations in the Atlantic Ocean; (B) 5 m depth concentrations of individual and $\sum_{24}$OPE (ng L^{-1}) in the Atlantic Ocean; (C) Location of stations in the Southern Ocean; and (D) 5 m depth concentrations of individual and $\sum_{24}$OPE (ng L^{-1}) in the Southern Ocean.

number of environmental variables affecting inputs and the biogeochemical cycling in the different oceanic regions. Surprisingly, OPE concentrations in the South Atlantic were not significantly different than those in the Southern Ocean, defying the expectation of lower concentrations in the latter due to its remote location.

Spearman correlation tests were conducted to assess the potential relationships between OPE concentrations at 5 m depth and environmental and biological variables **(Figure 2, and Table S11)**. Generally, individual OPEs were correlated among them, even though the relative abundance of individual OPEs were different in the Atlantic compared to the Southern Ocean. Bacterial abundance showed significant positive correlations with $\sum_{24}$OPE, TCEP, ∑TCPP, ∑TcPs (Cl-OPEs), and minor OPEs, whereas it was negatively correlated with TBEP. This could indicate that certain bacteria might be tolerant to OPEs toxicities, and although OPE background concentrations alone cannot explain the growth of some bacterial taxa, it suggests that OPEs can be used as cometabolite growth substrate for some bacterial taxa along with other organic compounds. Recently, the biodegradation potential at six oceanic sites from the same north-south transect have been reported[73], showing that short term (48 hours) microbial degradation of OPEs, especially for hydrophobic aryl-OPEs, occurs when bacterial production is higher. This trend is consistent with the observed negative correlations between bacterial production and TPhP.

Chlorophyll *a* exhibited a negative correlation with $\sum_{24}$OPE concentrations at 5 m depth, consistent with the biological pump removing OPEs from surface waters efficiently at sites with larger phytoplanktonic biomass. Specifically, Chlorophyll *a* was negatively correlated with the surface concentrations of TPhP, TNBP, ∑TCPP, and the group minor-OPEs.

Surface water and air temperatures were positively correlated to the concentrations of several OPEs, such as TPhP, ∑TCPP, TCEP, TNBP, and TiBP. To further explore these trends, a polynomial regression model was applied to log-transformed 5 m depth $\sum_{24}$OPE concentrations against latitude, revealing a quadratic distribution (R^2 = 0.39, p = 0.002) **(Figures 3 and S1, Table S11).**

OPE concentrations increased from the northern hemisphere subtropical regions to the equatorial region, peaking at 14°S, and then decreased at higher southern latitudes, with the lowest concentrations in the Southern Ocean. This latitudinal trend at surface was primarily due to the contribution of Cl-OPEs, confirmed with a significant quadratic correlation with latitude (R^2 = 0.42, p < 0.001) **(Table S12)**, but also observed for minor-OPES (R^2=0.58, p<0.001). Alkyl- and aryl-OPEs did not follow this trend at surface, but in some cases with correlations with latitude at other depths **(Table S12)**. This may be due to their lower persistence, and/or higher degradation and volatilization at high temperatures, as reported recently[73]. At low latitudes, the atmospheric and oceanic circulation close to the equator can bring OPEs from continents or proximate waters to this oceanic region. The decline of $\sum_{24}$OPE, particularly Cl-OPE (and aryl-OPEs at the DCM depth), concentrations towards the Southern Ocean suggests a combination of reduced inputs and a potential influence of the biological pump's removal of OPEs from surface waters **(Figure 3)**, consistent with the inverse correlation between OPEs concentration and chlorophyll a reported above. Such trend is more pronounced for Cl-OPEs than aryl-OPEs. Aryl-OPEs are generally more hydrophobic than Cl-OPEs, and are biodegraded to a higher extend in warmer Atlantic waters than in the Southern Ocean[73]. Still, at the DCM, aryl-OPEs decreased at the southernmost latitudes.

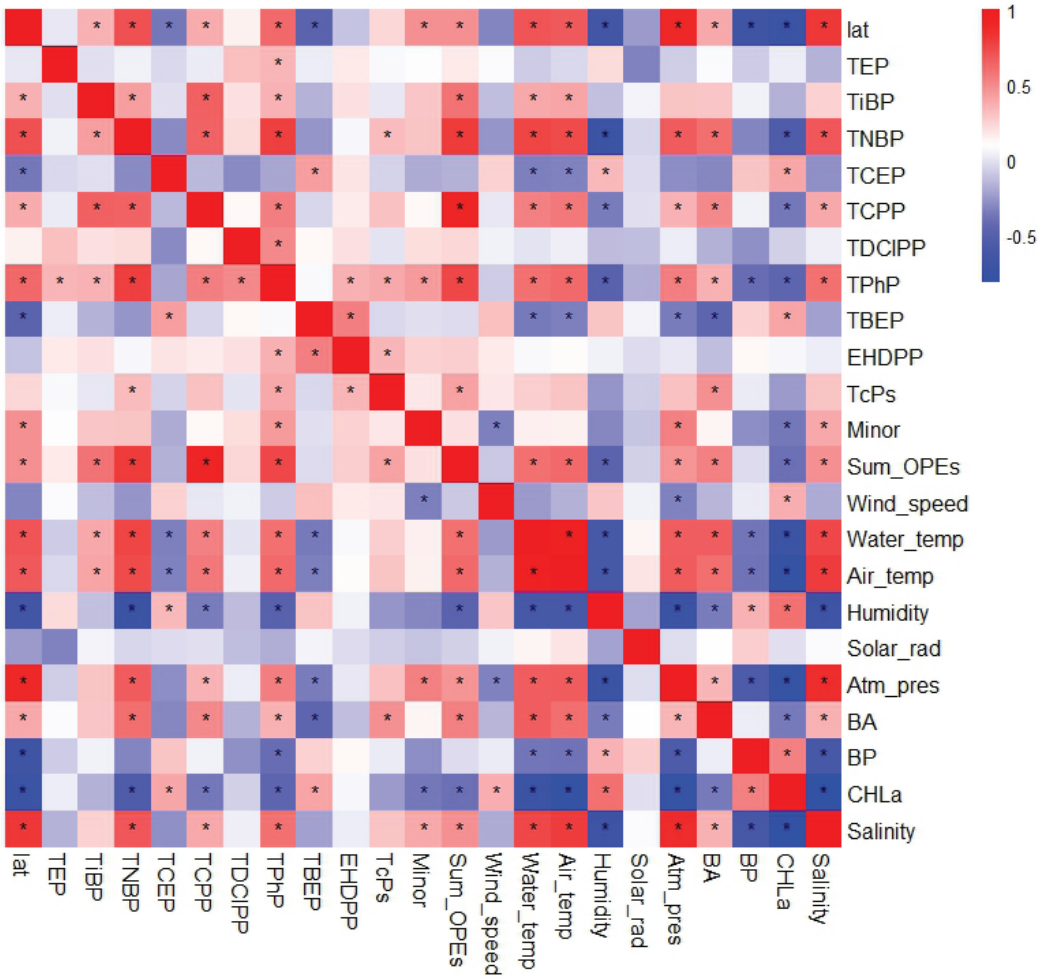


Figure 2 | Spearman correlation heatmap showing the correlations between individual OPEs, $\sum_{24}$OPE concentrations, and various biological (e.g., bacterial abundance, bacterial production, chlorophyll a) and environmental variables (e.g., water temperature, air temperature, and wind speed). Positive correlations are indicated in red and negative correlations are indicated in blue, with darker colors denoting stronger correlations. *The asterisks indicate statistically significant correlations (p<0.05).*

Thus, the interpretation of latitudinal trends is complex for polar and biodegradable contaminants, and do not follow a clear relationship with hydrophobicity as reported for legacy POPs[74].

The higher concentrations observed in equatorial and intertropical regions are consistent with these sites being receptors of the prevailing oceanic and atmospheric currents, which may bring OPEs from South America and Africa, for instance, from the Amazon River-influenced region. Furthermore, this region is one of the few oceanic regions that receives atmospheric inputs from rain events[75].

Wet deposition of OPEs

Wet deposition by rain is quantitatively important in some regions due to the high efficiency of raindrops scavenging air pollutants[75–77], leading to an amplification of concentrations in the receiving waters[69] .

The $\sum_{24}$OPE concentrations in the two rain samples collected in, or proximate to, the Intertropical Convergence Zone (ITCZ), were of 398.1 and 421.5 ng L^{-1} (averaging 409.86 ng L^{-1}), more than twenty fold higher than 5 m depth $\sum_{24}$OPE concentrations at the same stations (15.01 and 13.27 ng L^{-1}, respectively) **(Figure S2 and Table S13)**. ∑TCPP had a concentration of 270.4 ng L-1 and of 288.5 ng ng L^{-1}, accounting for 67.9% and 68.4% of $\sum_{24}$OPE, respectively for the two rain events. In both samples, EHDPP (12.9 and 14.0%, respectively), and TiBP (6.07% and 8.84%, respectively) showed high contributions to $\sum_{24}$OPE. The concentrations reported here for rain are one order of magnitude higher than the ones reported in Livingston Island (Antarctica)[69], but in the lower range than those reported in Germany and Italy, where TCPP concentrations in rainwater ranged from 46 to 2659 ng L^{-1} [78,79] and from 28 and 739 ng L^{-1} [80], respectively.

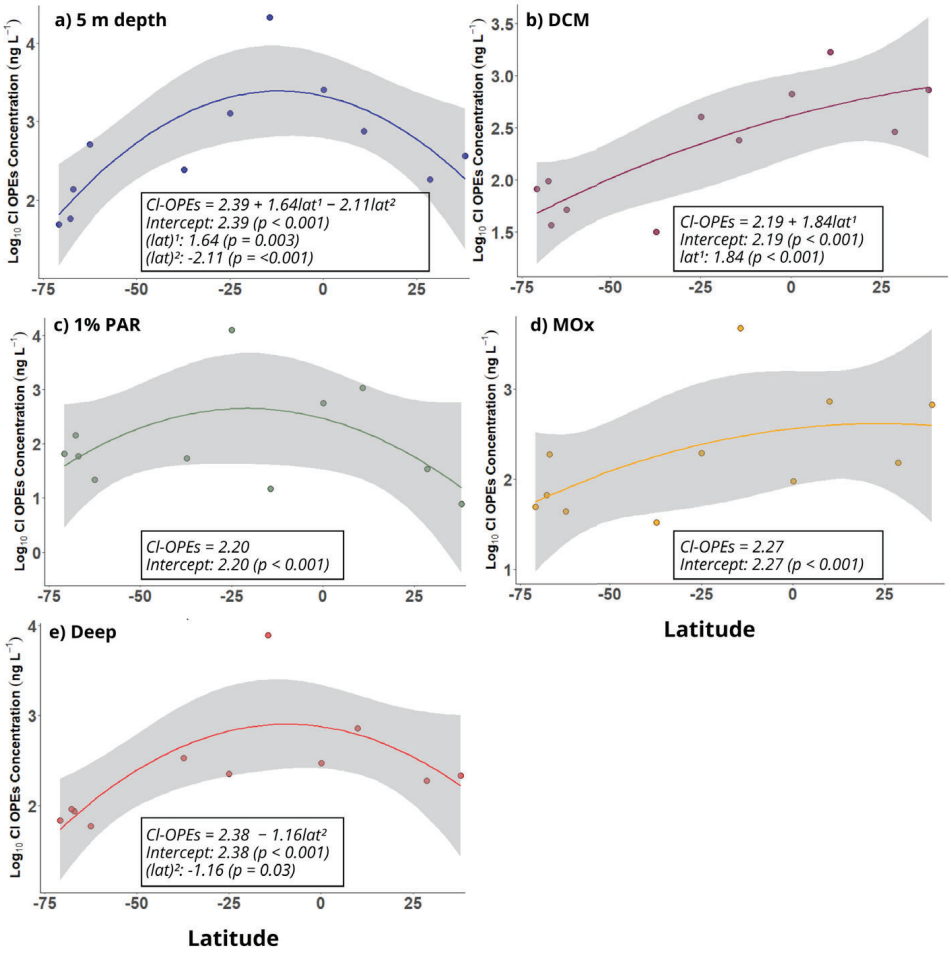


Figure 3 | Latitudinal distribution of log Cl-OPE concentrations (ng L^{-1}) at 5 m depth, at the deep chlorophyll maximum (DCM), at the depth with 1% of photosynthetically active radiation (1% PAR), and the minimum O2 depth (MOx), and at 2000 m depth (Deep). The significant variables (p<0.05) of the quadratic correlations with latitudes are shown **(Table S12)**.

The wet deposition fluxes (F_{WD}, ng m^{-2}) are given by:

$$F_{WD} = M_{rain}/A \quad [1]$$

where M_{rain} is the $\sum_{24}$OPE mass in rain (ng) and A (m^2) is the collecting area (stainless steel funnel of 0.2 m diameter). The F_{WD} of $\sum_{24}$OPE were of 12,679 ng m^{-2} and 13,426 ng m^{-2} for the two rain events, respectively. The obtained F_{WD} imply that every rain event can increase the total OPE amount in surface waters by few ng L^{-1}. These large fluxes confirm that wet deposition can be a relevant source in the region, and consistent with the high concentration of Cl-OPEs found close to the equator. Such fluxes are the result of the large washout ratios or rain-air partition constant, (K_{RP}), given by:

$$K_{RP} = C_{rain}/C_{aerosols} \quad [2]$$

Where C_{rain} and $C_{aerosols}$ are the concentrations in the rain (ng m^{-3}) and aerosol (ng m^{-3}) phase, respectively. We estimated K_{RP} using the C_{rain} measured here and $C_{aerosols}$ reported for the Atlantic Ocean in a previous work[81] **(Table S14)**. K_{RP} ranged from $3.67x10^3$ ± $1.59x10^3$ (TEHP) to $1.39x10^6$ ± $8.27x10^4$ (TPhP) for individual OPEs. Log K_{RP} ranged from 3.5 (TEHP) to 6.1 (TPhP) with an average of 4.9 **(Table S15)**. There were no significant correlations between K_{RP} and OPE's hydrophobicity. These K_{RP} are of similar magnitude than those reported before, which ranged from 4.1 to 7.3[69]. Nevertheless, the rain concentrations could have a contribution from gas-phase OPEs, not available in these estimates. Wet deposition has been identified as a dominant mechanism for the deposition of aerosol bound pollutants in the Atlantic Ocean[75], particularly in regions with high precipitation rates, such as the Intertropical Convergence Zone (ITCZ), where our samples were collected. Both the general circulation pattern of air masses, river inputs, and the importance of wet deposition could contribute to the high OPE concentrations at low latitudes.

OPEs in the top meters of the ocean

Generally, surface-named concentrations refer to seawater taken at 4-5 m depth, but not the real surface of the ocean, which cannot be sampled directly from an oceanographic ship. Recently, the concurrent OPE concentrations in the surface micro-layer (SML) and sub-surface layer (SSL) have been reported at 18 stations from the same transect[54]. This allows to compare the OPE concentrations at the sea skin (SML, top mm of the ocean), at 0.5 m depth (SSL) and at 5 m depth, providing insights on the dynamics of contaminants in the top meters of the ocean.

The surface microlayer is the interface between the atmosphere and the ocean, potentially concentrating OPEs due to their physicochemical properties, whereas the top meters of the ocean are continuously mixed by convection/turbulence driven by temperature and wind. In the field, the SML can be collected from an inflatable boat using a glass plate sampler[54]. The comparison of the OPE concentrations at SML, SSL and 5 m depth is done for 18 stations, nine stations at each ocean, where the three depths were sampled concurrently **(Figure S3).** In the Atlantic Ocean, the 5 m depth, SSL and SML average ± SD concentrations (ng L^{-1}) were 25.7 ± 22.4, 12.6 ± 7.54, and 24.7 ± 16.0, respectively. In the Southern Ocean, the 5 m depth, SSL, and SML average ± SD concentrations (ng L^{-1}) were 7.18 ± 3.42, 16.5 ± 9.17 and 193.0 ± 143.0, respectively. For the Atlantic Ocean, there were no significant $\sum_{24}$OPE concentration differences among the layers (Kruskal-Wallis, p = 0.09). Pairwise Wilcoxon tests revealed no significant differences between 5 m and SML (p = 0.93) or between 5 m and SSL (p = 0.08). However, the difference between SML and SSL was significant (p = 0.05), consistent with the enrichment factors generally higher than unity between the SML and SS[54].

In contrast, the Southern Ocean's concentrations showed significant differences between the 5 m depth and SML (p = 0.0001), the 5 m depth and SSL (p = 0.01), and the SML and SSL (p = 0.003). These results show an important gradient of OPEs in the top 5 m of the water column, which may be facilitated by gradients of salinity (from ice and snow melting), temperature, or higher biological activity leading to exudates of surfactant-like substances, in the Southern Ocean than in the Atlantic Ocean. Conversely, in tropical and subtropical waters, the top 5 m show moderately constant concentrations of OPEs, maybe related to temperature facilitating either degradation or volatilization of OPEs close to the surface interface, to a larger extend than at 5 meters.

OPE in the phytoplankton maximum (DCM depth)

DCM depths ranged from 34 to 145 m in the Atlantic, and from 19 to 57 m in the Southern Ocean. In the North Atlantic, $\sum_{24}$OPE mean concentrations at the DCM were 19.3 ng L^{-1}, not significantly different than at 5 m depth (mean 18.6 ng L^{-1} for the same stations), and neither for any individual OPE. However, in the South Atlantic, 5 m depth concentrations, averaging 27.6 ng L^{-1}, were significantly higher ($p < 0.05$) than in the DCM, with an average of 14.5 ng L^{-1} for $\sum_{24}$OPE, and also significantly different for TNBP, TCEP, TDCIPP, and EHDPP.

A significant positive correlation between latitude and log $\sum_{24}$OPE concentrations at the DCM (p = 0.002, R^2 = 0.34) was observed, with the highest concentrations in the northern hemisphere decreasing steadily towards

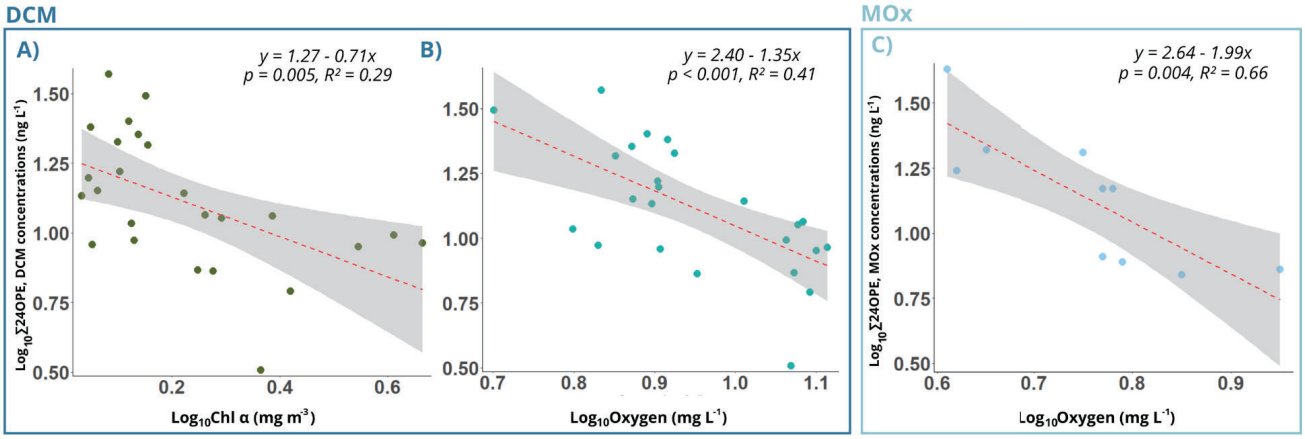


Figure 4 | Linear regressions between Σ_{24}OPE concentrations (ng L^{-1}) and Chl a (mg m^{-3}) (panel A), and oxygen levels (mg L^{-1}) at the DCM (panel B). Panel C shows the linear regression between Σ_{24}OPE concentrations (ng L^{-1}) and oxygen levels (mg L^{-1}) at the MOx layer (panel C). Red dashed lines represent the linear regression, and the shaded areas indicate the 95% confidence intervals. Linear regression equations and p-values are shown for each plot.

southern latitudes, with minimum concentrations in the Southern Ocean. This pattern was also significant for Cl-OPEs (R^2=0.36, p = 0.001) **(Figure 3)**, aryl-OPEs (R^2 = 0.41, p = 0.001) and minor-OPEs (R^2 = 0.36, p = 0.001). Such latitudinal trend could be related to the fact that the sampling was performed in different seasons, winter for the northern hemisphere samples (December 2020), and summer for the southern hemisphere samples (January 2020 and January-February 2022). This implies samples from different stages of the seasonal physical and biological succession. There were significant negative correlations between Chl a (mg m^{-3}) and $\sum_{24}$OPE concentrations (r = -0.54, p = 0.005) and between water oxygen (mg L^{-1}) and $\sum_{24}$OPE concentrations (r = -0.64, p = 0.0005) **(Figure 4)**. This trend is consistent with the negative correlation of OPEs and Chl *a* at 5 m depth reported above **(Figure 2)**. In the northern hemisphere, winter season during sampling, a lower phytoplankton biomass and a weakened biological pump likely reduced OPE removal, resulting in higher OPE concentrations at the DCM. In contrast, the lower OPE concentrations observed at lower latitudes (Southern and South Atlantic oceans) are consistent with an enhanced biological pump when biomass was higher (evidenced by higher Chl *a*). Similar trends have been observed for other pollutants, such as PFAS[19], which also tend to decrease from the surface to the DCM. It is also possible that higher bacterial abundances lead to increased degradation, though this may occur more slowly in colder waters. While some individual OPEs have been shown to serve as a phosphorus source[67], phosphorus is generally not a limiting nutrient in the Southern Ocean. On the other hand, microbial degradation of OPEs due to carbon demand has been suggested to be minimal in the Southern Ocean[73].

OPEs in the mesopelagic and deep ocean

Few works have reported OPEs at water layers below the photic zone. In addition to 5 m and DCM depths, OPEs were measured at the depth with the 1% photosynthetically active radiation (1%PAR), the oxygen minimum layer (MOx), and at 2000 m depth at eleven stations **(Tables S16-S18)**. In both the Atlantic and Southern Ocean, Cl-OPEs consistently accounted for the largest contribution to $\sum_{24}$OPE at all depths, but this contribution was lower in the Southern Ocean **(Table S17 and S18)**. Overall, OPE concentrations did not exhibit consistent trends with depth, as some stations showed a surface enrichment with depth depletion profile (station AN1_ST12) consistent with sources at surface and vertical transport due to the biological pump. Others depth profiles displayed both surface enrichment and an increase in concentrations with depth (station AN1_ST15), while some profiles showed no discernible pattern **(Figure 5 and S5)**. Overall, the biogeochemistry of polar, potentially biodegradable chemicals such as OPEs follow complex profiles following less prominent trends with depth, than when evaluated latitudinally for a single depth **(Figure 3).**

Cl-OPEs, alkyl-OPEs and aryl-OPEs at the 1%PAR depth showed no significant correlations with latitude **(Figure 3 and table S12)**, even though some decrease in concentrations in the Southern Ocean and northern hemisphere concentrations was observed. This contrast with the latitudinal trends at 5 m and DCM depths discussed above. At 1% PAR, the lower boundary of the euphotic zone, phytoplankton photosynthesis can still occur, but at minimal rates. Thus, depletion of dissolved-phase OPEs by the biological pump is likely to be minimal, with the latitudinal profile at this depth more closely resembling that observed at 5 meters

(source-influenced) than at the DCM (influenced by the biological pump).

From the concentrations at surface, the DCM and 1%PAR, and the volumes of the oceanic basins[82], a reservoir of 119, 190 and 273 Ktons of $\sum_{24}$OPE were estimated for the North Atlantic, South Atlantic and Southern Ocean, respectively. This reservoir is comparable to a lower-end estimate of the global annual production of OPEs of 598 Ktons[83]. The reservoir in the deep ocean cannot estimated because it would require a larger sampling resolution.

The MOx depth has received increasing attention during the last decade as a relevant biogeochemical layer[84,85], even though it has not yet been explored in terms of biogeochemical cycling of contaminants. At the MOx layer, oxygen levels fall below 80 µmol kg^{-1}, which limits oxygen-sensitive species, thus altering biogeochemical processes[86]. In addition, micro-anaerobic environments in marine snow aggregates may be feasible. Such low levels of O_2 can originate from remineralization (respiration) of sinking organic matter (OM). Such depletion of OM would induce a re-dissolution of OPEs due to particle-water partitioning since when OM

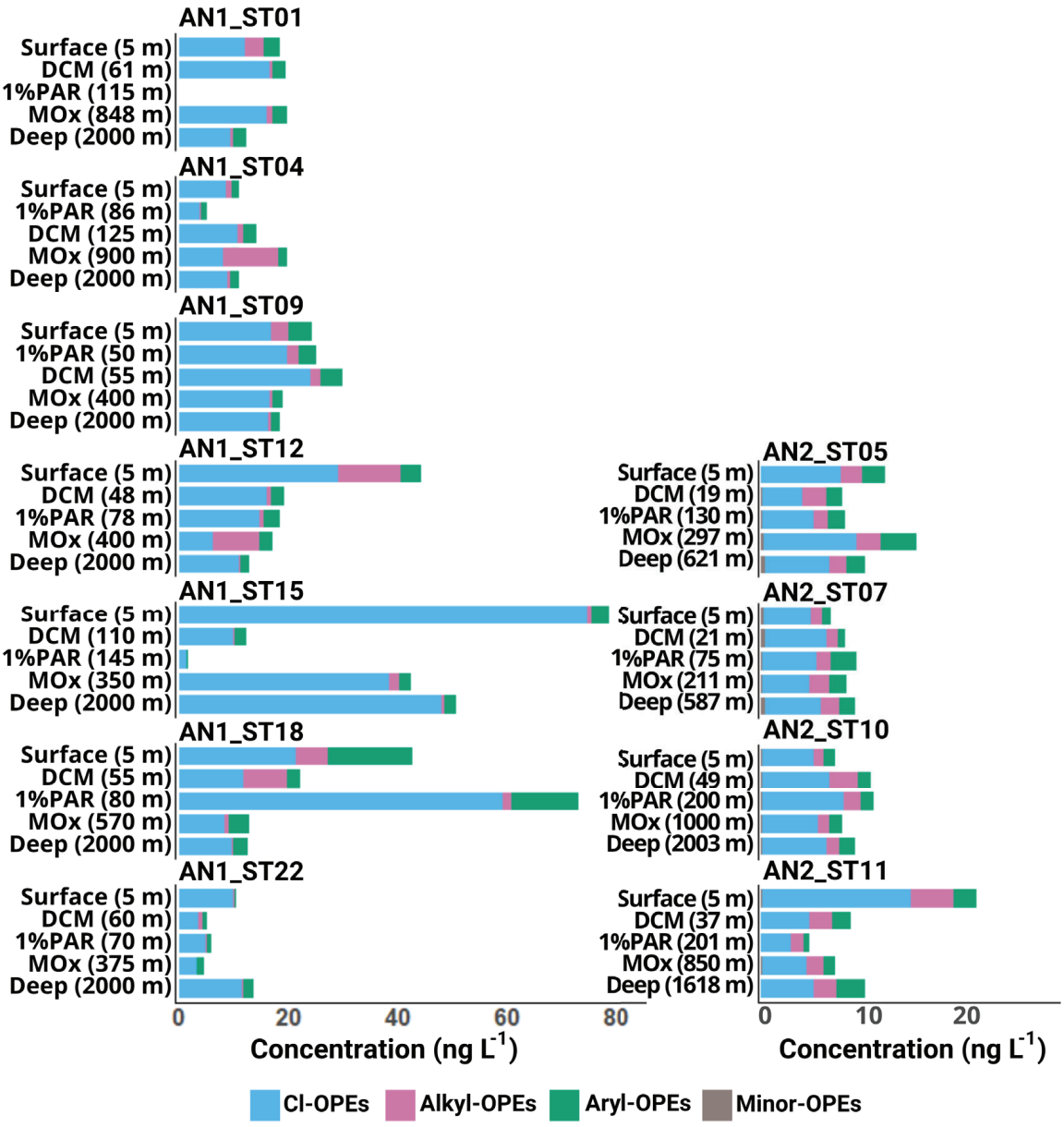


Figure 5 | Vertical profiles of concentrations (ng L^{-1}) of grouped OPEs categorized as alkyl-OPEs, aryl-OPEs, Cl-OPEs, and minor OPEs. The left panels show the vertical profiles sampled in the Atlantic Ocean, whereas the right panels show profiles sampled in the Southern Ocean. Please note that x-axis in left and right panels are not shown at the same scale.

decrease, there is a fugacity amplification of OPEs due to solvent depletion. A significant positive latitudinal trend for log-$\sum_{24}$OPE was observed (R^2 = 0.48, p = 0.03), indicating higher OPE concentrations in the northern hemisphere, and decreasing concentrations at the southernmost latitudes. A significant influence of latitude at MOX depth was also found for minor-OPES.

Additionally, a significant negative correlation between $\sum_{24}$OPE concentrations at MOx and oxygen levels (r = -0.81, p = 0.004) was found **(Figure 4),** suggesting higher OPE concentrations in oxygen-depleted regions. The latitudinal trend at the MOx layer is similar to that found at the DCM but different than at surface and 1%PAR. This is consistent with the OPE concentrations, reflecting the extend of the biological pump, with a fraction of the exported OPEs re-dissolved due to amplified fugacity and particle-water partitioning at the MOx layer. Nevertheless, further research is needed on the biogeochemistry of contaminants in O_2 depleted zones, which are increasing under the current scenario of global change[81].

The deep-water samples (2000 m depth) provide a long-term perspective of the accumulation of OPEs in the deep ocean. This layer integrates the signal over long time periods, as many biogeochemical processes are slow at this depth. Therefore, it reflects cumulative biogeochemical processes and OPEs received from over-lying waters over time, even though advection of deep water masses occurs, and this may lead to spatial changes in contaminant accumulation, variability, and differences between the geographic distribution at surface and at deep waters. A significant quadratic relationship (p = 0.03) was observed for Cl-OPE concentrations in deep-waters, analogous to that observed in surface waters, following an inverted U-shaped distribution across latitudes **(Figure 3)**. Additionally, a significant positive correlation was found between surface and deep concentrations for Cl-OPEs (r = 0.68, p = 0.03), aryl-OPEs (r = 0.63, p = 0.04) and minor-OPEs (r = 0.61, p = 0.04), suggesting that as surface concentrations reflect sources, deep waters integrate these sources over time, showing a similar latitudinal trend **(Figure S6)**. No significant correlations were observed for alkyl-OPEs, indicating different transport or degradation mechanisms. OPE concentrations at the MOx depth were also correlated with those at 2000 m depth (r = 0.76, p = 0.006), suggesting that deep waters not only reflect the OPE sources at surface, but also different vertical transport and biogeochemical mechanisms that impact OPE concentrations across multiple layers.

OPE distribution throughout the water column suggests that the surface layer, representing the primary and secondary sources of OPEs, plays a dominant role. The MOx layer, similar to DCM but influenced by surface processes, serves as a transitional zone. The biological pump plays a crucial role in transporting vertically OPEs attached to sinking organic matter, which when re-mineralized at deeper waters, can liberate OPEs back to the dissolved phase. This results in a mixed pattern in MOx and 1%PAR layers, but a clearer pattern in deep waters, which integrate sources and biogeochemistry, where OPE concentrations align with surface distributions. Over time, the biological pump removes OPEs from the surface and transports them to deeper layers, with microbial degradation probably influencing OPE distribution at intermediate depths, the elucidation of which will require future work. Research priorities should focus on the elucidation of the seasonal variability at different oceanic regions, as well a more detailed assessment of vertical distributions, and how particle-seawater varies with depth. The large latitudinal sampling effort performed here has proven useful at discerning patterns and the processes affecting OPEs in the Ocean, and shows that OPEs are mobile and persistent enough to reach the whole ocean.

ASSOCIATED CONTENT

Supporting Information

The Supporting Information is available free of charge. Additional text on methods **(note S1)**, additional figures showing concentrations and correlations **(Figures S1–S7),** and additional tables with ancillary data, quality assurance, target compounds information, individual OPEs concentrations, washout ratios, and correlations **(Tables S1–S18)** are provided.

ACKNOWLEDGMENTS

We thank the staff of the Marine Technology Unit (UTM-CSIC) and the crew of the research ships Sarmiento de Gamboa and Hespérides for their logistical support during the sampling campaigns. N.T.P. and JI acknowledge predoctoral fellowship (PRE2019-089641 and FPU19/02782) funded by the Spanish Ministry of Science, Innovation and Universities. This work was supported by the Spanish Research Agency through projects ANTOM (PGC2018-096612-B-I00), PANTOC (PID2021-127769NB-I00) and MIQAS (PID2021-128084OB-I00). The research group of Global Change and Genomic Biogeochemistry receives support from the Catalan Government (2021-SGR-00448).

REFERENCES

(1) Wang, Z.; Walker, G. W.; Muir, D. C. G.; Nagatani-Yoshida, K. Toward a Global Understanding of Chemical Pollution: A First Comprehensive Analysis of National and Regional Chemical Inventories. *Environ. Sci. Technol.* **2020**, 54 (5), 2575–2584. https://doi.org/10.1021/acs.est.9b06379.

(2) Lohmann, R.; Breivik, K.; Dachs, J.; Muir, D. Global Fate of POPs: Current and Future Research Directions. *Environ. Pollut.* **2007**, 150 (1), 150–165. https://doi.org/10.1016/j.envpol.2007.06.051.

(3) Zhang, X.; Li, L.; Xie, Z.; Ma, J.; Li, Y.-F.; Cai, M.; Ren, N.-Q.; Kallenborn, R.; Zhang, Z.-F.; Zhang, X.; Muir, D. C. G. Exploring Global Oceanic Persistence and Ecological Effects of Legacy Persistent Organic Pollutants across Five Decades. *Science Advances* **2024**; Vol. 10, eado5534. https://doi.org/ 10.1126/sciadv.ado5534

(4) Lohmann, R.; Markham, E.; Klanova, J.; Kukucka, P.; Pribylova, P.; Gong, X.; Pockalny, R.; Yanishevsky, T.; Wagner, C. C.; Sunderland, E. M. Trends of Diverse POPs in Air and Water across the Western Atlantic Ocean: Strong Gradients in the Ocean but Not in the Air. *Environ. Sci. Technol.* **2021**, 55 (14), 9498–9507. https://doi.org/10.1021/acs.est.0c04611.

(5) Berrojalbiz, N.; Dachs, J.; Del Vento, S.; Ojeda, M. J.; Valle, M. C.; Castro-Jiménez, J.; Mariani, G.; Wollgast, J.; Hanke, G. Persistent Organic Pollutants in Mediterranean Seawater and Processes Affecting Their Accumulation in Plankton. *Environ. Sci. Technol.* **2011**, 45 (10), 4315–4322. https://doi.org/10.1021/es103742w.

(6) Casal, P.; Casas, G.; Vila-Costa, M.; Cabrerizo, A.; Pizarro, M.; Jiménez, B.; Dachs, J. Snow Amplification of Persistent Organic Pollutants at Coastal Antarctica. *Environ. Sci. Technol.* **2019**, 53 (15), 8872–8882. https://doi.org/10.1021/acs.est.9b03006.

(7) Galbán-Malagón, C.; Gómez-Aburto, V. A.; Hirmas-Olivares, A.; Luarte, T.; Berrojalbiz, N.; Dachs, J. Dichlorodiphenyltrichloroethane (DDT) and Dichlorodiphenyldichloroethylene (DDE) Levels in Air and Surface Sea Waters along the Antarctic Peninsula. *Mar. Pollut. Bull.* **2023**, 197. https://doi.org/10.1016/j.marpolbul.2023.115699.

(8) Nizzetto, L.; Lohmann, R.; Gioia, R.; Jahnke, A.; Temme, C.; Dachs, J.; Herckes, P.; Di Guardo, A.; Jones, K. C. PAHs in Air and Seawater along a North-South Atlantic Transect: Trends, Processes and Possible Sources. *Environ. Sci. Technol.* **2008**, 42 (5), 1580–1585. https://doi.org/10.1021/es0717414.

(9) Lohmann, R.; Gioia, R.; Jones, K. C.; Nizzetto, L.; Temme, C.; Xie, Z.; Schulz-Bull, D.; Hand, I.; Morgan, E.; Jantunen, L. Organochlorine Pesticides and PAHs in the Surface Water and Atmosphere of the North Atlantic and Arctic Ocean. *Environ. Sci. Technol.* **2009**, 43 (15), 5633–5639. https://doi.org/10.1021/es901229k.

(10) González-Gaya, B.; Martínez-Varela, A.; Vila-Costa, M.; Casal, P.; Cerro-Gálvez, E.; Berrojalbiz, N.; Lundin, D.; Vidal, M.; Mompeán, C.; Bode, A.; Jiménez, B.; Dachs, J. Biodegradation as an Important Sink of Aromatic Hydrocarbons in the Oceans. *Nat. Geosci.* **2019**, 12 (2), 119–125. https://doi.org/10.1038/s41561-018-0285-3.

(11) Trilla-Prieto, N.; Vila-Costa, M.; Casas, G.; Jiménez, B.; Dachs, J. Dissolved Black Carbon and Semivolatile Aromatic Hydrocarbons in the Ocean: Two Entangled Biogeochemical Cycles? *Environ. Sci. Technol. Lett.* **2021**. https://doi.org/10.1021/acs.estlett.1c00658.

(12) Law, K. L. Plastics in the Marine Environment. Annual Review of Marine Science. *Annual Reviews Inc.* **2017**, pp 205–229. https://doi.org/10.1146/annurev-marine-010816-060409.

(13) Ostle, C.; Thompson, R. C.; Broughton, D.; Gregory, L.; Wootton, M.; Johns, D. G. The Rise in Ocean Plastics Evidenced from a 60-Year Time Series. *Nat. Commun.* **2019**, 10 (1). https://doi.org/10.1038/s41467-019-09506-1.

(14) Amelia, T. S. M.; Khalik, W. M. A. W. M.; Ong, M. C.; Shao, Y. T.; Pan, H. J.; Bhubalan, K. Marine Microplastics as Vectors of Major Ocean Pollutants and Its Hazards to the Marine Ecosystem and Humans. Progress in Earth and Planetary Science. *Springer Science and Business Media Deutschland* **2021** . https://doi.org/10.1186/s40645-020-00405-4.

(15) Dees, J. P.; Ateia, M.; Sanchez, D. L. Microplastics and Their Degradation Products in Surface Waters: A Missing Piece of the Global Carbon Cycle Puzzle. *Environ. Sci. Technol. Water.* **2021**, 1 (2), 214–216. https://doi.org/10.1021/acsestwater.0c00205.

(16) Bengtson Nash, S.; Rintoul, S. R.; Kawaguchi, S.; Staniland, I.; Hoff, J. Van Den; Tierney, M.; Bossi, R. Perfluorinated Compounds in the Antarctic Region: Ocean Circulation Provides Prolonged Protection from Distant Sources. *Environ. Pollut.* **2010**, 158 (9), 2985–2991. https://doi.org/10.1016/j.envpol.2010.05.024.

(17) Benskin, J. P.; Muir, D. C. G.; Scott, B. F.; Spencer, C.; De Silva, A. O.; Kylin, H.; Martin, J. W.; Morris, A.; Lohmann, R.; Tomy, G.; Rosenberg, B.; Taniyasu, S.; Yamashita, N. Perfluoroalkyl Acids in the Atlantic and Canadian Arctic Oceans. *Environ. Sci. Technol.* **2012**, 46 (11), 5815–5823. https://doi.

org/10.1021/es300578x.

(18) González-Gaya, B.; Dachs, J.; Roscales, J. L.; Caballero, G.; Jiménez, B. Perfluoroalkylated Substances in the Global Tropical and Subtropical Surface Oceans. *Environ. Sci. Technol.* **2014**, 48 (22), 13076–13084. https://doi.org/10.1021/es503490z.

(19) González-Gaya, B.; Casal, P.; Jurado, E.; Dachs, J.; Jiménez, B. Vertical Transport and Sinks of Perfluoroalkyl Substances in the Global Open Ocean. Environ. *Sci. Process. Impacts* **2019**, 21 (11), 1957–1969. https://doi.org/10.1039/c9em00266a.

(20) Zhang, X.; Lohmann, R.; Sunderland, E. M. Poly- And Perfluoroalkyl Substances in Seawater and Plankton from the Northwestern Atlantic Margin. *Environ. Sci. Technol.* **2019**, 53 (21), 12348–12356. https://doi.org/10.1021/acs.est.9b03230.

(21) Joerss, H.; Xie, Z.; Wagner, C. C.; Von Appen, W. J.; Sunderland, E. M.; Ebinghaus, R. Transport of Legacy Perfluoroalkyl Substances and the Replacement Compound HFPO-DA through the Atlantic Gateway to the Arctic Ocean - Is the Arctic a Sink or a Source? *Environ. Sci. Technol.* **2020**, 54 (16), 9958–9967. https://doi.org/10.1021/acs.est.0c00228.

(22) Casas, G.; Martínez-Varela, A.; Roscales, J. L.; Vila-Costa, M.; Dachs, J.; Jiménez, B. Enrichment of Perfluoroalkyl Substances in the Sea-Surface Microlayer and Sea-Spray Aerosols in the Southern Ocean. *Environ. Pollut.* **2020**, 267, 1–30. https://doi.org/10.1016/j.envpol.2020.115512.

(23) Han, T.; Chen, J.; Lin, K.; He, X.; Li, S.; Xu, T.; Xin, M.; Wang, B.; Liu, C.; Wang, J. Spatial Distribution, Vertical Profiles and Transport of Legacy and Emerging per- and Polyfluoroalkyl Substances in the Indian Ocean. *J. Hazard. Mater.* **2022**, 437 (June), 129264. https://doi.org/10.1016/j.jhazmat.2022.129264.

(24) Yamazaki, E.; Taniyasu, S.; Wang, X.; Yamashita, N. Per- and Polyfluoroalkyl Substances in Surface Water, Gas and Particle in Open Ocean and Coastal Environment. *Chemosphere* **2021**, 272, 129869. https://doi.org/10.1016/j.chemosphere.2021.129869.

(25) Bollmann, U. E.; Möller, A.; Xie, Z.; Ebinghaus, R.; Einax, J. W. Occurrence and Fate of Organophosphorus Flame Retardants and Plasticizers in Coastal and Marine Surface Waters. *Water. Res.* **2012**, 46 (2), 531–538. https://doi.org/10.1016/j.watres.2011.11.028.

(26) Li, J.; Xie, Z.; Mi, W.; Lai, S.; Tian, C.; Emeis, K. C.; Ebinghaus, R. Organophosphate Esters in Air, Snow, and Seawater in the North Atlantic and the Arctic. *Environ. Sci. Technol.* **2017**, 51 (12), 6887–6896. https://doi.org/10.1021/acs.est.7b01289.

(27) Gao, X.; Huang, P.; Huang, Q.; Rao, K.; Lu, Z.; Xu, Y.; Gabrielsen, G. W.; Hallanger, I.; Ma, M.; Wang, Z. Organophosphorus Flame Retardants and Persistent, Bioaccumulative, and Toxic Contaminants in Arctic Seawaters: On-Board Passive Sampling Coupled with Target and Non-Target Analysis. *Environ. Pollut.* **2019**, 253, 1–10. https://doi.org/10.1016/j.envpol.2019.06.094.

(28) Gao, X.; Xu, Y.; Ma, M.; Huang, Q.; Gabrielsen, G. W.; Hallanger, I.; Rao, K.; Lu, Z.; Wang, Z. Distribution, Sources and Transport of Organophosphorus Flame Retardants in the Water and Sediment of Ny-Ålesund, Svalbard, the Arctic. *Environ. Pollut.* **2020**, 264. https://doi.org/10.1016/j.envpol.2020.114792.

(29) McDonough, C. A.; De Silva, A. O.; Sun, C.; Cabrerizo, A.; Adelman, D.; Soltwedel, T.; Bauerfeind, E.; Muir, D. C. G.; Lohmann, R. Dissolved Organophosphate Esters and Polybrominated Diphenyl Ethers in Remote Marine Environments: Arctic Surface Water Distributions and Net Transport through Fram Strait. *Environ. Sci. Technol.* **2018**, 52 (11), 6208–6216. https://doi.org/10.1021/acs.est.8b01127.

(30) Schmidt, N.; Fauvelle, V.; Ody, A.; Castro-Jiménez, J.; Jouanno, J.; Changeux, T.; Thibaut, T.; Sempéré, R. The Amazon River: A Major Source of Organic Plastic Additives to the Tropical North Atlantic? *Environ. Sci. Technol.* **2019**, 53 (13), 7513–7521. https://doi.org/10.1021/acs.est.9b01585.

(31) Schmidt, N.; Castro-Jiménez, J.; Oursel, B.; Sempéré, R. Phthalates and Organophosphate Esters in Surface Water, Sediments and Zooplankton of the NW Mediterranean Sea: Exploring Links with Microplastic Abundance and Accumulation in the Marine Food Web. *Environ. Pollut.* **2021**, 272. https://doi.org/10.1016/j.envpol.2020.115970.

(32) Na, G.; Hou, C.; Li, R.; Shi, Y.; Gao, H.; Jin, S.; Gao, Y.; Jiao, L.; Cai, Y. Occurrence, Distribution, Air-Seawater Exchange and Atmospheric Deposition of Organophosphate Esters (OPEs) from the Northwestern Pacific to the Arctic Ocean. *Mar. Pollut. Bull.* **2020**, 157, 111243. https://doi.org/10.1016/j.marpolbul.2020.111243.

(33) Xie, Z.; Wang, P.; Wang, X.; Castro-Jiménez, J.; Kallenborn, R.; Liao, C.; Mi, W.; Lohmann, R.; Vila-Costa, M.; Dachs, J. Organophosphate Ester Pollution in the Oceans. *Nature Reviews Earth and Environment* **2022**, 309–322. https://doi.org/10.1038/s43017-022-00277-w.

(34) Andresen, J. A.; Grundmann, A.; Bester, K. Organophosphorus Flame Retardants and Plasticisers in Surface Waters. *Sci. Total Environ.* **2004**, 332 (1–3), 155–166. https://doi.org/10.1016/j.scitotenv.2004.04.021.

(35) van der Veen, I.; de Boer, J. Phosphorus Flame Retardants: Properties, Production, Environmental Occurrence, Toxicity and Analysis. *Chemosphere* **2012**, 88 (10), 1119–1153. https://doi.org/10.1016/j.chemosphere.2012.03.067.

(36) Wei, G. L.; Li, D. Q.; Zhuo, M. N.; Liao, Y. S.; Xie, Z. Y.; Guo, T. L.; Li, J. J.; Zhang, S. Y.; Liang, Z. Q. Organophosphorus Flame Retardants and Plasticizers: Sources, Occurrence, Toxicity and Human Exposure. *Environ. Pollut.* **2015**, pp 29–46. https://doi.org/10.1016/j.envpol.2014.09.012.

(37) Zhang, Y.; Su, H.; Ya, M.; Li, J.; Ho, S. H.; Zhao, L.; Jian, K.; Letcher, R. J.; Su, G. Distribution of Flame Retardants in Smartphones and Identification of Current-Use Organic Chemicals Including Three Novel Aryl Organophosphate Esters. *Sci. Total Environ.* **2019**, 693, 133654. https://doi.org/10.1016/j.scitotenv.2019.133654.

(38) Tran, C. M.; Lee, H.; Lee, B.; Ra, J. S.; Kim, K. T. Effects of the Chorion on the Developmental Toxicity of Organophosphate Esters in Zebrafish Embryos. *J. Hazard. Mater.* **2021**, 401, 123389. https://doi.org/10.1016/j.jhazmat.2020.123389.

(39) Wang, Y.; Li, W.; Martínez-Moral, M. P.; Sun, H.; Kannan, K. Metabolites of Organophosphate Esters in Urine from the United States: Concentrations, Temporal Variability, and Exposure Assessment. *Environ. Int.* **2019**, 122, 213–221. https://doi.org/10.1016/j.envint.2018.11.007.

(40) Greaves, A. K.; Letcher, R. J. A Review of Organophosphate Esters in the Environment from Biological Effects to Distribution and Fate. *Bull. Environ. Contam. Toxicol.* **2017**, 98 (1), 2–7. https://doi.org/10.1007/s00128-016-1898-0.

(41) Bekele, T. G.; Zhao, H.; Wang, Q. Tissue Distribution and Bioaccumulation of Organophosphate Esters in Wild Marine Fish from Laizhou Bay, North China: Implications of Human Exposure via Fish Consumption. *J. Hazard. Mater.* **2021**, 401, 123410. https://doi.org/10.1016/j.jhazmat.2020.123410.

(42) Ding, Y.; Han, M.; Wu, Z.; Zhang, R.; Li, A.; Yu, K.; Wang, Y.; Huang, W.; Zheng, X.; Mai, B. Bioaccumulation and Trophic Transfer of Organophosphate Esters in Tropical Marine Food Web, South China Sea. *Environ. Int.* **2020**, 143. https://doi.org/10.1016/j.envint.2020.105919.

(43) Garcia-Garin, O.; Sala, B.; Aguilar, A.; Vighi, M.; Víkingsson, G. A.; Chosson, V.; Eljarrat, E.; Borrell, A. Organophosphate Contaminants in North Atlantic Fin Whales. *Sci. Total Environ.* **2020**, 721. https://doi.org/10.1016/j.scitotenv.2020.137768.

(44) Wang, X.; Zhong, W.; Xiao, B.; Liu, Q.; Yang, L.; Covaci, A.; Zhu, L. Bioavailability and Biomagnification of Organophosphate Esters in the Food Web of Taihu Lake, China: Impacts of Chemical Properties and Metabolism. *Environ. Int.* **2019**, 125, 25–32. https://doi.org/10.1016/j.envint.2019.01.018.

(45) Sühring, R.; Diamond, M. L.; Scheringer, M.; Wong, F.; Pućko, M.; Stern, G.; Burt, A.; Hung, H.; Fellin, P.; Li, H.; Jantunen, L. M. Organophosphate Esters in Canadian Arctic Air: Occurrence, Levels and Trends. *Environ. Sci. Technol.* **2016**, 50 (14), 7409–7415. https://doi.org/10.1021/acs.est.6b00365.

(46) Schmidt, N.; Castro-Jiménez, J.; Fauvelle, V.; Ourgaud, M.; Sempéré, R. Occurrence of Organic Plastic Additives in Surface Waters of the Rhône River (France). *Environ. Pollut.* **2020**, 257. https://doi.org/10.1016/j.envpol.2019.113637.

(47) Marklund, A.; Andersson, B.; Haglund, P. Organophosphorus Flame Retardants and Plasticizers in Swedish Sewage Treatment Plants. *Environ. Sci. Technol.* **2005**, 39 (19), 7423–7429. https://doi.org/10.1021/es051013l.

(48) Meyer, J.; Bester, K. Organophosphate Flame Retardants and Plasticisers in Wastewater Treatment Plants. *J. Environ. Monit.* **2004**, 6 (7), 599–605. https://doi.org/10.1039/b403206c.

(49) Xie, C.; Qiu, N.; Xie, J.; Guan, Y.; Xu, W.; Zhang, L.; Sun, Y. Organophosphate Esters in Seawater and Sediments from the Low-Latitude Tropical Sea. *Sci. Total Environ.* **2024**, 907, 167930. https://doi.org/10.1016/j.scitotenv.2023.167930.

(50) Kim, U. J.; Kannan, K. Occurrence and Distribution of Organophosphate Flame Retardants/Plasticizers in Surface Waters, Tap Water, and Rainwater: Implications for Human Exposure. *Environ. Sci. Technol.* **2018**, 52 (10), 5625–5633. https://doi.org/10.1021/acs.est.8b00727.

(51) Sühring, R.; Diamond, M. L.; Bernstein, S.; Adams, J. K.; Schuster, J. K.; Fernie, K.; Elliott, K.; Stern, G.; Jantunen, L. M. Organophosphate Esters in the Canadian Arctic Ocean. *Environ. Sci. Technol.* **2021**, 55 (1), 304–312. https://doi.org/10.1021/acs.est.0c04422.

(52) Li, R.; Gao, H.; Hou, C.; Fu, J.; Shi, T.; Wu, Z.; Jin, S.; Yao, Z.; Na, G.; Ma, X. Occurrence, Source, and Transfer Fluxes of Organophosphate Esters in the South Pacific and Fildes Peninsula, Antarctic. *Sci. Total Environ.* **2023**, 894, 164263. https://doi.org/10.1016/j.scitotenv.2023.164263.

(53) Shi, T.; Li, R.; Fu, J.; Hou, C.; Gao, H.; Cheng, G.; Zhang, H.; Jin, S.; Kong, L.; Na, G. Fate of Organophosphate Esters from the Northwestern Pacific to the Southern Ocean: Occurrence, Distribution, and Fugacity Model Simulation. *J. Environ. Sci.* (China) **2024**, 137, 347–357. https://doi.org/10.1016/j.jes.2023.03.001.

(54) Trilla-Prieto, N.; Iriarte, J.; Berrojalbiz, N.; Casas, G.; Sobrino, C.; Vila-Costa, M.; Jiménez, B.; Dachs, J. Enrichment of Organophosphate Esters in the Sea Surface Microlayer from the Atlantic and Southern Oceans. *Environ. Sci. Technol. Lett.* **2024**. https://doi.org/10.1021/acs.estlett.4c00636.

(55) Dachs, J. , B. J. M. , A. J. Spatial Distribution, Vertical Profiles and Budget of Organochlorine Compounds in Western Mediterranean Seawater. *Environ. Sci. Technol.* **1997**, 57, 313–324. https://doi.org/10.1021/es960233j

(56) Dachs, J.; Bayona, J. M.; Raoux, C.; Albaigés, J. Spatial, Vertical Distribution and Budget of Polycyclic Aromatic Hydrocarbons in the Western Mediterranean Seawater. *Environ. Sci. Technol.* **1997**, 31 (3), 682–688. https://doi.org/10.1021/es960233j.

(57) Sun, C.; Soltwedel, T.; Bauerfeind, E.; Adelman, D. A.; Lohmann, R. Depth Profiles of Persistent Organic Pollutants in the North and Tropical Atlantic Ocean. *Environ. Sci. Technol.* **2016**, 50 (12), 6172–6179. https://doi.org/10.1021/acs.est.5b05891.

(58) Savvidou, E. K.; Sha, B.; Salter, M. E.; Cousins, I. T.; Johansson, J. H. Horizontal and Vertical Distribution of Perfluoroalkyl Acids (PFAAs) in the Water Column of the Atlantic Ocean. *Environ. Sci. Technol. Lett.* **2023**, 10 (5), 418–424. https://doi.org/10.1021/acs.estlett.3c00119.

(59) Cullen, J. J. The Deep Chlorophyll Maximum: Comparing Vertical Profiles of Chlorophyll a. Canadian *J. Fish. Aqua. Sci.* **1982**, 39 (5), 791–803. https://doi.org/10.1139/f82-108.

(60) Dachs, J.; Lohmann, R.; Mejanelle, L.; Eisenreich, S. J.; Jones, K. C. Oceanic Biogeochemical Controls on Global Dynamics of Persistent Organic Pollutants. *Environ. Sci. Technol.* **2002**, 36 (20), 4229–4237. http:77doi.org/ 10.1021/es025724k

(61) Berrojalbiz, N.; Dachs, J.; Ojeda, M. J.; Valle, M. C.; Castro-Jiménez, J.; Wollgast, J.; Ghiani, M.; Hanke, G.; Zaldivar, J. M. Biogeochemical and Physical Controls on Concentrations of Polycyclic Aromatic Hydrocarbons in Water and Plankton of the Mediterranean and Black Seas. *Global Biogeochem. Cycles* **2011**, 25 (4). https://doi.org/10.1029/2010GB003775.

(62) Galbán-Malagón, C. J.; Berrojalbiz, N.; Gioia, R.; Dachs, J. The "Degradative" and "Biological" Pumps Controls on the Atmospheric Deposition and Sequestration of Hexachlorocyclohexanes and Hexachlorobenzene in the North Atlantic and Arctic Oceans. *Environ. Sci. Technol.* **2013**, 47 (13), 7195–7203. https://doi.org/10.1021/es4011256.

(63) Galbán-Malagón, C.; Berrojalbiz, N.; Ojeda, M. J.; Dachs, J. The Oceanic Biological Pump Modulates the Atmospheric Transport of Persistent Organic Pollutants to the Arctic. *Nat. Commun.* **2012**, 3. https://doi.org/10.1038/ncomms1858.

(64) Regnery, J.; Püttmann, W. Occurrence and Fate of Organophosphorus Flame Retardants and Plasticizers in Urban and Remote Surface Waters in Germany. *Water Res.* **2010**, 44 (14), 4097–4104. https://doi.org/10.1016/j.watres.2010.05.024.

(65) Su, G.; Letcher, R. J.; Yu, H. Organophosphate Flame Retardants and Plasticizers in Aqueous Solution: PH-Dependent Hydrolysis, Kinetics, and Pathways. *Environ. Sci. Technol.* **2016**, 50 (15), 8103–8111. https://doi.org/10.1021/acs.est.6b02187.

(66) Cristale, J.; Dantas, R. F.; De Luca, A.; Sans, C.; Esplugas, S.; Lacorte, S. Role of Oxygen and DOM in Sunlight Induced Photodegradation of Organophosphorous Flame Retardants in River Water. *J. Hazard Mater.* **2017**, 323, 242–249. https://doi.org/10.1016/j.jhazmat.2016.05.019.

(67) Vila-Costa, M.; Sebastián, M.; Pizarro, M.; Cerro-Gálvez, E.; Lundin, D.; Gasol, J. M.; Dachs, J. Microbial Consumption of Organophosphate Esters in Seawater under Phosphorus Limited Conditions. *Sci. Rep.* **2019**, 9 (1), 1–11. https://doi.org/10.1038/s41598-018-36635-2.

(68) Reemtsma, T.; García-López, M.; Rodríguez, I.; Quintana, J. B.; Rodil, R. Organophosphorus Flame Retardants and Plasticizers in Water and Air I. Occurrence and Fate. *TrAC Trends Anal. Chem.* **2008**, 27 (9), 727–737. https://doi.org/10.1016/j.trac.2008.07.002.

(69) Casas, G.; Martinez-Varela, A.; Vila-Costa, M.; Jiménez, B.; Dachs, J. Rain Amplification of Persistent Organic Pollutants. *Environ. Sci. Technol.* **2021**, 55 (19), 12961–12972. https://doi.org/10.1021/acs.est.1c03295.

(70) Sühring, R.; Wolschke, H.; Diamond, M. L.; Jantunen, L. M.; Scheringer, M. Distribution of Organophosphate Esters between the Gas and Particle Phase-Model Predictions vs Measured Data. *Environ. Sci. Technol.* **2016**, 50 (13), 6644–6651. https://doi.org/10.1021/acs.est.6b00199.

(71) Ma, Y.; Xie, Z.; Lohmann, R.; Mi, W.; Gao, G. Organophosphate Ester Flame Retardants and Plasticizers in Ocean Sediments from the North Pacific

to the Arctic Ocean. *Environ. Sci. Technol.* **2017**, 51 (7), 3809–3815. https://doi.org/10.1021/acs.est.7b00755.

(72) Li, C.; Wei, G.; Chen, J.; Zhao, Y.; Zhang, Y. N.; Su, L.; Qin, W. Aqueous OH Radical Reaction Rate Constants for Organophosphorus Flame Retardants and Plasticizers: Experimental and Modeling Studies. *Environ. Sci. Technol.* **2018**, 52 (5), 2790–2799. https://doi.org/10.1021/acs.est.7b05429.

(73) Iriarte, J.; Trilla-Prieto, N.; Berrojalbiz, N.; Vila-Costa, M.; Dachs, J. Bacterial Production Modulates the Persistence of Organophosphate Ester Flame Retardants and Plasticizers in the Ocean. *Environ. Sci. Technol. Lett.* **2025**. https://doi.org/10.1021/acs.estlett.4c01128.

(74) Galbán-Malagón, C. J.; Del Vento, S.; Cabrerizo, A.; Dachs, J. Factors Affecting the Atmospheric Occurrence and Deposition of Polychlorinated Biphenyls in the Southern Ocean. *Atmos. Chem. Phys.* **2013**, 13 (23), 12029–12041. https://doi.org/10.5194/acp-13-12029-2013.

(75) Jurado, E.; Jaward, F.; Lohmann, R.; Jones, K. C.; Simó, R.; Dachs, J. Wet Deposition of Persistent Organic Pollutants to the Global Oceans. *Environ. Sci. Technol.* **2005**, 39 (8), 2426–2435. https://doi.org/10.1021/es048599g.

(76) Lei, Y. D.; Wania, F. Is Rain or Snow a More Efficient Scavenger of Organic Chemicals? *Atmos. Environ.* **2004**, 38 (22), 3557–3571. https://doi.org/10.1016/j.atmosenv.2004.03.039.

(77) Marlina, N.; Hassan, F.; Chao, H. R.; Latif, M. T.; Yeh, C. F.; Horie, Y.; Shiu, R. F.; Hsieh, Y. K.; Jiang, J. J. Organophosphate Esters in Water and Air: A Minireview of Their Sources, Occurrence, and Air–Water Exchange. *Chemosphere* **2024**, 356 (April), 141874. https://doi.org/10.1016/j.chemosphere.2024.141874.

(78) Mihajlović, I.; Fries, E. Atmospheric Deposition of Chlorinated Organophosphate Flame Retardants (OFR) onto Soils. *Atmos. Environ.* **2012**, 56, 177–183. https://doi.org/10.1016/j.atmosenv.2012.03.054.

(79) Regnery, J.; Püttmann, W. Organophosphorus Flame Retardants and Plasticizers in Rain and Snow from Middle Germany. *Clean (Weinh)* **2009**, 37 (4–5), 334–342. https://doi.org/10.1002/clen.200900050.

(80) Bacaloni, A.; Cucci, F.; Guarino, C.; Nazzari, M.; Samperi, R.; Laganà, A. Occurrence of Organophosphorus Flame Retardant and Plasticizers in Three Volcanic Lakes of Central Italy. *Environ. Sci. Technol.* **2008**, 42 (6), 1898–1903. https://doi.org/10.1021/es702549g.

(81) Castro-Jiménez, J.; González-Gaya, B.; Pizarro, M.; Casal, P.; Pizarro-Álvarez, C.; Dachs, J. Organophosphate Ester Flame Retardants and Plasticizers in the Global Oceanic Atmosphere. *Environ. Sci. Technol.* **2016**, 50 (23), 12831–12839. https://doi.org/10.1021/acs.est.6b04344.

(82) Costello, M. J.; Cheung, A.; De Hauwere, N. Surface Area and the Seabed Area, Volume, Depth, Slope, and Topographic Variation for the World's Seas, Oceans, and Countries. *Environ. Sci. Technol.* **2010**, 44 (23), 8821–8828. https://doi.org/10.1021/es1012752.

(83) Huang, J.; Ye, L.; Fang, M.; Su, G. Industrial Production of Organophosphate Flame Retardants (OPFRs): Big Knowledge Gaps Need to Be Filled? *Bull. Environ. Cont. Toxic.* **2022**, pp 809–818. https://doi.org/10.1007/s00128-021-03454-7.

(84) Löscher, C. R.; Bange, H. W.; Schmitz, R. A.; Callbeck, C. M.; Engel, A.; Hauss, H.; Kanzow, T.; Kiko, R.; Lavik, G.; Loginova, A.; Melzner, F.; Meyer, J.; Neulinger, S. C.; Pahlow, M.; Riebesell, U.; Schunck, H.; Thomsen, S.; Wagner, H. Water Column Biogeochemistry of Oxygen Minimum Zones in the Eastern Tropical North Atlantic and Eastern Tropical South Pacific Oceans. *Biogeosciences* **2016**, 13 (12), 3585–3606. https://doi.org/10.5194/bg-13-3585-2016.

(85) Stramma, L.; Johnson, G. C.; Sprintall, J.; Mohrholz, V. Expanding Oxygen-Minimum Zones in the Tropical Oceans. ***Science*** **2008**, 320 (5876), 652–655. https://doi.org/10.1126/science.1151751.

(86) Sarmiento, J. L. Ocean Biogeochemical Dynamics; *Princeton University Press*, **2006**. https://doi.org/10.1515/9781400849079.

PART 03 - CHAPTER 3. TRANSPORT AND BIOGEOCHEMISTRY OF OPES IN THE OCEANS

3.3.4. Paper IV. Supplementary Information

Notes S1 - S2

Figures S1 - S7

Tables S1 - S18.

Supplementary Material

Biogeochemical Controls on Latitudinal (42°N to 70°S) and Depth Distribution of Organophosphate Esters in the Atlantic and Southern Oceans

Núria Trilla-Prieto[1,2], Naiara Berrojalbiz[1], Jon Iriarte[1], Antonio Fuentes-Lema[3], Cristina Sobrino[4], Maria Vila-Costa[1], Begoña Jiménez[5], and Jordi Dachs[1]*

[1]Department of Environmental Chemistry, IDAEA-CSIC, 08034, Barcelona, Catalunya, Spain.
[2]Departament of Ecology, Faculty of Earth Sciences, Universitat de Barcelona, 08034, Barcelona, Catalunya, Spain.
[3]Centro de Investigación Mariña (CIM), Universidade de Vigo, 36310, Vigo, Spain
[4]Grupo de Oceanografía Biolóxica, Centro de Investigación Mariña (CIM), Universidade de Vigo, 36310, Vigo, Spain.
[5]Department of Instrumental Analysis and Environmental Chemistry, IQOG-CSIC, 28006, Madrid, Spain.

*Corresponding Author: jordi.dachs@idaea.csic.es.

Summary

Notes

Note S1. Analytical methodologies for Chlorophyll *a*, bacterial production (BP) and bacterial abundance (BA) measuring from seawater samples.

Figures

Figure S1. Log-transformed concentrations of grouped OPEs vs latitude, colored by depth (m). Panel top left plots Cl-OPES, top right Alkyl-OPEs, bottom left Aryl-OPEs and bottom right Minor-OPEs. The color gradient represents the sampling depth, with shallower depths depicted in yellow and deeper depths in purple. The shaded area around the regression line represents the 95% confidence interval.
Figure S2. Rainfall and 5 m depth seawater (Surface) individual and $\sum_{24}$OPE concentrations (ng L^{-1}) from Atlantic Ocean stations AN1_ST10 and AN1_ST11.
Figure S3. Surface microlayer (SML), subsurface layer (SSL), and 5m depth OPE concentrations (ng L^{-1}) of individual and $\sum_{24}$OPE at nine stations sampled in the Atlantic Ocean (top panel) and the Southern Ocean (bottom panel).
Figure S4. Scatter plots comparing the individual and $\sum_{24}$OPE log-transformed concentrations between the 5 m depth (Surface) and DCM layers across three ocean regions.
Figure S5. Vertical profiles of concentrations (in ng L^{-1}) of $\sum_{24}$OPEs plotted over the bathymetry of the sampling site where each vertical profile was sampled.
Figure S6. Log-transformed surface (5 m depth) and deep (2000 m) OPE concentrations for different OPE groups (Cl-OPEs, Alkyl-OPEs, Aryl-OPEs, and Minor OPEs). Spearman correlation coefficients (r) and p-values are displayed for each group.
Figure S7. Major ocean gyres (top) and global winds circulation (bottom).

Tables

Table S1. Stations information from the Atlantic Ocean (top table) and Southern Ocean (bottom table) where samples for OPE analysis were collected.
Table S2. Information of labelled OPE compounds used as surrogate (top table) and as Internal Standard (bottom table).
Table S3. Names, acronym molecular weight (MW) and Log KOW of the targeted compounds.
Table S4. Individual OPE contribution (%) to the total pool for each for the Atlantic and Southern Ocean samples.
Table S5. Field and procedural blanks OPE abundance (ng).
Table S6. Limits of quantification (LOQs) in ng.
Table S7. Surrogate and matrix spike recoveries (%) from the Atlantic Ocean samples (top table) and Southern Ocean samples (bottom table).
Table S8. Individual and $\sum_{24}$OPE concentration in surface and DCM samples from the Atlantic Ocean (ng L^{-1}).
Table S9. Mean and SD of surface and DCM concentrations (ng L^{-1}) in the three ocean basins sampled.
Table S10. Individual and $\sum_{24}$OPE concentration in surface and DCM samples from the Southern Ocean (ng L^{-1}).
Table S11. Environmental variables measured at surface waters and atmospheric conditions in the Atlantic and Southern Oceans.
Table S12. Summary of the polynomial regression models applied to log-transformed grouped OPEs concentrations across different depths (5 m, DCM, 1% PAR, MOx, and Deep) with latitude.
Table S13. Wet Deposition and related surface sample concentrations (in ng L-1) of individual and ∑24OPE in the Atlantic Ocean and calculation of EFWD (C_{WD}/C_{SURF}) for those samples.
Table S14. Atmospheric aerosol concentrations of $\sum_{14}$OPEs (ng m^{-3}) from Malaspina (Castro-Jiménez et al., 2016) from latitudes ranging between 7°N and 0°N (top table) and rain water $\sum_{14}$OPEs (ng m^{-3}) concentrations from AN1_ST10 and AN1_ST11 2021 Atlantic campaign.
Table S15. Log K_{RP} values from the Atlantic Ocean.
Table S16. Mean ± SD of group OPE concentrations (ng L^{-1}) separated by ocean and depth.
Table S17. Individual and $\sum_{24}$OPE concentration in vertical profiles from the Atlantic Ocean (ng L^{-1}).
Table S18. Individual and $\sum_{24}$OPE concentration in vertical profiles from the Southern Ocean (ng L^{-1}).

Note S1. Analytical methodologies for chlorophyll a, bacterial production and bacterial abundance measuring from seawater samples.

Chlorophyll *a* (Chl *a*) concentrations were measured in all samples. For each sample, 250 mL was gently filtered under dim light in triplicate through a size fraction cascade system with 20, 2 and 0.22 µm size pore 47-mm Filter-Lab polycarbonate filters and immediately stored at -20 °C until further analysis. Chl *a* extraction was carried out with 90% acetone, and the concentration in each sample (µg L^{-1}) was estimated following the acidification method described by Estrada (2012) using a Turner A10 fluorometer previously calibrated with a pure Chl *a* standard (SIGMA C5753-1 mg). Here, we provided the sum of the three fractions as a proxy for biomass and biological activity.

Bacterial Production (BP) (as Leucine Incorporation Rates (LIR)) was estimated as the incorporation of 3H-leucine into protein, as reported previously.2 Briefly, 1.2 mL quadruplicate live and duplicate killed (5% trichloroacetic acid (TCA)) subsamples were incubated with 3H-leucine (40 nM) for 4-5 hours at in situ temperature in the dark. Incubation was stopped by the addition of 120 µL of cold TCA 50% and then frozen (−20 °C) until further processing by centrifugation and TCA rinsing.

Prokaryotic cell abundance (Bacterial Abundance, BA) was determined using flow cytometry. Subsamples of 1.8 mL for quantification of prokaryote abundance were fixed with 1% buffered paraformaldehyde solution (pH 7.0) plus 0.05% glutaraldehyde, left at room temperature in the dark for 10 min, flash-frozen in N_2 (l), and stored at −80 °C. Prokaryotic cell abundance was estimated using flow cytometry, as described elsewhere 3. Briefly, the samples were run using a BD Accuri C6 Plus flow cytometer. The resulting cytograms were analyzed using FlowJo software to quantify the high-nucleic acid-containing (HNA) and the low-nucleic acid-containing (LNA) prokaryotes.

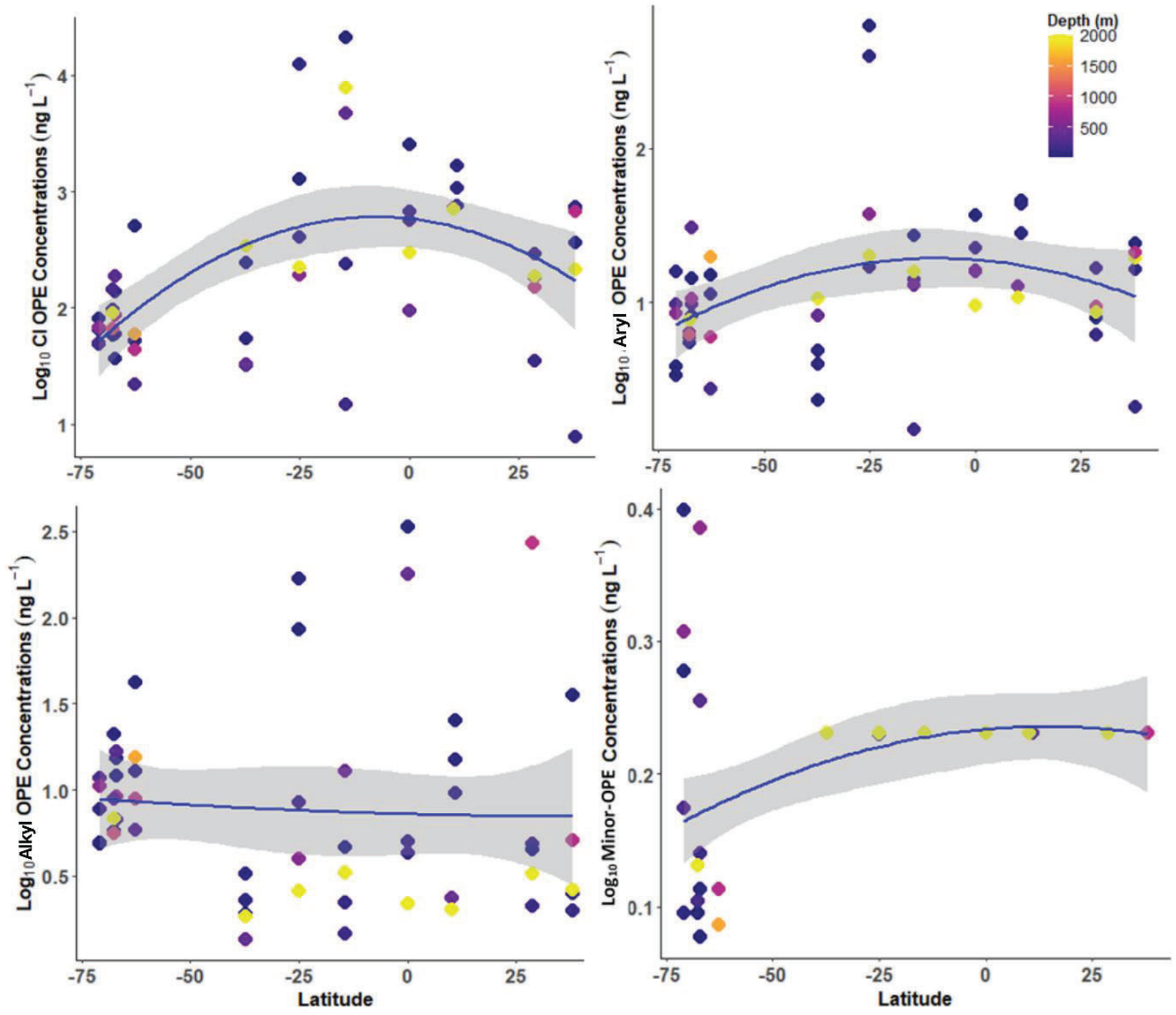


Figure S1. Log-transformed concentrations of grouped OPEs vs latitude, colored by depth (m). Panel top left plots Cl-OPES, top right Alkyl-OPEs, bottom left Aryl-OPEs and bottom right Minor-OPEs. The color gradient represents the sampling depth, with shallower depths depicted in purple and deeper depths in yellow. The shaded area around the regression line represents the 95% confidence interval.

Statistical results for polynomial regression model considering all samples (all depth. See Table S12 for correlations at each depth):

- **Cl-OPEs** show a significant, non-linear relationship with latitude ($p < 0.001$, $R^2 = 0.34$).
- **Aryl-OPEs** show a non-linear influence of latitude ($p < 0.001$, $R^2 = 0.16$).
- **Alkyl-OPEs** show no significant effects from latitude**.**
- **Minor-OPEs** show a significant positive linear relationship with latitude ($p < 0.001$, $R^2 = 0.58$).

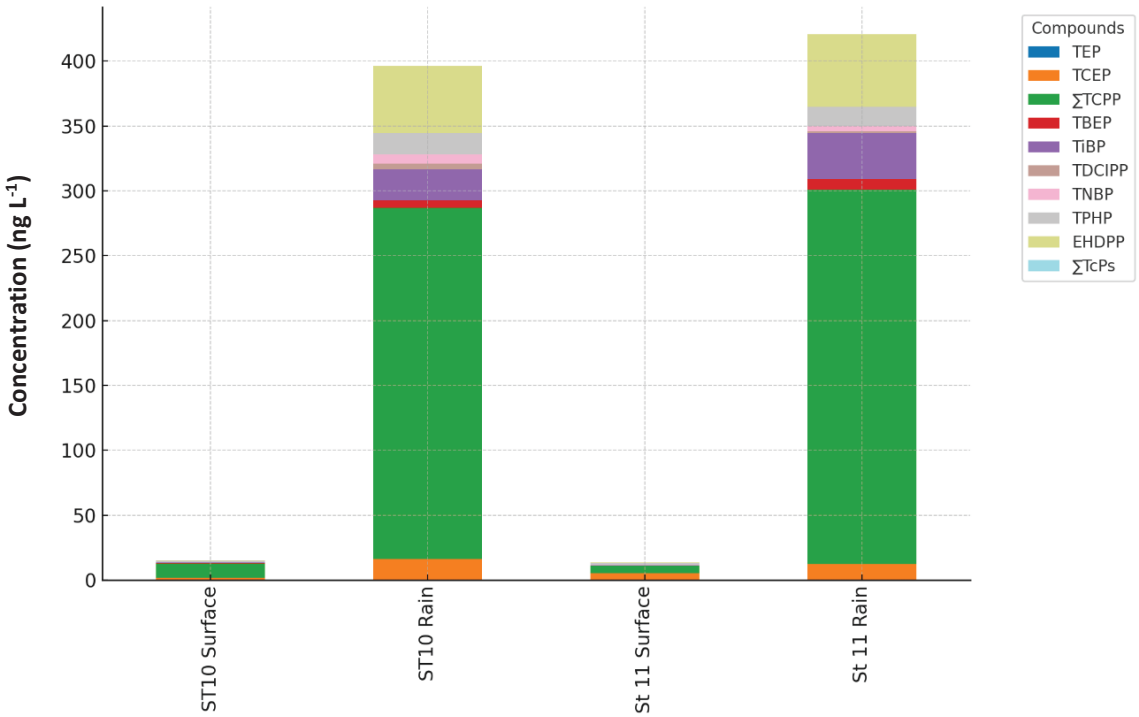


Figure S2. Rainfall and 5 m depth seawater (Surface) individual and $\sum_{24}$OPE concentrations (ng L^{-1}) from Atlantic Ocean stations AN1_ST10 and AN1_ST11.

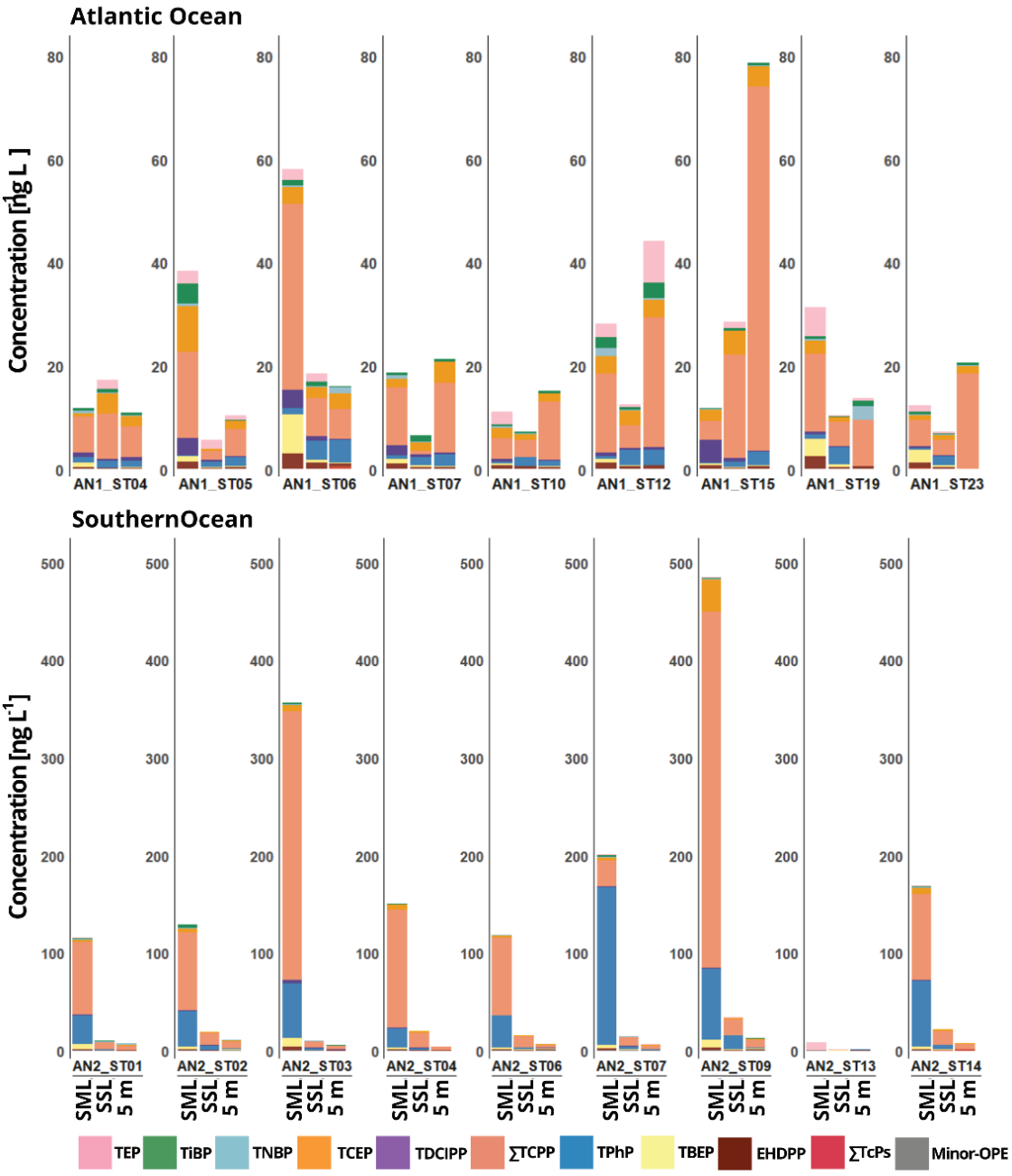


Figure S3 Surface microlayer (SML), subsurface layer (SSL), and 5m depth OPE concentrations (ng L^{-1}) of individual and $\sum_{24}$OPE at nine stations sampled in the Atlantic Ocean (top panel) and the Southern Ocean (bottom panel).

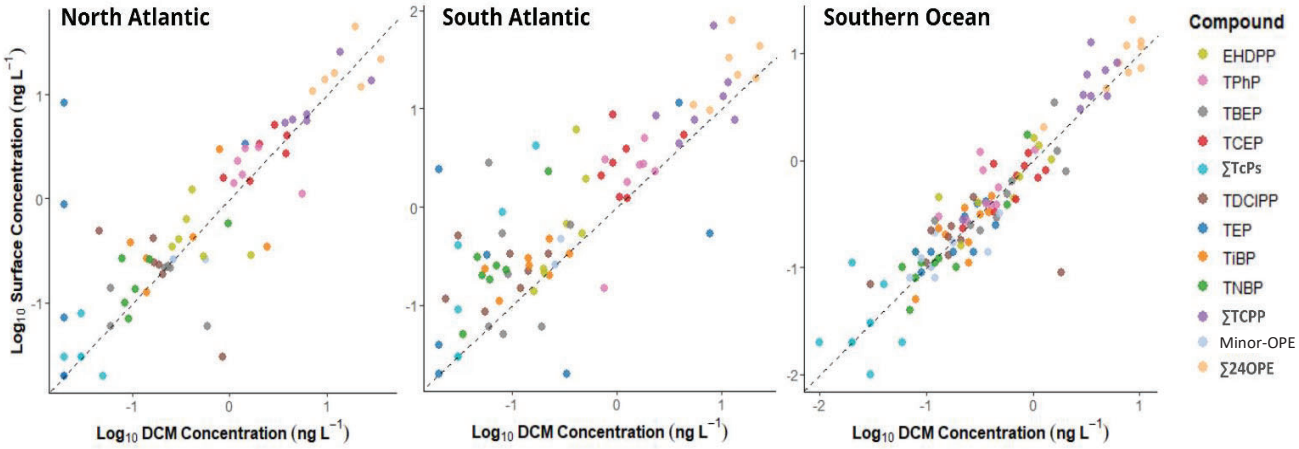


Figure S4. OPEs in surface versus DCM. Scatter plots comparing the individual and $\sum_{24}$OPE log-transformed concentrations between the 5 m depth (Surface) and DCM layers across three ocean regions: North Atlantic, South Atlantic, and Southern Ocean. The dashed line represents a 1:1 relationship between surface and DCM concentrations.

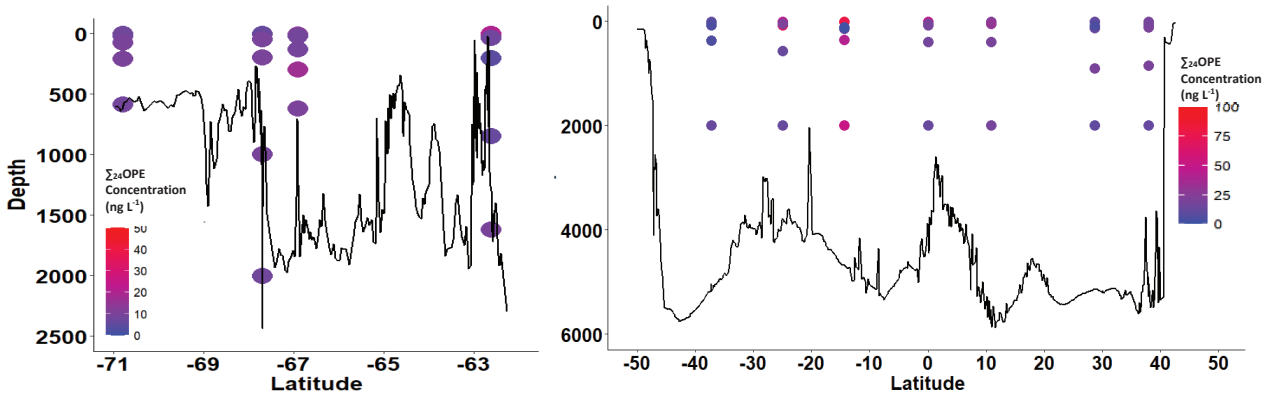
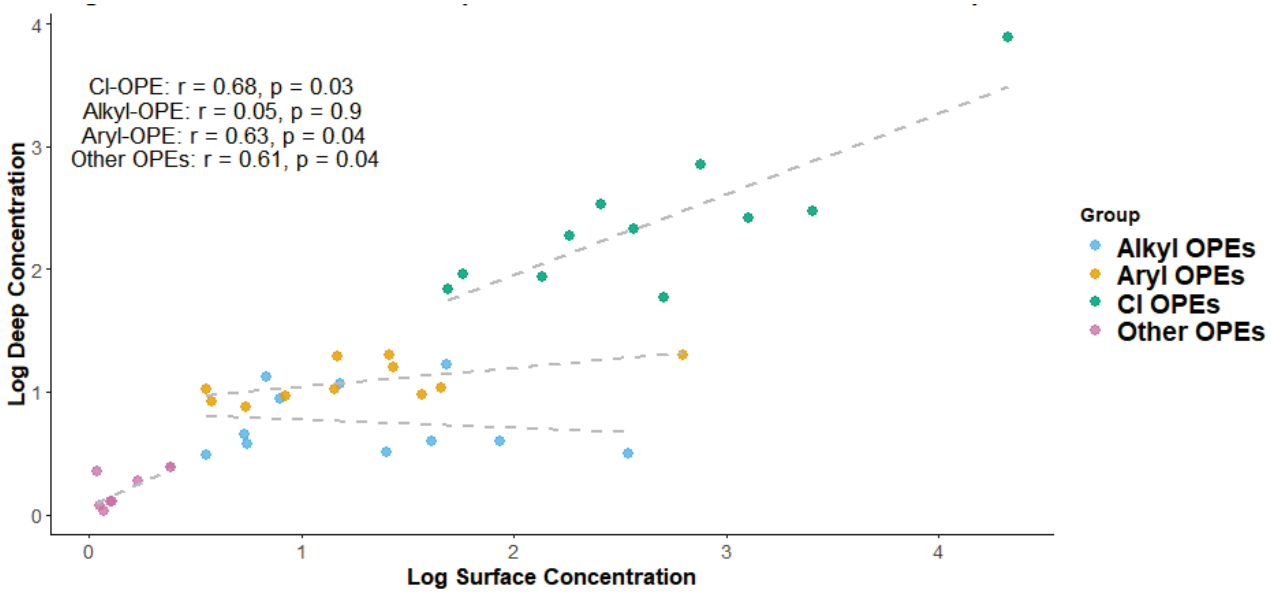


Figure S5. Vertical profiles of $\sum_{24}$OPE concentrations (in ng L^{-1}) plotted over the bathymetry during the transects for the ANTOM-1 and ANTOM-2 cruises. The left panel shows vertical profiles of concentrations sampled in the Southern Ocean (63°S to 71°S) and the right panel shows vertical profiles of concentrations sampled in the Atlantic Ocean (40°N to 40°S).

Figure S6. Log-transformed surface (5 m depth) versus deep (2000 m) OPE concentrations for different OPE groups (Cl-OPEs, Alkyl-OPEs, Aryl-OPEs, and Minor-OPEs). Spearman correlation coefficients (r) and p-values are displayed for each group.



Cl-OPEs, aryl-OPEs, and minor-OPEs show significant positive correlations between surface and deep concentrations (r = 0.68, p = 0.03, r = 0.63, p = 0.04, and r = 0.61, p = 0.04, respectively), while alkyl-OPEs exhibit weaker or no significant correlation.

Figure S7. Major ocean gyres.

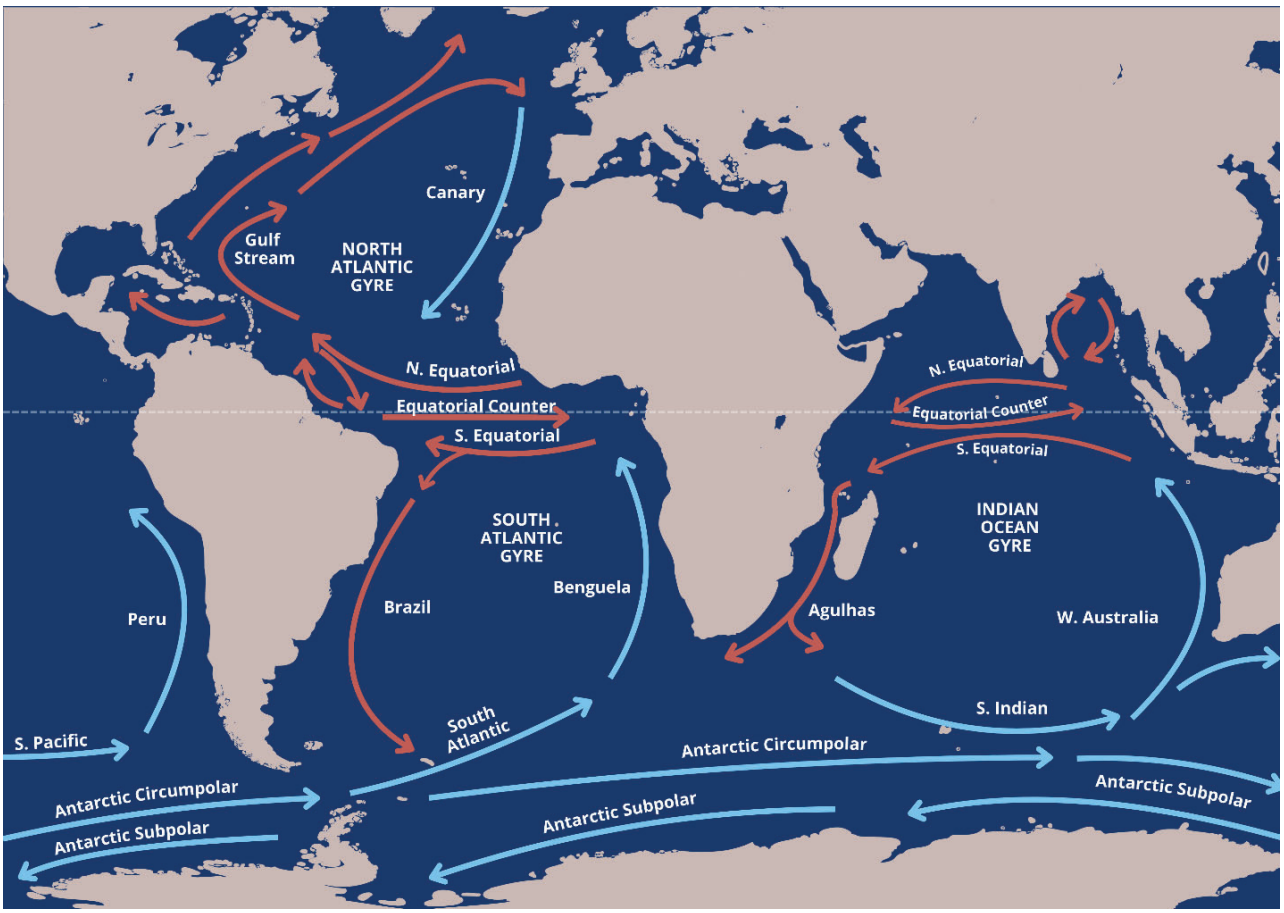


Table S1. List of samples, date and coordinates from the Atlantic Ocean (top table) and Southern Ocea (bottom table) where samples for OPE analysis were collected.

Station Code	Date	Latitude	Longitude	Surface sample	DCM sample	Vertical Profile	WD Sample
AN1_St01	18/12/2020	37.91	-15.97	x	x	x	
AN1_St02	19/12/2020	35.73	-19.06	x	x		
AN1_St03	20/12/2020	32.18	-21.53	x	x		
AN1_St04	21/12/2020	28.65	-23.39	x	x	x	
AN1_St05	22/12/2020	25.63	-24.89	x	x		
AN1_St06	23/12/2020	22.22	-26.63	x			
AN1_St07	24/12/2020	18.86	-28.31	x	x		
AN1_St08	25/12/2020	14.98	-28.77	x			
AN1_St09	26/12/2020	10.87	-29.23	x	x	x	
AN1_St10	27/12/2020	7.34	-29.58	x			x
AN1_St11	28/12/2020	3.82	-29.86	x	x		x
AN1_St12	29/12/2020	0.15	-30.50	x	x	x	
AN1_St13	30/12/2020	-2.97	-30.95	x			
AN1_St14	31/12/2020	-6.77	-31.33	x	x		
AN1_St15	02/01/2021	-14.36	-33.91	x	x	x	
AN1_St16	03/01/2021	-17.77	-35.26	x			
AN1_St17	04/01/2021	-21.29	-36.81	x	x		
AN1_St18	05/01/2021	-24.91	-38.71	x	x	x	
AN1_St19	06/01/2021	-27.79	-40.65	x			
AN1_St20	07/01/2021	-30.98	-42.96	x	x		
AN1_St21	08/01/2021	-34.40	-45.63	x			
AN1_St22	09/01/2021	-37.24	-48.09	x	x	x	
AN1_St23	11/01/2021	-43.79	-54.75	x			
AN1_St24	12/01/2021	-46.78	-58.46	x	x	x	

Station code	Date	Latitude	Longitude	Surface sample	DCM sample	Vertical Profile
AN2_St01	23/01/2022	-62.71	-60.64	X	X	
AN2_St02	24/01/2022	-62.92	-61.04	X	X	
AN2_St03	25/01/2022	-64.58	-62.57	X		
AN2_St04	26/01/2022	-65.15	-65.64	X	X	
AN2_St05	27/01/2022	-66.92	-69.10	X	X	X
AN2_St06	28/01/2022	-67.75	-68.03	X		
AN2_St07	30/01/2022	-70.85	-79.89	X	X	X
AN2_St08	30/01/2022	-70.85	-79.89	X		
AN2_St09	31/01/2022	-69.21	-78.84	X	X	
AN2_St10	01/02/2022	-67.70	-75.00	X	X	X
AN2_St11	04/02/2022	-62.57	-58.62	X	X	X
AN2_St13	05/02/2022	-62.97	-60.29	X	X	
AN2_St14	06/02/2022	-62.95	-60.64	X	X	

Table S2. Information of labelled OPEs used as surrogate (top table) and as Internal Standard (bottom table).

Compound name	Abbreviation	Concentration (ng μL^{-1})	V added (µL)	Mass added (ng)
Tri-n-buthyl phosphate - d27	TNBP-d27	1	50	50
Triphenyl phosphate - d15	TPhP-d15	1	50	50
Tris (2-chloroethyl) phosphate - d12	TCEP-d12	1	50	50
Tri-n-propyl phosphate - d21	TPrP-d21	1	50	50
Tris (2-chloroisoprpyl) phosphate - d18	TCPP-d18	1	50	50
Tris (2-ethylhexyl) phosphate - d51	TEHP-d51	1	50	50
Triphenylphosphine oxide - d15	TPPO-d15	1	50	50

Compound name	Abbreviation	Concentration (ng μL^{-1})	V added (µL)	Mass added (ng)
Tris (1.3-dichloro-2-propyl) phosphate - d15	TDCPP-d15	5	10	50
Tris (2-butoxyethyl) phosphate - $^{13}C_2$	M6TBEP	5	10	50
Triphenyl phosphate - $^{13}C_{18}$	MTPhP	5	10	50

Table S3. Names, acronym, molecular weight (MW) and Log K_{OW} of the targeted compounds.

Analyte	Acronym	MW (g mol^{-1})	Log K_{OW}
Tris (2-chloroethyl) phosphate	TCEP	285.5	1.6
Tris (2-choloroisopropyl) phosphate	TCPP-1.2.3	327.6	2.9
Tris (1.3-dichlor-2-propyl) phosphate	TDCIPP	430.9	3.7
Triethyl phosphate	TEP	182.2	0.9
Tripropyl phosphate	TPrP	224.2	2.1
Tris-iso-butyl phosphate	TiBP	266.3	3.6
Tri-n-butyl phosphate	TNBP	266.3	3.8
Tris (2-ehylhexyl) phosphate	TEHP	434.6	9.5
Tris (2-butoxyethyl) phosphate	TBEP	398.5	3.0
Triphenyl phosphate	TPhP	326.3	4.7
2-Ethylhexyldiphenyl phosphate	EHDPP	362.4	6.3
Tri-p-cresyl phosphate	TpCP	368.4	6.3
Tri-o-cresyl phosphate	ToCP	368.4	6.3
Tri-m-cresyl phosphate	TmCP	368.4	6.3
Tris (3.5-dimethylphenyl) phosphate	TDMPP	410.4	8.0
Tris (2-isopropylphenyl) phosphate	TPPP	452.5	9.1
Tris (4-tert-butylphenyl) phosphate	TTBPP	494.6	10.4
Tris (2.3-dibromopropyl) phosphate	TDBPP	697.6	9.1
Chlorpyrifos	Chlor	350.6	4.9
Triphenyl phosphine oxide	TPPO	278.3	**2.9**
Dioctylphenyl phosphonate	DOPP	382.5	7.5
Tributyl phosphine oxide	TBPO	218.3	3.9

Table S4. Individual OPE contribution (%) to the total pool of $\sum_{24}$OPE in the Atlantic and Southern Ocean samples.

Compound	∑TCPP	TCEP	TPhP	TEP	EHDPP	TBEP	TiBP	TNBP	TDCIPP	∑TcPs	TBPO	TPrP	TEHP	TDBPP	TPPP	Chlor	TTBPP	DOPP	TDMPP	TPPO
Atlantic	59.40	13.0	7.650	3.43	6.76	1.48	3.90	2.16	0.950	0.54	0.22	0.06	0.15	0.06	0.09	0.03	0.002	0.03	0.06	0.003
Southern	50.0	9.05	5.56	2.36	10.1	9.61	2.88	5.54	2.84	0.81	0.00	1.03	0.19	0.05	0.00	0.00	0.03	0.01	0.01	0.00
All	58.26	12.53	7.38	3.29	7.16	2.48	3.76	2.57	1.18	0.57	0.22	0.18	0.15	0.05	0.08	0.02	0.01	0.03	0.05	0.001

Grey area shows OPEs that on average contribute below 0.5% to the total pool and are grouped in this work as "minor-OPEs".

Table S5. Field and procedural blanks OPE abundance (ng).

Name	TEP	TPrP	TiBP	TNBP	TBPO	TCEP	TCPP1	TCPP2	TCPP3	Chlor	TDCIPP	TPhP	TBEP	EHDPP	TEHP	TPPO	ToCP	DOPP	TmCP	TpCP	TPPP	TDMPP	TDBPP	TTBPP
ANIWOPE_010	nd	0.01	nd	0.01	0.29	nd	0.27	0.04	nd	nd	0.01	0.03	0.11	0.02	nd	nd	nd	nd	nd	nd	nd	nd	nd	nd
ANIWOPE_024	nd	0.01	nd	0.02	0.05	nd	0.32	0.08	0.04	nd	0.02	0.11	nd	0.19	nd	nd	nd	nd	nd	nd	0.05	nd	0.02	nd
ANIWOPE_050	nd	0.03	0.07	0.06	0.11	0.16	1.32	0.30	0.02	nd	0.02	0.27	nd	0.40	nd	nd	nd	nd	nd	nd	nd	nd	nd	nd
ANIWOPE_051	nd	0.02	0.07	0.09	0.18	0.38	1.15	0.50	0.30	nd	0.01	0.16	nd	0.27	nd	nd	nd	nd	nd	nd	nd	nd	nd	nd
ANIWOPE_063	nd	0.01	nd	0.03	0.64	1.23	0.57	0.06	nd	nd	0.02	0.14	nd	0.10	nd	nd	nd	nd	nd	nd	nd	0.03	nd	nd
ANIWOPE_064	nd	0.01	nd	0.04	0.24	1.59	0.76	0.09	0.01	nd	0.01	0.16	nd	0.12	nd	nd	nd	nd	nd	nd	nd	nd	0.04	nd
ANIWOPE_066	nd	0.01	nd	0.08	0.55	nd	0.82	0.10	0.01	nd	0.06	0.33	nd	0.38	nd	nd	nd	nd	nd	nd	nd	nd	0.05	nd
ANIWOPE_082	nd	0.01	nd	0.04	0.40	0.28	0.45	0.11	0.01	nd	0.03	0.16	nd	0.21	nd	nd	nd	nd	nd	nd	nd	nd	nd	nd
ANIWOPE_083	0.01	0.02	nd	0.08	0.86	0.51	0.71	0.18	0.01	nd	nd	0.15	nd	0.15	nd	nd	nd	nd	nd	nd	nd	nd	nd	nd
ANIWOPE_090	nd	0.03	nd	0.03	0.14	0.30	0.91	0.51	0.03	nd	nd	0.14	nd	0.22	nd	nd	nd	nd	nd	nd	nd	nd	0.05	nd
ANIWOPE_121	nd	0.01	nd	0.03	0.23	5.13	0.54	0.06	nd	nd	0.02	0.07	nd	0.09	nd	nd	nd	nd	0.01	nd	0.01	0.03	nd	nd
ANIWOPE_134	nd	nd	nd	0.01	0.11	0.11	0.18	0.03	nd	nd	nd	0.06	nd	0.04	nd	nd	nd	nd	nd	nd	nd	0.03	0.03	nd
ANIWOPE_140	nd	nd	0.06	0.08	0.17	0.07	1.17	0.16	0.10	nd	nd	0.11	nd	0.10	nd	nd	nd	nd	nd	nd	nd	nd	nd	nd
ANIWOPE_142	nd	0.01	nd	0.02	0.12	nd	0.33	0.18	0.03	nd	nd	0.07	nd	0.03	nd	nd	nd	nd	nd	nd	nd	nd	nd	nd
ANIWOPE_143	nd	0.01	nd	0.25	nd	2.36	nd	2.09	0.18	nd	0.26	0.64	0.28	0.83	nd	nd	nd	nd	0.02	0.01	nd	nd	nd	nd
ANIWOPE_174	nd	0.01	0.02	0.04	0.23	0.02	0.40	0.04	0.02	nd	0.08	0.10	0.09	0.05	nd	nd	0.03	nd	0.02	0.01	0.01	0.04	nd	nd
ANIWOPE_175	nd	nd	nd	0.02	0.19	nd	0.17	0.11	0.01	nd	0.06	0.10	nd	0.09	nd	nd	nd	nd	nd	nd	nd	0.03	nd	nd
ANIWOPE_217	0.01	nd	0.01	0.01	0.08	nd	0.09	0.04	0.01	nd	nd	0.04	nd	0.01	nd	nd	nd	nd	nd	nd	nd	nd	nd	nd
ANIWOPE_219	0.01	0.01	nd	0.03	0.19	0.43	0.40	0.24	0.04	nd	nd	0.10	nd	0.03	nd	nd	nd	nd	nd	nd	nd	nd	nd	nd
ANIWOPE_248	0.07	0.01	0.01	0.01	nd	0.57	0.24	0.06	nd	nd	0.04	1.04	nd	0.59	nd	nd	nd	nd	nd	nd	0.09	nd	nd	nd
ANIWOPE_PB001	0.09	nd	0.02	0.37	nd	nd	0.10	0.02	0.13	nd	0.01	0.03	0.03	nd	nd	nd	nd	nd	nd	nd	nd	nd	nd	nd
ANIWOPE_PB002	0.05	nd	0.02	0.31	nd	nd	0.10	0.01	0.12	nd	0.02	0.03	0.05	0.01	nd	nd	nd	nd	nd	nd	nd	nd	nd	nd
ANIWOPE_PB003	nd	nd	0.03	0.36	nd	nd	0.08	0.01	0.10	nd	0.06	0.03	0.07	0.01	nd	nd	nd	nd	nd	nd	nd	nd	nd	nd
ANIWOPE_PB004	0.01	nd	0.04	0.45	nd	nd	0.16	0.03	0.19	nd	0.03	0.08	0.10	nd	nd	nd	nd	nd	0.01	nd	nd	nd	nd	nd
ANIWOPE_PB005	0.01	nd	0.03	0.51	nd	nd	0.13	nd	0.16	nd	nd	0.03	nd	nd	nd	nd	nd	nd	nd	nd	nd	nd	nd	nd
ANIWOPE_PB006	nd	nd	0.02	0.29	nd	nd	0.08	0.01	0.10	nd	0.01	0.03	0.05	0.01	nd	nd	nd	nd	nd	nd	nd	nd	nd	nd
ANIWOPE_PB007	nd	nd	0.08	0.86	nd	nd	nd	nd	0.05	nd	nd	0.02	nd	nd	nd	nd	nd	nd	nd	nd	nd	nd	nd	nd
ANIWOPE_PB008	nd	nd	0.02	0.24	nd	nd	0.05	0.06	0.06	nd	0.01	0.04	0.32	0.01	nd	nd	nd	nd	nd	nd	nd	nd	nd	nd
ANIWOPE_PB009	nd	nd	0.03	0.24	nd	nd	0.04	0.05	0.05	nd	0.01	0.04	nd	0.01	nd	nd	nd	nd	nd	nd	nd	nd	nd	nd
ANIWOPE_PB010	nd	nd	0.05	0.02	nd	nd	0.09	0.06	0.13	nd	0.01	0.01	nd	nd	nd	nd	nd	nd	nd	nd	nd	nd	nd	nd
ANIWOPE_PB011	nd	nd	0.03	0.01	nd	nd	0.05	0.02	0.07	nd	0.01	0.02	0.04	0.01	nd	nd	nd	nd	nd	nd	nd	nd	nd	nd
ANIWOPE_PB012	nd	nd	0.05	0.02	nd	nd	0.06	0.03	0.09	nd	0.01	0.01	0.16	nd	nd	nd	nd	nd	nd	nd	nd	nd	nd	nd
ANIWOPE_PB013	nd	nd	0.05	0.02	nd	nd	0.06	0.03	0.08	nd	0.01	0.01	0.07	0.01	nd	nd	nd	nd	nd	nd	nd	nd	nd	nd
ANIWOPE_PB014	nd	nd	0.06	0.38	nd	nd	0.07	0.09	0.09	nd	nd	0.02	0.24	nd	nd	nd	nd	nd	nd	nd	nd	nd	nd	nd
ANIWOPE_PB015	nd	nd	0.06	0.43	nd	nd	0.11	0.14	0.15	nd	nd	nd	nd	nd	nd	nd	nd	nd	nd	nd	nd	nd	nd	nd
ANIWOPE_PB016	nd	nd	0.06	0.10	nd	nd	0.03	0.03	0.04	nd	nd	nd	nd	nd	nd	nd	nd	nd	nd	nd	nd	nd	nd	nd
ANIWOPE_PB017	nd	nd	0.10	0.44	nd	nd	0.10	0.08	0.02	nd	nd	0.01	nd	nd	nd	nd	nd	nd	nd	nd	nd	nd	nd	nd
ANIWOPE_PB018	nd	nd	0.01	0.11	nd	nd	0.01	0.01	0.01	nd	0.01	0.02	nd	nd	nd	nd	nd	nd	nd	nd	nd	nd	nd	nd
ANIWOPE_PB019	nd	nd	0.01	0.12	nd	nd	0.01	0.01	0.01	nd	nd	0.01	nd	nd	nd	nd	nd	nd	0.06	nd	nd	nd	nd	nd
AN2WOPE_003	0.31	nd	0.13	nd	nd	0.04	1.35	0.12	0.06	nd	0.02	0.13	nd	nd	0.01	1.84	nd	nd	nd	nd	nd	nd	nd	nd
AN2WOPE_015	0.15	nd	0.06	0.05	nd	0.04	1.55	0.12	nd	nd	0.04	0.19	nd	nd	0.02	1.16	nd	nd	nd	nd	nd	nd	nd	nd
AN2WOPE_031	0.12	0.02	0.07	0.07	nd	0.02	0.82	0.08	0.05	nd	0.02	0.08	0.10	nd	0.01	1.17	nd	nd	nd	nd	nd	nd	nd	nd
AN2WOPE_032	0.06	0.02	0.04	0.04	nd	0.02	0.91	0.09	0.02	nd	0.02	0.15	0.11	nd	0.01	0.61	nd	nd	nd	nd	nd	nd	nd	nd
AN2WOPE_033	0.07	0.02	0.05	nd	nd	0.02	0.59	0.06	0.02	nd	nd	0.07	nd	nd	nd	1.34	nd	nd	nd	nd	nd	nd	nd	nd
AN2WOPE_042	0.04	0.01	0.02	0.06	nd	0.02	0.73	0.08	0.05	nd	0.01	0.09	nd	nd	nd	0.72	nd	nd	nd	nd	nd	nd	nd	nd
AN2WOPE_048	0.02	0.01	0.01	0.01	nd	0.02	0.19	0.03	0.03	nd	nd	0.06	0.04	nd	nd	0.18	nd	nd	nd	nd	nd	nd	nd	nd
AN2WOPE_097	0.07	nd	0.04	nd	nd	0.02	0.67	0.06	0.04	nd	nd	0.07	nd	nd	nd	0.86	nd	nd	nd	nd	nd	nd	nd	nd
AN2WOPE_141	0.21	0.01	0.02	0.01	nd	0.01	0.98	0.06	0.01	nd	0.01	0.35	nd	nd	0.01	0.28	nd	nd	nd	nd	nd	nd	nd	nd

**PB for Procedural blank, nd = non detected*

Table S6. Limits of quantification (LOQs) in ng.

OPE compound	LOQs Atlantic	LOQs Southern
TEP	0.064	0.272
TPrP	0.030	0.020
TiBP	0.110	0.126
TNBP	0.741	0.842
TBPO	0.713	0.001
TCEP	3.117	0.043
TCPP1	1.390	1.645
TCPP2	1.167	0.167
TCPP3	0.266	0.221
Chlorpyrifos	0.001	0.001
TDCIPP	0.153	0.052
TPhP	0.689	0.282
TBEP	0.282	0.286
EHDPP	0.638	0.013
TEHP	0.001	0.013
TPPO	0.001	1.846
ToCP	0.015	0.001
DOPP	0.001	0.001
TmCP	0.035	0.037
TpCP	0.007	0.001
TPPP	0.053	0.001
TDMPP	0.037	0.001
TDBPP	0.046	0.001
TTBPP	0.001	0.001

All samples consisted of 2 L of seawater, except the rain water samples that extracted 1 L of water. The limits of quantification (LOQs) were defined as the mean concentration plus three times the standard deviation of the blank response. For the analytes which were not found in procedural or field blanks, LOQs were derived from the lowest standard in the calibration curve.

Table S7. Mean surrogate (top table) and matrix spike (bottom table) recoveries (%) from the Atlantic Ocean and Southern Ocean samples.

Mean surrogate Recoveries (%)					
Atlantic Ocean					
	D27-TNBP	D12-TCEP	D18-TCPP	D15-TPHP	D51-TEHP
MEAN	45.9	68.2	28.2	88.0	127.7
SD	23.4	75.0	24.3	44.3	55.1
Southern Ocean					
	D27-TNBP	D12-TCEP	D18-TCPP	D15-TPHP	D51-TEHP
MEAN	64.9	56.7	60.7	82.2	107.0
SD	14.9	9.9	10.0	13.8	51.7

Mean Matrix Spike Recoveries (%)												
Atlantic Ocean (N=6)												
Name	TEP	TiBP	TNBP	TCEP	TCPP	TDCIPP	TPhP	TBEP	EHDPP	ToCP	TmCP	TpCP
Mean	18.28	43.41	31.99	55.02	21.93	67.52	64.32	95.01	144.63	81.47	94.54	138.63
Sd	2.79	8.20	5.07	10.51	3.68	7.12	5.48	11.29	13.25	3.39	19.89	18.30
Southern Ocean (N=4)												
	TEP	TiBP	TNBP	TCEP	TCPP	TDCIPP	TPhP	TBEP	EHDPP	ToCP	TmCP	TpCP
Mean	66.95	108.18	84.63	60.55	66.97	113.83	85.24	74.60	43.19	67.24	44.89	41.40
Sd	10.12	15.11	9.05	3.18	3.37	8.75	4.28	4.25	3.63	5.57	2.43	1.21

Table S8. Individual and $\sum_{24}$OPE concentration in surface and DCM samples from the Atlantic Ocean (ng L^{-1}).

station	type	depth (m)	date	lat	long	TEP	TCEP	∑TCPP	TBEP	TiBP	TDCIPP	TNBP	TPhP	EHDPP	∑TcPs	Minor-OPE	$\sum_{24}$OPES
AN1_ST01	5 m	4	20201218	37.92	-15.97	2.65	2.90	8.72	<loq	0.86	0.37	<loq	2.78	<loq	nd	nd	18.29
AN1_ST01	DCM	61	20221218	37.92	-15.97	<loq	3.81	12.38	0.18	0.23	0.35	<loq	1.88	0.46	<loq	nd	19.29
AN1_ST02	5 m	5	20201219	35.74	-19.07	nd	2.67	6.37	nd	0.34	nd	0.58	1.12	<loq	nd	nd	11.08
AN1_ST02	DCM	105	20201219	35.74	-19.07	nd	3.79	6.20	0.59	2.41	0.85	0.97	5.62	1.67	0.31	nd	22.41
AN1_ST03	5 m	5	20201220	35.74	-19.07	3.32	<loq	5.55	0.21	0.27	0.23	<loq	3.04	1.23	0.06	nd	13.91
AN1_ST03	DCM	115	20201220	35.74	-19.07	1.44	1.63	6.24	0.21	0.14	0.19	<loq	1.45	0.41	nd	nd	11.70
AN1_ST04	5 m	5	20201221	28.66	-28.41	<loq	2.00	5.99	0.20	0.51	0.59	<loq	1.18	<loq	nd	nd	10.48
AN1_ST04	DCM	86	20201221	28.66	-28.41	<loq	2.21	7.91	0.33	0.47	0.62	<loq	1.87	0.49	nd	nd	13.88
AN1_ST05	5 m	5	20201222	25.63	-24.90	0.88	1.57	5.31	0.22	0.13	0.24	<loq	1.70	0.35	<loq	nd	10.39
AN1_ST05	DCM	120	20201222	25.63	-24.90	<loq	<loq	3.74	0.23	0.14	0.17	<loq	1.35	<loq	0.03	nd	5.67
AN1_ST06	5 m	5	20201223	22.22	-26.63	<loq	3.06	5.78	0.22	0.18	0.25	1.20	4.28	0.64	0.43	0.03	16.08
AN1_ST07	5 m	5	20201224	18.87	-28.32	<loq	4.00	13.61	0.22	0.43	0.41	<loq	2.30	<loq	nd	nd	20.98
AN1_ST07	DCM	85	20201224	18.87	-28.32	<loq	3.88	29.10	0.25	0.42	0.16	<loq	1.22	0.54	nd	nd	35.58
AN1_ST08	5 m	5	20201225	14.97	-28.70	0.70	5.90	7.78	<loq	0.20	0.08	<loq	1.62	<loq	nd	nd	16.28
AN1_ST09	5 m	5	20201226	10.87	-29.23	1.21	7.42	9.10	0.17	0.61	0.26	1.08	3.15	0.71	0.40	nd	24.09
AN1_ST09	DCM	50	20201226	10.87	-29.23	0.92	11.01	12.68	0.20	0.24	0.41	<loq	3.15	0.84	0.16	nd	29.62
AN1_ST10	5 m	5	20201227	7.35	-29.58	<loq	1.61	11.29	<loq	0.44	0.11	<loq	1.16	0.40	<loq	nd	15.01
AN1_ST11	5 m	5	20201228	3.83	-29.86	0.07	5.12	5.68	<loq	0.38	0.19	<loq	1.41	0.41	nd	nd	13.27
AN1_ST11	DCM	77	20201228	3.83	-29.86	<loq	2.92	4.49	<loq	0.10	0.21	<loq	1.11	<loq	nd	nd	8.83
AN1_ST12	5 m	5	20201229	0.14	-30.50	8.20	3.37	25.20	<loq	2.97	0.49	<loq	3.13	0.63	nd	nd	43.98
AN1_ST12	DCM	48	20201229	0.14	-30.50	<loq	2.05	13.77	<loq	0.79	<loq	<loq	1.97	0.36	<loq	nd	18.94
AN1_ST13	5 m	5	20201230	-2.98	-30.95	0.47	2.65	17.74	0.44	0.39	0.42	<loq	4.81	0.94	0.81	nd	28.72
AN1_ST14	5 m	5	20201231	-6.78	-31.33	0.32	<loq	4.39	<loq	0.33	0.33	<loq	1.76	0.67	nd	nd	7.82
AN1_ST14	DCM	120	20201231	-6.78	-31.33	0.06	<loq	3.97	<loq	0.35	0.22	<loq	1.26	0.33	nd	nd	6.19
AN1_ST15	5 m	5	20210102	-14.37	-33.92	nd	3.87	70.56	0.21	0.47	0.22	<loq	2.64	0.53	nd	nd	78.50
AN1_ST15	DCM	110	20210102	-14.37	-33.92	<loq	<loq	8.41	<loq	0.23	0.14	<loq	1.66	0.47	<loq	nd	10.91
AN1_ST16	5 m	5	20210103	-17.78	-35.27	nd	8.19	27.87	2.07	0.72	nd	4.85	2.57	0.51	nd	nd	46.77
AN1_ST17	5 m	5	20210104	-21.30	-36.80	0.04	5.36	7.64	0.65	0.25	0.15	<loq	2.75	1.90	0.87	0.22	19.83
AN1_ST17	DCM	90	20210104	-21.30	-36.80	<loq	4.40	13.62	0.36	0.14	0.12	<loq	1.82	0.51	0.06	0.04	21.07
AN1_ST18	5 m	5	20210105	-24.91	-38.72	0.53	2.84	18.37	2.80	0.30	0.11	2.27	5.05	6.06	4.21	0.01	42.56
AN1_ST18	DCM	55	20210105	-24.91	-38.72	7.80	nd	11.56	nd	0.14	<loq	<loq	1.83	0.41	0.15	nd	21.90
AN1_ST19	5 m	5	20210106	-27.79	-40.65	0.50	nd	8.94	nd	0.95	nd	2.70	nd	0.61	nd	nd	13.71
AN1_ST20	5 m	5	20210107	-30.98	-42.96	2.40	2.10	13.35	0.54	0.11	0.33	<loq	2.30	<loq	nd	nd	21.12
AN1_ST20	DCM	110	20210107	-30.98	-42.96	<loq	<loq	10.57	<loq	0.08	0.10	<loq	2.31	<loq	<loq	nd	13.05
AN1_ST21	5 m	5	20210108	-34.40	-45.63	<loq	<loq	1.74	<loq	<loq	nd	<loq	0.38	<loq	nd	nd	2.12
AN1_ST22	5 m	5	20210109	-37.24	-48.09	<loq	<loq	8.51	<loq	0.20	0.09	<loq	nd	<loq	0.07	nd	8.87
AN1_ST22	DCM	60	20210109	-37.24	-48.09	0.33	<loq	2.37	<loq	0.23	<loq	<loq	0.75	<loq	nd	nd	3.68
AN1_ST23	5 m	5	20210111	-43.79	-54.75	nd	<loq	18.48	nd	0.63	nd	<loq	nd	nd	nd	nd	19.11
AN1_ST24	5 m	5	20210112	-46.79	-58.46	11.35	8.63	7.74	nd	0.24	0.51	<loq	3.00	<loq	0.39	nd	31.87
AN1_ST24	DCM	34	20210112	-46.79	-58.46	3.92	nd	5.51	0.19	0.06	nd	<loq	0.77	<loq	nd	nd	10.44

*Category "Minor-OPE" results from the sum of: TEHP, TPrP, TPPP, TBPO, Chlorpyrifos, DOPP, TPPO, TDMPP, TDBPP and TTBPP; nd = non detected; <loq = value below limit of quantification; ∑TCPP = sum of three TCPP isomers (TCPP1, TCPP2 and TCPP3); ∑TcPs = sum of three cresyl isomers (TpC, TmCP and TpCP).

Table S9. Mean and SD of 5 m depth and DCM concentrations (ng L^{-1}) in the three ocean basins sampled.

	North Atlantic				South Atlantic				Southern Ocean			
	5 m		DCM		5 m		DCM		5 m		DCM	
	Mean	SD	Mean	SD	Mean	SD	Mean	SD	Mean	SD	Mean	SD
TEP	1.43	2.40	0.29	0.52	1.31	3.23	1.74	3.03	0.21	0.11	0.25	0.11
TiBP	0.61	0.77	0.55	0.73	0.39	0.27	0.18	0.10	0.24	0.13	0.25	0.11
TNBP	0.52	0.30	0.44	0.20	1.10	1.44	0.37	0.00	0.52	0.36	0.49	0.15
TCEP	3.43	1.88	3.65	2.59	3.45	2.59	1.97	1.07	0.60	0.29	0.74	0.35
∑TCPP	9.20	5.66	10.70	7.82	17.10	18.40	8.00	4.19	5.10	2.94	3.65	1.54
TDCIPP	0.28	0.16	0.34	0.25	0.21	0.15	0.12	0.05	0.21	0.14	0.34	0.57
TPhP	2.24	1.03	2.18	1.43	2.19	1.65	1.49	0.58	0.54	0.33	0.42	0.26
TBEP	0.17	0.04	0.25	0.14	0.63	0.88	0.18	0.08	0.72	0.88	0.86	0.71
EHDPP	0.50	0.27	0.60	0.43	1.07	1.64	0.38	0.08	0.76	0.60	0.65	0.50
∑TcPs	0.27	0.18	0.27	0.19	0.14	0.06	0.12	0.02	0.09	0.07	0.14	0.14
Minor	0.09	0.15	0.07	0.10	0.54	1.20	0.04	0.05	0.14	0.32	0.01	0.01
$\sum_{24}$OPE	18.60	9.07	19.30	9.29	27.60	20.30	14.50	6.47	9.00	4.53	7.77	2.79

Table S10. Individual and $\sum_{24}$OPE concentration in surface and DCM samples from the Southern Ocean (ng L^{-1}).

Station	Type	Depth(m)	Date	LAT	LONG	TEP	TCEP	∑TCPP	TBEP	TiBP	TDCIPP	TNBP	TPHP	EHDPP	∑TcPs	Minor-OPE	$\sum_{24}$OPE
AN2_ST01	5 m	5.44	220123	-62.71	-60.64	0.30	0.72	4.01	0.22	0.33	0.13	1.73	0.38	0.14	0.01	0.09	8.06
AN2_ST01	DCM	25.19	220123	-62.71	-60.64	0.23	0.70	3.00	0.32	0.39	0.16	0.88	0.46	0.08	0.01	0.15	6.36
AN2_ST02	5 m	4.81	220124	-62.92	-61.04	0.25	0.80	6.91	0.64	0.46	0.18	<loq	1.24	0.44	0.00	0.18	11.10
AN2_ST02	DCM	29.48	220124	-62.92	-61.04	0.45	1.33	4.83	0.64	0.41	0.21	0.57	1.04	0.67	0.04	0.09	10.28
AN2_ST03	5 m	4.81	220125	-64.58	-62.57	<loq	0.53	3.23	0.24	0.13	0.51	<loq	0.48	0.24	0.00	0.01	5.37
AN2_ST04	5 m	4.55	220126	-65.15	-65.64	<loq	0.43	2.97	0.25	0.17	0.11	<loq	0.27	0.16	0.01	0.05	4.41
AN2_ST04	DCM	19.60	220126	-65.15	-65.64	<loq	0.69	2.82	0.26	0.25	0.10	<loq	0.24	0.21	0.00	0.05	4.62
AN2_ST05	5 m	7.44	220127	-66.92	-69.10	0.41	0.93	6.29	1.21	0.23	0.22	<loq	0.81	1.36	0.01	0.03	11.50
AN2_ST05	DCM	19.84	220127	-66.92	-69.10	0.36	0.43	3.24	1.70	0.13	0.11	<loq	0.34	1.14	0.00	0.05	7.51
AN2_ST06	5 m	5.06	220128	-67.75	-68.03	0.36	0.34	3.15	0.64	0.25	0.29	<loq	0.30	1.52	0.01	0.12	6.97
AN2_ST07	5 m	4.63	220130	-70.85	-79.89	0.39	0.33	4.00	0.29	0.20	0.09	<loq	0.39	0.40	0.00	0.26	6.35
AN2_ST07	DCM	21.90	220130	-70.85	-79.89	0.30	0.44	3.48	0.46	0.15	1.84	<loq	0.36	0.31	0.01	0.41	7.76
AN2_ST08	5 m	4.65	220130	-70.85	-79.89	0.30	0.57	4.73	0.67	0.42	0.25	<loq	0.51	1.72	0.56	0.11	9.83
AN2_ST09	5 m	5.45	220131	-69.21	-78.84	<loq	0.88	8.06	0.48	0.31	0.45	<loq	0.55	1.61	0.06	0.11	12.52
AN2_ST09	DCM	30.40	220131	-69.21	-78.84	<loq	0.84	6.14	0.57	0.32	0.28	<loq	0.48	1.02	0.03	0.34	10.03
AN2_ST10	5 m	5.77	220201	-67.70	-75.00	<loq	0.69	3.96	0.79	0.11	0.19	<loq	0.38	0.70	0.01	0.05	6.87
AN2_ST10	DCM	49.44	220201	-67.70	-75.00	0.28	1.11	5.03	2.03	0.25	0.16	<loq	0.40	0.76	0.01	0.05	10.08
AN2_ST11	5 m	4.94	220204	-62.57	-58.62	nd	1.16	12.57	3.46	0.36	0.24	<loq	1.20	1.01	0.02	0.08	20.09
AN2_ST11	DCM	37.43	220204	-62.57	-58.62	<loq	0.90	3.49	1.59	0.23	0.17	<loq	0.32	1.51	0.01	0.02	8.25
AN2_ST13	5 m	4.99	220205	-62.97	-60.29	<loq	0.23	<loq	0.27	<loq	0.07	<loq	0.30	0.45	0.09	0.01	1.42
AN2_ST13	DCM	57.83	220205	-62.97	-60.29	0.18	0.22	<loq	<loq	0.08	0.03	<loq	<loq	0.13	0.00	0.02	0.67
AN2_ST14	5 m	5.00	220206	-62.95	-60.64	<loq	0.22	5.56	nd	0.09	0.03	<loq	0.27	0.14	1.07	0.04	7.42

* Category "Minor-OPEs" results from the sum of: TEHP, TPrP, TPPP, TBPO, Chlorpyrifos, DOPP, TDMPP, TPPO, TDBPP and TTBPP; nd = non detected; <loq = value below limit of quantification; ∑TCPP = sum of three TCPP isomers (TCPP1, TCPP2 and TCPP3); ∑TcPs = sum of three cresyl isomers (TpC, TmCP and TpCP).

Table S11. Environmental variables measured at surface waters and atmospheric conditions in the Atlantic and Southern Oceans.

Station	Depth	Ocean	Latitude	Longitude	Wind speed	Water T°	Air T°	Humidity	Solar Radiation	Atmospheric Pressure	Bacterial Abundance	Bacterial Production	Chl *a*	Salinity
Units					$m\ s^{-1}$	°C	°C	%	$W\ m^{-2}$	hPa	$cells\ mL^{-1}$	$pmol\ Leu\ L^{-1}\ h^{-1}$	$\mu g\ L^{-1}$	PSU
AN1_ST01	5 m	Atlantic	37.92	-15.97	11.0	17.5	17.2	90.0	17.1	1027.9	6.47E+05	4.5	0.2	36.3
AN1_ST02	5 m	Atlantic	35.74	-19.07	4.3	17.8	17.2	72.1	100.6	1031.6	5.81E+05	8.2	0.1	36.3
AN1_ST03	5 m	Atlantic	32.18	-19.07	0.7	19.9	19.4	78.8	48.7	1034.5	5.27E+05	8.4	0.1	36.8
AN1_ST04	5 m	Atlantic	28.66	-28.41	4.4	21.4	21.0	66.2	368.3	1034.2	5.00E+05	8.7	0.1	37.1
AN1_ST05	5 m	Atlantic	25.63	-24.90	6.4	22.9	21.0	71.8	23.7	1030.9	6.39E+05	2.8	0.1	37.3
AN1_ST06	5 m	Atlantic	22.22	-26.63	3.0	23.6	21.8	56.6	38.9	1027.2	5.57E+05	12.5	0.2	37.0
AN1_ST07	5 m	Atlantic	18.87	-28.32	6.1	24.0	22.3	67.3	42.6	1023.2	6.45E+05	7.3	0.2	36.9
AN1_ST08	5 m	Atlantic	14.97	-28.70	4.0	25.5	23.2	65.3	132.2	1022.5	7.99E+05	14.7	0.2	35.5
AN1_ST09	5 m	Atlantic	10.87	-29.23	8.8	26.4	25.1	77.7	4.5	1020.6	7.85E+05	16.8	0.2	35.6
AN1_ST10	5 m	Atlantic	7.35	-29.58	2.0	27.5	26.5	82.2	185.9	1021.6	9.72E+05	23.9	0.2	35.0
AN1_ST11	5 m	Atlantic	3.83	-29.86	1.4	27.9	25.5	87.6	20.8	1021.1	8.18E+05	18.4	0.2	35.4
AN1_ST12	5 m	Atlantic	0.14	-30.50	7.7	27.0	26.7	80.2	120.8	1020.8	7.66E+05	5.7	0.2	36.3
AN1_ST13	5 m	Atlantic	-2.98	-30.95	9.2	26.9	26.6	81.4	135.3	1020.3	8.31E+05	16.3	0.1	36.2
AN1_ST14	5 m	Atlantic	-6.78	-31.33	9.1	27.5	27.0	74.3	295.7	1022.2	7.29E+05	13.7	0.1	36.5
AN1_ST15	5 m	Atlantic	-14.37	-33.92	5.2	26.9	26.7	64.2	241.2	1023.9	3.53E+05	21.5	0.1	37.3
AN1_ST16	5 m	Atlantic	-17.78	-35.27	7.3	27.5	26.6	69.2	514.5	1023.4	1.47E+06	32.2	0.5	37.3
AN1_ST17	5 m	Atlantic	-21.30	-36.80	7.7	27.2	26.5	77.1	434.2	1024.8	1.45E+06	16.2	0.2	37.2
AN1_ST18	5 m	Atlantic	-24.91	-38.72	11.6	26.2	26.5	77.3	221.1	1023.9	7.41E+05	18.3	0.2	36.3
AN1_ST19	5 m	Atlantic	-27.79	-40.65	3.2	24.4	24.8	89.3	160.2	1023.2	7.42E+05	26.8	0.1	36.3
AN1_ST20	5 m	Atlantic	-30.98	-42.96	2.6	23.6	21.7	86.9	44.9	1020.6	7.08E+05	17.4	0.1	36.1
AN1_ST21	5 m	Atlantic	-34.40	-45.63	6.5	23.9	23.6	80.2	358.9	1018.6	7.55E+05	14.9	0.1	37.0
AN1_ST22	5 m	Atlantic	-37.24	-48.09	9.6	19.4	19.0	65.8	322.6	1021.0		27.5	0.2	35.1
AN1_ST23	5 m	Atlantic	-43.79	-54.75	5.0	18.5	17.7	81.0	157.2	1014.6	2.29E+06	98.6	0.2	34.2
AN1_ST24	5 m	Atlantic	-46.79	-58.46	2.6	13.7	12.2	67.2	187.0	1015.6	2.64E+06	65.8	0.5	34.2
AN2_ST01	5 m	Southern	-62.71	-60.64	8.1	1.4	1.9	97.6	136.6	987.7	4.30E+05	29.2	0.7	34.1
AN2_ST02	5 m	Southern	-62.92	-61.04	1.8	1.4	1.3	96.7	122.5	982.4	4.12E+05	22.3	0.9	34.1
AN2_ST03	5 m	Southern	-64.58	-62.57	9.8	1.0	1.5	92.1	456.0	985.6	2.39E+05	5.3	1.2	34.0
AN2_ST04	5 m	Southern	-65.15	-65.64	6.3	1.0	0.2	81.4	217.7	990.8	2.15E+05	41.4	1.9	33.5
AN2_ST05	5 m	Southern	-66.92	-69.10	10.7	0.5	0.5	94.5	107.6	989.5	2.26E+05	86.2	2.9	33.4
AN2_ST06	5 m	Southern	-67.75	-68.03	3.6	0.3	0.0	81.5	179.3	998.9	2.13E+05	39.6	2.6	33.1
AN2_ST07	5 m	Southern	-70.85	-79.89	6.8	0.0	0.0	97.9	124.0	973.8	5.93E+05	57.1	3.6	33.1
AN2_ST08	5 m	Southern	-70.85	-79.89	6.8	0.0	0.0	92.6	182.0	975.2	5.58E+05	121.1	4.7	33.2
AN2_ST09	5 m	Southern	-69.21	-78.84	10.2	0.0	0.0	96.7	106.7	971.4	2.77E+05	34.0	0.7	33.6
AN2_ST10	5 m	Southern	-67.70	-75.00	11.4	0.7	0.0	88.2	45.6	969.5	1.77E+05	9.9	1.8	33.9
AN2_ST11	5 m	Southern	-62.57	-58.62	12.8	1.3	1.8	93.4	107.6	993.7	4.81E+05	48.7	2.7	34.3
AN2_ST13	5 m	Southern	-62.97	-60.29	7.9	0.3	1.5	98.8	106.9	996.0	2.45E+05	16.5	0.6	34.4
AN2_ST14	5 m	Southern	-62.95	-60.64	11.4	1.7	1.1	95.9	61.3	992.2	1.09E+06	27.2	1.0	34.0

Table S12. Summary of the polynomial regression models applied to log-transformed grouped OPE concentrations across different depths (5 m, DCM, 1% PAR, MOx, and Deep) with latitude.

Cl-OPEs	5 m	p	DCM	p	1%PAR	p	MOx	p	Deep	p
(a) Intercept	2.39	**< 0.001**	2.19	**< 0.001**	2.20	**< 0.001**	2.27	**< 0.001**	2.38	**< 0.001**
(b) (lat)^1	1.64	**0.003**	1.84	**< 0.001**						
(c) (lat)^2	-2.11	**< 0.001**							-1.16	**0.03**
Residual SD	0.5		0.48		0.86		0.57		0.43	
Multiple R^2	0.42		0.43		0.30		0.33		0.59	
F-statistic	12.8		8.54		1.93		2.03		5.67	
P-value	**< 0.001**		**0.002**		0.20		0.19		**0.03**	

Aryl-OPE	5 m	p	DCM	p	1%PAR	p	MOx	p	Deep	p
(a) Intercept	1.14	**< 0.001**	0.99	**< 0.001**	1.10	**< 0.001**	1.11	**< 0.001**	1.08	**< 0.001**
(b) (lat)^1			1.26	**< 0.001**						
(c) (lat)^2										
Residual SD	0.46		0.31		0.64		0.27		0.17	
Multiple R^2	0.21		0.42		0.21		0.08		0.07	
F-statistic	4.68		8.17		1.21		0.39		0.29	
P-value	**0.01**		**0.002**		0.34		0.69		0.76	

Alkyl-OPE	5 m	p	DCM	p	1%PAR	p	MOx	p	Deep	p
(a) Intercept	1.10	**< 0.001**	0.95	**< 0.001**	0.87	**< 0.001**	1.15	**0.001**	0.75	**< 0.001**
(b) (lat)^1									-0.69	**< 0.001**
(c) (lat)^2									0.41	**< 0.001**
Residual SD	0.54		0.44		0.32		0.68		0.12	
Multiple R^2	0.03		0.04		0.25		0.10		0.84	
F-statistic	0.68		0.42		1.51		0.44		21.5	
P-value	0.51		0.65		0.27		0.65		**< 0.001**	

Minor-OPE	5 m	p	DCM	p	1%PAR	p	MOx	p	Deep	p
(a) Intercept	0.14	**< 0.001**	0.15	**< 0.001**	0.13	**< 0.001**	0.16	**< 0.001**	0.18	**< 0.001**
(b) $(lat)_1$	0.41	**< 0.001**	0.29	**0.002**	0.05	**< 0.001**	0.23	**0.005**		
(c) $(lat)_2$	0.27	**< 0.001**	0.33	**0.001**	0.16	**0.013**	0.23	**0.006**	0.29	**0.01**
Residual SD	0.07		0.09		0.05		0.06		0.09	
Multiple R^2	0.58		0.53		0.9		0.77		0.59	
F-statistic	23.8		12.7		23.12		13.64		5.87	
P-value	**< 0.001**		**< 0.001**		**0.0002**		**0.002**		**0.02**	

The table shows the significant estimated coefficients for the intercept and the two polynomial terms of latitude, along with their corresponding p-values (p) for different depths and compounds. For each model, we fitted a quadratic polynomial regression equation of the form: OPE = Intercept + $a \cdot (lat)^1 + b \cdot (lat)^2$ where lat^1 and lat^2 are the first and second polynomial terms of latitude, respectively.

The residual standard deviation (SD), multiple R-squared, F-statistic, and overall model p-value are also provided for each depth. To interpret the coefficients, note that significant p-values ($p < 0.05$), which are bolded in the table, indicate a meaningful relationship between latitude and Cl-OPE concentrations at the given depth.

Table S13. Wet Deposition and related surface sample concentrations (in ng L^{-1}) of individual and $\sum_{24}$OPE in the Atlantic Ocean, and calculation of EF_{WD} (C_{WD}/C_{SURF}) for those samples.

Sample code	Date	LAT	LONG	TEP	TCEP	∑TCPP	TBEP	TiBP	TDCIPP	TNBP	TPHP	EHDPP	∑TcPs	Minor	$\sum_{24}$OPE
AN1_ST10_surface	20201227	7.3	-29.6	<loq	1.61	11.29	<loq	0.44	0.11	<loq	1.16	0.40	0.01	nd	15.01
AN1_ST10_WD	20201227	7.3	-29.6	<loq	16.33	270.39	5.83	24.18	4.21	7.15	16.42	51.51	0.16	1.96	398.14
AN1_ST11_surface	20201228	3.8	-29.8	0.07	5.12	5.68	<loq	0.38	0.19	<loq	1.41	0.41	nd	nd	13.27
AN1_ST11_WD	20201228	3.8	-29.8	0.23	12.15	288.46	8.53	35.22	1.39	3.79	15.10	55.74	0.16	0.80	421.58

**nd non detected; <loq: concentration below limit of quantification.*

Table S14. Atmospheric aerosol concentrations of $\sum_{14}$OPEs (ng m^{-3}) from *Malaspina* (Castro-Jiménez et al., 2016) from latitudes ranging between 7°N and 0°N (top table) and rain water $\sum_{14}$OPEs (ng m^{-3}) concentrations from AN1_ST10 and AN1_ST11 2021 Atlantic campaign.

Atmospheric Aerosol (ng m^{-3})												
Sample	LAT	LONG	TCEP	TDCP	∑TCPP	TiBP	TnBP	TPhP	EHDPP	TEHP	∑TCPs	$\sum_{14}$OPEs
MA6	6.06	-25.9	0.08	0.10	0.96	0.07	0.44	0.01	0.18	0.41	0.01	2.24
MA7	0.29	-26.0	0.16	0.06	0.71	0.13	0.37	0.01	0.18	0.31	0.01	1.93

Rainwater (ng m^{-3})												
Sample	LAT	LONG	TCEP	TDCP	∑TCPPs	TiBP	TnBP	TPhP	EHDPP	TEHP	∑TCPs	$\sum_{14}$OPEs
AN1_ST10	7.35	-29.58	16326.0	4211.7	270391.0	24176.8	7150.0	16420.4	51508.0	1957.9	158.7	392300.0
AN1_ST11	3.83	-29.86	12154.8	1391.2	288457.0	35219.0	3790.4	15097.6	55742.2	803.0	163.3	412818.0

Table S15. Log K_{RP} values from the Atlantic Ocean.

$LogK_{RP}$										
Site	**TCEP**	**TDCIPP**	**∑TCPP**	**TiBP**	**TNBP**	**TPhP**	**EHDPP**	**TEHP**	**∑TcPs**	**$\sum_{14}$OPEs**
1	5,3	4,6	5,4	5,5	4,2	6,2	5,5	3,7	4,1	5,2
2	4,9	4,3	5,6	5,4	4,0	6,1	5,5	3,4	4,2	5,3
MEAN	5,1	4,5	5,5	5,5	4,1	6,1	5,5	3,5	4,2	5,3
SD	0,3	0,2	0,1	0,1	0,1	0,0	0,0	0,2	0,0	0,1

Table S16. Mean ± SD concentrations for different OPEs groups (ng L^{-1}) by ocean and depth.

	Atlantic Ocean (N=7)				**Southern Ocean (N=4)**			
	Cl-OPEs	**Aryl-OPEs**	**Alkyl-OPEs**	**Minor-OPEs**	**Cl-OPEs**	**Aryl-OPEs**	**Alkyl-OPEs**	**Minor-OPEs**
Surface	16.8 ± 14.4	3.31 ± 3.01	3.08 ± 3.26	0.20 ± 0.15	5.91 ± 3.21	1.45 ± 0.76	1.69 ± 0.96	0.09 ± 0.07
DCM	12.7 ± 7.62	2.44 ± 1.55	1.94 ± 2.09	0.20 ± 0.16	4.73 ± 1.90	1.08 ± 0.60	1.84 ± 0.73	0.13 ± 0.14
1%PAR	17.7 ± 20.0	3.55 ± 4.05	1.47 ± 1.17	0.20 ± 0.16	5.12 ± 1.98	1.43 ± 0.74	1.68 ± 0.18	0.05 ± 0.02
MOx	14.2 ± 11.6	2.36 ± 0.76	3.62 ± 4.20	0.21 ± 0.17	5.63 ± 2.11	1.85 ± 1.06	1.91 ± 0.46	0.12 ± 0.08
Deep	16.4 ± 14.1	2.07 ± 0.47	0.75 ± 0.11	0.21 ± 0.17	5.54 ± 0.56	1.83 ± 0.56	2.00 ± 0.34	0.21 ± 0.18

Table S17. Individual and $\sum_{24}$OPE concentration in vertical profiles from the Atlantic Ocean (ng L^{-1}).

Station Code	Depth Code	Depth (m)	Date (yymmdd)	LAT	LONG	TEP	TCEP	∑TCPP	TBEP	TiBP	TDCIPP	TNBP	TPhP	EHDPP	∑TcPs	Minor-OPE	$\sum_{24}$OPE
	SURF	5	201218	37.92	-15.97	2.65	2.90	8.72	<loq	0.86	0.37	<loq	2.78	<loq	nd	nd	18.3
	DCM	61	201218	37.92	-15.97	<loq	3.81	12.38	0.18	0.23	0.35	<loq	1.88	0.46	<loq	nd	19.23
AN1_ST01	1%PAR	115	201218	37.92	-15.97	nd	nd	nd	nd	nd	nd	nd	nd	nd	nd	nd	0.00
	MOx	848	201218	37.92	-15.97	<loq	4.21	11.04	0.23	0.54	0.65	<loq	2.18	0.57	<loq	nd	19.4
	DEEP	2000	201218	37.92	-15.97	nd	2.38	6.74	0.21	0.21	0.17	<loq	2.31	<loq	0.03	nd	12.0
	SURF	5	201221	28.66	-28.41	<loq	2.00	5.99	0.20	0.51	0.59	<loq	1.18	<loq	nd	nd	10.5
	DCM	125	201221	28.66	-28.41	<loq	2.21	7.91	0.33	0.47	0.62	<loq	1.87	0.49	nd	nd	13.9
AN1_ST04	1%PAR	86	201221	28.66	-28.41	<loq	<loq	2.50	<loq	0.15	0.12	<loq	0.88	<loq	nd	nd	3.65
	MOx	900	201221	28.67	-28.41	9.99	1.79	5.88	<loq	0.10	0.16	<loq	1.42	<loq	nd	nd	19.3
	DEEP	2000	201221	28.67	-28.41	<loq	1.69	6.64	<loq	0.24	0.40	<loq	1.29	<loq	nd	nd	10.3
	SURF	5	201226	10.87	-29.23	1.21	7.42	9.10	0.17	0.61	0.26	1.08	3.15	0.71	0.40	nd	24.1
	DCM	55	201226	10.87	-29.23	0.92	11.01	12.68	0.20	0.24	0.41	<loq	3.15	0.84	0.16	nd	29.6
AN1_ST09	1%PAR	50	201226	10.87	-29.23	1.48	6.29	13.18	0.16	0.45	0.33	<loq	2.49	0.76	<loq	nd	25.1
	MOx	400	201226	10.04	-29.33	<loq	2.41	13.98	<loq	0.26	0.11	<loq	1.70	<loq	<loq	nd	18.4
	DEEP	2000	201226	10.04	-29.33	<loq	11.03	5.21	<loq	0.13	0.10	<loq	1.45	0.33	<loq	nd	18.2
	SURF	5	201229	0.14	-30.50	8.20	3.37	25.20	<loq	2.97	0.49	<loq	3.13	0.63	nd	nd	44.0
	DCM	48	201229	0.14	-30.50	<loq	2.05	13.77	<loq	0.79	<loq	<loq	1.97	0.36	<loq	nd	18.9
AN1_ST12	1%PAR	78	201229	0.14	-30.50	0.05	3.55	10.62	0.19	0.49	0.50	<loq	2.36	0.47	nd	nd	18.2
	MOx	400	201229	0.14	-30.52	8.01	1.90	4.18	<loq	0.22	0.13	<loq	2.08	<loq	<loq	nd	16.5
	DEEP	2000	201229	0.14	-30.52	<loq	3.78	6.90	<loq	0.10	0.15	<loq	1.31	0.32	<loq	nd	12.6
	SURF	5	210102	-14.37	-33.92	nd	3.87	70.56	0.21	0.47	0.22	<loq	2.64	0.53	nd	nd	78.5
	DCM	110	210102	-14.37	-33.92	<loq	<loq	8.41	<loq	0.23	0.14	<loq	1.66	0.47	<loq	nd	10.9
AN1_ST15	1%PAR	145	210102	-14.37	-33.92	0.07	nd	1.27	nd	<loq	nd	<loq	<loq	<loq	nd	nd	1.34
	MOx	350	210102	-14.37	-33.93	1.52	2.61	35.75	<loq	0.29	0.08	<loq	1.87	<loq	<loq	nd	42.1
	DEEP	2000	210102	-14.37	-33.93	0.06	6.12	41.54	<loq	0.35	0.29	<loq	1.93	0.32	0.05	nd	50.7
	SURF	5	210105	-24.91	-38.72	0.53	2.84	18.37	2.80	0.30	0.11	2.27	5.05	6.06	4.21	nd	42.5
	DCM	55	210105	-24.91	-38.72	7.80	nd	11.56	nd	0.14	<loq	<loq	1.83	0.41	0.15	nd	21.9
AN1_ST18	1%PAR	80	210105	-24.91	-38.72	<loq	28.59	29.58	0.16	0.37	1.01	0.98	10.07	0.86	1.48	nd	73.1
	MOx	570	210105	-24.94	-38.72	0.24	<loq	8.03	0.39	0.13	0.11	<loq	2.69	0.80	0.32	nd	12.7
	DEEP	2000	210105	-24.94	-38.72	<loq	<loq	8.41	0.16	0.25	0.18	<loq	2.20	0.44	0.03	nd	11.7
	SURF	5	210109	-37.24	-48.09	<loq	<loq	8.51	<loq	0.20	0.09	<loq	nd	<loq	0.07	nd	8.87
	DCM	60	210109	-37.24	-48.09	0.33	<loq	2.37	<loq	0.23	<loq	<loq	0.75	<loq	nd	nd	3.68
AN1_ST22	1%PAR	70	210109	-37.24	-48.09	<loq	1.61	2.99	nd	0.30	0.08	<loq	0.65	<loq	nd	nd	5.63
	MOx	375	210109	-37.24	-48.09	<loq	<loq	3.02	<loq	0.06	<loq	<loq	1.15	0.33	<loq	nd	4.57
	DEEP	2000	210109	-37.24	-48.09	0.07	4.62	6.75	<loq	0.06	0.16	<loq	1.42	0.34	<loq	nd	13.4

*Category "minor-OPE" results from the sum of: TEHP, TPrP, TPPP, TBPO, TPPO, Chlorpyrifos, DOPP, TDMPP, TDBPP and TTBPP; nd = non detected; <loq = value below limit of quantification; ∑TCPP = sum of three TCPP isomers (TCPP1, TCPP2 and TCPP3); ∑TcPs = sum of three cresyl isomers (TpCP, TmCP and TpCP).

Table S18. Individual and $\sum_{24}$OPE concentration in vertical profiles from the Southern Ocean (ng L^{-1}).

Station Code	Depth Code	Depth (m)	Date (yymmdd)	LAT	LONG	TEP	TCEP	∑TCPP	TBEP	TiBP	TDCIPP	TNBP	TPHP	EHDPP	∑TcPs	Minor-OPE	$\sum_{24}$OPE
AN2_ST05	SURF	7	220127	-66.92	-69.10	0.41	0.93	6.29	1.21	0.23	0.22	<loq	0.81	1.36	0.01	0.00	11.47
	DCM	19	220127	-66.92	-69.10	0.36	0.43	3.24	1.70	0.13	0.11	<loq	0.34	1.14	0.00	0.00	7.45
	1%PAR	130	220127	-66.92	-69.10	0.19	0.66	4.00	0.77	0.23	0.22	<loq	0.44	1.23	0.00	0.00	7.73
	MOx	297	220127	-66.92	-69.10	nd	1.51	6.79	1.27	0.68	0.42	<loq	0.71	2.67	0.02	0.00	14.1
	DEEP	621	220127	-66.92	-69.10	0.15	1.94	3.74	0.72	0.63	0.25	<loq	0.41	1.35	0.01	0.00	9.19
AN2_ST07	SURF	5	220130	-70.85	-79.89	0.39	0.33	4.00	0.29	0.20	0.09	<loq	0.39	0.40	0.00	0.00	6.09
	DCM	21	220130	-70.85	-79.89	0.30	0.44	3.48	0.46	0.15	1.84	<loq	0.36	0.31	0.01	0.00	7.35
	1%PAR	75	220130	-70.85	-79.89	0.28	0.46	4.44	0.83	0.18	0.22	<loq	0.66	1.64	0.01	0.00	8.72
	MOx	211	220130	-70.85	-79.89	<loq	0.38	3.89	0.69	0.33	0.16	0.75	0.41	1.25	0.00	0.00	7.87
	DEEP	587	220130	-70.85	-79.89	0.28	0.97	3.95	1.20	0.18	0.34	<loq	0.45	1.06	0.00	0.00	8.43
AN2_ST10	SURF	5	220201	-67.70	-75.00	<loq	0.69	3.96	0.79	0.11	0.19	<loq	0.38	0.70	0.01	0.00	6.82
	DCM	49	220201	-67.70	-75.00	0.28	1.11	5.03	2.03	0.25	0.16	<loq	0.40	0.76	0.01	0.00	10.0
	1%PAR	200	220201	-67.70	-75.00	<loq	1.81	5.66	1.21	0.13	0.20	<loq	0.50	0.71	0.01	0.00	10.2
	MOx	1000	220201	-67.70	-75.00	0.16	0.47	4.57	0.55	0.23	0.15	<loq	0.65	0.53	0.00	0.00	7.32
	DEEP	2003	220201	-67.70	-75.00	<loq	1.02	4.86	0.85	0.18	0.21	<loq	0.60	0.80	0.01	0.00	8.53
AN2_ST11	SURF	5	220204	-62.57	-58.62	nd	1.16	12.57	3.46	0.36	0.24	<loq	1.20	1.01	0.02	0.00	20.0
	DCM	37	220204	-62.57	-58.62	<loq	0.90	3.49	1.59	0.23	0.17	<loq	0.32	1.51	0.01	0.00	8.23
	1%PAR	201	220204	-62.57	-58.62	<loq	0.77	1.97	0.83	0.10	0.08	<loq	0.20	0.33	0.00	0.00	4.30
	MOx	850	220204	-62.57	-58.62	0.14	1.27	2.73	1.15	0.16	0.17	<loq	0.30	0.83	0.03	0.00	6.78
	DEEP	1618	220204	-62.57	-58.62	nd	1.28	3.39	1.60	0.25	0.22	<loq	0.39	1.91	0.34	0.00	9.38

**Category "minor-OPE" results from the sum of: TEHP, TPrP, TPPP, TBPO, TPPO, Chlorpyrifos, DOPP, TDMPP, TDBPP and TTBPP; nd = non detected; <loq = value below limit of quantification;* ∑TCPP = sum of three TCPP isomers (TCPP1, TCPP2, and TCPP3); ∑TcPs = sum of three cresyl isomers (TpCP, TmCP and TpCP). *Stations 10 and 11 showed strong mixing and weak MOx layer.*

References

Estrada, M. (2012) in Libro blanco de métodos y técnicas de trabajo oceanográfico en la Expedición Malaspina, 399-345.

Gasol, J. M.& Moran, X. A. G. (2015). Flow Cytometric Determination of Microbial Abundances and Its Use to Obtain Indices of Community Structure and Relative Activity. McGenity, T. J.; Timmis, K. N.; Nogales Fernández, B. Hydrocarbon and Lipid Microbiology Protocols. Biochemical Methods; Springer Protoc. Handbooks, 159-187.

Smith, D. C.& Farooq, A (1992). A simple, economical method for measuring bacterial protein synthesis rates in seawater using 3H-leucine. Environmental Science.





PART 03

CHAPTER 4.
SCIENTIFIC OUTREACH WITHIN ACADEMIA

3.4.1. Paper V. *Balancing the equation: A tool for evaluating effective scientific outreach*

3.4.2. Paper V. Supplementary Materials

PART 03 - CHAPTER 4. SCIENTIFIC OUTREACH WITHIN ACADEMIA

3.4.1. Paper V. *Balancing the equation: A tool for evaluating effective scientific outreach*

Núria Trilla-Prieto[1,2], Maria Paula Carrillo[1], Clara Serrano[1], Jon Iriarte[1], Jessica Patrone[1], Naiara Berrojalbiz[1]

[1]Department of Environmental Chemistry, IDAEA-CSIC, 08034, Barcelona, Catalunya, Spain, +34 934006100.

[2]Department of Evolutionary Biology, Ecology and Environmental Sciences, Faculty of Earth Sciences, Universitat de Barcelona, 08028, Barcelona, Catalunya, Spain, +34 934021336

*Corresponding author: nuria.trilla@idaea.csic.es, +34610342471.

ABSTRACT

Scientific outreach bridges science and society and fosters trust and societal progress. However, it is undervalued in academia because of its limited recognition, resources, and training. This study introduces a novel evaluation tool to assess the effectiveness of outreach across seven qualitative and quantitative parameters. Applied to diverse initiatives, it highlights successes and areas for improvement. Structured evaluations help prioritize impactful activities and refine strategies. Addressing barriers, such as time constraints and inadequate training through institutional support and professional collaborations, can elevate outreach quality. This framework empowers scientists to engage effectively and to build a more informed society.

INTRODUCTION

Scientific outreach, or science communication, aims to make scientific knowledge accessible and engage non-experts, including the public and policymakers (Burns, O'Connor, & Stocklmayer, 2003). This powerful mechanism fosters connections between the work of scientists and its broader societal impact, building public trust, informing policies, improving education, and inspiring social change (Hopf et al., 2019; Scheufele & Krause, 2019). By directly engaging with the public, scientists can play a critical role in filtering and clarifying information, countering misconceptions, and promoting a more informed and critically aware society.

On a personal level, scientists often find outreach deeply rewarding and beneficial. The motivation to engage in such activities frequently stems from intrinsic factors, such as a commitment to public education, a desire to emphasize the societal relevance of their work, or the satisfaction of influencing public discourse (Weingart & Guenther, 2016). Many scientists also find outreach enjoyable and fulfilling, adding to its appeal (Andrews et al., 2005; Woitowich et al., 2022). Moreover, outreach provides valuable opportunities to refine essential communication skills, enabling researchers to convey complex scientific ideas effectively to diverse audiences, including the public, funding bodies, and policymakers (Dudo, 2013; Jensen et al., 2008). It also serves as a platform for receiving constructive feedback, improving public engagement, and guiding future research, all while fostering a stronger connection between science and society (Andrews et al., 2005; Jensen et al., 2008).

Communication, however, is often undervalued in academia, where publishing and securing grants dominate the focus of curricula evaluations. Outreach is frequently perceived as a secondary responsibility within academic institutions, discouraging senior academics from investing time and effort in public engagement. In fact, evidence indicates that outreach activities are disproportionately undertaken by women and early-career researchers (Andrews et al., 2005; Ecklund, James, & Lincoln, 2012). Although many prestigious institutions claim that scientific outreach is a priority (Jensen et al., 2008), truth is that outreach is rarely rewarded, whether through recognition or economically, contributing to its perception as an optional rather than essential part of academic life. A survey carried out by the Royal Society in 2006 found that not only do scientists feel they receive little or no reward from their engagement in outreach, but their participation may even be detrimental to their careers. In addition, previous reports have shown that the main factors hindering participation in outreach activities include a lack of time and resources (Andrews et al., 2005; Hopf et al., 2019; Michelle, Pooni, & Hartfree, 2001; Woitowich et al., 2022) and a lack of preparation or effective interaction with the public (Jensen et al., 2008; Varner, 2014).

Formally recognizing outreach activities is essential for reshaping the current perspective. This would require the effective integration of outreach into the academic and research culture, with outreach efforts incorporated into academic evaluations to ensure they are valued alongside research achievements in grant assessments, promotion decisions, and performance reviews. Such an approach would incentivize scientists to engage in high-impact outreach, rewarding those who pursue strategic, in-depth public engagement over those who treat outreach as a mere formality. Institutions might implement appropriate evaluation tools that incorporate key parameters for objectively assessing outreach efforts. Establishing clear standards for meaningful outreach would further support its recognition, ensuring that valuable contributions to science communication are properly acknowledged by institutions and funding bodies.

Despite its crucial role, outreach is often approached with little formal planning or evaluation, as highlighted by Varner (2014), who argues that outreach must be practiced with the same rigor as the science itself. There is a significant lack of structured frameworks to systematically create, design, implement and evaluate the effectiveness of outreach activities. Furthermore, the absence of clear goals and evaluative frameworks limits the ability to compare different initiatives and improve outreach outcomes. A tool that incorporates these parameters can provide a clear assessment of outreach success and can allow a more realistic comparison across diverse activities, helping scientists allocate their efforts for maximum impact and, ultimately, increasing their participation in impactful outreach.

To the authors' knowledge, no current tools exist for a comprehensive, global, and qualitative evaluation of scientific outreach activities. Existing assessment methods often focus on quantitative reach, such as the number of people engaged, without fully accounting for other essential factors that influence the effectiveness of outreach. For instance, while it may be tempting to consider an activity that reaches 10,000 people more effectively than one that reaches only 20, the true value depends on multiple dimensions, including audience engagement and specificity, the time and resources invested, the depth of communication achieved, and the impact the activity has on the audience's future actions.

The **objectives** of this study are to: (a) propose a new, adaptable, and user-friendly qualitative tool to evaluate the effectiveness of scientific outreach activities for scientist and institutions, (b) validate the proposed evaluation method by applying it to real outreach activities, and (c) analyze the potential impact of several traditional and innovative outreach activities and highlight their respective pros and cons using the evaluation tool.

MATERIALS AND METHODS

Development of the evaluation tool. To establish a systematic approach to evaluating the effectiveness of outreach activities, a simple yet impactful qualitative assessment method was developed. Designed for universal application, this tool enables scientists and outreach professionals worldwide to assess and enhance their initiatives.

The evaluation tool operates as follows: after the first implementation of an outreach activity, the facilitator(s) must complete an evaluation form based on their experiences. The form evaluates the activity across seven categories: audience reach, engagement, time investment, economic investment, target audience specificity, long-term impact, and facilitator perception, assigning a score from one to five for each category based on predefined criteria **(Table S1)**. After scoring each category, the seven scores are summed to obtain a total score, which scales up to 35 points. This total score is used to classify the activity into a specific category of effectiveness and priority **(Table S2)**, helping facilitators identify strengths and areas for improvement. These selected categories encompass both qualitative and quantitative parameters, as well as objective and subjective criteria, the latter based on the facilitator's perception of the success of the activity. When multiple people are facilitating the same activity, each individual facilitator should independently complete the form. After all forms are filled out, the results are calculated by taking the average of all the individual responses. Additionally, it is recommended that during the first implementation of an outreach activity, a neutral observer also evaluates the activity using the same form. The final result should then include the average scores from both the facilitators and the neutral observer, providing a more comprehensive and balanced assessment. Other considerations regarding the use of the tool and its application in specific scenarios are detailed in **Note S1**. To facilitate the widespread use of this tool, a template for scientists and institutions to evaluate their own activities is provided in **Table S3**.

Validation of the evaluation tool, real-world outreach activities. To evaluate the functionality of the tool and demonstrate its utility, it was pilot tested on a diverse set of real-world outreach activities conducted by scientists. All activities were carried out as part of the Spanish National Project "PANTOC" (Persistent Anthropogenic Organic Carbon in the Oceans and Antarctica), aiming to understand the impact of chemical pollution and microbial interactions in marine environments, particularly relevant in the context of global environmental change. Activities were selected to ensure diversity in terms of format (e.g., in-person versus online), target audience (e.g., general public, school students, or professionals), and geographic reach. Facilitators evaluated these outreach activities using the evaluation tool. The results of these evaluations are presented in **Table S4.**

The primary communication focus of the PANTOC project was to create a social media channel to enhance science communication, specifically utilizing Instagram and TikTok under the name of the National Project (@pantoc_project). A detailed communication plan was developed and implemented, resulting in weekly publications in various formats, including posts, carousels, and reels. This strategy successfully engaged an audience of 1,000 followers and achieved a reach of nearly 100,000 people within a year. Additionally, virtual connections with Spanish Antarctic stations (BAE Juan Carlos I, and BAE Gabriel de Castilla, at Livingston and Deception Islands, respectively) were performed, featuring school talks and live sessions open to the public, which were announced in advance on the project's social media.

On the more innovative side, two novel activities were also designed and performed. The first involved partnering with an organization that creates 360º virtual experiences for elderly people (Amatller, 2024). Briefly, through this collaboration the PANTOC team documented an Antarctic campaign using 360º cameras, which resulted in an immersive video that highlighted life and research in Antarctica. This video was projected using Virtual Reality Glasses in nursing homes across the country. This allowed residents to explore and experience Antarctica without leaving their facilities.

The second activity was a pilot initiative, performed in collaboration with the city council of a Spanish city, aimed at integrating scientific learning into everyday activities, such as commuting. Briefly, the activity involved a team of three facilitators traveling along a metro line for three hours, engaging with passengers using a quiz about Antarctica and discussing their responses.

In addition to these innovative efforts, the project also included a variety of traditional outreach activities, performed multiple times and in different formats. These included online school talks, virtual sessions, in-person talks in museums, participation in science fairs, and other community events, ensuring a broad and diverse engagement with audiences of all ages **(Table S4).**

DISCUSSION

Framework for developing and evaluating outreach activities. The systematic evaluation of outreach activities is essential for enhancing their effectiveness and impact. The development of these activities typically involves three key stages: brainstorming, detailed planning, and implementation. While this progression is straightforward in theory, it is often hindered in practice by the tendency to repeat activities without substantial revision. This limits opportunities for refinement and improvement, reducing the potential impact of outreach efforts **(Figure 1).**

The proposed evaluation tool addresses this gap by integrating a structured assessment phase into the outreach process. Following the initial implementation of an activity, facilitators can utilize the tool to critically evaluate its performance and outcomes **(Figure 2).** This systematic approach allows facilitators to make informed decisions, including whether to adjust the activity for improvement, validate its success for further scaling, or discontinue efforts that do not meet desired standards. Such an iterative process fosters continuous improvement and ensures that only well-designed and impactful activities are prioritized for broader application.

By embedding evaluation into the outreach development cycle, the tool offers a transformative framework for science communication. It empowers facilitators to identify weaknesses, amplify strengths, and refine their strategies. Beyond improving individual activities, this approach establishes a culture of rigorous planning and systematic improvement. The resulting framework not only optimizes outreach efforts but also provides a valuable resource for institutions seeking to evaluate and prioritize initiatives. For funding bodies, this tool delivers insights into the success and societal impact of activities, moving beyond traditional metrics like the number of events conducted. Instead, it enables a nuanced assessment of engagement and long-term impact, ultimately fostering more meaningful and impactful connections between science and society.

Application of the Evaluation Tool. The application of the evaluation tool to real-life outreach activities demonstrated its utility in systematically assessing their effectiveness and impact, highlighting strengths, weaknesses, and opportunities for improvement. By categorizing activities based on their performance and analyzing specific parameters, the tool provided valuable insights into optimizing outreach efforts to maximize impact and better allocate resources.

The evaluated activities **(Table S4)** were classified into three of the six established groups: basic outreach impact with margins for improvement, moderately effective outreach activities, and highly effective outreach activities. These categories reflect varying levels of impact, engagement, and resource utilization, offering a framework for prioritizing and refining future initiatives.

Basic outreach impact with margins for improvement: the Science in the metro activity obtained the lowest score and was the only activity classified within this category. While this activity required minimal time and financial resources, it did not score positively on any other parameters, reflecting its limitations in approach, performance, engagement, and overall impact. Facilitators found it challenging to find individuals willing to participate and listen, as most passengers were apathetic and likely busy in their own activities such as reading, listening to music, chatting, or scrolling on the cell phone.

This suggests that scientific outreach may be less effective in contexts where the audience is focused on personal tasks or entertainment, rather than actively seeking scientific engagement. Therefore, the facilitators concluded the activity with the impression that the approach was neither functional nor successful. Such insights emphasize the importance of listening to facilitators, whose experiences provide critical indicators of an activity's success and guide its refinement or discontinuation.

Moderately effective outreach activities: talk-based activities assessed across various formats were rated within this category. These activities were cost-effective and helped foster critical thinking and environmental awareness. However, their impact on long-term engagement and audience reach remained limited. Talks were easy to prepare, with content and visuals structured efficiently, and typically required only one to two hours to deliver.

Certain lower-scoring parameters in the evaluation, such as limited audience reach in live school and museum talks, are inherent to the activity type and thus challenging to modify. One effective solution could be to perform the same activities in a virtual format, where a wider audience can be reached with minimal logistical requirements. However, online experiences tend to be less personal, and the public is more prone to disconnect than in-person interactions with smaller

groups. It has also been proven that in-school visits were more successful in engaging students from historically underrepresented backgrounds with STEM than open house events (Gall, Vollbrecht, & Tobias, 2020; Kaggwa et al., 2023; Vennix, den Brok, & Taconis, 2018). Consequently, efforts to enhance the impact of these activities should focus on modifiable aspects, such as fostering long-term partnerships with schools and museums or developing streaming formats that prioritize engagement.

Highly effective outreach activities: The project included two activities within this group, the social media approach and the virtual experience for the elderly. Both demonstrated strong engagement, long-term impact, and high value for both audiences and facilitators.

The social media initiative leveraged platforms such as Instagram and TikTok to communicate scientific content effectively. Although audience reach is a challenging parameter to optimize, social media remains a key tool for broadening reach and maximizing impact [Meyer et al., 2018]. It has been observed, for example, that young adults regularly use social media as a mean to engage with science and research (Hargittai, Füchslin, & Schäfer, 2018). Establishing a dedicated channel to share information about a specific scientific field has proven to be highly effective, relatively cost-free, and, when done well, can become a powerful tool to reach a wider audience (Stofer, Hecht, & Lundgren, 2023). Meyer et al. (2018) successfully created an outreach social media initiative to communicate oceanographic research. Over three years, they have engaged over 7,000 followers across 100 countries, with Instagram being the most successful platform for engaging young, science-oriented audiences. Their findings highlight the ability of social media to boost research visibility, engage with diverse demographics, and foster public trust in science by making complex topics more accessible.

This approach requires a significant but highly rewarding time allocation effort from communicators. It also was a link to many other activities and connections, that came from social media presence, and to date, the account remains active for future research projects. However, finding a balance between effective outreach and manageable workloads remains a challenge for many researchers, and even when approached as a team effort, it can be difficult to maintain a high publishing rate over extended periods.

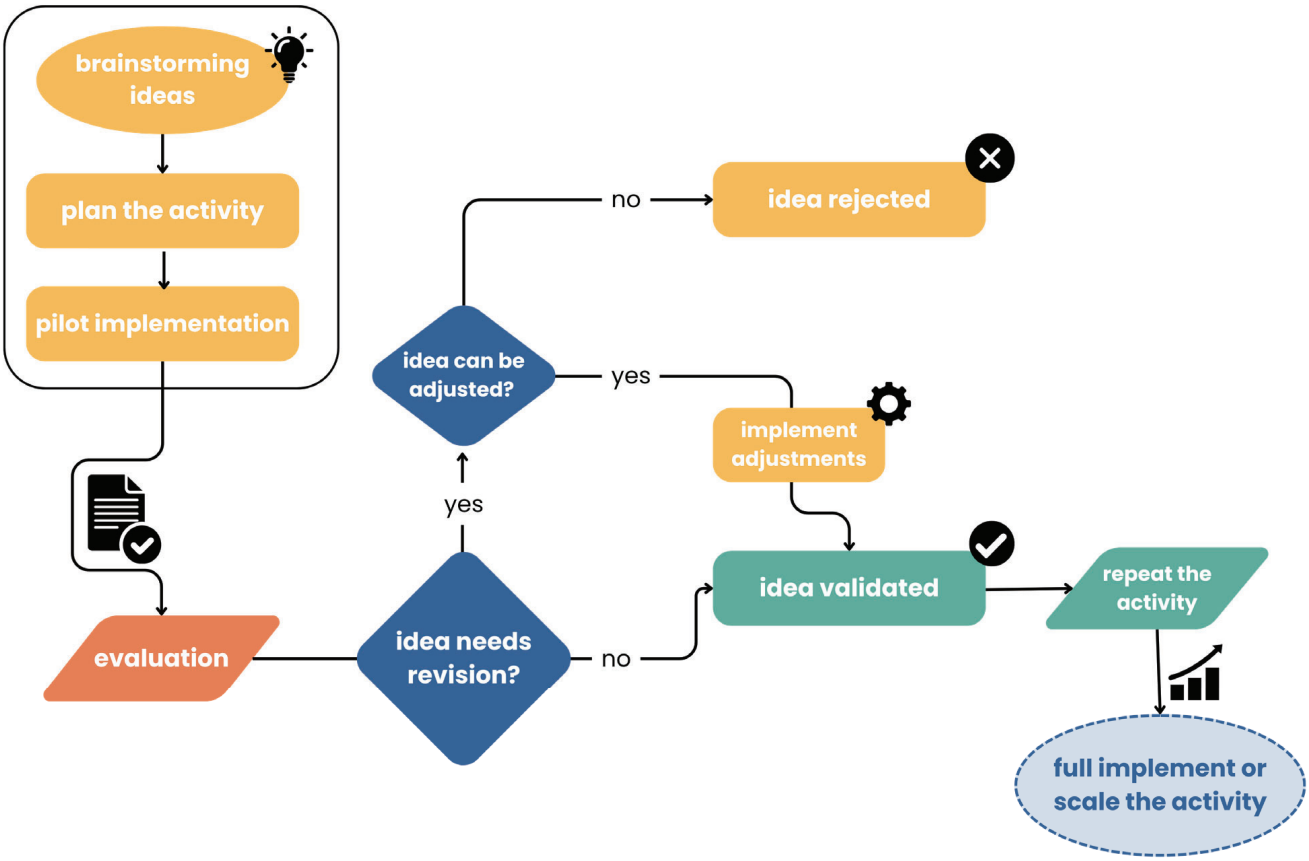


Figure 1 | Flowchart illustrating the ideal process for developing and refining outreach activities.

Moreover, research groups are still underrepresented on social media (Pavlov et al., 2018) as scientists often encounter difficulties convincing senior leaders to use social media for science outreach. Finally, creating engaging and catchy content must be balanced by maintaining accuracy and reliability, ensuring that the audience receives trustworthy and well-communicated information.

Finally, the highest scoring activity was the virtual experience for nursing homes. It provided an immersive Antarctic experience for elderly participants. Despite limitations in audience reach owing to restricted access to electronic devices, it demonstrated remarkable audience interaction and specificity. This particular case highlights the importance of collaboration in science outreach, since the investment of time and resources from the collaborators was key for recording and communicating the work. Likewise, without funding from the National Project, an Antarctic virtual experience would not have been possible.

Beyond traditional outreach activities, innovative approaches can serve as powerful channels for disseminating science. Unique formats—such as interactive exhibits in unexpected locations, science-themed art installations, documentaries or immersive experiences using virtual and augmented reality—can capture diverse audiences and engage people in novel ways [Rosin et al., 2023; Rosin et al., 2019; Sandu, Christensen, & Noirlab, 2011]. By integrating science into cultural events, such as art festivals, Rosin et al. successfully reached non-traditional audiences, demonstrating the effectiveness of participant-centered activities in inclusive science communication. Collaboration with non-traditional partners, such as city councils for public installations or local businesses for science pop-ups, further extends the reach and accessibility of scientific information. These creative approaches not only attract attention, but also deepen engagement, making scientific concepts more memorable and approachable for the public. Exploring innovative approaches beyond one-way communication, such as interactive and dialogic methods, has been shown to be more successful and effective in fostering mutual trust, enhancing knowledge retention, and generating enthusiasm among audiences (Rosin et al., 2023; Rosin et al., 2019; Sandu, Christensen, & Noirlab, 2011; Varner, 2014).

The evaluation of the project's real-life activities illustrates how this qualitative assessment enables (i) prioritization of high-impact activities and (ii) identification of areas for improvement in activities with suboptimal features. By systematically applying the tool, outreach efforts can be optimized to maximize their impact, ensuring that resources are allocated effectively and initiatives better meet the needs of their target audiences.

Potential use of the evaluation tool in academic institutions. To ensure that researchers' efforts to design and develop outreach projects are meaningful, institutions and scientists should prioritize activities that demonstrate measurable effectiveness and align with strategic goals. By employing tools such as this proposed evaluation framework, which objectively assesses outreach based on key parameters, scientists can identify activities that offer the highest value for the time and resources invested. Meanwhile, institutions can identify impactful activities in which to invest, thereby maximizing public engagement and enhancing the overall impact of science outreach.

Evaluating these activities provides the first step towards a more comprehensive view of scientific knowledge sharing within academic culture. Analyzing the effectiveness of the projects not only in terms of audience engagement but also scientists' effort investment allows for a greater emphasis on quality and accessibility in communication over simple productivity metrics. Emphasizing quality over quantity will ultimately foster sustainable, high-impact science communication that enriches both the society and the scientific community.

Institutions and funding bodies should establish clear standards to differentiate and recognize meaningful outreach efforts in scientific evaluations and professional criteria. The global, universal tool proposed in this study can serve this purpose by assessing the impact, strategy, and engagement of scientists, thus rewarding those attempting to maximize the impact of their outreach initiatives rather than those completing outreach as a mere formality. Financial support from institutions would help eliminate significant barriers and enable scientists to pursue public engagement without compromising their research funds.

In addition, formally recognizing outreach activities within official working hours is essential for fostering sustainable and balanced public engagement among scientists. By treating outreach as an integral component of professional responsibility, institutions would reinforce its value and legitimacy within the scientific profession. This acknowledgment would relieve scientists from choosing between advancing their research and dedicating their personal time to public engagement. A formal structure that accommodates outreach within academic duties would likely result in greater participation in and commitment to outreach activities, as scientists could pursue these initiatives with institutional support rather than as voluntary or extracurricular tasks. Furthermore, the successful implementation of impactful outreach ideas requires proper communication training. High-

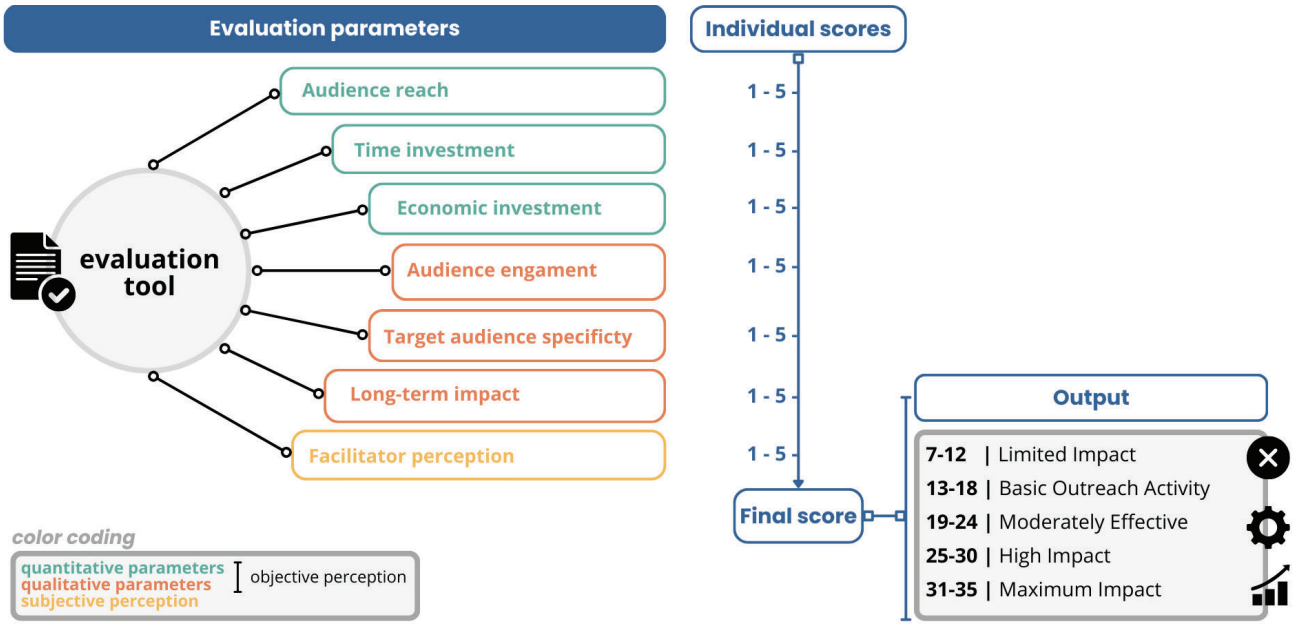


Figure 2 | Overview of the evaluation tool and scoring system for assessing scientific outreach activities.

quality courses should be offered regularly at both the undergraduate and professional scientific levels to equip scientists with essential public engagement skills. This training would prepare them to navigate the complexities of sharing scientific knowledge in an accessible, accurate, and engaging manner while keeping them up-to-date with best practices in science communication. Alternatively, institutions should consider investing in collaboration between scientists and professional communicators as a powerful combination. This partnership could result in outreach initiatives that are not only scientifically accurate, but also highly engaging for the public, thus amplifying the impact of scientific work.

CONCLUSIONS

To promote impactful and meaningful scientific outreach, it is essential to implement careful evaluation and planning as foundational steps. The qualitative evaluation scores demonstrate that, while many outreach activities have a significant impact, there is often room for improvement in their effectiveness and engagement. The proposed tool plays a critical role in this process, enabling researchers to identify the strengths and weaknesses of their initiatives. Structured evaluations can help scientists optimize their efforts and ensure that their activities are both effective and impactful.

The evaluation tool, not only does it serve as a resource for scientists and institutions to assess their own activities, but it can also be utilized for grant and project evaluations. This application can enhance the quality of parameters evaluated, providing higher scores for activities that consider diverse variables contributing to their success. By incorporating such an approach, the quality of scientific outreach activities can improve significantly.

Addressing barriers to impactful outreach, such as researchers' time constraints and lack of formal training, requires institutional support. This includes embedding communication training in education, recognizing outreach in academic evaluations, and allocating dedicated resources. Collaborative models, including hybrid roles and partnerships with professional communicators, can further enhance outreach quality and reach. By prioritizing these changes, institutions can empower scientists to engage more effectively with the public, bridging the gap between discovery and understanding while fostering a culture in which science actively supports societal progress.

ACKNOWLEDGMENTS

We would like to thank Prof. Jordi Dachs, Dr. Maria Vila-Costa, and all the researchers involved with the Global Change and Biogeochemistry Research Group (IDAEA-CSIC) for their support and collaboration in our outreach initiatives. We also thank the communication department of IDAEA-CSIC for their support and

initiative. N.T.P., M. P. C., and C. S. acknowledge a predoctoral fellowship (PRE2019-089641, FPU20/03595, and PRE2021-098386, respectively) from the Spanish Ministry of Science. This work was supported by the Spanish Research Agency through projects PANTOC (PID2021-127769NB-I00) and MIQAS (PID2021-128084OB-I00). The Global Change and Genomic Biogeochemistry Research Group received support from the Catalan Government (2021-SGR-00448).

Declaration of Conflicting Interest

The authors declared no potential conflicts of interest with respect to the research, authorship, and/or publication of this article.

Author Contributions

NTP conceived the work. NTP, MPC and CS wrote the manuscript. All authors contributed to the discussion and final version of the manuscript. All authors also contributed to perform the activities described and evaluated by the tool.

Supplementary Information

Supplementary Information such as details on the use of the Evaluation Tool, a template to use it, the results of our personal experience with the evaluation tool, and the details for scoring the parameters are presented in Supplementary Information **(Note 1, and Tables 1-4).**

REFERENCES

Amatller, D. (2024). Inclusive Communication. Més Que Ciència. Retrieved from https://www.mesqueciencia.cat/

Andrews, E., Weaver, A., Hanley, D., Shamatha, J., & Melton, G. (2005). Scientists and public outreach: Participation, motivations, and impediments. Journal of Geoscience Education, 53(3), 281–293.

Burns, T. W., O'Connor, D. J., & Stocklmayer, S. M. (2003). Science communication: A contemporary definition. Public Understanding of Science.

Dudo, A. (2013). Toward a Model of Scientists' Public Communication Activity: The Case of Biomedical Researchers. Science Communication, 35(4), 476–501.

Ecklund, E. H., James, S. A., & Lincoln, A. E. (2012). How academic biologists and physicists view science outreach. PLoS ONE, 7(5).

Gall, A. J., Vollbrecht, P. J., & Tobias, T. (2020). Developing outreach events that impact underrepresented students: Are we doing it right? European Journal of Neuroscience, 52(6), 3499–3506.

Hargittai, E., Füchslin, T., & Schäfer, M. S. (2018). How Do Young Adults Engage With Science and Research on Social Media? Some Preliminary Findings and an Agenda for Future Research. Social Media and Society, 4(3).

Hopf, H., Krief, A., Mehta, G., & Matlin, S. A. (2019). Fake science and the knowledge crisis: Ignorance can be fatal. Royal Society Open Science. Royal Society Publishing.

Jensen, P., Rouquier, J. B., Kreimer, P., & Croissant, Y. (2008). Scientists who engage with society perform better academically. Science and Public Policy, 35(7), 527–541.

Kaggwa, R. J., Blevins, A., Wester, E., Arango-Caro, S., Woodford-Thomas, T., & Callis-Duehl, K. (2023). STEM Outreach to Underresourced Schools: A Model for Inclusive Student Engagement. The Journal of STEM Outreach, 6(1).

Meyer, A., Pavlov, A. K., Rösel, A., Negrel, J., Itkin, P., Cohen, L., King, J., Gerland, S., Hudson, S. R., de Steur, L., Dood, P.A., Crews, L., Bratrein, M., Granskog, M.A., & Cobbing, N. (2018). Science outreach using social media: Oceanography from the lab to the public. Oceanography, 31(2 Special Issue), 11–15.

Michelle, C., Pooni, K., & Hartfree, Y. (2001). The role of scientists in public Debate. London: The Wellcome Trust.

Pavlov, A. K., Meyer, A., Rösel, A., Cohen, L., King, J., Itkin, P., Negrel, J., Gerland, S., Hudson, S.R., Dood, P.A., de Steur, L., Mathisen, S., Cobbing, N., & Granskog, M. A. (2018). Does your lab use social media? Sharing three years of experience in science communication. Bulletin of the American Meteorological Society. American Meteorological Society.

Rosin, M. S., Storksdieck, M., O'Connell, K., Keys, B., Hoke, K., & Lewenstein, B. V. (2023). Broadening participation in science through arts-facilitated experiences at a cultural festival. PLoS ONE, 18(5 May).

Rosin, M., Wong, J., O'Connell, K., Storksdieck, M., & Keys, B. (2019). Mark Rosin et al, Guerilla Science: Mixing Science with Art, Music and Play in Unusual Settings Guerilla Science: Mixing Science with Art, Music and Play in Unusual Settings.

Sandu, O., Christensen, L. L., & Noirlab, N. (2011). Outrageous Outreach-Unconventional Ways of Communicating Science. CAP Journal, 11, 22-30. Retrieved from https://www.researchgate.net/publication/253871076_Outrageous_Outreach_---_Unconventional_Ways_of_Communicating_Science

Scheufele, D. A., & Krause, N. M. (2019). Science audiences, misinformation, and fake news.

Proceedings of the National Academy of Sciences of the United States of America, 116(16), 7662–7669.

Stofer, K. A., Hecht, K., & Lundgren, L. (2023). Using Social Media to Engage Communities with Research: Accessibility. EDIS, 2023(1).

Varner, J. (2014). Scientific outreach: Toward effective public engagement with biological science. BioScience. Oxford University Press.

Vennix, J., den Brok, P., & Taconis, R. (2018). Do outreach activities in secondary STEM education motivate students and improve their attitudes towards STEM? International Journal of Science Education, 40(11), 1263–1283.

Weingart, P., & Guenther, L. (2016). Science communication and the issue of trust. Journal of Science Communication, 15(5), C01. https://jcom.sissa.it/article/pubid/JCOM_1505_2016_C01/

Woitowich, N. C., Hunt, G. C., Muhammad, L. N., & Garbarino, J. (2022). Assessing motivations and barriers to science outreach within academic science research settings: A mixed-methods survey. Frontiers in Communication, 7, 907762.

PART 03 - CHAPTER 4. SCIENTIFIC OUTREACH WITHIN ACADEMIA

3.4.2. Paper V. Supplementary Information

Note S1

Tables S1-S4

Balancing the equation: A tool for evaluating effective scientific outreach

Núria Trilla-Prieto[1,2]*, Maria Paula Carrillo[1], Clara Serrano[1], Jon Iriarte[1], Jessica Patrone[1], Naiara Berrojalbiz[1]

[1]Department of Environmental Chemistry, IDAEA-CSIC, 08034, Barcelona, Catalunya, Spain, +34 934006100.
[2]Department of Evolutionary Biology, Ecology and Environmental Sciences, Faculty of Earth Sciences, Universitat de Barcelona, 08028, Barcelona, Catalunya, Spain, +34 934021336

*Corresponding author: nuria.trilla@idaea.csic.es, +34610342471

Notes

Note S1. Details on the use of the evaluation tool.

Tables

Table S1. Evaluation criteria for scientific outreach activities. The table provides a description for each parameter evaluated to assess the execution and results of outreach activities. Each activity receives a score from 1 to 5 based on its performance relative to the criteria below.

Table S2. Summary of outreach activity scores and ranking. The table provides a proposed ranking based on the total scores from the evaluation in Table S1, guiding prioritization and assessing the overall impact and effectiveness of each outreach activity.

Table S3. Activity evaluation model.

Table S4. Evaluation of outreach activities conducted within our project. This table presents the parameters and scores for outreach activities that were implemented as part of our project, highlighting the performance of each real-world initiative.

Note S1. Details on the use of the evaluation tool.

This evaluation tool was designed to balance objectivity and practicality while accommodating the diverse contexts in which outreach activities occur. A key objective in its development was to ensure the tool remains simple, quick to implement, and easy to use, making it accessible and suitable for a wide range of scientists and institutions. Below are key considerations regarding its use and how the evaluation criteria are operationalized:

(a) Multiple Facilitators:
When more than one facilitator is involved in executing an activity, the final score for each category is calculated by taking the mean of the individual scores submitted by each facilitator. This approach ensures that the evaluation captures the collective experiences and perspectives of all facilitators without requiring additional complexity.

(b) Economic Investment:
The economic investment category considers the resources required to execute the activity, including financial costs, materials, and other logistical expenses. This category is highly context-dependent, as the level of investment can vary significantly between countries, depending on available resources, institutional support, and opportunities for collaboration with other entities. To address disparities, facilitators are encouraged to consider three distinct components:

a. Costs incurred by the individual or research group, excluding salaries but including transportation and materials.
b. Economic costs covered by collaborators, such as partner organizations or institutions.
c. Salaries for facilitators, if applicable, as a separate parameter.

Each of these components should be scored independently, and the final economic investment score is obtained by averaging the scores of the three parameters. This approach ensures a balanced evaluation that reflects both individual and collective efforts while accounting for variations in financial support and resource allocation. Facilitators are also encouraged to explore partnerships with local organizations, leverage existing resources, and seek external funding or sponsorships to minimize financial barriers.

(c) Audience Engagement, Target Audience Specificity, and Long-term Impact:
While these criteria include subjective elements, they are operationalized with specific guiding questions to make evaluations consistent and meaningful. Facilitators assess these categories as follows:

- Audience Engagement: Facilitators consider observable indicators such as active participation, questions asked, and audience demeanor during the activity. Engagement levels are categorized into degrees of interest—curious, active, and passionate—based on predefined examples provided in Table S1.
- Target Audience Specificity: This criterion evaluates how well the activity aligns with its intended audience. Facilitators reflect on whether the activity content, format, and communication style were tailored appropriately to the target demographic.

(d) Long-term Impact:
This category requires facilitators to reflect on whether the activity likely sparked curiosity, inspired further interest in science, or led to follow-up actions (e.g., participants engaging in additional science-related activities). Although facilitators cannot directly measure long-term retention, guiding questions help them infer potential impact based on audience behavior during and after the event. For institutional contexts, follow-up surveys or feedback from participants could be implemented to substantiate this assessment.

(e) Facilitator Perception:
This criterion explicitly captures the subjective impression of the facilitator regarding the success of the activity and audience response. While other criteria (e.g., engagement and long-term impact) are partially influenced by facilitator perception, this category is intended to provide a holistic, personal evaluation of the activity's overall success and reception.

(f) Secondary Audience Effects and Contextual Factors:
Secondary audience effects (e.g., participants sharing knowledge or experiences with others after the outreach activity) and in-kind support are valuable but challenging to quantify. While facilitators are encouraged to note these factors in their evaluation, they remain supplementary considerations rather than core scoring criteria to maintain simplicity and scalability of the tool.

(g) Independent Evaluators:
To enhance objectivity, it is recommended—though not mandatory—that an independent observer (neutral to the facilitation team) evaluates the activity during its first implementation. This observer would complete the same evaluation form, and their scores would be averaged with those of the facilitators to provide a balanced assessment. This recommendation is especially important when institutions use the tool to assess and compare outreach activities.

(h) Ease of Use and Accessibility:
The primary design principle of this tool was simplicity and practicality. It was intentionally developed to be easy to understand and quick to implement, minimizing the time burden on facilitators and institutions. By focusing on a streamlined process, the tool increases its suitability for widespread use, ensuring it remains accessible to scientists and institutions with varying levels of resources and experience in outreach evaluation.

By integrating these considerations, the evaluation tool ensures a structured yet adaptable framework for assessing outreach activities in diverse scenarios while retaining its simplicity. For more detailed examples and explanations, refer to the templates and criteria outlined in Table S1 and Table S3.

Table S1. Evaluation criteria for scientific outreach activities. The table provides a description for each parameter evaluated to assess the execution and results of outreach activities. Each activity receives a score from 1 to 5 based on its performance relative to the criteria below.

Evaluation category	Score		
	1	2	3
Audience reach			
Measures the number of people that participated in the activity.	< 10 people	10-50 people	50-250 people
Audience engagement			
Measures the degree of attentiveness, interaction, and active participation from the audience during an outreach activity. It assesses how effectively the activity captures and sustains the audience's interest, as well as the level of enthusiasm or response shown by participants.	Minimal Engagement with little or no participation or attention from the audience.	Low engagement, with limited interest and occasional attention.	Moderate engagement, where some audience members actively participate and ask questions, showing curiosity.
Time investment			
Measures the amount of time required by the facilitator to prepare and conduct the outreach activity. It evaluates whether the activity demands significant hours each week or is more time-efficient.	> 16 h / week	8-16 h / week	4-8 h / week
Economic cost*			
Assesses the financial resources required to execute the outreach activity.	> 1000 €	250 - 1000 €	50 - 250 €
Target audience specificity			
Measures how well the outreach activity is tailored to the specific needs, interests, and characteristics of the intended audience.	***Very general***: broad approach; minimal customization to any of the audience's needs or interests.	***General:*** moderately broad approach with limited focus on audience needs.	***Moderate***: balanced approach; focus on some specific audience needs or interests.
Long-term impact			
It evaluates the lasting effects of the outreach activity on participants.	***No impact:*** completed on the same day, with no follow-up, interest after the activity is finished or any lasting effect.	***Minimal impact:*** short-term interest (hours or days), with little retention or continued engagement.	***Moderate impact:*** interest /knowledge retained for a few weeks, but limited follow-up and fading engagement.
Facilitator perception			
Encompasses the personal sense of fulfillment, perceived audience engagement, and whether the effort felt worthwhile. It captures both the subjective impression of audience response and the facilitator's own satisfaction with the activity's impact and reception.	***Very negative***: the facilitator felt disengaged and sensed little to no interest from the audience. The activity felt unfulfilling, with minimal signs of audience attentiveness or enthusiasm. Overall, it felt like the effort was not worthwhile.	***Negative***: the facilitator perceived low interest and limited engagement from the audience. While there may have been some interaction, it was minimal, and the activity felt only slightly rewarding, falling short of expectations.	***Neutral***: the facilitator felt the experience was average. Audience engagement was moderate, with some interaction and attentiveness, though the activity didn't stand out as particularly impactful or rewarding. It felt somewhat worthwhile but not exceptional.

4	5
250-1000 people	> 1000 people
High engagement, with many participants interacting actively and asking thoughtful questions.	Exceptional engagement, where nearly all participants are highly involved, asking insightful questions, and demonstrating sustained enthusiasm throughout the activity.
2 - 4 h / week	< 2h / week
< 50 €	no cost
Specific: customized to the audience; content and activities that strongly resonate with them.	***Highly specific:*** deep customization to the audience; meeting all the audience needs and interests.

Significant impact: interest / knowledge retained for several months; curiosity and possible engagement in additional science activities.	***Lasting impact:*** sustained impact and long-term engagement; participants retain knowledge, show ongoing interest, and some follow science-related education or activities.
***Positive*:** the facilitator felt good about the activity, observing active audience engagement and genuine interest. The activity was fulfilling and felt impactful, with clear signs that the audience was receptive and interested. The experience felt worthwhile.	***Very positive***: the facilitator felt highly satisfied, noting strong engagement and enthusiasm from the audience. The activity was highly rewarding and impactful, exceeding expectations, and left the facilitator feeling that the effort was truly valuable and meaningful.

Table S2. Summary of outreach activity scores and ranking. The table provides a proposed ranking based on the total scores from the evaluation in Table 1, guiding prioritization and assessing the overall impact and effectiveness of each outreach activity.

Total score	Activity impact and performance
7-12	Limited Impact Outreach
13-18	Basic Outreach with margins for improves
19–24	Moderately Effective Activity
25–30	High-Impact, highly effective
31-35	Maximum Impact with lasting engagement

Table 3. Activity evaluation template.

Description		
Activity name		
Activity description		
Audience		
Date		
Duration		
Economic cost		
Facilitator/s		
Parameter	**Score**	**Comments**
Audience reach		
Audience engagement		
Time investment		
Economic cost		
Target audience specificity		
Long-term impact		
Facilitator perception		
Final score		

Table S4. Evaluation of outreach activities conducted within our project. This table presents the parameters and scores for outreach activities that were implemented as part of our project, highlighting the performance of each real-world initiative.

Activity	Parameter	Score	Analysis
Instagram profile	Audience reach	5	In addition to our 1,000 followers, our content reaches a broader audience through non-followers, resulting in a total reach up to 100 times greater than our follower base.
	Audience engagement	3	Followers respond quickly after a post, indicating attentiveness. Many engage further after discovering the profile, showing interest in future content.
	Time investment	2	Significant time investment is required to reach a wide audience, though shared among multiple people. More time invested generally yields better results, though the most active participants tend to be the same individuals.
	Economic cost	4	There was a small investment but it is not necessary.
	Audience specificity	3	Our target audience on social media is largely self-selected, as people choose to engage with content they are interested in. While most Instagram users are aged 18 to 34 (62.3%), the content also reaches people from a wide range of ages and backgrounds, showing diverse engagement.
	Long-term impact	4	Additional activities have emerged from this project, and interest has continued beyond the Antarctic campaign.
	Facilitator perception	5	Audience feedback has been entirely positive, making our efforts feel well-rewarded and motivating us to continue.
	Final score	**26**	
Science at Metro	Audience reach	2	No more than 50 people participated in the activity, most of the people in the metro showed no interest.
	Audience engagement	1	Everyone had to be approached. Some people showed interest after our introduction; others did not, often leading to uncomfortable situations.
	Time investment	3	The activity lasted 4 hours and a few hours were invested for previous preparation of materials and dynamics.
	Economic cost	4	Little money was invested in some supporting material during the activity.
	Audience specificity	1	The supporting materials and activities were designed for a general audience, not tailored to anyone specifically on the train.
	Long-term impact	1	Impact on the audience was not lasting longer than the interaction with us.
	Facilitator perception	1	The audience's limited interest in such an "out-of-context" setting made us feel intrusive, spending energy on an activity that had minimal impact.
	Final score	**13**	

Live school talk	Audience reach	2	Classes are usually integrated by 20-30 students.
	Audience engagement	4	Both teachers and students had prior knowledge of the topic, resulting in active engagement with the activity.
	Time investment	3	Preparing materials and activities from scratch requires significant time, though they become reusable afterward. The entire activity lasts at least 2 hours, including necessary commuting.
	Economic cost	5	Any investment had to be done.
	Audience specificity	5	Considering the audience's age, supporting materials used familiar examples and relatable comparisons.
	Long-term impact	2	No follow-up was planned between presenters and students, so retention was likely short-term, lasting probably only until a major academic event.
	Facilitator perception	3	The talk inspired those interested in the topic, though it did not capture everyone's attention, as we observed.
	Final score	**24**	
Streaming school talk	Audience reach	3	The open streaming connection allowed multiple classes to join the activity.
	Audience engagement	3	Both teachers and students had prior knowledge of the topic, however remote connection is less effective to engage public's attention than in live talks.
	Time investment	4	Commuting is unnecessary, reducing the time required from me as the speaker compared to in-person talks
	Economic cost	5	Any investment had to be done.
	Audience specificity	2	Specificity is limited in remote talks due to the wider range of ages and contexts.
	Long-term impact	2	With no planned follow-up, students likely retained the information only until a major academic event.
	Facilitator perception	3	Remote setup forces presenters to address a broad audience through a single screen, creating a palpable yet impersonal impact that might nonetheless enhance idea retention.
	Final score	**22**	

Museum talk	Audience reach	2	Convening power in the museum reached between 40-50 people.
	Audience engagement	4	Those interested in the topic chose to attend and actively participated.
	Time investment	3	Preparing materials and activities from scratch is time-intensive, though reusable. The full activity, including travel, takes at least two hours.
	Economic cost	5	Any investment had to be done.
	Audience specificity	2	Specificity is reduced because of the diverse range of ages and backgrounds involved.
	Long-term impact	3	Interested participants tend to retain information longer, though engagement likely diminishes over time.
	Facilitator perception	4	An engaged audience motivates the presenter, enhancing the energy and impact of the activity.
	Final score	**23**	
Virtual Antarctica in nursing homes	Audience reach	2	Groups visited at nursing homes did not exceed 50 people.
	Audience engagement	5	Most of the residents were emotionally engaged, actively asking questions and sharing their own knowledge with the group.
	Time investment	5	Filming the videos was efficient, and thanks to our collaboration with @mesqueciencia, no additional time was required from our team.
	Economic cost	4	Our collaborators provided the audiovisual devices, the video editing and the virtual reality glasses, through which residents viewed the images and heard the information.
	Audience specificity	5	This group, often excluded from advancements in science and technology, deserves the same access as others.
	Long-term impact	5	These residents tend to remember the experience longer than those who continuously receive input from social media and other channels.
	Facilitator perception	4	The activity was profoundly moving and enriching. The audience's emotional response fueled our enthusiasm and commitment to inclusive science outreach.
	Final score	**30**	

GENERAL DISCUSSION

04



PART 04. GENERAL DISCUSSION AND CONCLUSIONS

4.1. INTRODUCTION

The work performed within this doctoral thesis is the result of field, laboratory and conceptual work. Such extensive effort has allowed to better understand the occurrence and distribution of recalcitrant hydrocarbons, OPEs and PFAAs in the Atlantic and Southern Oceans. These three families of contaminants form a critical triad of anthropogenic perturbations due to their relatively higher concentrations and ubiquity, posing an increasing risk to marine ecosystems and global environmental health. This discussion aims to complement the discussion performed in the previous chapters by exploring the comparative environmental behavior of these chemical families, comparing their latitudinal distributions and apparent persistence at surface waters, with a focus on understanding their differences in transport mechanisms and accumulation, particularly in remote regions like Antarctica. The assessment of contaminants in vast oceanic regions is important not only in the context of global change, but also in the prioritization of contaminants, as only those chemicals with enough persistence will be ubiquitous globally. Such observations are often used to support the urgent need for global action on chemical pollution within international conventions and protocols.

Organophosphate esters (OPEs) and perfluoroalkyl acids (PFAAs) share several similarities in terms of properties and uses, while exhibiting notable differences regarding their sources, environmental behavior and sinks. Both chemical families are emerging contaminants are widely used in industrial and consumer products: OPEs as flame retardants and plasticizers, and PFAAs as components in water- and grease-resistant applications. Both are characterized by their notable persistence and widespread distribution in the oceans (Reemtsma et al., 2008; Ahrens et al., 2010; Glüge et al., 2020; Xie et al., 2022a; Cousins et al., 2022), but they differ in their physicochemical properties, environmental behavior, and legislative frameworks.

PFAAs, often referred to as "forever chemicals," are extraordinarily resistant to degradation due to the strong carbon-fluorine bonds and some of them are now considered legacy pollutants by part of the scientific community, even though there are thousands of them still treated as emerging pollutants.

In contrast, OPEs, which were developed many decades ago, but increasingly used as replacements for banned polybrominated diphenyl ethers (PBDEs), are less persistent but some of them show a higher potential for partitioning into organic phases, particularly in organisms. In this thesis, even though is it primarily centered in the study of contaminants in the dissolved phase, the accumulation in the ocean's surface microlayer has been evaluated for OPEs, a process also coupled to partitioning to organic lipids at the sea's surface. These contrasting properties make the study of both families crucial to understand the broad dynamic of chemical pollution in the marine environment.

4.1.1. DATA INTEGRATION AND SCOPE

The targeted compounds within the three studied families were selected for their environmental relevance. For **PFAAs**, nineteen compounds ($\sum_{19}$PFAAs) were analyzed, comprising six perfluoroalkyl sulfonates (PFSAs) and thirteen perfluoroalkyl carboxylates (PFCAs) **(Table 1.5)**. Among them, PFBA was excluded due to non-detection, and PFHxA was omitted because of analytical uncertainties linked to potential co-elutions, resulting in final concentrations of **$\sum_{17}$PFAAs,** including **$\sum_{6}$PFSAs and $\sum_{11}$PFCAs**.

For **OPEs**, twenty organophosphate esters plus four organophosphorus compounds were analyzed **(Tables 1.6 and 1.7)**. To simplify the discussion, all were named OPEs ($\sum_{24}$OPEs). These compounds can be classified by their chemical structures into: chlorinated OPEs (Cl-OPEs), aryl OPEs, alkyl OPEs, and brominated OPEs (Br-OPE). Among the analyzed compounds, TPPO and Chlorpyrifos were excluded due to analytical uncertainties and their absence in surface waters, respectively, resulting in the analysis of $\sum_{22}$OPEs.

The data presented in this thesis were obtained during two extensive oceanographic campaigns conducted as part of the ANTOM project. These campaigns covered a wide transect spanning from 37°N to 71°S, including some of the southernmost sampling locations ever reported for OPEs and PFAAs. Vertical profiles reaching depths of up to 2000 m provided unique insights into the behavior of these pollutants in the water column, data particularly scarce in the Southern Ocean.

Table 4.1 | Stations, coordinates and date of sampling (dd-mm-yyyy) of surface waters at 5 m depth, from the Atlantic Ocean (AN1_ST01 to ST24) and Southern Ocean (AN2_ST01 to AN2_ST12) where both PFAAs and OPEs were analyzed.

Station Code	Longitude	Latitude	Date (dd-mm-yyyy)
AN1_ST01	37,92	-15,97	18-12-2020
AN1_ST02	35,74	-19,07	19-12-2020
AN1_ST03	35,74	-19,07	20-12-2020
AN1_ST04	28,66	-28,41	21-12-2020
AN1_ST05	25,63	-24,90	22-12-2020
AN1_ST06	22,22	-26,63	23-12-2020
AN1_ST07	18,87	-28,32	24-12-2020
AN1_ST08	14,97	-28,70	25-12-2020
AN1_ST09	10,87	-29,23	26-12-2020
AN1_ST10	7,35	-29,58	27-12-2020
AN1_ST11	3,83	-29,86	28-12-2020
AN1_ST12	0,14	-30,50	29-12-2020
AN1_ST13	-2,98	-30,95	30-12-2020
AN1_ST14	-6,78	-31,33	31-12-2020
AN1_ST15	-14,37	-33,92	02-01-2021
AN1_ST17	-21,30	-36,80	04-01-2021
AN1_ST21	-34,40	-45,63	08-01-2021
AN1_ST23	-43,79	-54,75	11-01-2021
AN1_ST24	-46,79	-58,46	12-01-2021
AN2_ST01	-62,71	-60,64	23-01-2022
AN2_ST02	-62,92	-61,04	24-01-2022
AN2_ST03	-64,58	-62,57	25-01-2022
AN2_ST05	-66,92	-69,10	27-01-2022
AN2_ST07	-70,85	-79,89	30-01-2022
AN2_ST09	-69,21	-78,84	31-01-2022
AN2_ST10	-67,70	-75,00	01-02-2022
AN2_ST11	-62,57	-58,62	04-02-2022
AN2_ST12	-62,97	-60,29	05-02-2022

To enable meaningful comparisons, only stations where both OPEs and PFAAs were measured in surface waters (approximately 5 m depth) are considered in this discussion **(see Table 4.1).**

Polycyclic aromatic hydrocarbons (PAHs) were examined as a compilation of data from previously published studies, providing the first assessment of the relevance of PAHs and other SALCs as part of the broader dissolved black carbon (DBC) pool. This dataset complements the novel insights gained from OPEs and PFAAs, offering a comprehensive perspective on the behavior of both emerging pollutants and hydrocarbons in remote marine environments.

In Chapter 1, all available data on PAHs in surface waters of the global oceans (up to 2021, when the meta-analysis was performed) was systematically compiled.

To address variability in the specific number and identity of PAHs analyzed across studies, a standardized subset of four PAHs ($\sum_4$PAHs) —Anthracene, Phenanthrene, Pyrene, and Fluoranthene—was identified. This subset served as a consistent reference group, ensuring comparability across datasets, and by a conversion factor, estimates of total $\sum_{64}$PAHs concentrations were obtained. Such estimates are based on the previous measurements conducted by González-Gaya et al., 2016, from the Malaspina Circumnavigation Campaign from December 2010 until July 2011 **(Table 4.2)**; and second from Iriarte et al., 2023 from the Sentinel and Remarca Antarctic Campaigns at South and False Bays of Livingston Island, from December 2014 to March 2015, and from January to March 2018 **(Table 4.2)**. Here, the PAHs occurrence is compared with the measured concentrations of OPEs and PFAAs in the Atlantic and Southern Oceans from this work.

Table 4.1 | Stations and coordinates from González-Gaya, et al., 2016 and Iriarte et al., 2023 for PAH concentrations measured.

Ocean	Station name	Longitude	Latitude	Work
Atlantic Ocean	St01	34.58	-11.173	González-Gaya et al., 2016
Atlantic Ocean	St02	30.37	-16.6	González-Gaya et al., 2016
Atlantic Ocean	St03	26.452	-20.125	González-Gaya et al., 2016
Atlantic Ocean	St04	22.633	-22.658	González-Gaya et al., 2016
Atlantic Ocean	St05	19.063	-24.974	González-Gaya et al., 2016
Atlantic Ocean	St06	13.66	-25.999	González-Gaya et al., 2016
Atlantic Ocean	St07	8.571	-26.014	González-Gaya et al., 2016
Atlantic Ocean	St08	3.695	-25.998	González-Gaya et al., 2016
Atlantic Ocean	St09	-1.14	-26.481	González-Gaya et al., 2016
Atlantic Ocean	St10	-5.954	-28.709	González-Gaya et al., 2016
Atlantic Ocean	St11	-13.443	-30.443	González-Gaya et al., 2016
Atlantic Ocean	St12	-14.263	-32.659	González-Gaya et al., 2016
Atlantic Ocean	St13	-19.369	-35.114	González-Gaya et al., 2016
Atlantic Ocean	St14	-23.374	-38.086	González-Gaya et al., 2016
Atlantic Ocean	St15	-24.104	-37.53	González-Gaya et al., 2016
Atlantic Ocean	St16	-24.789	-33.485	González-Gaya et al., 2016
Atlantic Ocean	St17	-25.155	-31.647	González-Gaya et al., 2016
Southern Ocean	SO_St01 (Liv.-Emona Anchorage)	-62.76	-60.34	Iriarte et al., 2023
Southern Ocean	SO_St02 (Liv.-Johnsons)	-62.7	-60.35	Iriarte et al., 2023
Southern Ocean	SO_St03 (Liv.-Raquelias)	-62.76	-60.46	Iriarte et al., 2023
Southern Ocean	SO_St04 (Liv.-South Bay)	-62.729	-60.636	Iriarte et al., 2023

4.1.2. LATITUDINAL DISTRIBUTION AT SURFACE (5 M) WATERS

Organophosphate Esters (OPEs)

OPEs are typically reported in concentrations of ng L^{-1}, reflecting their higher occurrence in the environment compared to per- and polyfluoroalkyl acids, which are found at concentrations of pg L^{-1} in the open ocean. The concentrations of OPEs are in fact comparable, or even higher than those of hydrocarbons in the open ocean (González-Gaya et al. 2016). In order to facilitate the comparison, here we use concentrations of the three families in pg L^{-1}.

Total OPE concentrations ($\sum_{22}$OPE) across all sampled regions exhibited an average value of 17659 pg L^{-1}, with concentrations ranging from 1425 to 78751 pg L^{-1} (SD: 15131 pg L^{-1}) **(Figure 4.1)**. Among OPEs, Cl-OPEs were the most abundant, with a mean concentration of 13042 pg L^{-1}, followed by aryl-OPEs, 2411 pg L^{-1} and alkyl-OPE, 2206 pg L^{-1}. Br-OPEs were negligible on average.

OPE concentrations showed a non-normal distribution (Shapiro-Wilk normality test $W = 0.73$, $p < 0.05$). A Mann-Whitney U test comparing $\sum_{22}$OPEs concentrations between both oceans revealed a statistically significant difference ($W = 140$, $p = 0.006$) proving that $\sum_{22}$OPEs are significantly higher in the Atlantic Ocean (AO) than in the Southern Ocean (SO), consistent with the first being much closer to the source's regions of these contaminants. Pearson's correlation test revealed a significant positive correlation of total OPE concentrations with temperature ($r = 0.45$, $p = 0.01$), consistent with maximum concentrations being found at tropical latitudes.

A remarkable observation of the OPE distribution was their enrichment in the ocean's surface microlayer (SML). The SML, as a unique interface between the atmosphere and the ocean, has been shown to concentrate hydrophobic and semivolatile compounds, including OPEs (Trilla-Prieto et al., 2024, in this thesis found at Part 03 – Chapter 3 – Publication III). In particular, this doctoral thesis demonstrates that OPEs, particularly Cl-OPEs, are significantly enriched in the SML relative to underlying waters, with enrichment factors averaging 5.84 ± 8.97 in the Atlantic Ocean, and 9.10 ± 9.48 in the Southern Ocean. This enrichment is strongly correlated with chlorophyll α content, suggesting that biogenic surfactants play a critical role in the accumulation of OPEs at the SML. Moreover, the formation of sea spray aerosols (SSA), mediated by this enrichment in the SML, could act as

a pathway for atmospheric transport of semivolatile organic pollutants. Estimated enrichment factors in SSA ranged from 3.69 × 10^4 to 3.33 × 10^6, highlighting the importance of the SML-SSA interface in pollutant cycling.

Similarly, previous work by Casas et al. (2020) demonstrated that PFAS also accumulate in the SML, but with lower enrichment factors ranging from 1.2 to 5, compared to OPEs. Long-chain PFAS (such as PFOA, PFNA or PFDA) showed the highest enrichment. In SSA, PFAS exhibited enrichment factors between 522 and 4690, significantly lower than those observed for OPEs (3.69 × 10^4 to 3.33 × 10^6). These findings confirm that the SML acts as a critical interface for both OPEs and PFAS, though the extent of enrichment differs due to their distinct physicochemical properties. OPEs exhibit stronger partitioning into the SML, likely due to their higher hydrophobicity and interaction with biogenic surfactants. In contrast, PFAS show more moderate enrichment in the SML but undergo significant amplification in SSA, potentially due to their amphiphilic nature and affinity for aerosol organic matter. Both studies highlight the role of SSA as a potentially relevant vector for long-range atmospheric transport.

Traditionally, two main sinks were considered to be affecting OPE distribution: photodegradation (Cristale et al., 2017, Regnery et al., 2010; Su et al., 2016), and microbial degradation (Vila-Costa et al., 2019; Iriarte et al., 2025), but those are restricted to the photic zone, being more relevant in surface waters. Previous works have also underscored the role of the biological pump acting as a sink sequestrating legacy pollutant, such as PAHs, HCHs, PCBs or PFAAs (González-Gaya et al., 2019b; Berrojalbiz et al., 2011b; Galbán-Malagón et al., 2012; 2013). Our recent work (in this thesis found at Part 03 – Chapter 3 – Paper IV) suggests that this mechanism has also the potential to remove OPEs from surface waters. Lower OPE concentrations in southern latitudes (south Atlantic and Southern Ocean) might be attributed to an enhanced biological pump related to higher biomass (evidenced by higher Chl *a* in the Southern than in the Atlantic Ocean, 1.9 ± 1.3 µg L^{-1} and 0.2 ± 0.1 µg L^{-1}, respectively). The environmental fate of OPEs has some similarities with that of PAHs as reported elsewhere (Berrojalbiz et al. 2011, González-

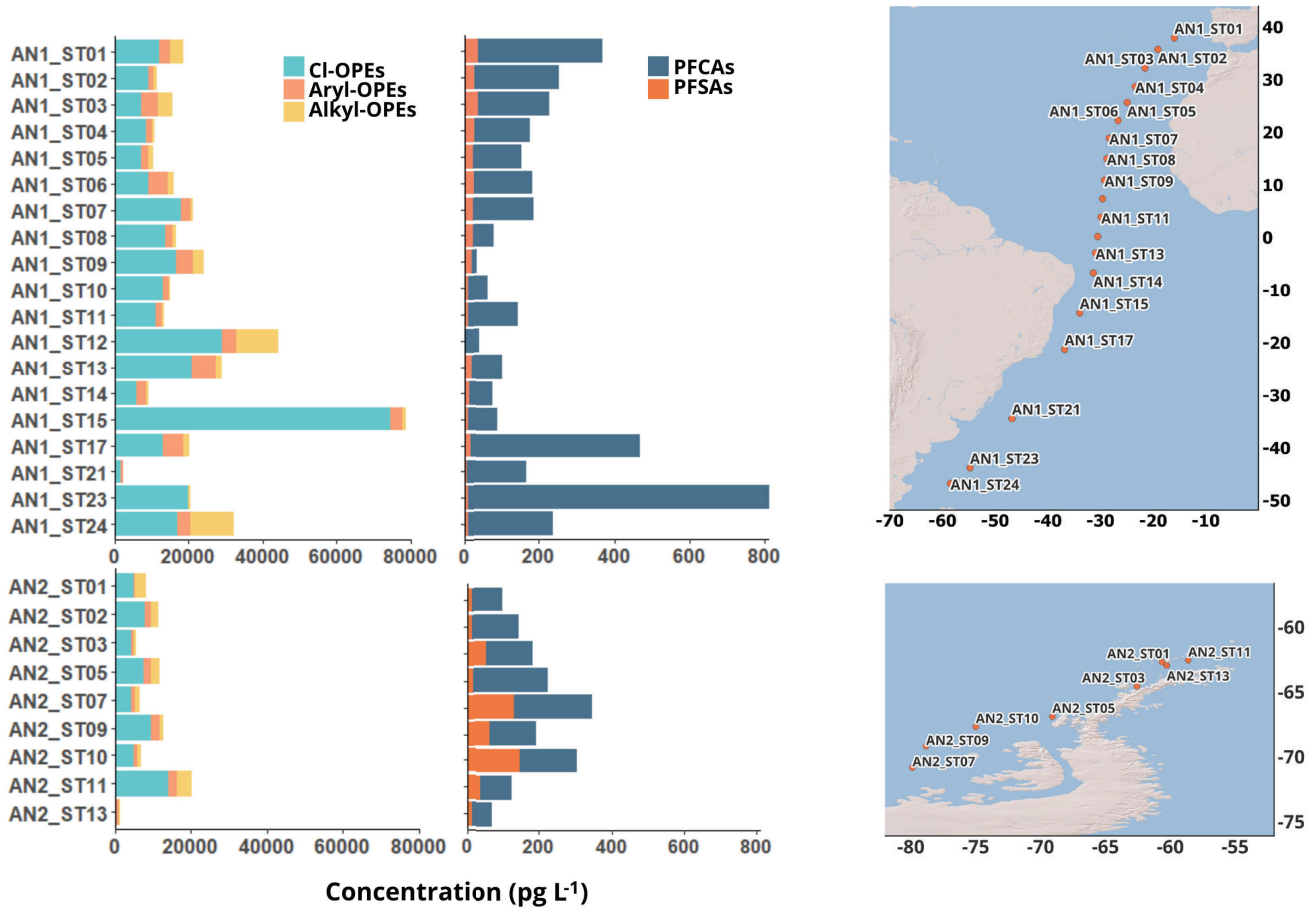


Figure 4.1 | $\sum_5$Cl-OPEs, $\sum_6$Alkyl-OPEs and $\sum_9$Aryl-OPEs concentrations (pg L-1) (left panels), and $\sum_6$PFSAs and $\sum_{11}$PFCAs concentrations (pg L^{-1}) (middle panels) across the Atlantic Ocean (top panel) and Southern Ocean (bottom panel). Right panels show the stations location in the Atlantic (top) and Southern Ocean (bottom).

Gaya et al. 2019). For PAHs, the biological pump is the main sink for the more hydrophobic compounds (more than 4 aromatic rings), while biodegradation is the key sink of the less hydrophobic, more soluble, hydrocarbons. For OPEs, degradation is also a sink in the environment, but contrary to PAHs, this has been reported to be more relevant for the more hydrophobic OPEs (Iriarte et al., 2025), especially aryl-OPEs. In this thesis, evidence of degradation of TPhP due to carbon demand was also observed. In addition, contrary to the trends for PAHs, the biological pump arises as relevant for Cl-OPEs which are not often the more hydrophobic OPEs. Therefore, there are considerable differences between the trends in terms of sinks between OPEs and PAHs. Specifically, for OPEs, the hydrophobic paradigm, in which the environmental behavior can be predicted from their physico-chemical properties such as K_{OA} or H' does not hold. The hydrophobic paradigm works well for other non-polar semi-volatile contaminants such as PCBs, in addition to PAHs. The results found here for OPEs shows that the hydrophobic paradigm is not a good predictor of the environmental transport and fate of OPEs, probably because these chemicals are polar, and their chemical structure is highly variable, affecting their accumulation, degradation and transport.

The distribution of OPEs in the studied oceans shows a clear latitudinal gradient, with significantly higher concentrations observed in the Atlantic Ocean compared to the Southern Ocean. The Atlantic's proximity to anthropogenic sources, as well as processes like wet deposition and riverine inputs, plays a major role in this pattern. Additionally, enrichment in the SML and subsequent atmospheric transport further highlight the complexity of OPE cycling. By contrast, the Southern Ocean's lower OPE concentrations reflect its remoteness from sources and the barrier effect of the Antarctic Circumpolar Current (ACC). This contrast with the extremely high concentrations of OPEs in the Southern Ocean's SML, showing an enrichment in this region larger than that observed for other legacy and emerging contaminants (Cincinelli et al., 2005; Stortini et al., 2009; Casas et al., 2020) and of a similar extend to other woks (Fuoco et al., 2005).

Perfluoroalkyl Acids (PFAAs)

Total PFAA concentrations ($\sum_{17}$PFAAs) across all regions averaged 198 pg L^{-1}, ranging from 36 to 810 pg L^{-1} (SD: 158 pg L^{-1}). No significant differences were found among $\sum_{17}$PFAA concentrations between the Atlantic and Southern Ocean (Wilcoxon rank sum test; W = 77, p = 0.71), which averaged (mean ± SD) 203 ± 183 and 184 ± 91 pg L^{-1}, respectively.

Among PFAS subclasses, perfluoroalkyl carboxylic acids ($\sum_{11}$PFCA) were the dominant contributors, with a mean concentration of 167.8 pg L^{-1} and average contributions of 85.6% and 74% in the Atlantic and Southern Oceans, respectively. On the other hand, perfluoroalkyl sulfonic acids ($\sum_{6}$PFSAs) showed an average of 30.5 pg L^{-1} **(Figure 4.1)**, and average contributions of 14.6 and 26% in the Atlantic and Southern Oceans.

Among the PFAAs group, perfluorooctane sulfonate (PFOS) and perfluorooctanoic acid (PFOA) are two of the most studied and widely detected compounds in marine environments. PFOA was detected in 65% of the surface samples. In the Atlantic Ocean, PFOA concentrations averaged 31.0 pg L^{-1}, with values ranging from 15.7 to 103.5 pg L^{-1}, while in the Southern Ocean, the average concentration was 58.8 pg L^{-1}(ranging from 18.0 to 115.5 pg L^{-1}). In contrast, PFOS was more prevalent, being found in 90% of the samples. PFOS concentrations averaged 3.5 pg L^{-1} (range: 2.25–5.25 pg L^{-1}) in the Atlantic Ocean and 45.4 pg L^{-1} (range: 8.25–123.7 pg L^{-1}) in the Southern Ocean **(Figure 4.2)**.

Given that PFAS have been in use and monitored for decades, we can now assess whether regulatory restrictions and phase-out efforts have effectively reduced their occurrence in the environment. Comparing our results (samples collected from 2020 to 2022), with data collected over a decade ago in the Atlantic Ocean provides valuable insight into temporal trends, allowing us to evaluate whether concentrations have declined, probably in response to these regulations. For instance, González-Gaya (2014) measured $\sum_{11}$PFAS in the Atlantic Ocean during the Malaspina 2010 expedition and found a range between 131 – 10900 pg L^{-1} (median = 645 pg L^{-1}), with maximums substantially higher than the ones presented in this thesis for $\sum_{17}$PFAAs in the Atlantic Ocean (ranging 36 - 810 pg L^{-1}, median = 165.8 ng L^{-1}), but with a consistent pattern of maximums found offshore Brazil. Moreover, in González-Gaya's measurements, PFOA showed a median of 44 and 58 pg L^{-1}, and PFOS showed a median of 59 and 742 pg L^{-1}, in the North and South Atlantic oceanic basins, respectively. In this work, performed a decade later, PFOA showed medians of 20.63 and 21.75 pg L^{-1} in the North, and South Atlantic basins, respectively, with a relatively consistent pattern along all the Atlantic transect, and slightly lower that the concentrations found in 2010. However, PFOS showed medians of 3.55 and 3.36 pg L^{-1} in the North, and South Atlantic basins, respectively, showing a clear decrease compared to the measurements done in 2010.

Benskin (2012) measured $\sum_{13}$PFAAs concentrations between 2005 and 2009 along the Atlantic Ocean and found concentrations ranging from 64 to 980 pg L^{-1}. In their results, maximums were found around the Canary Islands, at 28ºN (890 pg L^{-1}), and near Rio de la Plata (South America, 37ºS), which showed increased

concentrations of 540 and 360 pg L^{-1}, respectively. The spatial trend was consistent with this work's measurements, even though the concentrations ranges are very different. However, most sample's profiles were dominated by PFOS and PFOA, together accounting for 47-62% of total PFAAs, in the North Atlantic, and 43-71% in the South Atlantic. In this work, PFOA and PFOS together accounted for 5-16% and 3 – 23% in the North and South Atlantic basins, respectively, and 4 – 82% in the Southern Ocean.

In the marine environment, several recognized oceanic sinks for PFAAs exist, including vertical eddy diffusion (Lohmann et al., 2013), deep water formation (Lohmann et al., 2013; Armitage et al., 2009), and the settling of particle-bound PFAAs (referred to as the biological pump) (Casas et al., 2023; González-Gaya et al., 2019b; Casal et al., 2017). Despite these sinks, PFAAs are estimated to persist in the marine environment for periods ranging from decades to centuries (Muir & Miaz et al., 2021; Yamashita et al., 2008). The ban on PFOS production and use over 15 years ago has led to markedly lower concentrations in regions influenced by direct pollutant sources, such as the Atlantic Ocean, aligning with reduced emissions and global phase-out efforts. However, despite these regulatory measures, PFOS remains prevalent in the Southern Ocean, emphasizing the role of long-range atmospheric transport and oceanic circulation in its redistribution, and probably less efficient removal processes in the Southern Ocean. Processes such as sea spray formation, wet deposition, and the Antarctic Circumpolar Current (ACC) facilitate its accumulation in remote waters, where it persists. While microbial degradation of PFOS has been reported near Deception Island (Cerro-Gálvez et al., 2020), its significance in other Antarctic waters remains unclear. This persistence, coupled with the consistently higher concentrations of PFCAs relative to PFSAs in the global ocean, underscores the extreme longevity of these compounds and reinforces their status as truly 'forever chemicals' in the marine environment.

The findings in Chapter 2 highlight the extraordinary persistence of PFAAs, particularly PFCAs, distinguishing them from other legacy POPs. While the Antarctic Circumpolar Current is traditionally considered a barrier preventing north-south transport of contaminants, the detection of PFAAs at levels comparable to those found in the North Atlantic demonstrates their ability to cross this barrier through a combination of aerosolization via sea spray aerosols, atmospheric transport, and wet deposition processes. Once they reach Antarctic waters, the Antarctic Divergence traps them cycling in the Southern Ocean water column. Unlike other semi-volatile POPs, whose concentrations typically decrease in polar waters, the absence of effective sinks for PFAAs, such as microbial degradation or uptake by the biological pump, accentuates their accumulation in the Southern Ocean, unable to compensate for their

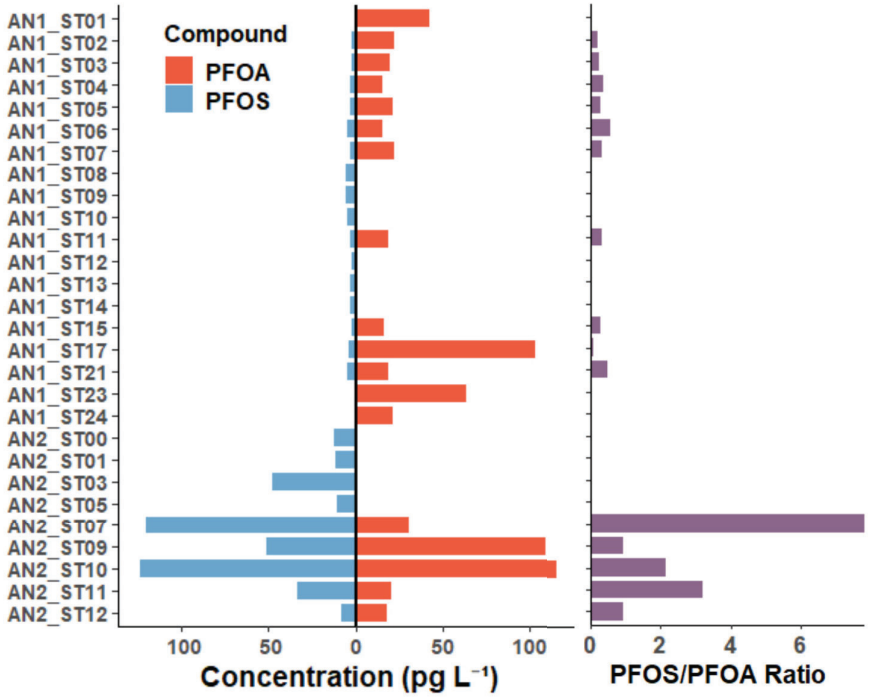


Figure 4.2 | Distribution of PFOS and PFOA concentrations (pg L^{-1}) across the Atlantic Ocean (AN1_ST01 to ST24) and Southern Ocean (AN2_ST00 to ST12) (left panel) and corresponding PFOS/PFOA ratios (right panel).

continuous inputs via atmospheric transport and wet deposition processes.

Additionally, the environmental fate and transport of PFAAs reported in this thesis challenge the traditional hydrophobic paradigm, as the octanol-water partition coefficient (K_{OW}) does not reliably predict the behavior of amphiphilic and non-volatile PFAS in the environment. However, the persistence of PFAAs, and PFAS in general, may be only a fraction of a much larger problem, as current analytical methods only capture a subset of the vast number of existing PFAS. Recent research has estimated the existence of over 7 million PFAS structures (Schymasnki et al., 2023), an alarming figure that suggests we may be underestimating their environmental presence and impact.

At the same time, the growing complexity and ubiquity of PFAS have led to calls for their regulation as a single class rather than as individual compounds (Cousins et al., 2022). This approach acknowledges their shared persistence, mobility, and bioaccumulative potential, reinforcing the urgency for global regulatory measures to curb emissions and prevent further contamination. Given their resistance to degradation and ability to accumulate in even the most remote environments, PFCAs emerge as the ultimate 'forever chemicals,' turning the Southern Ocean into both a receptor and long-term reservoir for these pollutants. This underscores the necessity for intensified international efforts to regulate and mitigate PFAS emissions globally before their environmental and ecological impacts become irreversible.

Aromatic Compounds

For polycyclic aromatic hydrocarbons (PAHs), seventeen stations from the Atlantic (37°N – 35°S), from González-Gaya et al., 2016 were compiled (see **Table 4.2, and Figure 4.3**). In the Southern Ocean, four locations were sampled over three years, resulting in a total of 38 samples. For this study, the final concentration at each location was calculated as the average of all samples collected from that sampling location. This approach allowed for meaningful comparisons of PAH concentrations in the surface waters of the Atlantic and Southern Ocean.

$\sum_{64}$PAH concentrations showed a consistent pattern across the transect. Briefly, concentrations from 35°N to 62°S ranged from 79.0 to 3674.9 pg L^{-1} (average 2302.2 ± 1083.7 pg L^{-1}, N = 17) in the Atlantic Ocean **(Figure 4.3)**, and from 877.7 to 3587.6 pg L^{-1} (average 1784.1 ± 1242.3 pg L^{-1}, N = 38) in the Southern Ocean **(Figure 4.3)**. Comparison of concentrations between oceans did not show statistically significant differences (Wilcoxon rank sum test, W = 41, p = 0.56) and maximum concentrations (around 3500 pg L^{-1}) were found in various stations across both oceans.

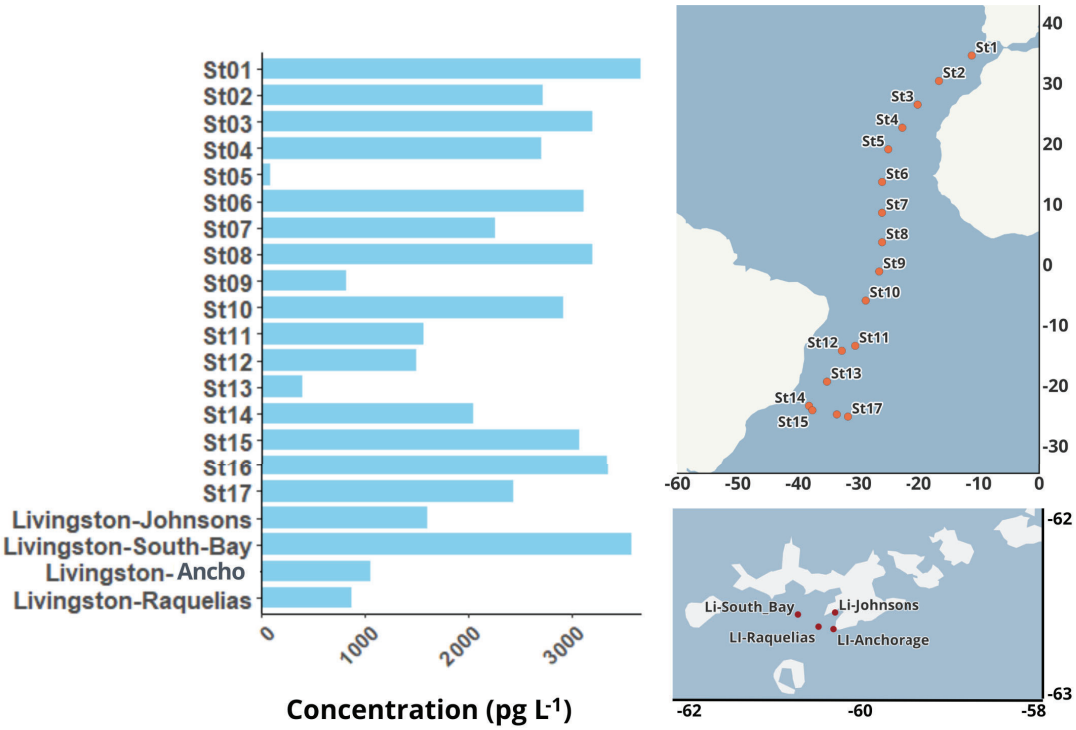


Figure 4.3 | $\sum_{64}$PAH concentrations (pg L^{-1}) (left panel) across the Atlantic Ocean (St 1 to 17) and Southern Ocean, sampled at four different stations around Livingston Island in the South Shetland Islands (Antarctic Peninsula) and maps of stations locations (right panels).

The behavior of PAHs and DBC in the global ocean highlights their complex fate and persistence. While PAHs are susceptible to biological and photodegradation processes (Dachs et al., 1997; Berrojalbiz et al., 2011a; Head et al., 2006; González-Gaya, et al., 2019), they exhibit a strong tendency to associate with particulate matter (Duran et al., 2016), which can influence their transport and removal pathways in the water column, as reported previously when assessing the role of the biological pump (González-Gaya et al. 2019, Berrojalbiz et al. 2011).

In our recent work (Trilla-Prieto et al., 2021; found at Part 01 – Chapter 1 – Paper I), further insights into the relationship between PAHs and DBC, were highlighted, suggesting that semivolatile aromatic-like compounds (SALCs), including PAHs, contribute significantly to the DBC pool in the ocean. A meta-analysis indicated that SALCs account for approximately 16% of DBC, with contributions ranging from 5% to 31%. This substantial contribution aligns with the large atmospheric input of SALCs, estimated at 400 Tg C y^{-1}.

The study also showed the importance of considering known inputs and sinks for PAHs when examining the DBC cycle. Processes such as diffusive air–water exchange and degradation, which are well-documented for PAHs, play a crucial role in the dynamics of DBC. Photodegradation at the ocean surface and microbial degradation in the water column are significant sinks for semivolatile DBC, consistent with the ubiquitous presence of degradation genes associated with aromatic hydrocarbon metabolic pathways.

In the case of PAHs, and probably other semivolatile aromatic hydrocarbons, the environmental transport and fate is highly dependent on K_{OW} and H', so these chemicals even though they are not strictly persistent, do follow the hydrophobic paradigm, and their environmental fate is more predictable than that of OPEs and PFAS.

4.1.3. COMPARISON OF THE LATITUDINAL DISTRIBUTION

The distribution of OPEs and PFAAs in the Atlantic and Southern Oceans revealed distinct patterns and spatial variability. Overall, OPEs displayed significantly higher concentrations, with peaks reaching up to 80,000 pg L^{-1}, up to three orders of magnitude compared to PFAA concentrations, that were consistently lower, peaking around 800 pg L^{-1}. Despite this difference, PFAAs exhibit a more uniform presence across regions, which may be due to their persistence, but probably also to different cycling in the water column.

PFAAs exhibited lower overall concentrations compared to OPEs, but their distribution revealed a distinct latitudinal trend. Concentrations decreased steadily from 37°N to 14°S, likely reflecting the increasing distance from major industrial and continental sources in the Northern Hemisphere. This decreasing pattern, however, was interrupted by two notable peaks of PFAAs (mainly driven by PFHpA, PFPeA, PFOA and PFNA) at 21°S and 43°S, where concentrations were surprisingly high. These peaks were attributed to the influence of direct inputs from continental sources, particularly riverine discharges and atmospheric deposition in heavily industrialized regions such as Brazil and Argentina. The Brazil Current might be facilitating the transport of these water masses, enhancing the observed concentrations near the South American coast.

A similar pattern was also observed for OPEs, which showed significant enrichment at mid-latitude stations in the Atlantic Ocean. Peak in OPE concentrations at station 15 (latitude 14°S) suggests that both pollutant families are influenced by shared sources, including direct riverine inputs and atmospheric deposition. Industrialized coastal areas serve as hotspots for pollutant release, where rivers act as transport pathways, delivering contaminants into adjacent marine systems. Atmospheric inputs further amplify these concentrations, particularly in regions experiencing intense human activity and industrial emissions.

Relative Ratios of OPEs and PAHs to PFAAs.

To further investigate the differences in the distribution and accumulation of these three pollutant families, several dimensionless ratios were calculated using concentrations (pg L^{-1}) of total PAHs ($\sum_{64}$PAHs), Cl-OPEs, total OPEs ($\sum_{22}$OPEs), and perfluoroalkyl carboxylic acids ($\sum_{17}$PFCAs), perfluoroalkyl sulfonic acids ($\sum_{11}$PFSAs), and total $\sum_{16}$PFAAs. All ratios used PFAAs as a reference framework to evaluate the relative contributions of OPEs and PAHs compared to the presence of PFAAs cross the transect **(Figures 4.4. and 4.5).**

In the Atlantic Ocean **(Figure 4.4)**, Cl-OPEs/PFAAs ratios exhibited a mean value of 167 ± 233, and OPEs/PFAAs ratio of 222 ± 298. Similarly, Cl-OPEs/PFCAs and OPEs/PFCAs ratios were 222 ± 329 and 299 ± 441, respectively. However, the Cl-OPEs/PFSAs and OPEs/PFSAs ratios were higher, with means of 1560 ± 2448 and 2113 ± 3445, consistent with PFSAs contributing less to the total pool of PFAAs, and being found in concentrations of a few pg L^{-1} in surface waters in the Atlantic Ocean.

In contrast, the Southern Ocean showed considerably lower ratios across all variables, indicating reduced concentrations of OPEs and Cl-OPEs relative to PFAAs

(Figure 4.4). The Cl-OPEs/PFAAs and OPEs/PFAAs ratios in this region were 39.3 ± 32.8 and 59.2 ± 46.3, respectively. Similarly, the Cl-OPEs/PFCAs and OPEs/PFCAs ratios were 53.5 ± 47.2 and 79.8 ± 66.2, while Cl-OPEs/PFSAs and OPEs/PFSAs ratios were 226 ± 205 and 346 ± 305.

For PAHs, the analysis of the ratios compared to PFAAs also highlighted distinct regional differences in pollutant distributions **(Figure 4.5)**. In the Atlantic Ocean, the mean PAH/PFCA ratio was 30.4 ± 38.6. The PAH/PFSA ratio was notably higher, averaging 212 ± 238, also significantly heterogeneous, and considerably higher due to the lower concentrations of PFSAs compared to PFCAs. The PAH/PFAA ratio showed the lowest mean of 21.9 ± 21.4. In the Southern Ocean, ratios were generally lower and less variable. The mean PAH/PFCA ratio was 24.1 ± 24.8, the PAH/PFSA ratio averaged 120 ± 104, and the mean PAH/PFAA ratio was 19.7 ± 20.2. These lower values in Antarctic waters are consistent with the lower concentrations found in such a remote and less impacted area from most pollutants' families. Processes such as biodegradation, and attachment to particles reduce the load of PAHs reaching the colder environment of the Southern Ocean. However, PFAAs, found in concentrations similar to the North Atlantic did not show as reduced concentrations as the PAHs, resulting in lower ratios in the SO than in the AO.

The explored ratios PAHs/PFAAs and OPEs/PFAAs show a remarkable variability. Probably, some the primary sources of the three families of pollutants are similar, as pollutant emissions depend strongly on population density and economic development. However, the OPEs/PFAAs ratios show that in the intertropical region OPES are much more abundant in comparison to PFAAs than at high latitudes or the Southern Ocean. This could be due to a higher contribution of OPEs than PFAAs at source regions and their transport to the tropical Atlantic. However, as noted above, the latitudinal distribution of PFAAs is more homogeneous, while OPEs show high concentrations at low latitudes. This different spatial pattern could be related to the higher persistence of PFAAs in comparison to OPEs, allowing them to reach distant regions due to their longer half-lives in the environment. The comparison of PAHs and PFAAs shows also some differences, but to lower extend than that of OPEs and PFAAs. For PAHs, the atmospheric transport is key to understand their global distribution, while for OPEs and PFAAs, as these are polar chemicals, more soluble compounds, the role of oceanic transport is more relevant. It is also possible, that the biological pump is a more relevant sink for OPES and PAHs than for PFAAs, further contributing to the more homogeneous PFAAs distribution found in the ocean.

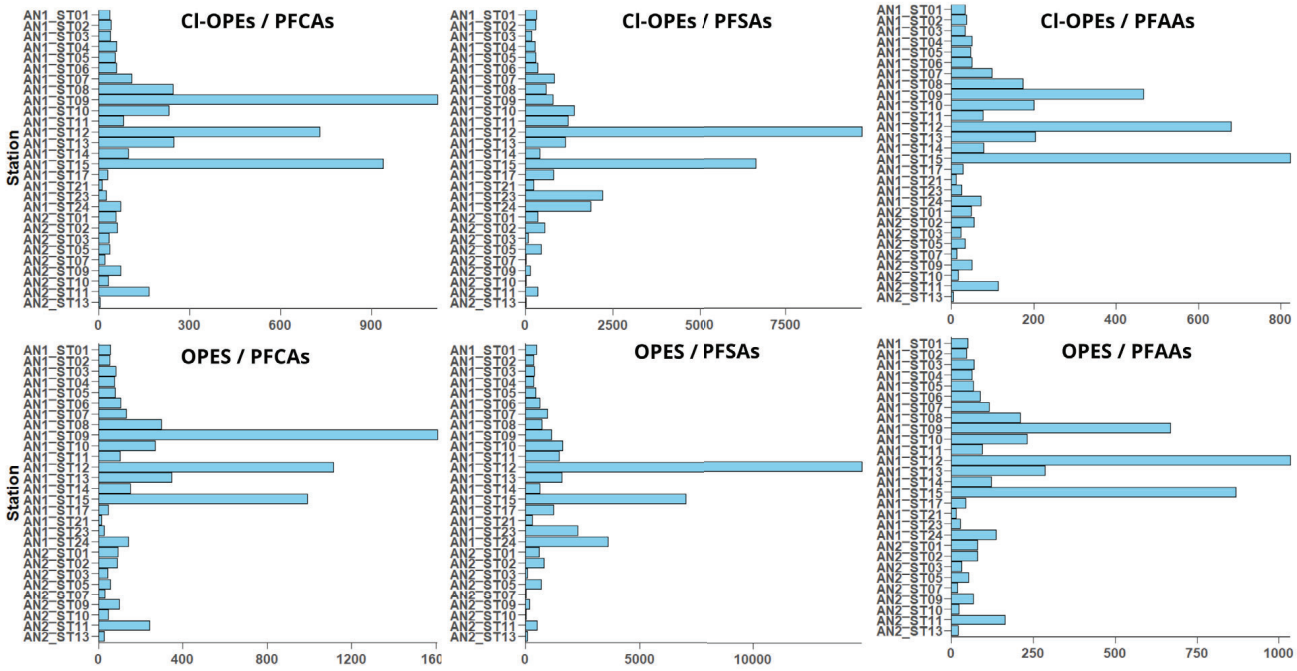


Figure 4.4 | Bar plots showing the ratios of $\sum_5$Cl-OPEs (Cl-OPEs) and total $\sum_{22}$OPEs (OPEs) relative to $\sum_{17}$PFAAs (PFAAs), $\sum_{11}$PFCAs (PFCAs), and $\sum_6$PFSAs (PFSAs) concentrations (pg L^{-1}) along an Atlantic Ocean (AN1, stations St01 to St24) and Southern Ocean (AN2 stations St01 to ST13) transects. Each panel represents a different ratio: Cl-OPEs/PFAAs, Cl-OPEs/PFCAs, Cl-OPEs/PFSAs, OPEs/PFAAs, OPEs/PFCAs, and OPEs/PFSAs.

As far as we know, this is the first time that large scale oceanic distributions are compared for different families of contaminants with significantly different properties. This comparison suggests that PFAAs, even at lower concentrations than OPEs and PAHs, have higher potential for long-range transport, thus being distributed globally. Even though PFAAs are non-volatile, while PAHs and OPEs are semivolatile, the strongest atmospheric component of the PAHs and OPEs cycle, does not compensate the influence of higher persistence of PFAAs, facilitating the global distribution of the latter. It could be also possible, that for semi-volatile compounds, their occurrence in the gas phase may facilitate their degradation by OH radical attack. While for PFAAs this process may not be relevant, or have a lower relevance. PFAAs are associated to sea spray aerosols which may protect them from efficient OH degradation. In any case, the comparison of the latitudinal distribution of OPEs, PAHs and PFAAs further suggest the key role that persistence plays in the global distribution of contaminants, and agrees with previous assessments (Cousins et al., 2020) suggesting that persistence is a key property to take into account when prioritizing chemicals of emerging concern up to the category of persistent organic pollutants.

4.1.4. BALANCING SCIENTIFIC OUTREACH WITH ACADEMIA

Scientific outreach has been an essential part of my work during the last five years, bridging the gap between research and societal awareness. Communicating the importance of studying man-made pollution in remote and vulnerable regions like Antarctica has been a priority. I've explored, with the help of the Global Change & Genomics Biogeochemistry research group, diverse formats, including public talks, educational workshops, visual campaigns, and interactive social media content. Each activity was tailored to engage specific audiences and to emphasize how persistent organic pollutants connect our actions to global environmental health.

Balancing these outreach efforts with academic responsibilities during my PhD has been challenging. Time management and strategic prioritization were crucial to ensure impactful outreach without compromising my research progress. Despite these challenges, engaging in outreach has enhanced my communication skills, broadened my perspective, and reinforced the scientific and societal relevance of my work.

To maximize the impact of these initiatives, our team developed an evaluation tool to assess the effectiveness of various formats (see Part 03 – Chapter 4). This tool measures reach, engagement,

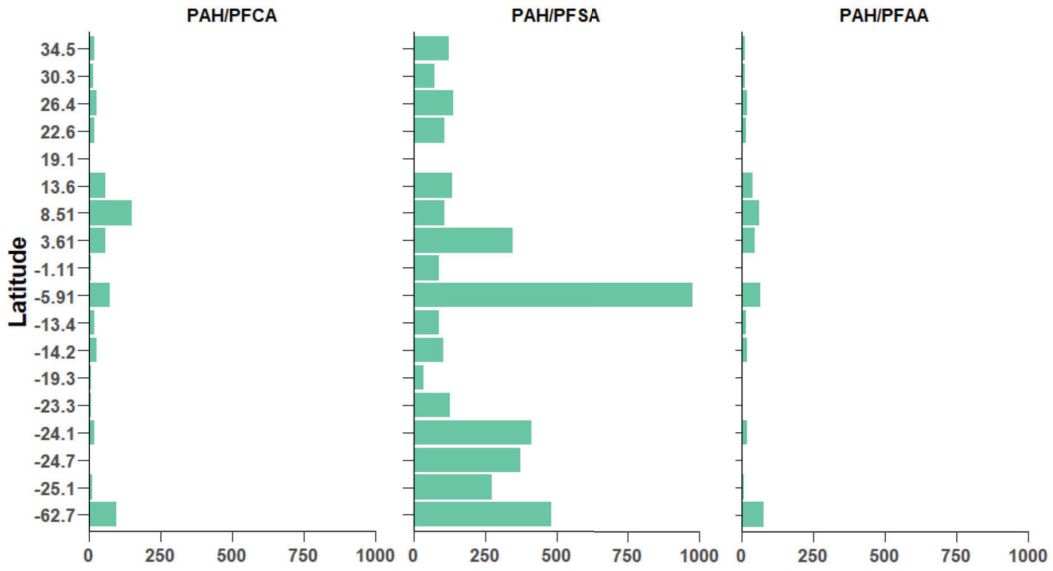


Figure 4.5 | Bar plots of pollutant ratios across latitude categories. The plots illustrate PAH/PFCA, PAH/PFSA, and PAH/PFAA ratios, respectively, from left to right. Each plot shares a consistent y-axis scale ranging from 0 to 1000 for easy comparison.

and educational value, helping to refine activities and allocate resources to the most impactful formats. For instance, comparing in-person workshops with online campaigns revealed valuable insights into audience preferences and engagement.

In a time of unprecedented global environmental challenges, communicating scientific findings effectively is more critical than ever. Outreach efforts on chemical pollution in the oceans and Antarctica highlight the interconnectedness of ecosystems and the urgent need for informed decision-making. By fostering trust in science and encouraging collaborative solutions, these initiatives emphasize that scientists are not just researchers but also advocates for sustainable change and sound environmental protection and management.

4.1.5. FUTURE PERSPECTIVES

This study represents a significant step forward in understanding the distribution and persistence of key organic pollutants in the marine environment. The wide transect, spanning multiple ocean zones, provided a comprehensive and unique dataset that includes a latitudinal and vertical assessment, up to 2000 m and the southernmost samples ever collected for OPEs and PFAAs at 70°S. The inclusion of vertical profiles in such remote and understudied regions offers a unique perspective on pollutant dynamics, such as the role of the biological pump sequestrating pollutants in the Atlantic and Southern oceans. These data fill critical gaps in our understanding of chemical pollution in extreme and remote environments.

However, challenges remain in capturing the full complexity of pollutant dynamics, particularly in the Southern Ocean, but also the deep ocean which remains understudied. Future research could benefit from the establishment of long-term temporal series, with data consistently collected along a standardized transect across multiple years. This approach would allow for a more robust assessment of temporal trends in pollutant concentrations, providing critical insights into the effectiveness of regulatory policies aimed at reducing the occurrence and impact of these compounds in the environment. Additionally, advanced technologies that allowed expanding vertical profiles to cover a continuum of depths, rather than sampling at only a limited number of depths, would offer a more comprehensive understanding of how pollutants are distributed through the water column and the processes driving their sequestration or persistence. Especially important would be to extend the vertical profiles to deeper waters, close to the sediment, to confirm the truly ubiquitous distribution of these contaminants.

Expanding beyond the current set of target compounds is another crucial avenue for future work. Non-target instrumental analysis, including high-resolution mass spectrometry (HRMS) approaches, could enable the identification of previously unmonitored or emerging pollutants. This methodology would help avoid the inherent limitations of focusing on predefined targeted compounds, allowing for a broader and more comprehensive assessment of the chemical burden in the environment. In combination with seasonal and inter-annual monitoring, non-target analysis could offer new insights into the evolving landscape of global chemical pollution and its interactions with climatic and oceanographic processes.

In summary, this study contributed significantly to the understanding of the occurrence and behavior of organic pollutants in the ocean, particularly in remote, high-latitude regions. By incorporating advanced technologies and non-target analytical approaches, future research can further illuminate the complex dynamics of pollutants and their environmental and ecological risks.

PART 04. GENERAL DISCUSSION AND CONCLUSIONS

4.2. CONCLUSIONS

1. Semivolatile aromatic-like compounds (SALCs) contribute significantly to dissolved black carbon (DBC) in the ocean, accounting for up to 16% of DBC concentrations, highlighting their interconnected biogeochemical cycles.

2. Microbial degradation is a key sink for SALCs, showing that there is a fraction of dissolved black carbon that is not refractory.

3. Generally, concentrations of organophosphate esters in the SML were higher than in the underlying waters, especially for the Southern Ocean.

4. OPE enrichment in sea spray aerosols (SSA), mediated by their concentration in the SML, highlights SSA formation as an important pathway for transfer of OPEs to the atmosphere.

5. OPEs exhibited widespread oceanic distribution at surface waters, with latitudinal gradients showing higher concentrations near the equator, compared to higher latitudes.

6. OPEs are persistent enough to reach all oceanic compartments, including the deep ocean.

7. The biological pump plays a significant role in OPE dynamics, through the depletion of OPEs from the photic zone and transfer to the deep ocean.

8. Perfluoroalkyl acids (PFAAs) showed a widespread and unexpected accumulation in Antarctic waters, with concentrations comparable to those observed in the North Atlantic.

9. A transport mechanism is suggested for PFAAs transport to the Southern Ocean, consisting in grasshopping mediated by sea spray aerosolization and wet deposition.

10. The persistence of PFAAs, driven by their resistance to biological degradation, lead to their long-term accumulation in Antarctic waters.

11. Ratios of PFAAs to other contaminants, such as PAHs and OPEs, reveal their unique persistence and low degradation rates, specifically for PFCAs.

12. Given their resistance to degradation and ability to accumulate in even the most remote environments, PFCAs emerge as the ultimate 'forever chemicals,' turning the Southern Ocean into both a receptor and long-term reservoir for these pollutants.

13. In a time when global change poses unprecedented challenges, the role of scientists extends beyond research to ensure their findings reach society effectively.

14. Outreach activities that communicate critical issues are essential for raising public awareness and fostering informed decision-making. For outreach efforts to maximize their impact, they must be well-planned, evidence-based, and subject to continuous evaluation.

REFERENCES

- A -

Ahrens, L., Xie, Z., & Ebinghaus, R. (2010). Distribution of perfluoroalkyl compounds in seawater from Northern Europe, Atlantic Ocean, and Southern Ocean. Chemosphere, 78(8), 1011–1016.

Armitage, J. M., Schenker, U. R. S., Scheringer, M., Martin, J. W., & Macleod, M. (2009). Modeling the Global Fate and Transport of Perfluorooctane Sulfonate (PFOS) and Precursor Compounds in Relation to Temporal Trends in Wildlife Exposure. 43(24), 9274–9280.

- B -

Benskin, J. P., Muir, D. C. G., Scott, B. F., Spencer, C., de Silva, A. O., Kylin, H., Martin, J. W., Morris, A., Lohmann, R., Tomy, G., Rosenberg, B., Taniyasu, S., & Yamashita, N. (2012). Perfluoroalkyl acids in the atlantic and Canadian arctic oceans. Environmental Science and Technology, 46(11), 5815–5823.

Berrojalbiz, N., Dachs, J., Ojeda, M. J., Valle, M. C., Castro-Jiménez, J., Wollgast, J., Ghiani, M., Hanke, G., & Zaldivar, J. M. (2011). Biogeochemical and physical controls on concentrations of polycyclic aromatic hydrocarbons in water and plankton of the Mediterranean and Black Seas. Global Biogeochemical Cycles, 25(4).

- C -

Casal, P., Zhang, Y., Martin, J. W., Pizarro, M., Jiménez, B., & Dachs, J. (2017). Role of Snow Deposition of Perfluoroalkylated Substances at Coastal Livingston Island (Maritime Antarctica). Environmental Science and Technology, 51(15), 8460–8470.

Casal, P., González-Gaya, B., Zhang, Y., Reardon, A. J. F., Martin, J. W., Jiménez, B., & Dachs, J. (2017). Accumulation of Perfluoroalkylated Substances in Oceanic Plankton. Environmental Science and Technology, 51(5), 2766–2775. https://doi.org/10.1021/acs.est.6b05821

Casas, G., Martínez-Varela, A., Roscales, J. L., Vila-Costa, M., Dachs, J., & Jiménez, B. (2020). Enrichment of perfluoroalkyl substances in the sea-surface microlayer and sea-spray aerosols in the Southern Ocean. Environmental Pollution, 267, 1–30.

Casas, G., Iriarte, J., D'Agostino, L. A., Roscales, J. L., Martinez-Varela, A., Vila-Costa, M., Martin, J. W., Jiménez, B., & Dachs, J. (2023). Inputs, amplification and sinks of perfluoroalkyl substances at coastal Antarctica. Environmental Pollution, 338.

Cerro-Gálvez, E., Roscales, J. L., Jiménez, B., Sala, M. M., Dachs, J., & Vila-Costa, M. (2020). Microbial responses to perfluoroalkyl substances and perfluorooctanesulfonate (PFOS) desulfurization in the Antarctic marine environment. Water Research, 171.

Cincinelli, A., Stortini, A. M., Checchini, L., Martellini, T., del Bubba, M., & Lepri, L. (2005). Enrichment of organic pollutants in the sea surface microlayer (SML) at Terra Nova Bay, Antarctica: Influence of SML on superficial snow composition. Journal of Environmental Monitoring, 7(12), 1305–1312.

Cousins, I. T., Dewitt, J. C., Glüge, J., Goldenman, G., Herzke, D., Lohmann, R., Ng, C. A., Scheringer, M., & Wang, Z. (2020). The high persistence of PFAS is sufficient for their management as a chemical class. In Environmental Science: Processes and Impacts, 22, 12, 2307–2312.

Cousins, I. T., Johansson, J. H., Salter, M. E., Sha, B., & Scheringer, M. (2022). Outside the Safe Operating Space of a New Planetary Boundary for Per- and Polyfluoroalkyl Substances (PFAS). In Environmental Science and Technology, 56, 16, 11172–11179.

Cristale, J.; Dantas, R. F.; De Luca, A.; Sans, C.; Esplugas, S.; Lacorte, S. Role of Oxygen and DOM in Sunlight Induced Photodegradation of

Organophosphorous Flame Retardants in River Water. J Hazard Mater 2017, 323, 242–249.

- D -

Dachs, J., Bayona, J. M., Raoux, C., & Albaigés, J. (1997). Spatial, vertical distribution and budget of polycyclic aromatic hydrocarbons in the western Mediterranean seawater. Environmental Science and Technology, 31(3), 682–688.

Duran, R., & Cravo-Laureau, C. (2016). Role of environmental factors and microorganisms in determining the fate of polycyclic aromatic hydrocarbons in the marine environment. In FEMS Microbiology Reviews, 40, 6, 814–830.

-F -

Fuoco,R.,Giannarelli,S.,Wei,Y.,Abete,C.,Francesconi, S., & Termine, M. (2005). Polychlorobiphenyls and polycyclic aromatic hydrocarbons in the sea-surface micro-layer and the water column at Gerlache Inlet, Antarctica. Journal of Environmental Monitoring, 7(12), 1313–1319.

-G -

Galbán-Malagón, C., Berrojalbiz, N., Ojeda, M. J., & Dachs, J. (2012). The oceanic biological pump modulates the atmospheric transport of persistent organic pollutants to the Arctic. Nature Communications, 3.

Galbán-Malagón, C. J., Berrojalbiz, N., Gioia, R., & Dachs, J. (2013). The "degradative" and "biological" pumps controls on the atmospheric deposition and sequestration of hexachlorocyclohexanes and hexachlorobenzene in the North Atlantic and Arctic Oceans. Environmental Science and Technology, 47(13), 7195–7203.

Glüge, J. et al. An overview of the uses of per- And polyfluoroalkyl substances (PFAS). Environmental Sciences Processes and Impacts 22, 2345–2373 (2020).

González-Gaya, B., Dachs, J., Roscales, J. L., Caballero, G., & Jiménez, B. (2014). Perfluoroalkylated substances in the global tropical and subtropical surface oceans. Environmental Science and Technology, 48(22), 13076–13084.

González-Gaya, B., Fernández-Pinos, M. C., Morales, L., Méjanelle, L., Abad, E., Piña, B., Duarte, C. M., Jiménez, B., & Dachs, J. (2016). High atmosphere-ocean exchange of Semivolatile Aromatic hydrocarbons. Nature Geoscience, 9(6), 438–442.

González-Gaya, B., Martínez-Varela, A., Vila-Costa, M., Casal, P., Cerro-Gálvez, E., Berrojalbiz, N., Lundin, D., Vidal, M., Mompeán, C., Bode, A., Jiménez, B., & Dachs, J. (2019). Biodegradation as an important sink of aromatic hydrocarbons in the oceans. Nature Geoscience, 12(2), 119–125.

Grunfeld, D. A., Gilbert, D., Hou, J., Jones, A. M., Lee, M. J., Kibbey, T. C. G., & Carroll, D. M. O. (2024). Underestimated burden of per- and polyfluoroalkyl substances in global surface waters and groundwaters. Nature Geoscience, 17, 340-346

- H -

Head, I. M., Jones, D. M. & Röling, W. F. M. (2006). Marine microorganisms make a meal of oil. Nature Reviews Microbioogy, 4, 173–182 (2006).

- I -

Iriarte, J., Dachs, J., Casas, G., Martínez-Varela, A., Berrojalbiz, N., & Vila-Costa, M. (2023). Snow-Dependent Biogeochemical Cycling of Polycyclic Aromatic Hydrocarbons at Coastal Antarctica. Environmental Science and Technology, 57(4), 1625–1636.

Iriarte, J., Trilla-Prieto, N., Berrojalbiz, N., Vila-Costa, M., & Dachs, J. (2025). Bacterial Production Modulates the Persistence of Organophosphate Ester Flame Retardants and Plasticizers in the Ocean. Environmental Science and Technology Letters.

- L -

Lindstrom, A. B., Strynar, M. J. & Libelo, E. L. (2011). Polyfluorinated compounds: Past, present, and future. Environmental Science and Technology, 45, 7954–7961.

Lohmann, R., Jurado, E., Dijkstra, H. A., & Dachs, J. (2013). Vertical eddy diffusion as a key mechanism for removing perfluorooctanoic acid (PFOA) from the global surface oceans. Environmental Pollution, 179, 88–94.

- M -

Muir, D., & Miaz, L. T. (2021). Spatial and Temporal Trends of Perfluoroalkyl Substances in Global Ocean and Coastal Waters. Environmental Science and Technology, 55(14), 9527–9537.

- N -

Nizzetto, L., Lohmann, R., Gioia, R., Jahnke, A., Temme, C., Dachs, J., Herckes, P., di Guardo, A., & Jones, K. C. (2008). PAHs in air and seawater along a North-South Atlantic transect: Trends, processes and possible sources. Environmental Science and Technology, 42(5), 1580–1585.

- R -

Reemtsma, T., García-López, M., Rodríguez, I., Quintana, J. B., & Rodil, R. (2008). Organophosphorus flame retardants and plasticizers in water and air I. Occurrence and fate. TrAC - Trends in Analytical Chemistry, 27(9), 727–737.

- S -

Schymanski, E. L., Zhang, J., Thiessen, P. A., Chirsir, P., Kondic, T., & Bolton, E. E. (2023). Per- and Polyfluoroalkyl Substances (PFAS) in PubChem: 7 Million and Growing. Environmental Science and Technology, 57(44), 16918–16928.

Stortini, A. M., Martellini, T., del Bubba, M., Lepri, L., Capodaglio, G., & Cincinelli, A. (2009). n-Alkanes, PAHs and surfactants in the sea surface microlayer and sea water samples of the Gerlache Inlet sea (Antarctica). Microchemical Journal, 92(1), 37–43.

Su, G., Letcher, R. J., & Yu, H. (2016). Organophosphate Flame Retardants and Plasticizers in Aqueous Solution: PH-Dependent Hydrolysis, Kinetics, and Pathways. Environmental Science and Technology, 50(15), 8103–8111.

- T -

Trilla-Prieto, N., Vila-Costa, M., Casas, G., Jiménez, B., & Dachs, J. (2021). Dissolved Black Carbon and Semivolatile Aromatic Hydrocarbons in the Ocean: Two Entangled Biogeochemical Cycles? Environmental Science and Technology Letters, 8, 918-923.

Trilla-Prieto, N., Iriarte, J., Berrojalbiz, N., Casas, G., Sobrino, C., Vila-Costa, M., Jiménez, B., & Dachs, J. (2024). Enrichment of Organophosphate Esters in the Sea Surface Microlayer from the Atlantic and Southern Oceans. Environmental Science and Technology Letters, 11, 1008-1015.

- U -

UNEP. (2009, 2019). Stockholm Convention on Persistent Organic Pollutants. United Nations Environment Programme.

- V -

van der Veen, I., & de Boer, J. (2012). Phosphorus flame retardants: Properties, production, environmental occurrence, toxicity and analysis. Chemosphere, 88(10), 1119–1153.

Vila-Costa, M.; Sebastián, M.; Pizarro, M.; Cerro-Gálvez, E.; Lundin, D.; Gasol, J. M. & Dachs, J. (2020). Microbial Consumption of Organophosphate Esters in Seawater under Phosphorus Limited Conditions. Scientific Reports, 9 (1), 1–11.

- W -

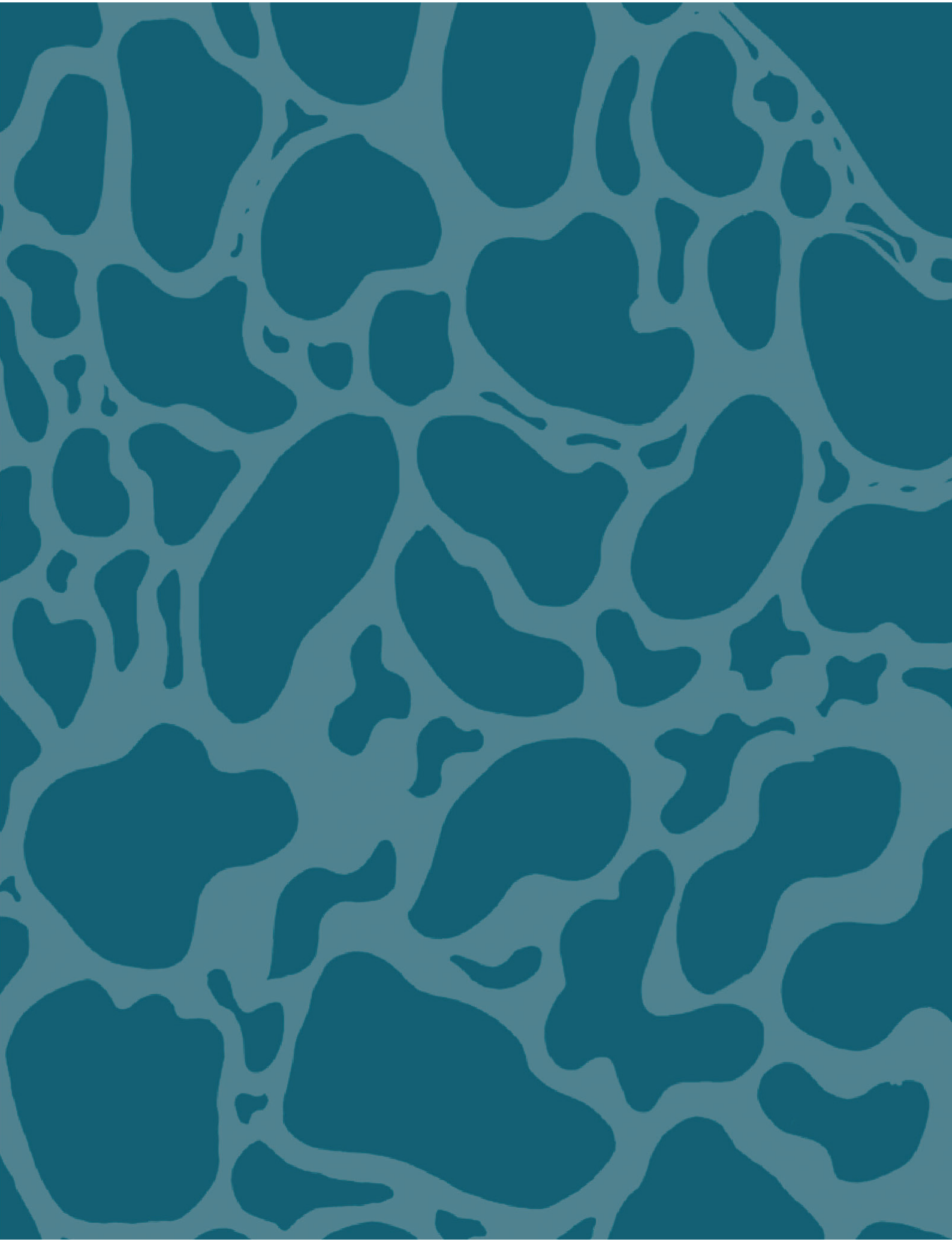
Wei, G. L., Li, D. Q., Zhuo, M. N., Liao, Y. S., Xie, Z. Y., Guo, T. L., Li, J. J., Zhang, S. Y., & Liang, Z. Q. (2015). Organophosphorus flame retardants and plasticizers: Sources, occurrence, toxicity and human exposure. In Environmental Pollution, 196, 29–46.

- X -

Xie, Z., Wang, P., Wang, X., Castro-Jiménez, J., Kallenborn, R., Liao, C., Mi, W., Lohmann, R., Vila-Costa, M., & Dachs, J. (2022). Organophosphate ester pollution in the oceans. Nature Reviews Earth and Environment, 3, 5, 309–322.

- Y -

Yamashita, N., Taniyasu, S., Petrick, G., Wei, S., Gamo, T., Lam, P. K. S., & Kannan, K. (2008). Perfluorinated acids as novel chemical tracers of global circulation of ocean waters. Chemosphere, 70(7), 1247–1255.





AKNOWLEDGEMENTS
AGRAÏMENTS
AGRADECIMIENTOS

Els darrers quatre anys i mig han estat un batut d'emocions difícils de d'explicar, però deixeu-me que ho intenti. Per una banda, fer una tesi doctoral ha estat un cami complex, intens, però profundament enriquidor. He pogut treballar del que m'agrada, fer ciència, comunicar-la, viure EL mar i viure AL mar. He complert un propòsit i ho he fet envoltada dels millors companys i companyes de feina, i tot això em fa sentir molt feliç i afortunada.

Per altra banda, aquests quatre anys i mig també han estat una de les etapes més complicades de la meva vida, ja que he hagut de transitar la malaltia i la pèrdua de la meva mare, la Chus. Aquesta vivència ha acompanyat cada moment d'aquest període, i em porta aquí a voler donar gràcies a totes les persones que han estat al meu costat, tant a la feina com fora: ensenyant-me, inspirant-me, ajudant-me, sostenint-me, i sent una xarxa que m'ha salvat de caure. Aquesta tesi és gràcies a totes vosaltres.

Com sabeu, la música banya la meva vida cada dia. Per això, cada una de les cançons que veureu escrites, per algun motiu em ressonen a vosaltres, o les hem gaudit, descobert o cantat juntes. Aquí va també el meu wrapped de la tesi.

Ara si, començo... Primer de tot vull agrair al Jordi i la Begoña per donar-me aquesta oportunitat que m'ha permès crèixer com a científica, i comunicadora, i viure unes de les experiències que més recordaré al llarg de la meva vida. Anar a **l'Antàrtida** era un somni per mi, i gràcies a aquesta feina hi he pogut anar no una, sinó dues vegades. Espero poder-hi tornar, però, si no, serà sempre un dels meus tresors més preuats. *Tierra del Hielo, de Clara Peya i Alessio Arena.*

Jordi, gràcies per la teva orientació, per la comprensió, per les idees brillants i per enssenyar-me a explicar històries. Gràcies també per la confiança i pels consells. He après tantes coses en aquests anys que em quedaria curta anomenant-les. De veritat, gràcies. He tingut molta sort de caure en aquest grup, de qualitat científica i humana inmillorable. *Born to Run, de Bruce Springsteen.*

Begoña, guardo con mucho cariño nuestras conversaciones por Skype, siempre positiva, animándome y mandándome energía. Gracias por tu cariño y por ser tan humana. Gracias también por tus consejos y revisiones escribiendo y por tu sabiduría con los PFAS. ¡Fue fantástico compartir unos meses contigo y tu equipo en 2022! *Pongamos que hablo de Madrid, de Joaquín Sabina.*

Maria, que divertit coincidir amb tu en aquesta etapa, quina qualitat, energia, motivació i ganes de fer les coses. M'has ensenyat que és possible fer ciència i també divulgar-la. Gràcies! *Cant de Lluita, de Roba Estesa.*

Nai, gracias por la paciencia, las ganas, y la escucha (que ha sido mucha), me alegro mucho de haber podido aprender contigo. Y también gracias, por las risas, por los talleres de InDesign, por las anécdotas, el cotilleo puro, los cafés (o matchas) y snacks después de comer, los descubrimientos musicales y los planes after-work... *Disco 2000, de Pulp.*

Jonsito, emprender este viaje de 5 años de lado (o de espaldas) ha sido una suerte inmensa. Un poco el ying y el yang, tu temple y mi energía... una combinación divertidísima! Gracias por la comprensión, por la escucha, por aprender juntos y enseñarnos. No podría haber pedido un compi de tesis mejor. El químico haciendo la tesis en biología, y la bióloga haciendo la tesis en química. ¿Qué podía salir mal? Eskerrik asko eta faltan botako zaitut. *Libre, de Izaro y Cris (Belako).*

Claudichi, coincidir en ANTOM y compartir camarote contigo fué un sueño. Gràcies pels mimos, per escoltar-me, per compartir amb mi les misèries quan no podíem més, i ajudar-nos a veure la llum. Ets una artista de cap a peus. Gracias también por esta maravillosa portada. Te quiero y can't wait a hacer proyectos juntis!!! *Piropo, de Tronco.*

Gemma i **Ali**, les meves seniors els dos primers anys de tesi. Gràcies per la saviesa, pels warnings, per l'ajuda i per l'experiència. No m'oblido de les fondues i raclettes a casa en Jordi fent cates de vins i menjant fins a no poder més. Ni de les sessions de ioga durant o pre-campanya (jeje). *Perra, de Rigoberta Bandini.*

A **Belén y Paulo**, los séniors - séniors, por forjar el camino sobre el que ha rodado esta tesis. I a todxs lxs que habéis pasado por el grupo a lo largo de estos cinco años... **Isa, Maria petita, Marta, Mar, Elisa, Laura, Júlia (y más...).** Gracias por las comidas, los cafés... ¡de todas he aprendido algo nuevo! I a la **Montse**, gràcies per la tutorització de la tesi! *Under Pressure, de Queen i el David Bowie.*

Berta, crec que no hagués anat a ANTOM-II si no fos per tu. I els que estaven allà i em van sentir cridar a través de les parets de l'Hotel Bagu ho poden corroborar. Gràcies per salvar-me el genoll a dues hores d'embarcar a l'Hespèrides per anar a l'Antàrtida. Ha estat un plaer coincidir amb tu a ANTOM-II, conduir juntes a Cartagena, cantar Manel fent anar el Baker, i compartir despatx i lab a l'IDAEA. *Benvolgut, de Manel.*

ANTOM collegues... qué loco confinarnos en Vigo y en Ushuaia, que loco embarcarnos en el Sarmiento cuando el mundo estaba en pandemia, qué loco el cruce del ecuador o la barbacoa en el estrecho de Gerlache. Visto con perspectiva, fue muy fuerte. Las campañas son para mí recuerdos tan preciados que me acompañaran toda la vida, y vosotroxs estaréis siempre en ellos. Gracias por ayudarme en mi vuelta a la ciencia, y por las fiestitas también. Espero volverme a embarcar en otras campañas con vosotrxs. *El Invento, de José González.*

A todo el equipo del **IQOG-CSIC** de Madrid: Pere, Juan, María, Cielo, Alba, Alice. Gracias por esos meses compartidos en Madrid. Fue un verdadero placer descubrir otra ciudad y otro labo con vosotrxs. *El Fin del Mundo, de La La Love You.*

Ah, i a la **Roser** i la **Sagrario** per ajudar-me quan començava a injectar i semblava que parlavem idiomes diferents. Gràcies per la paciencia. *Comèdia Dramàtica, de la Fúmiga.*

I a les noves fornades… **Clara y Jessica,** compartir tres días (TRES DÍAS?!!!) en Isla Decepción con vosotras fué un regalo de fin de tesis inmejorable. Descubrirnos en pequeño comité y como co-jefas en ese contexto en que parecía un videojuego lleno de trabas, fue increíble. Gracias por el trabajo bien hecho, por aprender las unas de las otras, pero también por los paseos, las volcadas de datos, los trasnochones y madrugones, por nuestra mesita de medio metro en nuestra pequeña casita de nuestro pequeño pueblito en la Antártida. De verdad que fue un regalo. *Rikiti de Mama Dousha.*

Y **Mapis**, gracias por tu energía, por tus recomendaciones, por tus correos de buenos días. Ha sido una gran sorpresa encontrarme con alguien (en la selva de la ciencia) que entiende la vida de una forma tan parecida a como la entiendo yo. Gracias!!! *Nuevayol, de Bad Bunny.*

Gracias también a Mapis, Jessica, Clara y Jon por decir SÍ cuando propuse la idea loca de crear un proyecto de divulgación científica sobre PANTOC. Fue luz en un momento bastante gris. El camino de aprender juntxs a hablar y posar ante una cámara, editar, subtitular, sintetizar, ha sido increíble y ha

dado a luz a un bebé histórico. No lo dejéis perder!!!! El capítulo 4 de esta tesis es de todas nosotras. Y, por supuesto, gracias también por nuestro viaje a la Toscana, un sueño, la verdad. Grazie mile! *Quando, quando, quando de Tony Renis.*

A la dotación del **Sarmiento de Gamboa** y **UTM** que participaron en la campaña ANTOM-I, gracias. Por llevarnos a cruzar el Atlántico, y por descubrirme la navegación de una forma tan divertida. Por bautizarnos en nuestro primer cruce por el ecuador, y por dejarme jugar con un sextante por primera vez. *Patagonia, de Xoel López.*

Gracias a la tripulación del **Hespérides** presentes en ANTOM-II (XXXIV Campaña Antártica), por el trabajo en el barco y por llevarnos tan al sur, tan al sur, como nunca antes había llegado el Hespérides. *Morriña, de Baiuca.*

Y al personal del ET y compañerxs científxs de la **Bae Gabriel de Castilla** en Isla Decepción en la XXXVI campaña antártica. Fue un placer descubrir la Antártida desde tierra, y aprender de todxs vosotrxs. Nunca, nunca olvidaré la vista, el olor y la sensación de acercarse a una pingüinera por primera vez. ¡Gracias! *Glaciar, de Xoel López.*

Aquest camí laboral ha estat sempre envoltat de company/es de feina increïbles, però a fora, m'esperava la meva xarxa que m'ha tret de la cova quan més necessitava veure la llum:

Núr, Mònica, Massi, Lau, Anna, Aïda, Gemma, Alba i Memé. Fa tants anys que ens coneixem que us heu convertit en casa. Sou la ZONA DE COMFORT, en majúscules. L'abraçada, les cançons que ens sabem de memòria, la birra freda, els vinets. Gràcies, perquè seguir compartint la vida i creixent juntes és una sort. Gràcies també per viure amb mi aquesta aventura, per escoltar-me, per rajar juntes de la sala blanca, i per dir-me moltes, moltes vegades que estic boja per voler anar a l'Antàrtida. Ja sabeu que si pogués us portaria amb mi cada vegada. I que bé ens ho passaríem!!! Us estimo i amb vosaltres me'n vaig a la fi del món! *La Gent Normal, versió de Manel.*

A la **Cris Ru, la Clara, el Marc i la Lauri.** Gràcies per ser els millors exemples de com comunicar ciència de la millor manera. Treballar amb vosaltres va ser un premi, i un aprenentatge, i ara, seguir creixent junts i dir cada vegada que ens veiem, que com l'equip del cosmo, no en trobarem cap altre és una sort immensa. *Petar-ho, d'Oques Grasses.*

Teresa, Clara, Mimi, Vir, Judith, Ivonne, Maria i Xènia: que feliç d'haver-vos conegut ja fa 8 anys! Sou energia fresca i renovada, idees bojes, estius infinits. Tan de bo poder desdoblar-me i tenir una part de mi sempre a Sant Antoni. I a l'squad, gràcies també, que divertit i refrescant compartir els estius amb vosaltres. *Volcans, de Buhos.*

Al **Jazel, el Marc, la Lucía, l'Alessandra**, gràcies per compartir dues aficions tan importants: la música i el mar. Gràcies pels Michael Collins, i per descobrir-me La Ludwig Band, la banda sonora de l'últim any de tesis. I gràcies també per les sortides a dins i a fora del mar. *Desembre, de La Ludwig Band.*

A la **Carlota, l'Helena i la Cris**, perquè tot i no veure'ns cada setmana, la complicitat i l'afecte fa que cada cop que ens veiem sigui com si encara tinguèssim 15 anys. *Roma, de Manel.*

A **Ses Calces**, per fer-me complir un altre somni: pujar un escenari i cantar davant de 1000 persones. Quina sort aprendre i fer-ho amb vosaltres. I quina bogeria tan xula ha estat!!! *El Lado Mes Bestia de la Vida, de l'Albert Pla i Still Young, de The Cat Empire.*
A **furgos**, per què sempre és divertit i energitzant trobar-me a un bar o festa amb vosaltres. *Nòmada, d'Adala.*I als **plomez**, per què sou la xarxa del papa i la mama, i la meva família postissa. Gràcies per fer-me sentir tan valorada. *Qualsevol Nit Pot Sortir el Sol de Jaume Sisa.*

A la **Karmen, la Laia, l'Estel, l'Ibai, el Jordi, la Pepi, la Marta, en Jaume i en Marcel**. Fa 8 anys que us heu convertit en una segona família. Gràcies per l'acollida i per convidar-me des del primer dia a les paelles al vostre meravellós jardí. *Ilargia de Ken Zazpi.*

Maria, iaia, iaio, avi, àvia, Montse, Alberto, Maria, Joan, Isabel, David i Olga, gràcies per l'amor, els jocs, la confiança i l'estabilitat en la que he tingut la sort de créixer i desenvolupar-me. Pels estius a Sant Antoni i els hiverns a Vallgorguina. Em sento orgullosa de dir que la sang catalana, i també la extremenya corre per les meves venes. *En el Borde del Mundo, de Valeria Castro.*

A la **Duna i la Oliveta**, per fer-me la millor de les companyies en les últimes setmanes d'escriure aquesta tesi i per omplir-me la casa d'energia, amor i caricies des de fa dos anys. Al **Nabiu i la Kiwi**, per omplir-li la caseta de bogeria i adicció per les plantes a l'Anna. I la **Petita**, **el Lur i l'Apache**, per ser tan caparruts i divertits com l'Odei. *Spirit Bird - Xavier Rudd.*

Papa, gràcies per ser inspiració, per creure en mi, i per fer de terapeuta cada cop que necessito desfogar-me. No em cansaré de dir-ho, ets la roca que ens sustenta. Gràcies també per encoratjar-me, per fardar de mi, i pel suport infinit. I gràcies per transmetre'ns des de petites l'amor per la muntanya, i les ganes d'aprendre. Crec que fer-nos nedar fins la ratlla de petites em va despertar les ganes de treballar vinculada al mar. *Nina de Miraguano, de Orquestra de Fireluche i Pau Riba.*

I **Anna**, gràcies a tu i a la vida per fer-nos crèixer juntes, per crear espais amb mi en els que la feina no formava part del discurs i per compartir tantes, tantes, taaantes coses. Per pujar a un escenari i cantar juntes, volar amb les teles, descobrir botiguetes, viatjar, bussejar, teixir, cosir, pintar o parlar de gats. I gràcies també per ser la viva imatge de la mare que ens va parir. *La Complicidad, de Perota Chingó.* Soc molt afortunada d'haver nascut entre vosaltres. La nostra Sagrada Família de quatre. Us estimo. *Historietes + Himne dels Pirates, de Dagoll Dagom.*

Odei, quin viatge!!!! Gràcies per inspirar-me, per buscar sempre el cantó positiu a les coses, per creure tant en mi (més del que jo hi crec a vegades), per trobar les coses boniques de cada situació, per ser llum i claredat i pau mental. Per ser casa. Per construir amb mi un lloc segur, amb la Duna i la Oliveta. Per acompanyar-me amb les idees boges, i deixar-me que t'acompanyi jo amb les teves. Per recórrer junts el món. Per recordar-me cada dia que l'amor és quotidià, és dolç i és fàcil. Gràcies, perquè aquests vuit anys de fer la vida junts (i els que venen) son tot el que podia demanar. T'estimo oceans. *Que Electricidad de Carlos Sadness + Sort De Tu d'Oques Grasses*

I **Mama**, a tu que has marxat durant aquest camí... gràcies per l'amor, el suport i la tendresa. Gràcies per enssenyar-me el que son les cures a la teva xarxa. I gràcies perquè, tot i ser una mare patidora, em vas encoratjar a embarcar-me en un vaixell a creuar l'Atlàntic, o a anar de campanya al lloc més llunyà i remot de tot el planeta terra. Sé que no va ser fàcil. *Vida, versió de Rita Payés i Pol Batlle*

Algú em va dir un dia: "*som filles de les mares que ens van parir, i si tu, Núria, ets una tia vital, forta i amb ganes de vida... només em puc imaginar que la teva mare és exactament igual*", i quanta raó... Crec que de tu he rebut les dues parts: la vital i aventurera, i la patidora. Quina barreja!

Ara només em queda aferrar-me a que des d'allà on siguis, saps aquesta tesi és per tu i gràcies a tu. I que soc qui soc gràcies a la seguretat i la base sòlida en la que he tingut la sort de créixer. Gràcies infinites. T'enyoro i t'estimo. Més que res en el món.

GRÀCIES!

THANK YOU!

¡GRACIAS!

FEMALE LEADERS

in oceanography, pollution and polar research

Thank you also to all the amazing **women** (among many others) who have fought and faced challenges in science, often receiving different treatment than their male colleagues. You paved the way for all of us who came after you...

France. Pioneer in marine biology; invented aquaria for observing marine life.



Spanish engineer and naval architect; significant contribution to maritime engineering.



Environmental scientist from the **US** and author of Silent Spring, sparking the modern environmental movement.





France. First woman to circumnavigate the globe, disguised as a man to join Bougainville's expedition.



Early coral reef **british** researcher, pioneered marine biological study in natural habitats.



France's first female oceanographer; documented and raised awareness about marine ecosystems.



Spanish marine biologist, discovered numerous marine species and advanced plankton studies.

US geologist and oceanographer. Created first global ocean floor maps, revealing the Mid-Atlantic Ridge.



Marine biologist from the **US** and ocean advocate, pioneer in underwater exploration.



Antarctic **US** researcher; first American woman to overwinter in Antarctica, studied marine physiology.



Spanish and **Catalan** oceanographer and marine biologist, participated in early Spanish Antarctic expeditions in 1984.





Marine biologist from the **US**. Known as "*Shark Lady*," conducted pioneering research on shark behavior.



Antarctic **US** geochemist; led first all-women expedition to Antarctica.



First Spanish and **Catalan** woman to lead Antarctic research; marine biologist focused on microbiology.

...and to all the women I have shared this journey, worked and laughed with, and befriended over these years... you are amazing!

